

Dissertation zur Erlangung des Doktorgrades
der Fakultät für Chemie und Pharmazie
der Ludwig-Maximilians-Universität München

**THE VERSATILITY OF TETRACOORDINATED BORON-CENTERED
SALTS FOR TRANSITION-METAL FREE C-C BOND FORMATIONS IN
ORGANOMETALLIC- AND ELECTRO-CHEMISTRY**

von

Arif Music

aus

Oberhausen

2020

ERKLÄRUNG

Diese Dissertation wurde im Sinne von § 7 der Promotionsordnung vom 28. November 2011 von Herrn Dr. Dorian Didier betreut.

EIDESSTATTLICHE VERSICHERUNG

Diese Dissertation wurde eigenständig und ohne unerlaubte Hilfe erarbeitet.

München, den 15.07.2020

.....
(Arif Music)

Dissertation eingereicht am: 26.05.2020
1. Gutachter: Dr. Dorian Didier
2. Gutachter: Prof. Dr. Oliver Trapp
Mündliche Prüfung am: 26.06.2020

Acknowledgements

This work was carried out from November 2017 to May 2020 under the guidance of Dr. Dorian Didier at the Department of Chemistry of the Ludwig-Maximilians-University, Munich.



Initially, I would like to thank Dr. Dorian Didier for being my Ph.D. supervisor and for allowing me to freely conduct my research. He navigated me through my Master and Ph.D. studies and has always been a supportive and reliable mentor. I always appreciated working on new topics and enjoyed the freedom of developing my own ideas. In addition, I want to thank him for being the first reviewer of this thesis.

Moreover, I likewise want to thank the other members of my Ph.D. defense committee, Prof. Dr. Oliver Trapp, Prof. Dr. Konstantin Karaghiosoff, Prof. Dr. Franz Bracher, Dr. Armin Ofial and Prof. Dr. Klaus T. Wanner. I also want to thank Michael Eisold, Marcel Leroux, Andreas Baumann, Felix Reiners, Alexandre Desaintjean, Ferdinand Lutter, Hendrik Schulz and Pascal Probst for proofreading this thesis.

A special thank you goes out to the cooking team and its chefs Micha, Andi, Marcel and Niels; I am a profound food lover and you helped me escape from the unbearable food in our canteen. A great thank you to the rest of the Didier/Knochel group as well, who made the daily lab-life in spite of all obstacles a pleasant experience.

I want to thank the members of the analytical department of the LMU Munich, Dr. David Stephenson, Claudia Ober, Sonja Kosak, Dr. Werner Spahl and Dr. Peter Mayer for measuring even the most “challenging” samples without any complaints.

Additionally, I would like to acknowledge my interns Clement Hoarau, Nicolas Hilgert, Phillip Spieß, Allan Plantefol and Yannick Lemke. They all did an amazing job in the lab and were essential in finishing the projects that are presented in this thesis.

I would like to specifically thank Andi, Micha and Marcel for the unforgettable time and memories we experienced together. As crazy as we all are, you guys had my back and stood by my side when things took the wrong turn. I will always appreciate your friendship.

Lastly, I want to express thanks to my siblings and parents for all the love and sacrifices they had to make to allow me to chase my dreams. And finally, I want to thank my dazzling girlfriend Charlotte, who was the person that inspired me to pursue chemistry in the first place; words cannot describe what you mean to me. This thesis would not have been written without any of these people and I will forever be grateful to them.

Parts of this Ph.D. Thesis have been published:

- 1) “One-Pot Preparation of Stable Organoboronate Reagents for the Functionalization of Unsaturated Four- and Five-Membered Carbo- and Heterocycles” A. N. Baumann[‡]; M. Eisold[‡]; A. Music[‡]; D. Didier; *Synthesis* **2018**, *50*, 3149–3160.
- 2) “Single-Pot Access to Bisorganoborinates: Applications in Zweifel Olefination” A. Music[‡]; A. N. Baumann[‡]; P. Spieß; N. Hilgert; M. Köllen; D. Didier, *Org. Lett.* **2019**, *21*, 2189–2193.
- 3) “Catalyst-Free Enantiospecific Olefination with *in situ* Generated Organocerium Species” A. Music; C. Hoarau; N. Hilgert; F. Zischka; D. Didier, *Angew. Chem. Int. Ed.* **2019**, *58*, 1188–1192.
- 4) “Organocerium: A New Contender for Halogen–Metal Exchanges” A. Music; D. Didier, *Synlett* **2019**, *30*, 1843–1849.
- 5) “Electrochemical Synthesis of Biaryls *via* Oxidative Intramolecular Coupling of Tetra(hetero)arylborates” A. Music; A. N. Baumann; P. Spieß; A. Plantefol; T. C. Jagau; D. Didier, *J. Am. Chem. Soc.* **2020**, *142*, 4341–4348.
- 6) “Electro-Olefination – A Catalyst Free, Stereoconvergent Strategy for the Functionalization of Alkenes” A. N. Baumann[‡], A. Music[‡], J. Dechent, N. Müller, T. C. Jagau, D. Didier, *Chem. Eur. J.* **2020**, *26*, 8382–8387.

[‡] *These authors have contributed equally to the published work.*

Parts of this thesis have been presented at scientific conferences:

BOSS XV - 16th Belgian Organic Synthesis Symposium

Enantioselective C-C-Bond Formation *via* Organocerium Species in Zweifel Olefinations
Brussel, Belgium, 2018.

SFB749 - Meeting at Venice International University

Single-Pot Access to Bisorganoborinates: Applications in Zweifel Olefination
Venice, Italy, 2019.

ESOC – 21st European Symposium of Organic Chemistry

Biaryl Coupling of Tetra(hetero)aryl borates *via* Electrochemical Oxidations
Vienna, Austria, 2019.

This project was also presented at the Hochschule-trifft-Industrie Meeting 2019 in Darmstadt (Merck KGaA).

Za Nanu.

*„Ich habe keine besondere Begabung,
sondern bin nur leidenschaftlich neugierig.“*

Albert Einstein

Abstract

The construction of carbon-carbon bonds has played and will play a central role in the development of future organic chemistry, as carbon frameworks represent vital motifs in natural and material sciences. For this reason, the field of synthetic organic chemistry is under constant pressure to produce novel methods that outcompete previous generations in terms of cost, atom-economy and sustainability. While this area of research is currently dominated by indispensable transition-metal catalyzed cross-coupling methods, there will always be demand for the development of complementary approaches and alternatives, which embodies the main objective of this thesis. Therefore, this work outlines transition-metal free C-C coupling reactions bearing tetrahedrally coordinated boron species at their reaction core. In a first step, the access toward those species as well as their robustness and usefulness in transition-metal free reactions is displayed and generalized. Novel organometallic species based on the earth-abundant lanthanide metal cerium are then established and their reactivity and advantages over other organometallics in organic transformations are explored. Lastly, the gained knowledge is translated to electrochemical processes, in which tetrahedrally coordinated boron salts enable versatile C-C bond forming reactions through oxidative electrocoupling chemistry.

Kurzfassung

Der Aufbau von Kohlenstoff-Kohlenstoff-Bindungen hat und wird eine zentrale Rolle in der zukünftigen Entwicklung der organischen Chemie spielen, da Kohlenstoff-Gerüste elementare Struktur motive in Natur- und Materialwissenschaften darstellen. Aus diesem Grund ist das Gebiet der synthetischen organischen Chemie unter ständigem Druck, neue Methoden zu entwickeln, die vorangegangene Systeme in Bezug auf Kosten, Atomökonomie und Nachhaltigkeit übertreffen. Obwohl dieses Forschungsgebiet derzeit von unverzichtbaren Übergangsmetall-katalysierten Kreuzkupplungsmethoden dominiert ist, wird es immer erforderlich sein, komplementäre Ansätze und Alternativen zu entwickeln, welches das Hauptziel dieser Arbeit darstellt. In dieser Arbeit werden daher übergangsmetallfreie C-C-Kupplungsreaktionen vorgestellt, deren Reaktionszentrum tetraedrisch koordinierte Borspezies darstellen. In einem ersten Schritt wird der synthetische Zugang zu diesen Spezies sowie ihre Robustheit und Nutzbarkeit in übergangsmetallfreien Reaktionen vorgestellt und verallgemeinert. Anschließend werden neuartige metallorganische Spezies auf Basis des am häufigsten vorkommenden Lanthanoids Cer hergestellt und ihre Reaktivität und Vorteile gegenüber anderen metallorganischen Verbindungen in organischen Reaktionen untersucht. Schließlich wird das gewonnene Wissen auf elektrochemische Prozesse übertragen, bei denen tetraedrisch koordinierte Borsalze vielseitige Reaktionen zur Bildung von C-C-Bindungen durch oxidative Elektrokupplungschemie ermöglichen.

Abbreviations

acac	acetylacetonate	dppf	1,1-bis(diphenylphosphino)ferrocene
aq.	aqueous	<i>dr</i>	diastereomeric ratio
Ar	aryl substituent	<i>E</i>	entgegen (opposite), <i>trans</i>
As	ampere seconds	E-X	electrophile
ATB	Alkenyltriarylborate	<i>ee</i>	enantiomeric excess
ATR	attenuated total reflection (IR)	<i>e.g.</i>	<i>exempli gratia</i> , for example
BARF	polyfluorinated tetraarylborate	EI	electron ionization
BDD	boron-doped diamond	<i>er</i>	enantiomeric ratio
BHT	dibutylhydroxytoluene	ESI	electron spray ionization
Boc	<i>tert</i> -butyloxycarbonyl	Et	ethyl
br	broad (NMR or IR spectroscopy)	<i>et al.</i>	<i>et alumni</i> , and others
Bu	butyl	equiv	equivalents
χ	electronegativity	F	Faraday
calcd	calculated	FCC	flash column chromatography
CAN	cerium ammonium nitrate	F_{eff}	Faradaic efficiency
CCDC	cambridge crystallographic data centre	FG	functional group
cm^{-1}	wavenumber	GC	gas chromatography
COVID-19	corona virus disease 2019	GCE	glassy carbon electrode
δ	chemical shift (NMR spectroscopy)	h	hour(s)
d	doublet (NMR spectroscopy)	Het	heteroaryl substituent
DavePhos	2-dicyclohexylphosphino-2'-(<i>N,N</i> ,dimethylamino)biphenyl	HFIP	hexafluoroisopropanol
dba	(1 <i>E</i> ,4 <i>E</i>)-1,5-diphenylpenta-1,4-dien-3-one	$h\nu$	photo irradiation
DCM	dichloromethane	HRMS	high resolution mass spectrometry
DDQ	2,3-dichloro-5,6-dicyano-1,4-benzoquinone	<i>i</i>	<i>iso</i>
DEP	direct evaporation probe	<i>J</i>	coupling constant (NMR)
DHEA	androst-5-en-3 β -ol-17-onr	K	Kelvin
DIPA	diisopropylamine	LDA	lithium diisopropylamide
DME	dimethoxyethane	LRMS	low resolution mass spectrometry
DMF	dimethylformamide	M	metal
DMG	directing metalation group	M	molar ($\text{mol}\cdot\text{L}^{-1}$)
DMSO	dimethylsulfoxide	m	medium (IR spectroscopy)
DoM	directed <i>ortho</i> -metalation	m	multiplet (NMR spectroscopy)

<i>m</i>	<i>meta</i>	quint	quintet (NMR spectroscopy)
mA	milliampere	R	organic substituent
Me	methyl	<i>R_f</i>	retention factor
MeLi	methylolithium	rpm	revolutions per minute
mg	milligrams	rt	room temperature
MHz	megahertz	RuPhos	2-dicyclohexylphosphino-2',6'-diisopropoxybiphenyl
MIDA	methyliminodiacetic acid	RVC	reticulated vitreous carbon
min	minutes	s	singlet (NMR spectroscopy)
mmol	millimole	s	strong (IR spectroscopy)
mol%	equiv•10 ²	sat.	saturated
MP	melting point	<i>s</i> -BuLi	<i>sec</i> -butyllithium
MS	mass spectrometry	SCE	saturated calomel electrode
<i>n</i> -BuLi	<i>n</i> -butyllithium	SD	standard
n.d.	not determined	SM	starting material
neopent	neopentyl	t	triplet (NMR spectroscopy)
NHC	<i>N</i> -heterocyclic carbene	TAB	tetraarylborate
nm	nanometre	<i>t</i> -BuLi	<i>tert</i> -butyllithium
NMP	<i>N</i> -methyl-2-pyrrolidone	TBHP	<i>tert</i> -butyl hydroperoxide
NMR	nuclear magnetic resonance	TBS	<i>tert</i> -butyldimethylsilyl
NOE	nuclear overhauser effect	TEMPO	(2,2,6,6-tetramethylpiperidin-1-yl)oxyl
NOESY	NOE spectroscopy	Tf	triflyl
<i>o</i>	<i>ortho</i>	tfp	tri(2-furyl)phosphine
<i>o/n</i>	overnight	THF	tetrahydrofuran
Ox	oxidation	THP	tetrahydropyran
<i>p</i>	<i>para</i>	TLC	thin layer chromatography
PAA	<i>para</i> -anisaldehyde	TM	transition metal
Ph	phenyl	TMEDA	<i>N,N,N',N'</i> -tetramethylethylenediamine
PIDA	(diacetoxyiodo)benzene	TMS	trimethylsilyl
pin	pinacol	TOB	tetraorganoborate
PMDTA	<i>N,N,N',N'',N'''</i> -pentamethyldiethylenetriamine	UV	ultraviolet
ppm	parts per million	V	volt
Pr	propyl	v/v	volume ratio
Py	pyridyl	vs, vw	very strong, very weak (IR)
q	quartet (NMR spectroscopy)	Z	zusammen (together), <i>cis</i>

TABLE OF CONTENTS

ACKNOWLEDGEMENTS	III
ABSTRACT	VII
KURZFASSUNG	VII
ABBREVIATIONS	VIII
A. INTRODUCTION	1
1 GENERAL INTRODUCTION	2
2 ORGANOMETALLIC CHEMISTRY	3
2.1 Overview.....	3
2.2 Halogen-Metal Exchange Reactions.....	6
2.3 Transmetalation.....	12
3 ORGANOBORON CHEMISTRY	15
3.1 Overview.....	15
3.2 Tetracoordinated Organoboron Salts.....	16
3.3 The Suzuki-Miyaura Cross-Coupling.....	21
3.4 Transition-metal free C-C bond formations – Zweifel Olefination.....	25
4 ELECTROCHEMISTRY	29
4.1 Overview.....	29
4.2 Oxidative C-C Couplings.....	31
4.3 Tetracoordinated Boron Salts.....	33
5 OBJECTIVES	37
B. RESULTS AND DISCUSSION	39
1 ONE-POT PREPARATION OF STABLE ORGANOBORONATE REAGENTS FOR THE FUNCTIONALIZATION OF UNSATURATED FOUR- AND FIVE-MEMBERED CARBO- AND HETEROCYCLES	40
1.1 Relevance.....	40
1.2 Preamble.....	40
2 SINGLE-POT ACCESS TO BISORGANOBORINATES: APPLICATIONS IN ZWEIFEL OLEFINATION	50
2.1 Relevance.....	50
2.2 Preamble.....	50

3	CATALYST-FREE ENANTIOSPECIFIC OLEFINATION WITH <i>IN SITU</i> GENERATED ORGANOCERIUM SPECIES	56
3.1	Relevance	56
3.2	Preamble	56
4	ELECTROCHEMICAL SYNTHESIS OF BIARYLS <i>VIA</i> OXIDATIVE INTRAMOLECULAR COUPLING OF TETRA(HETERO)ARYLBORATES	62
4.1	Relevance	62
4.2	Preamble	62
5	ELECTRO-OLEFINATION – A CATALYST FREE, STEREOCONVERGENT STRATEGY FOR THE FUNCTIONALIZATION OF ALKENES	71
5.1	Relevance	71
5.2	Preamble	71
6	CONCLUSIONS	78
6.1	Summary	78
6.2	Outlook	81
	C. EXPERIMENTAL PART	83
1	GENERAL CONSIDERATIONS	84
1.1	Solvents	84
1.2	Reagents	84
1.3	Chromatography	85
1.4	Analytical data	85
1.5	Single Crystal X-Ray Diffraction Studies	87
2	ONE-POT PREPARATION OF STABLE ORGANOBORONATE REAGENTS FOR THE FUNCTIONALIZATION OF UNSATURATED FOUR- AND FIVE-MEMBERED CARBO- AND HETEROCYCLES	87
2.1	General Procedures	87
2.2	Representative NMR Spectra	88
2.3	Single X-Ray Diffraction	89
3	SINGLE-POT ACCESS TO BISORGANOBORINATES: APPLICATIONS IN ZWEIFEL OLEFINATION	92
3.1	¹¹ B NMR Analysis	92
3.2	Synthesis of Organometallic Reagents	93
3.3	General Procedures	94
3.4	Experimental Data	99

3.5 Representative NMR Spectra	113
4 CATALYST-FREE ENANTIOSPECIFIC OLEFINATION WITH <i>IN SITU</i> GENERATED ORGANOCERIUM SPECIES	114
4.1 Synthesis of the Exchange Reagent.....	114
4.2 General Procedures.....	114
4.3 Optimizations	116
4.4 Experimental Data.....	116
4.5 Raman Spectroscopy	143
4.6 Representative NMR Spectra	147
4.7 Chiral HPLC Analysis.....	149
5 ELECTROCHEMICAL SYNTHESIS OF BIARYLS <i>VIA</i> OXIDATIVE INTRAMOLECULAR COUPLING OF TETRA(HETERO)ARYLBORATES	154
5.1 General Procedures.....	154
5.2 Formation of TAB Salt 1a by ¹¹ B NMR.....	157
5.3 Optimizations	158
5.4 NMR Experiments.....	160
5.5 Experimental Data.....	162
5.6 Decagram Scale Reaction of 2a.....	188
5.7 Cyclic Voltammetry	189
5.8 Calculations	191
5.9 Single X-Ray Diffraction	194
5.10 Unsuccessful Transformations and Limitations	197
5.11 Representative NMR Spectra	198
6 ELECTRO-OLEFINATION – A CATALYST FREE STEREOCONVERGENT STRATEGY FOR THE FUNCTIONALIZATION OF ALKENES	199
6.1 General Procedures.....	199
6.2 Formation of ATB salt 2a by ¹¹ B NMR	201
6.3 Optimizations	201
6.4 Experimental Data.....	202
6.5 Cyclic Voltammetry	221
6.6 Calculations	222
6.7 Single Crystal X-Ray Diffraction.....	224
6.8 Representative NMR Spectra	225

A. INTRODUCTION

1 General Introduction

"One thing appears to be unmistakably certain. Namely, we will always need, perhaps increasingly so with time, the uniquely creative field of synthetic organic and organometallic chemistry to prepare both new and existing organic compounds for the benefit and well-being of mankind."¹ (Ei-ichi Negishi, Nobel Lecture, 08.12.2010)

Over the last century, organic synthesis has – driven by tremendous efforts and creativity – flourished from a primitive and limited field to an area of research that allows chemists with sufficient resources and patience to synthesize virtually any conceivable molecule. Especially the ground-breaking discovery of transition-metal catalyzed cross-coupling reactions in the 1970s,² which was awarded with the Nobel Prize in Chemistry in 2010, has changed the way chemists think about synthesis in general, as they allow for the simple – yet essential – formation of carbon-carbon bonds. The development of reliable, efficient, economical and eco-compatible methods for those C-C bond formations is of utmost importance to humankind, as they represent key steps in the synthesis of bioactive, highly complex molecules developed as pharmaceutically active ingredients and agrochemicals as well as in the building of novel optoelectronic materials and devices.³

Since our globalized society is growing rapidly and is forecast to peak at around 11 billion people in 2100⁴, recent studies suggest that agricultural production has to increase by 1.1 percent every year to meet the rising food demand.⁵ As food consumption is in addition expected to increase by up to 80% in underdeveloped countries by 2100, as we are facing challenges like global warming⁶ and pandemic outbreaks such as most recently COVID-19⁷, there is extreme political and societal pressure on agricultural and pharmaceutical chemistry to provide solutions to those threats.⁸ Hence, the main goal of modern organic chemistry is to build upon the countless discoveries from the past and come up with fast synthetic answers that meet ecological and economical restrictions. In modern 21st century organic chemistry, it will therefore no longer be sufficient to simply be “the first” to synthesize the desired needed compound; the success of a methodology will largely depend on how efficiently and straightforward a compound can be prepared to ultimately find the “flawless” synthesis.^{1,9}

¹ E. Negishi, *Angew. Chem. Int. Ed.* **2011**, *50*, 6738–6764.

² a) N. Miyaura, A. Suzuki, *J. Chem. Soc., Chem. Commun.* **1979**, 866–867; b) N. Miyaura, K. Yamada, A. Suzuki, *Tetrahedron Letters* **1979**, *20*, 3437–3440; c) A. O. King, N. Okukado, E.-i. Negishi, *J. Chem. Soc., Chem. Commun.* **1977**, 683–684; d) R. F. Heck, J. P. Nolley, *J. Org. Chem.* **1972**, *37*, 2320–2322.

³ A. Suzuki, *Angew. Chem. Int. Ed.* **2011**, *50*, 6722–6737.

⁴ United Nations, Dept of Economic and Social Affairs, “*World Population Prospects*”, **2019**.

⁵ N. Alexandratos, J. Bruinsma, *ESA Working Paper* **2012**, 12-03.

⁶ J. Cook, et al., *Environ. Res. Lett.* **2016**, *11*, 048002.

⁷ R. Li, S. Pei, B. Chen, Y. Song, T. Zhang, W. Yang, J. Shaman, *Science* **2020**, *368*, 489–493.

⁸ a) P. S. Baran, *J. Am. Chem. Soc.* **2018**, *140*, 4751–4755; b) L. Depenbusch, S. Klasen, *PLOS ONE* **2019**, *14*, e0223188; c) W. Willett, et al., *The Lancet* **2019**, *393*, 447–492.

⁹ J. M. Smith, S. J. Harwood, P. S. Baran, *Acc. Chem. Res.* **2018**, *51*, 1807–1817.

2 Organometallic Chemistry

2.1 Overview

Organometallic compounds are molecules with at least one carbon-metal (C-M) or carbon-metalloid bond, therefore including elements such as boron (C-B). Even though the first syntheses of organometallic compounds trace back to the 18th century¹⁰, their use was popularized by the pioneering work on organomagnesium compounds by Victor Grignard in 1900¹¹, which was awarded with the Nobel Prize in 1912. More than a hundred years later, countless compounds containing C-M bonds have been produced and studied, including a wide range of alkaline, earth alkaline and transition metals and great structural diversity on the organic counterpart.¹²

What makes organometallic compounds appealing is the inherent polarization of the C-M bond, which can be best described by the difference in electronegativity between the two atoms. With an electronegativity of 2.55 on the Pauling scale¹³, the carbon atom is more electronegative than any known metal or metalloid, thereby generally acting as a nucleophile when bound to a metal (Figure 1). The greater the difference between the two atoms, the higher the ionic character of the C-M bond, resulting in a more reactive species. For this reason, organolithium compounds are highly reactive species that even act as nucleophiles toward ethereal solvents at ambient temperature and lack functional group tolerance.¹⁴ In contrast, Grignard reagents show lower reactivity than organolithium compounds and can be stored in ethereal solvents at room temperature but are in return more tolerant for functional groups.¹⁵ Lastly, organoboron compounds have a strong covalent character, showcasing exceptional functional group tolerance. However, their limited reactivity often requires additional activation.¹⁶

Further tendencies for reactivity and tolerance are observed when altering the hybridization of the organometallic species. In general, the reactivity of organometallics increases from C_{sp}-M to C_{sp}²-M to C_{sp}³-M species, as stabilization of the nucleophilic carbon atom from the nuclei is reduced with increasing p-orbital character.¹⁷

¹⁰ a) D. Seyferth, *Organometallics* **2001**, 20, 1488–1498; b) K. C. Nicolaou, *Angew. Chem. Int. Ed.* **2013**, 52, 131–146.

¹¹ V. Grignard, *Compt. Rend. Acad. Sci. Paris* **1900**, 130, 1322–1324.

¹² a) K. C. Nicolaou, D. Vourloumis, N. Winssinger, P. S. Baran, *Angew. Chem. Int. Ed.* **2000**, 39, 44–122; b) A. Boudier, L. O. Bromm, M. Lotz, P. Knochel, *Angew. Chem. Int. Ed.* **2000**, 39, 4414–4435; c) K. C. Nicolaou, P. G. Bulger, D. Sarlah, *Angew. Chem. Int. Ed.* **2005**, 44, 4442–4489; d) S. D. Robertson, M. Uzelac, R. E. Mulvey, *Chem. Rev.* **2019**, 119, 8332–8405.

¹³ a) L. Pauling, *J. Am. Chem. Soc.* **1932**, 9, 3570–3582; b) A. L. Allred, *J. Inorg. Nucl. Chem.* **1961**, 17, 215–221.

¹⁴ P. Stanetty, M. D. Mihovilovic, *J. Org. Chem.* **1997**, 62, 1514–1515.

¹⁵ D. Seyferth, *Organometallics* **2009**, 28, 1598–1605.

¹⁶ a) N. Miyaura, A. Suzuki, *Chem. Rev.* **1995**, 95, 2457–2483; b) A. F. Littke, G. C. Fu, *Angew. Chem. Int. Ed.* **2002**, 41, 4176–4211.

¹⁷ a) D. Hauk, S. Lang, A. Murso, *Org. Process Res. Dev.* **2006**, 10, 733–738.

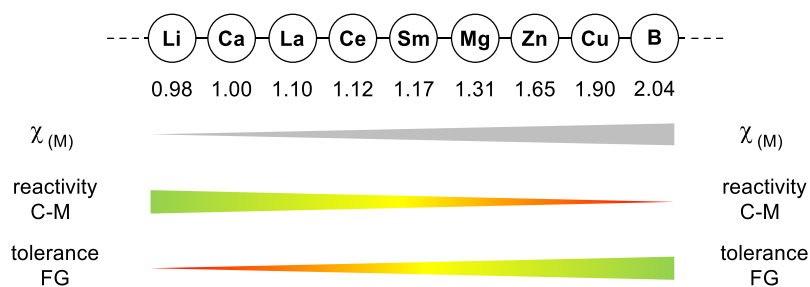


Figure 1: Comparison of electronegativity, reactivity and functional group (FG) tolerance of various organometallics on the Pauling scale.¹⁸

The first general route toward organometallic reagents was established by Frankland¹⁹ and Grignard¹¹ in the second half of the 19th century and involves the oxidative insertion of a metal such as zinc¹⁹, lithium²⁰ and magnesium¹¹ into a carbon-halogen bond, which in case of magnesium is widely believed to follow a radical SET mechanism.²¹ However, most recent quantum-chemical calculations have shown that several processes are of importance, including a nucleophilic pathway.²² In order to facilitate the reaction progress, the usually oxidized and therefore passivated magnesium turnings or powder has to be activated, *e.g.* with iodine or 1,2-dibromoethane.²³ While the original procedure with **1** in diethyl ether is performed in refluxing solvent, a stronger activation by reduction of magnesium salt (*e.g.* MgCl₂) with an alkaline metal (*e.g.* Li, K) results in the much more reactive Rieke-Magnesium (Mg*), enabling the insertion at cryogenic temperatures and allowing for the tolerance of a wider range of functional groups, such as ester-substituted arene **3** (Scheme 1).²⁴ Lastly, the presence of equimolar amount of LiCl in THF greatly enhances the oxidative insertion of magnesium, presumably due to solubilization and coordination effects at the heterogenic reaction surface.²⁵ This mild LiCl mediated magnesium insertion by Knochel and co-workers therefore conveniently allows for the preparation of Grignard reagents at ambient temperature, resulting in a high functional group tolerance exemplified in **5**.²⁶

¹⁸ Figure adapted from: A. Music, D. Didier, *Synlett* **2019**, 30, 1843–1849.

¹⁹ E. Frankland, *Liebigs Ann. Chem.* **1849**, 71, 171–213.

²⁰ M. Schlosser, *Organometallics in Organic Synthesis*, 2nd Ed., **2002**, Wiley, New York.

²¹ a) H. R. Rogers, C. L. Hill, Y. Fujiwara, R. J. Rogers, H. L. Mitchell, G. M. Whitesides, *J. Am. Chem. Soc.* **1980**, 102, 217–226; b) H. M. Walborsky, J. Rachon, *J. Am. Chem. Soc.* **1989**, 111, 1897–1900; c) Z.-N. Chen, G. Fu, X. Xu, *Org. Biomol. Chem.* **2012**, 10, 9491–9500.

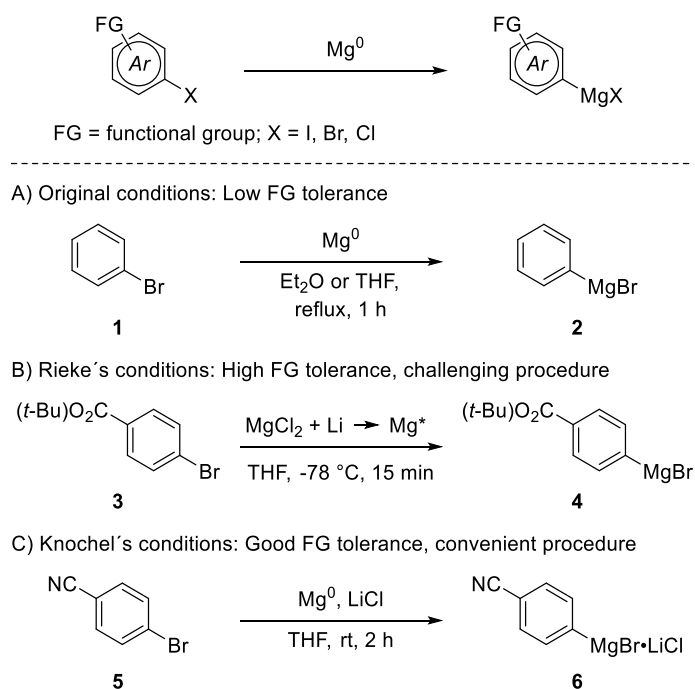
²² R. M. Peltzer, J. Gauss, O. Eisenstein, M. Cascella, *J. Am. Chem. Soc.* **2020**, 142, 2984–2994.

²³ a) H. Gilman, R. H. Kirby, *Rec. Trav. Chim. Pays-Bas* **1935**, 54, 577–582; b) D. E. Pearson, D. Cowan, J. D. Beckler, *J. Org. Chem.* **1959**, 24, 504–509; c) U. Tilstam, H. Weinmann, *Org. Proc. Res. Dev.* **2002**, 6, 906–910.

²⁴ a) T. P. Burns, R. D. Rieke, *J. Org. Chem.* **1987**, 52, 3674–3680; b) R. D. Rieke, *Science* **1989**, 246, 1260–1264; c) J.-S. Lee, R. Velarde-Ortiz, A. Guijarro, J. R. Wurst, R. D. Rieke, *J. Org. Chem.* **2000**, 65, 5428–5430.

²⁵ a) C. Reichardt, *Solvents and Solvent Effects in Organic Chemistry*, **2003**, Wiley-VCH, Weinheim; b) C. Feng, D. W. Cunningham, Q. T. Easter, S. A. Blum, *J. Am. Chem. Soc.* **2016**, 138, 11156–11159.

²⁶ F. M. Piller, P. Appukkuttan, A. Gavryushin, M. Helm, P. Knochel, *Angew. Chem. Int. Ed.* **2008**, 47, 6802–6806.



Scheme 1: Different methods for the oxidative addition of magnesium into carbon-halogen bonds.²⁷

A complementary approach is the directed metalation originating from the pioneering work of Schlenk in 1928, in which alkyl metal or metal amide bases cleave a C-H bond heterolytically.²⁸ The deprotonation step is hereby usually controlled by a directing metalation group (DMG), resulting in selective C-H metalation adjacent to the DMG.²⁹ This directed *ortho*-metalation (DoM) can either be enabled by kinetic effects, in which the Lewis basic DMG acts as coordination anchor for the organometallic base, or by electronic effects of the then electron-withdrawing DMG itself.³⁰ Importantly, the concept of directed metalation can be applied to heterocycles. For instance, the coordinative influence of heteroatoms in furans **7**, thiophenes **8** and pyrroles **9** enables smooth *ortho*-metalation.²⁰ As an example, the McMillan group exploited this property to synthesize the naturally occurring (+)-minfiensine **14** (Scheme 2) by direct *ortho*-metalation of the corresponding protected indole moiety **12**.³¹ In addition, non-aromatic surrogates such as vinyl ethers **10** and **11** can be readily metalated in the respective *ortho*-position of the DMG with simple alkylmetal bases such as *n*-BuLi.³²

The last two major methods for the preparation of organometallics, the halogen-metal exchange and the transmetalation, will be discussed in detail as they are the most frequently used methods for the preparation of organometallics in this work.

²⁷ Scheme adapted from: M. A. Ganiak, Dissertation, LMU Munich, **2018**.

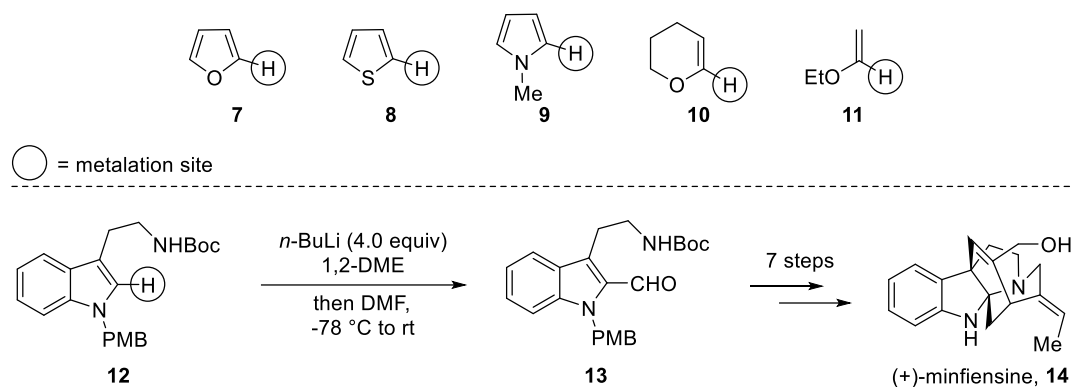
²⁸ W. Schlenk, E. Bergmann, *Justus Liebigs Ann. Chem.* **1928**, 463, 98–227.

²⁹ a) E. J.-G. Anctil, V. Sniekus, *J. Organomet. Chem.* **2002**, 653, 150–160; b) F. F. Wagner, D. L. Comins *Eur. J. Org. Chem.* **2006**, 3562–3565.

³⁰ a) V. Sniekus, *Chem. Rev.* **1990**, 90, 879–933; b) M. C. Whisler, S. MacNeil, V. Snieckus, P. Beak, *Angew. Chem. Int. Ed.* **2004**, 43, 2206–2225.

³¹ S. B. Jones, B. Simmons, D. W. C. MacMillan, *J. Am. Chem. Soc.* **2009**, 131, 13606–13607.

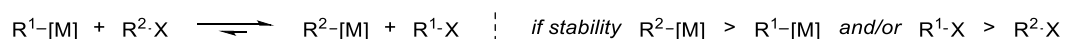
³² V. Hornillos, M. Giannerini, C. Vila, M. Fananas-Mastral, B. Feringa, *Chem. Sci.* **2015**, 6, 1394–1398.



Scheme 2: Preferred metalation sites on heterocycles and non-aromatic systems (top) and synthetic application to minfiensine (bottom).

2.2 Halogen-Metal Exchange Reactions³³

The halogen-metal exchange is one of the most convenient and fastest routes toward organometallic reagents. Since the discovery of bromine-magnesium exchange reactions by Prevost in 1931³⁴, numerous other metals including transition metals and lanthanides have shown to partake in metal-exchange chemistry. Hereby, a halogen-metal exchange is a reaction in equilibrium between an organometallic species and an organic halide (Scheme 3). The direction of this equilibrium is displaced with respect to the relative stability of the different carbon-metal bonds, favoring the formation of the most stable organometallic reagent.³⁵ As already described, the stability of the formed organometallic strongly depends on the hybridization of the carbon atom and additional stabilizing mesomeric and inductive effects ($sp > sp^2_{\text{vinyl}} > sp^2_{\text{aryl}} > sp^3_{\text{prim}} > sp^3_{\text{sec}} > sp^3_{\text{tert}}$).¹⁷ Although the direction of the exchange is mainly controlled by the nature of the organic part, its rate strongly depends on the electronegativity of the metal, so that a halogen-lithium exchange proceeds faster than the corresponding halogen-magnesium exchange.³⁶



Scheme 3: A typical halogen-metal exchange reaction.

Among all metal-halogen exchange reactions, the lithium-halogen exchange discovered by Wittig³⁷ and Gilman³⁸ in 1938/39 is one of the most utilized, since the fast reaction rate allows for the rapid formation of organolithium compounds. As organolithium reagents rank among the most reactive organometallic

³³ This chapter has been adapted from: A. Music, D. Didier, *Synlett* **2019**, 30, 1843–1849.

³⁴ C. Prévost, *Bull. Soc. Chim. Fr.* **1931**, 49, 1372–1381.

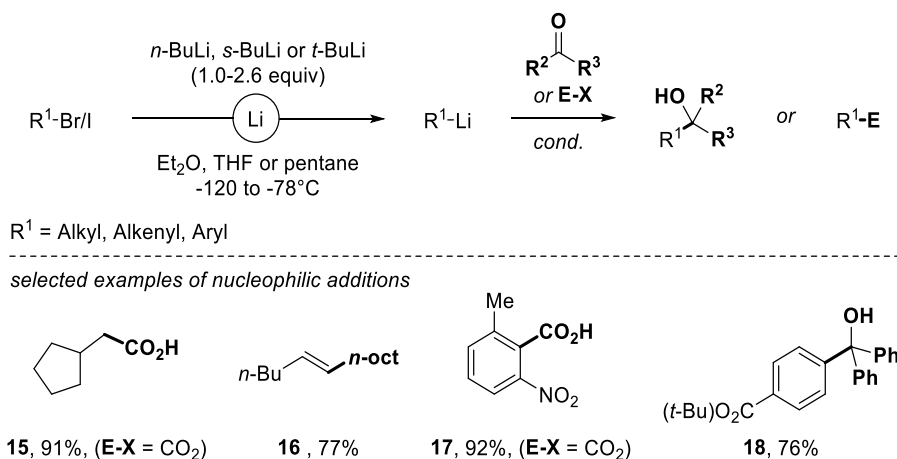
³⁵ a) H. J. S. Winkler, H. Winkler, *J. Am. Chem. Soc.* **1966**, 88, 964969; b) H. J. S. Winkler, H. Winkler, *J. Am. Chem. Soc.* **1966**, 88, 969–974.

³⁶ L. Anthore-Dalion, A. D. Benischke, B. Wei, G. Berionni, P. Knochel, *Angew. Chem. Int. Ed.* **2019**, 58, 4046–4050.

³⁷ G. Wittig, U. Pockels, H. Dröge, *Chem. Ber.* **1938**, 71, 1903–1912.

³⁸ a) H. Gilman, W. Langham, A. L. Jacoby, *J. Am. Chem. Soc.* **1939**, 61, 106109; b) R. G. Jones, H. Gilman, *Org. React.* **1951**, 6, 339–366.

species and functional group tolerance can be problematic, transmetalation of the generated organolithium toward smoother and more stable reagents is usually privileged for further applications (see chapter 2.3).³⁹ Nevertheless, this type of exchange was used in some total syntheses⁴⁰ and several exchange reactions featuring diverse C_{sp}²- and C_{sp}³-halides (**15**, **16**) are reported, which can even tolerate nitro- (**17**) and ester-substituted arenes (**18**) at very low reaction temperatures (Scheme 4).⁴¹



Scheme 4: Examples for halogen-lithium exchange reactions.

In contrast to lithium-halogen exchange chemistry, organomagnesium compounds are – due to their well-balanced reactivity and functional group tolerance – the most represented organometallics generated from halogen-metal exchange.⁴² As demonstrated by the groups of Cahiez and Knochel, iodine-magnesium exchange reactions with *i*-PrMgBr or (*i*-Pr)₂Mg on sensitive arenes bearing nitrile, ethyl ester and amide functionalities proceed smoothly at –40 °C.⁴³ However, those exchange-reagents struggle with the replacement of bromides, if the system is not activated by additional electron-deficient groups. While other exchange reagents such as aryl magnesium bromides⁴⁴ and mixed metal species like (*n*-Bu)₃MgLi⁴⁵ have to be mentioned, the introduction of the “Turbo-Grignard” *i*-PrMgCl•LiCl

³⁹ L. E. Overmann, D. J. Ricca, V. D. Tran, *J. Am. Chem. Soc.* **1997**, *119*, 12031–12040.

⁴⁰ a) J. E. Toth, P. L. Fuchs, *J. Org. Chem.* **1986**, *52*, 473–475; b) M. Bogenstatter, A. Limberg, L. E. Overman, A. L. Tomasi, *J. Am. Chem. Soc.* **1999**, *121*, 12206–12207; c) A. G. Myers, S. D. Goldberg, *Angew. Chem. Int. Ed.* **2000**, *39*, 2732–2735.

⁴¹ a) G. Köbrich, P. Buck, *Chem. Ber.* **1970**, *103*, 1412–1419; b) W. E. Parham, L. D. Jones, *J. Org. Chem.* **1976**, *41*, 2704–2706; c) H. Neumann, D. Seebach, *Tetrahedron Lett.* **1976**, *17*, 4839–4842; d) W. F. Bailey, E. R. Punzalan, *J. Org. Chem.* **1990**, *55*, 5404–5406.

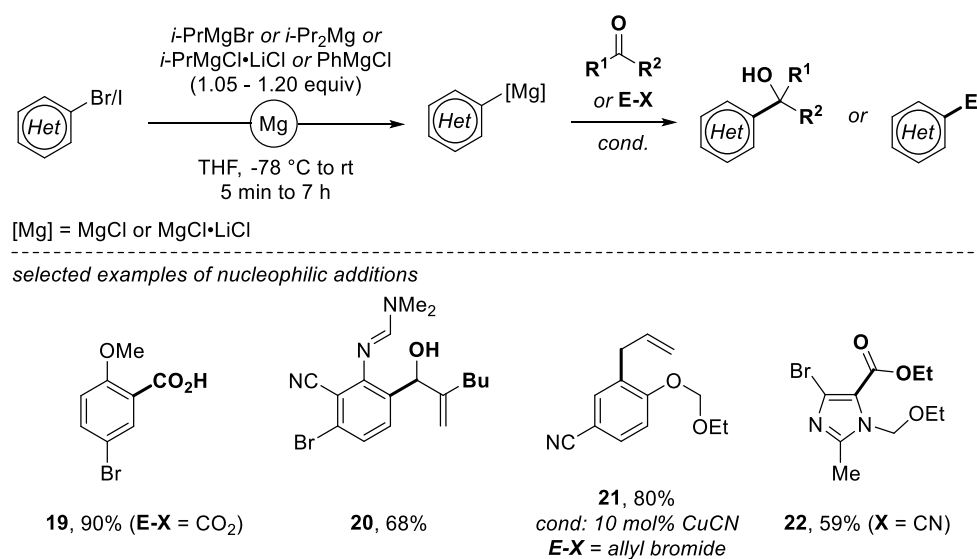
⁴² a) P. Knochel, W. Dohle, N. Gommermann, F. F. Kneisel, F. Kopp, T. Korn, I. Sapoutnis, V. A. Vu, *Angew. Chem. Int. Ed.* **2003**, *42*, 4302–4320; b) N. M. Barl, V. Werner, C. Sämam, P. Knochel, *Heterocycles* **2014**, *88*, 827–844; c) D. S. Ziegler, B. Wei, P. Knochel, *Chem. Eur. J.* **2019**, *25*, 2695–2703.

⁴³ a) L. Boymond, M. Rottländer, G. Cahiez, P. Knochel, *Angew. Chem. Int. Ed.* **1998**, *37*, 1701–1703; b) M. Abarbri, F. Dehmel, P. Knochel, *Tetrahedron Lett.* **1999**, *40*, 7449–7453; c) G. Varchi, A. Ricci, G. Cahiez, P. Knochel, *Tetrahedron* **2000**, *56*, 2727–2731; d) G. Varchi, A. E. Jensen, W. Dohle, A. Ricci, G. Cahiez, P. Knochel, *Synlett* **2001**, *4*, 477–480.

⁴⁴ a) I. Sapountzis, P. Knochel, *Angew. Chem. Int. Ed.* **2002**, *41*, 1610–1611; b) I. Sapountzis, H. Dube, R. Lewis, P. Knochel, *J. Org. Chem.* **2005**, *70*, 2445–2454.

⁴⁵ a) K. Kitagawa, A. Inoue, H. Shinokubo, K. Oshima, *Angew. Chem. Int. Ed.* **2000**, *39*, 2481–2483; b) A. Inoue, K. Kitagawa, H. Shinokubo, K. Oshima, *J. Org. Chem.* **2001**, *66*, 4333–4339.

popularized magnesium-bromine exchanges.⁴⁶ Similar to the use of LiCl in Grignard reactions, the additional salt helps breaking aggregates in solution, allowing for a consequent decrease in reaction times and higher yields compared to *i*-PrMgCl itself.



Scheme 5: Overview of halogen-magnesium exchange chemistry.

As depicted in Scheme 5, the formed organomagnesium species can be trapped with various electrophiles, showcasing good functional group tolerance for compounds **19**, **21**, **22**. In addition, these reagents proved to preferably perform 1,2-addition over 1,4-addition, resulting in **20** employing a Michael acceptor electrophile. More recently, the group of Knochel reported a novel halogen-magnesium exchange in toluene rather than commonly used THF, employing the exchange-reagents *s*-BuMgOR·LiOR (R = 2-ethylhexyl) and *s*-Bu₂Mg·2LiOR, respectively. The exchange rates for these transformations are very high and the reactions completed within a few minutes, even when using challenging electron-rich arenes. Notably, the addition of the additive PMDTA allowed for the first chlorine-magnesium exchange on electron-rich substrates.⁴⁷

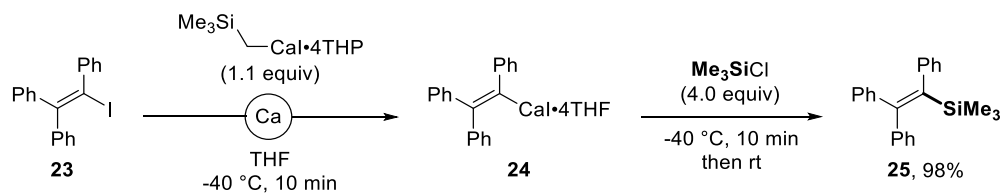
Other than the two presented and well-established classes of metal-exchange reagents, more exotic metal-exchange reagents have been designed. For example, the iodine-calcium exchange was recently described by the group of Westerhausen (Scheme 6).⁴⁸ (Trimethylsilyl)methylcalcium iodide was identified as a privileged exchange reagent for aryl-, alkenyl- (**23**), and cyclopropyl iodide substrates. The nucleophilic addition of the reactive intermediate organocalcium reagent **24** was performed on Me₃SiCl, furnishing corresponding organosilicon compounds such as **25** in excellent yields. With calcium having

⁴⁶ a) A. Krasovskiy, P. Knochel, *Angew. Chem. Int. Ed.* **2004**, *43*, 3333–3336; b) A. Krasovskiy, B. F. Straub, P. Knochel, *Angew. Chem. Int. Ed.* **2006**, *45*, 159–162; c) L. Shit, Y. Chu, P. Knochel, H. Mayr, *Angew. Chem. Int. Ed.* **2008**, *47*, 202–204; d) C. Sämann, B. Haag, P. Knochel, *Chem. Eur. J.* **2012**, *18*, 16145–16152.

⁴⁷ D. S. Ziegler, K. Karaghiosoff, P. Knochel, *Angew. Chem. Int. Ed.* **2018**, *57*, 6701–6704.

⁴⁸ A. Koch, M. Wirgenings, S. Kriek, H. Görls, G. Pohnert, M. Westerhausen, *Organometallics* **2017**, *36*, 3981–3986.

a low electronegativity – very close to lithium – organocalcium reagents are expected to be very reactive, hence the limited number of examples described until now.



Scheme 6: Generation and trapping reaction of organocalcium species with TMSCl.

As another example, Knochel and co-workers developed the first halogen-lanthanide exchange reagent, $(n\text{-Bu})_2\text{LaMe}\cdot 5\text{LiCl}$. In a double halogen-lanthanide exchange, aryl- and heteroaryl iodides and bromides were employed furnishing organolanthanides that were previously only accessible *via* transmetalation of organolithium compounds with the appropriate lanthanide salt (see chapter 2.3).⁴⁹ Since all known lanthanides display electronegativities in the range between lithium ($\chi = 0.98$) and magnesium ($\chi = 1.31$),¹³ a fast exchange within 5 minutes at $-50\text{ }^\circ\text{C}$ was observed. Remarkably, not only trapping reactions with ketones (**26**), but also sequences with Weinreb amides (**27**) and cross-coupling procedures (**28**) were tolerated (Scheme 7).

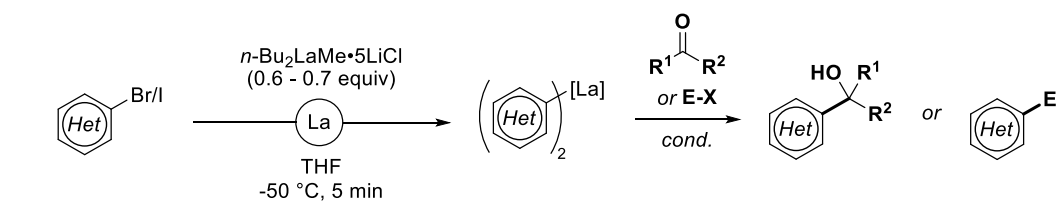
$(n\text{-Bu})_2\text{LaMe}\cdot 5\text{LiCl}$ was also used to promote exchanges on 2-bromobiaryls. Interestingly, a C-H metalation of the formed 2-biaryllanthanum compound onto the other arene was observed and the resulting organometallic was trapped with various electrophiles yielding polyfunctional biaryls such as **29**.⁵⁰ In addition, the 2nd generation exchange reagents $\text{Ph}_3\text{La}\cdot 5\text{LiCl}$ and $(m\text{-xylyl})_3\text{La}\cdot 5\text{LiCl}$ were developed, exhibiting greater functional group tolerance and thermal properties than the previously described reagent as well as enabling a triple halogen-lanthanide exchange.⁵¹

Most recently, the same group subsequently proposed the alternative oligoalkyl samarium reagents $(n\text{-Bu})_2\text{SmCl}\cdot 4\text{LiCl}$ and $(n\text{-Bu})_3\text{Sm}\cdot 5\text{LiCl}$ to perform double or triple halogen-samarium exchanges giving products **30–32**. Similar to their results on organolanthanum chemistry, the exchanges occurred at high rates and could be performed at slightly elevated temperatures. The authors proposed that tuning the electronegativity of the chosen metal greatly influences the rate of the exchange, but also the reactivity and stability of the corresponding organometallic species. Importantly, they demonstrated the synthetic utility of their approach by highlighting that product **31** was not accessible employing organolithium reagents under identical conditions (Scheme 8).³⁶

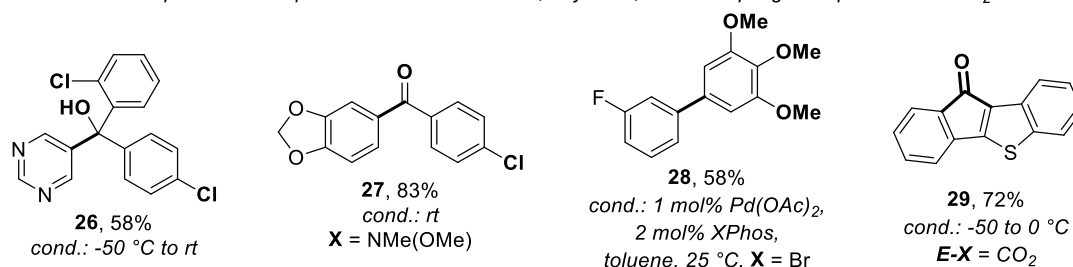
⁴⁹ A. D. Benischke, L. Anthore-Dalion, G. Berionni, P. Knochel, *Angew. Chem. Int. Ed.* **2017**, *56*, 16390–16394.

⁵⁰ B. Wei, D. Zhang, Y.-H. Chen, A. Lei, P. Knochel, *Angew. Chem. Int. Ed.* **2019**, *58*, 15631–15635.

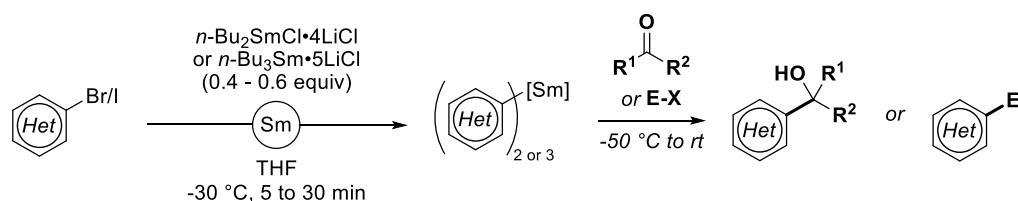
⁵¹ A. D. Benischke, L. Anthore-Dalion, F. Kohl, P. Knochel, *Chem. Eur. J.* **2018**, *24*, 11103–11109.



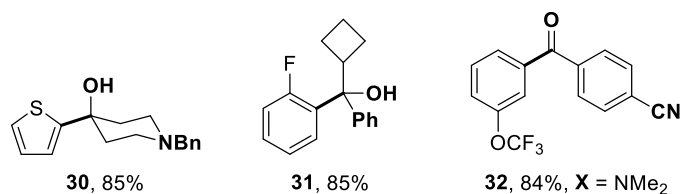
selected examples of nucleophilic additions to ketones, acylation, cross-coupling and quench with CO₂



Scheme 7: Halogen-lanthanum exchange and following transformations.



selected examples of nucleophilic additions to ketones and acylation



Scheme 8: Halogen-samarium exchange and following trapping sequence.

In contrast to these novel organolanthanide exchange reagents, the field of halogen-zinc exchange chemistry is well-established and was pioneered by Oku in 1989,⁵² even though earlier reports by Furukawa *et al.* on improved Simmons-Smith reaction⁵³ conditions in 1966 might be considered the first example of an iodine-zinc exchange.⁵⁴ While the group of Oku mainly demonstrated the reaction to be useful for generating stable carbenoid derivatives for further functionalization,^{52,55} the group of Knochel was able to perform the exchange with similar zincate reagents on functionalized alkyl groups, showing the high tolerance of such organozinc species.⁵⁶ Again, this tolerance stems from the relatively weak

⁵² T. Harada, K. Hattori, T. Katsuhira, A. Oku, *Tetrahedron Lett.* **1989**, *30*, 6035–6038.

⁵³ H. E. Simmons, R. D. Smith, *J. Am. Chem. Soc.* **1959**, *81*, 4256–4264.

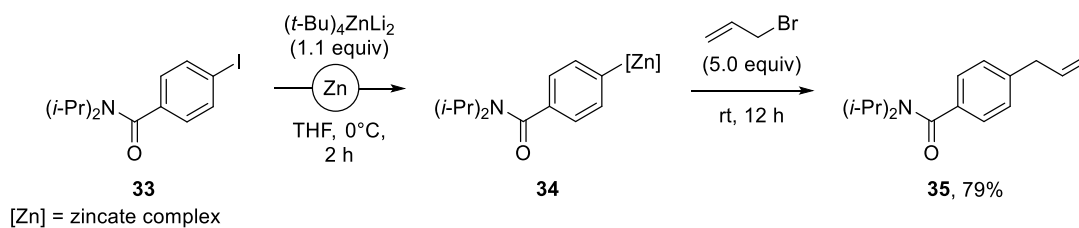
⁵⁴ a) J. Furukawa, N. Kawabata, J. Nishimura, *Tetrahedron Lett.* **1966**, *28*, 3353–3354; b) J. Furukawa, N. Kawabata, J. Nishimura, *Tetrahedron* **1968**, *24*, 53–58.

⁵⁵ T. Harada, Y. Kotani, T. Katsuhira, A. Oku, *Tetrahedron Lett.* **1991**, *32*, 1573–1576.

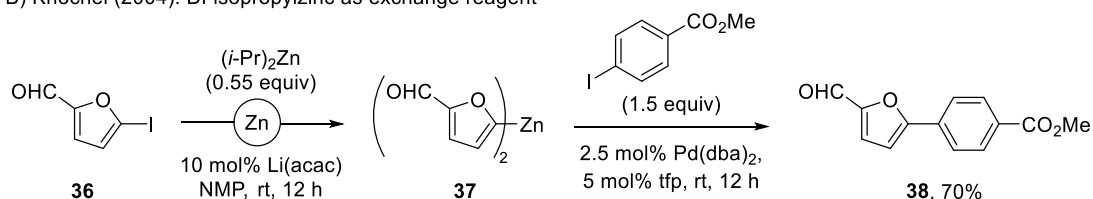
⁵⁶ a) I. Klement, P. Knochel, K. Chau, G. Cahiez *Tetrahedron Lett.* **1994**, *35*, 1177–1180; b) L. Micouin, P. Knochel, *Synlett* **1997**, 327–328.

polarization of the C-Zn bond as a result of zinc's inherently high electronegativity and enables ambient temperature exchange chemistry.

A) Uchiyama (2006): Tetraalkyldilithiumzincates as exchange reagents



B) Knochel (2004): Di-isopropylzinc as exchange reagent



Scheme 9: Iodine-zinc exchange reactions and following transformations.

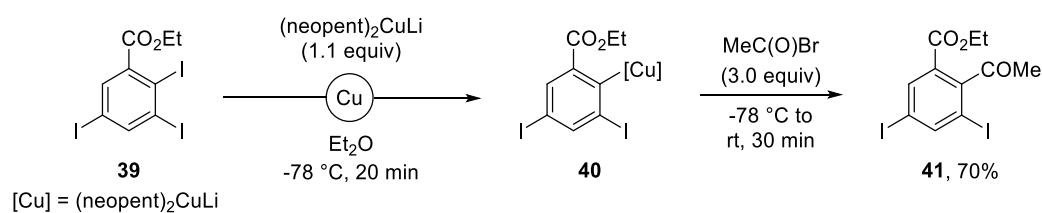
In 1994, Uchiyama and co-workers described the first iodine-zinc exchange of aryl iodides (**33**) with lithium trimethylzincate species. In the following two decades, organozinc derivatives (**34**) proved to be reactive toward the addition of allyl halides giving products such as **35** (Scheme 9A) and to be efficient in Negishi cross-coupling reactions.⁵⁷ Later, the group of Knochel elaborated a strategy for iodine-zinc exchange using diisopropylzinc reagents and catalytic amounts of Li(acac) in a solvent mixture containing NMP at room temperature. Allylation- and cross-coupling reactions were performed on various substrates possessing sensitive groups such as aldehydes and esters (**38**) with good yields (Scheme 9B).⁵⁸ More recent contributions from the groups of Gros, Mongin, Fort, and Uchiyama demonstrated the usefulness of homoleptic lithium polyalkyl zincates for halogen-metal exchanges on bromopyridine derivatives.⁵⁹ Lastly, the group of Hevia showed the applicability of structurally defined magnesium-zincates for iodine-zinc exchanges.⁶⁰

⁵⁷ a) Y. Kondo, N. Takazawa, C. Yamazaki, T. Sakamoto, *J. Org. Chem.* **1994**, *59*, 4717–4718; b) M. Uchiyama, T. Miyoshi, Y. Kajihara, T. Sakamoto, Y. Otani, T. Ohwada, Y. Kondo, *J. Am. Chem. Soc.* **2002**, *124*, 8514–8515; c) M. Uchiyama, T. Furuyama, M. Kobayashi, Y. Matsumoto, K. Tanaka, *J. Am. Chem. Soc.* **2006**, *128*, 8404–8405; d) M. Uchiyama, Y. Kobayashi, T. Furuyama, S. Nakamura, Y. Kajihara, T. Miyoshi, T. Sakamoto, Y. Kondo, K. Morokuma, *J. Am. Chem. Soc.* **2008**, *130*, 472–480; e) S. Nakamura, C.-Y. Liu, A. Muranaka, M. Uchiyama, *Chem. Eur. J.* **2009**, *15*, 5686–5694.

⁵⁸ a) F. F. Kneisel, M. Dochnahl, P. Knochel, *Angew. Chem. Int. Ed.* **2004**, *43*, 1017–1021; b) L.-Z. Gong, P. Knochel, *Synlett* **2005**, 267–270.

⁵⁹ N. T. T. Chau, M. Meyer, S. Komagawa, F. Chevallier, Y. Fort, M. Uchiyama, F. Mongin, P. C. Gros, *Chem. Eur. J.* **2010**, *16*, 12425–12433.

⁶⁰ a) E. Hevia, J. Z. Chua, P. García-Álvarez, A. R. Kennedy, M. D. McCall, *Proc. Natl. Acad. Sci. U.S.A.* **2010**, *107*, 5294–5299; b) T. D. Bluemke, W. Clegg, P. García-Álvarez, A. R. Kennedy, K. Koszinowski, M. D. McCall, L. Russo, E. Hevia, *Chem. Sci.* **2014**, *5*, 3552–3562.



Scheme 10: Halogen-copper exchange and following trapping sequence.

The last major transition metal that partakes in halogen-metal exchange reactions is copper. In 1968, Corey *et al.* described the first example of halogen-copper exchange using dialkyl cuprates.⁶¹ In this report, alkyl-, alkenyl-, allyl-, and aryl iodides, bromides, and even chlorides were shown to proceed through halogen-copper permutations. Organocuprates are known to be reactive nucleophiles toward alkyl halides through nucleophilic substitutions. As primary alkyl halides are produced during the reaction of exchange, a major drawback happens to be the alkylation of the generated organocopper species with this alkyl halide. To tackle this problem, Knochel and co-workers later used bulkier alkyl copper species to avoid the parasitic alkylation reaction. Dineopentylcuprate species were used on olefinic, aromatic and heteroaromatic bromides and iodides. Interestingly, besides exhibiting excellent functional group tolerance, dineopentylcuprate reagents showed exceptional regioselectivity in case of polyhalogenated compounds (**39**), which was attributed to the presence of a coordinating group such as an ester or a sulfone, directing the exchange to the favorable *ortho*-position (**40**) and yielding the desired compound **41** in high yield (Scheme 10).⁶²

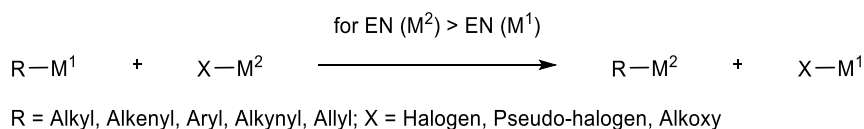
2.3 Transmetalation

Since many organometallic compounds cannot be prepared by either oxidative insertion, directed metalation or halogen-metal exchange reactions, transmetalation proved to be a convenient alternative. In principle, every organometallic reagent that is generated by one of the methods mentioned above can be transmetalated to another organometallic compound by treatment with the desired metal salt, as long as the cation in the salt has a higher electronegativity than the metal in the starting organometallic reagent. This process is thermodynamically favored and therefore usually irreversible, as the more covalent C-M bond in addition to the more ionic and thus stable metal salt is formed (Scheme 11).⁶³

⁶¹ a) E. J. Corey, G. H. Posner, *J. Am. Chem. Soc.* **1968**, *90*, 5615–5616; b) Y. Kondo, T. Matsudaira, J. Sato, N. Maruka, T. Sakamoto, *Angew. Chem. Int. Ed. Engl.* **1996**, *35*, 736–738.

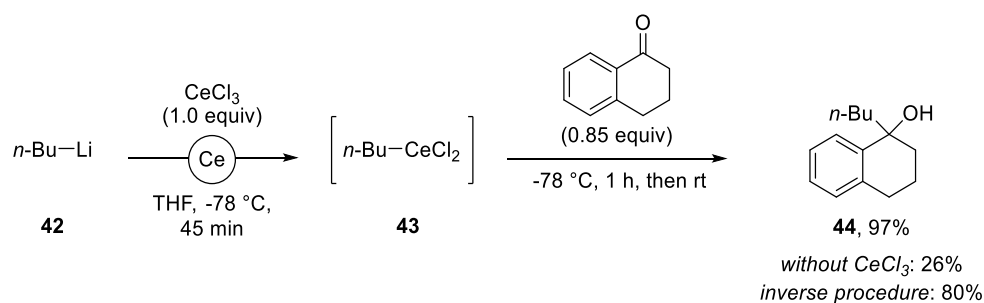
⁶² a) C. Piazza, P. Knochel, *Angew. Chem. Int. Ed.* **2002**, *41*, 3263–3265; b) X. Yang, T. Rotter, C. Piazza, P. Knochel, *Org. Lett.* **2003**, *5*, 1229–1231; c) X. Yang, A. Althammer, P. Knochel, *Org. Lett.* **2004**, *6*, 1665–1667.

⁶³ a) G. O. Spessard, G. L. Miessler, *Organometallic Chemistry* **2010**, Oxford University Press, New York; b) C. Elschenbroich, *Organometallic Chemie 6. Auflage* **2008**, Teubner, Wiesbaden.



Scheme 11: The general mechanism of transmetalation reactions.

Transmetalations have two main purposes: First, otherwise unstable organometallic reagents can be transformed to more stable, functional group tolerant species with altered reactivity.⁶⁴ Frequent metal salts used are LiCl complexed MgCl₂, ZnCl₂ or CuCN. Upon transmetalation, the resulting organometallic species enable specific reactions such as Negishi cross-coupling reactions or copper-catalyzed allylations,⁶⁵ in which transmetalation reactions also play an important role for the catalytic cycle (see chapter 3.3).⁶⁶ Second, rapid formation of organolithium or organomagnesium compounds followed by transmetalation is usually much faster than other preparative methods for the synthesis of more covalent organometallic species such as organo-boron, -silicon or -tin compounds and is also popular in organolanthanide chemistry.⁶⁷ A common example was developed within the pioneering work of Imamoto, in which transmetalation of *n*-BuLi with CeCl₃ (**43**) enabled the selective 1,2-addition to easily enolizable ketones such as α -tetralone in up to 97% yield (Scheme 12). Importantly, the absence of CeCl₃ resulted in a significantly lower yield of 26% for tertiary alcohol **44**, as – due to enolization – significant amounts of the starting ketone were recovered. However, premixing of the ketone with CeCl₃ also proved to be feasible and the corresponding alcohol was isolated in 80%, since coordination of the Lewis acidic cerium salt to the ketone favors 1,2-addition.⁶⁸



Scheme 12: Transmetalation of *n*-BuLi with CeCl₃ and 1,2-addition to α -tetralone.

⁶⁴ K. Osakada, *Fundamentals of Molecular Catalysis* **2003**, Elsevier, Amsterdam.

⁶⁵ a) A. Metzger, F. M. Piller, P. Knochel, *Chem. Commun.* **2008**, 5824–5826; b) F. M. Piller, A. Metzger, M. A. Schade, B. A. Haag, A. Gavryushin, P. Knochel, *Chem. Eur. J.* **2009**, *15*, 7192–7202; c) A. Frischmuth, M. Fernández, N. M. Barl, F. Achraimer, H. Zipse, G. Berionni, H. Mayr, K. Karaghiosoff, P. Knochel, *Angew. Chem. Int. Ed.* **2014**, *53*, 7928–7932.

⁶⁶ a) E. Negishi, *Acc. Chem. Res.* **1982**, *15*, 340–348; b) A. J. J. Lennox, G. C. Lloyd-Jones, *Chem. Soc. Rev.* **2014**, *43*, 412–443.

⁶⁷ a) T. Imamoto, T. Kusumoto, M. Yokoyama, *J. Chem. Soc. Chem. Commun.* **1982**, 1042–1044; b) T. Imamoto, Y. Sugiura, *J. Phys. Org. Chem.* **1989**, *2*, 93–102; c) G. A. Molander, *Chem. Rev.* **1992**, *92*, 29–68; d) V. Alexander, *Chem. Rev.* **1995**, *95*, 273–342.

⁶⁸ N. Takeda, T. Imamoto, *Org. Synth.* **1999**, *76*, 228.

3 Organoboron Chemistry

3.1 Overview

Throughout the majority of the last century, organoboron chemistry was almost irrelevant to the scientific community. However, the ground-breaking work by Brown and co-workers in the early 1960s on hydroboration of alkynes and alkenes,⁷² which was awarded the Nobel Prize in Chemistry in 1979, completely revolutionized the field as organoboranes were readily accessible and demonstrated to furnish synthetically useful intermediates. In analogy to this pioneering work, transition-metal catalyzed carboborations and haloborations as well as borylations for the preparation of bench-stable boronic acids and related compounds such as pinacol boronic esters were developed in the last decades, since traditional organoboranes usually exhibit pyrophoricity.⁷³ The growth in the field was even more accelerated, when – amongst others – Suzuki and Miyaura developed their cross-coupling protocol allowing for the formation of ubiquitous C-C bonds.^{2,3}

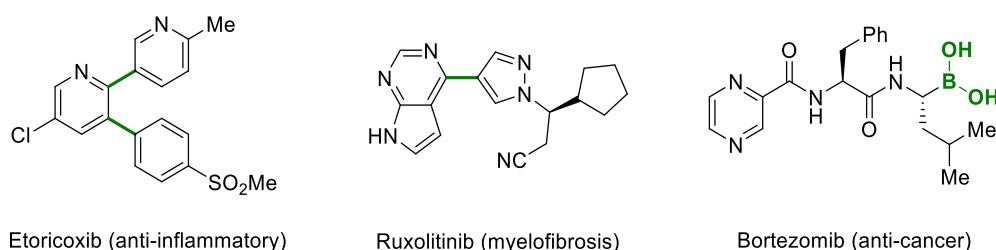


Figure 2: Examples of drugs either synthesized by Suzuki-Miyaura coupling or bearing an organoboron moiety.⁷⁴

Nowadays, organoboron reagents are essential and indispensable tools in any organic chemist's toolbox. Arguably, they are the most studied and applied class of reagents in organic synthesis and represent a rapidly expanding field, since they do not only offer a wide reactivity profile but are in addition popular due to their non-toxic nature and excellent functional group tolerance.^{16a,75} Moreover, boronic and boronic acids and esters thereof have shown their potential beyond acting as substrates in C-C bond forming reactions and are regularly used in catalysis, *e.g.* Corey's CBS reduction⁷⁶, or in drug discovery and material science.^{3,77} In combination with the importance of the Suzuki-Miyaura cross-coupling in those fields (Figure 2), there is an ever-growing importance for the straightforward and elegant preparation of organoboron compounds.

⁷² a) H. C. Brown, G. Zweifel, *J. Am. Chem. Soc.* **1961**, *83*, 3834–3840; b) H. C. Brown, S. K. Gupta, *J. Am. Chem. Soc.* **1971**, *93*, 1816–1818; c) K. Burgess, M. J. Ohlmeyer, *Chem. Rev.* **1991**, *91*, 1179–1191.

⁷³ a) A. Suzuki, *Heterocycles* **2010**, *80*, 15–43; b) E. Negishi, G. Wang, H. Rao, Z. Xu, *J. Org. Chem.* **2010**, *75*, 3151–3182; c) M. Sugimoto, *Chem. Rec.* **2010**, *10*, 348–358; d) J. R. Lawson, R. L. Melen, *Inorg. Chem.* **2017**, *56*, 8627–8643.

⁷⁴ P. Schäfer, T. Palacin, M. Sidera, S. P. Fletcher, *Nat. Commun.* **2017**, *8*, 15762.

⁷⁵ J. W. B. Fyfe, A. J. B. Watson, *Chem* **2017**, *3*, 31–55.

⁷⁶ a) E. J. Corey, R. K. Bakshi, S. Shibata, *J. Am. Chem. Soc.* **1987**, *109*, 5551–5553; b) L. Deloux, M. Srebnik, *Chem. Rev.* **1993**, *93*, 763–784; c) E. J. Corey, C. J. Helal, *Angew. Chem. Int. Ed.* **1998**, *37*, 1986–2012.

⁷⁷ D. G. Brown, J. Boström, *J. Med. Chem.* **2016**, *59*, 4443–4458.

3.2 Tetracoordinated Organoboron Salts

Debatably the most classical synthesis of organoboron compounds lies in the addition of organolithium and organomagnesium reagents to trialkylborates, which generates a tetracoordinated boron center.⁷⁸ Even though traditional organoboron chemistry disregarded those species and routinely converted them into the corresponding boronic acids by acid hydrolysis, more recent studies by the groups of Mayr, Aggarwal, Morken and many more have shown the importance of such tetracoordinated boron centers.⁷⁹ As trivalent organoboron species – due to their electronic structure and trigonal planar geometry – act as electrophiles in chemical transformations, their tetrahedral equivalents exhibit nucleophilic character, fundamentally changing their properties and reactivity.⁸⁰ The influence on the nucleophilic character of the ligands surrounding the boron core was thoroughly described by Mayr and his group on their nucleophilicity scale. The authors investigated furyl boronic acid derivatives and engaged those with different benzhydrylium cations, while carefully measuring the kinetics. From this data, respective nucleophilicities (N) were derived, which are summarized in Figure 3.⁸¹

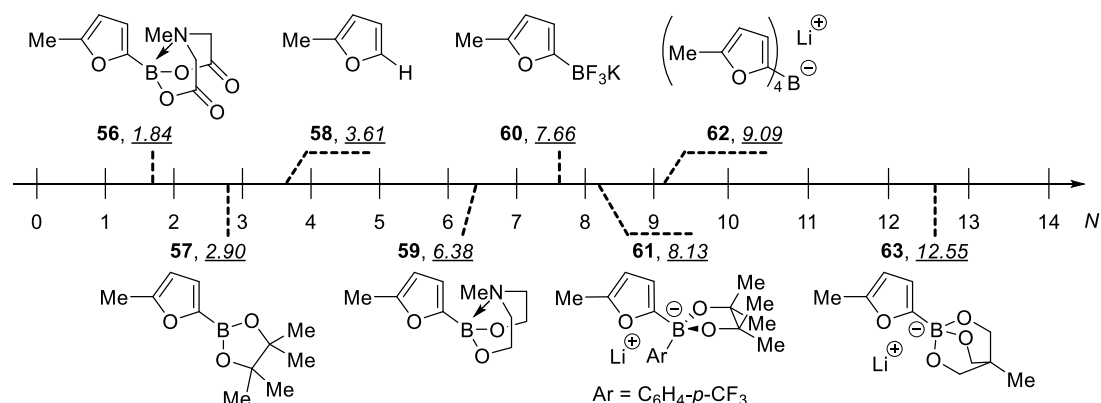


Figure 3: Selection of furyl boronic acid derivatives by Mayr *et al.* and their calculated nucleophilicities.

As seen above, the pinacol boronic ester **57** is less reactive toward carbocations than the unsubstituted 2-methylfuran **58** itself. Moreover, intramolecular coordination of an additional alkoxide (**63**) or amino group in **59** drastically increases the nucleophilicity of the compound. This general trend of increasing nucleophilicity by tetrahedral assembly onto the boron center holds true for potassium trifluoroborate **60** as well as bisorganoborinate **61** and tetraorganoborate **62** and has its sole exception in MIDA

⁷⁸ a) H. C. Brown, T. E. Cole, *Organometallics* **1983**, *2*, 1316–1319; b) H. C. Brown, N. Bhat, M. Srebnik, *Tetrahedron Lett.* **1988**, *29*, 2631–2634; c) H. C. Brown, M. V. Rangaishenvi, *Tetrahedron Lett.* **1990**, *31*, 7113–7114; d) H. C. Brown, M. V. Rangaishenvi, *Tetrahedron Lett.* **1990**, *31*, 7115–7118.

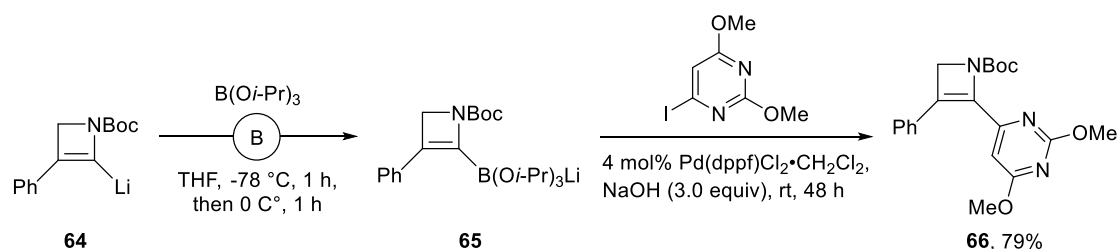
⁷⁹ a) K. Feeney, G. Berionni, H. Mayr, V. K. Aggarwal, *Org. Lett.* **2015**, *17*, 2614–2617; b) C. Garcia-Ruiz, J. L.-Y. Chen, C. Sandford, K. Feeney, P. Lorenzo, G. Berionni, H. Mayr, V. K. Aggarwal, *J. Am. Chem. Soc.* **2017**, *139*, 15324–15327; c) C. Shu, A. Noble, V. K. Aggarwal, *Angew. Chem. Int. Ed.* **2019**, *58*, 3870–3874; d) A. Fawcett, T. Biberger, V. K. Aggarwal, *Nat. Chem.* **2019**, *11*, 117–122; e) S. Namirembe, J. P. Morken, *Chem. Soc. Rev.* **2019**, *48*, 3464–3474.

⁸⁰ R. N. Dhital, H. Sakurai, *Asian J. Org. Chem.* **2014**, *3*, 668–684.

⁸¹ a) G. Berionni, B. Maji, P. Knochel, H. Mayr, *Chem. Sci.* **2012**, *3*, 878–882; b) G. Berionni, A. I. Leonov, P. Mayer, A. R. Ofial, H. Mayr, *Angew. Chem. Int. Ed.* **2015**, *54*, 2780–2783.

boronate **56**, as the electron-withdrawing effect of the carbonyl groups outcompetes the coordination effect and results in an attenuated nucleophilicity.⁸¹

As a recent example for the addition of organolithium reagents to trialkylborates like B(O*i*-Pr)₃, Didier and co-workers, amongst others, showed that a highly reactive Boc-protected azetinyllithium compound **64** – generated and only stable at cryogenic temperatures – can be transmetalated to the corresponding 4-azetinyboronate **65**, which is stable at room temperature. These compounds were for instance engaged in Suzuki-Miyaura cross-couplings (chapter 3.3), yielding compounds such as **66** in high yields (Scheme 15).⁸²



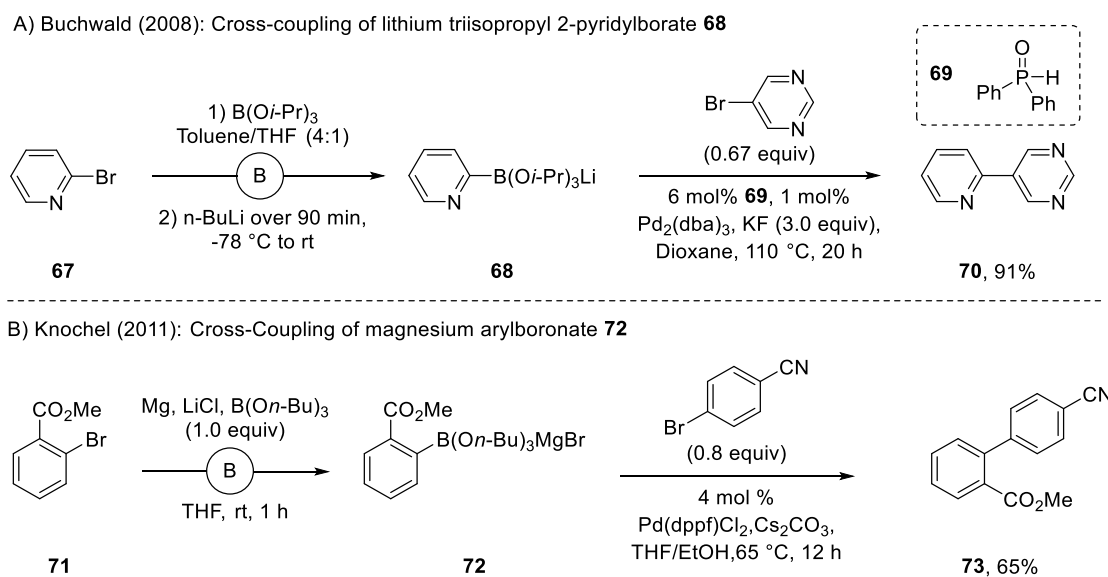
Scheme 15: Reaction of **53** with B(O*i*-Pr)₃ and subsequent Suzuki-Miyaura cross-coupling.

Contrary to the reaction in Scheme 15, in which the transmetalating agent is added after completed formation of the organometallic species, the group of Buchwald presented an *in situ* transmetalation process.⁸³ Hereby, 2-bromopyridines (**67**) and B(O*i*-Pr)₃ were dissolved in THF/toluene mixtures and *n*-BuLi was added slowly over the course of 30 min. Due to kinetic effects, the bromine-lithium exchange is favored over the competing nucleophilic attack onto the borate (Scheme 16A). The resulting triisopropyl 2-pyridylborate **68** was then submitted to a Suzuki-Miyaura cross-coupling yielding compound **70** in 91%. As other typical boron-based esters failed to perform the desired cross-coupling, this report highlights the importance of tetracoordinated boron species. In a similar fashion, Knochel and co-workers demonstrated that *in situ* transmetalation of Grignard reagents toward organozinc compounds was feasible.⁶⁵ The same group showed furthermore, that B(*On*-Bu)₃ greatly enhanced the insertion process, enabling a fast transmetalation toward the organoborate **72** within 1 h (Scheme 16B). A comparable transmetalation with ZnCl₂ was only completed after 3 h and other borate sources such as B(OEt)₃ or B(OMe)₃ gave worse results, as transesterification with sensitive substrates such as ester **71** were observed. The cross-coupled product **73** was isolated in 65% yield.⁸⁴

⁸² a) Y. Yamamoto, M. Takizawa, X.-Q. Yu, N. Miyaura, *Angew. Chem. Int. Ed.* **2008**, *47*, 928–931; b) M. A. Oberli, S. L. Buchwald, *Org. Lett.* **2012**, *14*, 4606–4609; c) A. N. Baumann, M. Eisold, A. Music, G. Haas, Y. M. Kiw, D. Didier, *Org. Lett.* **2017**, *19*, 5681–5684; d) A. Music, A. N. Baumann, M. Eisold, D. Didier, *J. Org. Chem.* **2018**, *83*, 783–792.

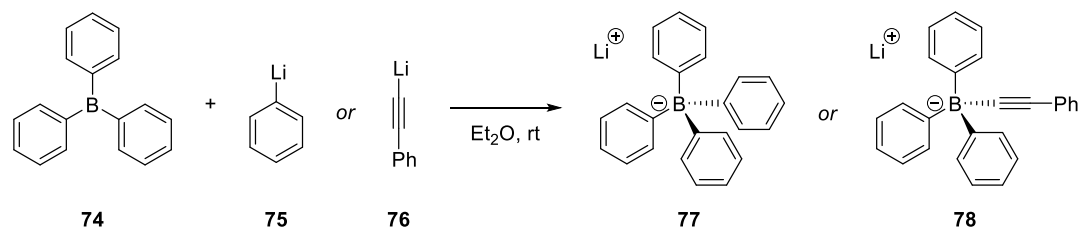
⁸³ a) W. Li, D. P. Nelson, M. S. Jensen, R. S. Hoerner, D. Cai, R. D. Larsen, P. J. Reider, *J. Org. Chem.* **2002**, *67*, 5394–5397; b) Billingsley, K. L.; Buchwald, S. L. *Angew. Chem., Int. Ed.* **2008**, *47*, 4695–4698.

⁸⁴ a) B. A. Haag, C. Sämann, A. Jana, P. Knochel, *Angew. Chem. Int. Ed.* **2011**, *50*, 7290–7294; b) E. Demory, V. Blandin, J. Einhorn, P. Y. Chavant, *Org. Process Res. Dev.* **2011**, *15*, 710–716.



Scheme 16: Buchwald's and Knochel's approaches toward *in situ* transmetalated organoborates.

Coming back from those more elaborate structures, one of the earliest reports of an addition reaction to a tricoordinated boron species was reported by Wittig and co-workers in 1949.⁸⁵ In their study, triphenylborane **74** was treated with phenyllithium **75** at ambient temperature, generating lithium tetraphenylborate **77** for the first time (Scheme 17). Two years later, the same group demonstrated that the methodology was applicable to synthesize mixed tetraorganoborate **78** utilizing lithium phenylacetylide **76**.⁸⁶



Scheme 17: First synthesis of symmetrical and mixed lithium tetraorganoborates.

Exploiting this methodology, Hirao and co-workers later showed that tetraorganoborates **77** and **78** were prone to oxidation by organovanadium compounds.⁸⁷ Hereby, the strong oxidant $\text{VO}(\text{OEt})\text{Cl}_2$ is reduced from vanadium(V) to vanadium(III), oxidizing the tetraorganoborate and ultimately furnishing biphenyl and diphenylacetylene in a selective intramolecular oxidative coupling reaction, a process also enabled by other molecular oxidants.⁸⁸ Based on this concept, Hirao's group extended their work to

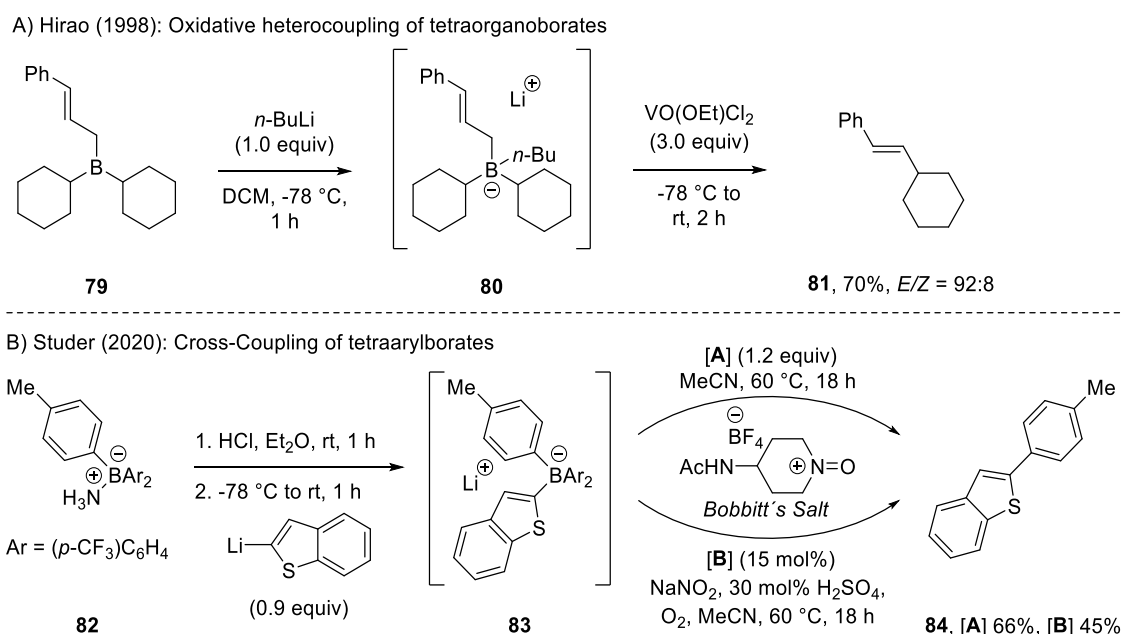
⁸⁵ G. Wittig, G. Keicher, A. Rückert, P. Raff, *Liebigs Ann. Chem.* **1949**, 563, 110–126.

⁸⁶ G. Wittig, P. Raff, *Liebigs Ann. Chem.* **1951**, 573, 195–209.

⁸⁷ a) H. Mizuno, H. Sakurai, T. Amaya, T. Hirao, *Chem. Commun.* **2006**, 48, 5042–5044; b) M. Asay, B. Donnadieu, T. Amaya, Y. Tsukamura, T. Hirao, *Adv. Synth. Catal.* **2009**, 351, 1025–1028.

⁸⁸ a) P. Abley, J. Halpern, *J. Chem. Soc. D* **1971**, 1237–1238; b) H. Sakurai, C. Morimoto, T. Hirao, *Chem. Lett.* **2001**, 30, 1084–1085; c) Z. Lu, R. Lavendomme, O. Burghaus, J. R. Nitschke, *Angew. Chem. Int. Ed.* **2019**, 58, 9073–9077.

olefinations and showed that organoborane **79**, prepared by hydroboration of dicycloborane and phenylacetylene, could be treated with *n*-BuLi to synthesize the tetracoordinated organoborate salt **80**, followed by stereoselective oxidation with VO(OEt)Cl₂ to yield olefin **81** in good yield (Scheme 18A).⁸⁹ Most recently, Studer and co-workers showcased the selective cross-coupling of tetraarylborates. The highly reactive and unstable triarylborane could be prepared *in situ* from the ammonium protected salt **82** by treatment with hydrochloric acid (Scheme 18B). After addition of an aromatic organolithium or organomagnesium species, the desired mixed tetraorganoborate **83** was prepared. Interestingly, an organic oxoammonium salt (Bobbitt's salt)⁹⁰ could either be used as a stoichiometric oxidant or employed catalytically with NO₂/O₂ as additional oxidants to yield (hetero)biaryls like **84**.⁹¹



Scheme 18: Hirao's and Studer's methods for the oxidation of tetraorganoborates.

A complementary pathway for the synthesis of tetrahedral organoborates, which enjoyed great popularity in cross-coupling chemistry over the last decades,⁹² stems from direct ligand-exchange on already

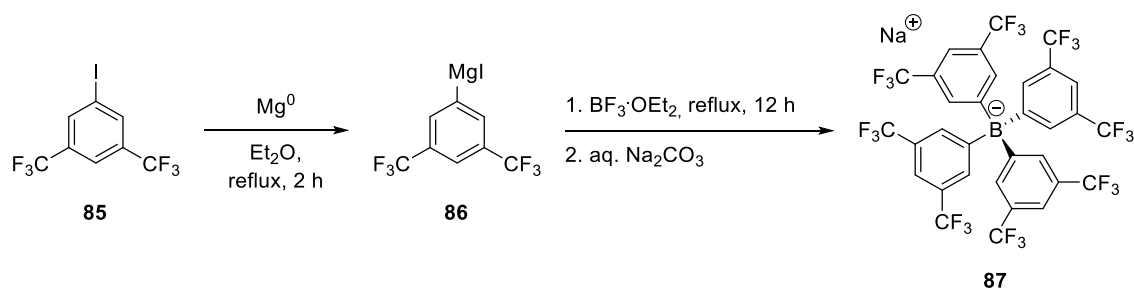
⁸⁹ T. Ishikawa, S. Nonaka, A. Ogawa, T. Hirao, *Chem. Commun.* **1998**, 1209–1210.

⁹⁰ a) J. M. Bobbitt, *J. Org. Chem.* **1998**, *63*, 9367–9374; b) N. Merbouh, J. M. Bobbitt, C. Brückner, *Org. Prep. Proced. Int.* **2004**, *36*, 1–31; c) M. A. Mercadante, C. B. Kelly, J. M. Bobbitt, L. J. Tilley, N. E. Leadbeater, *Nat. Protoc.* **2013**, *8*, 666–676.

⁹¹ C. Gerleve, A. Studer, *Angew. Chem. Int. Ed.* **2020**, *accepted manuscript*, doi.org/10.1002/ange.202002595.

⁹² a) K. Siegmann, P. S. Pregosin, L. M. Venanzi, *Organometallics* **1989**, *8*, 2659–2664; b) P. G. Ciattini, E. Morera, G. Ortar, *Tetrahedron Lett.* **1992**, *33*, 4815–4818; c) N. A. Bumagin, V. V. Bykov, *Tetrahedron* **1997**, *53*, 14437–14450; d) D. Villemin, M. J. Gómez-Escalonilla, J.-F. Saint-Clair, *Tetrahedron Lett.* **2001**, *42*, 635–637; e) T. Ohe, S. Uemura, *Bull. Chem. Soc. Jpn.* **2003**, *76*, 1423–1431; f) J. R. Gardinier, P. J. Pellechia, M. D. Smith, *J. Am. Chem. Soc.* **2005**, *127*, 12448–12449; g) J. Yan, W. Hu, G. Rao, *Synthesis* **2006**, *6*, 943–945; h) L. Bai, J.-X. Wang, *Adv. Synth. Catal.* **2008**, *350*, 315–320; i) H. Zeng, R. Hua, *J. Org. Chem.* **2008**, *73*, 558–562; j) W. W. Schoeller, G. Bertrand, *Angew. Chem. Int. Ed.* **2009**, *48*, 4796–4799; k) W.-J. Zhou, K.-H. Wang, J.-X. Wang, Z.-R. Gao, *Tetrahedron* **2010**, *66*, 7633–7641; l) N. Ishida, W. Ikemoto, M. Narumi, M. Murakami, *Org. Lett.* **2011**, *13*, 3008–3011; m) R. B. Bedford, P. B. Brenner, E. Carter, J. Clifton, P. M. Cogswell, N. J. Gower, M. F. Haddow, J. N. Harvey, J. A. Kehl, D. M. Murphy, E. C. Neeve, M. L. Neidig, J. Nunn, B. E. R. Snyder, J. Taylor, *Organometallics* **2014**, *33*, 5767–5780.

tetracoordinated potassium trifluoroborate salts. The discovery of this reactivity again dates back to Wittig and co-workers in 1951, who demonstrated that up to four consecutive transmetalations with phenyllithium could be performed on $\text{BF}_3 \cdot \text{Et}_2\text{O}$ to yield lithiumtetraphenylborate **77**.⁸⁶ Adapting this method and using pentafluorophenyllithium, Massey and Park prepared the first BARF-anion (nick-name for polyfluorinated tetraarylborate anions) lithium tetra(pentafluorophenyl)borate,⁹³ followed by Kobayashi and co-workers in 1984 who synthesized a variety of BARF-anions from Grignard reagents (**86**), including compound **87** (Scheme 19).⁹⁴ These anions are particularly useful as they exhibit a very low nucleophilicity and therefore reformed the class of weakly coordinating anions. The four aromatic rings in addition to the fluorine substituents effectively shield the borate anion, therefore allowing for the study of highly electrophilic cations.⁹⁵



Scheme 19: Synthesis of BARF-anion **73** by magnesium insertion and following transmetalation sequence.

More recent procedures employing potassium trifluoroborate salts are focused on the synthesis of sophisticated organoboron complexes.⁹⁶ Interestingly, the work of Soós and others showed that treatment of the initial tetrahedral trifluoroborate salt **88** results in the corresponding triarylborane **90**, since the di-*ortho* substituted arylmagnesium reagent **89** is not able to perform three consecutive transmetalations. Thus, a halogenated and sterically interlocked organoborane is obtained, that can be further used in frustrated Lewis pair chemistry (Scheme 20).⁹⁷

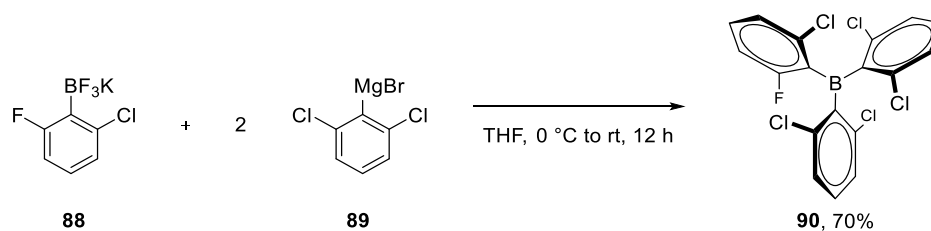
⁹³ A. G. Massey; A. J. Park, *J. Organometal. Chem.* **1964**, *2*, 245.

⁹⁴ a) H. Nishida, N. Takada, M. Yoshimura, T. Sonoda, H. Kobayashi, *Bull. Chem. Soc. Jpn.* **1984**, *57*, 2600–2604; b) N. A. Yakelis, R. G. Bergman, *Organometallics* **2005**, *24*, 3579–3581.

⁹⁵ a) S. G. Weber, D. Zahner, F. Rominger, B. F. Staub, *Chem. Comm.* **2012**, *48*, 11325–11327; b) N. Hafezi, J. M. Holcroft, K. J. Hartlieb, E. J. Dale, N. A. Vermeulen, C. L. Stern, A. A. Sarjeant, J. F. Stoddard, *Angew. Chem. Int. Ed.* **2015**, *54*, 456–461; c) P. Pommerening, J. Mohr, J. Friebe, M. Oestreich, *Eur. J. Org. Chem.* **2017**, 2312–2316; d) L. Carreras, L. Rovira, M. Vaquero, I. Mon, E. Martin, J. Benet-Buchholz, A. Vidal-Ferran, *RSC Adv.* **2017**, *7*, 32833–32841.

⁹⁶ a) K. Schickedanz, J. Radkte, M. Bolte, H.-W. Lerner, M. Wagner, *J. Am. Chem. Soc.* **2017**, *139*, 2841–2851; b) S. Konishi, T. Iwai, M. Sawamura, *Organometallics* **2018**, *37*, 1876–1883; c) A. B. Saida, A. Chardon, A. Osi, N. Tumanov, J. Wouters, A. I. Adjieufack, B. Champagne, G. Berionni, *Angew. Chem. Int. Ed.* **2019**, *58*, 16889–16893; d) S. Atsushi, *JP2016150925*, **2016**.

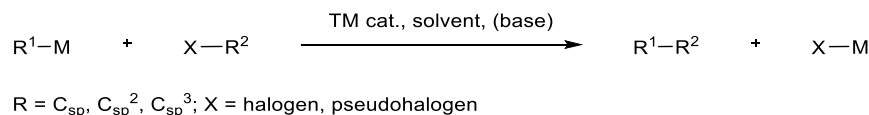
⁹⁷ a) Á. Gyömöre, M. Bakos, T. Földes, I. Pápai, A. Domján, T. Soós, *ACS Catal.* **2015**, *5*, 5366–5372; b) É. Dorkó, M. Szabó, B. Kótai, I. Pápai, A. Domján, T. Soós, *Angew. Chem. Int. Ed.* **2017**, *56*, 9512–9516.



Scheme 20: Formation of triarylborane **90** by Soós.

3.3 The Suzuki-Miyaura Cross-Coupling

In the history of organic synthesis, only a few reactions can compete with the novelty and importance of C-C cross-coupling chemistry. These schematically simple reactions, which enable the formation of diversely hybridized carbon-carbon bonds by coupling of organometallic reagents with organic (pseudo)halides under transition-metal catalysis, enjoy great popularity due to their broad applicability and generality (Scheme 21).^{1,3,16,66,73}



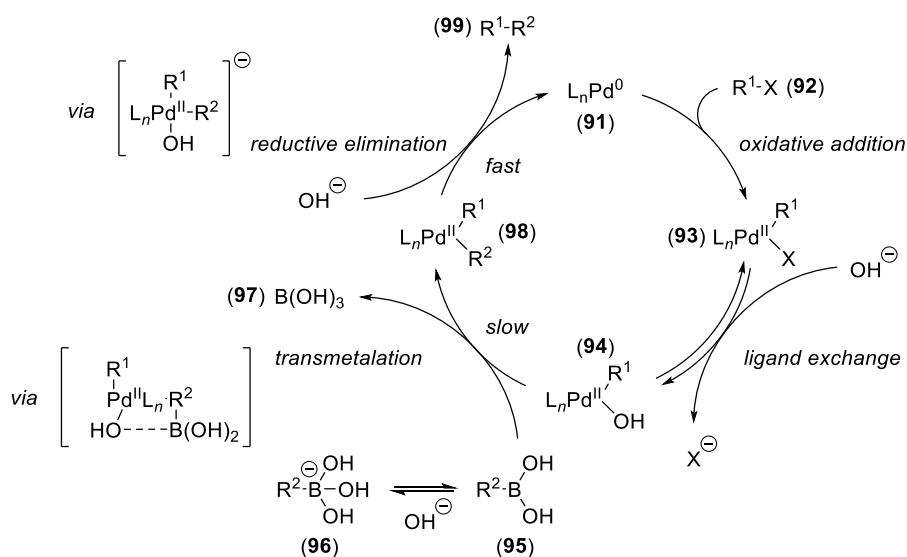
Scheme 21: Schematic representation of a C-C cross-coupling.

Even though several organometallic reagents have proven to participate in these transformations, including exceptional contributions by Negishi (Zn, Al, Zr), Stille (Sn), Hiyama (Si), Corriu and Kumada (Mg), the Suzuki-Miyaura coupling utilizing organoboron compounds is arguably the most-sought-after.^{75,98} The main reasons for this are the high availability, water and air stability of the used organoboron compounds in addition to mild and non-inert reaction conditions, resulting in exceptional functional group tolerance, regio- and stereoselectivity as well as high yields.^{3,16}

Traditionally, the Suzuki-Miyaura coupling is performed using boronic acids or esters thereof, which are coupled to organohalides *via* palladium catalysis under basic conditions. From a mechanistic perspective, a Pd⁰ catalyst **91** – either prepared *in situ* from the corresponding metal salt and a ligand or directly used as Pd⁰, *e.g.* Pd(PPh₃)₄ – undergoes oxidative insertion to the organohalide **92**, forming palladium(II) complex **93**, which then performs a reversible ligand exchange with the base to provide **94**, thus enhancing the electrophilicity of the complex. In the next crucial and rate-determining transmetalation step, the somewhat nucleophilic boronic acid **95** and the electrophilic palladium complex **94** react to furnish palladium(II) complex **98** and boric acid **97** as a side product. Importantly, the tetracoordinated boronate **96** generated from **95** and base was found to be inactive in the catalytic cycle, even though it exhibits a much higher nucleophilicity than the boronic acid **95**. As this process is

⁹⁸ C. C. C. Johansson Seechurn, M. O. Kitching, T. J. Colacot, V. Snieckus, *Angew. Chem. Int. Ed.* **2012**, *51*, 5062–5085.

reversible, a careful balance between base, catalyst and substrate loading is required to maximize the turnover of the desired cycle.⁹⁹ Lastly, base-assisted reductive elimination yields the desired cross-coupled compound **99** and recovers the initial catalyst for another cycle (Scheme 22).^{66b,99}



Scheme 22: The catalytic cycle of a Suzuki-Miyaura cross-coupling.

While boronic acids perform well in the Suzuki-Miyaura couplings, their use has fallen out of favor in the cross-coupling community, because they are difficult to purify and tend to form trimeric anhydrides, which makes it hard to estimate exact stoichiometries.¹⁰⁰ Moreover, boronic acids suffer from protodeborylation in aqueous solutions, rendering them useless in the catalytic process.⁹⁹ Therefore, pinacol boronic esters serve today as the preferred boron source and are readily available. However, the inherently lower reactivity of boronic esters (see Figure 3), coupled with a lack of atom-economy, motivated researchers to find alternative solutions. In the early 2000s, the group of Molander started engaging potassium trifluoroborate salts in Pd-catalyzed cross-coupling reactions.^{100,101} These salts can be conveniently prepared from boronic acids or esters in a one-pot procedure, which was first described by Vedejs *et al.*,¹⁰² and are exceptionally stable toward air, moisture and oxidation. In addition, they reliably form crystalline monomeric materials and can be seen as precursors to boronic acids, as they were found to slowly hydrolyze under Suzuki-Miyaura reaction conditions.^{99e,103} From this perspective,

⁹⁹ a) C. Amatore, A. Jutand, G. Le Duc, *Chem. Eur. J.* **2011**, *17*, 2492–2503; b) B. P. Carrow, J. F. Hartwig, *J. Am. Chem. Soc.* **2011**, *133*, 2116–2119; c) C. Amatore, G. Le Duc, A. Jutand, *Chem. Eur. J.* **2013**, *19*, 10082–10093; d) A. J. J. Lennox, G. C. Lloyd-Jones, *Angew. Chem., Int. Ed.* **2013**, *52*, 7362–7370; e) G. A. Molander, *J. Org. Chem.* **2015**, *80*, 7837–7848; f) A. A. Thomas, S. E. Denmark, *Science* **2016**, *352*, 329–332.

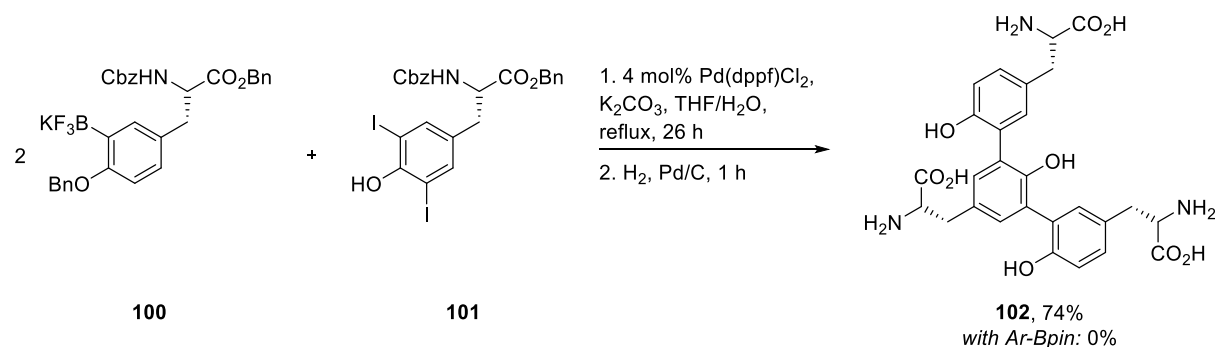
¹⁰⁰ G. A. Molander, N. Ellis, *Acc. Chem. Res.* **2007**, *40*, 275–286.

¹⁰¹ G. A. Molander, T. Ito, *Org. Lett.* **2001**, *3*, 393–396.

¹⁰² E. Vedejs, R. W. Chapman, S. C. Fields, S. Lin, M. R. Schrimpf, *J. Org. Chem.* **1995**, *60*, 3020–3027.

¹⁰³ a) G. A. Molander, B. Biolatto, *J. Org. Chem.* **2003**, *68*, 4302–4312; b) R. Ting, C. W. Harwig, J. Lo, Y. Li, M. J. Adam, T. J. Ruth, D. M. Perrin, *J. Org. Chem.* **2008**, *73*, 4662–4670; c) Z. Liu, D. Chao, Y. Li, R. Ting, J. Oh, D. M. Perrin, *Chem. Eur. J.* **2015**, *21*, 3924–3928; d) A. J. J. Lennox, G. C. Lloyd-Jones, *J. Am. Chem. Soc.* **2012**, *134*, 7431–7441.

potassium trifluoroborate salts combine the advantages of pinacol boronic esters and boronic acids,¹⁰⁴ which was for instance experimentally demonstrated in the synthesis of trityrosine by Hutton and co-workers (Scheme 23).¹⁰⁵ While the Suzuki-Miyaura reaction of the potassium tyrosine-3-trifluoroborate **100** enabled a double cross-coupling on the diiodotyrosine derivative **101** and furnished the expected trityrosine **102** in 74% overall yield, the same reaction with the analogous pinacol boronic ester did not result in any product formation. Since then, potassium trifluoroborate salts have demonstrated to resemble versatile substrates in Suzuki-Miyaura couplings.¹⁰⁶



Scheme 23: Double Suzuki-Miyaura coupling for the formation of trityrosine **87**.

More recent advances in the field focus on the relative reactivity of the used substrates, enabling selectivity in iterative and tandem cross-coupling reactions.⁷⁵ For instance, Watson and co-workers¹⁰⁷ demonstrated that conjunctive dihalide components in combination with an aryl pinacol boronic ester and aryl MIDA (methyliminodiacetic acid) boronate allow for the chemoselective formation of two C-C bonds in one operation.¹⁰⁸ While electrophile selectivity for the oxidative addition is well-defined ($\text{I} > \text{Br} > \text{Cl}$) and the bromide on quinoline **104** reacts faster than the chloride, MIDA-substituted organoboron compounds are usually not nucleophilic enough (see Figure 3) to perform in Suzuki-Miyaura couplings and therefore serve as protecting groups. As boric acid pinacol ester is released in the first cross-coupling cycle with pyridyl boron pinacol ester **103**, a rapid transesterification takes place, activating the other MIDA substrate **105** for the second cross-coupling cycle (Scheme 24A).¹⁰⁷ A similar protection/deprotection strategy for the activation of MIDA-substituted organoboron compounds was

¹⁰⁴ M. Butters, J. N. Harvey, J. Jover, A. J. J. Lennox, G. C. Lloyd-Jones, P. M. Murray, *Angew. Chem. Int. Ed.* **2010**, *49*, 5156–5160.

¹⁰⁵ O. Skaff, K. A. Jollioffe, C. A. Hutton, *J. Org. Chem.* **2005**, *70*, 7353–7363.

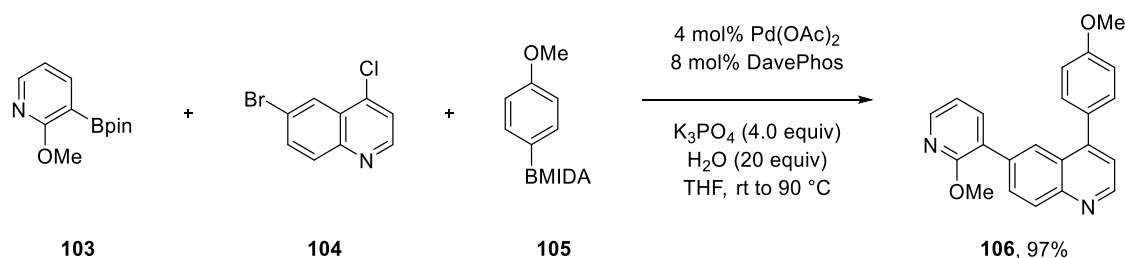
¹⁰⁶ a) G. A. Molander, B. W. Katona, F. Machrouhi, *J. Org. Chem.* **2002**, *67*, 8416–8423; b) T. E. Barder, S. L. Buchwald, *Org. Lett.* **2004**, *6*, 2649–2652; c) M. Mizuta, K. Seio, K. Miyata, M. Sekine, *J. Org. Chem.* **2007**, *72*, 5046–5055; d) M. Achmatowicz, J. Chan, P. Wheeler, L. Liu, M. M. Faul, *Tetrahedron Lett.* **2007**, *48*, 4825–4829; e) S. Darses, J.-P. Genet, *Chem. Rev.* **2008**, *108*, 288–325; f) S. D. Dreher, S.-E. Lim, D. L. Sandrock, G. A. Molander, *J. Org. Chem.* **2009**, *74*, 3626–3631.

¹⁰⁷ C. P. Seath, J. W. B. Fyfe, J. J. Molloy, A. J. B. Watson, *Angew. Chem. Int. Ed.* **2015**, *54*, 9976–9979.

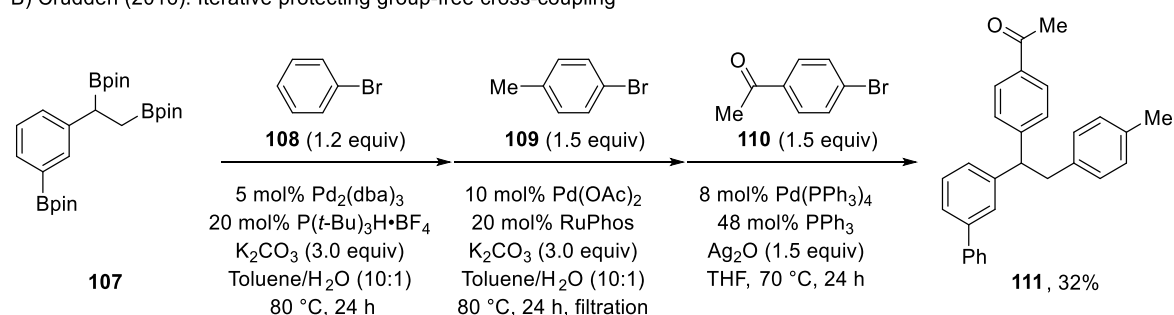
¹⁰⁸ a) E. P. Gillis, M. D. Burke, *J. Am. Chem. Soc.* **2007**, *129*, 6714–6717; b) E. P. Gillis, M. D. Burke, *J. Am. Chem. Soc.* **2008**, *130*, 14084–14085; c) S. J. Lee, K. C. Gray, J. S. Paek, M. D. Burke, *J. Am. Chem. Soc.* **2008**, *130*, 466–468; d) J. Li, M. D. Burke, *J. Am. Chem. Soc.* **2011**, *133*, 13774–13777; e) J. P. G. Rygus, C. M. Crudden *J. Am. Chem. Soc.* **2017**, *139*, 18124–18137.

showcased by Burke and co-workers, who designed an automated process allowing for several selective C-C bond formations in one operation.¹⁰⁹ Lastly, Crudden *et al.* displayed that exploiting simple nucleophilicity trends of carbon hybridization ($C_{sp^2} > C_{sp^3} > C_{sp^3}^{benz}$) in substrate **107** allowed for the selective formation of highly functionalized carbogenic frameworks such as **111** without protection of the organoboron species (Scheme 24B).¹¹⁰

A) Watson (2015): Chemoselective tandem Suzuki-Miyaura cross-coupling



B) Crudden (2016): Iterative protecting group-free cross-coupling



Scheme 24: Modern approaches to Suzuki-Miyaura cross-couplings.

Even if palladium-catalyzed Suzuki-Miyaura couplings are among the most elaborate and utilized transformations, there are significant drawbacks with the metal itself: palladium is not only very rare and thus expensive, it is also subject of strict regulations in the pharmaceutical industry due to potential health risks.^{111,112} Although significant improvements in catalyst loadings down to the lower ppm level have been achieved, more environmentally benign metals are of interest.¹¹³ Nickel as a replacement metal for palladium solves the problem of price, but its use is limited due to severe toxicity issues.¹¹⁴

¹⁰⁹ J. Li, S. G. Ballmer, E. P. Gillis, S. Fujii, M. J. Schmidt, A. M. E. Palazzolo, J. W. Lehmann, G. F. Morehouse, M. D. Burke, *Science* **2015**, *347*, 1221–1226.

¹¹⁰ C. M. Crudden, C. Ziebenhaus, J. P. G. Rygus, K. Ghazati, P. J. Unsworth, M. Nambo, S. Voth, M. Hutchinson, V. S. Laberge, Y. Maekawa, D. Imao, *Nat. Commun.* **2016**, *7*, 11065.

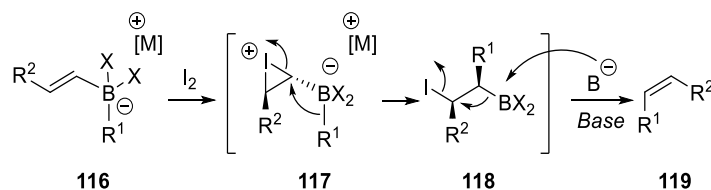
¹¹¹ S. Asghar, S. B. Tailor, D. Elorriaga, R. B. Bedford, *Angew. Chem. Int. Ed.* **2017**, *56*, 16367–16370.

¹¹² a) Á. Molnár, *Chem. Rev.* **2011**, *111*, 2251–2320; b) A. Biffis, P. Centomo, A. Del Zotto, M. Zecca, *Chem. Rev.* **2018**, *118*, 2249–2295.

¹¹³ a) A. Piontek, E. Bisz, M. Szostak, *Angew. Chem. Int. Ed.* **2018**, *57*, 11116–11128; b) S. E. Hooshmand, B. Heidari, R. Sedghi, R. S. Varma, *Green Chem.* **2019**, *21*, 381–405.

¹¹⁴ a) T. Clarkson, G. F. Nordberg, P. R. Sager, *Reproductive and Developmental Toxicity of Metals* **1983**, Springer, Berlin; b) F.-S. Han, *Chem. Soc. Rev.* **2013**, *42*, 5270–5298.

Friedel-Crafts reaction are well-described,¹²¹ but also oxidative coupling reactions instancing hypervalent-iodine species or DDQ are worthy of note.¹²²



Scheme 26: General mechanism of the Zweifel olefination.¹⁸

In the field of olefination reactions, those that create a carbon-carbon double bond or introduce it into a target molecule, Wittig's outstanding work from 1954 has to be mentioned.¹²³ Awarded the Nobel Prize in Chemistry in 1979, this reaction named after him allows for the transformation of a carbonyl moiety into the desired olefin using phosphonium ylides, giving triphenylphosphine oxide as the side product.¹²⁴ In addition to several more contributions by others in the next decades,¹²⁵ the Zweifel olefination represents a powerful and often times overlooked method for the stereoselective formation of alkenes.¹²⁶ Pioneered by Zweifel and co-workers, only iodine and a base are required for this olefination to occur.¹²⁷ Mechanistically, the iodine coordinates to the pre-existing C-C double bond of a preactivated tetracoordinated organoboron species **116**, thus forming the iodonium intermediate **117**, which provokes the formation of **118** via a stereospecific 1,2-metalate rearrangement. Lastly, the so-formed β -iodo organoboron species undergoes antiperiplanar β -elimination promoted by the base, resulting in the desired olefin **119** (Scheme 26). Importantly, this transformation is stereospecific, meaning that initial (*E*)-alkenes are transferred to (*Z*)-olefins and *vice versa*.^{18,126} Notably, Zweifel later also showed that by replacement of iodine with cyanogen bromide the selectivity is switched as syn-periplanar elimination was observed.¹²⁸

¹²¹ a) E. Buncl, J. M. Dust, F. Terrier, *Chem. Rev.* **1995**, *95*, 2261–2280; b) T. B. Poulsen, K. A. Jørgensen, *Chem. Rev.* **2008**, *108*, 2903–2915.

¹²² C.-L. Sun, Z.-J. Shi, *Chem. Rev.* **2014**, *114*, 9219–9280.

¹²³ a) G. Wittig, U. Schöllkopf, *Chem. Ber.* **1954**, *87*, 1318–1330; b) G. Wittig, W. Haag, *Chem. Ber.* **1955**, *88*, 1654–1666.

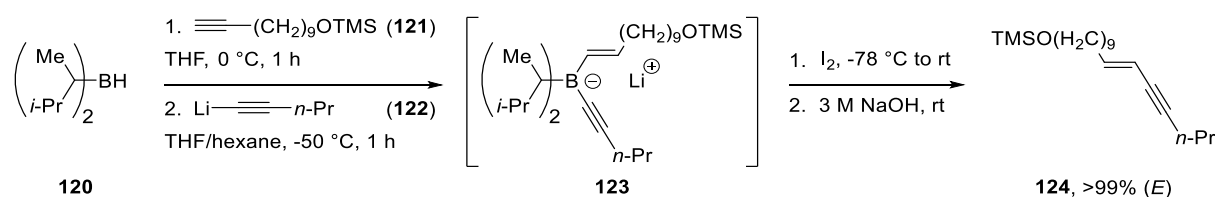
¹²⁴ a) B. E. Maryanoff, A. B. Reitz, *Chem. Rev.* **1989**, *89*, 863–927; b) R. W. Hoffmann, *Angew. Chem. Int. Ed.* **2001**, *40*, 1411–1416.

¹²⁵ a) D. J. Peterson, *J. Org. Chem.* **1968**, *33*, 780–784; b) F. N. Tebbe, G. W. Parshall, G. S. Reddy, *J. Am. Chem. Soc.* **1978**, *100*, 3611–3613; c) L. Horner, H. Hoffmann, H. G. Wippel, *Chem. Ber.* **1958**, *91*, 61–63; d) W. S. Wadsworth, W. D. Emmons, *J. Am. Chem. Soc.* **1961**, *83*, 1733–1738; e) K. Takai, K. Nitta, K. Utimoto, *J. Am. Chem. Soc.* **1986**, *108*, 7408–7410; f) J. E. McMurry, M. P. Fleming, *J. Am. Chem. Soc.* **1974**, *96*, 4708–4709; g) M. Julia, Y.-M. Paris, *Tetrahedron Lett.* **1973**, *14*, 4833–4836.

¹²⁶ R. J. Armstrong, V. K. Aggarwal, *Synthesis* **2017**, *49*, 3323–3336.

¹²⁷ a) G. Zweifel, H. Arzoumanian, C. C. Whitney, *J. Am. Chem. Soc.* **1967**, *89*, 3652–3653; b) G. Zweifel, N. L. Polston, C. C. Whitney, *J. Am. Chem. Soc.* **1968**, *90*, 6243–6245.

¹²⁸ a) G. Zweifel, R. P. Fisher, J. T. Snow, C. C. Whitney, *J. Am. Chem. Soc.* **1972**, *94*, 6560–6561; b) R. J. Armstrong, C. García-Ruiz, E. L. Myers, V. K. Aggarwal, *Angew. Chem. Int. Ed.* **2017**, *56*, 786–790.



Scheme 27: Zweifel olefination within the synthesis of bombykol by Negishi and co-workers.

The Zweifel olefination was picked up early by Negishi *et al.* for the total synthesis of bombykol.¹²⁹ As at that time vinyl borane intermediates were only accessible by Brown's hydroboration method, the sequence toward bombykol starts with the reaction of alkyne **121** with borane **120**, followed by addition of alkynyllithium species **122**, generating the tetracoordinated organoborane salt **123**, which after Zweifel olefination yields **124** as the single (*E*)-isomer (Scheme 27). After second hydroboration, hydrolysis and subsequent protodeborylation bombykol is generated (see Figure 4).¹

In the same year, Brown and co-workers also showed that the Zweifel olefination can be applied to the synthesis of alkynes not bearing an olefin, a procedure that was readily utilized in total syntheses.^{126,130} In addition, Evans and Matteson presented the potential of boronic esters to participate in this type of olefination, thus greatly enhancing the viability of the approach.¹³¹ Exploiting those findings, Aggarwal and co-workers highlighted that the Zweifel olefination is not only stereospecific, but also enantiospecific.

Performing the olefination on enantiomerically enriched benzylic tertiary boronic esters like **127** furnished the desired coupling products (**129**) in 100% enantiospecificity (Scheme 28A), which also held true for alkylic tertiary boronic esters as substrates.¹³² Hereby, a very reactive and unstable vinyl lithium species **126** was generated *via* transmetalation from tetravinyltin **125** to access bisorganoborinate **128**. Moreover, it was demonstrated by the same group that more stable organomagnesium instead of usually employed organolithium compounds could be used in Zweifel olefinations.¹³³ In case of alkenylmagnesium compounds (**131**) however, over-addition of the organometallic was observed onto the pinacol boronic ester **130**, resulting in the formation of tetraorganoboronate **133** and full conversion was therefore only achieved using 4.0 equivalents of the organometallic species. This problem was circumvented

¹²⁹ E. Negishi, G. Lew, T. Yoshida, *J. Chem. Soc. Chem. Commun.* **1973**, 874–875.

¹³⁰ a) A. Suzuki, N. Miyaura, S. Abiko, M. Itoh, H. C. Brown, J. A. Sinclair, M. M. Midland, *J. Am. Chem. Soc.* **1973**, *95*, 3080–3081; b) A. Suzuki, N. Miyaura, S. Abiko, M. Itoh, M. M. Midland, J. A. Sinclair, H. C. Brown, *J. Org. Chem.* **1986**, *51*, 4507–4511; c) M. Naruse, K. Utimoto, H. Nozaki, *Tetrahedron* **1974**, *30*, 2159–2163; d) M. Naruse, K. Utimoto, H. Nozaki, *Tetrahedron Lett.* **1973**, *14*, 2741–2744; e) A. Pelter, R. A. Drake, *Tetrahedron Lett.* **1988**, *29*, 4181–4184; f) J. A. Sikorski, N. G. Bhat, T. E. Cole, K. K. Wang, H. C. Brown, *J. Org. Chem.* **1986**, *51*, 4521–4525; g) D. P. Canterbury, G. C. Micalizio, *J. Am. Chem. Soc.* **2010**, *132*, 7602–7604.

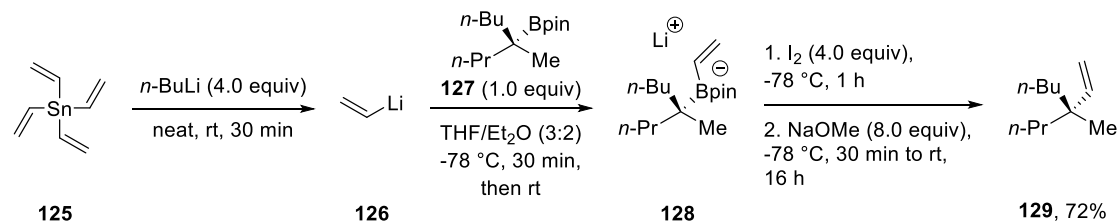
¹³¹ a) D. S. Matteson, P. K. Jesthi, *J. Organomet. Chem.* **1976**, *110*, 25–37; b) D. A. Evans, R. C. Thomas, J. A. Walker, *Tetrahedron Lett.* **1976**, *17*, 1427–1430; c) D. A. Evans, T. C. Crawford, R. C. Thomas, J. A. Walker, *J. Org. Chem.* **1976**, *41*, 3947–3953; d) H. C. Brown, N. G. Bhat, *J. Org. Chem.* **1988**, *53*, 6009–6013.

¹³² a) A. P. Pulis, D. J. Blair, E. Torres, V. K. Aggarwal, *J. Am. Chem. Soc.* **2013**, *135*, 16054–16057; b) D. J. Blair, D. Tanini, J. M. Bateman, H. K. Scott, E. L. Myers, V. K. Aggarwal, *Chem. Sci.* **2017**, *8*, 2898–2903.

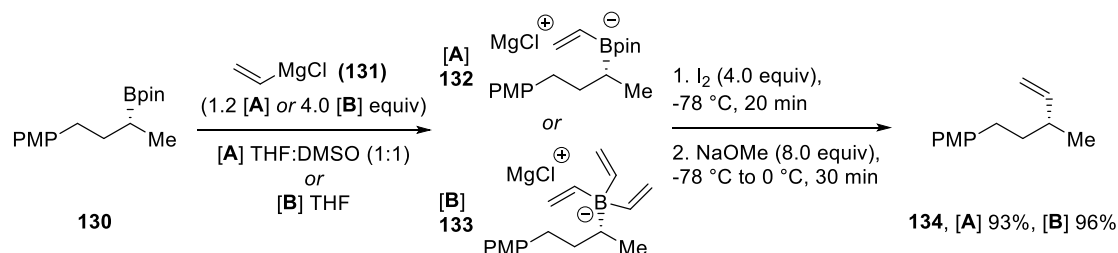
¹³³ a) R. P. Sonawane, V. Jheengut, C. Rabalakos, R. Larouche-Gauthier, H. K. Scott, V. K. Aggarwal, *Angew. Chem. Int. Ed.* **2011**, *50*, 3760–3763; b) M. Shimizu, *Angew. Chem. Int. Ed.* **2011**, *50*, 5998–6000.

by the addition of DMSO, which precipitated the desired salt **132** from solution and thereby rendered it unreactive for further additions. The olefinated compound **134** was isolated in excellent yields of up to 96% (Scheme 28B).¹³⁴

A) Aggarwal (2013): Stereospecific Zweifel olefination



B) Aggarwal (2017): Zweifel olefination employing vinylmagnesium reagents



Scheme 28: Recent developments in Zweifel olefinations by Aggarwal and co-workers.

As olefins represent valuable and important structural motifs in nature, it is not surprising that Zweifel olefinations have been applied in natural product syntheses. Even though it remains in steady competition with the pervasive Suzuki-Miyaura cross-coupling,^{3,12c,16,135} many reports – starting with Negishi's bombykol synthesis – have implemented the Zweifel olefination as a transition-metal free alternative into their protocol. While most reports convert the alkenyl moiety toward the final steps of their total synthesis *via* hydrogenations, epoxidations or cyclizations, some of them preserve it.¹³⁶ These efforts are summarized in Figure 4.^{129,137}

¹³⁴ R. J. Armstrong, W. Niwetmarin, V. K. Aggarwal, *Org. Lett.* **2017**, *19*, 2762–2765.

¹³⁵ a) S. R. Chemler, D. Trauner, S. J. Danishefsky, *Angew. Chem. Int. Ed.* **2001**, *40*, 4544–4568; b) R. Jana, T. P. Pathak, M. S. Sigman, *Chem. Rev.* **2011**, *111*, 1417–1492.

¹³⁶ a) D. J. Blair, C. J. Fletcher, K. M. P. Wheelhouse, V. K. Aggarwal, *Angew. Chem. Int. Ed.* **2014**, *53*, 5552–5555; b) F. Meng, K. P. McGrath, A. H. Hoveyda, *Nature* **2014**, *513*, 367–374; c) T. P. Blaisdell, J. P. Morken, *J. Am. Chem. Soc.* **2015**, *137*, 8712–8715; d) R. A. Kleinnijenhuis, B. J. J. Timmer, G. Lutteke, J. M. M. Smits, R. de Gelder, J. H. van Maarseveen, H. Hiemstra, *Chem. Eur. J.* **2016**, *22*, 1266–1269; e) J. A. M. Mercer, C. M. Cohen, S. R. Shuken, S. R. Wagner, M. W. Smith, F. R. Moss, M. D. Smith, R. Vahala, A. Gonzalez-Martinez, S. G. Boxer, N. Z. Burns, *J. Am. Chem. Soc.* **2016**, *138*, 15845–15848; f) A. Varela, L. K. B. Garve, D. Leonori, V. K. Aggarwal, *Angew. Chem. Int. Ed.* **2017**, *56*, 2127–2131.

¹³⁷ a) S. Xu, C.-T. Lee, H. Rao, E. Negishi, *Adv. Synth. Catal.* **2011**, *353*, 2981–2987; b) A. Noble, S. Roesner, V. K. Aggarwal, *Angew. Chem. Int. Ed.* **2016**, *55*, 15920–15924.

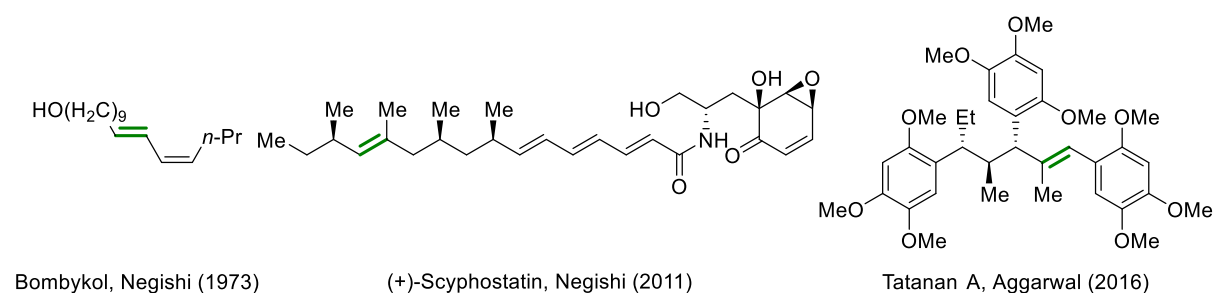


Figure 4: Examples of Zweifel olefinations in natural product syntheses with preserved alkenyl moiety.

4 Electrochemistry

4.1 Overview

The manipulation of an organic molecule under reductive or oxidative conditions is one of the most fundamental principles in organic chemistry.¹³⁸ While these processes are traditionally facilitated by molecular oxidizing or reducing agents like transition-metal catalysts (Suzuki-Miyaura coupling, section 3.3) or organic molecules like iodine (Zweifel Olefination, section 3.4), electrochemistry can be considered the simplest, most eco-friendly and atom-economic operation to remove or add electrons from or to an organic molecule, as stoichiometric amounts of reagent waste are avoided.¹³⁹ The direct control over current and potential and consequential tuneability from very mild to forcing oxidizing and reducing conditions at reusable anodes and cathodes are innate advantages of electrochemical setups. Moreover, the inherently safe, sustainable and “green” reaction conditions in addition to economic aspects and easy scalability are key factors that make electrochemical transformations desirable.¹⁴⁰ Even though well-established in industrial applications, electrochemistry was considered a niche technology in the organic community throughout the majority of the last century, largely due to complex reaction systems and numerous optimization parameters.¹⁴¹ It is currently experiencing a renaissance, since more user-friendly and simple setups have paved the way for regular organic chemists to implement electrochemical processes into their protocols.^{138,142} Ground-breaking work by the groups of

¹³⁸ a) J. Yoshida, K. Kataoka, R. Horcajada, A. Nagaki, *Chem. Rev.* **2008**, *108*, 2265–2299; b) M. Yan, Y. Kawamata, P. S. Baran, *Chem. Rev.* **2017**, *117*, 13230–13319.

¹³⁹ a) A. Wiebe, T. Gieshoff, S. Möhle, E. Rodrigo, M. Zirbes, S. R. Waldvogel, *Angew. Chem. Int. Ed.* **2018**, *57*, 5594–5619; b) S. Möhle, M. Zirbes, E. Rodrigo, T. Gieshoff, A. Wiebe, S. R. Waldvogel, *Angew. Chem. Int. Ed.* **2018**, 6018–6041.

¹⁴⁰ a) S. R. Waldvogel, S. Lips, M. Selt, B. Riehl, C. J. Kampf, *Chem. Rev.* **2018**, *118*, 6706–6765; b) M. D. Kärkäs, *Chem. Soc. Rev.* **2018**, *47*, 5786–5865; c) J. L. Röckl, D. Pollok, R. Franke, S. R. Waldvogel, *Acc. Chem. Res.* **2020**, *53*, 45–61.

¹⁴¹ a) J. B. Sperry, D. L. Wright, *Chem. Soc. Rev.* **2006**, *35*, 605–621; b) E. J. Horn, B. R. Rosen, P. S. Baran, *ACS Cent. Sci.* **2016**, *2*, 302–308; c) D. S. P. Cardoso, B. Sljukic, D. M. F. Santos, C. A. C. Sequeira, *Org. Process Res. Dev.* **2017**, *21*, 1213–1226.

¹⁴² C. Kingston, M. D. Palkowitz, Y. Takahira, J. C. Vantourout, B. K. Peters, Y. Kawamata, P. S. Baran, *Acc. Chem. Res.* **2020**, *53*, 72–83.

Yoshida¹⁴³, Waldvogel¹⁴⁰, Baran¹⁴⁴ and many more has not only demonstrated to mimic conventional organic synthesis but has displayed novel reactivity patterns by rethinking essential mechanistic pathways and transposing those from two- to one-electron processes, usually enabling more step-economic syntheses.¹⁴⁵ In recent years, electrochemistry has emerged in the fields of natural product synthesis, organocatalysis and flow electrochemistry.^{139b,140c,146} As excessive energy consumption and environmental considerations are major topics of current political and social discourse, the use of “green” electrochemistry from renewable energy sources will most certainly become increasingly important in 21st century organic synthesis.^{139a}

Dating back to the invention of the “Volta pile”, the first battery in 1800,¹⁴⁷ the basic principle behind electroorganic synthesis lies in the constant movement of electrons through a circuit.^{138b} For this reason, sufficient conductivity in solution between anode and cathode has to be ensured, which is usually guaranteed by addition of a supporting electrolyte to a solvent with a high dielectricity constant and electrochemical stability. As electroorganic synthesis essentially resembles redox chemistry, both anodic oxidation and cathodic reduction have to occur simultaneously. The most prominent electrodes are made from non-destructive carbon-based materials or noble metals. Modern electrochemical transformations favor a simple undivided cell-setup, meaning that both electrodes reside in the same chamber, and run the reaction under constant current (galvanostatic) conditions, while more sophisticated and complex divided-cell setups and constant potential (potentiostatic) reaction conditions are used less frequently, as they require a third reference electrode and additional porous materials that separate the anodic and cathodic compartments. Constant current conditions are additionally operatively convenient, as they allow for the precise addition of electrons to the system.^{138b,140,142}

$$\text{reaction time (s)} = n \cdot \frac{F}{I} \quad (\text{with } F = N_A \cdot e \approx 96485 \frac{\text{As}}{\text{mol}}) \quad (\text{equation 1})$$

Faraday’s constant (F , equation 1) resembles the equivalent to one mole of electrons and can therefore be used to calculate the time needed for the electrochemical setup to add the desired number of

¹⁴³ a) J. Yoshida, Y. Ashikari, K. Matsumoto, T. Nokami, *J. Synth. Org. Chem., Jpn.* **2013**, *71*, 1136–1144; b) J. Yoshida, A. Shimizu, R. Hayashi, *Chem. Rev.* **2018**, *118*, 4702–4730.

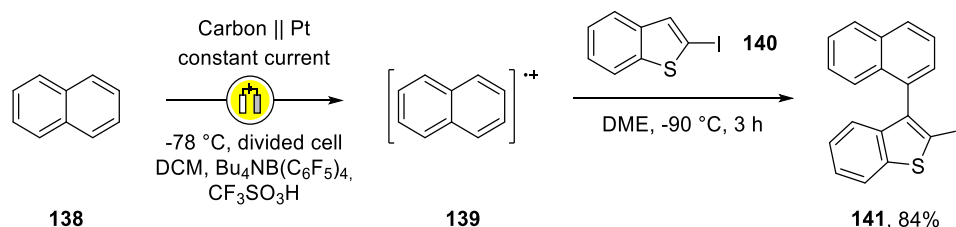
¹⁴⁴ a) E. J. Horn, B. R. Rosen, Y. Chen, J. Tang, K. Chen, M. D. Eastgate, P. S. Baran, *Nature* **2016**, *533*, 77–81; b) J. Xiang, M. Shang, Y. Kawamata, H. Lundberg, S. H. Reisberg, M. Chen, P. Mykhailiuk, G. Beutner, M. R. Collins, A. Davies, M. Del Bel, G. M. Gallego, J. E. Spangler, J. Starr, S. Yang, D. G. Blackmond, P. S. Baran, *Nature* **2019**, *573*, 398–402; c) B. K. Peters, K. X. Rodriguez, S. H. Reisberg, S. B. Beil, D. P. Hickey, Y. Kawamata, M. Collins, J. Starr, L. Chen, S. Udyavara, K. Klunder, T. J. Gorey, S. L. Anderson, M. Neurock, S. D. Minter, P. S. Baran, *Science* **2019**, *363*, 838–845.

¹⁴⁵ a) M. Yan, J. C. Lo, J. T. Edwards, P. S. Baran, *J. Am. Chem. Soc.* **2016**, *138*, 12692–12714; b) P. S. Baran, et al., *Angew. Chem. Int. Ed.* **2018**, *57*, 14560–14565; c) P. S. Baran, et al., *Angew. Chem. Int. Ed.* **2019**, *58*, 2454–2458; d) P. S. Baran, et al., *J. Am. Chem. Soc.* **2019**, *141*, 6392–6402; e) P. S. Baran, et al., *J. Am. Chem. Soc.* **2019**, *141*, 6726–6739; f) Y. Yuan, A. Lei, *Acc. Chem. Res.* **2019**, *52*, 3309–3324; g) K. Yamamoto, M. Kuriyama, O. Onomura, *Acc. Chem. Res.* **2020**, *53*, 105–120.

¹⁴⁶ a) C. Gütz, A. Stenglein, S. R. Waldvogel, *Org. Process Res. Dev.* **2017**, *21*, 771–778; b) A. Shatskiy, H. Lundberg, M. Kärkäs, *ChemElectroChem* **2019**, *6*, 4067–4092; c) A. Lipp, M. Selt, D. Ferenc, D. Schollmeyer, S. R. Waldvogel, T. Opatz, *Org. Lett.* **2019**, *21*, 1828–1831.

¹⁴⁷ a) A. G. A. Volta, *Nat. Philos. Chem. Arts* **1800**, *4*, 179–187; b) H. Lund, *J. Electrochem. Soc.* **2002**, *149*, 21–33.

the potential have to be chosen carefully in order to dial in the perfect conditions that minimize side product formation, which can result in laborious optimizations.¹⁴² In general, the molecule with the highest electron-density will get oxidized first, while the molecule with the highest electron-deficiency will be reduced first. The oxidizing or reducing power of the electrochemical system is defined by its potential, meaning that a high voltage results in a strong redox environment and *vice versa*.^{141b,142}



Scheme 29: An example of C-C cross-coupling enabled by Yoshida’s cation pool method.

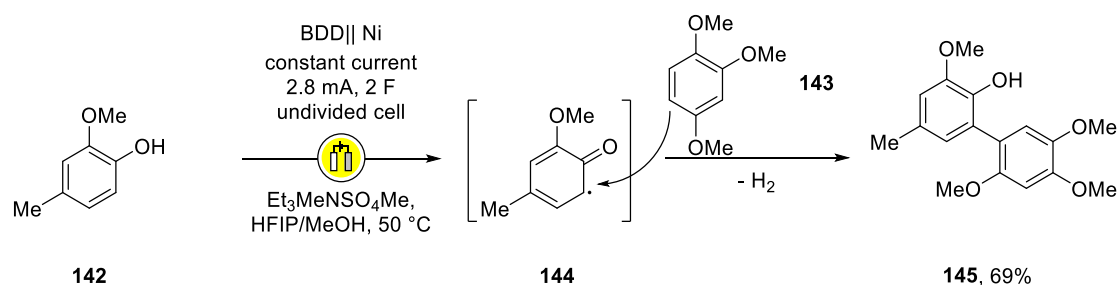
Adhering to this fundamental groundwork, the last two decades of electrochemical organic synthesis have produced tremendous developments, especially in the field of oxidative C-C cross-couplings.^{138b,140} For instance, Yoshida and co-workers established the “cation pool method” in 1999, in which *via* anodic oxidation cations are cumulated in a divided cell setup and then reacted with respective nucleophiles under non-electrochemical conditions to yield the desired coupled products.¹⁵¹ By separating the oxidation and coupling events, unwanted overoxidation of the substrates and homocoupling side-reactions are elegantly suppressed. More recently, the same authors were able to expand the scope of their reaction to radical arene cations, as treatment of naphthalene **138** at cryogenic temperatures yielded cation **139**, which was then further reacted with heteroarene **140** to yield the cross-coupled product **141** in high yields (Scheme 29).¹⁵² However, using this “radical cation pool method” the temperature has to be kept very low and BARF anions have to be used to tame the reactivity of the synthesized intermediates. An elaborate divided cell-setup must be employed to generate a selective coupling process, making this method less attractive for large-scale synthesis.^{139a,b}

In a different approach toward electrochemical aryl-aryl cross-couplings, Waldvogel and co-workers highlighted the advantages of boron-doped diamond (BDD) electrodes over different anodes and hexafluoroisopropanol (HFIP) over other solvents for the cross-coupling of phenols and arenes. The unique electrochemical stability, solvation and stabilization capability of radicals by HFIP allow for the selective oxidation of phenol **142** over electron-rich arene **143** in an undivided cell *via* hydrogen-bonding

¹⁵¹ a) J. Yoshida, S. Suga, S. Suzuki, N. Kinomura, A. Yamamoto, K. Fujiwara, *J. Am. Chem. Soc.* **1999**, *121*, 9546–9549; b) J. Yoshida, S. Suga, *Chem. Eur. J.* **2002**, *8*, 2650–2658; c) S. Suga, T. Nishida, D. Yamada, A. Nagaki, J. Yoshida, *J. Am. Chem. Soc.* **2004**, *126*, 14338–14339; d) S. Suga, S. Suzuki, A. Yamamoto, J. Yoshida, *J. Am. Chem. Soc.* **2000**, *122*, 10244–10245; e) T. Nokami, T. Watanabe, N. Musya, T. Morofuji, K. Tahara, Y. Tobe, J. Yoshida, *Chem. Commun.* **2011**, *47*, 5575–5577; f) R. Hayashi, A. Shimizu, J. Yoshida, *J. Am. Chem. Soc.* **2016**, *138*, 8400–8403; g) T. Maruyama, Y. Mizuno, I. Shimizu, S. Suga, J. Yoshida, *J. Am. Chem. Soc.* **2007**, *129*, 1902–1903.

¹⁵² a) T. Morofuji, A. Shimizu, J. Yoshida, *Angew. Chem. Int. Ed.* **2012**, *51*, 7259–7262; b) T. Arai, H. Tateno, K. Nakabayashi, T. Kashiwagi, M. Atobe, *Chem. Commun.* **2015**, *51*, 4891–4894.

interactions, even though both compounds exhibit similar electron-densities and oxidation potentials.^{140a,c} The formed radical **144** is then selectively attacked in *ortho*-position by arene **143** instead of phenol **142** preventing homo-coupling, as the former is only weakly solvated by HFIP resulting in a highly nucleophilic species. Importantly, the *ortho*-selectivity was only observed at BDD anodes and was related to their high electrochemical stability and overpotential for oxygen evolution in aqueous media.^{139b} The resulting cross-coupled biaryl **145** (Scheme 30) is only one product of a diverse library of compounds accessible *via* this method,¹⁵³ allowing for the synthesis of biphenols¹⁵⁴, protected bi-aniline derivatives¹⁵⁵, bi(hetero)aryls¹⁵⁶ and also terphenyls¹⁵⁷ *via* double anodic C-C couplings. The Waldvogel group has therefore impressively demonstrated that the discrimination for oxidation between two species with similar oxidation potentials *via* solvation can be achieved with HFIP and BDD electrodes, resulting in a versatile and general procedure, which can be conveniently run at ambient temperature in an undivided cell.^{139a}



Scheme 30: Selective electrochemical cross-coupling of phenols and arenes by Waldvogel.

4.3 Tetracoordinated Boron Salts

In addition to their work on HFIP assisted C-C cross-couplings, the group of Waldvogel also devised a boron templated method for the regioselective coupling of phenols in MeCN without the necessity of HFIP as a solvent. Hereby, various symmetrical tetraphenoxy borate salts were synthesized (**146**) and subsequently oxidized at a platinum electrode in an undivided cell under constant current to yield intermediate **147**. This oxidation was found to proceed solely through an intramolecular pathway, yielding the homocoupled biphenol **148** after acidic workup with citric acid (Scheme 31). Interestingly, no

¹⁵³ a) A. Kirste, G. Schnakenburg, F. Stecker, A. Fischer, S. R. Waldvogel, *Angew. Chem. Int. Ed.* **2010**, *49*, 971–975; b) A. Kirste, B. Elsler, G. Schnakenburg, S. R. Waldvogel, *J. Am. Chem. Soc.* **2012**, *134*, 3571–3576.

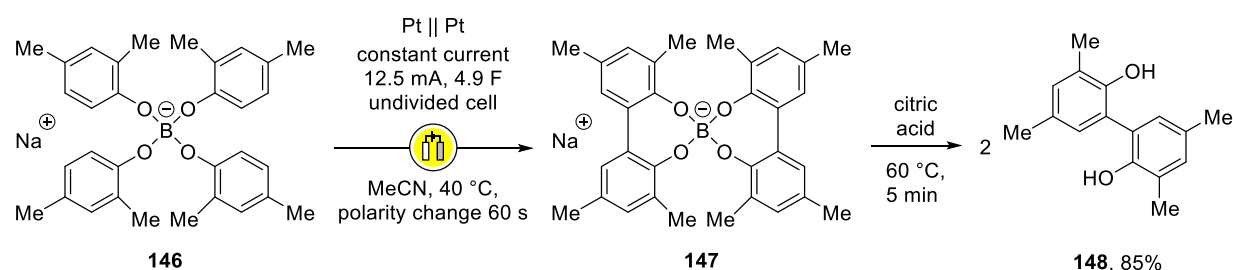
¹⁵⁴ a) B. Elsler, D. Schollmeyer, K. M. Dyballa, R. Franke, S. R. Waldvogel, *Angew. Chem. Int. Ed.* **2014**, *53*, 5210–5213; b) A. Wiebe, D. Schollmeyer, K. M. Dyballa, R. Franke, S. R. Waldvogel, *Angew. Chem. Int. Ed.* **2016**, *55*, 11801–11805.

¹⁵⁵ L. Schulz, M. Enders, B. Elsler, D. Schollmeyer, K. M. Dyballa, R. Franke, S. R. Waldvogel, *Angew. Chem. Int. Ed.* **2017**, *56*, 4877–4881.

¹⁵⁶ A. Wiebe, S. Lips, D. Schollmeyer, R. Franke, S. R. Waldvogel, *Angew. Chem. Int. Ed.* **2017**, *56*, 14727–14731.

¹⁵⁷ a) S. Lips, A. Wiebe, B. Elsler, D. Schollmeyer, K. M. Dyballa, R. Franke, S. R. Waldvogel, *Angew. Chem. Int. Ed.* **2016**, *55*, 10872–10876; b) A. Wiebe, B. Riehl, S. Lips, R. Franke, S. R. Waldvogel, *Sci. Adv.* **2017**, *3*, ea03920.

additional electrolyte was needed as the borate salt itself served as one and the procedure was easily scaled up to a multikilogram scale.¹⁵⁸



Scheme 31: Intramolecular oxidation of tetraphenoxy borate anions to biphenols.

Additionally, fundamental work by Schlegel and Schäfer showed that otherwise inactive triorganoboranes are activated for oxidation after addition of a nucleophile to form the tetraorganoborate. Importantly, the donating character of the nucleophile influences the oxidation potential so that weakly nucleophilic THF- and F-coordinated tri-*n*-butylborane complexes **149** and **150** exhibit high oxidation potentials, whereas strong and electron-rich nucleophiles like cyanide and hydroxide anions yield complexes **151** and **152**, which undergo more facile anodic oxidation (Figure 6). Subsequently, the authors showcased that tetraorganoborates of type **152** could be oxidized to yield the corresponding aliphatic hydrocarbons. However, no cross-coupling products could be detected in useful yields, as deboronative alkyl radical formations were observed, thereby disassembling the selectivity-enabling boron-template and yielding almost statistical distributions of homo- and heterocoupling products.¹⁵⁹

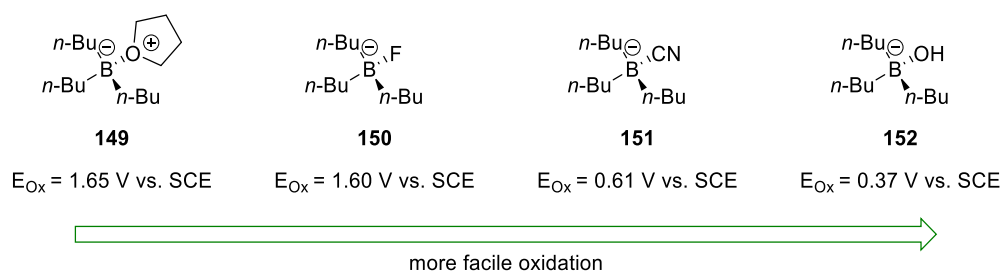


Figure 6: Influence of the substituents on the oxidation potential of the tetraorganoborate.

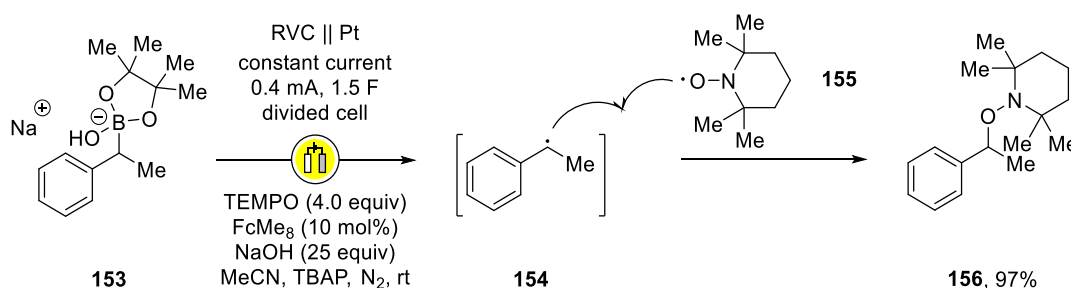
In the emerging field of photoredox catalysis, which is closely related to electrochemistry as typically one-electron processes are studied,^{120b,160} such deboronative alkyl radical formations of tetracoordinated

¹⁵⁸ a) I. M. Malkowsky, C. E. Rommel, R. Fröhlich, U. Griesbach, H. Pütter, S. R. Waldvogel, *Chem. Eur. J.* **2006**, *12*, 7482–7488; b) I. M. Malkowsky, R. Fröhlich, U. Griesbach, H. Pütter, S. R. Waldvogel, *Eur. J. Inorg. Chem.* **2006**, 1690–1697.

¹⁵⁹ a) G. Schlegel, H. J. Schäfer, *Chem. Ber.* **1984**, *117*, 1400–1423; b) J. H. Morris, H. J. Gysling, D. Reed, *Chem. Rev.* **1985**, *85*, 51–76.

¹⁶⁰ a) J. M. R. Narayanam, C. R. J. Stephenson, *Chem. Soc. Rev.* **2011**, *40*, 102–113; b) C. K. Prier, D. A. Rankic, D. W. C. MacMillan, *Chem. Rev.* **2013**, *113*, 5322–5363.

organoboron compounds are frequently used to trigger follow-up transformations.^{79c,161} Moreover, Stahl's group recently highlighted that redox inactive benzylic boronic esters can be activated by addition of sodium hydroxide and further used in electrochemical processes. In a ferrocene-mediated¹⁶² anodic oxidation of the tetraorganoboronate **153** under potentiostatic conditions in a divided cell setup the resulting benzylic radical **154** was trapped almost quantitatively employing TEMPO **155** to yield **156** (Scheme 32).¹⁶³



Scheme 32: *In situ* quench of electrochemically generated benzyl radicals by Stahl and co-workers.

The electrochemical properties of related tetraarylborates are already well-studied.¹⁶⁴ Initial data on the electrochemical synthesis of biaryls from tetraphenylborate salts was provided by Geske and co-workers. In their pioneering studies the tetraphenylborate ion **77** was found to be oxidized at a platinum anode to form biphenyl.¹⁶⁵ Similar to the later work by Hirao and others (chapter 3.2), in which molecular oxidants promoted the oxidation of tetraarylborate salts,^{87,88,89} an intramolecular two-electron process was proposed and control experiments using fully deuterated tetraphenylborate were conducted to exclude intermolecular pathways.¹⁶⁶ However, the possibility of a one-electron process was neglected at that time,¹⁶⁷ even though seminal work by Doty *et al.* on photochemical oxidation of the tetraphenylborate anion with *in situ* generated singlet oxygen suggested the possibility of a one-electron

¹⁶¹ a) Y. Yasu, T. Koike, M. Akita, *Adv. Synth. Catal.* **2012**, *354*, 3414–3420; b) J. C. Tellis, D. N. Primer, G. A. Molander, *Science* **2014**, *345*, 433–436; c) H. Huang, G. Zhang, L. Gong, S. Zhang, Y. Chen, *J. Am. Chem. Soc.* **2014**, *136*, 2280–2283; d) H. Huang, K. Jia, Y. Chen, *Angew. Chem. Int. Ed.* **2015**, *54*, 1881–1884; e) D. N. Primer, I. Karakaya, J. C. Tellis, G. A. Molander, *J. Am. Chem. Soc.* **2015**, *137*, 2195–2198; f) F. Lima, M. A. Kabeshov, D. N. Tran, C. Battilocchio, J. Sedelmeier, G. Sedelmeier, B. Schenkel, S. V. Ley, *Angew. Chem. Int. Ed.* **2016**, *55*, 14085–14089; g) H. Huo, K. Harms, E. Meggers, *J. Am. Chem. Soc.* **2016**, *138*, 6936–6939; h) D. N. Primer, G. A. Molander, *J. Am. Chem. Soc.* **2017**, *139*, 9847–9850; i) F. Lima, U. K. Sharma, L. Grunenberg, D. Saha, S. Johannsen, J. Sedelmeier, E. V. Van der Eycken, S. V. Ley, *Angew. Chem. Int. Ed.* **2017**, *56*, 15136–15140; j) S. B. Lang, R. J. Wiles, C. B. Kelly, G. A. Molander, *Angew. Chem. Int. Ed.* **2017**, *56*, 15073–15077; k) W. Liu, P. Liu, L. Lv, C. Li, *Angew. Chem. Int. Ed.* **2018**, *57*, 13499–13503; l) H. Yan, Z.-W. Hou, H.-C. Xu, *Angew. Chem. Int. Ed.* **2019**, *131*, 4640–4643.

¹⁶² a) J.-M. Savéant, *Chem. Rev.* **2008**, *108*, 2348–2378; b) R. Francke, R. D. Little, *Chem. Soc. Rev.* **2014**, *43*, 2492–2521.

¹⁶³ A. J. J. Lennox, J. E. Nutting, S. S. Stahl, *Chem. Sci.* **2018**, *9*, 356–361.

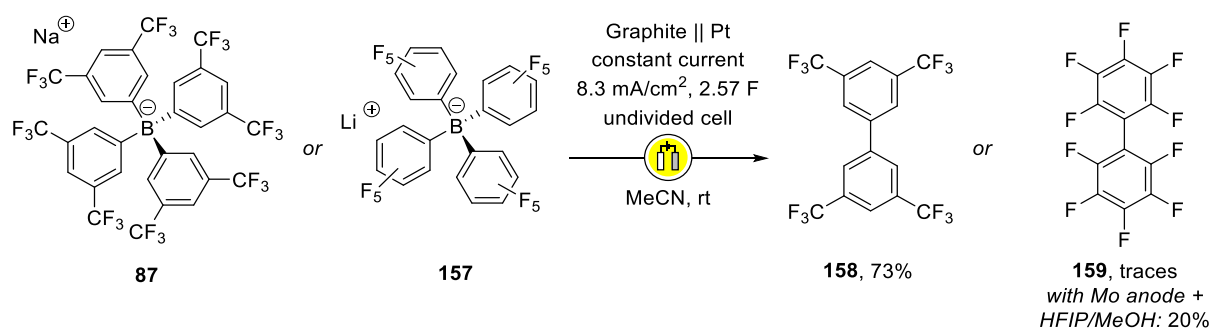
¹⁶⁴ a) F. Barrière; W. E. Geiger, *J. Am. Chem. Soc.* **2006**, *128*, 3980–3989; b) W. E. Geiger; F. Barrière, *Acc. Chem. Res.* **2010**, *43*, 1030–1039.

¹⁶⁵ D. H. Geske, *J. Phys. Chem.* **1959**, *63*, 1062–1070.

¹⁶⁶ D. H. Geske, *J. Phys. Chem.* **1962**, *66*, 1743–1744.

¹⁶⁷ W. R. Turner, P. J. Elving, *Anal. Chem.* **1965**, *37*, 207–211.

pathway.¹⁶⁸ Almost a decade later, Janzen and co-workers supported this idea with spin-trapping experiments and proved the presence of radical species in solution.¹⁶⁹ Most recently, Waldvogel and co-workers reassured Geske's fundamental work and demonstrated the electrochemical instability of tetraarylborates toward oxidation on two BARF substrates (Scheme 33). While BARF anion **87** was smoothly oxidized to the homocoupled biaryl **158** in 73% yield at a graphite anode, the expected biaryl **159** from oxidation of BARF anion **157** was only observed in traces. Even after extensive optimizations, biaryl **159** was only obtained in 20% yield at a molybdenum anode, presumably due to its very high oxidation potential (see Figure 6). Although radical trapping and crossover experiments were performed, the exact mechanistic pathway remained unsolved, as both cationic and radical pathway were imaginable.¹⁷⁰



Scheme 33: Oxidation of symmetrical tetraarylborates toward homocoupled biaryls.

¹⁶⁸ a) J. C. Doty, P. J. Grisdale, T. R. Evans, J. L. R. Williams, *J. Organomet. Chem.* **1971**, 32, C35–C37; b) A. Pelter, R. T. Pardasani, P. Pardasani, *Tetrahedron* **2000**, 56, 7339–7369.

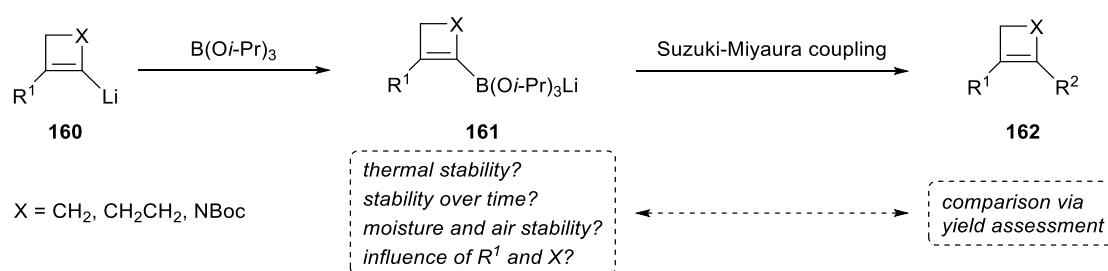
¹⁶⁹ a) E. E. Bancroft, H. N. Blount, E. G. Janzen, *J. Am. Chem. Soc.* **1979**, 101, 3692–3694; b) P. K. Pal, S. Chowdhury, M. G. B. Drew, D. Datta, *New. J. Chem.* **2002**, 26, 367–371.

¹⁷⁰ S. B. Beil, S. Möhle, P. Enders, S. R. Waldvogel, *Chem. Comm.* **2018**, 54, 6128–6131.

5 Objectives

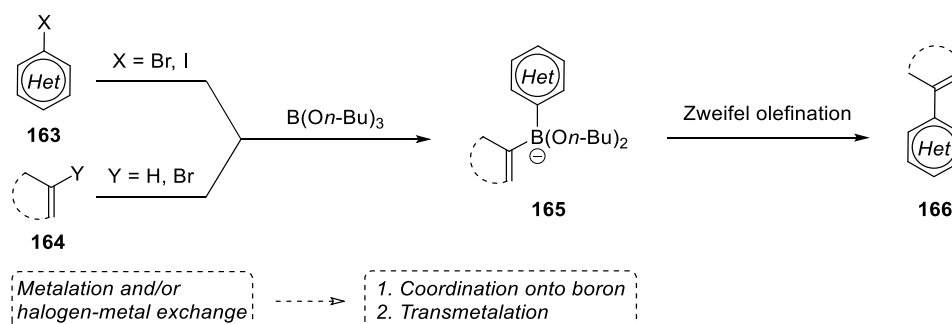
This work should present complementary approaches to fundamental and well-established methods relying on organoboron chemistry, such as Suzuki-Miyaura cross-couplings. The reliance on potentially toxic, hazardous and expensive transition-metal catalysts is the major drawback of these powerful and incredibly versatile methods. Therefore, this work will heavily focus on the extension of more environmentally benign strategies, involving underestimated transition-metal free olefinations and electrochemical alternatives, circumventing the use of transition-metal catalysis.

For this reason, the preparation and stability of tetracoordinated organoboron salts should be investigated first. Based on previous results, highly strained cyclic carbenoid and therefore reactive organometallic intermediates **160** shall be trapped with borontrialkoxides to yield the corresponding organoboronate salts **161**. These salts will then be stored under different conditions for varying amounts of time to determine their stability, which will be measured by comparing the residual conversion in subsequent Suzuki-Miyaura cross-couplings toward **162** (Scheme 34).



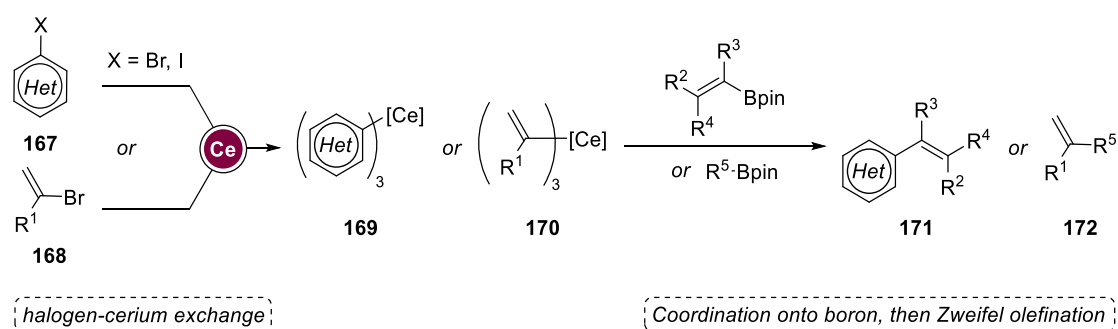
Scheme 34: Synthesis and stability assessment of organoboronates **161**.

In a second step, the usefulness of such salts should be examined in Zweifel olefinations. Since modern Zweifel olefinations mostly employ pinacol boronic esters, their applicability is limited as especially more sophisticated substrates tend to be expensive or unavailable. Therefore, it is highly desirable to develop a general methodology that allows for the rapid formation of diverse bisorganoborinates **165** *via* metalation, metal-exchange and transmetalation strategies onto inexpensive borontrialkoxides for their implementation in Zweifel olefinations (Scheme 35).



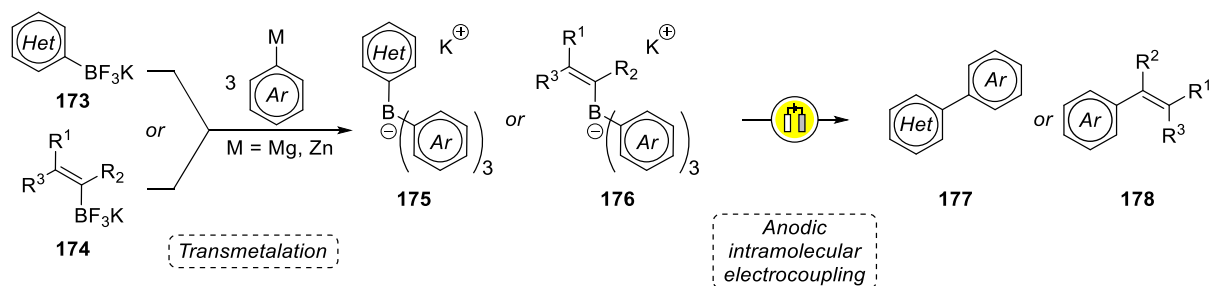
Scheme 35: Access to bisorganoborinates **165** *via* organometallic methods and follow-up Zweifel olefination.

Furthermore, there is significant interest in the development of novel organometallics that might fill gaps and combine functional group tolerance and reactivity. For instance, most examples of Zweifel olefination rely on the use of highly reactive organolithium species for smooth addition onto the boron pinacol ester. While functional group tolerance is therefore limited, additions of milder arylmagnesium compounds to boron pinacol esters tend to be problematic and the use of alkenylmagnesium species usually results in overaddition. Based on previous results, organolanthanide reagents show promising behavior with balanced functional group tolerance and reactivity due to intermediate electronegativities compared to magnesium and lithium. For this reason, a halogen-metal exchange reagent from the most abundant and cheap lanthanide metal cerium should be developed and its reactivity and tolerance tested in Zweifel olefination chemistry and related nucleophilic additions (Scheme 36).



Scheme 36: Halogen-cerium exchange and subsequent Zweifel olefination.

The last aim of this work is to expand the applicability of tetrahedrally coordinated boron salts to C-C bond formations other than olefination reactions. As biaryl frameworks pose as essential moieties in pharmaceutical and agricultural industries, they will serve as eligible products. Based on fundamental previous work, it is envisioned to first synthesize mixed or unsymmetrical tetraarylborates **175** from commercially available potassium trifluoroborates **173** via simple transmetalation chemistry. Those salts shall then be anodically oxidized employing “green” electrochemistry, resulting in intramolecularly cross-coupled (hetero)biaryls **177**. Envisioning a radical pathway, this electrocoupling concept should then be expanded to olefinations, which in theory should lead to a transition-metal free method for the functionalization of alkenes **178** (Scheme 37).



Scheme 37: Envisioned electrocoupling and electro-olefination of potassium tetraorganoborate salts.

B. RESULTS AND DISCUSSION

1 One-Pot Preparation of Stable Organoboronate Reagents for the Functionalization of Unsaturated Four- and Five-Membered Carbo- and Heterocycles

1.1 Relevance

Saturated four- and five-membered carbo- and heterocycles are ubiquitous in nature and important motifs for the pharmaceutical industry, most prominently in the area of β -lactams.¹⁷¹ In addition, their unique range of reactivity caused by the inherent ring-strain makes them valuable intermediates, which was recently highlighted by the groups of Baran and Carreira, who demonstrated applications of propellanes¹⁷², azetidines¹⁷³ and oxetanes¹⁷⁴ in synthesis.

However, unsaturated analogues are scarcely represented in natural products and synthesis, mainly due to their even higher reactivity, resulting instability and lack of synthetic protocols. Even though some representative examples are found in nature, the addition of an internal C-C double bond to an already strained cyclic system makes those compounds privileged intermediates for further transformations.^{82d,175} While organometallic chemistry involving such structures is challenging and has to be usually performed at cryogenic temperatures, this chapter presents a method that allows for the formation of room temperature stable organoboronates, which can be used as building blocks for further applications.

1.2 Preamble

The following work was reprinted with permission from A. N. Baumann, M. Eisold, A. Music and D. Didier, *Synthesis* **2018**, *50*, 3149–3160. The manuscript is presented as a modified version compared to the original publication online in order to prevent copyright infringement with the Georg Thieme Verlag, Stuttgart – New York. The project was conducted in equal contribution with A. N. Baumann and M. Eisold.

¹⁷¹ a) B. Alcaide, P. Almendros, C. Aragoncillo, *Chem. Rev.* **2007**, *107*, 4437–4492; b) C. R. Pitts, T. Lectka, *Chem. Rev.* **2014**, *114*, 7930–7953; c) D. Didier, A. N. Baumann, M. Eisold, *Tetrahedron Lett.* **2018**, *59*, 3975–3987.

¹⁷² a) P. S. Baran, et al., *Science* **2016**, *351*, 241–246; b) P. S. Baran, et al., *J. Am. Chem. Soc.* **2017**, *139*, 3209–3226.

¹⁷³ a) Y. Dejaegher, N. M. Kuz'menok, A. M. Zvonok, N. De Kimpe, *Chem. Rev.* **2002**, *102*, 29–60; b) J. Burkhard, E. M. Carreira, *Org. Lett.* **2008**, *10*, 3525–3526; c) J. A. Burkhard, C. Guérot, H. Knust, M. Rogers-Evans, E. M. Carreira, *Org. Lett.* **2010**, *12*, 1944–1947; d) J. A. Burkhard, B. Wagner, H. Fischer, F. Schuler, K. Müller, E. M. Carreira, *Angew. Chem. Int. Ed.* **2010**, *49*, 3524–3527.

¹⁷⁴ a) G. Wuitschik, M. Rogers-Evans, K. Müller, H. Fischer, B. Wagner, F. Schuler, L. Polonchuk, E. M. Carreira, *Angew. Chem. Int. Ed.* **2006**, *45*, 7736–7739; b) G. Wuitschik, M. Rogers-Evans, A. Buckl, M. Bernasconi, M. Märki, T. Godel, H. Fischer, B. Wagner, I. Parrilla, F. Schuler, J. Schneider, A. Alker, W. B. Schweizer, K. Müller, E. M. Carreira, *Angew. Chem. Int. Ed.* **2008**, *47*, 4512–4515; c) G. Wuitschik, E. M. Carreira, B. Wagner, H. Fischer, I. Parrilla, F. Schuler, M. Rogers-Evans, K. Müller, *J. Med. Chem.* **2010**, *53*, 32273246; d) J. A. Bull, R. A. Croft, O. A. Davis, R. Doran, K. F. Morgan, *Chem. Rev.* **2016**, *116*, 12150–12233.

¹⁷⁵ a) A. N. Baumann, M. Eisold, D. Didier, *Org. Lett.* **2017**, *19*, 2114–2117; b) A. N. Baumann, F. Reiners, T. Juli, D. Didier, *Org. Lett.* **2018**, *20*, 6736–6740.

One-pot Preparation of Stable Organoboronate Reagents for the Functionalization of Unsaturated Four- and Five-Membered Carbo- and Heterocycles

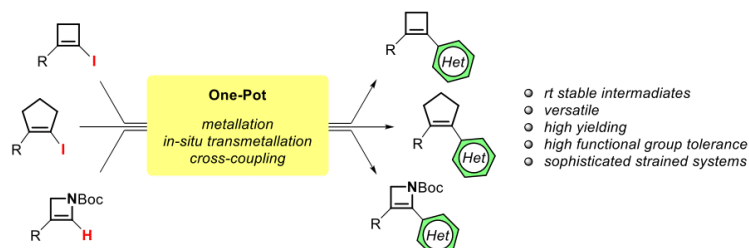
Andreas N. Baumann[†]
 Michael Eisold[†]
 Arif Music[‡]
 Dorian Didier^{*}

University Ludwig-Maximilians, Department of Chemistry and Pharmacy, Butenandtstraße 5-13, 81377 Munich, Germany

dorian.didier@cup.uni-muenchen.de

[†] These authors contributed equally to this work.

Published as part of the Special Topic *Modern Coupling Approaches and their Strategic Applications in Synthesis*



Received: 23.02.2018

Accepted after revision: 03.04.2018

Published online: 14.05.2018

DOI: 10.1055/s-0036-1592004; Art ID ss-2018-c0107-st

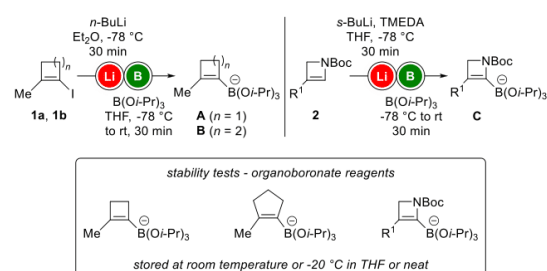
Abstract Combining a facile preparation of organoboronates with their remarkable stability and functional group tolerance allows for the straightforward synthesis of four- and five-membered carbo- and heterocycles. While most strategies rely on the ex situ preparation of boronic acids as isolated intermediates, we demonstrate that in situ transmetalation of sensitive organometallics with boron alkoxides can lead to great stabilization of such species at room temperature. A considerable extension of the library of unsaturated strained structures is achieved through these sequences, expanding the potential applicability of such unusual building blocks.

Key words cyclobutenes, cyclopentenones, azetines, organoboronates, one-pot sequences

The transition-metal-catalyzed cross-couplings of organoboronic acids with organic halides, a process developed by Suzuki et. al.¹ has become one of the most powerful tools for the creation of C-C bonds.² Both simplicity and functional group tolerance have made it a privileged method³ for assembling complex structures in many fields of chemistry such as drug discovery,⁴ materials science⁵, chemosensors⁶ and total synthesis.⁷ Spurred on by the particular stability of organoboron species, we took on the challenge of generalizing the access to classes of molecules that have been scarcely reported: strained cyclobutenes, cyclopentenones and 2-azetines. Due to their commercial availability, organoboronic acids are employed as stable substrates for numerous cross-coupling reactions. For more elaborated scaffolds however, tailor-made boronic acids must be prepared ex situ in order to be engaged in a subsequent reaction through a two-step process. For the sake of step-economy, we needed to develop a more straightforward access to the targeted compounds, avoiding an extra purification of intermediate boronic acids. Taking into account the recent work of Buchwald and co-workers on direct cross-coupling of lithium

organoboronates,⁸ Miyaura et al. on base-free coupling of triolborates,⁹ Cammidge on coupling of ex situ generated trihydroxyborates,¹⁰ and Knochel's group and the in situ generation of magnesium bis-organoboronates,¹¹ we designed different strategies in which the cross-coupling reaction would be relayed by the in situ formation of a stable intermediate boron species. Our first objective was to demonstrate the long-term stability of such strained organoboron derivatives over time, opening the strategy to reagent storage; secondly, we aimed to explore the scope and limitations of the method to complete a large library of new building blocks, being hitherto difficult to access.

Cyclobutene and cyclopentene iodides **1a,b** were readily prepared from procedures originally described by Negishi et. al involving π -cyclization of *gem*-bismetallated alkenes,¹² which we recently applied to the synthesis of alkylidenecyclobutanes and fused four-membered rings.¹³ Halogen-lithium exchanges on **1a** and **1b** were performed employing *n*-BuLi in diethylether at -78 °C (as THF led to further alkylation of the newly formed cycloalkenyllithium) and the corresponding cycloalkenylboronates **A** and **B** were generated by addition of B(O*i*-Pr)₃ in THF (Scheme 1).

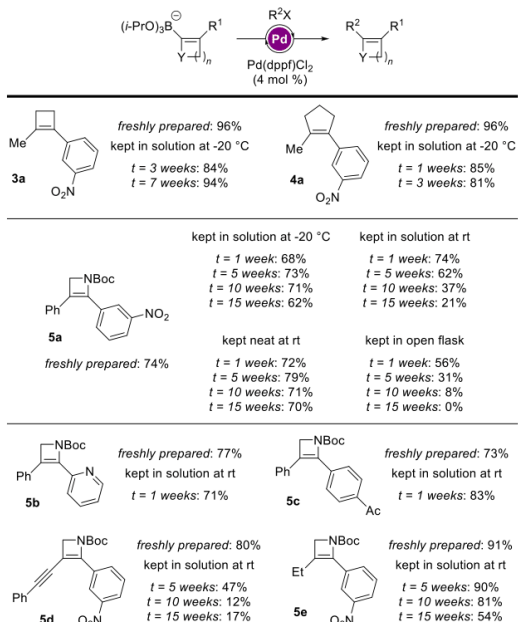


Scheme 1 Organoboronate synthesis through Li/I exchange-transmetalation or α -lithiation-transmetalation

Azetinyl lithium reagents were generated by α -lithiation of in situ formed azetines **2** using *s*-BuLi in the presence of TMEDA in

THF at $-78\text{ }^{\circ}\text{C}$ ¹⁴ and subsequently trapped with boron isopropoxide to give **C**.¹⁵

Organoboronates **A**, **B** and **C** were then stored either in solution or neat at $-20\text{ }^{\circ}\text{C}$ or room temperature before being engaged in Suzuki cross-couplings (Scheme 2).

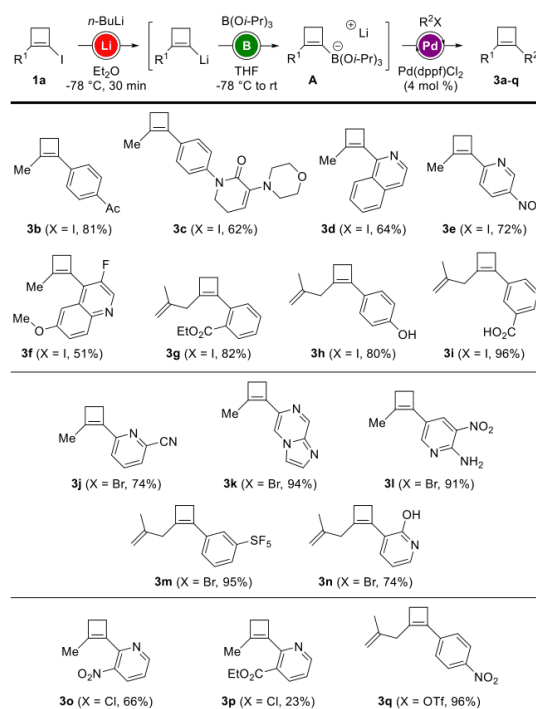


Scheme 2 Stability testing of four- and five-membered carbo- and heterocyclic organoboronates

Cyclobutenyl- and cyclopentenylboronates **A** and **B** were coupled with 1-iodo-3-nitrobenzene as a test partner. From freshly prepared solutions, both products **3a**¹⁶ and **4a** were obtained in excellent yields (96%). Keeping solutions at $-20\text{ }^{\circ}\text{C}$ showed constancy in reactivity, delivering **3a** in 94% yield after seven weeks and **4a** (81%) after three weeks. Diverse conditions were evaluated for storage of azetinyboronates **C**. When kept in an open flask, the yields decreased drastically after only one week of storage, and a fast decrease in reactivity was also observed on storing **C** in solution at room temperature. However, reproducible results were obtained when the boronate salts were kept either in solution at $-20\text{ }^{\circ}\text{C}$ (as for **A** and **B**), or neat at room temperature. Products **5a** were isolated in constant, reasonable yields (up to 70% after fifteen weeks). Stock solutions of azetinyboronate reagents were prepared and further used in cross-coupling reactions after different storage times at room temperature. In some cases (**5b**, **5c** and **5e**), the salts gave reproducible yields after one or ten weeks of storage, showing the great potential of such reagents as building blocks. In some other cases (**5d**), the solution showed a rapid decrease of reactivity, furnishing only a 47% yield of the desired product.

Having established the stability of strained organoboronates, we next investigated the scope of the transformation toward a new library of cyclobutenes. The protocol of Scheme 1 was used to generate in situ the cyclobutenylboronate **A**, which was then engaged directly in cross-coupling reactions in the presence of $\text{Pd}(\text{dppf})\text{Cl}_2 \cdot \text{CH}_2\text{Cl}_2$ (Scheme 3). Aromatic and heteroaromatic iodides bearing ketone, ester, nitro or amide moieties led to the

expected arylcyclobutenes **3b–g** in moderate to good yields (51 to 82%). Interestingly, an unprotected phenol and a benzoic acid furnished the desired products **3h** and **3i** in excellent yields up to 80% and 96%, respectively. Not only iodides, but bromides could be engaged as cross-coupling partners with similar efficacy, furnishing **3j–n** with up to 95% yield and with exceptional functional group tolerance (SF_5 , NH_2 , OH). Alternatively, an aryl triflate gave a similar result (**3q**, 96%) while aryl chlorides showed decreased efficiency (**3o,p**, 23 to 66%).



Scheme 3 In situ preparation and further Suzuki cross-coupling of cyclobutenylboronates

The study was then pursued with five-membered rings, utilizing cyclopentenyl iodides as starting materials¹⁷ in a similar one-pot sequence (Scheme 4). Halogen-lithium exchange on **1b** was followed by transmetalation with $\text{B}(\text{O}i\text{-Pr})_3$ and further palladium-catalyzed cross-coupling with diverse aromatic halides. A comparable functional group tolerance was observed for these larger cycloalkenylboronates, as ketone, nitro, amide and aldehyde moieties could be introduced, giving a wide range of unique functionalized cyclopentenenes **4a–h** in moderate to excellent yields (52 to 96%). When β -styryl iodide was used, the reaction resulted in partial double bond isomerization and **4i** was obtained in 95% yield and 82:18 *E/Z* ratio.

Next, we investigated the iodine/lithium exchange in the presence of boron isopropoxide. Given that the exchange reaction should proceed at higher rate than the nucleophilic addition of *n*-BuLi to the boron atom, the presence of boron species should not perturb the exchange reaction, but rather promote the direct transmetalation of the newly generated lithium species (Scheme 5), as previously exemplified by Li et al.¹⁸ As a result, the undesired alkylation reaction was to be suppressed without

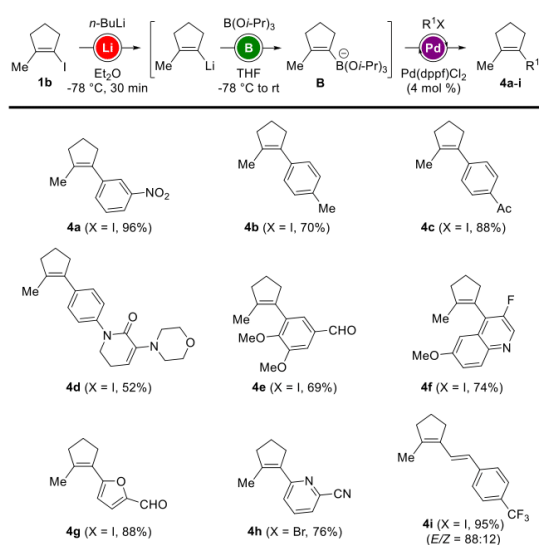
Synthesis

Special Topic

having to use Et₂O, avoiding the previously required mixture of solvents.

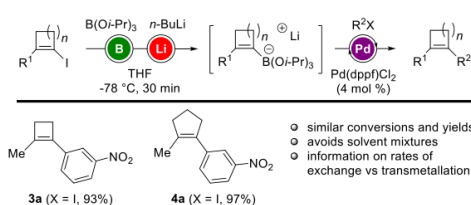
As a proof of concept, the halogen-metal exchange was performed on **1a** and **1b** in the presence of B(O*i*-Pr)₃ at -78 °C, and ultimately engaged in the cross-coupling reaction with a representative partner (1-iodo-3-nitrobenzene). Similar results were collected from this simplified procedure (93 to 96% yield).

Toward a more convenient setup, a step further was then taken by developing conditions that would not require low temperatures for the formation of organoboronates. We envisioned that room temperature metal insertion in the presence of boron alkoxides should lead to the expected intermediate boron species through in situ transmetalation of the transitional cycloalkenylmagnesium species (Scheme 6).



Scheme 4 In situ preparation and further Suzuki cross-coupling of cyclopentenyboronates

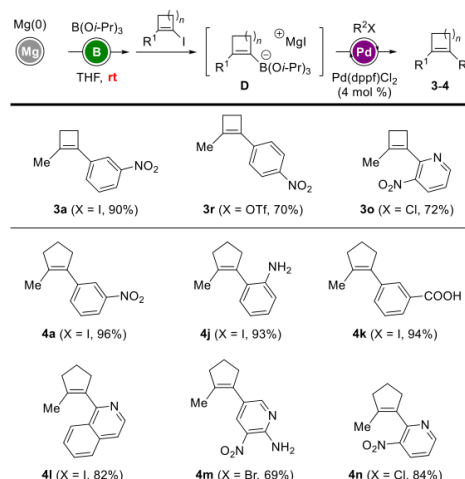
Magnesium powder was then employed, furnishing the intermediary magnesium salt **D**, being an analog of **A** and **B**. Performing the full sequence at room temperature afforded the desired cross-coupling products in excellent yields, comparable to those obtained via the lithium path (up to 96%). The reaction also showed similarly high functional group tolerance, with the ability to introduce unprotected amines (**4j**, **4m**: 69 to 93%) and a carboxylic acid (**4k**, 94%).



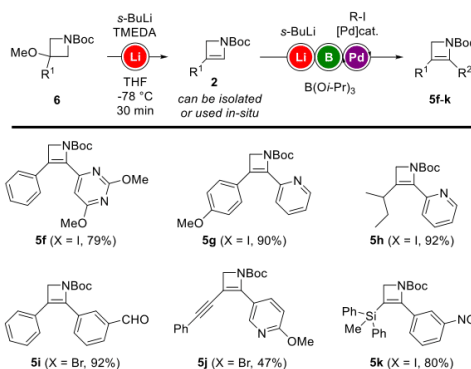
Scheme 5 Iodine-lithium exchange in the presence of B(O*i*-Pr)₃ for direct transmetalation

In addition, we recently demonstrated the potential of in situ generated azetinyboronates to undergo unprecedented cross-coupling, transposing the methodology to heterocyclic four-

membered structures. A one-pot sequence was designed to access the desired boronates through a double α -lithiation of readily available azetidines **6**, followed by trapping with boron isopropoxide and palladium-catalyzed cross-coupling. Representative examples are given in Scheme 7. Alkyl, aryl, alkynyl and silyl groups were introduced at position 3, and the cross-coupling was performed using a large range of functionalized aromatic halides.¹⁵



Scheme 6 Formation of organoboronates through magnesium insertion and in situ transmetalation

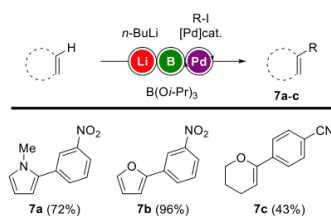


Scheme 7 Single-pot access to 3,4-disubstituted azetidines through lithiation/transmetalation/cross-coupling sequence

Furthermore, we showed the applicability of such strategy to pyrroles, furans and hydroxyranes to open the scope to a larger array of heterocyclic scaffolds. A simple metalation with *n*-BuLi was performed to access the initial organometallic derivatives, before transmetalation with B(O*i*-Pr)₃. Heteroaromatic starting materials furnished the desired cross-coupled compounds **7a**¹⁶ and **7b** in good yields (up to 96%). However, employing hydrofuran resulted in only 43% of the substituted styrene derivative **7c** (Scheme 8).

In conclusion, we have assembled a new efficient one-pot sequence for the synthesis of cyclobutenes, cyclopentenes and azetidines by using in situ prepared boron alkoxides possessing a remarkable functional group tolerance. Diverse conditions were successfully developed relying either on halogen/metal

exchanges or on an advantageous room temperature insertion/transmetalation procedure. Through the intermediate formation of stable organoboronate building blocks, we unlocked a wide library of unexplored strained architectures, opening modern organic chemistry to new classes of modules for further applications.



Scheme 8 Extension to other heterocycles

Commercially available starting materials were used without further purification unless otherwise stated. All reactions were carried out under N_2 atmospheres in flame-dried glassware. Syringes, which were used to transfer anhydrous solvents or reagents, were purged with nitrogen prior to use. CH_2Cl_2 was predried over $CaCl_2$ and distilled from CaH_2 . THF was refluxed and distilled from sodium benzophenone ketyl under nitrogen. Et_2O was predried over $CaCl_2$ and passed through activated Al_2O_3 (using a solvent purification system SPS-400-2 from Innovative Technologies Inc.). Toluene was predried over $CaCl_2$ and distilled from CaH_2 . $n-BuLi$ was purchased from Rockwood Lithium GmbH; [$n-BuLi$] = 2.44 M in hexane (titration with isopropanol / 1,10-phenanthroline)

Chromatography purifications were performed using silica gel (SiO_2 , 0.040-0.063 mm, 230-400 mesh ASTM) from Merck. The spots were visualized under UV (254 nm) or by staining the TLC plate with $KMnO_4$ solution [K_2CO_3 (10 g), $KMnO_4$ (1.5 g), H_2O (150 mL), $NaOH$ (10% in H_2O , 1.25 mL)] or p -anisaldehyde (PAA) solution [concd H_2SO_4 (10 mL), $EtOH$ (200 mL), $AcOH$ (3 mL), p -anisaldehyde (4 mL)]. Melting points were determined on a Büchi B-540 apparatus and are uncorrected. Diastereoisomeric ratios were determined by 1H NMR and ^{13}C NMR spectroscopy. 1H and ^{13}C NMR spectra were recorded on VARIAN Mercury 200, BRUKER ARX 300, VARIAN VXR 400 S and BRUKER AMX 600 instruments. Chemical shifts are reported as δ values in ppm relative to the residual solvent peak (1H NMR) or the solvent peak (^{13}C NMR) in deuterated chloroform ($CDCl_3$: δ 7.26 for 1H NMR and δ 77.16 for ^{13}C NMR). Abbreviations for multiplicities are as follows: s (singlet), d (doublet), t (triplet), q (quartet), quin (quintet), m (multiplet) and br (broad). Reaction endpoints were determined by GC monitoring. Gas chromatography was performed with an Agilent Technologies 7890 instrument, using a column of type HP 5 (Agilent 5% phenylmethylpolysiloxane; length: 15 m; diameter: 0.25 mm; film thickness: 0.25 μm) or Hewlett-Packard 6890 or 5890 series II instruments, using a column of type HP 5 (HewlettPackard, 5% phenylmethylpolysiloxane; length: 15 m; diameter: 0,25 mm; film thickness: 0.25 μm). High-resolution mass spectra (HRMS) and low-resolution mass spectra (LRMS) were recorded on Finnigan MAT 95Q, Finnigan MAT 90 or JEOL JMS-700 instruments. Single crystals (for X-ray analysis) were grown in small quench vials with a volume of 5.0 mL from slow evaporation of dichloromethane/hexanes mixtures at room temperature. Suitable single crystals were then introduced into perfluorinated oil and mounted on top of a thin glass wire. Data collection was performed at 100 K with a Bruker D8 Venture TXS equipped with a Spellman generator (50 kV, 40 mA) and a Kappa CCD detector operating with Mo- $K\alpha$ radiation ($\lambda = 0.71071 \text{ \AA}$).

General Procedure A

To a solution of cycloalkenyliodide (1.00 equiv) in diethyl ether (0.5 M) was slowly added a solution of $n-BuLi$ (2.44 M in hexane, 1.10 equiv) at $-78^\circ C$. After stirring for 30 min at aforementioned temperature, $B(OiPr)_3$ (1.15 equiv) and THF (total concn 0.25 M) were added and the resulting mixture stirred for an additional 1 h at room temperature. $Pd(dppf)Cl_2 \cdot CH_2Cl_2$ (4 mol%), the cross-coupling partner (aromatic or

vinylid iodide, bromide, tosylate or chloride) (0.90 equiv) and an aqueous solution of $NaOH$ (1.5 equiv 1.00 M) were subsequently added and the reaction mixture stirred overnight. The crude material was extracted with Et_2O (3×20 mL), washed with a saturated aqueous solution of sodium chloride (20 mL), dried with magnesium sulfate, filtered, concentrated and purified via flash column chromatography.

General Procedure B

Magnesium powder (1.30 equiv) and $LiCl$ (1.10 equiv) were placed in a reaction tube and flame dried in vacuo three times. After cooling to ambient temperature, enough THF was added to cover the solids. The magnesium was activated by addition of a few drops of dibromoethane and heating. After cooling back to ambient temperature $B(OiPr)_3$ (1.00 equiv) was added. The cycloalkenyliodide was added dropwise as a solution in THF (1.00 equiv, 0.5 M) and the resulting solution stirred for 2 h, after which a grey suspension had formed, which was divided into equimolar portions into new reaction tubes. To the portions was then added $Pd(dppf)Cl_2 \cdot CH_2Cl_2$ (4 mol%), cross-coupling partner (aromatic iodide, bromide, tosylate or chloride) (0.80 equiv) and an aqueous solution of $NaOH$ (1.5 equiv 1.00 M). The reaction mixture stirred overnight and then extracted with Et_2O (3×20 mL), washed with a saturated aqueous solution of sodium chloride (20 mL), dried with magnesium sulfate, filtered, concentrated and purified via flash column chromatography.

1-Iodo-2-methylcyclopent-1-ene (1b)

Commercially available 5-iodopent-1-yne (1.93 g, 10 mmol, 1.0 equiv) was dissolved in 30 mL dry pentane and cooled to $-78^\circ C$. $n-BuLi$ (2.39 M, 10 mmol, 1.0 equiv) was then added dropwise and the reaction mixture was stirred for 30 min before being warmed to $-50^\circ C$ for 5 min. The mixture was then cooled back to $-78^\circ C$ and dimethylaluminum chloride (1 M in CH_2Cl_2 , 10 mmol, 1.0 equiv) was added dropwise and the resulting mixture stirred for a further 30 minutes. The reaction mixture was then allowed to reach room temperature. In another Schlenk flask, zirconocene dichloride (2.93 g, 10 mmol, 1.0 equiv) was dissolved in 25 mL DCM and trimethyl aluminium (2 M, 20 mmol, 2.0 equiv) was added at room temperature and the mixture stirred for 1 h. The first Schlenk flask was then cooled back to $-78^\circ C$ before dropwise addition of the solution from the second Schlenk flask. The combined reaction mixture was allowed to reach room temperature and stirred for 1 h. The solvent was then removed in vacuo and a red solid remained, which was dissolved in THF (50 mL). After 30 minutes, complete conversion into the cyclized pentene was confirmed by GC-MS. The reaction mixture was cooled to $-78^\circ C$ and iodine (5.58 g, 22 mmol, 2.2 equiv) was added portionwise. The mixture was allowed to reach room temperature and then poured into 200 mL of ice-cold 2 M HCl . The layers were separated and the aqueous layer was extracted with hexane (2×100 mL). The combined organics were washed with a saturated sodium thiosulfate solution. The organics were dried over $MgSO_4$, filtered and the solvent evaporated at $20^\circ C$ (60 mbar) due to the volatility of the desired product. Column chromatography in hexane yielded the desired product as a colorless oil, which was stored at $-20^\circ C$ to avoid undesired decomposition.

Yield: 1.48 g (7.09 mmol, 71%); $R_f = 0.79$ (hexane, UV, $KMnO_4$, PAA).

1H NMR (400 MHz, $CDCl_3$): $\delta = 2.74 - 2.54$ (m, 2H), 2.31 (t, $J = 8.5$ Hz, 2H), 2.04 - 1.82 (m, 2H), 1.80 - 1.72 (m, 3H).

Spectroscopic data in agreement with previously reported characterization.¹⁷

1-(2-Methylcyclobut-1-en-1-yl)-3-nitrobenzene (3a)

Using 1-iodo-2-methylcyclobut-1-ene and 1-iodo-3-nitrobenzene according to general procedure A provided **3a** as a yellow solid.

Yield: 49 mg, 0.26 mmol (96%); $R_f = 0.32$ (hexane/ $EtOAc$ 98:2; UV, $KMnO_4$, PAA).

1H NMR (400 MHz, $CDCl_3$): $\delta = 8.09$ (t, $J = 2.0$ Hz, 1H), 8.01 (ddd, $J = 8.1$, 2.4, 1.0 Hz, 1H), 7.60 (dt, $J = 7.7$, 1.4 Hz, 1H), 7.47 (t, $J = 7.9$ Hz, 1H), 2.70 - 2.63 (m, 2H), 2.52 - 2.42 (m, 2H), 2.08 - 1.99 (m, 3H).

Synthesis

Special Topic

¹³C NMR (101 MHz, CDCl₃): δ = 148.6, 143.0, 137.7, 135.7, 131.2, 129.3, 121.0, 120.0, 30.2, 26.3, 16.5.

MS (EI): *m/z* (%) = 189 (11) [M]⁺, 172 (43), 141 (67), 128 (100), 115 (58).

HRMS (EI): *m/z* [M]⁺ calcd for C₁₁H₁₁NO₂: 189.0790; found: 189.0783.

Compound **3a** was also synthesized according to general procedure B.

Yield: 41 mg, 0.22 mmol (90%); mp 115–117 °C.

1-(4-(2-Methylcyclobut-1-en-1-yl)phenyl)ethan-1-one (3b)

Using 1-iodo-2-methylcyclobut-1-ene and 1-(4-iodophenyl)ethan-1-one according to general procedure A provided **3b** as a colorless oil.

Yield: 30 mg, 0.16 mmol (81%); *R*_f = 0.5 (hexane/EtOAc 95:5, UV, KMnO₄, PAA).

¹H NMR (400 MHz, CDCl₃): δ = 7.91 (d, *J* = 8.4 Hz, 2H), 7.37 (d, *J* = 8.4 Hz, 2H), 2.66–2.63 (m, 2H), 2.58 (s, 3H), 2.49–2.44 (m, 2H), 2.05–2.02 (m, 3H).

¹³C NMR (101 MHz, CDCl₃): δ = 197.7, 143.4, 140.7, 137.1, 134.9, 128.7, 125.4, 30.3, 26.7, 26.2, 16.7.

MS (EI): *m/z* (%) = 186 [M]⁺ (30), 171 (20), 143 (80), 128 (100), 115 (40).

HRMS (EI): *m/z* [M]⁺ calcd for C₁₃H₁₄O: 186.1045; found: 186.1037.

1-(4-(2-Methylcyclobut-1-en-1-yl)phenyl)-3-morpholino-5,6-dihydropyridin-2(1H)-one (3c)

Using 1-iodo-2-methylcyclobut-1-ene and 1-(4-iodophenyl)-3-morpholino-5,6-dihydropyridin-2(1H)-one according to general procedure A provided **3c** as a colorless oil.

Yield: 40 mg, 0.12 mmol (62%); *R*_f = 0.2 (hexane/EtOAc 6:4, UV, KMnO₄, PAA).

¹H NMR (400 MHz, CDCl₃): δ = 7.37–7.27 (m, 4H), 5.63 (t, *J* = 4.7 Hz, 1H), 3.84–3.80 (m, 4H), 3.78 (t, *J* = 6.7 Hz, 2H), 2.93–2.86 (m, 4H), 2.64–2.55 (m, 2H), 2.48 (td, *J* = 6.7, 4.6 Hz, 2H), 2.44–2.39 (m, 2H), 2.00–1.94 (m, 3H).

¹³C NMR (101 MHz, CDCl₃): δ = 161.3, 143.8, 140.8, 139.0, 137.0, 134.1, 125.6, 124.7, 114.2, 66.7, 50.5, 48.6, 29.8, 26.1, 23.4, 16.2.

1-(2-Methylcyclobut-1-en-1-yl)isoquinoline (3d)

Using 1-iodo-2-methylcyclobut-1-ene and 1-iodoisoquinoline according to general procedure A provided **3d** as a colorless oil.

Yield: 25 mg, 0.13 mmol (64%); *R*_f = 0.3 (hexane/EtOAc 9:1, UV, KMnO₄, PAA).

¹H NMR (400 MHz, CDCl₃): δ = 8.52 (d, *J* = 5.6 Hz, 1H), 8.30 (d, *J* = 8.5 Hz, 1H), 7.80 (d, *J* = 7.0 Hz, 1H), 7.67–7.63 (m, 1H), 7.56 (ddd, *J* = 8.2, 6.8, 1.3 Hz, 1H), 7.50 (d, *J* = 5.6 Hz, 1H), 3.11–3.06 (m, 2H), 2.63–2.57 (m, 2H), 2.02 (s, 3H).

¹³C NMR (101 MHz, CDCl₃): δ = 155.3, 147.5, 142.5, 137.8, 136.8, 129.9, 127.1, 126.9, 126.7, 126.6, 119.2, 31.1, 29.9, 17.2.

MS (EI): *m/z* (%) = 194 [M – H]⁺ (100), 180 (100), 167 (30), 154 (20).

HRMS (EI): *m/z* [M – H]⁺ calcd for C₁₄H₁₂N: 194.0970; found: 194.0962.

2-(2-Methylcyclobut-1-en-1-yl)-5-nitropyridine (3e)

Using 1-iodo-2-methylcyclobut-1-ene and 2-iodo-5-nitropyridine according to general procedure A provided **3e** as a yellow oil.

Yield: 27 mg, 0.14 mmol (72%); *R*_f = 0.5 (hexane/EtOAc 9:1, UV, KMnO₄, PAA).

¹H NMR (400 MHz, CDCl₃): δ = 9.37 (d, *J* = 2.6 Hz, 1H), 8.39 (dd, *J* = 8.7, 2.7 Hz, 1H), 7.26 (d, *J* = 8.7 Hz, 1H), 2.81–2.70 (m, 2H), 2.59–2.49 (m, 2H), 2.21 (t, *J* = 1.9 Hz, 3H).

¹³C NMR (101 MHz, CDCl₃): δ = 159.2, 153.3, 145.5, 141.5, 136.8, 131.4, 119.6, 31.1, 26.1, 17.2.

MS (EI): *m/z* (%) = 190 [M]⁺ (40), 175 (100), 143 (60), 129 (70).

HRMS (EI): *m/z* [M – H]⁺ calcd for C₁₀H₉N₂O₂: 189.0664; found: 189.0656.

3-Fluoro-6-methoxy-4-(2-methylcyclobut-1-en-1-yl)quinoline (3f)

Using 1-iodo-2-methylcyclobut-1-ene and 3-fluoro-4-iodo-6-methoxyquinoline according to general procedure A provided **3f** as a colorless oil.

Yield: 25 mg, 0.10 mmol (51%); *R*_f = 0.3 (hexane/EtOAc 9:1, UV, KMnO₄, PAA).

¹H NMR (400 MHz, CDCl₃): δ = 8.60 (d, *J* = 1.7 Hz, 1H), 7.97 (d, *J* = 9.1 Hz, 1H), 7.30 (dd, *J* = 9.1, 2.8 Hz, 1H), 7.26 (d, *J* = 4.1 Hz, 1H), 3.92 (s, 3H), 2.98–2.89 (m, 2H), 2.72–2.58 (m, 2H), 1.84 (d, *J* = 1.3 Hz, 3H).

¹³C NMR (101 MHz, CDCl₃): δ = 158.6, 154.0 (d, *J* = 254.5 Hz), 148.4, 141.8 (d, *J* = 2.3 Hz), 138.6 (d, *J* = 29.3 Hz), 131.4, 130.2, 128.3 (d, *J* = 3.4 Hz), 124.8 (d, *J* = 12.7 Hz), 120.8 (d, *J* = 2.7 Hz), 103.9 (d, *J* = 5.4 Hz), 103.8, 55.6, 32.0, 30.5 (d, *J* = 2.8 Hz), 17.4 (d, *J* = 2.1 Hz).

MS (EI): *m/z* (%) = 243 [M]⁺ (90), 228 (70), 212 (100), 200 (30).

HRMS (EI): *m/z* [M]⁺ calcd for C₁₅H₁₄FNO: 243.1059; found: 243.1053.

Ethyl 2-(2-(2-methylallyl)cyclobut-1-en-1-yl)benzoate (3g)

Using 1-iodo-2-(2-methylallyl)cyclobut-1-ene and ethyl 2-iodobenzoate according to general procedure A provided **3g** as a colorless oil.

Yield: 42 mg, 0.16 mmol (82%*), *with minor impurities due to the starting material (aryl-I); *R*_f = 0.6 (hexane/EtOAc 9:1, UV, KMnO₄, PAA).

¹H NMR (400 MHz, CDCl₃): δ = 7.67 (d, *J* = 7.6 Hz, 1H), 7.39 (t, *J* = 8.1 Hz, 1H), 7.31–7.19 (m, 2H), 4.74 (d, *J* = 6.8 Hz, 2H), 4.31 (q, *J* = 7.1 Hz, 2H), 2.85 (s, 2H), 2.68–2.61 (m, 2H), 2.46–2.36 (m, 2H), 1.68 (s, 3H), 1.34 (t, *J* = 7.1 Hz, 3H).

¹³C NMR (101 MHz, CDCl₃): δ = 168.6, 142.9, 141.9, 140.2, 136.1, 131.1, 130.3, 129.6, 129.4, 126.7, 111.6, 61.3, 38.2, 29.2, 28.7, 23.0, 14.4.

MS (EI): *m/z* (%) = 256 [M]⁺ (10) 241 (5), 227 (5), 209 (30), 195 (100), 181 (20).

HRMS (EI): *m/z* [M]⁺ calcd for C₁₇H₂₀O₂: 256.1463; found: 256.1458.

4-(2-(2-Methylallyl)cyclobut-1-en-1-yl)phenol (3h)

Using 1-iodo-2-(2-methylallyl)cyclobut-1-ene and 4-iodophenol according to general procedure A provided **3h** as a colorless oil.

Yield: 32 mg, 0.16 mmol (80%); *R*_f = 0.3 (hexane/EtOAc 8:2, UV, KMnO₄, PAA).

¹H NMR (400 MHz, CDCl₃): δ = 7.25–7.21 (m, 2H), 6.83–6.76 (m, 2H), 4.81 (d, *J* = 5.6 Hz, 3H), 3.04 (s, 2H), 2.64–2.59 (m, 2H), 2.47–2.40 (m, 2H), 1.78 (s, 3H).

¹³C NMR (101 MHz, CDCl₃): δ = 154.4, 142.9, 138.6, 137.7, 129.4, 127.2, 115.3, 111.5, 39.0, 28.3, 26.2, 23.1.

MS (EI): *m/z* (%) = 200 [M]⁺ (30), 185 (80), 171 (20), 158 (100), 144 (30).

HRMS (EI): *m/z* [M]⁺ calcd for C₁₄H₁₆O: 200.1201; found: 200.1195.

3-(2-(2-Methylallyl)cyclobut-1-en-1-yl)benzoic acid (3i)

Using 1-iodo-2-(2-methylallyl)cyclobut-1-ene and 3-iodobenzoic acid according to general procedure A provided **3i** as a colorless oil.

Yield: 44 mg, 0.19 mmol (96%); *R*_f = 0.3 (hexane/EtOAc 95:5, UV, KMnO₄, PAA).

¹H NMR (400 MHz, CDCl₃): δ = 8.07 (s, 1H), 7.95 (d, *J* = 7.7 Hz, 1H), 7.57 (d, *J* = 7.7 Hz, 1H), 7.43 (t, *J* = 7.7 Hz, 1H), 4.84 (s, 2H), 3.13 (s, 2H), 2.73–2.67 (m, 2H), 2.53–2.46 (m, 2H), 1.80 (s, 3H).

¹³C NMR (101 MHz, CDCl₃): δ = 172.3, 142.4, 142.2, 138.2, 136.4, 129.5, 128.7, 128.3, 127.4, 111.9, 39.1, 28.6, 26.2, 23.1.

MS (EI): *m/z* (%) = 228 [M]⁺ (5), 212 (10), 183 (100), 167 (20), 155 (50).

HRMS (EI): *m/z* [M]⁺ calcd for C₁₅H₁₆O₂: 228.1150; found: 228.1143.

6-(2-Methylcyclobut-1-en-1-yl)picolinonitrile (3j)

Using 1-iodo-2-methylcyclobut-1-ene and 6-bromopicolinonitrile according to general procedure A provided **3j** as a colorless oil.

Yield: 25 mg, 0.15 mmol (74%); R_f = 0.5 (hexane/EtOAc 8:2, UV, KMnO₄, PAA).

¹H NMR (400 MHz, CDCl₃): δ = 7.72 (t, J = 7.8 Hz, 1H), 7.44 (d, J = 7.6 Hz, 1H), 7.31 (d, J = 8.1 Hz, 1H), 2.73 – 2.63 (m, 2H), 2.53 – 2.44 (m, 2H), 2.16 (s, 3H).

¹³C NMR (101 MHz, CDCl₃): δ = 155.9, 149.6, 137.0, 136.2, 133.6, 125.4, 123.0, 117.8, 30.6, 26.0, 16.8.

MS (EI): m/z (%) = 170 [M]⁺ (20), 155 (100), 142 (10), 129 (10), 115 (10).

HRMS (EI): m/z [M]⁺ calcd for C₁₁H₁₀N₂: 170.0844; found: 170.0843.

6-(2-Methylcyclobut-1-en-1-yl)imidazo[1,2-*a*]pyrazine (3k)

Using 1-iodo-2-methylcyclobut-1-ene and 6-bromoimidazo[1,2-*a*]pyrazine according to general procedure A provided **3k** as a yellowish oil.

Yield: 35 mg, 0.19 mmol (94%); R_f = 0.1 (hexane/EtOAc 5:5, UV, KMnO₄, PAA).

¹H NMR (400 MHz, CDCl₃): δ = 9.06 (s, 1H), 7.85 (s, 1H), 7.75 (s, 1H), 7.63 (s, 1H), 2.72 – 2.61 (m, 2H), 2.55 – 2.43 (m, 2H), 2.15 (s, 3H).

¹³C NMR (101 MHz, CDCl₃): δ = 144.5, 143.3, 139.8, 137.5, 135.7, 133.7, 114.1, 113.7, 30.5, 25.7, 16.5.

MS (EI): m/z (%) = 185 [M]⁺ (70), 184 (100), 170 (100), 157 (5), 144 (5).

HRMS (EI): m/z [M]⁺ calcd for C₁₁H₁₀N₃: 184.0875; found: 184.0869.

5-(2-Methylcyclobut-1-en-1-yl)-3-nitropyridin-2-amine (3l)

Using 1-iodo-2-methylcyclobut-1-ene and 5-bromo-3-nitropyridin-2-amine according to general procedure A provided **3l** as a yellow oil.

Yield: 37 mg, 0.18 mmol (91%); R_f = 0.1 (hexane/EtOAc 8:2, UV, KMnO₄, PAA).

¹H NMR (400 MHz, CDCl₃): δ = 8.40 (d, J = 2.2 Hz, 1H), 8.25 (d, J = 2.1 Hz, 1H), 6.69 (s, 2H), 2.66 – 2.56 (m, 2H), 2.50 – 2.40 (m, 2H), 1.99 (s, 3H).

¹³C NMR (101 MHz, CDCl₃): δ = 153.3, 151.7, 140.2, 132.8, 130.5, 128.0, 123.7, 30.4, 26.1, 16.5.

MS (EI): m/z (%) = 205 [M]⁺ (100), 190 (90), 176 (40), 157 (60), 144 (60).

HRMS (EI): m/z [M]⁺ calcd for C₁₀H₁₁N₃O₂: 205.0851; found: 205.0840.

Pentafluoro(3-(2-(2-methylallyl)cyclobut-1-en-1-yl)phenyl)- λ^6 -sulfane (3m)

Using 1-iodo-2-(2-methylallyl)cyclobut-1-ene and (3-bromophenyl)pentafluoro- λ^6 -sulfane according to general procedure A provided **3m** as a colorless oil.

Yield: 59 mg, 0.19 mmol (95%); R_f = 0.6 (hexane, UV, KMnO₄, PAA).

¹H NMR (400 MHz, CDCl₃): δ = 7.68 (s, 1H), 7.59 – 7.53 (m, 1H), 7.45 – 7.36 (m, 2H), 4.83 (d, J = 9.7 Hz, 2H), 3.08 (s, 2H), 2.73 – 2.63 (m, 2H), 2.52 – 2.44 (m, 2H), 1.78 (s, 3H).

¹³C NMR (101 MHz, CDCl₃): δ = 154.3, 143.4, 142.0, 137.7, 136.8, 128.8, 128.5, 123.9, 123.3, 112.1, 39.1, 28.9, 26.2, 23.0.

MS (EI): m/z (%) = 310 [M]⁺ (60), 295 (60), 282 (10), 269 (5), 253 (5).

HRMS (EI): m/z [M]⁺ calcd for C₁₄H₁₅F₅S: 310.0815; found: 310.0807.

3-(2-(2-Methylallyl)cyclobut-1-en-1-yl)pyridin-2-ol (3n)

Using 1-iodo-2-(2-methylallyl)cyclobut-1-ene and 3-bromopyridin-2-ol according to general procedure A provided **3n** as a colorless oil.

Yield: 30 mg, 0.15 mmol (74%); R_f = 0.1 (hexane/EtOAc 7:3, UV, KMnO₄, PAA).

¹H NMR (400 MHz, CDCl₃): δ = 7.31 (dd, J = 7.0, 2.0 Hz, 1H), 7.21 (dd, J = 6.5, 2.0 Hz, 1H), 6.25 (t, J = 6.7 Hz, 1H), 4.79 – 4.74 (m, 2H), 3.29 (s, 2H), 2.68 – 2.63 (m, 2H), 2.45 – 2.39 (m, 2H), 1.75 (s, 3H).

¹³C NMR (101 MHz, CDCl₃): δ = 162.8, 144.5, 143.9, 137.0, 135.0, 132.4, 127.7, 111.2, 106.8, 40.3, 28.5, 26.9, 23.1.

MS (EI): m/z (%) = 201 [M]⁺ (100) 186 (50), 167 (30), 134 (30).

HRMS (EI): m/z [M]⁺ calcd for C₁₃H₁₅NO: 201.1154; found: 201.1149.

2-(2-Methylcyclobut-1-en-1-yl)-3-nitropyridine (3o)

Using 1-iodo-2-methylcyclobut-1-ene and 2-chloro-3-nitropyridine according to general procedure A provided **3o** as a yellowish oil.

Yield: 25 mg, 0.13 mmol (66%).

Compound **3o** was also synthesized according to general procedure B.

Yield: 32 mg, 0.17 mmol (72%); R_f = 0.6 (hexane/EtOAc 8:2, UV, KMnO₄, PAA).

¹H NMR (400 MHz, CDCl₃): δ = 8.72 (dd, J = 4.7, 1.6 Hz, 1H), 7.92 (dd, J = 8.1, 1.6 Hz, 1H), 7.21 (dd, J = 8.2, 4.7 Hz, 1H), 2.72 – 2.61 (m, 2H), 2.55 – 2.46 (m, 2H), 2.10 (s, 3H).

¹³C NMR (101 MHz, CDCl₃): δ = 153.6, 151.9, 147.2, 144.4, 133.6, 131.4, 120.8, 31.6, 27.5, 17.2.

MS (EI): m/z (%) = 172 (5), 160 (950), 145 (30), 130 (90), 117 (100).

HRMS (EI): m/z [M]⁺ calcd for C₁₀H₉N₂O₂: 189.0664; found: 189.0657.

Ethyl 2-(2-methylcyclobut-1-en-1-yl)nicotinate (3p)

Using 1-iodo-2-methylcyclobut-1-ene and ethyl 2-chloronicotinate according to general procedure A provided **3p** as a yellowish oil.

Yield: 10 mg, 0.05 mmol (23%); R_f = 0.6 (hexane/EtOAc 8:2, UV, KMnO₄, PAA).

¹H NMR (400 MHz, CDCl₃): δ = 8.65 (dd, J = 4.8, 1.8 Hz, 1H), 7.87 (dd, J = 7.8, 1.8 Hz, 1H), 7.13 (dd, J = 7.8, 4.8 Hz, 1H), 4.36 (q, J = 7.2 Hz, 2H), 2.76 – 2.71 (m, 2H), 2.48 – 2.42 (m, 2H), 2.01 (s, 3H), 1.38 (t, J = 7.2 Hz, 3H).

¹³C NMR (101 MHz, CDCl₃): δ = 168.0, 152.9, 151.1, 148.6, 137.0, 136.9, 126.0, 120.4, 61.8, 30.8, 28.3, 16.7, 14.4.

MS (EI): m/z (%) = 217 [M]⁺ (10), 187 (100), 174 (15).

HRMS (EI): m/z [M]⁺ calcd for C₁₃H₁₅NO₂: 217.1103; found: 217.1099.

1-(2-(2-Methylallyl)cyclobut-1-en-1-yl)-4-nitrobenzene (3q)

Using 1-iodo-2-(2-methylallyl)cyclobut-1-ene and 4-nitrophenyl trifluoromethanesulfonate according to general procedure A provided **3q** as a colorless oil.

Yield: 44 mg, 0.19 mmol (96%); R_f = 0.7 (hexane/EtOAc 9:1, UV, KMnO₄, PAA).

¹H NMR (400 MHz, CDCl₃): δ = 8.17 (d, J = 8.8 Hz, 2H), 7.42 (d, J = 8.8 Hz, 2H), 4.83 (d, J = 16.7 Hz, 2H), 3.12 (s, 2H), 2.84 – 2.61 (m, 2H), 2.58 – 2.41 (m, 2H), 1.79 (s, 3H).

¹³C NMR (101 MHz, CDCl₃): δ = 146.9, 146.0, 141.9, 141.6, 137.8, 126.1, 124.0, 112.2, 39.3, 29.1, 26.1, 23.1.

MS (EI): m/z (%) = 229 [M]⁺ (2), 212 (90), 182 (100), 168 (50), 153 (50).

HRMS (EI): m/z [M]⁺ calcd for C₁₄H₁₅NO₂: 229.1103; found: 229.1102.

1-(2-Methylcyclobut-1-en-1-yl)-4-nitrobenzene (3r)

Using 1-iodo-2-methylcyclobut-1-ene and 4-nitrophenyl trifluoromethanesulfonate according to general procedure B provided **3r** as a yellow oil.

Yield: 32 mg, 0.17 mmol (70%); R_f = 0.29 (hexane/EtOAc 98:2, UV, KMnO₄, PAA).

¹H NMR (400 MHz, CDCl₃): δ = 8.19 – 8.09 (m, 1H), 7.46 – 7.28 (m, 1H), 2.76 – 2.57 (m, 1H), 2.57 – 2.40 (m, 1H), 2.15 – 1.96 (m, 2H).

¹³C NMR (101 MHz, CDCl₃): δ = 145.9, 145.8, 142.3, 136.3, 125.7, 124.0, 30.6, 26.2, 16.7.

MS (EI): m/z (%) = 189 (23), 172 (34), 143 (63), 128 (100), 115 (50), 102 (14).

HRMS (EI): m/z [M]⁺ calcd for C₁₁H₁₁NO₂: 189.0790; found: 189.0783.

1-(2-Methylcyclopent-1-en-1-yl)-3-nitrobenzene (4a)

Using 1-iodo-methylcyclopent-1-ene and 1-iodo-3-nitrobenzene according to general procedure A provided **4a** as a light yellow oil.

Yield: 39 mg, 0.19 mmol (96%); $R_f = 0.2$ (hexane/EtOAc 99:1, UV, KMnO₄, PAA).

¹H NMR (400 MHz, CDCl₃): $\delta = 8.13$ (t, $J = 1.9$ Hz, 1H), 8.04 (dd, $J = 9.1, 2.1$ Hz, 1H), 7.59 (d, $J = 7.8$ Hz, 1H), 7.48 (t, $J = 7.9$ Hz, 1H), 2.80 – 2.72 (m, 2H), 2.54 (t, $J = 7.9$ Hz, 2H), 1.94 (quin, $J = 7.5$ Hz, 2H), 1.88 (s, 3H).

¹³C NMR (101 MHz, CDCl₃): $\delta = 148.3, 140.5, 138.7, 133.7, 133.0, 129.0, 122.4, 120.9, 40.4, 37.2, 21.9, 15.6$.

MS (EI): m/z (%) = 203 [M]⁺ (80), 188 (100), 156 (20), 141 (78), 128 (58), 115 (81).

HRMS (EI): m/z [M]⁺ calcd for C₁₂H₁₃NO₂: 203.0946; found: 203.0939.

Compound **4a** was also synthesized according to general procedure B.

Yield: 39 mg, 0.19 mmol (96%).

1-Methyl-4-(2-methylcyclopent-1-en-1-yl)benzene (4b)

Using 1-iodo-2-methylcyclopent-1-ene and 1-iodo-4-methylbenzene according to general procedure A provided **4b** as a colorless oil.

Yield: 24 mg, 0.14 mmol (70%); $R_f = 0.7$ (hexane, UV, KMnO₄, PAA).

¹H NMR (400 MHz, CDCl₃): $\delta = 7.44 - 7.29$ (m, 4H), 2.95 – 2.86 (m, 2H), 2.73 – 2.60 (m, 2H), 2.52 (s, 3H), 2.07 (t, $J = 7.5$ Hz, 2H), 2.05 – 1.99 (m, 3H).

¹³C NMR (101 MHz, CDCl₃): $\delta = 135.9, 135.7, 134.7, 134.6, 128.8, 127.6, 40.2, 37.4, 22.0, 21.3, 15.6$.

MS (EI): m/z (%) = 172 [M]⁺ (70), 157 (100), 142 (40), 129 (40), 115 (30).

HRMS (EI): m/z [M]⁺ calcd for C₁₃H₁₆: 172.1252; found: 172.1245.

1-(4-(2-Methylcyclopent-1-en-1-yl)phenyl)ethan-1-one (4c)

Using 1-iodo-methylcyclopent-1-ene and 1-(4-iodophenyl)ethan-1-one according to general procedure A provided **4c** as a colorless oil.

Yield: 35 mg, 0.18 mmol (88%); $R_f = 0.3$ (hexane/EtOAc 95:5, UV, KMnO₄, PAA).

¹H NMR (400 MHz, CDCl₃): $\delta = 7.93$ (d, $J = 8.4$ Hz, 2H), 7.37 (d, $J = 8.4$ Hz, 2H), 2.80 – 2.71 (m, 2H), 2.60 (s, 3H), 2.53 (t, $J = 7.1$ Hz, 2H), 1.97 – 1.90 (m, 2H), 1.88 (s, 3H).

¹³C NMR (101 MHz, CDCl₃): $\delta = 197.9, 143.9, 138.5, 134.8, 134.2, 128.3, 127.7, 40.5, 37.1, 26.7, 22.0, 15.9$.

MS (EI): m/z (%) = 200 [M]⁺ (57), 185 (100), 157 (22), 142 (25), 128 (32).

HRMS (EI): m/z [M – H]⁺ calcd for C₁₄H₁₆O: 200.1201; found: 200.1195.

1-(4-(2-Methylcyclopent-1-en-1-yl)phenyl)-3-morpholino-5,6-dihydropyridin-2(1H)-one (4d)

Using 1-iodo-methylcyclopent-1-ene and 1-(4-iodophenyl)-3-morpholino-5,6-dihydropyridin-2(1H)-one according to general procedure A provided **4d** as a light yellow sticky oil.

Yield: 35 mg, 0.10 mmol (52%); $R_f = 0.3$ (hexane/EtOAc 1:1, UV, KMnO₄, PAA).

¹H NMR (400 MHz, CDCl₃): $\delta = 7.35 - 7.25$ (m, 4H), 5.63 (t, $J = 4.7$ Hz, 1H), 3.84 – 3.76 (m, 6H), 2.91 (t, $J = 4.4$ Hz, 4H), 2.75 – 2.66 (m, 2H), 2.53 – 2.43 (m, 4H), 1.95 – 1.84 (m, 2H), 1.84 (s, 3H).

¹³C NMR (101 MHz, CDCl₃): $\delta = 161.5, 143.9, 140.6, 136.6, 135.6, 134.3, 128.0, 124.5, 114.2, 66.9, 50.6, 48.7, 40.2, 37.3, 23.5, 21.9, 15.6$.

MS (EI): m/z (%) = 338 [M]⁺ (14), 320 (100), 307 (20), 281 (35), 253 (34), 239 (31), 207 (55).

HRMS (EI): m/z [M]⁺ calcd for C₂₁H₂₆N₂O₂: 338.1994; found: 338.1988.

3,4-Dimethoxy-5-(2-methylcyclopent-1-en-1-yl)benzaldehyde (4e)

Using 1-iodo-methylcyclopent-1-ene and 3-iodo-4,5-dimethoxybenzaldehyde according to general procedure A provided **4e** as a colorless oil.

Yield: 34 mg, 0.14 mmol (69%); $R_f = 0.35$ (hexane/EtOAc 9:1, UV, KMnO₄, PAA).

¹H NMR (400 MHz, CDCl₃): $\delta = 9.87$ (s, 1H), 7.34 (d, $J = 1.9$ Hz, 1H), 7.24 (d, $J = 1.9$ Hz, 1H), 3.92 (s, 3H), 3.79 (s, 3H), 2.76 – 2.61 (m, 2H), 2.47 (t, $J = 7.0$ Hz, 2H), 1.95 (quin, $J = 7.5$ Hz, 2H), 1.65 (s, 3H).

¹³C NMR (101 MHz, CDCl₃): $\delta = 191.6, 153.6, 152.7, 138.0, 133.6, 132.1, 132.1, 127.6, 108.7, 60.8, 56.1, 38.9, 37.8, 22.7, 15.4$.

MS (EI): m/z (%) = 246 [M]⁺ (100), 231 (27), 217 (18), 203 (18), 189 (24), 161 (26), 115 (35).

HRMS (EI): m/z [M]⁺ calcd for C₁₅H₁₈O₃: 246.1256; found: 246.1250.

3-Fluoro-6-methoxy-4-(2-methylcyclopent-1-en-1-yl)quinoline (4f)

Using 1-iodo-methylcyclopent-1-ene and 3-fluoro-4-iodo-6-methoxyquinoline according to general procedure A provided **4f** as a colorless oil.

Yield: 38 mg (0.15 mmol, 74%); $R_f = 0.3$ (hexane/EtOAc 9:1, UV, KMnO₄, PAA).

¹H NMR (400 MHz, CDCl₃): $\delta = 8.62$ (d, $J = 9.2$ Hz, 1H), 8.00 (d, $J = 9.2$ Hz, 1H), 7.31 (dd, $J = 9.2, 2.8$ Hz, 1H), 6.99 (d, $J = 2.8$ Hz, 1H), 3.89 (s, 3H), 2.86 – 2.74 (m, 1H), 2.71 – 2.66 (m, 1H), 2.62 (t, $J = 7.3$ Hz, 2H), 2.20 – 1.99 (m, 2H), 1.56 (s, 3H).

¹³C NMR (101 MHz, CDCl₃): $\delta = 158.9, 154.3$ (d, $J = 252.4$ Hz), 142.0, 141.9, 138.9 (d, $J = 29.3$ Hz), 131.7, 129.4 (d, $J = 3.6$ Hz), 128.8 (d, $J = 14.4$ Hz), 126.7, 120.8 (d, $J = 3.2$ Hz), 104.1 (d, $J = 5.9$ Hz), 55.9, 39.2, 37.8 (d, $J = 2.1$ Hz), 23.5, 15.9.

MS (EI): m/z (%) = 257 [M]⁺ (100), 242 (25), 226 (20), 214 (40), 198 (22), 184 (36), 172 (20).

HRMS (EI): m/z [M]⁺ calcd for C₁₆H₁₆FNO: 257.1216; found: 257.1210.

5-(2-methylcyclopent-1-en-1-yl)furan-2-carbaldehyde (4g)

Using 1-iodo-methylcyclopent-1-ene and 5-iodofuran-2-carbaldehyde according to general procedure A provided **4g** as a crystalline solid.

Yield: 31 mg, 0.18 mmol (88%); mp 93–97 °C; $R_f = 0.2$ (hexane/EtOAc 98:2, UV, KMnO₄, PAA).

¹H NMR (400 MHz, CDCl₃): $\delta = 9.56$ (s, 1H), 7.23 (d, $J = 3.7$ Hz, 1H), 6.34 (d, $J = 3.7$ Hz, 1H), 2.80 – 2.65 (m, 2H), 2.60 – 2.48 (m, 2H), 2.12 (quin, $J = 1.6$ Hz, 3H), 1.93 (quin, $J = 7.6$ Hz, 2H).

¹³C NMR (101 MHz, CDCl₃): $\delta = 177.0, 159.1, 151.2, 144.1, 124.1, 123.4, 109.4, 40.9, 34.4, 22.1, 16.4$.

MS (EI): m/z (%) = 176 [M]⁺ (100), 161 (50), 147 (78), 129 (21), 119 (46), 105 (22).

HRMS (EI): m/z [M]⁺ calcd for C₁₁H₁₂O₂: 176.0837; found: 176.0831.

6-(2-Methylcyclopent-1-en-1-yl)picolinonitrile (4h)

Using 1-iodo-methylcyclopent-1-ene and 6-bromopicolinonitrile according to general procedure A provided **4h** as a colorless oil.

Yield: 28 mg, 0.15 mmol (76%); $R_f = 0.3$ (hexane/EtOAc 95:5, UV, KMnO₄, PAA).

¹H NMR (400 MHz, CDCl₃): $\delta = 7.74$ = (t, $J = 7.9$ Hz, 1H), 7.46 (d, $J = 7.6$ Hz, 1H), 7.41 (d, $J = 8.1$ Hz, 1H), 2.85 – 2.76 (m, 2H), 2.58 (t, $J = 7.4$ Hz, 2H), 2.10 (s, 3H), 1.92 (quin, $J = 7.6$ Hz, 2H).

¹³C NMR (101 MHz, CDCl₃): $\delta = 158.8, 145.2, 136.9, 133.1, 132.4, 125.2, 125.1, 117.8, 41.3, 35.8, 21.7, 16.4$.

MS (EI): m/z (%) = 184 [M]⁺ (70), 169 (100), 155 (46), 142 (36), 129 (13), 118 (12), 103 (17).

HRMS (EI): m/z [M]⁺ calcd for C₁₂H₁₂N₂: 184.1000; found: 184.0994.

(E)-1-[2-(2-Methylcyclopent-1-en-1-yl)vinyl]-4-(trifluoromethyl)benzene (4i)

Using 1-iodo-methylcyclopent-1-ene and (*Z*)-1-(2-iodovinyl)-4-(trifluoromethyl)benzene according to general procedure A provided **4i** (*E/Z* = 88:12 by crude GC, isolated *E/Z* = 56:44) as a colorless oil.

Yield: 48 mg, 0.19 mmol (95%); *R*_f = 0.56/0.68 (hexane, UV, KMnO₄, PAA).

¹H NMR (400 MHz, CDCl₃): δ = 7.59 – 7.46 (m, 3H), 7.37 – 7.30 (m, 1H), 6.46 – 6.33 (m, 2H), 2.36 – 2.28 (m, 2H), 2.22 – 2.11 (m, 2H), 1.75 (quin, *J* = 7.4 Hz, 2H), 1.67 (s, 3H).

¹³C NMR (101 MHz, CDCl₃): δ = 142.6 (*d*, *J* = 1.6 Hz), 142.3, 133.8, 129.2, 128.7 (*d*, *J* = 5.0 Hz), 128.0, 125.9, 124.7 (*q*, *J* = 3.8 Hz), 123.1 (*d*, *J* = 1.5 Hz), 38.6, 35.8, 22.8, 15.1.

MS (EI): *m/z* (%) = 252 [M]⁺ (91), 237 (100), 209 (75), 183 (53), 159 (35), 141 (34), 115 (22).

HRMS (EI): *m/z* [M]⁺ calcd for C₁₅H₁₅F₃: 252.1126; found: 252.1119.

2-(2-Methylcyclopent-1-en-1-yl)aniline (4j)

Using 1-iodo-methylcyclopent-1-ene and 2-iodoaniline according to general procedure B provided **4j** as a light yellow oil.

Yield: 32 mg, 0.19 mmol (93%); *R*_f = 0.2 (hexane/EtOAc 95:5, UV, KMnO₄, PAA).

¹H NMR (400 MHz, CDCl₃): δ = 7.07 (td, *J* = 7.8, 1.5 Hz, 1H), 6.98 (dd, *J* = 7.5, 1.4 Hz, 1H), 6.79 – 6.69 (m, 2H), 3.66 (s, 2H), 2.68 – 2.57 (m, 2H), 2.48 (t, *J* = 7.3 Hz, 2H), 1.96 (quin, *J* = 7.5 Hz, 2H), 1.61 (s, 3H).

¹³C NMR (101 MHz, CDCl₃): δ = 143.6, 136.9, 133.4, 129.3, 127.7, 124.9, 118.2, 115.2, 38.8, 37.9, 22.6, 15.2.

MS (EI): *m/z* (%) = 173 [M]⁺ (67), 158 (22), 144 (100), 130 (53), 117 (22), 77 (20).

HRMS (EI): *m/z* [M]⁺ calcd for C₁₂H₁₅N: 173.1204; found: 173.1198.

3-(2-Methylcyclopent-1-en-1-yl)benzoic acid (4k)

Using 1-iodo-methylcyclopent-1-ene and 3-iodobenzoic acid according to general procedure B provided **4k** as a light brown solid.

Yield: 38 mg, 0.19 mmol (94%); mp 116–120 °C; *R*_f = 0.4 (hexane/1% MeOH, UV, KMnO₄, PAA).

¹H NMR (400 MHz, CDCl₃): δ = 11.39 (s, 1H), 8.01 (s, 1H), 7.91 (*d*, *J* = 7.6 Hz, 1H), 7.47 (*d*, *J* = 7.4 Hz, 1H), 7.36 (t, *J* = 7.3 Hz, 1H), 2.72 (s, 2H), 2.49 (s, 2H), 1.90 (quin, *J* = 7.2 Hz, 2H), 1.83 (s, 3H).

¹³C NMR (101 MHz, CDCl₃): δ = 172.8, 139.1, 136.7, 134.1, 132.7, 129.9, 129.4, 128.2, 127.9, 40.3, 37.3, 22.0, 15.6.

MS (EI): *m/z* (%) = 202 [M]⁺ (100), 187 (81), 157 (52), 128 (77), 115 (67), 77 (28).

HRMS (EI): *m/z* [M]⁺ calcd for C₁₃H₁₄O₂: 202.0994; found: 202.0989.

1-(2-Methylcyclopent-1-en-1-yl)isoquinoline (4l)

Using 1-iodo-methylcyclopent-1-ene and 1-iodoisoquinoline according to general procedure B provided **4l** as a light yellow oil.

Yield: 34 mg, 0.16 mmol (82%); *R*_f = 0.2 (hexane/EtOAc 9:1, UV, KMnO₄, PAA).

¹H NMR (400 MHz, CDCl₃): δ = 8.53 (*d*, *J* = 5.7 Hz, 1H), 7.97 (*d*, *J* = 8.4 Hz, 1H), 7.82 (*d*, *J* = 8.2 Hz, 1H), 7.70 – 7.62 (m, 1H), 7.57 – 7.51 (m, 2H), 2.97 – 2.82 (m, 2H), 2.62 (t, *J* = 7.1 Hz, 2H), 2.09 (quin, *J* = 7.5 Hz, 2H), 1.55 (s, 3H).

¹³C NMR (101 MHz, CDCl₃): δ = 160.2, 142.5, 139.9, 136.5, 134.5, 130.1, 127.5, 127.1, 127.0, 126.9, 119.3, 39.4, 38.6, 22.9, 15.6.

MS (EI): *m/z* (%) = 208 [M-H]⁺ (100), 191 (11), 180 (40), 167 (15).

HRMS (EI): *m/z* [M-H]⁺ calcd for C₁₅H₁₄N: 208.1126; found: 208.1120.

5-(2-Methylcyclopent-1-en-1-yl)-3-nitropyridin-2-amine (4m)

Using 1-iodo-methylcyclopent-1-ene and 5-bromo-3-nitropyridin-2-amine according to general procedure B provided **4m** as a yellow solid.

Yield: 30 mg, 0.14 mmol (69%); mp 177–180 °C; *R*_f = 0.2 (hexane/EtOAc 9:1, UV, KMnO₄, PAA).

¹H NMR (400 MHz, CDCl₃): δ = 8.36 (*d*, *J* = 2.1 Hz, 1H), 8.31 (*d*, *J* = 2.0 Hz, 1H), 6.70 (s, 2H), 2.76 – 2.64 (m, 2H), 2.51 (t, *J* = 7.1 Hz, 2H), 1.93 (quin, *J* = 7.5 Hz, 2H), 1.86 (s, 3H).

¹³C NMR (101 MHz, CDCl₃): δ = 155.1, 151.7, 137.6, 133.0, 129.7, 127.9, 125.4, 40.2, 36.9, 21.8, 15.7.

MS (EI): *m/z* (%) = 219 [M]⁺ (100), 204 (67), 173 (22), 158 (30).

HRMS (EI): *m/z* [M]⁺ calcd for C₁₁H₁₃N₃O₂: 219.1008; found: 219.0992.

2-(2-Methylcyclopent-1-en-1-yl)-3-nitropyridine (4n)

Using 1-iodo-methylcyclopent-1-ene and 2-chloro-3-nitropyridine according to general procedure B provided **4n** as a yellow oil.

Yield: 26 mg, 0.17 mmol (84%); *R*_f = 0.3 (hexane/EtOAc 8:2, UV, KMnO₄, PAA).

¹H NMR (400 MHz, CDCl₃): δ 8.79 = (dd, *J* = 4.7, 1.6 Hz, 1H), 8.15 (dd, *J* = 8.2, 1.6 Hz, 1H), 7.34 (dd, *J* = 8.2, 4.7 Hz, 1H), 2.84 – 2.70 (m, 2H), 2.50 (t, *J* = 8.0 Hz, 2H), 2.01 (quin, *J* = 7.5 Hz, 2H), 1.61 (s, 3H).

¹³C NMR (101 MHz, CDCl₃): δ = 152.9, 152.6, 146.5, 142.1, 132.2, 132.0, 121.8, 39.4, 36.7, 22.8, 15.0.

MS (EI): *m/z* (%) = 187 (70), 174 (35), 156 (95), 147 (100), 130 (75), 117 (65), 103 (23).

HRMS (EI): *m/z* [M-H]⁺ calcd for C₁₁H₁₁N₂O₂: 203.0821; found: 203.0814.

1-Methyl-2-(3-nitrophenyl)-1H-pyrrole (7a)

To a solution of 1-methyl-1H-pyrrole (90 μL, 1.014 mmol) and TMEDA (200 μL, 1.33 mmol, 1.33 equiv) in Et₂O (2 mL, 0.5 M) was slowly added a solution of *n*-BuLi (410 μL, 2.44 M in hexane, 1.00 equiv) at 0 °C. After stirring for 2 h at ambient temperature, B(OiPr)₃ (230 μL, 1.00 mmol, 1.00 equiv) and THF (2 mL) were added and the resulting mixture stirred for another 1 h at room temperature. Pd(dppf)Cl₂ dichloromethane adduct (16 mg, 4 mol%), 1-iodo-3-nitrobenzene (125 mg, 0.5 mmol, 0.5 equiv) and an aqueous solution of sodium hydroxide (1.5 mL, 1.5 equiv 1.00 M) were subsequently added and the reaction mixture stirred overnight. The mixture was extracted with Et₂O (3 × 20 mL), washed with a saturated aqueous solution of sodium chloride (20 mL), dried over magnesium sulfate, filtrated, concentrated and purified via flash column chromatography. Compound **7a** was obtained as a yellow solid.

Yield: 73 mg, 0.36 mmol (72%); mp 73–75 °C; *R*_f = 0.09 (hexane/EtOAc 98:2, UV, KMnO₄, PAA).

¹H NMR (400 MHz, CDCl₃): δ = 8.27 (t, *J* = 2.0 Hz, 1H), 8.13 (ddd, *J* = 8.3, 2.3, 1.1 Hz, 1H), 7.74 (ddd, *J* = 7.7, 1.7, 1.1 Hz, 1H), 7.57 (t, *J* = 8.0 Hz, 1H), 6.79 (t, *J* = 2.3 Hz, 1H), 6.36 (dd, *J* = 3.7, 1.8 Hz, 1H), 6.24 (dd, *J* = 3.7, 2.7 Hz, 1H), 3.73 (s, 3H).

¹³C NMR (101 MHz, CDCl₃): δ = 148.5, 135.0, 134.1, 132.1, 129.5, 125.4, 122.8, 121.4, 110.4, 108.5, 35.4.

MS (EI): *m/z* (%) = 202 (100) [M]⁺, 156 (45), 141 (11), 128 (35), 115 (25).

HRMS (EI): *m/z* [M]⁺ calcd for C₁₁H₁₀N₂O₂: 202.0742; found: 204.0736.

2-(3-Nitrophenyl)furan (7b)

To a solution of furan (75 μL, 1.014 mmol) in Et₂O (2 mL, 0.5 M) was slowly added a solution of *n*-BuLi (410 μL, 2.44 M in hexane, 1.00 equiv) at 0 °C. After stirring for 1 h at ambient temperature, B(OiPr)₃ (230 μL, 1.00 mmol, 1.00 equiv) and THF (2 mL) were added and the resulting mixture stirred for another 1 h at room temperature. Pd(dppf)Cl₂ dichloromethane adduct (16 mg, 4 mol%), 1-iodo-3-nitrobenzene (125 mg, 0.5 mmol, 0.5 equiv) and an aqueous solution of sodium hydroxide (1.5 mL, 1.5 equiv 1.00 M) were subsequently added and the mixture stirred overnight. The mixture was extracted with Et₂O (3 × 20 mL), washed with a saturated aqueous solution of sodium chloride (20 mL), dried over magnesium sulfate, filtered, concentrated and purified via flash column chromatography. Compound **7b** was obtained as

Synthesis

Special Topic

a colorless oil.

Yield: 91 mg, 0.48 mmol (96%); R_f = 0.14 (hexane/EtOAc 98:2, UV, KMnO₄, PAA).

¹H NMR (400 MHz, CDCl₃): δ = 8.46 (t, J = 1.9 Hz, 1H), 8.06 (dd, J = 8.2, 1.7 Hz, 1H), 7.93 (d, J = 7.8 Hz, 1H), 7.57 – 7.42 (m, 2H), 6.79 (d, J = 3.5 Hz, 1H), 6.52 (dd, J = 3.4, 1.8 Hz, 1H).

¹³C NMR (101 MHz, CDCl₃): δ = 151.6, 148.8, 143.4, 132.4, 129.8, 129.3, 121.7, 118.5, 112.2, 107.4.

MS (EI): m/z (%) = 189 (100) [M]⁺, 143 (23), 131 (10), 115 (100), 102 (7).

HRMS (EI): m/z [M]⁺ calcd for C₁₀H₇NO₃: 189.0426; found: 189.0420.

4-(3,4-Dihydro-2H-pyran-6-yl)benzoxazole (7c)

To a solution of 3,4-dihydro-2H-pyran (90 μ L, 1.014 mmol) and TMEDA (50 μ L, 0.33 mmol, 0.33 equiv) in Et₂O (2 mL, 0.5 M) was slowly added a solution of *n*-BuLi (550 μ L, 2.44 M in hexane, 1.34 equiv) at ambient temperature. After stirring for 30 min, B(O*i*Pr)₃ (230 μ L, 1.00 mmol, 1.00 equiv) and THF (2 mL) were added and the resulting mixture stirred for 1 h at room temperature. Pd(dppf)Cl₂ dichloromethane adduct (16 mg, 4 mol%), 4-bromobenzonitrile (91 mg, 0.5 mmol, 0.5 equiv) and an aqueous solution of sodium hydroxide (1.5 mL, 1.5 equiv, 1.00 M) were subsequently added and the mixture stirred overnight. The mixture was extracted with Et₂O (3 \times 20 mL), washed with a saturated aqueous solution of sodium chloride (20 mL), dried over magnesium sulfate, filtered, concentrated and purified via flash column chromatography. Compound **7c** was obtained as a yellow oil.

Yield: 40 mg, 0.22 mmol, 43%; R_f = 0.17 (hexane/EtOAc 98:2, UV, KMnO₄, PAA).

¹H NMR (400 MHz, CDCl₃): δ = 7.65 – 7.59 (m, 1H), 7.59 – 7.54 (m, 1H), 5.50 (t, J = 4.2 Hz, 1H), 4.17 (t, J = 5.3 Hz, 1H), 2.24 (td, J = 6.4, 4.1 Hz, 1H), 1.96 – 1.85 (m, 1H).

¹³C NMR (101 MHz, CDCl₃): δ = 150.2, 140.5, 132.0, 124.7, 119.2, 110.9, 101.0, 66.7, 22.2, 21.0.

MS (EI): m/z (%) = 185 (56), 170 (9), 156 (6), 140 (7), 130 (100), 116 (5), 102 (44).

HRMS (EI): m/z [M]⁺ calcd for C₁₂H₁₁NO: 185.0841; found: 185.0834.

Funding Information

A.N.B., M.E., A.M. and D.D. are grateful to the Fonds der Chemischen Industrie, the Deutsche Forschungsgemeinschaft (DFG grant: DI 2227/2–1) and the SFB749 for Ph.D. funding and financial support.

Supporting Information

Supporting information for this article is available online at <https://doi.org/10.1055/s-0036-1592004>.

References

- (1) (a) Miyaura, N.; Suzuki, A. *J. Chem. Soc. Chem. Commun.* **1979**, 866. (b) Miyaura, N.; Yamada, K.; Suzuki, A. *Tetrahedron Lett.* **1979**, 36, 3437. (c) Suzuki, A. *Angew. Chem. Int. Ed.* **2011**, 50, 6722.
- (2) (a) Lennox, A. J. J.; Lloyd-Jones, G. C. *Chem. Soc. Rev.* **2014**, 43, 412. (b) Maluenda, I.; Navarro, O. *Molecules* **2015**, 20, 7528. (c) Han, F.-S. *Chem. Soc. Rev.* **2013**, 42, 5270.
- (3) (a) Synthesis and Application of Organoboron Compounds, In *Topics in Organometallic Chemistry*, Vol. 49; Fernández, E.; Whiting, A., Eds.; Springer, **2015**. (b) Brown, H. C.; Cole, T. C. *Organometallics* **1983**, 2, 1316. (c) *Boronic Acids: Preparation, Applications in Organic Synthesis and Medicine*; Hall, D. G., Ed.; Wiley-VCH: Weinheim, **2005**.
- (4) (a) Trippier, P. C.; McGuigan, C. *MedChemComm* **2010**, 1, 183. (b) Draganov, A.; Wang, D.; Wang, B. In *Atypical Elements in Drug Design*, Vol. 17; Schwarz, J., Ed.; Springer, **2014**.
- (5) Brooks, W. L. A.; Sumerlin, B. S. *Chem. Rev.* **2016**, 116, 1375.
- (6) Bull, S. D.; Davidson, M. G.; van den Elsen, J. M. H.; Fossey, J. S.; Jenkins, A. T. A.; Jiang, Y.-B.; Kubo, Y.; Marken, F.; Sakurai, K.; Zhao, J.; James, T. D. *Acc. Chem. Res.* **2013**, 46, 312.
- (7) Nicolaou, K. C.; Bulger, P. G.; Sarlah, D. *Angew. Chem. Int. Ed.* **2005**, 44, 4442.
- (8) (a) Billingsley, K. L.; Buchwald, S. L. *Angew. Chem. Int. Ed.* **2008**, 47, 4695. (b) Oberli, M. A.; Buchwald, S. L. *Org. Lett.* **2012**, 14, 4606.
- (9) (a) Yamamoto, Y.; Takizawa, M.; Yu, X.-Q.; Miyaura, N. *Angew. Chem. Int. Ed.* **2008**, 47, 928. (b) Yamamoto, Y.; Iikizakura, K.; Ito, H.; Miyaura, N. *Molecules* **2013**, 18, 430.
- (10) Cammidge, A. N.; Goddard, V. H. M.; Gopee, H.; Harrison, N. L.; Hughes, D. L.; Schubert, C. J.; Sutton, B. M.; Watts, G. L.; Whitehead, A. J. *Org. Lett.* **2006**, 8, 4072.
- (11) Haag, B. A.; Sämman, C.; Jana, A.; Knochel, P. *Angew. Chem. Int. Ed.* **2011**, 50, 7290.
- (12) (a) Boardman, L. D.; Bagheri, V.; Sawada, H.; Negishi, E.-i. *J. Am. Chem. Soc.* **1984**, 106, 6105. (b) Liu, F.; Negishi, E.-i. *Tetrahedron Lett.* **1997**, 38, 1149.
- (13) (a) Eisold, M.; Didier, D. *Angew. Chem. Int. Ed.* **2015**, 54, 15884. (b) Eisold, M.; Kiefl, G. M.; Didier, D. *Org. Lett.* **2016**, 18, 3022. (c) Eisold, M.; Baumann, A. N.; Kiefl, G. M.; Emmerling, S. T.; Didier, D. *Chem. Eur. J.* **2017**, 23, 1634. (d) Baumann, A. N.; Eisold, M.; Didier, D. *Org. Lett.* **2017**, 19, 2114. (e) Eisold, M.; Didier, D. *Org. Lett.* **2017**, 19, 4046.
- (14) Hodgson, D. M.; Pearson, C. I.; Kazmi, M. *Org. Lett.* **2014**, 16, 856.
- (15) Baumann, A. N.; Eisold, M.; Music, A.; Haas, G.; Kiw, Y. M.; Didier, D. *Org. Lett.* **2017**, 19, 5681.
- (16) CCDC 1825251 (**3a**), CCDC 1826225 (**4g**) and CCDC 1825250 (**7a**) contain the supplementary crystallographic data for this manuscript. The data can be obtained free of charge from The Cambridge Crystallographic Data Centre via www.ccdc.cam.ac.uk/getstructures. See the Supporting Information for details.
- (17) Negishi, E.-i.; Sawada, H.; Tour, J. M.; Wei, Y. *J. Org. Chem.* **1988**, 53, 915.
- (18) Li, W.; Nelson, D. P.; Jensen, M. S.; Hoerrner, R. S.; Cai, D.; Larsen, R. D.; Reider, P. J. *J. Org. Chem.* **2002**, 67, 5394.

2 Single-Pot Access to Bisorganoborinates: Applications in Zweifel Olefination

2.1 Relevance

The vast majority of Zweifel olefinations performed in recent publications utilizes alkyl, alkenyl or aryl pinacol boronic esters as substrates.¹²⁶ Especially sp^2 -configured substrates are directly available *via* a variety of pathways, including transition-metal catalyzed borylations of aryl halides¹⁷⁶ and ethers¹⁷⁷, transition-metal free alternatives thereof¹⁷⁸ and transition-metal catalyzed C-H borylations¹⁷⁹ with bis(pinacolato)diboron or pinacolborane. Nevertheless, the arguably still most utilized and rapid access toward pinacol boronic esters is represented by the addition of a borontrialkoxide to an organolithium species.^{75,180} However, such a process is not step-economic, as after generation of the tetracoordinated organoborate those species are usually hydrolyzed and then protected with pinacol to furnish the desired pinacol boronic ester.¹⁸⁰ In the next step, the ester is engaged with another organometallic compound to form the tetracoordinated bisorganoborinate, which is only then applicable in Zweifel olefinations. To facilitate the synthesis of bisorganoborinates and improve step-economy in follow-up Zweifel transformations, an inexpensive protocol is herein reported, in which the addition of two organometallic reagents onto borontrialkoxides directly furnishes bisorganoborinates in an *in situ* single-pot process.

2.2 Preamble

The following work was reprinted with permission from Arif Music, A. N. Baumann, P. Spieß, N. Hilgert, M. Köllen and D. Didier, *Org. Lett.* **2019**, *21*, 2189–2193. Copyright© 2019 American Chemical Society. The project was conducted in equal contribution with A. N. Baumann.

¹⁷⁶ a) T. Ishiyama, M. Murata, M. Miyaura, *J. Org. Chem.* **1995**, *60*, 7508–7510; b) M. Murata, *Heterocycles* **2012**, *85*, 1795–1819; c) T. Niwa, H. Ochiai, Y. Watanabe, T. Hosoya, *J. Am. Chem. Soc.* **2015**, *137*, 14313–14318.

¹⁷⁷ C. Zarate, R. Manzano, R. Martin, *J. Am. Chem. Soc.* **2015**, *137*, 6754–6757.

¹⁷⁸ a) E. Yamamoto, K. Izumi, Y. Horita, H. Ito, *J. Am. Chem. Soc.* **2012**, *134*, 19997–20000; b) M.-A. Légaré, M.-A. Courtemanche, É. Rochette, F.-G. Fontaine, *Science* **2015**, *349*, 513–516; c) K. Chen, S. Zhang, P. He, P. Li, *Chem. Sci.* **2016**, *7*, 3676–3680; d) A. M. Mfuh, J. D. Doyle, B. Chhetri, H. D. Arman, O. V. Larionov, *J. Am. Chem. Soc.* **2016**, *138*, 2985–2988.

¹⁷⁹ a) C. N. Iverson, M. R. Smith, *J. Am. Chem. Soc.* **1999**, *121*, 7696–7697; b) S. Shimada, A. S. Batsanov, J. A. K. Howard, T. B. Marder, *Angew. Chem. Int. Ed.* **2001**, *40*, 2168–2171; c) T. Ishiyama, J. Tagaki, K. Ishida, N. Miyaura, N. R. Anastasi, J. F. Hartwig, *J. Am. Chem. Soc.* **2002**, *124*, 390–391; d) I. A. I. Mkhaliid, J. H. Barnard, T. B. Marder, J. M. Murphy, J. F. Hartwig, *Chem. Rev.* **2010**, *110*, 890–931; e) H.-X. Dai, J.-Q. Yu, *J. Am. Chem. Soc.* **2012**, *134*, 134–137; f) M. A. Larsen, J. F. Hartwig, *J. Am. Chem. Soc.* **2014**, *136*, 4287–4299.

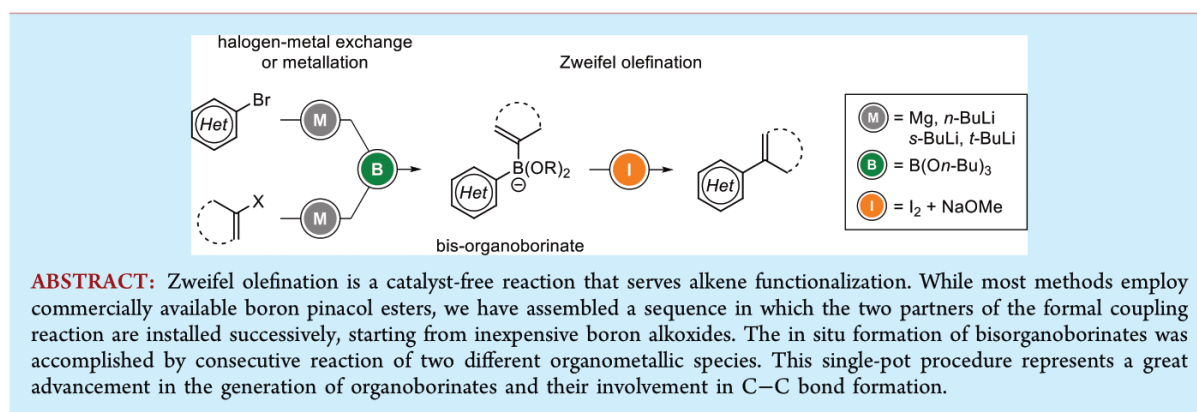
¹⁸⁰ W. C. Chow, O. Y. Yuen, P. Y. Choy, C. M. So, C. P. Lau, W. T. Wong, F. Y. Kwong, *RSC Advances* **2013**, *3*, 12518–12539.

Single-Pot Access to Bisorganoborinates: Applications in Zweifel Olefination

Arif Music,[†] Andreas N. Baumann,[†] Philipp Spieß, Nicolas Hilgert, Martin Köllen, and Dorian Didier*[✉]

Department of Chemistry and Pharmacy, Ludwig-Maximilians-Universität München, Butenandtstraße 5-13, 81377 Munich, Germany

S Supporting Information



The use of boron in synthesis has spanned the community of organic chemists for a few decades. Boron-based reagents have been employed in quite a number of transformations such as stereo- and regioselective hydroborations,¹ highly functional group tolerant Suzuki cross-coupling reactions,² stereospecific homologations pioneered by Matteson,³ and recently revisited by the group of Aggarwal,⁴ and Zweifel olefinations.⁵

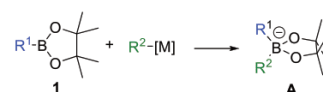
With dependable boron-related strategies in hand, we previously set out to tackle challenging strained ring-system syntheses. While boron homologations were employed to stereoselectively access alkylidenecyclobutanes⁶ and cyclopropanes,⁷ stable boronate complexes enabled the formation of scarcely described substituted cyclobutenes and 2-azetines.⁸

Although Zweifel olefination is an established transformation, for which we recently developed alternative organocerium reagents,⁹ most reports describe the use of commercial organoboron pinacol esters **1**.¹⁰ However, this strategy is currently limited by the availability of those reagents and their price. To overcome the need of using boron pinacol esters **1**, we thought of employing in situ generated trialkoxyorganoboronates **B** as intermediates for bisorganoborinates **C**, considering the pseudometallic character of boron to displace one of the alcoholate ligands (Scheme 1b).

Given that organoboronates **A** and **B** can be generated quantitatively by addition of boron alkoxides to organometallic species ($R^1-[M]$),¹¹ such a protocol would constitute a solid base as the first step in the in situ formation of

Scheme 1. Our Approach to Bisorganoborinates^a

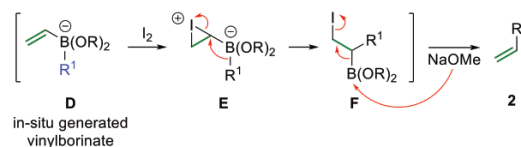
a) classical access to bis-organoborinates



b) our approach



c) Zweifel olefination

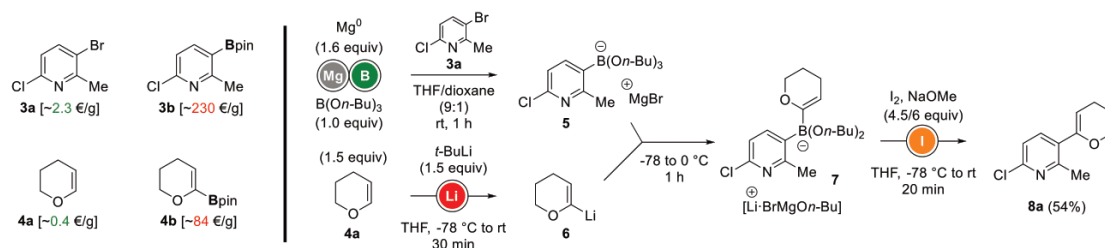


^aCounter-cations have been omitted for more clarity.

bisorganoborinates **C**. With the possibility of performing a ligand exchange on the intermediate organoboronates, an economic alternative to the use of commercially available

Received: February 6, 2019

Published: March 13, 2019

Scheme 2. Proof of Concept: Coordination–Ligand Exchange–Zweifel Olefination Sequence¹¹

boron pinacol esters **1** (Scheme 1a) would be unlocked with inexpensive boron alkoxides.

In the Zweifel olefination, an alkenyl-organoboronate **D** (Scheme 1c) reacts with iodine, giving an intermediate iodonium species **E** that triggers a 1,2-metalate rearrangement toward the neutral compound **F**, upon which the addition of a base promotes a β -elimination that ultimately leads to the olefin **2**.¹² The efficient formation of **D** stands as a key step in this transformation. We describe herein a one-pot sequence toward alkenyl-organoboronates **D** and their subsequent involvement in Zweifel olefination reactions.

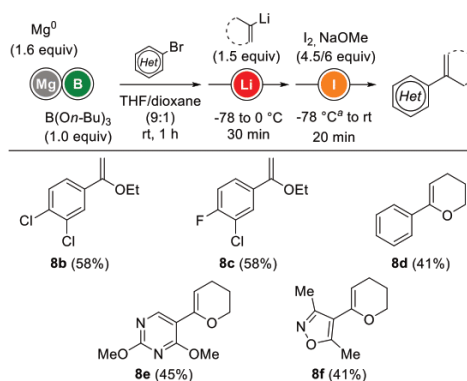
As a proof of concept, we envisioned the formation of a Csp^2 – Csp^2 bond between a pyridine moiety **3** and a 3,4-dihydropyran **4** (Scheme 2).

Via known strategies, the reaction requires the use of expensive boron pinacol esters (either **3b** or **4b**), while our method enables the use of cheaper substrates such as **3a** and **4a**. The intermediate 3-pyridylboronate **5** is generated by adding **3a** to a suspension of magnesium in the presence of boron *n*-butoxide (0.15 €/g),^{11c,13} the reaction proceeding through metal insertion followed by coordination to the boron atom at room temperature. The presence of dioxane during this step proved to be essential to avoid formation of undesired boron species.^{14,15} An ex-situ prepared solution of (3,4-dihydro-2*H*-pyran-6-yl)lithium **6**¹⁶ is added to perform the ligand exchange, releasing an equivalent of butylate salt and giving access to the alkenylboronate **7** (Scheme 2). The intramolecular alkenylation proceeds upon addition of iodine, furnishing the heterocyclic compound **8a** in 54% yield.

As described by the group of Aggarwal,^{5g} no excessive amount of alkenyllithium reagent was required for full consumption of the intermediate trialkoxyboronate as shown by ¹¹B NMR measurements.¹⁵

With a proof of concept in hand, we started exploring the in situ formation of bisorganoboronates through magnesium insertion/trapping reaction and further ligand exchange with alkenyllithium. Reasonable yields were obtained for insertions onto aromatic and heteroaromatic derivatives, in combination with acyclic (**8b–c**) and cyclic (**8d–f**) alkenyl ethers (Scheme 3).

However, when the ligand exchange of the second step was performed using organomagnesium reagents, an excess of the latter was required for the Zweifel product to be obtained with maximum efficiency. Three equivalents were needed in order to generate a proposed tetrakis-organoboron complex containing three alkenyl groups. ¹¹B NMR studies also demonstrated that the intermediate organoboronate species such as **B** (Scheme 1b) would remain unconsumed with lower excesses of organomagnesium reagents.¹⁴ The boron-relayed room-temperature magnesium insertion/trapping reaction was performed on a wide range of aryl and heteroaryl bromides and

Scheme 3. Mg Insertion/Ligand Exchange with Alkenyllithium Reagents/Zweifel Olefination Sequence^a

^aConducting the addition of iodine at 0 °C resulted in lower yields.

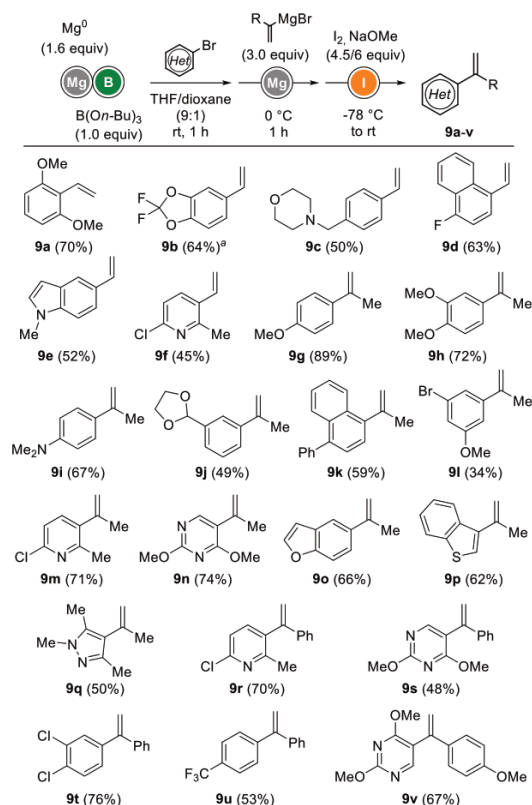
followed by exchanges of alkoxide ligands with alkenylmagnesium species (Scheme 4). The scope of the reaction was evaluated with vinyl (**9a–f**), isopropenyl (**9g–q**), and α -styrylmagnesium reagents (**9r–v**) in 45 to 89% yield. Interestingly, valuable heteroaromatic derivatives were successfully engaged in this procedure, affording sophisticated structures such as alkenyl pyrazole **9q** (50%) or pyrimidines **9n**, **9s**, and **9v** (48 to 74%).

Next, we envisioned that a Br/Li exchange (instead of Mg insertion) as a first step could be used in the formation of intermediate organoboronates (Scheme 5). *n*-Butyllithium was introduced at -78 °C on different aryl bromides, and—after formation of the organoboronate species via addition of boron butylate—the sequence was continued as above, with further introduction of 3 equiv of ex situ generated alkenylmagnesium stock solutions.

Phenanthryl, naphthyl, and carbazolyl substrates led to olefins **10a–c** in good yields up to 80%, validating the process to work with a first step of organolithium addition. The transformation being quite efficient, we pushed the challenge further and set out to perform a double, yet unprecedented Zweifel olefination on bisbrominated substrates. Double Br/Li exchange was undertaken using 2 equiv of *n*-BuLi at -78 °C. Twice the amount of further reagents was subsequently needed to drive the reaction to completion, affording bisolefinated products **10d–f** in good yields (up to 63%).

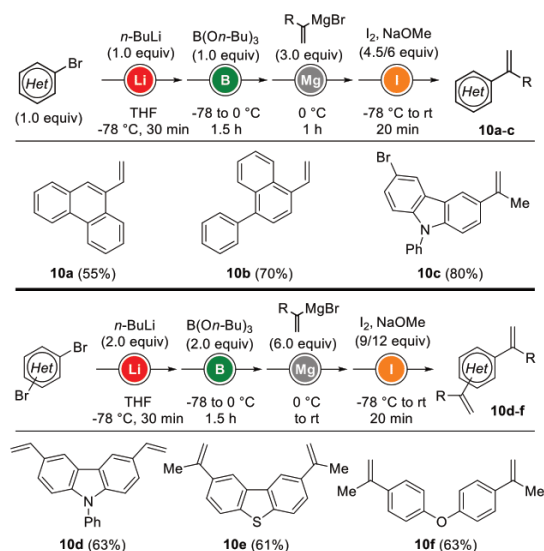
In consideration of previous results, it was expected that a procedure using sequentially two organolithium reagents would lead to desired products, and compounds **11a** and **b** were isolated in moderate yields (Scheme 6). Importantly, such a protocol allowed us to use 2 equiv of the same olefin to

Scheme 4. Mg Insertion/Ligand Exchange with Alkenylmagnesium Reagents/Zweifel Olefination Sequence



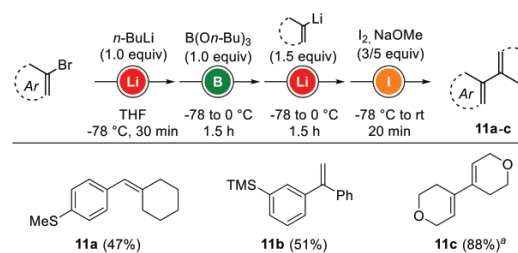
^aYield was determined by ¹⁹F NMR vs C₆F₆ as internal standard.

Scheme 5. Br/Li Exchange/Ligand Exchange with Alkenylmagnesium Reagents/Zweifel Olefination Sequence



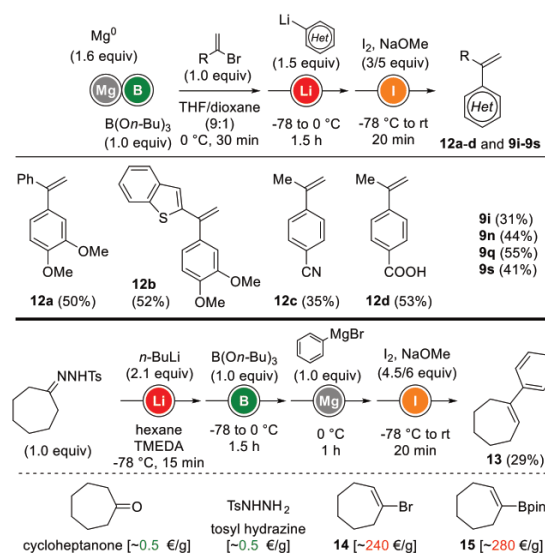
undergo formal dimerization (**11c**) in 88% yield, opening an efficient route toward functionalized dienes.

Scheme 6. Br/Li Exchange/Ligand Exchange with Alkenyllithium Reagents/Zweifel Olefination Sequence



^a**11c** was made from 4-(3,6-dihydro-2H-pyran)yllithium and 0.5 equiv of B(On-Bu)₃ (see S1).

We finally explored the possibility of an inverse procedure in which the alkenyl group would be introduced in the first step (Scheme 7). In this case, considerable savings of alkenylmag-

Scheme 7. Zweifel Olefinations with In Situ Generated Alkenylboronates¹¹

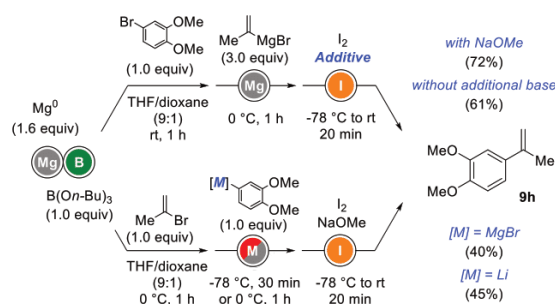
nesium reagent—previously required in excess—would be achieved. Such a challenge was undertaken by generating an alkenylboronate from the corresponding alkenyl bromide, in the presence of magnesium and boron *n*-butoxide. An aryllithium species was then added (1.5 equiv), followed by iodine and sodium methoxide. This procedure allowed for the formation of *gem*-bisarylated alkenes **12a** and **b** in moderate yields.

In addition, this reverse alternative provides an access to compounds that could not be obtained via previous routes, such as the nitrile derivative **12c** (35%). A challenging unprotected carboxylic acid was also engaged in the second step of the olefination reaction. In this case, 2 equiv of *n*-BuLi was used: one to deprotonate the carboxylic acid and one to perform a halogen–metal exchange. **12d** was obtained in 53% yield. To push the methodology further, we employed a Shapiro rearrangement to produce an alkenyllithium reagent to be engaged in the Zweifel olefination. Cycloheptanyl hydrazone was chosen as a representative example, as classical

alternatives would require expensive starting materials such as 1-cycloheptyl bromide **14** or boron pinacol ester **15**. Even though **13** was obtained in 29% yield, only inexpensive cycloheptanone and tosylhydrazine were needed as substrates in this multistep one-pot sequence.

We have shown that different transition-metal-free paths can be taken to synthesize arylated olefins without the need of purchasing expensive boron pinacol esters. In Scheme 8, we

Scheme 8. Comparison of Different Methods to Access 9h



summarize and compare some of these methods, having an in situ magnesium insertion/trapping reaction as the first step. Employing classical conditions described in Scheme 4 afforded **9h** in 72% yield.

Importantly, when performing the ligand exchange in the second step on the intermediate organoboronate, magnesium butoxide (*n*-BuOMgBr) is released in the reaction mixture, and we hypothesized that this alcoholate could be used as the required base in the elimination step. Avoiding the addition of sodium methanolate confirmed this hypothesis, as **9h** was isolated in 61% yield. Alternatively, the first insertion step could be performed on the alkenyl part, preventing the use of an excessive amount of the corresponding Grignard reagent in the second step. Similar yields were obtained using either arylmagnesium or aryllithium species (40–45%).

In conclusion, we have demonstrated that a stoichiometrically controlled generation of hetero bisorganoborinates could be turned into a powerful tool for C–C bond formation. By unlocking new and complementary paths toward diversely substituted boron species, a wide array of functionalized olefins were developed, employing inexpensive substrates and reagents in combination with catalyst-free Zweifel conditions.

■ ASSOCIATED CONTENT

Supporting Information

The Supporting Information is available free of charge on the ACS Publications website at DOI: 10.1021/acs.orglett.9b00493.

Experimental procedures and characterization (IR, HRMS, and ¹H and ¹³C NMR data) for all new compounds (PDF)

■ AUTHOR INFORMATION

Corresponding Author

*E-mail: dorian.didier@cup.uni-muenchen.de.

ORCID

Andreas N. Baumann: 0000-0002-2811-1787

Dorian Didier: 0000-0002-6358-1485

Author Contributions

†A.M. and A.N.B. contributed equally.

Notes

The authors declare no competing financial interest.

■ ACKNOWLEDGMENTS

D.D., A. M., and A.N.B. are grateful to the Fonds der Chemischen Industrie, the Deutsche Forschungsgemeinschaft (DFG grant: DI 2227/2-1), the SFB749, and the Ludwig-Maximilians University for PhD funding and financial support. Dr. Christoph Sämann (Bayer Crop Science, Dormagen) is kindly acknowledged for fruitful discussions.

■ REFERENCES

- (a) Hurd, D. T. *J. Am. Chem. Soc.* **1948**, *70*, 2053–2055. (b) Brown, H. C.; Subba Rao, B. C. *J. Am. Chem. Soc.* **1956**, *78*, 2582–2588. (c) Brown, H. C.; Subba Rao, B. C. *J. Am. Chem. Soc.* **1956**, *78*, 5694–5695. (d) Brown, H. C.; Subba Rao, B. C. *J. Am. Chem. Soc.* **1959**, *81*, 6423–6428. (e) Brown, H. C. *Tetrahedron* **1961**, *12*, 117–138. (f) Evans, D. A.; Fu, G. C.; Hoveyda, A. H. *J. Am. Chem. Soc.* **1992**, *114*, 6671–6679.
- (a) Miyaura, N.; Yamada, K.; Suzuki, A. *Tetrahedron Lett.* **1979**, *20*, 3437–3440. (b) Suzuki, A. *Acc. Chem. Res.* **1982**, *15*, 178–184. (c) Lennox, A. J. J.; Lloyd-Jones, G. C. *Chem. Soc. Rev.* **2014**, *43*, 412–443.
- (a) Matteson, D. S.; Mah, R. H. W. *J. Am. Chem. Soc.* **1963**, *85*, 2599–2603. (b) Matteson, D. S.; Ray, R. *J. Am. Chem. Soc.* **1980**, *102*, 7590–7591. (c) Matteson, D. S.; Ray, R.; Rocks, R. R.; Tsai, D. J. *Organometallics* **1983**, *2*, 1536–1543. (d) Matteson, D. S.; Sadhu, K. M. *J. Am. Chem. Soc.* **1983**, *105*, 2077–2078. (e) Matteson, D. S. *Acc. Chem. Res.* **1988**, *21*, 294–300. (f) Matteson, D. S. *Chem. Rev.* **1989**, *89*, 1535–1551. (g) Matteson, D. S. *Tetrahedron* **1989**, *45*, 1859–1885. (h) Matteson, D. S. *Pure Appl. Chem.* **1991**, *63*, 339–344. (i) Matteson, D. S. *Tetrahedron* **1998**, *54*, 10555–10607.
- (a) Fang, G. Y.; Aggarwal, V. K. *Angew. Chem., Int. Ed.* **2007**, *46*, 359–362. (b) Stymiest, J. L.; Dutheuil, G.; Mahmood, A.; Aggarwal, V. K. *Angew. Chem., Int. Ed.* **2007**, *46*, 7491–7494. (c) Burns, M.; Essafi, S.; Bame, J. R.; Bull, S. P.; Webster, M. P.; Balieu, S.; Dale, J. W.; Butts, C. P.; Harvey, J. N.; Aggarwal, V. K. *Nature* **2014**, *513*, 183–188. (d) Roesner, S.; Blair, D. J.; Aggarwal, V. K. *Chem. Sci.* **2015**, *6*, 3718–3723. (e) Thomas, S. P.; French, R. M.; Jheengut, V.; Aggarwal, V. K. *Chem. Rec.* **2009**, *9*, 24–39.
- (a) Zweifel, G.; Arzoumanian, H.; Whitney, C. C. *J. Am. Chem. Soc.* **1967**, *89*, 3652–3653. (b) Zweifel, G.; Polston, N. L.; Whitney, C. C. *J. Am. Chem. Soc.* **1968**, *90*, 6243–6245. (c) Negishi, E.; Lew, G.; Yoshida, T. *J. Chem. Soc., Chem. Commun.* **1973**, *22*, 874–875. (d) Evans, D. A.; Crawford, T. C.; Thomas, R. C.; Walker, J. A. *J. Org. Chem.* **1976**, *41*, 3947–3953. (e) Brown, H. C.; Bhat, N. G. *J. Org. Chem.* **1988**, *53*, 6009–6013. (f) Armstrong, R. J.; Aggarwal, V. K. *Synthesis* **2017**, *49*, 3323–3336. (g) Armstrong, R. J.; Niwetmarin, W.; Aggarwal, V. K. *Org. Lett.* **2017**, *19*, 2762–2765.
- (a) Eisold, M.; Didier, D. *Angew. Chem., Int. Ed.* **2015**, *54*, 15884–15887. (b) Eisold, M.; Kiefl, G. M.; Didier, D. *Org. Lett.* **2016**, *18*, 3022–3025. (c) Eisold, M.; Baumann, A. N.; Kiefl, G. M.; Emmerling, S. T.; Didier, D. *Chem. - Eur. J.* **2017**, *23*, 1634–1644. (d) Eisold, M.; Didier, D. *Org. Lett.* **2017**, *19*, 4046–4049.
- Baumann, A. N.; Music, A.; Karaghiosoff, K.; Didier, D. *Chem. Commun.* **2016**, *52*, 2529–2532.
- Baumann, A. N.; Eisold, M.; Music, A.; Didier, D. *Synthesis* **2018**, *50*, 3149–3160.
- Music, A.; Hoarau, C.; Hilgert, N.; Zischka, F.; Didier, D. *Angew. Chem., Int. Ed.* **2019**, *58*, 1188–1192.
- (10) For recent applications of Zweifel's olefination in synthesis, see: (a) Blair, D. J.; Fletcher, C. J.; Wheelhouse, K. M. P.; Aggarwal, V. K. *Angew. Chem., Int. Ed.* **2014**, *53*, 5552–5555. (b) Blaisdell, T. P.; Morken, J. P. *J. Am. Chem. Soc.* **2015**, *137*, 8712–8715. (c) Mercer, J. A. M.; Cohen, C. M.; Shuken, S. R.; Wagner, A. M.; Smith, M. W.;

Organic Letters

Letter

Moss, F. R.; Smith, M. D.; Vahala, R.; Gonzalez-Martinez, A.; Boxer, S. G.; Burns, N. Z. *J. Am. Chem. Soc.* **2016**, *138*, 15845–15848.

(11) (a) Yamamoto, Y.; Takizawa, M.; Yu, X.-Q.; Miyaura, N. *Angew. Chem., Int. Ed.* **2008**, *47*, 928–931. (b) Billingsley, K. L.; Buchwald, S. L. *Angew. Chem., Int. Ed.* **2008**, *47*, 4695–4698. (c) Haag, B. A.; Sämann, C.; Jana, A.; Knochel, P. *Angew. Chem., Int. Ed.* **2011**, *50*, 7290–7294. (d) Oberli, M. A.; Buchwald, S. L. *Org. Lett.* **2012**, *14*, 4606–4609.

(12) Matteson, D. S.; Liedtke, J. D. *J. Am. Chem. Soc.* **1965**, *87*, 1526–1531.

(13) For references in prices, see ABCR GmbH (<https://www.abcr.de/>).

(14) Addition of dioxane to the reaction mixture proved to avoid the undesired formation of bisorganoboron species by inducing precipitation of mono-organoboronates in the first coordination step.

(15) See [Supporting Information](#).

(16) Hornillos, V.; Giannerini, M.; Vila, C.; Fananas-Mastral, M.; Feringa, B. L. *Chem. Sci.* **2015**, *6*, 1394–1398.

3 Catalyst-Free Enantiospecific Olefination with *in situ* Generated Organocerium Species

3.1 Relevance

While lanthanides are often called rare-earth metals, they are not so rare after all.¹⁸¹ In fact, the most naturally occurring – cerium – with its abundance of approximately 66 ppm in the earth's crust is more abundant than other frequently encountered metals in organometallic chemistry such as cobalt, tin and zinc.^{69b} In addition, cerium is relatively non-toxic and can therefore be considered an environmentally sound alternative to other transition-metals.¹⁸² Since the lanthanides main difference to other metals is the existence of electrons in f-orbitals, their reactivity and chemical properties are uniquely different. For example, organocerium reagents were found to represent non-basic but highly nucleophilic and oxophilic reagents, which makes them highly selective for 1,2-additions to carbonyl or imine substrates.^{67,69,183} Those additions in complex substrates with traditional organolithium or organomagnesium reagents typically cause multiple side reactions such as reduction, self-condensation and enolization.^{69a} However, in this case superior organocerium species can be easily synthesized by transmetalation from the respective organometallics (see chapter A, 2.3). Moreover, organocerium compounds display significant scope and have therefore been utilized in several total syntheses, making them valuable alternatives to conventional organometallics.¹⁸⁴ In order to broaden the access toward those species, this chapter presents the generation of organocerium reagents by novel halogen-cerium exchange chemistry and their use in Zweifel olefinations.

3.2 Preamble

The following work was reprinted with permission from A. Music, C. Hoarau, N. Hilgert, F. Zischka and D. Didier, *Angew. Chem. Int. Ed.* **2019**, *58*, 1188–1192. Copyright© 2019 Wiley-VCH Verlag GmbH & Co. KGaA, Weinheim.

¹⁸¹ R. Anwander, M. Dolg, F. T. Edlmann, *Chem. Soc. Rev.* **2017**, *46*, 6697–6709.

¹⁸² T. Imamoto, *Lanthanides in Organic Synthesis* **1994**, Academic Press, New York.

¹⁸³ a) T. Imamoto, Y. Sugiura, N. Takiyama, *Tetrahedron Lett.* **1984**, *25*, 4233–4236; b) T. Imamoto, T. Kusumoto, Y. Tawarayama, Y. Sugiura, T. Mita, Y. Hatanaka, M. Yokoyama, *J. Org. Chem.* **1984**, *49*, 3904–3912; c) T. Imamoto, *Pure & Appl. Chem.* **1990**, *62*, 747–752; d) M. Badioli, R. Ballini, M. Bartolacci, G. Bosica, E. Torregiani, E. Marcantoni, *J. Org. Chem.* **2002**, *67*, 8938–8942; e) S. E. Denmark, J. P. Edwards, T. Weber, D. W. Piotrowski, *Tetrahedron Asymmetry* **2010**, *21*, 1278–1302; f) J. E. Kim, A. V. Zabula, P. J. Carroll, E. J. Schelter, *Organometallics* **2016**, *35*, 2086–2091; g) K.-J. Xiao, A.-E. Wang, P.-Q. Huang, *Angew. Chem. Int. Ed.* **2012**, *51*, 8314–8317; h) N. E. Behnke, J. H. Siitonen, S. A. Chamness, L. Kürti, *Org. Lett.* **2020**, *accepted manuscript*, doi.org/10.1021/acs.orglett.0c01229.

¹⁸⁴ a) C. M. J. Fox, R. M. Hiner, U. Warrior, J. D. White, *Tetrahedron Lett.* **1988**, *29*, 2923–2926; b) F. E. Ziegler, C. A. Metcalf III, A. Nangia, G. Schulte, *J. Am. Chem. Soc.* **1993**, *115*, 2581–2589; c) S. F. Martin, W. C. Lee, G. J. Pacofsky, R. P. Gist, T. A. Mulhern, *J. Am. Chem. Soc.* **1994**, *116*, 4674–4688; d) J. Boukouvalas, Y. X. Cheng, J. Robichaud, *J. Org. Chem.* **1998**, *63*, 228–229; e) D. Crich, S. Natarajan, *J. Chem. Soc., Chem. Commun.* **1995**, 85–86; f) M. Kurosu, L. R. Marcin, T. J. Grinsteiner, Y. Kishi, *J. Am. Chem. Soc.* **1998**, *120*, 6627–6628; g) M. Kurosu, Y. Kishi, *Tetrahedron Lett.* **1998**, *39*, 4793–4796; h) A. Fürstner, H. Weintritt, *J. Am. Chem. Soc.* **1998**, *120*, 2817–2825; i) C. L. Martin, L. E. Overman, J. M. Rohde, *J. Am. Chem. Soc.* **2008**, *130*, 7568–7569.

Halogen–Cerium Exchange

International Edition: DOI: 10.1002/anie.201810327
German Edition: DOI: 10.1002/ange.201810327

Catalyst-Free Enantiospecific Olefination with In Situ Generated Organocerium Species

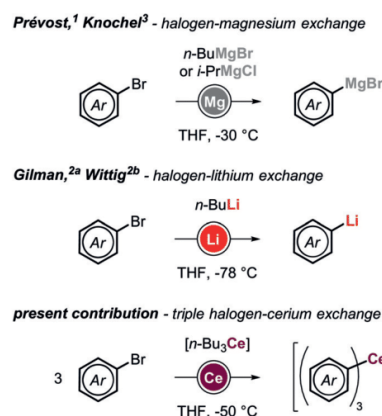
Arif Music, Clément Hoarau, Nicolas Hilgert, Florian Zischka, and Dorian Didier*

Dedicated to Professor Henri Kagan

Abstract: Described is the in situ formation of triorgano-cerium reagents and their application in catalyst-free Zweifel olefinations. These unique cerium species were generated through novel exchange reactions of organohalides with $n\text{-Bu}_3\text{Ce}$ reagents. The adequate electronegativity of cerium allowed for compensating the disadvantages of both usually functional-group-sensitive organolithium species and less reactive organomagnesium reagents. Exchange reactions were performed on aryl and alkenyl bromides, enabling enantio-specific transformations of chiral boron pinacol esters. Finally, these new organocerium species were engaged in selective 1,2-additions onto enolisable and sterically hindered ketones.

Halogen–metal exchange is one of the most efficient routes to preparing organometallic species. Following early findings of Prévost on bromide–magnesium permutation,^[1] Gilman and Wittig subsequently described what would later become the halogen–lithium exchange.^[2] Building upon these reliable methods, the group of Knochel engineered and popularized the efficient “Turbo-Grignard reagent” ($i\text{-PrMgCl-LiCl}$), which considerably facilitated access to organomagnesium intermediates and their implications in organic transformations.^[3] Although zinc and copper species can also be generated through exchange reactions,^[4] convenient transmetalations with ZnCl_2 or copper salts have usually been favoured. The endeavour to tune the reactivity of organometallic reagents was recently taken on by the same group, describing an interesting process to generate C_{sp^2} organo-lanthanum reagents through double exchange.^[5]

While organolithium species have proven to be very reactive, functional group tolerance has often been a major drawback in structural diversification. In comparison, organomagnesium reagents are usually more functional-group-tolerant, while showing decreased reactivity (Scheme 1). The Zweifel olefination is a typical illustration of this lower reactivity.^[6] The issue arises from the difficulty of achieving full conversion into the key boron-ate complex intermediates.



Scheme 1. Halogen–metal exchange: From the discovery to our contribution.

Elegant alternatives have been developed by the group of Aggarwal, who showed that addition of DMSO could drive the reaction to completion,^[7] and the group of Morcken, who used sodium triflate as a “Grignard activator”.^[8]

Aiming to find reagents that would balance the advantages of reactive organolithium reagents and functional-group-tolerant organomagnesium species, we began our quest towards unexplored organometallic species from across the periodic table. We envisioned that choosing an element with an intermediate Pauling electronegativity between those of lithium ($\chi = 0.98$) and magnesium ($\chi = 1.31$) would be a first step in this ambitious study. As many elements could fulfil this condition, we logically selected the most abundant and inexpensive cerium atom ($\chi = 1.12$) for the generation of new organometallic species.^[9] To the best of our knowledge, while organocerium derivatives have already been obtained by transmetalations by the group of Imamoto, no example of halogen–cerium exchanges had ever been reported, hence the interest in our method. Importantly, organocerium reagents have rarely been employed in reactions other than 1,2-additions to carbonyl compounds.^[10]

Our results are twofold. First, optimisations were undertaken by changing both the nature and the amount of the alkylcerium species used in the formation of alkylcerium derivatives in order to investigate their efficiency in halogen–cerium exchange. Second, in situ generated aryl- and alkenylcerium species were employed in Zweifel olefinations. Aryl and alkenyl bromides were used in this catalyst-free

[*] A. Music, N. Hilgert, F. Zischka, Dr. D. Didier
Department Chemie, Ludwig-Maximilians-Universität
Butenandtstraße 5–13, 81377 Munich (Germany)
E-mail: dorian.didier@cup.uni-muenchen.de

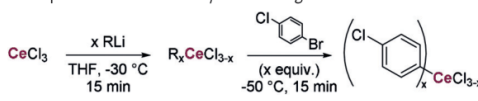
C. Hoarau
Ecole Polytechnique
Route de Saclay, 91128 Palaiseau Cedex (France)

Supporting information and the ORCID identification number(s) for the author(s) of this article can be found under:
<https://doi.org/10.1002/anie.201810327>.

transformation, to ultimately showcase enantiospecific transformations of chiral organoboronates.

The exchange reagents $R_x\text{CeCl}_{3-x}$ were generated in situ by mixing the alkyl lithium species (RLi) and CeCl_3 for 15 min at -30°C in THF. They were further used for Br/Ce exchange with 1-bromo-4-chlorobenzene as a test substrate. As shown in Table 1, moderate exchange conversions were observed

Table 1: Optimisation of the Br/Ce exchange.



RLi	x (equiv)	$R_x\text{CeCl}_{3-x}$	Conv. [%] ^[a]
<i>n</i> -BuLi	1 (1.1)	<i>n</i> -BuCeCl ₂	97
<i>n</i> -BuLi	2 (2.2)	<i>n</i> -Bu ₂ CeCl	95
<i>n</i> -BuLi	3 (3.3)	<i>n</i> -Bu ₃ Ce	93 (86) ^[b,c]
MeLi	3 (3.3)	Me ₃ Ce	30
<i>s</i> -BuLi	3 (3.3)	<i>s</i> -Bu ₃ Ce	55

[a] Determined by GC analysis after hydrolysis with H_2O . [b] Yield of isolated **6a** after Zweifel olefination with (3,6-dihydro-2H-pyran-4-yl)boronic ester. [c] The reaction performed in the absence of cerium chloride only afforded **6a** in 75% yield.

when employing secondary alkyl or methylcerium reagents. Improved results were observed with mono-, di-, and tri-*n*-butylcerium species. For the sake of atom economy, the best-performing tributylcerium reagent was chosen to pursue our study. The initial formation of alkyl cerium species was supported by Raman spectroscopy, which excluded the presence of parasitic *n*-BuLi in the reaction (Figure 1).^[11]

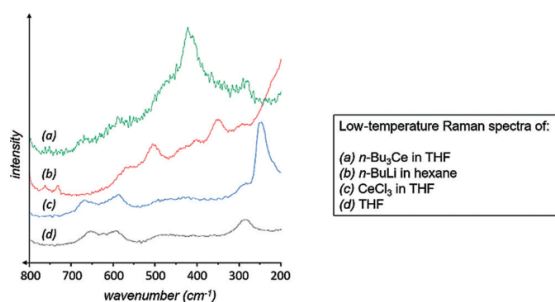
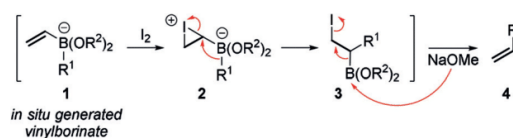


Figure 1. Comparative Raman spectra of different metal salts and organometallic species.

Measuring samples at low temperature allowed us to directly compare the spectra of *n*-BuLi (b) and a mixture (a) of *n*-BuLi (3 equiv) and CeCl_3 . While none of the representative bands of *n*-BuLi at wavenumbers of 350 and 500 cm^{-1} were detected in (a), the Raman spectrum showed a new significant band appearing at 420 cm^{-1} , indicating the formation of a novel species. This observation and the absence of both CeCl_3 and *n*-BuLi vibrations pointed to the existence of an alkyl–cerium bond, which was additionally supported by theoretical calculations.^[12]

In the Zweifel olefination, recently revisited by Aggarwal and co-workers,^[6,7] an in situ generated vinylorganoboronate **1** reacts with iodine at the electron-rich alkenyl moiety to form an iodonium intermediate **2**, which triggers a 1,2-metallate rearrangement of R^1 (Scheme 2). A β -elimination takes place upon addition of a base (NaOMe), yielding the formal coupling product **4**.

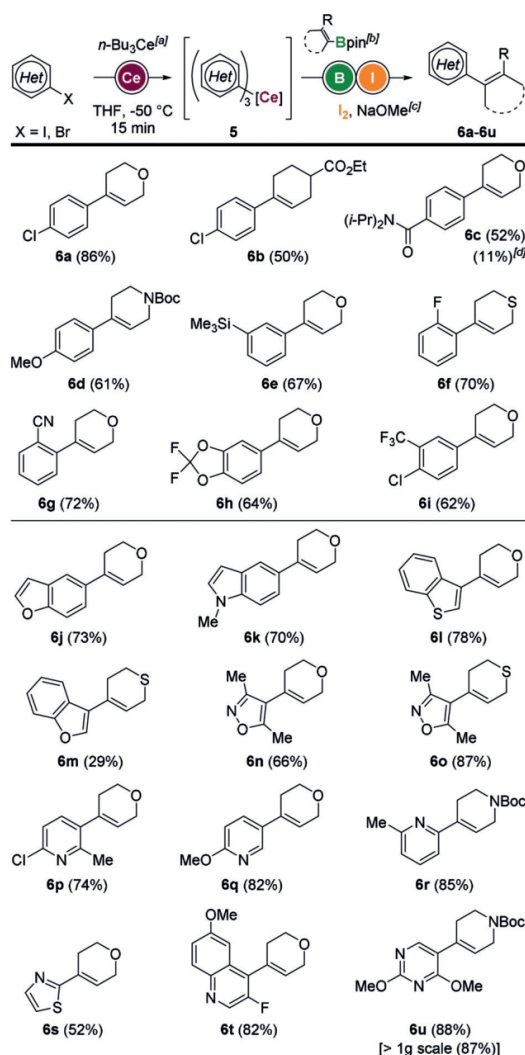


Scheme 2. General mechanism of the Zweifel olefination.

On the basis of the aforementioned optimisations (Table 1), 1-bromo-4-chlorobenzene (1.0 equiv) was used in the presence of 0.37 equiv of *n*-Bu₃Ce to perform a triple exchange to give the triaryl cerium species **5** (Scheme 3). Interestingly, this unprecedented species reacted quantitatively with a cyclic alkenyl boronic ester to in situ generate the alkenyl borinate intermediate. After successive addition of iodine and sodium methylate, the olefinated product **6a** was isolated in 86% yield. An excess amount of the organocerium reagent was not needed to complete the transformation, which thus provides an elegant alternative that balances reactivity and functional group tolerance.

With a successful proof of concept in hands, we started exploring the scope of the transformation. A carbonyl-substituted alkenyl boronic ester afforded the desired product **6b** in 50% yield. Importantly, we could demonstrate the difference in functional group tolerance between cerium and lithium species by employing an amide-substituted substrate. The organocerium reagent furnished the desired product **6c** in 52% yield while the corresponding organolithium species only gave the product in 11% yield. With electron-rich aromatic rings (*p*-OMe), *N*-Boc tetrahydropyridyl (**6d**) reacted similarly, giving the expected product in good yields (61%). Other electron-donating or -withdrawing substituents on the starting aryl bromides did not influence the outcome of the transformation as the *m*-silyl, *o*-fluoro, and *o*-cyano variants yielded **6e–g** in 67–72% yield, and disubstituted aryl precursors gave **6h** and **6i** in 64 and 62% yield, respectively. Heteroaromatics were also engaged in the exchange/Zweifel sequence, furnishing the 5-benzofuranyl, 5-indolyl, 3-benzothiophenyl, and 3-benzofuranyl products **6j–m** in up to 78% yield. Moreover, substituted isoxazole, thiazole, pyridine, and quinoline derivatives afforded the corresponding trisubstituted alkenes **6n–t** in high yields of up to 87%. Full conversion was also observed with a more challenging dimethoxypyrimidine derivative, giving **6u** in 88% yield. Importantly, a similar yield was obtained on 5 mmol scale (1.2 g, 87%).

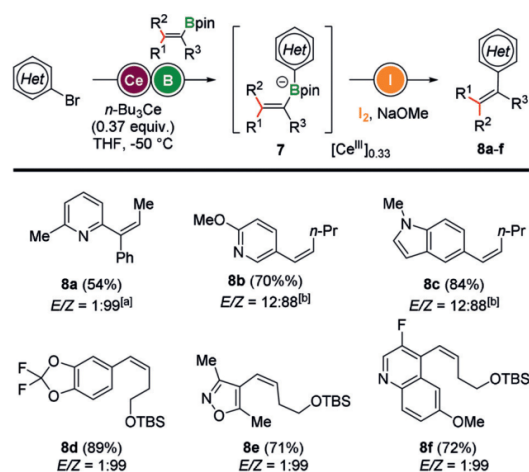
Acyclic alkenyl boronic esters were examined next. Following the same procedure for the in situ generation of the aryl cerium species, reactions were pursued with the introduction of stereodefined alkenyl boron derivatives.^[13] Further rearrangement of the ate complex in the presence



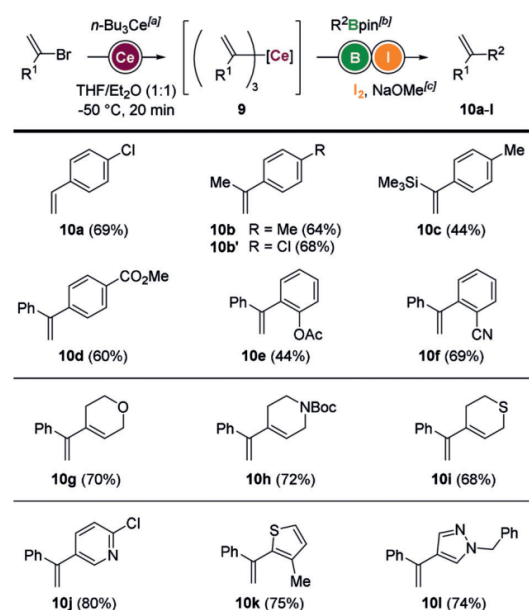
Scheme 3. Zweifel olefination of aryl cerium species generated in situ through triple halogen–cerium exchange. [a] 0.37 equiv. [b] 0.85 equiv of the alkenyl boronic ester; THF, -50°C to RT, 40 min. [c] I_2 (1.5 equiv), 0°C , 15 min; then NaOMe (5.0 equiv), to RT, 30 min. [d] Yield of isolated product when the reaction was performed in the absence of $\text{CeCl}_3 \cdot 2\text{LiCl}$.

of iodine and base gave the desired polysubstituted alkenes **8a–f** with the expected inversion of configuration (Scheme 4) in high yields of up to 89% and *E/Z* ratios of up to 1:99.^[12]

While we had demonstrated organocerium reagents to be more reactive than organomagnesium and more tolerant than organolithium species, the challenge was not restricted to the use of aryl groups for the exchange/Zweifel sequence. Next, we examined the propensity of alkenyl bromides to undergo permutations, and engage in subsequent catalyst-free coupling reactions (Scheme 5). α -Bromostyrene was used as a model substrate in this transformation, aside from the parent vinyl bromide and propenyl bromide.



Scheme 4. Zweifel olefination of stereodefined alkenyl boronic esters. [a] Same conditions as in Scheme 2; *E/Z* ratios determined by GC analysis. [b] Starting from the alkenyl boron pinacol ester with *E/Z* = 88:12.



Scheme 5. Zweifel olefination of alkenyl cerium species generated in situ through triple halogen–cerium exchange. [a] 0.37 equiv. [b] 0.85 equiv of the aryl boronic ester; THF/ Et_2O (1:1), -50°C to RT, 40 min. [c] I_2 (1.5 equiv), -50°C , 15 min; then NaOMe (5.0 equiv), to RT, 30 min.

Trialkenyl cerium species **9** were generated under the optimized conditions (see Table 1) and used in situ for the formation of the corresponding alkenyl borinates with aryl boronic esters. The reaction of trivinylcerium with a chlorinated aryl boron pinacol ester afforded product **10a** in 69% after successive addition of iodine and base. Consistent results

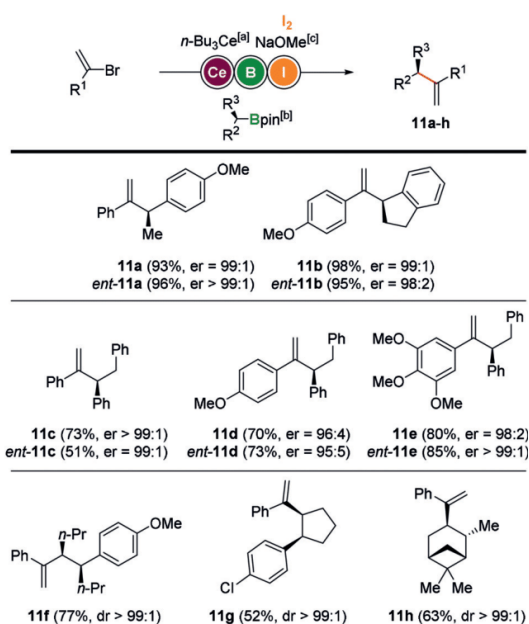
were observed when propenyl bromide and 1-(bromovinyl)-trimethylsilane were used as the substrates in the exchange reactions as **10b** and **10c** were obtained in up to 68% yield. The procedure proved to be quite functional-group-tolerant as diversely substituted aromatics furnished the corresponding products in reasonable yields (**10d–f**, 44–69%), including those with nitrile (**10f**) and ester (**10d,e**) substituents, when employing α -bromostyrene. Our procedure also allowed for the efficient formation of functionalized heterocyclic dienes (**10g–i**) in good yields of up to 72% from alkenyl boronic esters. The introduction of heteroaryl boronic esters for the intermediate formation of the boron-ate complexes with in situ generated trialkenyl cerium species led to the corresponding heteroaryl alkenes. The alkenyl pyridine, thiophene, and pyrazole derivatives **10j–l** were isolated in good yields of up to 80%.

Next, we examined the propensity of alkenyl cerium reagents to undergo stereospecific Zweifel olefinations with stereodefined organoboronic esters. Enantioenriched secondary alkyl boron species were synthesized following the copper-catalyzed enantioselective hydroboration of alkenes described by Lee, Yun, and co-workers.^[14] Halogen–cerium exchange was performed, followed by conversion into the bisorganoborinate and subsequent iodonium formation to trigger a stereospecific 1,2-metallate rearrangement. Addition of the base led to regeneration of the double bond by β -elimination. Enantioenriched benzylic boron pinacol esters furnished the Zweifel products **11a–e** with complete retention of configuration (> 99:1 er) and high yields (up to 98%) for both enantiomers (Scheme 6).

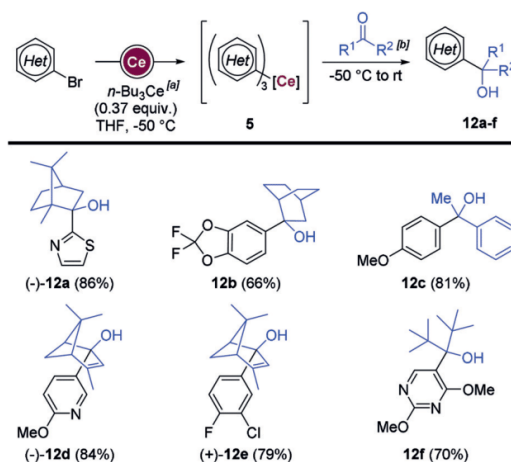
In addition, diastereomerically pure boronic esters^[15] were also employed in this catalyst-free olefination, giving the desired alkenes in moderate to good yields and with total retention of the diastereomeric ratios (> 99:1 dr). Cyclic and acyclic substrates gave access to the functionalized alkyl systems **11f** and **11g** in up to 77% yield. Employing a naturally occurring α -pinene derivative^[16] in the sequence afforded **11h** as a single enantiomer and diastereoisomer in 63% yield.

Taking advantage of the efficient preparation of organocerium species, we finally set out to demonstrate their more general applicability as nucleophiles in 1,2-additions onto diverse ketones. Cerium salts have been used in the past to selectively promote nucleophilic additions of organometallic reagents to hindered carbonyl systems, avoiding parasitic enolisation or conjugate additions.^[10] (+)-Camphor was first employed as a hindered ketone. As shown in Scheme 7, the tertiary alcohol **12a**, resulting from the addition of tri(thiazolyl)cerium species, was obtained in 86% yield. Other enolisable systems such as bicyclo[2.2.2]octan-2-one and acetophenone also gave reasonable yields in the formation of the corresponding alcohols (**12b,c**). (–)-Verbenone was used as an α,β -unsaturated ketone, and products **12d** and **12e** were selectively obtained in good yields of up to 84%, showing no trace of the Michael addition product. Finally, good conversion into the tertiary alcohol **12f** was achieved with hindered hexamethylacetone as the electrophile.

In summary, we have achieved a step forward in the challenge of combining reactivity and functional group



Scheme 6. One-pot stereospecific Zweifel olefination of alkenyl cerium species. [a] 0.37 equiv. [b] 0.85 equiv of the boronic ester; THF/Et₂O (1:1), –50 °C to RT, 40 min. [c] I₂ (1.5 equiv), –50 °C, 15 min; then NaOMe (5.0 equiv), to RT, 30 min.



Scheme 7. One-pot sequence of Br/Ce exchange and 1,2-addition onto ketones. [a] 0.37 equiv. [b] 0.85 equiv of the ketone, THF, –50 °C to RT.

tolerance, enabling considerable scope extensions of sensitive reactions. The development of a synthetic method to access unprecedented organometallic species through very efficient triple halogen–cerium exchange allowed for a wide exemplification of the catalyst-free Zweifel olefination. Additionally, we demonstrated the ability of these unique in situ generated organocerium reagents to undergo stereospecific transformations in one-pot sequences, as well as selective 1,2-additions to challenging ketones.

Acknowledgements

Prof. Andreas Kornath (LMU Munich) is gratefully acknowledged for his help with Raman spectroscopy and for technical support. We would like to thank the Chemical Industry Fund (FCI), the Deutsche Forschungsgemeinschaft (DFG grant DI 2227/2-1, Sonderforschungsbereich SFB749), and the Ludwig-Maximilians-Universität München (LMU) for financial support.

Conflict of interest

The authors declare no conflict of interest.

Keywords: catalyst-free reactions · enantiospecificity · halogen-metal exchange · organocerium compounds · Zweifel olefination

How to cite: *Angew. Chem. Int. Ed.* **2019**, *58*, 1188–1192
Angew. Chem. **2019**, *131*, 1200–1204

- [1] C. Prévost, *Bull. Soc. Chim. Fr.* **1931**, *49*, 1372.
- [2] a) H. Gilman, W. Langham, A. L. Jacoby, *J. Am. Chem. Soc.* **1939**, *61*, 106–109; b) G. Wittig, G. Fuhrmann, *Ber. Dtsch. Chem. Ges.* **1940**, *73*, 1197–1218.
- [3] a) L. Boymond, M. Rottländer, G. Cahiez, P. Knochel, *Angew. Chem. Int. Ed.* **1998**, *37*, 1701–1703; *Angew. Chem.* **1998**, *110*, 1801–1803; b) A. Inoue, K. Kitagawa, H. Shinokubo, K. Oshima, *J. Org. Chem.* **2001**, *66*, 4333–4339.
- [4] a) F. F. Kneisel, M. Dochnahl, P. Knochel, *Angew. Chem. Int. Ed.* **2004**, *43*, 1017–1021; *Angew. Chem.* **2004**, *116*, 1032–1036; b) T. Harada, Y. Kotani, T. Katsuhira, A. Oku, *Tetrahedron Lett.* **1991**, *32*, 1573–1576.
- [5] a) A. D. Benischke, L. Anthore-Dalio, G. Berionni, P. Knochel, *Angew. Chem. Int. Ed.* **2017**, *56*, 16390–16394; *Angew. Chem.* **2017**, *129*, 16608–16612; b) A. D. Benischke, L. Anthore-Dalio, F. Kohl, P. Knochel, *Chem. Eur. J.* **2018**, *24*, 11103–11109.
- [6] a) R. J. Armstrong, V. K. Aggarwal, *Synthesis* **2017**, *49*, 3323–3336; b) R. J. Armstrong, C. Sandford, C. García-Ruiz, V. K. Aggarwal, *Chem. Commun.* **2017**, *53*, 4922–4925.
- [7] R. J. Armstrong, W. Niwetmarin, V. K. Aggarwal, *Org. Lett.* **2017**, *19*, 2762–2765.
- [8] G. J. Lovinger, M. D. Aparece, J. P. Morken, *J. Am. Chem. Soc.* **2017**, *139*, 3153–3160.
- [9] L. Pauling, *J. Am. Chem. Soc.* **1932**, *54*, 3570–3582.
- [10] a) T. Imamoto, T. Kusumoto, M. Yokoyama, *J. Chem. Soc. Chem. Commun.* **1982**, 1042–1044; b) T. Imamoto, Y. Sugiura, N. Takiyama, *Tetrahedron Lett.* **1984**, *25*, 4233–4236; c) Y. Tamura, M. Sasho, S. Akai, H. Kishimoto, J.-I. Sekihachi, Y. Kita, *Chem. Pharm. Bull.* **1987**, *35*, 1405–1412; d) T. Imamoto, Y. Sugiura, *J. Phys. Org. Chem.* **1989**, *2*, 93–102; e) K. Nagasawa, K. Ito, *Heterocycles* **1989**, *28*, 703–706; f) G. A. Molander, *Chem. Rev.* **1992**, *92*, 29–68; g) G. Bartoli, M. Bosco, J. V. Beek, L. Sambri, *Tetrahedron Lett.* **1996**, *37*, 2293–2296; h) N. Greeves, J. E. Pease, *Tetrahedron Lett.* **1996**, *37*, 5821–5824; i) M. G. Banwell, D. C. R. Hockless, J. W. Holman, R. W. Longmore, K. J. McRae, H. T. T. Pham, *Synlett* **1999**, *9*, 1491–1494; j) H.-J. Liu, K.-S. Shia, X. Shang, B.-Y. Zhu, *Tetrahedron* **1999**, *55*, 3803–3830; k) G. Bartoli, M. Bosco, E. Di Martino, E. Marcantoni, L. Sambri, *Eur. J. Org. Chem.* **2001**, 2901–2909; l) N. Takeda, T. Imamoto, *Org. Synth.* **2004**, *10*, 200.
- [11] K. Nakamoto, *Infrared and Raman Spectra of Inorganic and Coordination Compounds, Part B*, 6th ed., Wiley, Hoboken, **2009**.
- [12] See the Supporting Information.
- [13] For the preparation of stereodefined alkenyl boronic esters, see: S. Hong, W. Zhang, M. Liu, Z.-J. Yao, W. Deng, *Tetrahedron Lett.* **2016**, *57*, 1–4.
- [14] For the preparation of enantiomerically pure alkyl boronic esters, see: D. Noh, S. K. Yoon, J. Won, J. Y. Lee, J. Yun, *Chem. Asian J.* **2011**, *6*, 1967–1969.
- [15] For the preparation of diastereomerically pure alkyl boronic esters, see: a) K. M. Logan, S. R. Sardini, S. D. White, M. K. Brown, *J. Am. Chem. Soc.* **2018**, *140*, 159–162; b) K. M. Logan, M. K. Brown, *Angew. Chem. Int. Ed.* **2017**, *56*, 851–855; *Angew. Chem.* **2017**, *129*, 869–873.
- [16] C. Gerleve, M. Kischkewitz, A. Studer, *Angew. Chem. Int. Ed.* **2018**, *57*, 2441–2444; *Angew. Chem.* **2018**, *130*, 2466–2469.

Manuscript received: September 7, 2018

Revised manuscript received: November 22, 2018

Accepted manuscript online: November 23, 2018

Version of record online: December 17, 2018

4 Electrochemical Synthesis of Biaryls *via* Oxidative Intramolecular Coupling of Tetra(hetero)arylborates

4.1 Relevance

Out of the top 50 small molecule pharmaceuticals sorted by retail sales, six molecules hold bi(hetero)aryl moieties within their molecular structure, highlighting their key role in drug discovery processes (Figure 7).¹⁸⁵ Additionally, aryl moieties play an outstanding role in material sciences and nanotechnology, as they represent great building blocks for the formation of complex, non-symmetric structures.^{135a,186}

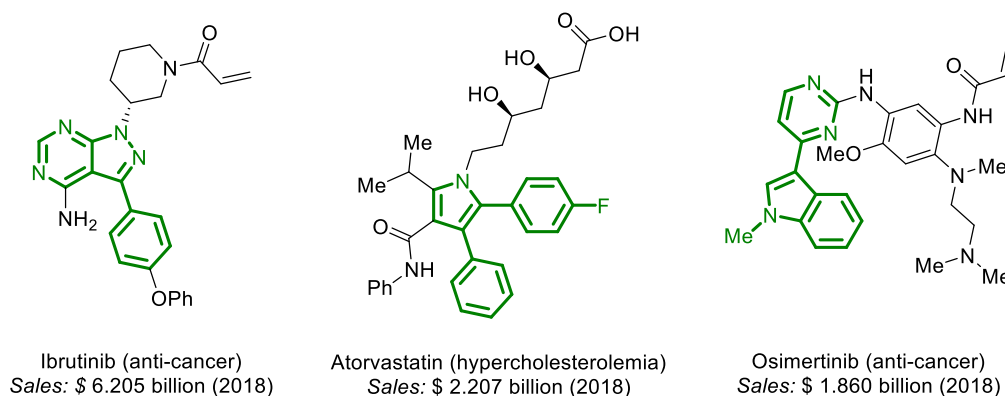


Figure 7: Top-selling drugs (small molecules) with bi(hetero)aryl moieties in 2018 by retail sales. Data was captured from the Njardarson group.¹⁸⁷

Based on their importance, a plethora of methods already exists to create such structures, but none of them can cope with the generality and diversity of transition-metal catalyzed cross-coupling chemistry.¹⁸⁸ This chapter presents an electrochemical and transition-metal free alternative that replaces the need for transition-metals with tetracoordinated organoborates, which serve as mediators for C-C bond formations.

4.2 Preamble

The following work was reprinted with permission from A. Music, A. N. Baumann, P. Spieß, A. Plante-fof, T. C. Jagau and D. Didier, *J. Am. Chem. Soc.* **2020**, *142*, 4341–4348. Copyright© 2020 American Chemical Society.

¹⁸⁵ Njardarson Web site. <https://njardarson.lab.arizona.edu/content/top-pharmaceuticals-poster> (accessed 1st May 2020)

¹⁸⁶ a) S. P. Stanforth, *Tetrahedron* **1997**, *54*, 263–303; b) R. Franke, D. Selent, A. Börner, *Chem. Rev.* **2012**, *112*, 5675–5732; c) K. Okamoto, J. Zhang, J. B. Housekeeper, S. R. Marder, C. K. Luscombe, *Macromolecules* **2013**, *46*, 8059–8078.

¹⁸⁷ N. A. McGrath, M. Bricchacek, J. T. Njardarson, *J. Chem. Educ.* **2010**, *87*, 1348–1349.

¹⁸⁸ a) J. A. Ashenhurst, *Chem. Soc. Rev.* **2010**, *39*, 540–548; b) A. H. Cherney, N. T. Kadunce, S. E. Reisman, *Chem. Rev.* **2015**, *115*, 9587–9652.

Electrochemical Synthesis of Biaryls via Oxidative Intramolecular Coupling of Tetra(hetero)arylborates

Arif Music, Andreas N. Baumann, Philipp Spieß, Allan Plantefol, Thomas C. Jagau, and Dorian Didier*

Cite This: *J. Am. Chem. Soc.* 2020, 142, 4341–4348

Read Online

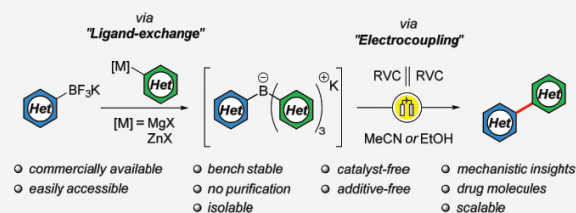
ACCESS |

Metrics & More

Article Recommendations

Supporting Information

ABSTRACT: We report herein versatile, transition metal-free and additive-free (hetero)aryl–aryl coupling reactions promoted by the oxidative electrocoupling of unsymmetrical tetra(hetero)arylborates (TABs) prepared from ligand-exchange reactions on potassium trifluoroarylborates. Exploiting the power of electrochemical oxidations, this method complements the existing organoboron toolbox. We demonstrate the broad scope, scalability, and robustness of this unconventional catalyst-free transformation, leading to functionalized biaryls and ultimately furnishing drug-like small molecules, as well as late stage derivatization of natural compounds. In addition, the observed selectivity of the oxidative coupling reaction is related to the electronic structure of the TABs through quantum-chemical calculations and experimental investigations.



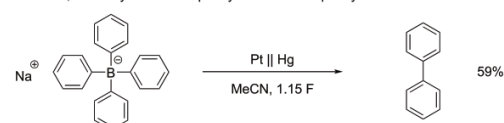
INTRODUCTION

Scientific progress is not linear. Even the most trusted and acknowledged chemical transformations deserve to be examined and leave room for new ideas. As cross-coupling reactions have undoubtedly changed the way organic chemists think about C–C bond formation, they represent an essential tool for synthesis and are one of the most used transformations in organic chemistry.^{1,2} Since their discovery in the late 1970s,³ countless modifications, extensions, and improvements of the pioneering Suzuki–Miyaura coupling have been reported, which have led to a library of available metal catalysts, ligands, and organoboron species, as well as detailed mechanistic insights into this remarkable coupling process.^{1,4–7}

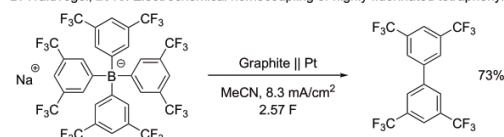
As electrochemistry has recently been welcomed by the community of synthetic chemists as an innately sustainable route to forge new C–C bonds, this work introduces a complementary approach to original transition-metal catalysis by merging the potential of organoboron and electrochemistry.^{8,9} Remarkable advances in the field by Baran,⁹ Yoshida,¹⁰ and many more^{11–13} have led to a revival of vintage electrochemistry from the early 19th century. In an early report from the 1950s, Geske (Scheme 1A) discovered that the tetraphenylborate anion undergoes formation of biphenyl under electrochemical conditions using a rotating platinum disc electrode.¹⁴ More recently, the Waldvogel group was able to demonstrate the electrochemical instability of highly fluorinated commercial tetraphenylborates, resulting interestingly in the formation of homocoupling products (Scheme 1B).¹⁵ They revealed that the oxidative process had to be intramolecular, as only traces of free radical species were detected in solution. In addition, the same group was able to observe one heterocoupling product by GC-MS analysis.^{16,17}

Scheme 1. Precedence in Electrocoupling

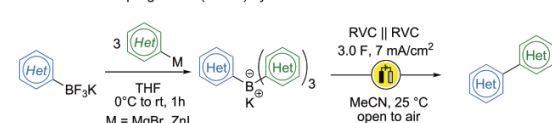
A: Geske, 1959: Synthesis of biphenyl from the tetraphenyl borate anion



B: Waldvogel, 2018: Electrochemical homocoupling of highly fluorinated tetraphenyl borates



C: This work: Coupling of tetra(hetero)aryl borates via electrochemical oxidation



The exact mechanism of the reaction remained however unclear, as both cationic and radical pathways are conceivable.^{15,18,19}

These findings motivate the present work. We envision that “unsymmetrical TAB salts” consisting of three identical aryl

Received: November 26, 2019

Published: February 10, 2020

moieties and a fourth more electron-rich aryl moiety (Scheme 1C) would be prone to selectively achieve electrochemical heterocoupling reactions. While this work does not attempt to compete with the well-established Suzuki–Miyaura coupling, it represents an alternative way to think about coupling reactions in general, in which the C–C forming step is enabled by assembling the components onto boron instead of a transition metal as a templating scaffold. We hypothesize that the most electron-rich aromatic ring gets oxidized first, which then triggers an intramolecular, yet unusual, 1,2-rearrangement of one of the remaining aromatics and therefore prevents undesired homocoupling side reactions.^{18,20}

The synthesis of symmetrical tetra(hetero)arylborates (TABs) was established by Wittig and co-workers²¹ and is performed using organometallic reagents and alkali tetrafluoroborates or boron trifluoride diethyl etherate, performing up to four B–F exchange reactions.^{22,23} We were surprised that, to the best of our knowledge, such methods were not reported for unsymmetrical TABs. Most of the literature relies on the use of highly unstable and oxygen-sensitive triarylboranes via addition of an organometallic reagent, which usually result in low yields and are synthetically unpractical.^{17,24}

Preliminary Findings. We were pleased to find that bench-stable potassium trifluoroarylborates, mainstreamed by the group of Molander,²⁵ undergo rapid ligand-exchange reactions with Grignard reagents under mild conditions, an approach already utilized in the synthesis of sterically demanding triarylboranes and the design of borate ligand/catalyst systems.^{26,27} Following ¹¹B NMR, complete formation of the desired unsymmetrical TAB salt **1a** was observed within an hour at room temperature with stoichiometric amounts of Grignard reagents.²⁸ After an aqueous workup, the air-stable salt was dissolved in MeCN and subjected to nondestructive electrochemical oxidation. Carbon-based electrodes proved to be the most reliable, and the best results were obtained with reticulated vitreous carbon (RVC) electrodes, probably due to their greater working surface. To gain more insight into the reaction pathway, the oxidation process was followed by ¹H NMR spectroscopy in deuterated MeCN (Scheme 2). We found that, in agreement with the results of Waldvogel et al.¹⁵ on homocoupled products, TAB salt **1a** was consumed after 2.5 F. In addition, the reaction proceeded very selectively, as only traces of the undesired homocoupled product were obtained, yielding **2a** as the sole product.

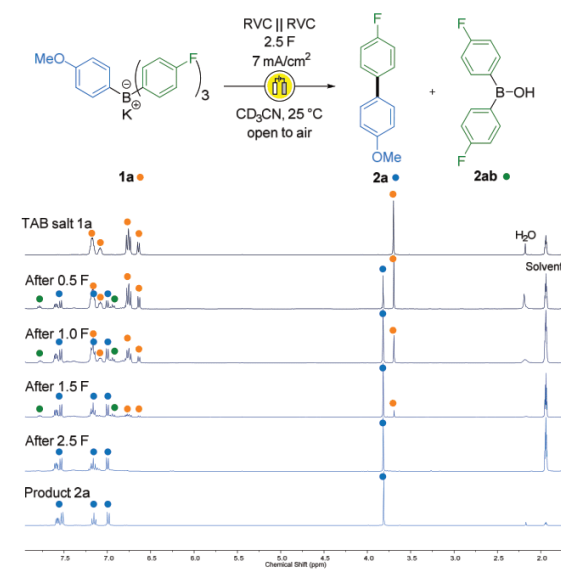
The formation of bis(4-fluorophenyl)borinic acid **2ab** as the major side product was also observed in the ¹H NMR spectra, but its instability under electrochemical conditions did not allow for its quantitative isolation. Interestingly, water did not disturb the reaction process but was consumed during the electrochemical oxidation, indicating its importance in the reaction mechanism.

As neither inert conditions nor the presence of an electrolyte influenced the conversion into **2a**, we decided to routinely perform the electrochemical oxidations in an open-flask setup without electrolyte in wet acetonitrile. The reactions were conducted in an undivided cell under galvanostatic conditions applying a constant current of 7 mA/cm².

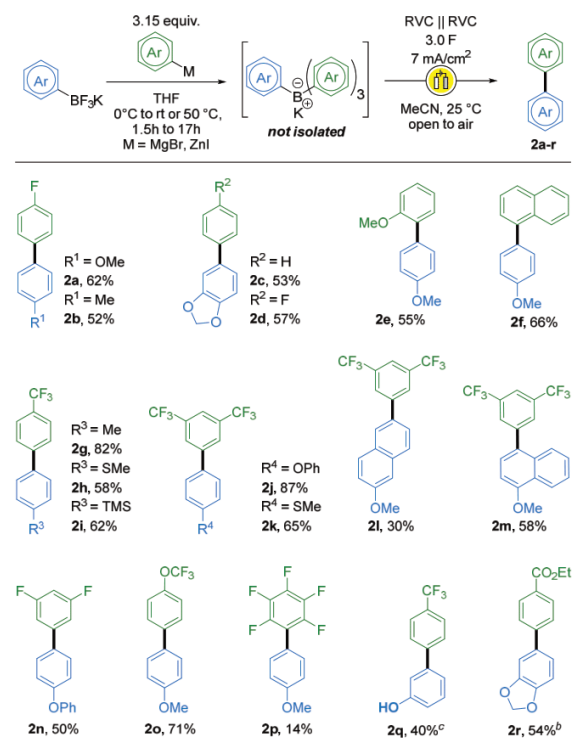
RESULTS AND DISCUSSION

Aryl–Aryl Electrocouplings. As depicted in Scheme 3, various substituted biaryls were synthesized with this procedure, for which no isolation of the intermediate TAB salt was required. 4-Fluoro-4'-methyl-1,1'-biphenyl (**2b**) and

Scheme 2. NMR Study on Oxidative Coupling



Scheme 3. Oxidative Heterocoupling of TAB Salts^a



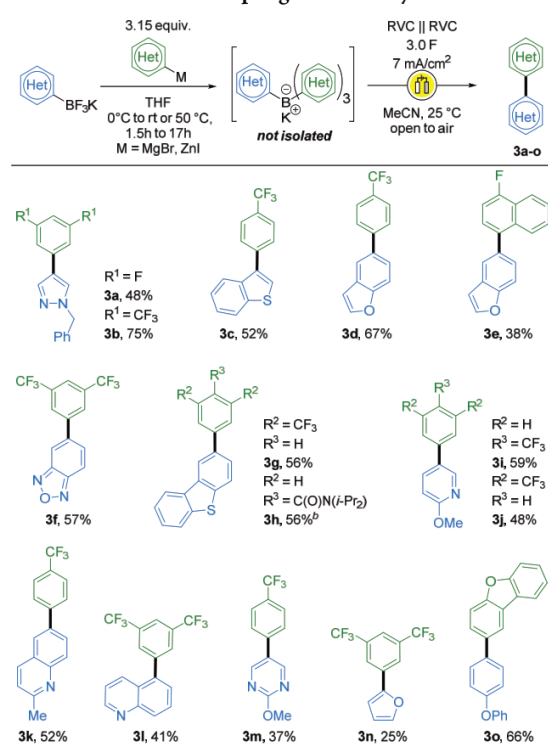
^aYields are stated as isolated yields over two steps. ^bReactions performed using 3.15 equiv of arylzinc reagents. ^c4.20 equiv of aryl-Grignard reagent was used.

three other electron-rich compounds (**2a**, **2c,d**) were isolated in 52–62% yield over two steps. Interestingly, the oxidation process was found to be generally preferred in *p*-position compared to *o*-position, furnishing products **2e,f** in 55–66%

yield. Using *p*-(4-(trifluoromethyl)phenyl)- (2*g*–*i*), 3,5-bis(trifluoromethyl)- (2*j*–*m*), (3,5-difluorophenyl)- (2*n*), and 4-(trifluoromethoxy)phenyl)-magnesium bromide (2*o*), diversely substituted biaryls were isolated in up to 87% yield. As seen for products 2*l* and 2*m*, the position of the methoxy moiety was crucial to navigate the oxidation toward the right aromatic ring within the naphthyl group. A more sterically demanding substrate leading to product 2*p* gave a diminished yield of 14%. Interestingly, the process proved to tolerate free alcohol moieties, as shown by example 2*q*, isolated in 40% yield. Lastly, sensitive functional groups were introduced using organozinc chemistry in the first step. To ensure full conversion into the TAB salts, the reaction mixtures employing arylzinc reagents were heated to 50 °C for 16 h. After successful electrochemical oxidations, ester-substituted product 2*r* was isolated in 54% yield.

(Hetero)aryl–(Hetero)aryl Electrocouplings. With these results in hands, we decided to question the reactivity of heterocyclic derivatives. The smooth formation of the heterocyclic TAB salts was completed within 1 h employing aryl-Grignard reagents. A broad range of electron-rich heterocycles was tolerated (Scheme 4), resulting in 4-1*H*-

Scheme 4. Oxidative Coupling of Heterocyclic TAB Salts^a



^aYields are stated as isolated yields over two steps. ^bReactions performed using 3.15 equiv of arylzinc reagents.

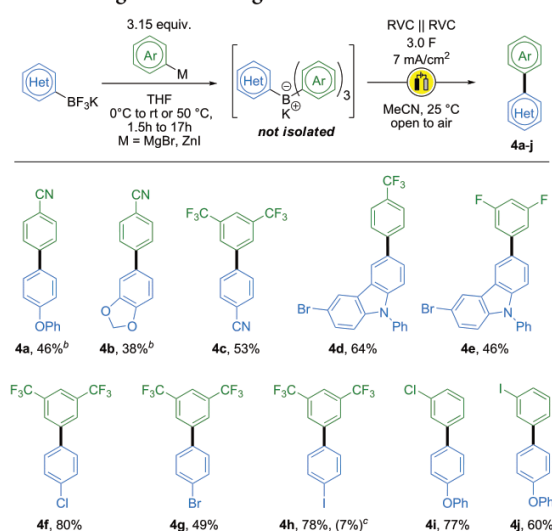
pyrazolyl (3a–b), 3-benzothiophenyl (3c), 5-benzofuranyl (3d,e), and 5-benzo[*c*][1,2,5]oxadiazolyl (3f) substituted biaryl products in 38% to 75% yield. Moreover, dibenzo[*b,d*]-thiophenyl (3g) derivatives afforded the corresponding (hetero)aryl–aryl coupling products in up to 56% yield, including a diisopropylamide group (3h).

Next, we examined electron-poor heterocyclic trifluoroborate salts. Implementation of substituted 3-pyridyl, 5- and 6-quinolinyl, and 5-pyrimidinyl building blocks allowed us to synthesize compounds 3i–m in moderate to good yields of up to 59% over two steps. Unsubstituted five-membered heterocycles such as furanes (3n) resulted in reduced yields of 25% due to polymerization and employing dibenzo[*b,d*]furan-2-ylmagnesium bromide as the corresponding Grignard reagent enabled the synthesis of product 3o in 66%.

Electrocoupling of (Pseudo)halogenated Substrates.

In order to evaluate the feasibility of the electrocoupling in the presence of potentially sensitive halogens and pseudo-halogen groups, a library of new borate salts was in situ created from the corresponding organotrifluoroborates and organometallic reagents (Scheme 5). Following the precedent procedure,

Scheme 5. Electrocoupling Reactions of Halogen- and Pseudo-halogen Containing Substrates^a



^aYields are stated as isolated yields over two steps. ^bReactions performed using 3.15 equiv of arylzinc reagents. ^cUsing Suzuki–Miyaura conditions: boronic acid (1 equiv, in blue), Pd(PPh₃)₄ (5 mol %), K₂CO₃ (2.7 equiv), dioxane/H₂O (2:1, 0.05 M), 70 °C, 24 h, GC yield.

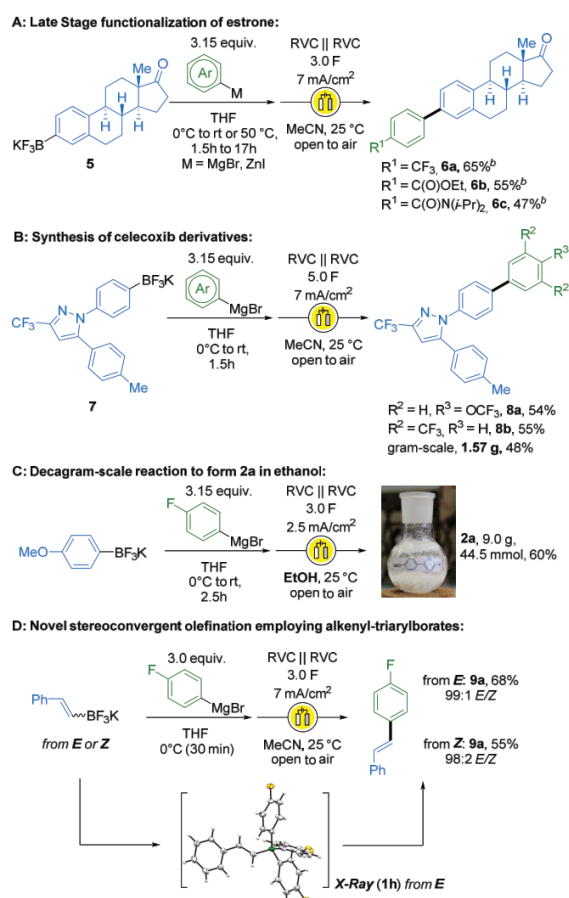
these salts were submitted to electrochemical oxidation without purification. The nitrile group was tested first, giving biaryls 4a,b in 38–46% yield. We attribute such moderate yield to the lower reactivity of the cyano-substituted organozinc reagent in the ligand-exchange reaction to form the intermediate borate salt. The reaction is therefore improved when the cyano group is attached to the organotrifluoroborate (4c, 53%). Starting from a bromo-substituted carbazole-BF₃K derivative, the electrocoupling furnished compounds 4d,e in 46–64% yield. With a chloride substituent in the para-position, the biaryl product 4f was isolated in 80% yield. Remarkably, bromide and iodide were also tolerated in this reaction as compounds 4g and 4h were obtained in moderate to good yield (49–78%).

As compounds 4f–h were generated from the halogenated organotrifluoroborates, we set out to employ a procedure in which the halogens would be introduced from the organometallic reagents. Therefore, meta-substituted chlorinated and

iodinated Grignard reagents were engaged in the electrocoupling reaction, giving **4i** and **4j** in good yields (60–77%). Suzuki–Miyaura cross-coupling conditions only yielded 7% of the desired compound **4h**.

Scope Extension. Having proven the robustness and versatility of this novel approach, we set out to tackle some more interesting molecular architectures. Simple functionalization of estrone derivative **5** was carried out by employing the established two-pot procedure to furnish biaryl compounds in good yields of up to 65%, utilizing organozinc reagents (**6a–c**, Scheme 6A).²⁹ In addition, the trifluoroborate salt **7** derived

Scheme 6. Extension to Drug-like Compounds, Decagram-scale Reactions, and Olefinations^a

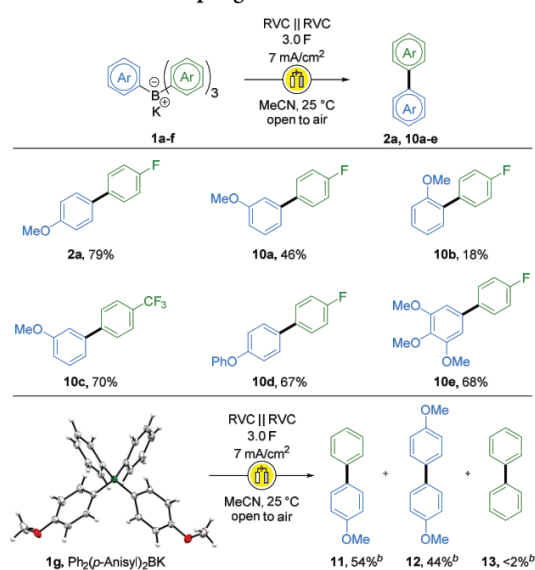


from celecoxib was engaged in the oxidative coupling process,³⁰ delivering two drug-like analogs **8a,b** in 54% and 55%, respectively. The reaction was successfully scaled up to 6 mmol, yielding product **8b** on a gram scale (1.57 g, 48%, Scheme 6B) and an additional decagram-scale process was designed.²⁸ The initial test substrate **1a** was considered for this experiment, and acetonitrile was replaced by ethanol as a more environmentally benign solvent.³¹ The crude material was simply plugged through a short pad of silica to remove residual salts, and product **2a** was isolated in 60% yield (9.0 g, Scheme

6C). To further showcase the potential of boron as a templating scaffold, we engaged *E*- and *Z*-styryltrifluoroborate salts as coupling partners in our sequential approach (Scheme 6D). The existence of those novel tetraorganoborate salts was confirmed by X-ray of intermediate **1h**. Performing the subsequent electrochemical olefination, only the thermodynamically favored product **9a** was isolated with high selectivity in up to 68% yield, resulting in a stereoconvergent method. We propose that the intermediate radical species is allowed to freely rotate around the oxidized C–C double bond.

Trends in Selectivity. In order to support our postulate that electronic effects play a determinant role in the selectivity of the electrochemical process, we set out to isolate selected organoborate salts and run the electrocoupling on pure compounds (Scheme 7). TAB salt **1a** bearing a *p*-anisyl

Scheme 7. Electrocoupling of Pure Salts^a



^aTAB salts were isolated by precipitation.²⁸ ^bGC ratios determined from crude mixtures using *n*-undecane as an internal standard.

group was prepared, as well as its *m*- (**1b**) and *o*-anisyl (**1c**) isomers. As seen in Scheme 7, the yields decreased from 79% to 18% going from *para*- over *meta*- to *ortho*-substituted compounds (**2a**, **10a,b**), while increasing amounts of homocoupling products were observed. While the lower yield in the case of *ortho*-substituted substrates was attributed to steric hindrance, the destabilizing effects of a *meta*-methoxy group provoked a slight decrease in selectivity. However, this negative effect was compensated when replacing the *p*-fluoride of the electron-deficient aryl groups on the borate by electron-poorer moieties such as *p*-(trifluoromethyl)phenyl. In this case, product **10c** was isolated in 70% yield. Increasing the electron-richness of the partner gave similar results (**10d,e**). Careful choice of the aromatic residues and accompanied balance of the electronic properties can clearly overcome most limitations even though some challenges still need to be tackled.²⁸ We last submitted the C₂-symmetrical potassium bis(4-methoxyphenyl)diphenylborate **1g** to the electrocoupling conditions in order to evaluate the propensity of the remaining unoxidized aryl groups to undergo C–C bond formation. As

expected, the experiment resulted in trace amounts of biphenyl 13. However, an almost statistical distribution of homocoupled 4,4'-dimethoxy-1,1'-biphenyl 12 and the desired heterocoupled product 11 was observed, which indicates that the migratory step is extremely fast and therefore leads to a lack of selectivity (Scheme 7).

MECHANISTIC STUDY

CV and Computational Data. Consequently, we became interested in a greater understanding of our electrocoupling reaction. Thus, next paragraphs will be devoted to creating a mechanistic picture of the oxidative transformation. In order to assess the influence of substituents borne by the aryl groups in the first oxidation step, we conducted quantum-chemical calculations based on coupled-cluster and density functional theory (DFT). These theoretical results correlate with experimental values for oxidation potential studies of salts 1a–g, measured by cyclic voltammetry (Figure 1B).²⁸ These

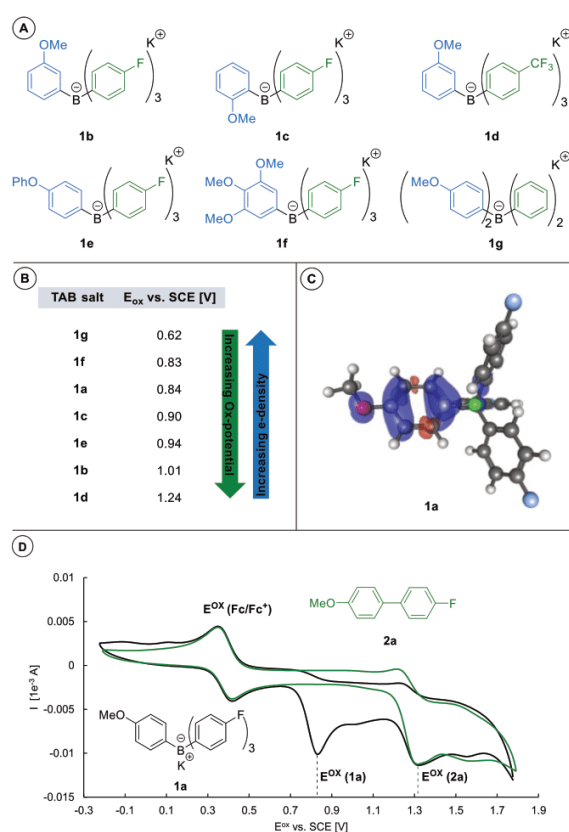


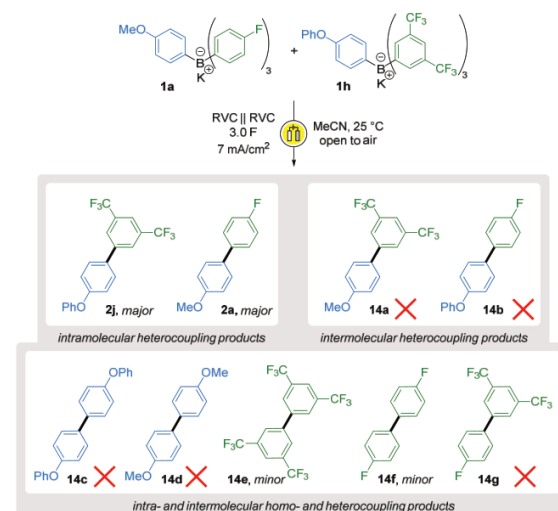
Figure 1. TAB salts 1b–g (A), experimental oxidation potentials of TAB salts 1a–g (B) with spin density after oxidation of 1a (C) and cyclic voltammetry of TAB salt 1a (D) calibrated to the reversible ferrocene oxidation (Fc/Fc⁺).

results also adhere to the correlation between electron-richness of the different aromatic patterns of the TAB salts and a decrease in their oxidation potentials. It is important to note that cyclic voltammetry performed on all salts only revealed one significant oxidation value within the measured range (Figure 1D).²⁸ To characterize the change in the electronic

structure upon oxidation of the TAB salts (1a–g), spin and charge densities were computed based on Mulliken population analysis of the DFT results. Charge densities were additionally computed using the ChElPG approach.²⁸ These analyses indicate that only the most electron-rich aromatic ring is selectively oxidized in all cases, while the charge and spin densities of the other aromatic substituents only change insignificantly and thereby confirm our assumptions. This is illustrated for TAB salt 1a in Figure 1C, where blue and red areas represent positive and negative spin densities after oxidation.

Investigative Work. As a next step, crossover experiments were performed in order to confirm or exclude the possibility of intermolecular couplings (Scheme 8). For this purpose, two

Scheme 8. Crossover Experiments⁴²



⁴²TAB salts were generated in situ.

nonsymmetrical borate salts 1a and 1h bearing different aryl groups were generated from the corresponding organotrifluoroborates and submitted to the electrocoupling reaction together. If one assumes that the reaction is exclusively intramolecular, the only products of the reaction are heterocoupling products 2j and 2a, and homocoupling 14e and 14f. As previously discussed, homocoupling products result from an unselective oxidation and are only observed as the minor biaryl in the reaction. However, if the intramolecular reaction were to be in competition with an intermolecular process, one can expect products 14a, 14b, 14c, 14d, and 14g. Submitting 1a and 1h to electrochemical conditions revealed the exclusive formation of 2j and 2a in major amounts and 14e and 14f as minor products. The absence of other products in the reaction mixture brings additional proof that the transformation goes through an intramolecular rearrangement, excluding any possibility of intermolecular coupling.

To reveal the one- or two-electron character of the electrocoupling reaction, several tests were conducted building on the cyclic voltammetry data, as it has shown that only one oxidation potential can be observed in the measurement window (Figure 1, D). To advocate this hypothesis, we performed potentiostatic experiments on 1a in which the voltage was set up to the constant value of 1.6 V (vs SCE). The

same conversion as for galvanostatic conditions into the biaryl **2a** was detected, indicating a one-electron process. To support this first assumption, a detailed look at the conversion rates during the electrocoupling reaction of TAB salt **1a** was carried out. Therefore, a sample with an internal standard was gradually taken during the electrochemical oxidation process (Figure 2). As highlighted in Figure 2, the transformation at 1

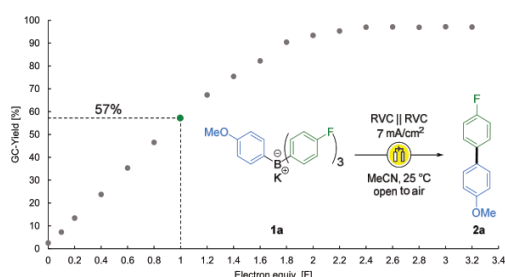


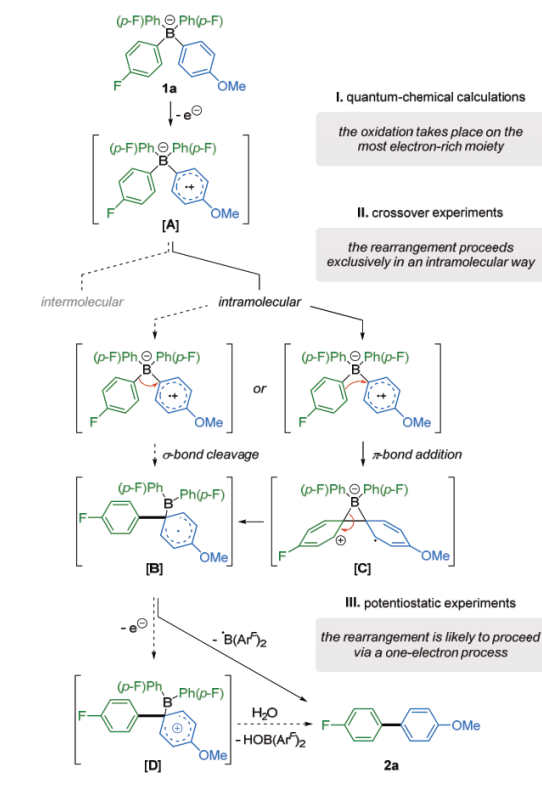
Figure 2. Measured GC yields during the electrochemical oxidation of **1a** toward **2a** with *n*-undecane as an internal standard.

F already results in a GC yield of 57% for **2a**, which assists the hypothesis of a one-electron process. Even in the unlikely scenario in which every electron performs the oxidation on one borate molecule, the conversion in a two-electron pathway after 1 F cannot exceed 50%.

The oxidative coupling of **1a** toward the formation of **2a** can also be promoted under non-electrochemical conditions with chemical oxidants such as CAN, PIDA, and ferrocenium. However, while ferrocenium furnished comparable results, CAN and PIDA gave significantly lower selectivity and yields.²⁸ Although those one-electron oxidants showcased similar reactivity to our electrochemical procedure, the use of two-electron oxidants such as I₂ or NBS resulted in the decomposition of our salts.

Summarized Mechanism. Even though a two-electron process is still conceivable, all indications (theoretical calculations, crossover experiments, cyclic voltammetry, potentiostatic/chemical experiments, and conversion rates) contribute and support the mechanistic pathway proposed in Scheme 9. The reaction starts with the selective oxidation of the most electron-rich aromatic ring of **1a** (supported by quantum-chemical calculations, as shown in Figure 1, giving intermediate [A]) and is followed by a pseudo-1,2-metalate rearrangement. This can be done via σ -bond cleavage or through π -addition, given that the reaction proceeds exclusively in an intramolecular way (as demonstrated with crossover experiments, Scheme 8). Although no calculations could be performed on this step, we assume, for geometric reasons, that the rearrangement takes place through π -orbitals and gives the radical cationic boracyclopropane species [C]. Such intermediate was already proposed in previous literature reports.^{18,19} It is important to note however that a σ -bond cleavage would result in the same intermediate [B]. Two different pathways can follow in the elimination/rearomatization process. Either an additional electron abstraction can occur (second oxidation, [D]) or a direct elimination of a boron-radical species can occur. As supported by galvanostatic experiments (Figure 2) and tests under chemical oxidation, we assume that the rearomatization likely occurs through a one-electron process, furnishing the biaryl compound **2a**.

Scheme 9. Proposed Mechanism for the Electrocoupling of TAB Salt **1a**



CONCLUSIONS

In summary, we have demonstrated that a broad range of heterosubstituted TAB salts are accessible using simple and rapid ligand-exchange reactions on potassium trifluoroborates. We have furthermore shown, that these salts are smoothly oxidized exploiting the power of electrochemistry to furnish substituted heterocyclic biaryl systems without the necessity of any additives or transition metals. This conceptual two-pot approach has shown to be robust toward moisture and air and therefore allowed us to routinely synthesize small drug-like molecules on gram scale. A great variety of functional groups were tolerated, including several heterocyclic systems. Lastly, theoretical calculations analyzing the electronic structure of these systems combined with measured oxidation potentials, crossover, and potentiostatic experiments allowed us to rationalize the outcome of the oxidative electrocoupling presented.

ASSOCIATED CONTENT

Supporting Information

The Supporting Information is available free of charge at <https://pubs.acs.org/doi/10.1021/jacs.9b12300>.

Experimental procedures, compound characterization, theoretical calculation, cyclic voltammetry, X-ray diffraction data (PDF)

Structure of **1g** (CIF)

Structure of **1h** (CIF)

AUTHOR INFORMATION

Corresponding Author

Dorian Didier – Ludwig-Maximilians-Universität München, Department Chemie, 81377 München, Germany; orcid.org/0000-0002-6358-1485; Email: dorian.didier@cup.uni-muenchen.de

Authors

Arif Music – Ludwig-Maximilians-Universität München, Department Chemie, 81377 München, Germany; orcid.org/0000-0002-4786-1268

Andreas N. Baumann – Ludwig-Maximilians-Universität München, Department Chemie, 81377 München, Germany; orcid.org/0000-0002-2811-1787

Philipp Spieß – Ludwig-Maximilians-Universität München, Department Chemie, 81377 München, Germany

Allan Plantefol – Sorbonne University, 75005 Paris, France

Thomas C. Jagau – Ludwig-Maximilians-Universität München, Department Chemie, 81377 München, Germany; orcid.org/0000-0001-5919-424X

Complete contact information is available at:

<https://pubs.acs.org/10.1021/jacs.9b12300>

Notes

The authors declare no competing financial interest.

ACKNOWLEDGMENTS

Dr. Robert Francke (University Rostock) is gratefully acknowledged for his help with initial electrochemical measurements and for technical support. Dr. Peter Mayer (LMU München) is kindly acknowledged for help with X-ray diffraction data. Robert J. Mayer (LMU Munich) is kindly acknowledged for help with cyclic voltammetry data. We thank the Chemical Industry Fund (FCI), the Deutsche Forschungsgemeinschaft (DFG grant DI 2227/2-1 + JA 2794/1-1), Sonderforschungsbereich SFB749), and the Ludwig-Maximilians-Universität München (LMU) for financial support.

REFERENCES

- (1) Biffis, A.; Centomo, P.; Del Zotto, A.; Zecca, M. Pd Metal Catalysts for Cross-Couplings and Related Reactions in the 21st Century: A Critical Review. *Chem. Rev.* **2018**, *118*, 2249–2295.
- (2) Brown, D. G.; Boström, J. Analysis of Past and Present Synthetic Methodologies on Medicinal Chemistry: Where Have All the New Reactions Gone? *J. Med. Chem.* **2016**, *59*, 4443–4458.
- (3) (a) Miyaura, N.; Suzuki, A. Stereoselective Synthesis of Arylated (E)-Alkenes by the Reaction of Alk-1-enylboranes with Aryl Halides in the Presence of Palladium Catalyst. *J. Chem. Soc., Chem. Commun.* **1979**, 866–867. (b) Miyaura, N.; Yamada, K.; Suzuki, A. A New Stereospecific Cross-Coupling by the Palladium-Catalyzed Reaction of 1-Alkenylboranes with 1-Alkynyl Halides. *Tetrahedron Lett.* **1979**, *20*, 3437–3440.
- (4) For reviews on organoboron chemistry, see: (a) Fyfe, J. W. B.; Watson, A. J. B. Recent Developments in Organoboron Chemistry: Old Dogs, New Tricks. *Chem.* **2017**, *3*, 31–55. (b) Miyaura, N.; Suzuki, A. Palladium-Catalyzed Cross-Coupling Reactions of Organoboron Compounds. *Chem. Rev.* **1995**, *95*, 2457–2483.
- (5) (a) Roy, D.; Uozumi, Y. Recent Advances in Palladium-Catalyzed Cross-Coupling Reactions at ppm to ppb Molar Catalyst Loadings. *Adv. Synth. Catal.* **2018**, *360*, 602–625. (b) Asghar, S.; Tailor, S. B.; Elorriaga, D.; Bedford, R. B. Cobalt-Catalyzed Suzuki Biaryl Coupling of Aryl Halides. *Angew. Chem., Int. Ed.* **2017**, *56*, 16367–16370.
- (6) For reviews on (radical) C–H activation, see: (a) Gandeepan, P.; Müller, T.; Zell, D.; Cera, G.; Warratz, S.; Ackermann, L. 3d Transition Metals for C–H Activation. *Chem. Rev.* **2019**, *119*, 2192–2452. (b) Yi, H.; Zhang, G.; Wang, H.; Huang, Z.; Wang, J.; Singh, A. K.; Lei, A. Recent Advances in Radical C–H Activation/Radical Cross-Coupling. *Chem. Rev.* **2017**, *117*, 9016–9085.
- (7) (a) Liu, W.; Li, J.; Querard, P.; Li, C.-J. Transition-Metal-Free C–C, C–O, and C–N Cross-Couplings Enabled by Light. *J. Am. Chem. Soc.* **2019**, *141*, 6755–6764. (b) Yan, H.; Hou, Z.-W.; Xu, H.-C. Photoelectrochemical C–H Alkylation of Heteroarenes with Organotrifluoroborates. *Angew. Chem., Int. Ed.* **2019**, *58*, 4592–4595. (c) Wiebe, A.; Schollmeyer, D.; Dyballa, K. M.; Franke, R.; Waldvogel, S. R. Selective Synthesis of Partially Protected Non-symmetric Biphenols by Reagent- and Metal-Free Anodic Cross-Coupling Reaction. *Angew. Chem., Int. Ed.* **2016**, *55*, 11801–11805. (d) Sun, C.-L.; Shi, Z.-J. Transition-Metal-Free Coupling Reactions. *Chem. Rev.* **2014**, *114*, 9219–9280.
- (8) For reviews on electrochemistry, see: (a) Wiebe, A.; Gieshoff, T.; Möhle, S.; Rodrigo, E.; Zirbes, M.; Waldvogel, S. R. Electrifying Organic Synthesis. *Angew. Chem., Int. Ed.* **2018**, *57*, 5594–5619. (b) Möhle, S.; Zirbes, M.; Rodrigo, E.; Gieshoff, T.; Wiebe, A.; Waldvogel, S. R. Photoelectrochemical C–H Alkylation of Heteroarenes with Organotrifluoroborates. *Angew. Chem., Int. Ed.* **2018**, *57*, 6018–6041. (c) Lennox, A. J. J.; Nutting, J. E.; Stahl, S. S. Selective electrochemical generation of benzylic radicals enabled by ferrocene-based electron-transfer mediators. *Chem. Sci.* **2018**, *9*, 356–361. (d) Schlegel, G.; Schäfer, H. J. Anodische Oxidation von Organoborverbindungen. *Chem. Ber.* **1984**, *117*, 1400–1423.
- (9) (a) Yan, M.; Kawamata, Y.; Baran, P. S. Synthetic Organic Electrochemical Methods Since 2000: On the Verge of a Renaissance. *Chem. Rev.* **2017**, *117*, 13230–13319. (b) Horn, E. J.; Rosen, R. R.; Baran, P. S. Synthetic Organic Electrochemistry: An Enabling and Innately Sustainable Method. *ACS Cent. Sci.* **2016**, *2*, 302–308.
- (10) (a) Yoshida, J.-i.; Shimizu, A.; Hayashi, R. Electrogenerated Cationic Reactive Intermediates: The Pool Method and Further Advances. *Chem. Rev.* **2018**, *118*, 4702–4730. (b) Morofuji, T.; Shimizu, A.; Yoshida, J.-i. Electrochemical C–H Amination: Synthesis of Aromatic Primary Amines via N-Arylpyridinium Ions. *J. Am. Chem. Soc.* **2013**, *135*, 5000–5003. (c) Yoshida, J.-i.; Nishiwaki, K. Redox selective reactions of organo-silicon and -tin compounds. *J. Chem. Soc., Dalton Trans.* **1998**, 2589–2596.
- (11) (a) Elsler, B.; Schollmeyer, D.; Dyballa, K. M.; Franke, R.; Waldvogel, S. R. Metal- and Reagent-Free Highly Selective Anodic Cross-Coupling Reaction of Phenols. *Angew. Chem., Int. Ed.* **2014**, *53*, 5210–5213. (b) Kirste, A.; Elsler, B.; Schnakenburg, G.; Waldvogel, S. R. Efficient Anodic and Direct Phenol-Arene C,C Cross-Coupling: The Benign Role of Water or Methanol. *J. Am. Chem. Soc.* **2012**, *134*, 3571–3576.
- (12) Shono, T.; Hamaguchi, H.; Matsumura, Y. Electroorganic Chemistry. Anodic Oxidation of Carbamates. *J. Am. Chem. Soc.* **1975**, *97*, 4264–4268.
- (13) For a review on electrochemical C–H functionalization, see: Kärkäs, M. D. Electrochemical strategies for C–H functionalization and C–N bond formation. *Chem. Soc. Rev.* **2018**, *47*, 5786–5865.
- (14) Geske, D. H. The Electrooxidation of the Tetraphenylborate Ion; An Example of a Secondary Chemical Reaction Following the Primary Electrode Process. *J. Phys. Chem.* **1959**, *63*, 1062.
- (15) Beil, S. B.; Möhle, S.; Enders, P.; Waldvogel, S. R. Electrochemical instability of highly fluorinated tetraphenyl borates and syntheses of their respective biphenyls. *Chem. Commun.* **2018**, *54*, 6128–6131.
- (16) Lu, Z.; Lavendomme, R.; Burghaus, O.; Nitschke, J. R. A Zn₄L₆ Capsule with Enhanced Catalytic C–C Bond Formation Activity upon C₆₀ Binding. *Angew. Chem., Int. Ed.* **2019**, *58*, 9073–9077.
- (17) Mizuno, H.; Sakurai, H.; Amaya, T.; Hirao, T. Oxovanadium(V)-catalyzed oxidative biaryl synthesis from organoborate under O₂. *Chem. Commun.* **2006**, *48*, 5042–5044.
- (18) For a review on oxidative organoboron coupling, see: Sakurai, H.; Dhital, R. N. Oxidative Coupling of Organoboron Compounds. *Asian J. Org. Chem.* **2014**, *3*, 668–684.

(19) (a) Geiger, W. E.; Barrière, F. Organometallic Electrochemistry Based on Electrolytes Containing Weakly-Coordinating Fluoroarylborate Anions. *Acc. Chem. Res.* **2010**, *43*, 1030–1039. (b) Pal, P. K.; Chowdhury, S.; Drew, M. G. B.; Datta, D. The electrooxidation of the tetraphenylborate ion revisited. *New J. Chem.* **2002**, *26*, 367–371. (c) Sakurai, H.; Morimoto, C.; Hirao, T. Oxidative Ligand Coupling of Tetraarylborates Promoted by Chlorosilane and Molecular Oxygen. *Chem. Lett.* **2001**, *30*, 1084–1085. (d) Abley, P.; Halpern, J. Oxidation of Tetraphenylborate by Hexachloroiridate(IV). *J. Chem. Soc. D* **1971**, *20*, 1238–1239. (e) Geske, D. H. Evidence for the Formation of Biphenyl by Intramolecular Dimerization in the Electrooxidation of Tetraphenylborate Ion. *J. Phys. Chem.* **1962**, *66*, 1743–1744.

(20) For a review on metalate shifts in organoboron chemistry, see: Namirembe, S.; Morken, J. P. Reactions of organoboron compounds enabled by catalyst-promoted metalate shifts. *Chem. Soc. Rev.* **2019**, *48*, 3464–3474.

(21) Wittig, G.; Keicher, G.; Rückert, A.; Raff, P. Über Boralkalimetall-organische Komplexverbindungen. *Liebigs Ann. Chem.* **1949**, *563*, 110–126.

(22) Vasu, D.; Yorimitsu, H.; Osuka, A. Palladium-Assisted “Aromatic Metamorphosis” of Dibenzothiophenes into Triphenylenes. *Angew. Chem., Int. Ed.* **2015**, *54*, 7162–7166.

(23) Wittig, D.; Raff, P. Über Komplexbildung mit Triphenylbor. *Liebigs Ann. Chem.* **1951**, *573*, 195–209.

(24) Siegmann, K.; Pregosin, P. S.; Venanzi, L. M. Reaction of Organoboron Compounds with Platinum(II) Disolvento Complexes. *Organometallics* **1989**, *8*, 2659–2664.

(25) For a review on organotrifluoroborates, see: Molander, G. A.; Ellis, N. Organotrifluoroborates: Protected Boronic Acids That Expand the Versatility of the Suzuki Coupling Reaction. *Acc. Chem. Res.* **2007**, *40*, 275–286.

(26) (a) Schickedanz, K.; Radtke, J.; Bolte, M.; Lerner, H.-W.; Wagner, M. Facile Route to Quadruply Annulated Borepins. *J. Am. Chem. Soc.* **2017**, *139*, 2842–2851. (b) Dorkó, E.; Szabó, M.; Kótai, B.; Pápai, I.; Domján, A.; Soós, T. Expanding the Boundaries of Water-Tolerant Frustrated Lewis Pair Hydrogenation: Enhanced Back Strain in the Lewis Acid Enables the Reductive Amination of Carbonyls. *Angew. Chem., Int. Ed.* **2017**, *56*, 9512–9516. (c) Gyömöre, Á.; Bakos, M.; Földes, T.; Pápai, I.; Domján, A.; Soós, T. Moisture-Tolerant Frustrated Lewis Pair Catalyst for Hydrogenation of Aldehydes and Ketones. *ACS Catal.* **2015**, *5*, 5366–5372.

(27) (a) Ben Saida, A. B.; Chardon, A.; Osi, A.; Tumanov, N.; Wouters, J.; Adjieufack, A. I.; Champagne, B.; Berionni, G. Pushing the Lewis Acidity Boundaries of Boron Compounds with Non-Planar Triarylboranes Derived from Triptycenes. *Angew. Chem., Int. Ed.* **2019**, *58*, 16889. (b) Konishi, S.; Iwai, T.; Sawamura, M. Synthesis, Properties, and Catalytic Application of a Triptycene-Type Borate-Phosphine Ligand. *Organometallics* **2018**, *37*, 1876–1883. (c) Atsushi, S. JP2016150925, 2016.

(28) For further details, see the [Supporting Information](#).

(29) van der Born, D.; Sewing, C.; Herscheid, J. K. D. M.; Windhorst, A. D.; Orru, R. V. A.; Vugts, D. J. A Universal Procedure for the [¹⁸F]Trifluoromethylation of Aryl Iodides and Aryl Boronic Acids with Highly Improved Specific Activity. *Angew. Chem., Int. Ed.* **2014**, *53*, 11046–11050.

(30) He, Z.; Song, F.; Sun, H.; Huang, Y. Transition-Metal-Free Suzuki-Type Cross-Coupling Reaction of Benzyl Halides and Boronic Acids via 1,2-Metalate Shift. *J. Am. Chem. Soc.* **2018**, *140*, 2693–2699.

(31) (a) Clarke, C. J.; Tu, W.-C.; Levers, O.; Bröhl, A.; Hallett, J. P. Green and Sustainable Solvents in Chemical Processes. *Chem. Rev.* **2018**, *118*, 747–800. (b) Byrne, F. P.; Jin, S.; Paggiola, G.; Petchey, T. H. M.; Clark, J. H.; Farmer, T. J.; Hunt, A. J.; McElroy, C. R.; Sherwood, J. Tools and techniques for solvent selection: green solvent selection guides. *Sustainable Chem. Processes* **2016**, *4*, 7.

5 Electro-Olefination – a Catalyst Free, Stereoconvergent Strategy for the Functionalization of Alkenes

5.1 Relevance

Convergent protocols are highly respected synthetic tools, as they allow for the transformation of racemic compounds into stereo- or even enantio-enhanced and more valuable products.¹⁸⁹ Exceptional synthetic and mechanistic contributions by the Fu group and others have shown the power of nickel catalysis in combination with chiral ligands to perform stereo- and enantioconvergent cross-coupling chemistry. While alkyl-aryl¹⁹⁰, alkyl-alkyl¹⁹¹, aryl-alkynyl¹⁹² couplings are well-described, convergent protocols involving and preserving alkenyl-moieties are still rare.¹⁹³

Even though radical intermediates with Ni(I), Ni(II) and Ni(III) species are believed to play key roles in all of those transformations¹⁹⁴ and the group of Molander has demonstrated the applicability of stereoconvergent strategies in SET photoredox/nickel dual catalysis,^{161b,195} there are very few reports of electrochemical olefination chemistry and none on stereoconvergent and transition-metal free variants thereof.¹⁹⁶ To fill this gap, the following chapter presents a stereoconvergent and transition-metal free electrochemical formation of arylated alkenes *via* tetracoordinated organoborates.

5.2 Preamble

The following work was reprinted with permission from A. N. Baumann, A. Music, J. Dechent, N. Müller, T. C. Jagau and D. Didier, *Chem. Eur. J.* **2020**, *26*, 8382–8387. Copyright© 2020 Wiley-VCH Verlag GmbH & Co. KGaA, Weinheim. The project was conducted in equal contribution with A. N. Baumann.

¹⁸⁹ a) Y. Apeloig, Z. Rappoport, *J. Am. Chem. Soc.* **1979**, *101*, 5095–5098; b) J. K. Park, H. H. Lackey, B. A. Ondrusek, D. T. McQuade, *J. Am. Chem. Soc.* **2011**, *133*, 2410–2413.

¹⁹⁰ a) P. M. Lundin, G. C. Fu, *J. Am. Chem. Soc.* **2010**, *132*, 11027–11029; b) S. L. Zultanski, G. C. Fu, *J. Am. Chem. Soc.* **2011**, *133*, 15362–15364; c) Y. Liang, G. C. Fu, *J. Am. Chem. Soc.* **2015**, *137*, 9523–9526; d) A. Varenikov, M. Gandelman, *J. Am. Chem. Soc.* **2019**, *141*, 10994–10999.

¹⁹¹ a) B. Saito, G. C. Fu, *J. Am. Chem. Soc.* **2008**, *130*, 6694–6695; b) Z. Lu, A. Wilsily, G. C. Fu, *J. Am. Chem. Soc.* **2011**, *133*, 8154–8157; c) A. Wilsily, F. Tramutola, N. A. Owston, G. C. Fu, *J. Am. Chem. Soc.* **2012**, *134*, 5794–5797; d) C. J. Cordier, R. J. Lundgren, G. C. Fu, *J. Am. Chem. Soc.* **2013**, *135*, 10946–10949.

¹⁹² a) S. W. Smith, G. C. Fu, *J. Am. Chem. Soc.* **2008**, *130*, 12645–12647; b) N. D. Schley, G. C. Fu, *J. Am. Chem. Soc.* **2014**, *136*, 16588–16593.

¹⁹³ a) J. Choi, P. Martín-Gago, G. C. Fu, *J. Am. Chem. Soc.* **2014**, *136*, 12161–12165; b) Z. Wang, H. Yin, G. C. Fu, *Nature* **2018**, *563*, 379–383.

¹⁹⁴ H. Yin, G. C. Fu, *J. Am. Chem. Soc.* **2019**, *141*, 15433–15440.

¹⁹⁵ O. Gutierrez, J. C. Tellis, D. N. Primer, G. A. Molander, M. C. Kozlowski, *J. Am. Chem. Soc.* **2015**, *137*, 4896–4899.

¹⁹⁶ a) C. Amatore, C. Cammoun, A. Jutand, *Adv. Synth. Catal.* **2007**, *349*, 292–296; b) E. E. López-López; J. A. Pérez-Bautista, F. Sartillo-Piscil, B. A. Frontana-Urbe, *Beilstein J. Org. Chem.* **2018**, *14*, 547–552; c) B. Chakraborty, A. Kostenko, P. W. Menezes, M. Driess, *Chem. Eur. J.* **2020**, 10.1002/chem.202001654.

Electrochemistry

Electro-Olefination—A Catalyst Free Stereoconvergent Strategy for the Functionalization of Alkenes

Andreas N. Baumann⁺, Arif Music⁺, Jonas Dechent, Nicolas Müller, Thomas C. Jagau, and Dorian Didier^{*[a]}

In memoriam to Professor Rolf Huisgen

Abstract: Conventional methods carrying out C(sp²)–C(sp²) bond formations are typically mediated by transition-metal-based catalysts. Herein, we conceptualize a complementary avenue to access such bonds by exploiting the potential of electrochemistry in combination with organoboron chemistry. We demonstrate a transition metal catalyst-free electrocoupling between (hetero)aryls and alkenes through readily available alkenyl-tri(hetero)aryl borate salts (ATBs) in a stereoconvergent fashion. This unprecedented transformation was investigated theoretically and experimentally and led to a library of functionalized alkenes. The concept was then carried further and applied to the synthesis of the natural product pinosylvin and the derivatization of the steroidal dehydroepiandrosterone (DHEA) scaffold.

Despite its young history of only a few decades, the Suzuki–Miyaura reaction is one of the most utilized reactions in modern organic chemistry.^[1,2] The palladium-catalyzed coupling of boronic acids with organohalides was not only awarded with the Nobel prize in 2010, in fact, a recent study ranks the Suzuki–Miyaura coupling as one of the most frequently used reactions (5th place) in medicinal chemistry.^[1] Besides, many other transition-metal-mediated cross-couplings, namely Stille, Heck, Negishi, Sonogashira, Hiyama and Kumada are likewise powerful tools to forge new C–C bonds.^[3] Such indispensable strategies undoubtedly display many advantages and have inspired us to challenge the formation of C–C bonds without the need of the commonly used transition-metal cata-

lysts, thus breaking new grounds in the field of cross-coupling reactions. We first started our ambitious concept by replacing the catalyst with an electrochemical setup. Innate advantages, including the use of inexpensive and reusable electrodes, reaction tuneability and scalability do not only rely on the modern and cutting-edge work from Baran, but trace back to many other advances in electrochemical synthesis since the pioneering works of Volta and Faraday in the 19th century.^[4]

We already employed electrochemistry to initiate aryl–aryl bond formation, inspired by the work of Geske^[5] and Waldvogel^[6] (Scheme 1 A), introducing new hetero-substituted tetraarylborate salts (TABs). We demonstrated that the formation of „unsymmetrical“ TAB salts is enabled by a triple ligand exchange reaction on commercially available organotrifluoroborate species employing aryl–Grignard reagents. Submitting those TABs to mild electrochemical oxidation led to the selective formation of heterocoupled biaryls (Scheme 1 B).^[7]

As an alternative route to conventional cross coupling reactions, the catalyst free Zweifel olefination cannot be neglected.^[8] This powerful methodology enables the stereospesific

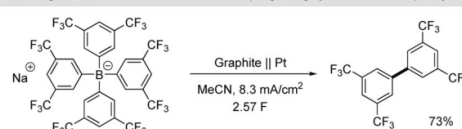
[a] A. N. Baumann,⁺ A. Music,⁺ J. Dechent, N. Müller, Dr. T. C. Jagau, Dr. D. Didier
Department of Chemistry and Pharmacy
Ludwig-Maximilians-University Munich
Butenandtstraße 5–13, Haus F, 81377 Munich (Germany)
E-mail: Dorian.Didier@cup.uni-muenchen.de

[†] These authors contributed equally to this work.

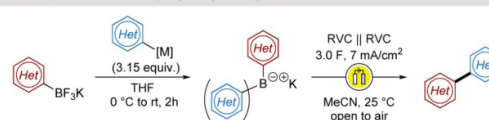
Supporting information and the ORCID identification number(s) for the author(s) of this article can be found under:
<https://doi.org/10.1002/chem.202001394>.

© 2020 The Authors. Published by Wiley-VCH Verlag GmbH & Co. KGaA. This is an open access article under the terms of the Creative Commons Attribution License, which permits use, distribution and reproduction in any medium, provided the original work is properly cited.

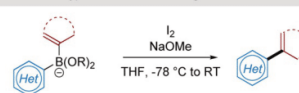
A - Waldvogel, 2018 - Electrochemical homocoupling of highly fluorinated tetraphenyl borates



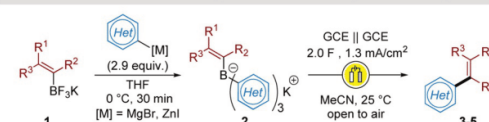
B - Didier, 2020 - Electrocoupling using tetraaryl borates under electrochemical oxidation



C - Aggarwal, 2017 - Zweifel-type olefination of bisorganoborinates



D - This work - Electro-olefination using bench-stable or in-situ generated tetraorgano borates



Scheme 1. Electrochemical/ Transition-metal catalyst-free C–C couplings.

formation of alkenes from the corresponding alkenyl-organo-borinates, as exemplified recently by the groups of Aggarwal and Morken (Scheme 1 C).^[9] In addition, we demonstrated that the logical combination of different organometallic reagents^[10] with boron alkoxides could lead to the formation of the required bis-organo-borinates in an efficient one-pot process.^[11] Based on these findings, we decided to examine the reactivity of alkenyl-triaryl borate salts (ATBs) to develop an electro-olefination reaction (Scheme 1 D).

ATBs (**2**) are underexplored salts, the only representative compound being triphenylvinyl borate which can be synthesized by treatment of tetravinyltin with triphenylborane.^[12] To investigate the electro-olefination and expand the structural variety of ATBs, we aimed to simplify their access. Therefore, we built on our previously described strategy for the synthesis of hetero-substituted tetraarylborate salts (TABs), and decided to make ATBs accessible by a triple ligand exchange reaction onto the corresponding potassium alkenyl-trifluoroborates **1** (Molander salts),^[13] employing *ex situ* generated Grignard or organozinc reagents.^[14]

We anticipated that the removal of an electron through an oxidation process should occur preferentially on the alkenyl moiety, avoiding the energetically disfavored dearomatization of one of the aryl groups. As a proof of concept, we first synthesized the model systems **2a**^[15] and **2b**, possessing, respectively *para*-fluorophenyl and phenyl moieties in addition to the β -styryl substituent (Figure 1). To describe the change in the electronic structure upon oxidation of **2a** and **2b**, spin and

charge densities were computed based on Mulliken population analysis of the DFT results. Charge densities were additionally computed using the CHarges from Electrostatic Potentials using a Grid-based (ChElPG) method.^[14] Blue areas (Figure 1 A) represent positive spin densities after oxidation. Only the alkenyl substituent is selectively oxidized in both cases whereas the charge and spin densities of the other aromatic substituents only change insignificantly, confirming our assumptions.

The oxidation potentials of ATB salts **2a** and **2b** were determined by cyclic voltammetry and compared to the value measured for commercial sodium tetraphenyl borate (Figure 1 B). With a fluoride atom present on each of the aryl groups, an E^{ox} value of +0.81 V vs. SCE was measured for **2a**, similar to the one of **2c** (+0.82 V vs. SCE). However, in the absence of electron-withdrawing substituents, the oxidation potential of **2b** was decreased to +0.67 V vs. SCE. As expected, it can be concluded that alkenyl groups are easier to oxidize and that the oxidation potential varies with the electronic nature of substituents on the moieties surrounding the boron atom. From a chemoselectivity perspective, the favorable oxidation of the olefin leaves no other path for the reaction but to transfer one of the remaining aryl moieties, thereby avoiding the undesirable formation of biaryl homocoupling compounds.

2a was chosen to test and optimize the reaction conditions.^[14] Inexpensive and reusable glassy carbon electrodes (GCE) proved to deliver the desired stilbene derivative **3a** with optimal conversions in acetonitrile at 25 °C. Following the transformation by ¹H NMR (Scheme 2) showed that the borate salt **2a** is selectively oxidized into product **3a**. Full conversion can be observed after 2.2 F in ¹H NMR studies and conversion-rate experiments of the electro-olefination using GC revealed that an optimal yield was obtained after 2 F. Remarkably, further oxidation resulted in consumption of the reaction product. Although no biaryl byproduct was detected in ¹H NMR, traces were found in GC. Interestingly, a third minor compound **3ab** can be observed, which was identified as the epoxy-stilbene derivative of **3a**. This side reaction will be discussed later with the mechanistic considerations (Scheme 7).

The synthesis of alkenyl-borate salts can be followed by ¹¹B NMR and proved quantitative when employing either Grignard reagents or—in cases of sensitive functional groups—organozinc species.^[14]

Therefore, we started investigating the scope of the transformation using borate salts without prior purification. The reaction was first evaluated engaging (*E*)-alkenyltrifluoroborates **1a–g** as starting materials in this two-pot sequence. Upon generation of the desired borate intermediates, those were treated with an aqueous solution to remove remaining inorganic salts and were subjected to electrochemical oxidation conditions after switching the solvent to acetonitrile. The results are depicted in Scheme 3. With electron-withdrawing substituents present on the aryl moieties, (*E*)-alkenes **3a–b** were obtained in up to 69% yield over two steps. In the case of *p*-CN-substituted phenyl groups, the corresponding organozinc species had to be employed, lowering the overall yield of the 2-pot procedure (**3c**, 29%). This consequent decrease in yield can be attributed to the lower reactivity of organozinc deriva-

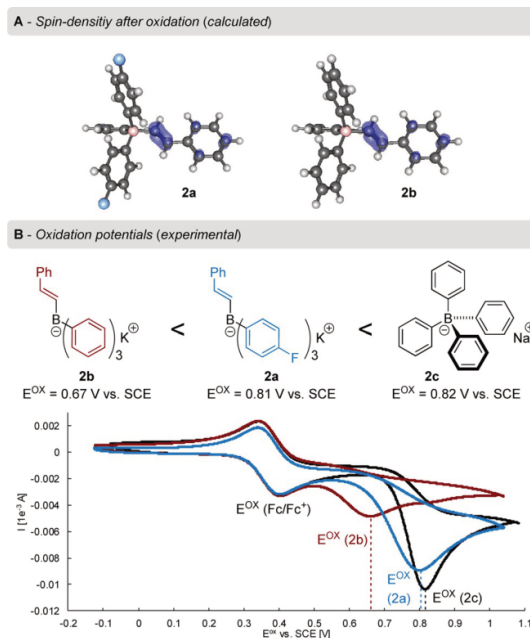
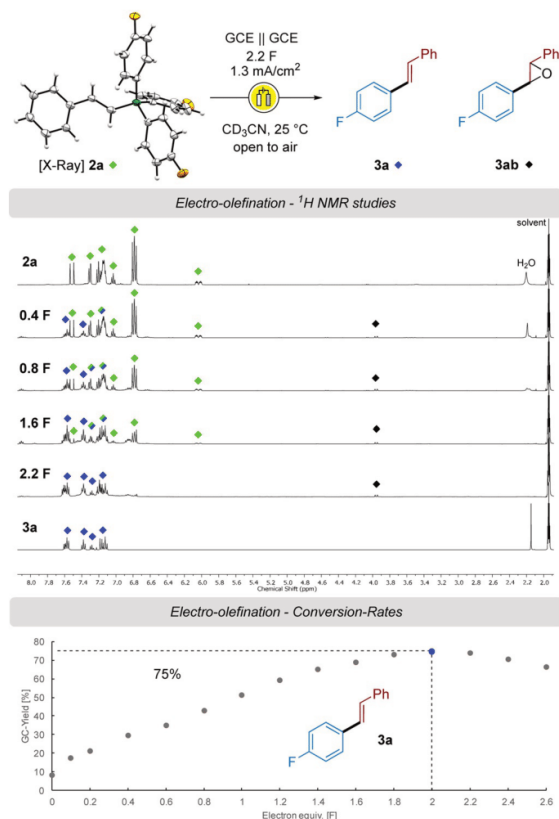


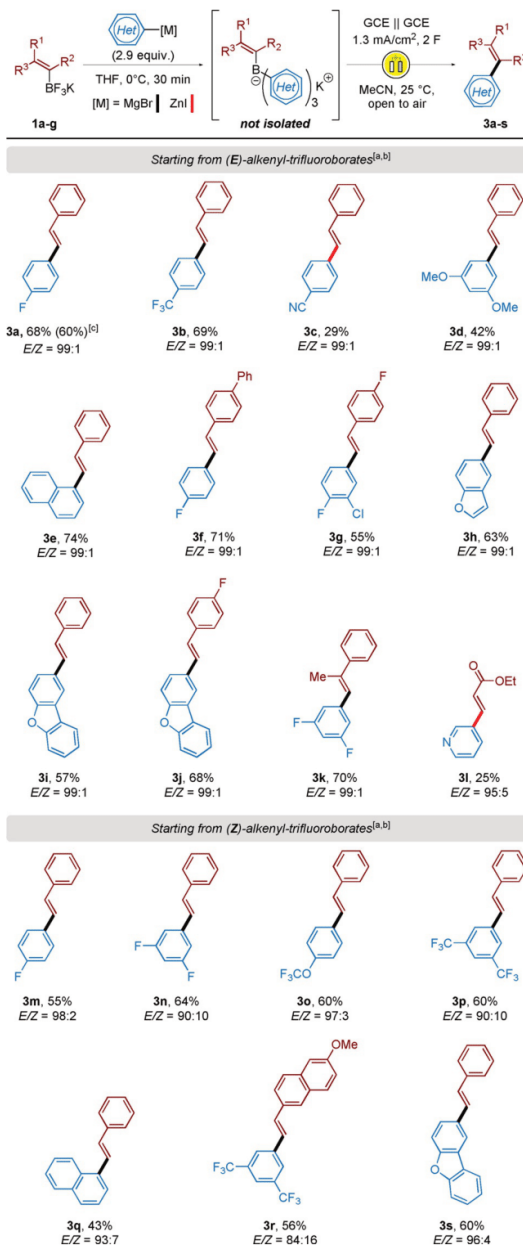
Figure 1. A) Spin density after oxidation of **2a** and **2b**. B) ATB salts **2a**, **2b** and tetraphenyl borate with experimental oxidation potentials and cyclic voltammetry calibrated to the reversible ferrocene oxidation (Fc/Fc^+).



Scheme 2. ¹H NMR studies of the transformation of **2a** into **3a** and **3ab** under electrochemical oxidation and conversion-rate (galvanostatic) experiment with *n*-undecane as internal standard.

tives in ligand exchange reactions. Electron-donating and neutral aryl substituents furnished the desired (*E*)-alkenes **3d–e** in moderate to good yields (42 and 74%). Varying the substitution pattern on the alkenyl moiety did not influence the course of the reaction, and **3f–g** were isolated in 55 to 71%. Heteroaryl groups were also tolerated in the electro-olefination process, furnishing structures **3h–j** in up to 68% yield. Interestingly, trisubstituted double bonds also led to the corresponding olefinated aryl derivative **3k** in good yield (70%). The formation of the borate salt proved however difficult when an acrylate derivative was used. The introduction of 3-pyridylzinc onto a trifluoroboryl acrylate and subsequent electro-olefination only gave 25% of product **3l**. Notably, all derivatives were obtained with excellent (*E/Z*) ratios, up to 99:1

Z-alkenyl trifluoroborates were employed next. Following the same two-pot protocol, the freshly generated *Z*-alkenyl-triaryl borates were engaged crude in the electro-olefination under oxidative conditions. Diversely substituted aryl moieties were able to perform the coupling reaction, furnishing compounds **3m–s** in reasonable yields (43 to 64%). It is however interesting to notice that all derivatives were isolated as *trans*-isomers. Given that either of the starting material (*E* or *Z*) gives



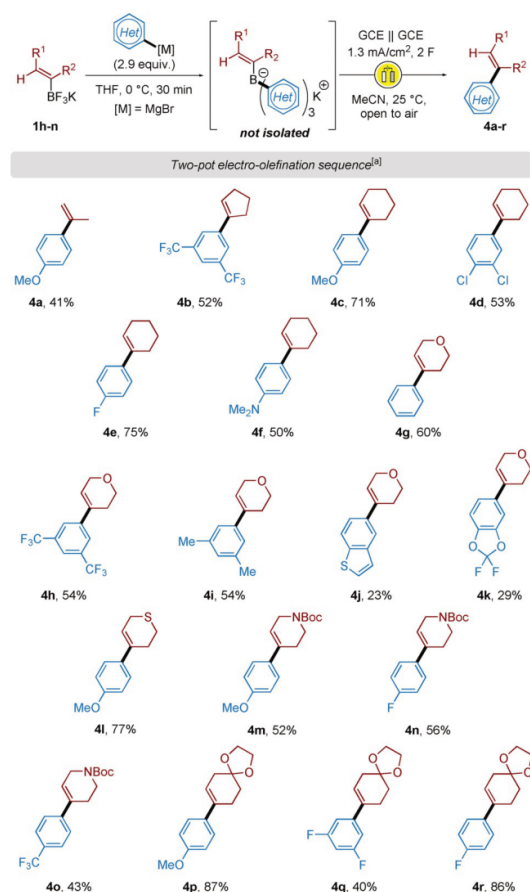
Scheme 3. Two-pot borate salt formation/ electro-olefination sequence—Synthesis of acyclic alkenes. [a] Yields are stated as isolated yields over two-steps. [b] GC-ratios determined from crude mixtures. [c] Electrochemical oxidation in EtOH as solvent instead of MeCN at 25 °C and open to air.

the same thermodynamic *E* isomers after electro-coupling, the strategy is stereoconvergent (Scheme 3). As it will be discussed in the mechanistic part, we assume that the oxidation of the double bond into a radical cationic species allows for the resulting bonding system to freely rotate and adopt the thermo-

dynamically more stable configuration before abstraction of the boron-containing moiety (Scheme 7).

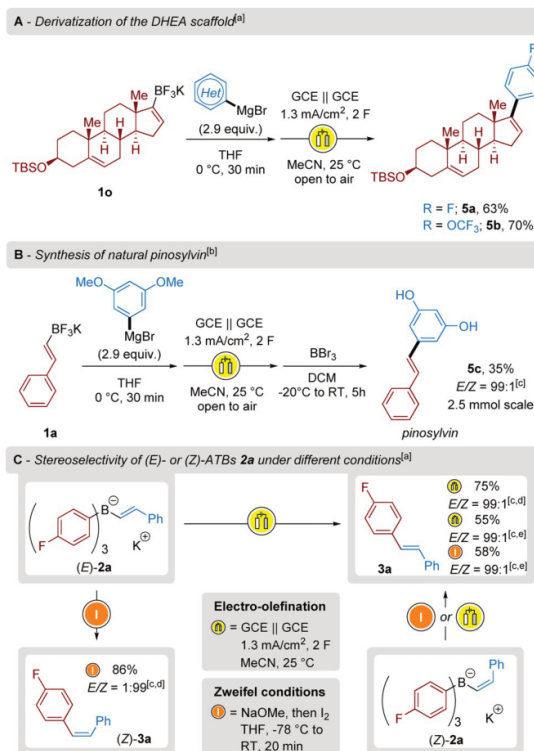
Our study of the electro-olefination was pursued with the use of α -substituted alkenyl borates (Scheme 4). The simple acyclic isopropenyl borate salt delivered product **4a** in 41% yield. Cyclic alkenyl groups were then investigated in the presence of electron-rich, -neutral and -poor aromatic systems, and gave compounds **4b–f** with up to 75% yield. Borate salts containing heteroatoms in the cycloalkenyl scaffolds such as 3,6-dihydro-2*H*-pyranyl, -thiopyranyl and 1,2,3,6-tetrahydropyridinyl underwent successful electro-olefinations, delivering trisubstituted olefins **4g–o** in moderate to good yields. We lastly demonstrated the reaction to be compatible in the presence of ketal functionalities (**4p–r**, up to 86%).

Next, we applied the method to the derivatization of more challenging structures to demonstrate the synthetic potential of our ATB salts. Dehydroepiandrosterone (DHEA) was derivatized into a TBS-protected ether and the carbonyl function transformed into the corresponding alkenyltrifluoroborate **1o**.



Scheme 4. Two-pot borate salt formation/ electro-olefination sequence—Synthesis of cyclic alkenes. [a] Yields are stated as isolated yields over two steps.

The addition of arylmagnesium bromide reagents to **1o**, followed by electro-olefination under the optimized oxidative conditions described above furnished functionalized molecules **5a** and **5b** in up to 70% yield (Scheme 5A). In addition, β -styryltrifluoroborate **1a** was employed as substrate for the synthesis of the natural product pinosylvin (Scheme 5B). 3,5-Dimethoxyphenylmagnesium bromide was introduced to perform the triple ligand exchange reaction and gave the intermediate alkenyltriaryl borate species. Subsequent electro-olefination and demethylation with BBr_3 furnished **5c** in 35% yield over three steps with perfect control of the diastereoselectivity ($E/Z = 99:1$). Furthermore, the chemoselectivity was investigated on our benchmark salt **2a** under distinct oxidative conditions (Scheme 5C). As already mentioned before, the electro-olefination occurs in a stereoconvergent manner. We selectively obtain the stilbene derivative **3a** using (*E*)-**2a** or (*Z*)-**2a** in moderate to good yields. In contrast, typical Zweifel conditions led to a stereospecific inversion of the double bond configuration, as the reaction proceeds through two consecutive stereospecific steps (1,2-metallate rearrangement and anti-periplanar β -elimination). The (*Z*)-isomer can therefore be synthesized using Zweifel conditions (Scheme 5C) and (*Z*)-**3a** was isolated in 86% yield (E/Z ratio < 1:99). Noteworthy, stereodivergent Zweifel protocols have been developed. Even though



Scheme 5. [a] Yields are stated as isolated yields over two steps. [b] Yield over three steps. [c] GC-ratios determined from crude mixtures. [d] Starting from **2a**. [e] Starting from (*Z*)-**2a**.

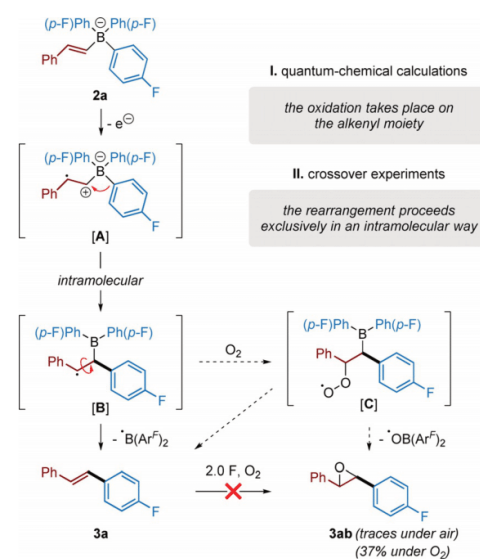
the presented method might be less versatile than these contributions, our strategy avoids the use of highly toxic chemicals such as BrCN and PhSeCl.^[16]

Lastly, we set out to ascertain the mechanism of this intriguing reaction, building on conversion experiments, cyclic voltammetry and theoretical considerations (Figure 1 and Scheme 2). Crossover experiments were conducted by mixing different borate salts under electrochemical conditions, confirming the absence of products resulting from intermolecular reactions and ruling out the possibility of intermolecular processes.^[14]

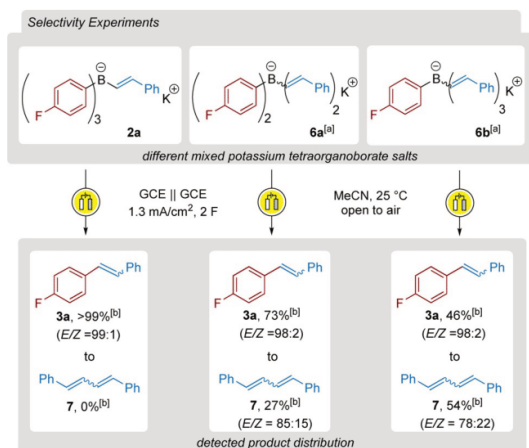
After selective oxidation of the alkenyl moiety, a rearrangement takes place. To study the nature of this rearrangement, we synthesized borate salts containing more than a single styryl group (**6a–b**, Scheme 6), employing styryl-Grignard reagents as (*E/Z*)-mixtures, and submitted them to our electrocoupling conditions. As a reference, the desired compound **3a** was obtained as the sole compound from **2a**. With a salt bearing two styryl groups (**6a**), a product ratio of 73:27 of **3a** and the diene **7** was obtained (*E/Z* = 85:15). This result points out that the transfer of a vinyl group is not preferred over the transfer of an aryl group, and therefore indicates that the rearrangement is more likely to go through a σ -bond breaking process rather than a π -addition, as for the latter an unfavorable dearomatization has to occur. Example **6b** (possessing three styryl moieties) further supports this hypothesis, as **7** was obtained in 54% and **3a** in 46% GC-ratio. The non-statistical distribution of products **3a** and **7** in both experiments also indicates that the aryl moiety is—in such cases—a better transferable ligand than the styryl group.

In summary, the alkenyl moiety is more prone to oxidation than the aryl groups (as concluded from quantum-chemical calculations and selectivity experiments, see Figure 1 and

Scheme 6) and leads to an intermediate alkyl radical cationic species [A] (Scheme 7). We then propose that further intramolecular σ -addition of one of the aryl moieties undergoes a rearrangement^[17] towards intermediate [B] in which the C–C alkyl radical bond can freely rotate and lead to the thermodynamically favored *trans* product (*E*)-**3a**. Oxygen probably interacts with the reaction intermediates under formation of structure [C], as **3ab** was observed in traces under air and isolated in



Scheme 7. Proposed mechanism for the electro-olefination of ATB **2a**.



Scheme 6. Electrocoupling of different mixed potassium tetraorganoborate salts. [a] In situ generated following general procedure **D**^[14] as follows for **6a**: 0.5 mmol **1p** and 1.0 mmol styrylmagnesium bromide. For **6b**: 0.5 mmol potassium trifluoro(4-fluorophenyl)borate and 1.5 mmol styrylmagnesium bromide. [b] Product distribution ratios are determined by GC analysis on crude mixtures without isolation. Homocoupled biaryls are omitted and not included in the GC-ratios for more clarity.

37% yield when the reaction was carried out under oxygen atmosphere. It is however important to note that product **3ab** does not come from the oxidation of product **3a** under electrochemical conditions, as confirmed by control experiments, indicating a radical pathway.^[14] Based on cyclic voltammetry (Figure 1), galvanostatic experiments (Scheme 2) and our findings in the previous work on biaryl electro-coupling,^[7] we assume that no second oxidation has to occur during the formation of the desired product **3a**.

In conclusion, we have developed a new conceptual approach to alkene derivatives through electro-olefination. A simple strategy was assembled for the synthesis of alkenylborate salts (ATBs) through ligand exchanges on potassium trifluoroborates. No purification of these salts was required for the sequence to be pursued and deliver the expected coupling compounds in moderate to good yields under electrochemical oxidation. Such method represents an original and stereoconvergent alternative to the formation of functionalized olefins, opening new ways of thinking about C–C bond disconnections.

Acknowledgements

Robert J. Mayer (LMU Munich) is kindly acknowledged for his help with cyclovoltammetry, as well as Hendrik Eijsberg (UCLdV, Poitiers) for helpful comments in the preparation of this manuscript. We thank the Chemical Industry Fund (FCI), the Deutsche Forschungsgemeinschaft (DFG grant DI 2227/2-1 + JA 2794/1-1, SFB749), and the Ludwig-Maximilians University, Munich (LMUExcellent) for financial support.

Conflict of interest

The authors declare no conflict of interest.

Keywords: catalyst-free • electrochemistry • olefination • organoborates • stereoconvergent

- [1] D. G. Brown, J. Boström, *J. Med. Chem.* **2016**, *59*, 4443.
- [2] a) N. Miyaura, A. Suzuki, *J. Chem. Soc. Chem. Commun.* **1979**, 866; b) N. Miyaura, K. Yamada, A. Suzuki, *Tetrahedron Lett.* **1979**, *20*, 3437.
- [3] a) D. Milstein, J. K. Stille, *J. Am. Chem. Soc.* **1978**, *100*, 3636; b) R. F. Heck, J. P. Nolley, *J. Org. Chem.* **1972**, *37*, 2320; c) A. O. King, N. Okukado, E.-i. Negishi, *J. Chem. Soc. Chem. Commun.* **1977**, 683; d) K. Sonogashira, Y. Tohda, N. Hagihara, *Tetrahedron Lett.* **1975**, *16*, 4467; e) Y. Hatanaka, T. Hiyama, *J. Org. Chem.* **1988**, *53*, 918; f) K. Tamao, K. Sumitani, M. Kumada, *J. Am. Chem. Soc.* **1972**, *94*, 4374.
- [4] a) E. J. Horn, B. R. Rosen, P. S. Baran, *ACS Cent. Sci.* **2016**, *2*, 302; b) M. Yan, Y. Kawamata, P. S. Baran, *Chem. Rev.* **2017**, *117*, 13230; c) C. Kingston, M. D. Palkowitz, Y. Takahira, J. C. Vantourout, B. K. Peters, Y. Kawamata, P. S. Baran, *Acc. Chem. Res.* **2020**, *53*, 72; d) J.-I. Yoshida, A. Shimizu, R. Hayashi, *Chem. Rev.* **2018**, *118*, 4702; e) B. Elsler, D. Schollmeyer, K. M. Dyballa, R. Franke, S. R. Waldvogel, *Angew. Chem. Int. Ed.* **2014**, *53*, 4979; *Angew. Chem.* **2014**, *126*, 5311; f) T. Shono, H. Hamaguchi, Y. Matsumura, *J. Am. Chem. Soc.* **1975**, *97*, 4264; g) M. D. Kärkäs, *Chem. Soc. Rev.* **2018**, *47*, 5786; h) A. G. A. Volta, *Nat. Philos. Chem. Arts* **1800**, *4*, 179; i) M. Faraday, *Ann. Phys. Leipzig* **1834**, *47*, 438.
- [5] D. H. Geske, *J. Phys. Chem.* **1959**, *63*, 1062.
- [6] S. B. Beil, S. Möhle, P. Enders, S. R. Waldvogel, *Chem. Commun.* **2018**, *54*, 6128.
- [7] A. Music, A. N. Baumann, P. Spieß, A. Plantefol, T.-C. Jagau, D. Didier, *J. Am. Chem. Soc.* **2020**, *142*, 4341.
- [8] a) G. Zweifel, H. Arzoumanian, C. C. Whitney, *J. Am. Chem. Soc.* **1967**, *89*, 3652; b) G. Zweifel, N. L. Polston, C. C. Whitney, *J. Am. Chem. Soc.* **1968**, *90*, 6243; c) E.-i. Negishi, G. Lew, T. J. Yoshida, *Chem. Soc. Chem. Commun.* **1973**, 874; d) D. A. Evans, T. C. Crawford, R. C. Thomas, J. A. Walker, *J. Org. Chem.* **1976**, *41*, 3947; e) H. C. Brown, N. G. Bhat, *J. Org. Chem.* **1988**, *53*, 6009.
- [9] a) D. J. Blair, C. J. Fletcher, K. M. P. Wheelhouse, V. K. Aggarwal, *Angew. Chem. Int. Ed.* **2014**, *53*, 5552; *Angew. Chem.* **2014**, *126*, 5658; b) T. P. Blaisdell, J. P. Morken, *J. Am. Chem. Soc.* **2015**, *137*, 8712; c) R. J. Armstrong, V. K. Aggarwal, *Synthesis* **2017**, *49*, 3323; d) R. J. Armstrong, W. Niwetmarin, V. K. Aggarwal, *Org. Lett.* **2017**, *19*, 2762.
- [10] A. Music, C. Hoarau, N. Hilgert, F. Zischka, D. Didier, *Angew. Chem. Int. Ed.* **2019**, *58*, 1188; *Angew. Chem.* **2019**, *131*, 1200.
- [11] A. Music, A. N. Baumann, P. Spieß, N. Hilgert, M. Köllen, D. Didier, *Org. Lett.* **2019**, *21*, 2189.
- [12] D. Seyferth, M. A. Weiner, *J. Am. Chem. Soc.* **1961**, *83*, 3583.
- [13] a) G. A. Molander, N. Ellis, *Acc. Chem. Res.* **2007**, *40*, 275; b) Shiraiishi Atsushi, JP2016150925, **2016**.
- [14] For further details see the Supporting Information.
- [15] CCDC 1964338 contain the supplementary crystallographic data for this paper. These data are provided free of charge by The Cambridge Crystallographic Data Centre.
- [16] a) G. Zweifel, R. P. Fisher, J. T. Snow, C. C. Whitney, *J. Am. Chem. Soc.* **1972**, *94*, 6560; b) R. J. Armstrong, C. Garcia-Ruiz, E. L. Myers, V. K. Aggarwal, *Angew. Chem. Int. Ed.* **2017**, *56*, 786.
- [17] S. Namirembe, J. P. Morken, *Chem. Soc. Rev.* **2019**, *48*, 3464.

Manuscript received: March 20, 2020

Accepted manuscript online: March 23, 2020

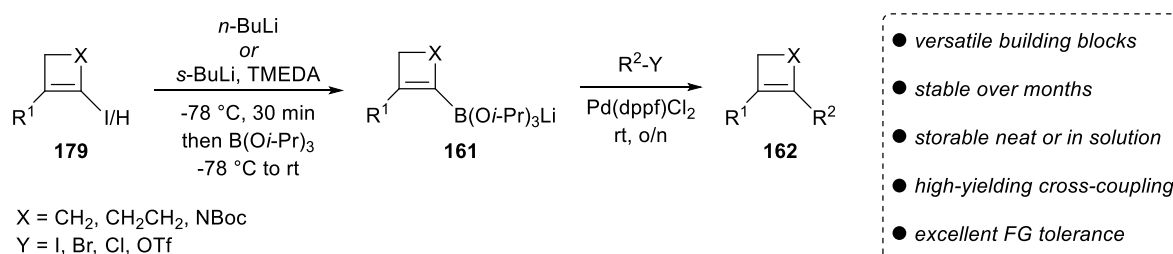
Version of record online: June 25, 2020

6 Conclusions

6.1 Summary

This work has presented several methods based on organometallic principles, which enable the formation of fundamental C-C bonds without the need of transition-metals. A major part of this thesis has been dedicated to the synthesis and generalized access toward tetrahedrally coordinated organoboronates, bisorganoboronates and tetraorganoborates, all bearing the boron atom rather than a transition-metal as their reaction center. It has been demonstrated that molecular oxidants such as iodine in combination with a base in Zweifel olefinations or electrons themselves as the most frugal oxidants *via* anodic electrochemical oxidation in combination with the mentioned organoboron reagents offer appealing alternatives to transition-metal catalysis.

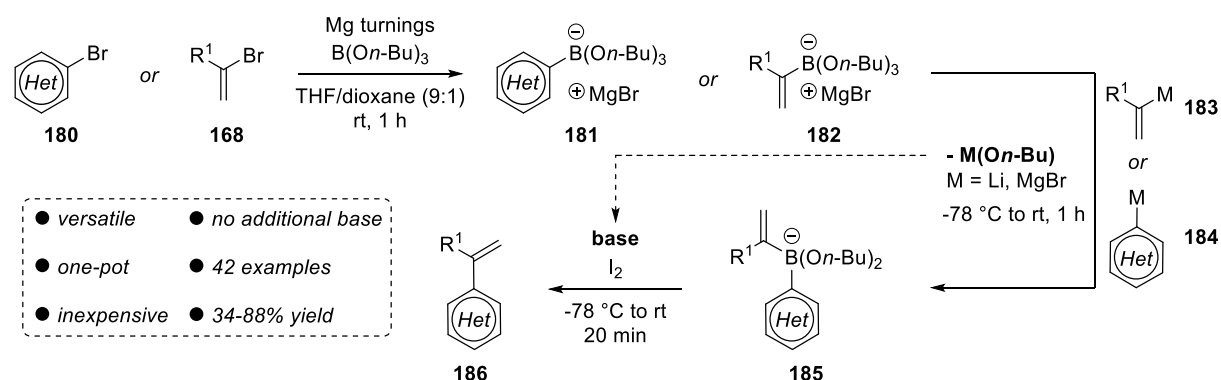
The starting point for this work was set at the synthesis of variously substituted and highly strained cyclobutenyl- and cyclopentenylboronates *via* halogen-metal exchange on the corresponding iodides with *n*-BuLi under cryogenic temperatures and following addition of borontriisopropoxide. The resulting reagents showed remarkable stability in solution at $-20\text{ }^{\circ}\text{C}$ or neat at room temperature under inert atmosphere, which was measured with conversion data in follow-up Suzuki-Miyaura cross-couplings. Importantly, this concept has been successfully applied to even more reactive azetynylboronates generated *via* metalation with TMEDA complexed *s*-BuLi, forming stable boronate building blocks **161** that exhibit excellent functional group tolerance and yields in cross-coupling reactions toward **162**. Importantly, this sequence could also be conveniently run as a one-pot protocol (Scheme 38).



Scheme 38: Versatile preparation of organoboronates and their application in Suzuki-Miyaura cross-coupling chemistry.

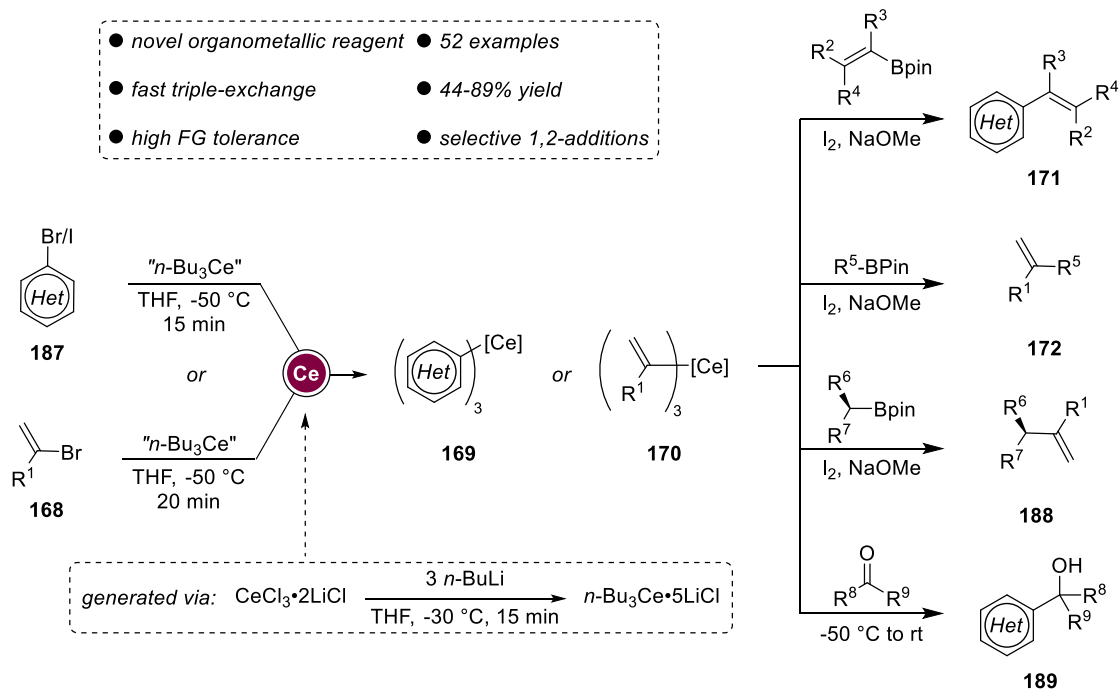
Having established the stability of such systems, a one-pot sequence for the assembly of structurally related bisorganoboronates has been designed. After generation of the required aryl- and alkenyl organomagnesium and organolithium species *via* metalation and halogen-metal exchanges, the first addition of an organometallic to the boronalkoxide proved to selectively form the intermediate organoboronate (**181** or **182**), while the second addition of another organometallic proceeded selectively *via* transmetalation resulting in ligand-exchanges at the boron-center and yielding bisorganoboronate **185**. While all four possible options to assemble two different organometallics onto boronalkoxides toward bisorganoboronates were viable, the most convenient and rapid method was found to be the direct insertion of

magnesium into a carbon-halogen bond in the presence of tributylborate, which facilitated the insertion by immediate formation of the desired organoboronate of type **181** or **182**. The use of 1,4-dioxane as cosolvent has been crucial to prevent overaddition, as the organoboronate instantly precipitated out of solution, thereby preventing further transmetalation. After consecutive formation of the bisorganoboronate of type **185**, these salts have shown to be excellent precursors for Zweifel olefinations and olefinated arenes of type **186** were isolated in good yields in an overall five-step *in situ* sequence (Scheme 39). Notably, the addition of additional base has not been necessary employing this procedure, as one equivalent of basic metal methoxide salt is released during the transmetalation step, making this process an atom-economic and inexpensive alternative to usually employed boron pinacol esters.



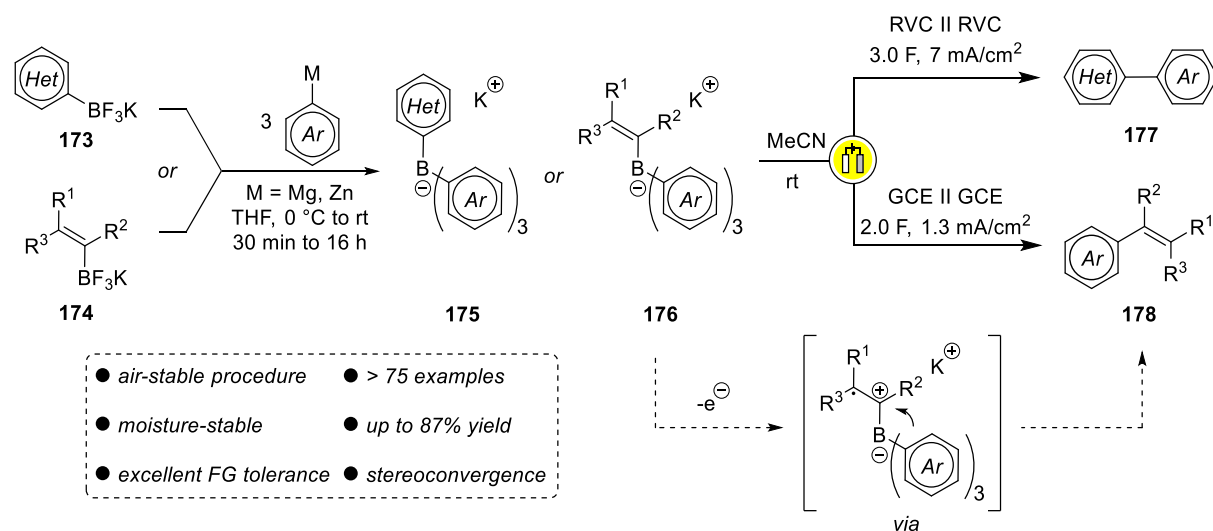
Scheme 39: One-pot sequence toward stable bisorganoborinates and subsequent Zweifel olefination.

Moreover, the role of the employed organometallics within the formation of bisorganoborinates has been studied in more detail. Organolithium species were the only reliable organometallics to add onto alkenyl- and arylboron pinacol esters, as especially alkenyl- and arylmagnesium species were prone to either overaddition or leading to complex product mixtures. In order to fill this gap between organomagnesium and more reactive organolithium species, the novel halogen-metal exchange reagent “*n*-Bu₃Ce” was developed by transmetalation from dry CeCl₃ and *n*-BuLi. A fast triple halogen-cerium exchange was observed at -50 °C within 20 min with (hetero)aryl bromides and iodides **187** as well as alkenylbromides of type **168**, whilst tolerating a broad range of functional groups. These species have then been added onto aryl, alkenyl and alkyl boron pinacol esters, selectively forming the bisorganoborinates and ultimately enabling the enantiospecific synthesis of olefins from sterically enhanced boron pinacol esters (**188**). Lastly, additions onto easily enolizable and sterically hindered ketones have been described, which selectively favor the formation of products *via* 1,2-additions (**189**, Scheme 40).



Scheme 40: Development of the novel “*n*-Bu₃Ce” exchange reagent, exchanges with various aryl- and alkenyl halides and further transformations in Zweifel olefinations and 1,2-additions to ketones.

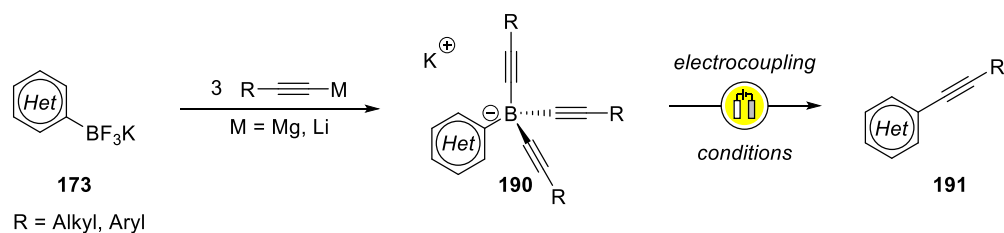
In the last part of this work, the electrochemical properties of unsymmetrical potassium tetra(hetero)arylborate of type **175** and alkenyltri(hetero)arylborate of type **176** salts have been extensively studied. Hereby, those unprecedented tetraorganoborate salts were first synthesized from commercially available potassium aryl- and alkenyltrifluoroborates (**173** and **174**) in triple-ligand exchanges onto boron *via* transmetalations with arylmagnesium or arylzinc reagents. A great diversity of salts has been found to be prone to oxidation, in which the most electron-rich aromatic system is oxidized first. Likely following a one-electron radical process, which was supported by theoretical calculations, an intramolecular rearrangement of one of the remaining less electron-rich aromatics is then taking place, which after elimination has yielded (hetero)biaryls of type **177** or olefinated arenes of type **178** in a chemoselective fashion. In case of the electro-olefination the reaction was found to proceed in a stereoconvergent manner, exclusively forming the thermodynamically favored (*E*)-olefins (Scheme 41). Importantly, even the most sophisticated tetraorganoborate salts have showcased excellent stability at ambient atmosphere and temperature, therefore allowing for the reaction to be conducted in protic and “green” solvents such as ethanol and without the necessity of an inert atmosphere. Finally, in conventional cross-couplings problematic polyhalogenated substrates have been tolerated in the electrocoupling protocol, presenting otherwise inaccessible chemical space.



Scheme 41: Electrocoupling and electro-olefination of diverse tetraorganoborates for the synthesis of (hetero)biaryls and olefinated arenes.

6.2 Outlook

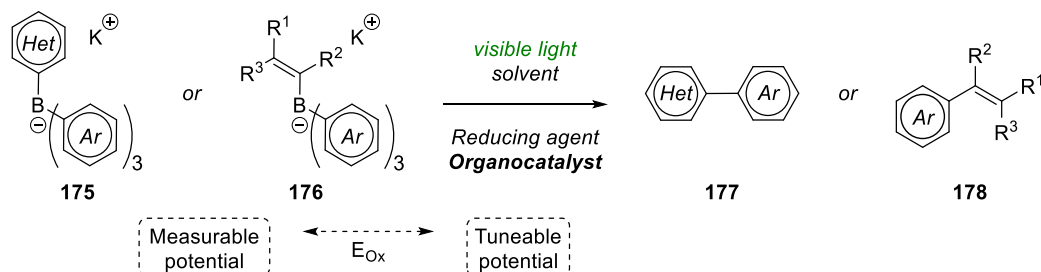
In order to generalize the presented electrochemical methods, the extension of the electrocoupling toward other C-C bond formations should be investigated. As alkyl borates tend to undergo homolytic C-B bond cleavage upon oxidation and are therefore not suitable for selective intramolecular couplings, the focus should be set onto alkylation chemistry. In order to obtain selectivity in these reactions, the tetraorganoborate should consist of one aryl and three alkynyl moieties, as a single-electron oxidation should be preferred in the sp^2 -hybridized aromatic rather than the sp -hybridized alkyne. Following the previous procedures, a triple transmetalation of alkynylmetal species onto potassium aryl trifluoroborates **173** should lead to unprecedented aryltrialkynylborates **190**, which could then be studied in electrocoupling reactions for the formation of alkynylated arenes **191** (Scheme 42).



Scheme 42: Potential extension of the electrocoupling toward alkylation.

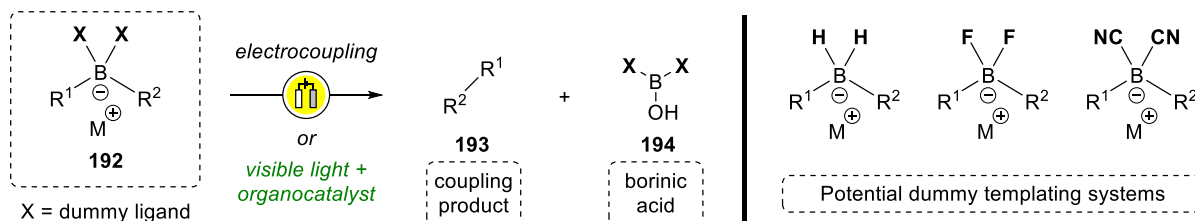
In addition, the tendencies of tetraorganoborates to perform transformations in photochemical oxidations could be analyzed, since those transformations are strongly related to single-electron transfers in electrochemical reactions and can be considered as another environmentally benign strategy to forge C-C bonds. Especially the area of organophotoredox catalysis has produced a great variety of catalysts with a broad range of oxidation potentials, which could enable the coupling of tetrahedrally coordinated

borates. As organophotoredox catalysis is usually performed under very mild conditions, more sensitive functional groups compared to electrochemical oxidations might be tolerated. Importantly, selectivity for the desired heterocoupling might be achieved, since every organocatalyst shows a defined oxidizing and reducing potential, which could be tailored to a specific borate substrate (Scheme 43).



Scheme 43: Envisioned photochemical oxidation of potassium tetraorganoborate salts.

Even though oxidative intramolecular couplings of tetraorganoborates constitute a novel addition to the C-C bond formation toolbox, their applicability is limited by one obvious drawback: Two of the three organometallic aromatics required in the borate salt formation are wasted in the coupling process. For this reason, the development of non-transferrable “dummy” ligands on the boron-temple (192) would be highly desirable. Besides fixing the problem of atom-economy, those novel species should greatly enlarge the scope of the electrocoupling and eliminate homocoupling side reactions completely, since no discrimination for oxidizable between the two coupling partners would be necessary (Scheme 44).



Scheme 44: Extension and improvement of the electrocoupling approach and potential photochemical oxidations employing dummy ligands.

C. EXPERIMENTAL PART

1 General Considerations

All reactions involving organometallic compounds were carried out using standard Schlenk-techniques in flame-dried glassware equipped with rubber septum and magnetic stirring bars under nitrogen atmosphere. Syringes for transferring anhydrous solvents or reagents were purged with nitrogen prior to use. Reaction endpoints were determined by GC, TLC or ^{11}B NMR monitoring of the reactions. Yields are referred to isolated compounds with a purity >95% as determined by ^1H -NMR (25 °C) or capillary GC. Counteractions are usually omitted for more clarity. The experimental part contains general experimental procedures, condensed data and selected spectral data for each topic discussed. The numbering is in accordance with the published data found in section B of this work. Starting material synthesis is abbreviated with **SM** and numbered continuously. Compounds synthesized by equally contributing co-authors are marked (*). The full supporting information for each publication can be downloaded free of charge on the corresponding website of the publishing company.

1.1 Solvents

For the preparation of anhydrous solvents, the crude solvents were first purified by distillation and then dried according to standard methods by distillation from drying agents as stated below and were stored under nitrogen. Non-anhydrous solvents were obtained from commercial sources and used without further purification. Solvents for column chromatography were distilled prior to use.

THF was continuously refluxed and freshly distilled from sodium benzophenone ketyl under nitrogen and stored over molecular sieves.

DCM was predried over CaCl_2 , continuously refluxed and freshly distilled from CaH_2 under nitrogen.

Et₂O was predried over CaCl_2 and passed through activated Al_2O_3 (using a solvent purification system SPS-400-2 from Innovative Technologies Inc.).

Toluene was predried just like DCM over CaCl_2 and distilled from CaH_2 .

MeCN was purchased in HPLC gradient grade ($\geq 99.9\%$) from Fisher Scientific.

1.2 Reagents

Commercially available starting materials were used without further purification unless otherwise stated.

***i*PrMgCl•LiCl** was prepared by careful addition of *i*-PrCl (78.5 g, 91.3 mL, 1.00 mol, 1.00 equiv) to a suspension of Mg turnings (26.7 g, 1.10 mol, 1.10 equiv) and LiCl (46.63 g, 1.10 mol, 1.10 equiv) in dry THF (900 mL). The reaction mixture was stirred for 12 h after which the floating particles were filtered. The solution was cannulated into a flame-dried and nitrogen flushed Schlenk flask and the concentration of the active species was determined by titration against I_2 in THF.¹⁹⁷

¹⁹⁷ A. Krasovskiy, P. Knochel, *Synthesis* **2006**, 5, 890–891.

***n*-BuLi**, ***s*-BuLi** and **MeLi** were purchased as solutions in cyclohexane/hexanes mixtures from Rockwood Lithium GmbH or Albemarle. The concentration was determined by titration against *N*-benzylbenzamide in THF at 0 °C or by titration of *isopropyl* alcohol using the indicator 1,10-phenanthroline in THF at –78 °C.¹⁹⁸ **Organozinc** and **Grignard** reagents were freshly prepared and titrated against iodine at room temperature.¹⁹⁷

1.3 Chromatography

Flash-column chromatography (FCC) was performed using silica gel 60 (SiO₂, 0.040–0.063 mm, 230–400 mesh ASTM) from Merck. Thin layer chromatography (TLC) was performed using aluminum plates covered with SiO₂ (Merck 60, F–254). Spots were visualized by UV light irradiation (254 nm) and/or by staining of the TLC plate with one of the solutions below, followed by careful warming with a heat gun.

KMnO₄ solution: KMnO₄ (1.50 g), K₂CO₃ (10.0 g) and NaOH (0.15 g) in water (150 mL).

***p*-Anisaldehyde solution:** conc. H₂SO₄ (10 mL), EtOH (200 mL), AcOH (3 mL), *p*-anisaldehyde (4 mL).

1.4 Analytical data

NMR spectra were recorded on Varian Mercury 200 or Bruker AC 300, Avance III HD 400 and AMX 600 instruments. Chemical shifts are reported as δ -values in parts per million (ppm) relative to the residual solvent peak: CDCl₃ (δ_{H} : 7.26; δ_{C} : 77.16), DMSO-*d*₆ (δ_{H} : 2.50; δ_{C} : 39.52), C₆D₆ (δ_{H} : 7.16; δ_{C} : 128.06), CD₃CN (δ_{H} : 1.94; δ_{C} : 1.39 and 118.69) and (CD₃)₂CO (δ_{H} : 2.05; δ_{C} : 29.84 and 206.26). For the observation of the signal multiplicities, the following abbreviations and combinations thereof were used: s (singlet), d (doublet), t (triplet), q (quartet), quint (quintet), sext (sextet), sept (septet), m (multiplet) and br (broad). If not otherwise noted, the coupling constants given are either H-H or H-F coupling constants for proton signals, C-F coupling constants for carbon signals and fluorine signals and B-F coupling constants for boron signals.

Melting points are uncorrected and were measured on a Büchi B.540 apparatus.

Infrared spectra were recorded from 4000–650 cm⁻¹ on a Perkin Elmer Spectrum BX-59343 instrument. For detection a Smiths Detection DuraSample IR II Diamond ATR sensor was used. The main absorption peaks are reported in cm⁻¹. Samples were measured neat and abbreviations for intensity were as follows: vs (very strong; maximum intensity), s (strong; above 75% of max. intensity), m (medium; from 50% to 75% of max. intensity), w (weak; below 50% of max. intensity) and br (broad).

Gas chromatography (GC) was performed with instruments of the type Hewlett-Packard 5890/6850/6890 Series II, using a column of the type HP 5 (Hewlett-Packard, 5% phenylmethylpolysiloxane; length: 10 m, diameter: 0.25 mm, film thickness 0.25 μm). The detection was accomplished using a flame ionization detector.

¹⁹⁸ A. F. Burchat, J. M. Chong, N. Nielsen, *J. Organomet. Chem.* **1997**, 542, 281–283.

For the combination of **gas chromatography with mass spectroscopic (LRMS)** detection, a GC–MS of the type Hewlett-Packard 6890/MSD 5793 networking was used (column: HP 5–MS, Hewlett–Packard; 5% phenylmethylpolysiloxane; length: 15 m, diameter: 0.25 mm, film thickness: 0.25 μm).

High resolution mass spectra (HRMS) were recorded on a Finnigan MAT 95Q, Finnigan MAT 90 or JEOL JMS-700 instrument for electron impact ionization (EI). Electron spray ionization (ESI) high resolution mass spectra were measured on a Thermo Finnigan LTQ FT Ultra High-Performance Mass Spectrometer with a resolution of 100.000 at m/z 400. The spray-capillary voltage of the IonMax ESI-unit is set to 4 kV while the heating-capillary temperature is set to 250 $^{\circ}\text{C}$.

Enantiomeric excess (*ee*) of chiral products was determined *via* chiral HPLC analysis on a Shimadzu Prominence 20A HPLC system running LabSolutions V5.42SP5. For developing a chiral resolution method, different chiral normal phase columns (Daicel Chemical Industries Chiralcel OD-H, OB-H) were tested with *n*-heptane and *i*-PrOH as mobile phase (*isocratic*) using a racemic mixture of the compound.

The **diastereomeric ratio (*dr*)** was determined either by NMR, GC or HPLC analysis.

Specific rotation $[\alpha]_{\text{D}}^{20}$ values of chiral products were measured in DCM at 20 $^{\circ}\text{C}$ using a wavelength of $\lambda = 589$ nm and a P8000-P8100-T polarimeter from A. Kruss Optronic, running software V3.0 with 5 cm path length. The sample concentration was 0.01 g/mL and the values are reported in $^{\circ}\cdot\text{mL}\cdot\text{dm}^{-1}\cdot\text{g}^{-1}$.

Low temperature raman measurements were performed on a Bruker MultiRAM FT-Raman spectrometer with a Nd:YAG laser excitation ($\lambda = 1064$ nm).

Electrochemical oxidations on scales smaller than 1.0 mmol were performed on the IKA Electra-Syn 2.0. All used electrodes were purchased from IKA, except the RVC (reticulated vitreous carbon) electrodes which were obtained from Goodfellow (Carbon – Vitreous – 3000C Foam, Thickness: 6.35 mm, Bulk density: 0.05 g/cm³, Porosity: 96.5%, Pores/cm: 24). Electrochemical Oxidations on a scale greater than 1.0 mmol were performed on an Atlas 0931 Potentiostat – Galvanostat using a two-electrode undivided cell setup.

Cyclic voltammetry measurements were performed in MeCN containing 0.1 M NBu₄ClO₄ with the TAB salt (**1a–g**) ($c \approx 3.4 \times 10^{-4}$ M) and ferrocene ($c = 3.8 \times 10^{-4}$ M) as an internal standard. The $E_{1/2}(\text{fc}^+/\text{fc}$ in MeCN) = +0.382 V was used to calibrate E_{p}^{Ox} (in MeCN) vs SCE.¹⁹⁹ The experiments were performed on a CH Instruments 630E electrochemical analyzer using a 2 mm diameter platinum working electrode, a platinum wire counter electrode and an Ag wire pseudo-reference electrode applying a scan rate of 0.1 V/s.

¹⁹⁹ J. R. Aranzaes, M.-C. Daniel, D. Astruc, *Can. J. Chem.* **2006**, *84*, 288–299.

1.5 Single Crystal X-Ray Diffraction Studies²⁰⁰

Single crystals suitable for X-ray diffraction were obtained by slow solvent evaporation. The crystals were introduced into perfluorinated oil and a suitable single crystal was carefully mounted on the top of a thin glass wire. Data collection was performed on a Bruker D8 Venture TXS diffractometer using Mo-K α radiation ($\lambda = 0.71073 \text{ \AA}$). The structures were solved by direct methods (SHELXT)²⁰¹ and refined by full-matrix least squares techniques against F_o^2 (SHELXL-2014/7)²⁰².

2 One-Pot Preparation of Stable Organoboronate Reagents for the Functionalization of Unsaturated Four- and Five-Membered Carbo- and Heterocycles²⁰³

2.1 General Procedures

The general procedures and analytical data for this chapter can be found in section B, chapter 1.1 of this work. They are printed as a direct part of the published manuscript. Therefore, only one exemplary spectral characterization (Figure 8) and crystallographic data (Table 1–Table 3) are shown below.

²⁰⁰ X-Ray measurements, data collection and processing were performed by Dr. Peter Mayer, Department of Chemistry, LMU Munich.

²⁰¹ Sheldrick, G. M. (2015). *Acta Cryst. A* **71**, 3–8.

²⁰² Sheldrick, G. M. (2015). *Acta Cryst. C* **71**, 3–8.

²⁰³ The full supporting information can be found under the following link: <https://doi.org/10.1055/s-0036-1592004>. This project was conducted in equal contribution with M. Eisold and A. N. Baumann.

2.2 Representative NMR Spectra

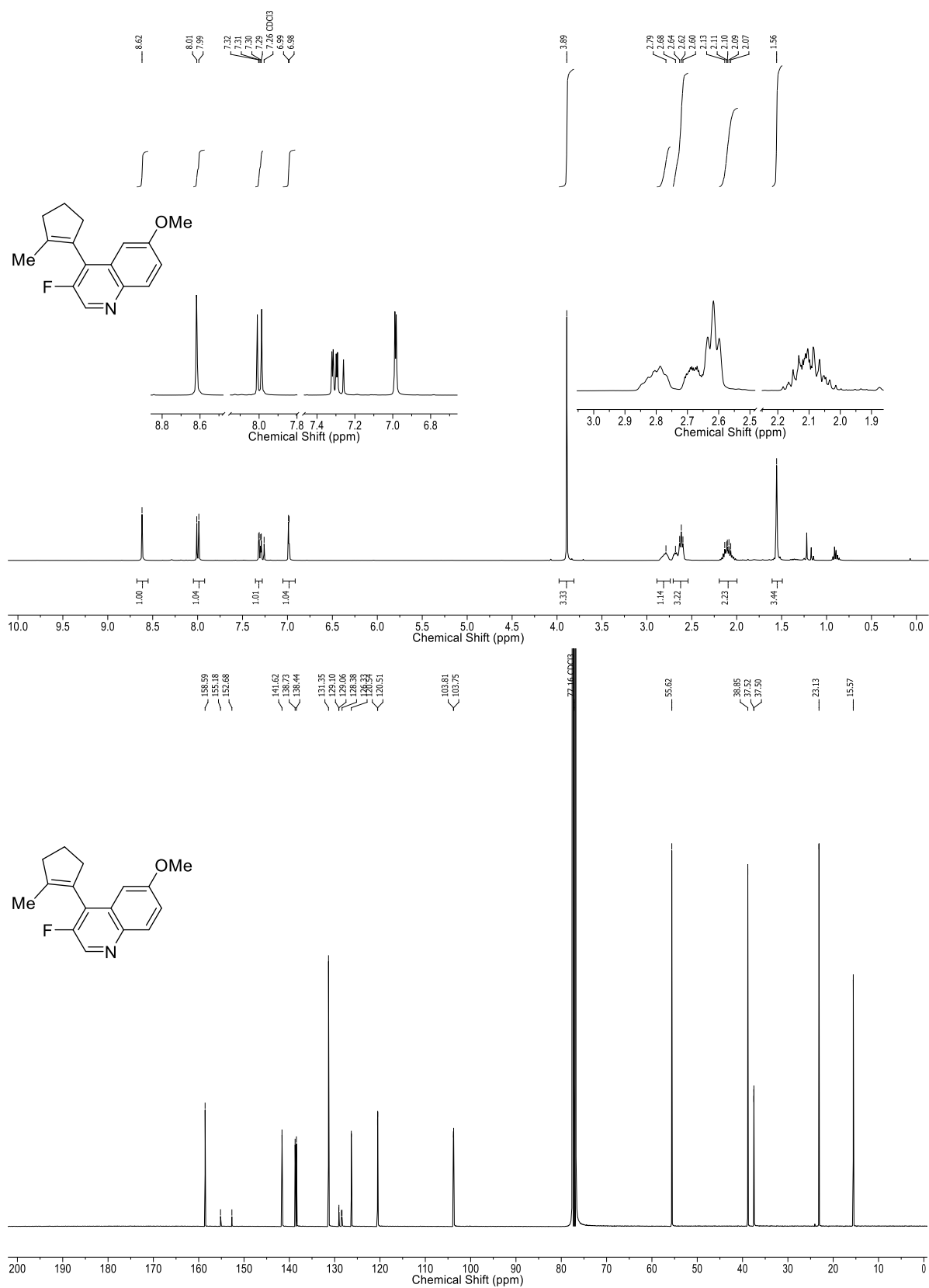
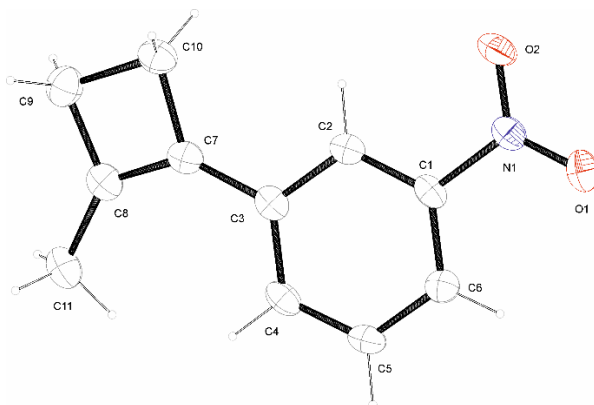


Figure 8: ¹H NMR (400 MHz, CDCl₃) and ¹³C NMR (101 MHz, CDCl₃) of 3-Fluoro-6-methoxy-4-(2-methylcyclopent-1-en-1-yl)quinoline (**4f**).

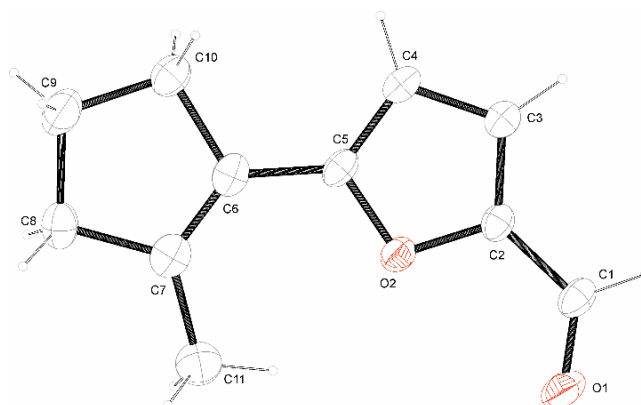
2.3 Single X-Ray Diffraction

Supporting Information available: Crystallographic data has been deposited with the Cambridge Crystallographic Data Centre: CCDC-1825251 for **3a**, CCDC-1826225 for **4g** and CCDC-1825250 for **7a**. Copies of the data can be obtained free of charge: <https://www.ccdc.cam.ac.uk/structures/>.

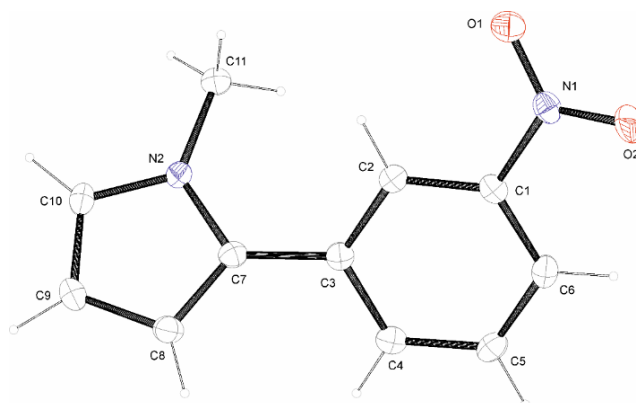
Table 1: Crystallographic data for compound **3a**.



Compound 3a			
net formula	C ₁₁ H ₁₁ NO ₂	absorption correction	Multi-Scan
CCDC	1825251	transmission factor range	0.90–1.00
M_r /g mol ⁻¹	189.21	refls. measured	10601
crystal size/mm	0.080 × 0.050 × 0.020	R_{int}	0.0669
T /K	103.(2)	mean $\sigma(I)/I$	0.0468
radiation	MoK α	θ range	3.146–25.349
diffractometer	'Bruker D8 Venture TXS'	observed refls.	1236
crystal system	<i>orthorhombic</i>	x, y (weighting scheme)	0.0447, 1.6457
space group	'P b c a'	hydrogen refinement	constr
$a/\text{\AA}$	8.2178(10)	refls in refinement	1710
$b/\text{\AA}$	13.1821(16)	parameters	128
$c/\text{\AA}$	17.446(2)	restraints	0
$\alpha/^\circ$	90	$R(F_{obs})$	0.0551
$\beta/^\circ$	90	$R_w(F^2)$	0.1340
$\gamma/^\circ$	90	S	1.056
$V/\text{\AA}^3$	1889.9(4)	shift/error _{max}	0.001
Z	8	max electron density/e \AA^{-3}	0.254
calc. density/g cm ⁻³	1.330	min electron density/e \AA^{-3}	-0.220
μ/mm^{-1}	0.092		

Table 2: Crystallographic data for compound **4g**.

Compound 4g			
net formula	$C_{11}H_{12}O_2$	absorption correction	Multi-Scan
$M_r/g\ mol^{-1}$	176.21	transmission factor range	0.89–1.00
crystal size/mm	$0.100 \times 0.090 \times 0.020$	refls. measured	6569
T/K	100.(2)	R_{int}	0.0280
radiation	MoK α	mean $\sigma(I)/I$	0.0279
diffractometer	'Bruker D8 Venture TXS'	θ range	3.548–26.371
crystal system	monoclinic	observed refls.	1640
space group	'P 1 21/c 1'	x, y (weighting scheme)	0.0506, 0.7671
$a/\text{\AA}$	7.6659(4)	hydrogen refinement	constr
$b/\text{\AA}$	8.1023(3)	refls in refinement	1867
$c/\text{\AA}$	14.9034(7)	parameters	119
$\alpha/^\circ$	90	restraints	0
$\beta/^\circ$	98.931(2)	$R(F_{obs})$	0.0498
$\gamma/^\circ$	90	$R_w(F^2)$	0.1297
$V/\text{\AA}^3$	914.45(7)	S	1.047
Z	4	shift/error $_{max}$	0.001
calc. density/ $g\ cm^{-3}$	1.280	max electron density/ $e\ \text{\AA}^{-3}$	0.473
μ/mm^{-1}	0.087	min electron density/ $e\ \text{\AA}^{-3}$	-0.227

Table 3: Crystallographic data for compound **7a**.**Compound 7a**

net formula	$C_{11}H_{10}N_2O_2$	absorption correction	Multi-Scan
$M_r/g\ mol^{-1}$	202.21	transmission factor range	0.97–1.00
crystal size/mm	$0.080 \times 0.060 \times 0.020$	refls. measured	17906
T/K	100.(2)	R_{int}	0.0370
radiation	MoK α	mean $\sigma(I)/I$	0.0192
diffractometer	'Bruker D8 Venture TXS'	θ range	3.393–26.372
crystal system	<i>orthorhombic</i>	observed refls.	1696
space group	'P b c a'	x, y (weighting scheme)	0.0406, 1.0718
$a/\text{\AA}$	7.0425(2)	hydrogen refinement	constr
$b/\text{\AA}$	14.7911(4)	refls in refinement	1942
$c/\text{\AA}$	18.2537(6)	parameters	137
$\alpha/^\circ$	90	restraints	0
$\beta/^\circ$	90	$R(F_{obs})$	0.0363
$\gamma/^\circ$	90	$R_w(F^2)$	0.0930
$V/\text{\AA}^3$	1901.42(10)	S	1.073
Z	8	shift/error $_{max}$	0.001
calc. density/ $g\ cm^{-3}$	1.413	max electron density/ $e\ \text{\AA}^{-3}$	0.208
μ/mm^{-1}	0.100	min electron density/ $e\ \text{\AA}^{-3}$	-0.254

3 Single-Pot Access to Bisorganoborinates: Applications in Zweifel Olefination²⁰⁴

3.1 ¹¹B NMR Analysis

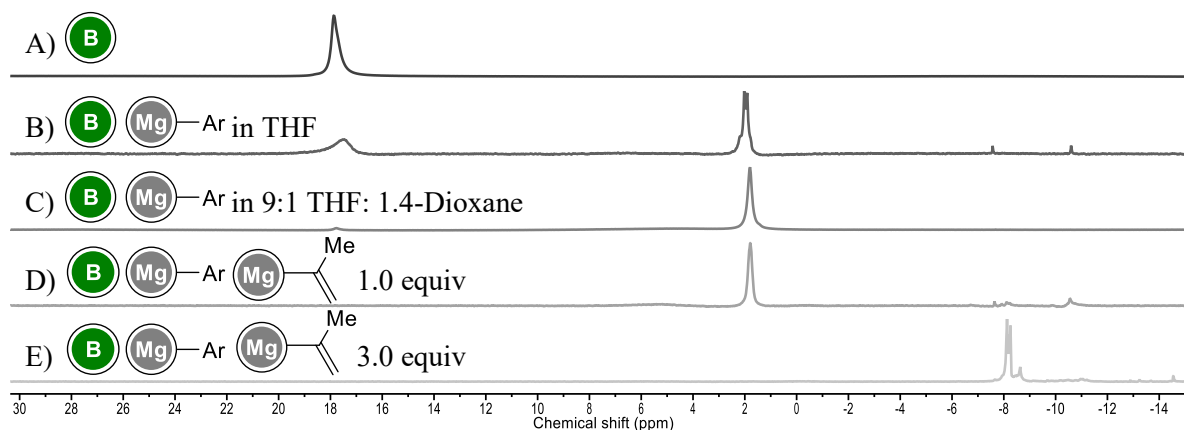


Figure 9: ¹¹B NMR Analysis of the transmetalation of B(*On*-Bu)₃ with Grignard reagents.

¹¹B NMR studies were performed under inert conditions at room temperature in non-deuterated solvents and CDCl₃ (5:2 v/v), see Figure 9 and Figure 10. In all cases, 4-bromo-1,2-dimethoxybenzene was used as the arylbromide for insertions with magnesium (general procedure C) or exchange reactions with *n*-BuLi (general procedure F). As a test substrate for alkenyl magnesium ligand exchanges prop-1-en-2-ylmagnesium bromide (SM1) was used, whereas (1-ethoxyvinyl)lithium (SM5) was used as a test substrate for alkenyl lithium ligand exchanges.

A) Reference NMR of B(*On*-Bu)₃.

B) Magnesium insertion of the aryl bromide in the presence of equimolar amounts of B(*On*-Bu)₃ in pure THF shows incomplete consumption of the B(*On*-Bu)₃. Two closely related peaks were detected, which were attributed to the monoorganoboronate and bisorganoborinate (2.02 and 1.91 ppm).

C) In the presence of 1,4-dioxane (1:9 v/v), full conversion of the B(*On*-Bu)₃ into the monoorganoboronate is observed.

D) 1.0 equiv of alkenyl magnesium reagent (SM1) result in no significant change of the measured boron species. The spectrum is almost identical to spectrum C).

E) 3.0 equiv of alkenyl magnesium reagent (SM1) result in full conversion of the monoorganoboronate. Four new signals are detected (−8.12, −8.21, −8.26, −8.63 ppm), which were all attributed to boron species with up to three consecutive ligand exchanges.

²⁰⁴ The full supporting information can be found under the following link: <https://doi.org/10.1021/acs.orglett.9b00493>. This project was conducted in equal contribution with A. N. Baumann.

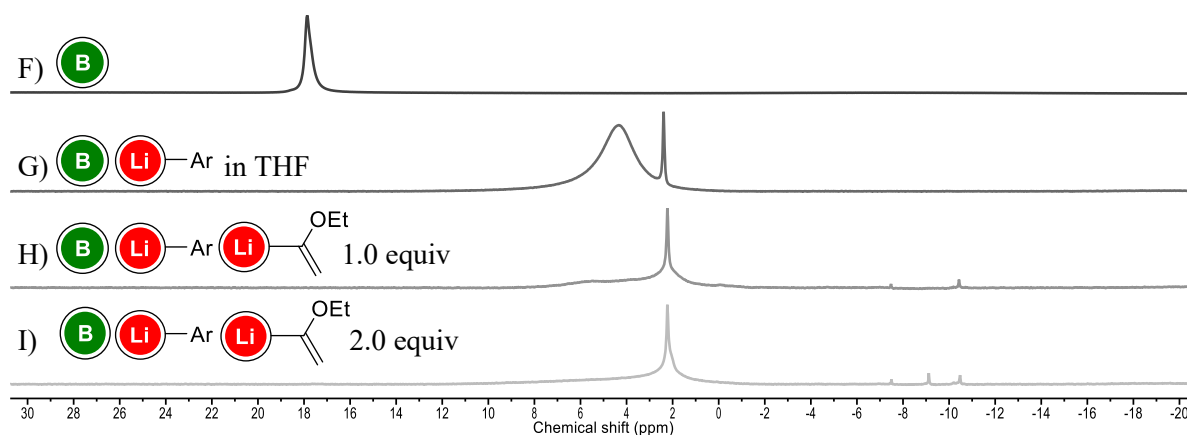


Figure 10: ^{11}B NMR Analysis of the transmetalation of $\text{B}(\text{On-Bu})_3$ with organolithium reagents.

F) Reference NMR of $\text{B}(\text{On-Bu})_3$.

G) Lithium exchange of the aryl bromide followed by addition of equimolar amounts of $\text{B}(\text{On-Bu})_3$ in pure THF. Complete consumption of the $\text{B}(\text{On-Bu})_3$ was observed. Again, two closely related peaks were detected, which were attributed to the monoorganoboronate and bisorganoborinate (4.38 and 2.39 ppm, 9:1 ratio by integration). Unfortunately, addition of 1,4-dioxane did not improve the selectivity toward the formation of the monoorganoboronate.

H) 1.0 equiv of alkenyl lithium reagent (**SM5**) result in nearly full consumption of the monoorganoboronate and the desired bisorganoborinate is detected (2.23 ppm).

I) 2.0 equiv of alkenyl lithium reagent (**SM5**) result in full consumption of the monoorganoboronate and the desired bisorganoborinate is detected (2.23 ppm).

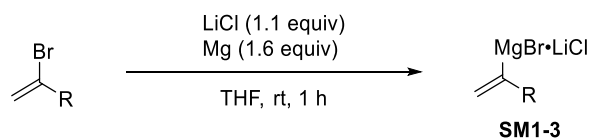
3.2 Synthesis of Organometallic Reagents

Prop-1-en-2-ylmagnesium bromide (**SM1**), vinylmagnesium bromide (**SM2**), (1-phenylvinyl)magnesium bromide (**SM3**) and (3,4-dimethoxyphenyl)magnesium bromide (**SM8**) were prepared according to literature.²⁰⁵ (3,4-Dihydro-2*H*-pyran-6-yl)lithium (**SM4**), (1-ethoxyvinyl)lithium (**SM5**) and (cyclohexylidenemethyl)lithium (**SM6**) were prepared according to literature.³² (1-Phenylvinyl)lithium (**SM7**) was prepared *via* the same protocol.

²⁰⁵ F. M. Piller, P. Appukkuttan, A. Gavryushin, M. Helm, P. Knochel, *Angew. Chem.* **2008**, *120*, 6907–6911.

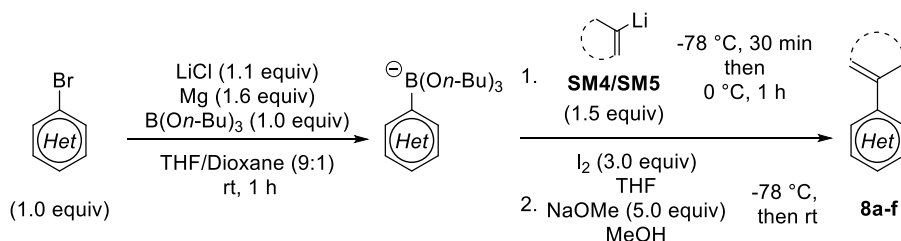
3.3 General Procedures

3.3.1 General Procedure A: Synthesis of Alkenylmagnesium Reagents



A Schlenk flask was charged with LiCl (1.17 g, 27.5 mmol, 1.1 equiv) and magnesium turnings (972 mg, 40 mmol, 1.6 equiv). LiCl and magnesium were dried *in vacuo* using a heat gun (600 °C, 2 × 5 min). After addition of THF (5.0 mL) and 1,2-dibromoethane (2 drops), the mixture was heated to boil with a heat gun to activate the magnesium. The bromoalkene (25 mmol, 1.0 equiv) was dissolved in THF (20.0 mL) and added to the activated magnesium suspension dropwise. After completion of the addition, the mixture was stirred for one hour at room temperature to yield a THF-solution of the alkenylmagnesium reagents **SM1–3**.

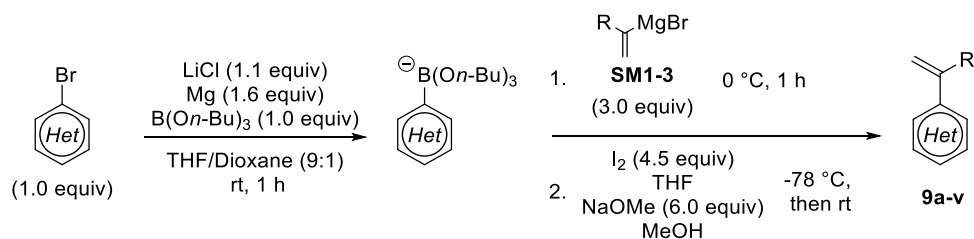
3.3.2 General Procedure B: Mg-Insertion / Transmetalation / Ligand Exchange with Alkenyllithium Reagents / Zweifel Olefination Sequence



A reaction flask was charged with LiCl (47 mg, 1.1 mmol, 1.1 equiv) and magnesium turnings (39 mg, 1.6 mmol, 1.6 equiv). LiCl and magnesium were dried *in vacuo* using a heat gun (600 °C, 2 × 5 min). After addition of THF (0.8 mL) / Dioxane (0.2 mL) and 1,2-dibromoethane (1 drop), the mixture was heated to boil with a heat gun to activate the magnesium, before tributylborate (270 μL, 1.0 mmol, 1.0 equiv) was added at once. The (hetero)aryl bromide (1.0 mmol, 1.0 equiv) was dissolved in THF (1.0 mL) and added dropwise to the activated magnesium suspension at room temperature (a water bath was used to keep the solution at ~23 °C). The mixture was then stirred for one hour at ~23 °C to yield a THF-solution of the magnesium organoboronate. The solution was cooled to –78 °C, before the solution of alkenyllithium reagent **SM4/SM5** (1.0–2.0 mmol, 1.0–2.0 equiv) was added dropwise. After half an hour, the reaction was warmed to 0 °C and stirred for 1 h. Then, after cooling back to –78 °C, iodine (761 mg, 3.0 mmol, 3.0 equiv) dissolved in THF (2.0 mL), was added dropwise to the solution. After 20 min a suspension of sodium methoxide (270 mg, 5.0 mmol, 5.0 equiv) in methanol (2.0 mL) was added at once. The reaction was allowed to reach room temperature, after which it was completed. The reaction was then quenched by the addition of sat. aq. Na₂S₂O₃ and extracted with diethyl ether (3 × 20 mL). The combined organic phases were dried over MgSO₄, filtered and concentrated under

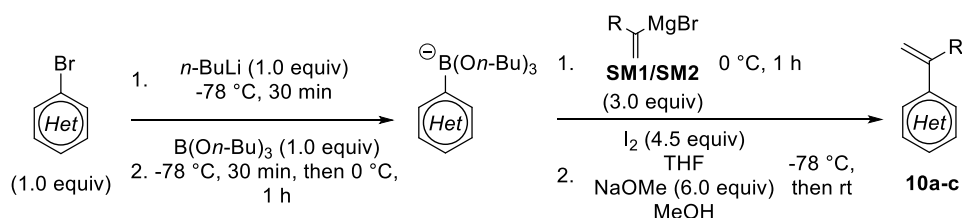
reduced pressure. The crude product was purified by column chromatography on silica gel to yield compounds **8a–f**.

3.3.3 General Procedure C: Mg-Insertion / Transmetalation / Ligand Exchange with Alkenylmagnesium Reagents / Zweifel Olefination Sequence



A reaction flask was charged with LiCl (47 mg, 1.1 mmol, 1.1 equiv) and magnesium turnings (39 mg, 1.6 mmol, 1.6 equiv). LiCl and magnesium were dried *in vacuo* using a heat gun (600 °C, 2 × 5 min). After addition of THF (0.8 mL) / Dioxane (0.2 mL) and 1,2-dibromoethane (1 drop), the mixture was heated to boil with a heat gun to activate the magnesium, before tributylborate (270 μL, 1.0 mmol, 1.0 equiv) was added at once. The (hetero)aryl bromide (1.0 mmol, 1.0 equiv) was dissolved in THF (1.0 mL) and added to the activated magnesium suspension at room temperature dropwise (to keep the solution at ~23 °C a water bath was used). The mixture was then stirred for one hour at ~23 °C to yield a THF-solution of the magnesium organoboronate. A solution of alkenylmagnesium reagent **SM1–3** (3.0 mmol, 3.0 equiv) was then added dropwise at 0 °C and stirred for another 1 h at 0 °C. Then, after the mixture was cooled back to –78 °C, iodine (1.142 g, 4.5 mmol, 4.5 equiv) dissolved in THF (2.0 mL), was added dropwise to the solution. After 20 min a suspension of sodium methoxide (348 mg, 6.0 mmol, 6.0 equiv) in methanol (2.0 mL) was added at once. The reaction was allowed to reach room temperature, after which it was completed. The reaction was then quenched by the addition of sat. aq. Na₂S₂O₃ and extracted with diethyl ether (3 × 20 mL). The combined organic phases were dried over MgSO₄, filtered and concentrated under reduced pressure. The crude product was purified by column chromatography on silica gel to yield **9a–v**.

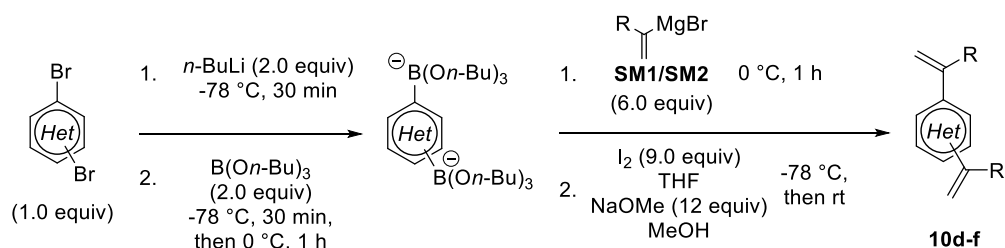
3.3.4 General Procedure D: Br/Li Exchange / Transmetalation / Ligand Exchange with Alkenylmagnesium Reagents / Zweifel Olefination Sequence



Under inert atmosphere, (hetero)aryl bromide (1.0 mmol, 1.0 equiv) was dissolved in a reaction flask in THF (1.0 mL) and the solution was cooled down to –78 °C before adding a solution of *n*-BuLi in hexanes (1.0 mmol, 2.45 M, 1.0 equiv) dropwise. The mixture was stirred for 30 min before

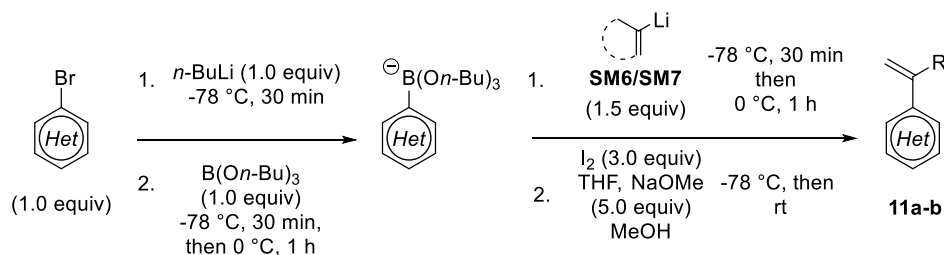
tributylborate (270 μL , 1.0 mmol, 1.0 equiv) was added dropwise at $-78\text{ }^\circ\text{C}$. The mixture was stirred for 30 min at $-78\text{ }^\circ\text{C}$ before warming to $0\text{ }^\circ\text{C}$ and stirred for another 1 h. A solution of alkenylmagnesium reagent **SM1/SM2** (3.0 mmol, 3.0 equiv) was then added dropwise at $0\text{ }^\circ\text{C}$ and stirred for another 1 h at $0\text{ }^\circ\text{C}$. Then, after cooling back to $-78\text{ }^\circ\text{C}$, iodine (1.142 g, 4.5 mmol, 4.5 equiv) dissolved in THF (2.0 mL), was added dropwise to the solution. After 20 min a suspension of sodium methoxide (348 mg, 6.0 mmol, 6.0 equiv) in methanol (2.0 mL) was added at once. The reaction was allowed to reach room temperature, after which it was completed. The reaction was then quenched by the addition of sat. aq. $\text{Na}_2\text{S}_2\text{O}_3$ and extracted with diethyl ether ($3 \times 20\text{ mL}$). The combined organic phases were dried over MgSO_4 , filtered and concentrated under reduced pressure. The crude product was purified by column chromatography on silica gel to yield **10a–c**.

3.3.5 General Procedure E: Double Br/Li exchange / Transmetalation / Ligand Exchange with Alkenylmagnesium Reagents / Zweifel Olefination Sequence



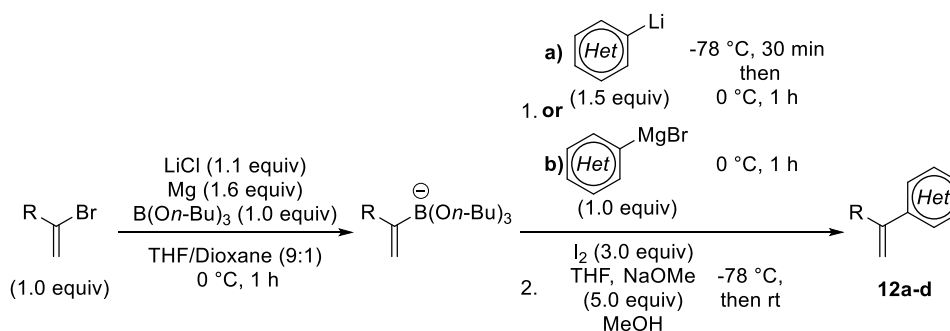
Under inert atmosphere, (hetero)aryl bromide (2.0 mmol, 1.0 equiv) was dissolved in a reaction flask in THF (2.0 mL) and the solution was cooled down to $-78\text{ }^\circ\text{C}$ before adding a solution of $n\text{-BuLi}$ in hexanes (2.0 mmol, 2.45 M, 1.0 equiv) dropwise. The mixture was stirred for 30 min before tributylborate (540 μL , 2.0 mmol, 1.0 equiv) was added dropwise at $-78\text{ }^\circ\text{C}$. The mixture was stirred for 30 min at $-78\text{ }^\circ\text{C}$ before warming to $0\text{ }^\circ\text{C}$ and stirred for another 1 h. A solution of alkenylmagnesium reagent **SM1/SM2** (6.0 mmol, 3.0 equiv) was then added dropwise at $0\text{ }^\circ\text{C}$ and stirred for another 1 h at $0\text{ }^\circ\text{C}$. Then, after cooling back to $-78\text{ }^\circ\text{C}$, iodine (2.284 g, 9.0 mmol, 9.0 equiv) dissolved in THF (2.0 mL), was added dropwise to the solution. After 20 min a suspension of sodium methoxide (648 mg, 12.0 mmol, 12 equiv) in methanol (2.0 mL) was added at once. The reaction was allowed to reach room temperature, after which it was completed. The reaction was then quenched by the addition of sat. aq. $\text{Na}_2\text{S}_2\text{O}_3$ and extracted with diethyl ether ($3 \times 20\text{ mL}$). The combined organic phases were dried over MgSO_4 , filtered and concentrated under reduced pressure. The crude product was purified by column chromatography on silica gel to yield **10d–f**.

3.3.6 General procedure F: Br/Li-Exchange / Transmetalation / Ligand Exchange with Alkenyllithium Reagents / Zweifel Olefination Sequence



Under inert atmosphere, (hetero)aryl bromide (2.0 mmol, 1.0 equiv) was dissolved in a reaction flask in THF (2.0 mL) and the solution was cooled down to $-78\text{ }^\circ\text{C}$ before adding a solution of $n\text{-BuLi}$ in hexanes (2.0 mmol, 2.45 M, 1.0 equiv) dropwise. The mixture was stirred for 30 min before tributylborate (540 μL , 2.0 mmol, 1.0 equiv) was added dropwise at $-78\text{ }^\circ\text{C}$. The mixture was stirred for 30 min at $-78\text{ }^\circ\text{C}$ before warming to $0\text{ }^\circ\text{C}$ and stirred for another 1 h. The solution was cooled to $-78\text{ }^\circ\text{C}$, before the solution of alkenyllithium reagent **SM6/SM7** (1.5 mmol, 1.5 equiv) was added dropwise. After half an hour, the reaction was warmed to $0\text{ }^\circ\text{C}$ and stirred for 1 h. Then, after cooling back to $-78\text{ }^\circ\text{C}$, iodine (761 mg, 3.0 mmol, 3.0 equiv) dissolved in THF (2.0 mL), was added dropwise to the solution. After 20 min a suspension of sodium methoxide (270 mg, 5.0 mmol, 5.0 equiv) in methanol (2.0 mL) was added at once. The reaction was allowed to reach room temperature, after which it was completed. The reaction was then quenched by the addition of sat. aq. $\text{Na}_2\text{S}_2\text{O}_3$ and extracted with diethyl ether ($3 \times 20\text{ mL}$). The combined organic phases were dried over MgSO_4 , filtered and concentrated under reduced pressure. The crude product was purified by column chromatography on silica gel to yield **11a-b**.

3.3.7 General Procedure G: Mg-Insertion / Transmetalation / Ligand Exchange with (Hetero)Aryl-Lithium or -Magnesium Reagents / Zweifel Olefination Sequence



A reaction flask was charged with LiCl (47 mg, 1.1 mmol, 1.1 equiv) and magnesium turnings (39 mg, 1.6 mmol, 1.6 equiv). LiCl and magnesium were dried *in vacuo* using a heat gun ($600\text{ }^\circ\text{C}$, $2 \times 5\text{ min}$). After addition of THF (0.8 mL) / Dioxane (0.2 mL) and 1,2-dibromoethane (1 drop), the mixture was heated to boil with a heat gun to activate the magnesium, before tributylborate (270 μL , 1.0 mmol, 1.0 equiv) was added at once. Alkenylbromide (1.0 mmol, 1.0 equiv) was dissolved in THF (1.0 mL)

and added to the activated magnesium suspension at 0 °C. The mixture was then stirred for 1 h at 0 °C to yield a THF-solution of the magnesium organoboronate.

a) Use of (hetero)aryl lithium reagent

In the meantime, a solution of (hetero)aryl lithium was prepared by using the corresponding bromide (1.5 mmol, 1.5 equiv) in THF (2.0 mL) followed by the dropwise addition of a solution of *n*-BuLi in hexanes (1.5 mmol, 1.5 equiv) at -78 °C. This solution was stirred for 30 min. The prior formed organoboronate was then slowly added to the (hetero)aryl lithium species at -78 °C. The combined mixture was stirred for 30 min at -78 °C before warming to 0 °C and being stirred for another 1 h.

b) Use of (hetero)aryl magnesium reagent

A prior synthesized and titrated (hetero)aryl magnesium reagent was prepared by charging a Schlenk flask with LiCl (448 mg, 11 mmol, 1.1 equiv) and magnesium turnings (389 mg, 16 mmol, 1.6 equiv). LiCl and magnesium were dried *in vacuo* using a heat gun (600 °C, 2 × 5 min). After addition of THF (5.0 mL) and 1,2-dibromoethane (2 drops), the mixture was heated to boil with a heat gun to activate the magnesium. The corresponding (hetero)aryl bromide (10 mmol, 1.0 equiv) was dissolved in THF (5.0 mL) and added to the activated magnesium suspension dropwise. After completion of the addition, the mixture was stirred for one hour at room temperature to yield a THF-solution of the organomagnesium reagent. Then, after cooling back to -78 °C, iodine (761 mg, 3.0 mmol, 3.0 equiv) dissolved in THF (2.0 mL), was added dropwise to the solution. After 20 min a suspension of sodium methoxide (270 mg, 5.0 mmol, 5.0 equiv) in methanol (2.0 mL) was added at once. The reaction was allowed to reach room temperature. After reaching room temperature the reaction is completed. The reaction was then quenched by the addition of sat. aq. Na₂S₂O₃ and extracted with diethyl ether (3 × 20 mL). The combined organic phases were dried over MgSO₄, filtered and concentrated under reduced pressure. The crude product was purified by column chromatography on silica gel to yield **12a-d**.

3.3.8 Optimizations for General Procedure G (b):

GC-ratios were determined by comparing to *n*-undecane as internal standard (SD). As shown in Table 4, no significant increase in product formation of **9h** was observed with increasing amount of aryl magnesium reagent **SM8**.

Table 4: Influence of added equivalents of Grignard **SM8** on conversion rates.

Entry	SM8 (equiv)	GC-ratio 9h : SD (%)
1	1.0	37 : 63
2	2.0	36 : 64
3	3.0	39 : 61

3.4 Experimental Data

6-Chloro-3-(3,4-dihydro-2H-pyran-6-yl)-2-methylpyridine (**8a**)

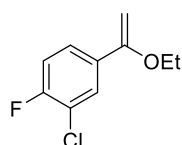
Using 3-bromo-6-chloro-2-methylpyridine and (3,4-dihydro-2H-pyran-6-yl)lithium (**SM4**) according to general procedure **B**, provided **8a** (0.54 mmol, 114 mg, 54%) as orange oil. $R_f = 0.40$ (hexane/EtOAc 95:5 and 1 % NEt₃, UV, PAA, KMnO₄). ¹H NMR (400 MHz, CDCl₃) δ 7.53 – 7.51 (d, $J = 8.1$ Hz, 1H), 7.12 – 7.10 (d, $J = 8.0$ Hz, 1H), 4.89 – 4.87 (t, $J = 3.9$ Hz, 1H), 4.15 – 4.13 (t, $J = 5.1$ Hz, 2H), 2.55 (s, 3H), 2.21 – 2.17 (td, $J = 6.4, 3.9$ Hz, 2H), 1.96 – 1.90 (m, 2H) ppm. ¹³C NMR (101 MHz, CDCl₃) δ 157.8, 150.9, 149.3, 139.0, 131.3, 120.9, 96.9, 66.3, 23.2, 22.5, 22.1 ppm. LRMS (DEP/EI-Orbitrap): m/z [%]: 209.1 (100), 194.1 (19), 180.1 (45), 166.1 (24), 154.0 (95). HRMS (EI-Orbitrap): m/z calcd for C₁₁H₁₂ClNO⁺: 209.0607; found: 209.0596. IR (Diamond-ATR, neat) $\tilde{\nu}_{max}$ (cm⁻¹): 2939 (s), 2935 (m), 2872 (m), 1714 (w), 1690 (s). Fast decomposition in chloroform was observed.

1,2-Dichloro-4-(1-ethoxyvinyl)benzene (**8b**)

Using 4-bromo-1,2-dichlorobenzene and (1-ethoxyvinyl)lithium (**SM5**) according to general procedure **B**, provided **8b** (0.58 mmol, 125 mg, 58%) as colorless liquid. $R_f = 0.50$ (hexane and 1 % NEt₃, UV, PAA, KMnO₄). ¹H NMR (400 MHz, CDCl₃) δ 7.71 (d, $J = 2.0$ Hz, 1H), 7.45 (dd, $J = 8.4, 2.0$ Hz, 1H), 7.38 (d, $J = 8.4$ Hz, 1H), 4.64 (d, $J = 3.0$ Hz, 1H), 4.24 (d, $J = 3.0$ Hz, 1H), 3.91 (q, $J = 7.0$ Hz, 2H), 1.42 (t, $J = 7.0$ Hz, 3H) ppm. ¹³C NMR (101 MHz, Benzene-d₆) δ 157.9, 137.1, 132.8, 132.6, 130.3, 127.6, 124.9, 83.5, 63.5, 14.3 ppm. LRMS

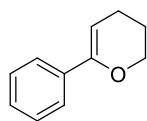
(DEP/EI-Orbitrap): m/z [%]: 216.0 (8), 188.0 (23), 175.0 (64), 173.0 (100), 146.0 (19), 109.0 (6). **HRMS** (EI-Orbitrap): m/z calcd for $C_{10}H_{10}Cl_2O^+$: 216.0109; found: 216.0104. **IR** (Diamond-ATR, neat) $\tilde{\nu}_{max}$ (cm^{-1}): 2977 (w), 2932 (w), 2886 (w), 1724 (w), 1693 (m), 1584 (w), 1557 (w), 1469 (s), 1378 (m), 1268 (s), 1240 (s), 1122 (s), 1050 (s).

2-Chloro-4-(1-ethoxyvinyl)-1-fluorobenzene (**8c**)*



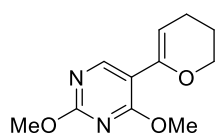
Using 4-bromo-2-chloro-1-fluorobenzene and (1-ethoxyvinyl)lithium (**SM5**) according to general procedure **B**, provided **8c** (0.58 mmol, 116 mg, 58%) as colorless oil. R_f = 0.41 (hexane, UV, PAA, $KMnO_4$). **1H NMR** (400 MHz, C_6D_6) δ 7.72 (dd, J = 7.2, 2.2 Hz, 1H), 7.19 (m, 1H), 6.61 (t, J = 8.7 Hz, 1H), 4.38 (d, J = 2.9 Hz, 1H), 3.95 (d, J = 2.9 Hz, 1H), 3.43 (q, J = 7.0 Hz, 2H), 1.03 (t, J = 7.0 Hz, 3H) ppm. **^{13}C NMR** (101 MHz, C_6D_6) δ 158.5 (d, J = 249.8 Hz), 158.1 (d, J = 0.8 Hz), 134.3 (d, J = 3.9 Hz), 125.5, 125.4, 121.2 (d, J = 18.0 Hz), 116.3 (d, J = 21.2 Hz), 82.9 (d, J = 1.4 Hz), 63.5, 14.3 ppm. **LRMS** (DEP/EI-Orbitrap): m/z [%]: 200.0 (7), 174.0 (14), 172.0 (19), 159.0 (33), 158.0 (7), 157.0 (100), 156 (11), 130.0 (11), 129.0 (35). **HRMS** (EI-Orbitrap): m/z calcd for $C_{10}H_{10}ClFO^+$: 200.0404; found: 200.0396. **IR** (Diamond-ATR, neat) $\tilde{\nu}_{max}$ (cm^{-1}): 2976 (w), 2279 (w), 1692 (w), 1593 (w).

6-Phenyl-3,4-dihydro-2H-pyran (**8d**)*



Using bromobenzene and (3,4-dihydro-2H-pyran-6-yl)lithium (**SM4**) according to general procedure **B**, provided **8d** (0.41 mmol, 66 mg, 41%) as colorless oil. R_f = 0.65 (hexane/EtOAc 95:5, UV, $KMnO_4$). **1H NMR** (400 MHz, C_6D_6) δ 7.72 – 7.64 (m, 2H), 7.21 – 7.12 (m, 2H), 7.10 – 7.00 (m, 1H), 5.22 (t, J = 4.0 Hz, 1H), 3.83 (t, J = 6.2, 4.7 Hz, 2H), 1.86 (td, J = 6.4, 4.0 Hz, 2H), 1.51 – 1.39 (m, 2H) ppm. **LRMS** (DEP/EI-Orbitrap): m/z [%]: 160.1 (65), 131.1 (15), 115.1 (10), 105.1 (100), 77.1 (45), 51.1 (15). Analytical data in accordance to literature.²⁰⁶

5-(3,4-Dihydro-2H-pyran-6-yl)-2,4-dimethoxypyrimidine (**8e**)

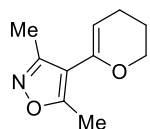


Using 5-bromo-2,4-dimethoxypyrimidine and (3,4-dihydro-2H-pyran-6-yl)lithium (**SM4**) according to general procedure **B**, provided **8e** (0.45 mmol, 101 mg, 45%) as yellowish oil. Repeated in 10 mmol gram scale provided **8e** (4.20 mmol, 933 mg, 42%) as yellowish oil. R_f = 0.30 (hexane/EtOAc 95:5 and 1 % NEt_3 , UV, PAA, $KMnO_4$). **1H NMR** (400 MHz, $CDCl_3$) δ 8.42 (s, 1H), 5.50 – 5.48 (t, J = 4.0 Hz, 1H), 4.15 – 4.13 (t, J = 5.2 Hz, 2H), 4.02 (s, 3H), 3.99 (s, 3H), 2.23 – 2.19 (td, J = 6.4, 4.1 Hz, 2H), 1.93 – 1.87 (dt, J = 11.7, 6.3 Hz, 2H) ppm. **^{13}C NMR** (101 MHz, $CDCl_3$) δ 167.8, 164.0, 156.5, 145.7, 111.7, 102.5, 66.6, 54.9, 54.3, 22.4, 20.9 ppm. **LRMS** (DEP/EI-Orbitrap): m/z [%]: 222.2 (98), 207.1 (14), 193.0 (19), 167.1 (100). **HRMS** (EI-Orbitrap): m/z calcd for $C_{11}H_{14}N_2O_3^+$: 222.1004; found: 222.0997. **IR** (Diamond-ATR, neat) $\tilde{\nu}_{max}$

²⁰⁶ U. Lehmann, S. Awasthi, T. Minehan, *Org. Lett.*, **2003**, *5*, 2405–2408.

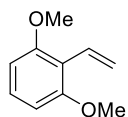
(cm^{-1}): 2928 (m), 2870 (w), 1733 (vw), 1717 (w), 1691 (w). Fast decomposition in chloroform was observed.

4-(3,4-Dihydro-2H-pyran-6-yl)-3,5-dimethylisoxazole (8f)



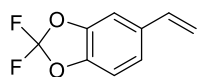
Using 4-bromo-3,5-dimethylisoxazole and (3,4-dihydro-2H-pyran-6-yl)lithium (**SM4**) according to general procedure **B**, provided **8f** (0.41 mmol, 74 mg, 41%) as orange oil. $R_f = 0.40$ (hexane/EtOAc 95:5 and 1 % NEt_3 , UV, PAA, KMnO_4). $^1\text{H NMR}$ (400 MHz, CDCl_3) δ 4.80 – 4.78 (t, $J = 3.9$ Hz, 1H), 4.11 – 4.09 (t, $J = 5.1$ Hz, 2H), 2.41 (s, 3H), 2.26 (s, 3H), 2.19 – 2.15 (td, $J = 6.4, 3.9$ Hz, 2H), 1.92 – 1.87 (m, 2H) ppm. $^{13}\text{C NMR}$ (101 MHz, CDCl_3) δ 166.3, 158.7, 144.9, 113.1, 101.1, 66.4, 22.4, 20.7, 12.3, 11.5 ppm. **LRMS** (DEP/EI-Orbitrap): m/z [%]: 179.1 (100), 149.8 (21), 135.9 (90), 123.9 (38), 108.9 (22). **HRMS** (EI-Orbitrap): m/z calcd for $\text{C}_{10}\text{H}_{13}\text{NO}_2^+$: 179.0946; found: 179.0938. **IR** (Diamond-ATR, neat) $\tilde{\nu}_{\text{max}}$ (cm^{-1}): 2929 (w), 2848 (w), 1672 (m), 1653 (w), 1646 (w). Fast decomposition in chloroform was observed.

1,3-Dimethoxy-2-vinylbenzene (9a)*



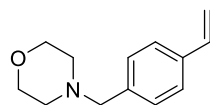
Using 2-bromo-1,3-dimethoxybenzene and vinylmagnesium bromide (**SM2**) according to general procedure **C**, provided **9a** (0.70 mmol, 115 mg, 70%) as yellow oil. $R_f = 0.67$ (hexane/EtOAc 98:2, UV, PAA, KMnO_4). $^1\text{H NMR}$ (400 MHz, CDCl_3) δ 7.04 (t, $J = 8.3$ Hz, 1H), 6.88 (dd, $J = 18.0, 12.1$ Hz, 1H), 6.44 (d, $J = 8.4$ Hz, 2H), 5.98 (dd, $J = 18.0, 2.8$ Hz, 1H), 5.35 (dd, $J = 12.2, 2.8$ Hz, 1H), 3.72 (s, 6H) ppm. **LRMS** (DEP/EI-Orbitrap): m/z [%]: 164.1 (75), 149.1 (100), 121.1 (30), 105.1 (10), 91.1 (95), 78.1 (25), 63.1 (12), 51.1 (10). Analytical data in accordance to literature.²⁰⁷

2,2-Difluoro-5-vinylbenzo[d][1,3]dioxole (9b)*



Using 5-bromo-2,2-difluorobenzo[d][1,3]dioxole and vinylmagnesium bromide (**SM2**) according to general procedure **C**, provided **9b** (0.64 mmol, 118 mg, 64% yield determined by $^{19}\text{F NMR}$ vs internal standard hexafluorobenzene) as colorless oil. $R_f = 0.68$ (pentane, UV, PAA, KMnO_4). $^1\text{H NMR}$ (400 MHz, CDCl_3) δ 7.16 (d, $J = 1.6$ Hz, 1H), 7.07 (dd, $J = 8.2, 1.7$ Hz, 1H), 7.00 (d, $J = 8.3$ Hz, 1H), 6.66 (dd, $J = 17.5, 10.8$ Hz, 1H), 5.66 (d, $J = 17.5$ Hz, 1H), 5.25 (d, $J = 10.8$ Hz, 1H) ppm. **LRMS** (DEP/EI-Orbitrap): m/z [%]: 184.1 (95), 118.1 (10), 89.1 (100), 63.1 (30), 51.1 (10). Analytical data in accordance to literature.²⁰⁸

4-(4-Vinylbenzyl)morpholine (9c)



Using 4-(4-bromobenzyl)morpholine and vinylmagnesium bromide (**SM2**) according to general procedure **C**, provided **9c** (0.502 mmol, 102 mg, 50%) as colorless oil. $R_f = 0.26$ (hexane/EtOAc 7:3, UV, PAA, KMnO_4). $^1\text{H NMR}$ (400 MHz, CDCl_3)

²⁰⁷ B. Bieszczad, M. Barbasiewicz, *Chem. Eur. J.* **2015**, *21*, 10322–10325.

²⁰⁸ G. Wang, R. Shang, Y. Fu, *Org. Lett.* **2018**, *20*, 888–891.

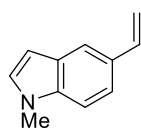
δ 7.30 (d, $J = 8.1$ Hz, 2H), 7.22 (d, $J = 8.0$ Hz, 2H), 6.64 (dd, $J = 17.6, 10.9$ Hz, 1H), 5.67 (d, $J = 17.6$ Hz, 1H), 5.16 (d, $J = 10.8$ Hz, 1H), 3.64 (t, $J = 4.6$ Hz, 4H), 3.41 (s, 2H), 2.48 – 2.30 (m, 4H) ppm. ^{13}C NMR (101 MHz, CDCl_3) δ 137.5, 136.6, 129.5, 128.3, 126.2, 113.7, 67.1, 63.2, 53.7 ppm. LRMS (DEP/EI-Orbitrap): m/z [%]: 203.2 (40), 172.2 (25), 130.1 (10), 117.1 (100), 100.1 (5), 86.1 (25), 56.1 (8). HRMS (EI-Orbitrap): m/z calcd for $\text{C}_{13}\text{H}_{17}\text{NO}^+$: 203.1310; found: 203.1306. IR (Diamond-ATR, neat) $\tilde{\nu}_{\text{max}}$ (cm^{-1}): 2958 (vw), 2853 (w), 2805 (w), 2360 (vw), 1511 (vw), 1454 (w), 1395 (vw), 1349 (w), 1288 (w), 1116 (vs), 1007 (m), 913 (m), 866 (s), 741 (vw), 668 (vw).

1-Fluoro-4-vinylnaphthalene (9d)*



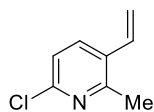
Using 1-bromo-4-fluoronaphthalene and vinylmagnesium bromide (**SM2**) according to general procedure C, provided **9d** (0.63 mmol, 109 mg, 63%) as colorless oil. $R_f = 0.79$ (pentane, UV, PAA, KMnO_4). ^1H NMR (400 MHz, CDCl_3) δ 8.17 – 8.08 (m, 2H), 7.63 – 7.52 (m, 3H), 7.41 (dd, $J = 17.3, 10.9$ Hz, 1H), 7.14 (dd, $J = 10.4, 8.0$ Hz, 1H), 5.76 (dd, $J = 17.2, 1.5$ Hz, 1H), 5.47 (dd, $J = 10.9, 1.4$ Hz, 1H) ppm. LRMS (DEP/EI-Orbitrap): m/z [%]: 171.1 (100), 151.1 (5), 85.1 (10), 75.1 (4). Analytical data in accordance to literature.²⁰⁹

1-Methyl-5-vinyl-1H-indole (9e)



Using 5-bromo-1-methyl-1H-indole and vinylmagnesium bromide (**SM2**) according to general procedure C provided **9e** (0.52 mmol, 82 mg, 52%) as colorless oil. $R_f = 0.32$ (hexane, UV, PAA, KMnO_4). ^1H NMR (400 MHz, CDCl_3): δ 7.65 (s, 1H), 7.39 (dd, $J = 8.5, 1.5$ Hz, 1H), 7.28 (d, $J = 8.5$ Hz, 1H), 7.04 (d, $J = 3.1$ Hz, 1H), 6.86 (dd, $J = 17.6, 10.9$ Hz, 1H), 6.49 – 6.48 (m, 1H), 5.72 (dd, $J = 17.6, 1.0$ Hz, 1H), 5.15 (dd, $J = 10.9, 0.9$ Hz, 1H), 3.79 (s, 3H) ppm. LRMS (DEP/EI-Orbitrap): m/z [%]: 158.1 (11), 157.1 (100), 156.1 (33), 154 (12), 130.1 (8), 115.1 (13). Analytical data in accordance to literature.²¹⁰

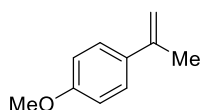
6-Chloro-2-methyl-3-vinylpyridine (9f)



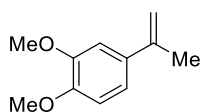
Using 3-bromo-6-chloro-2-methylpyridine and vinylmagnesium bromide (**SM2**) according to general procedure C, provided **9f** (0.45 mmol, 69 mg, 45%) as colorless oil. $R_f = 0.25$ (hexane/EtOAc 95:5, UV, KMnO_4). ^1H NMR (400 MHz, CDCl_3) δ 7.68 (d, $J = 8.1$ Hz, 1H), 7.15 (d, $J = 8.2$ Hz, 1H), 6.83 (dd, $J = 17.4, 11.0$ Hz, 1H), 5.66 (dd, $J = 17.5, 0.9$ Hz, 1H), 5.42 (dd, $J = 11.0, 0.8$ Hz, 1H), 2.55 (s, 3H) ppm. ^{13}C NMR (101 MHz, CDCl_3) δ 156.5, 149.2, 135.7, 132.3, 131.0, 122.0, 117.9, 22.4 ppm. LRMS (DEP/EI-Orbitrap): m/z [%]: 153.1 (100), 116.1 (50), 91.1 (25), 77.1 (25), 63.1 (20), 51.1 (25). HRMS (EI-Orbitrap): m/z calcd for $\text{C}_8\text{H}_8\text{ClN}^+$: 153.0345; found: 153.0340. IR (Diamond-ATR, neat) $\tilde{\nu}_{\text{max}}$ (cm^{-1}): 2924 (vw), 1692 (vw), 1625 (w), 1575 (m), 1441 (vs), 1252 (w), 1146 (s), 986 (m), 893 (vs), 829 (s), 738 (w) 664 (vw).

²⁰⁹ C. Yang, J. Han, Y. Zhang, H. Yu, S. Hu, X. Wang, *Chem. Eur. J.* **2018**, *24*, 10324–10328.

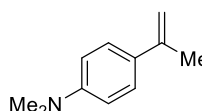
²¹⁰ J. J. Molloy, C. P. Seath, M. J. West, C. McLaughlin, N. J. Fazakerley, A. R. Kennedy, D. J. Nelson, A. J. B. Watson, *J. Am. Chem. Soc.* **2018**, *140*, 126–130.

1-Methoxy-4-(prop-1-en-2-yl)benzene (9g)

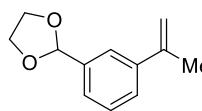
Using 1-bromo-4-methoxybenzene and prop-1-en-2-ylmagnesium bromide (**SM1**) according to general procedure **C** provided **9g** (0.89 mmol, 187 mg, 89%) as colorless solid. $R_f = 0.20$ (pentane/Et₂O 9:1, UV, PAA, KMnO₄). ¹H NMR (400 MHz, CDCl₃) δ 7.43 – 7.41 (d, $J = 8.8$ Hz, 2H), 6.88 – 6.86 (d, $J = 8.8$ Hz, 2H), 5.29 (s, 1H), 4.99 (s, 1H), 3.82 (s, 3H), 2.13 (s, 3H) ppm. LRMS (DEP/EI-Orbitrap): m/z [%]: 148.1 (100), 133.1 (82), 115.0 (11), 105.1 (24). Analytical data in accordance to literature.²¹¹

1,2-Dimethoxy-4-(prop-1-en-2-yl)benzene (9h)*

Using 4-bromo-1,2-dimethoxybenzene and prop-1-en-2-ylmagnesium bromide (**SM1**) according to general procedure **C** provided **9h** (0.72 mmol, 128 mg, 72%) as colorless oil. General procedure **C** without base (**NaOMe**) provided **9h** in 61%. General procedure **G (a)** provided **9h** in 45%. General procedure **G (b)** using (3,4-dimethoxyphenyl)magnesium bromide (**SM8**) provided **9h** in 40% $R_f = 0.79$ (hexane/EtOAc 96:4, UV, PAA, KMnO₄). ¹H NMR (400 MHz, CDCl₃) δ 7.04 – 7.00 (m, 2H), 6.83 (d, $J = 8.8$ Hz, 1H), 5.30 (s, 1H), 5.02 (s, 1H), 3.91 (s, 3H), 3.89 (s, 3H), 2.14 (s, 3H) ppm. LRMS (DEP/EI-Orbitrap): m/z [%]: 178.2 (100), 163.1 (35), 135.1 (14), 115.1 (11), 107.1 (18), 91.1 (36), 77.1 (16). Analytical data in accordance to literature.²¹²

***N,N*-Dimethyl-4-(prop-1-en-2-yl)aniline (9i)**

Using 4-bromo-*N,N*-dimethylaniline and prop-1-en-2-ylmagnesium bromide (**SM2**) according to general procedure **C** provided **9i** (0.63 mmol, 101 mg, 63%) as colorless oil. General procedure **G (a)** provided **9i** in 31%. $R_f = 0.11$ (hexane/EtOAc 99:1, UV, PAA, KMnO₄). ¹H NMR (400 MHz, CDCl₃) δ 7.41 (d, $J = 9.0$ Hz, 2H), 6.71 (d, $J = 9.0$ Hz, 2H), 5.28 (s, 1H), 4.93 (s, 1H), 2.97 (s, 6H), 2.14 (s, 3H) ppm. LRMS (DEP/EI-Orbitrap): m/z [%]: 161.1 (100), 146.1 (42), 129.9 (10), 114.9 (13), 102.9 (9), 77.1 (11). Analytical data in accordance to literature.²¹³

2-(3-(Prop-1-en-2-yl)phenyl)-1,3-dioxolane (9j)

Using 2-(3-bromophenyl)-1,3-dioxolane and prop-1-en-2-ylmagnesium bromide (**SM1**) according to general procedure **C**, provided **9j** (0.49 mmol, 93 mg, 49%) as colorless oil. $R_f = 0.20$ (hexane, UV, PAA KMnO₄). ¹H NMR (400 MHz, CDCl₃) δ 7.57 (s, 1H), 7.47 (dt, $J = 7.4, 1.7$ Hz, 1H), 7.41 – 7.32 (m, 2H), 5.83 (s, 1H), 5.39 (s, 1H), 5.10 (t, $J = 1.5$ Hz, 1H), 4.18 – 4.01 (m, 4H), 2.16 (s, 3H) ppm. ¹³C NMR (101 MHz, CDCl₃) δ 143.1, 141.6, 137.9, 128.4, 126.5, 125.6, 123.7, 113.0, 103.9, 65.5, 22.0 ppm. LRMS (DEP/EI-Orbitrap): m/z [%]:

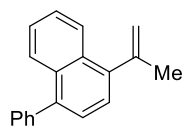
²¹¹ W. J. Kerr, A. J. Morrison, M. Pazicky, T. Weber, *Org. Lett* **2012**, *14*, 2250–2253.

²¹² A. Flores-Gaspar, R. Martin, *Adv. Synth. Catal.* **2011**, *353*, 1223–1228.

²¹³ E. Peyroux, F. Berthiol, H. Doucet, M. Santelli, *Eur. J. Org. Chem.* **2004**, 1075–1082.

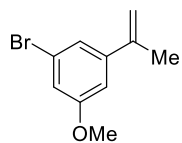
189.2 (100), 175.1 (25), 162.1 (25), 145.1 (65), 134.1 (20), 118.1 (75), 103.1 (15), 91.1 (35), 77.1 (15), 73.1 (60), 63.1 (10), 51.1 (10). **HRMS** (EI-Orbitrap): m/z calcd for $C_{12}H_{14}O_2^+$: 190.0994; found: 190.0998. **IR** (Diamond-ATR, neat) $\tilde{\nu}_{max}$ (cm^{-1}): n.d.

1-Phenyl-4-(prop-1-en-2-yl)naphthalene (9k)*



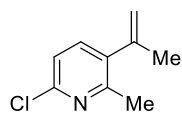
Using 1-bromo-4-phenylnaphthalene and prop-1-en-2-ylmagnesium bromide (**SM1**) according to general procedure **C** provided **9k** (0.59 mmol, 133 mg, 59%) as colorless oil. $R_f = 0.75$ (hexane, UV, PAA $KMnO_4$). **1H NMR** (400 MHz, $CDCl_3$) δ 8.25 (dd, $J = 8.5, 1.3$ Hz, 1H), 8.08 – 8.01 (m, 1H), 7.63 – 7.55 (m, 6H), 7.54 – 7.45 (m, 3H), 5.56 (s, 1H), 5.24 (s, 1H), 2.37 (s, 3H) ppm. **^{13}C NMR** (101 MHz, $CDCl_3$) δ 144.9, 142.0, 141.0, 139.5, 132.0, 131.2, 130.2, 128.4, 127.3, 126.6, 126.5, 126.2, 125.9, 125.8, 124.2, 116.4, 25.5 ppm. **LRMS** (DEP/EI-Orbitrap): m/z [%]: 244.2 (70), 229.2 (100), 215.1 (5), 202.1 (15), 165.1 (15), 152.1 (8), 113.1 (8), 101.1 (5), 91.1 (6). **HRMS** (EI-Orbitrap): m/z calcd for $C_{19}H_{16}^+$: 244.1252; found: 244.1250. **IR** (Diamond-ATR, neat) $\tilde{\nu}_{max}$ (cm^{-1}): 1492 (vw), 1443 (w), 1370 (vw), 1157 (vw), 1031 (w), 902 (m), 842 (m), 767 (vs), 701 (vs).

1-Bromo-3-methoxy-5-(prop-1-en-2-yl)benzene (9l)

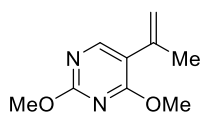


Using 1,3-dibromo-5-(prop-1-en-2-yl)benzene and prop-1-en-2-ylmagnesium bromide (**SM1**) according to general procedure **D** provided **9l** (0.34 mmol, 154 mg, 34%) as colorless oil. $R_f = 0.59$ (hexane/EtOAc 98:2, UV, PAA, $KMnO_4$). **1H NMR** (400 MHz, $CDCl_3$) δ 7.17 (t, $J = 1.6$ Hz, 1H), 6.94 (t, $J = 2.0$ Hz, 1H), 6.89 (t, $J = 1.9$ Hz, 1H), 5.34 (s, 1H), 5.09 (s, 1H), 3.79 (s, 3H), 2.09 (s, 3H) ppm. **^{13}C NMR** (101 MHz, $CDCl_3$) δ 160.3, 144.4, 142.1, 122.8, 121.4, 115.7, 114.0, 111.0, 55.6, 21.9 ppm. **LRMS** (DEP/EI-Orbitrap): m/z [%]: 229.0 (11), 228.0 (98), 227.0 (11), 226 (100), 188.0 (15), 186.0 (15). **HRMS** (EI-Orbitrap): m/z calcd for $C_{10}H_{11}BrO^+$: 225.9993; found: 225.9995. **IR** (Diamond-ATR, neat) $\tilde{\nu}_{max}$ (cm^{-1}): 2938 (br/w), 1599 (m), 1557 (vs), 1560 (s).

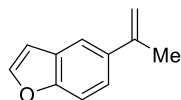
6-Chloro-2-methyl-3-(prop-1-en-2-yl)pyridine (9m)



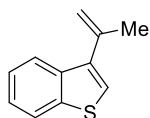
Using 3-bromo-6-chloro-2-methylpyridine and prop-1-en-2-ylmagnesium bromide (**SM1**) according to general procedure **C** provided **9m** (0.71 mmol, 119 mg, 71%) as yellow oil. $R_f = 0.50$ (hexane/EtOAc 9:1 UV, PAA, $KMnO_4$). **1H NMR** (400 MHz, $CDCl_3$) δ 7.37 – 7.35 (d, $J = 8.0$ Hz, 1H), 7.12 – 7.10 (d, $J = 8.0$ Hz, 1H), 5.27 (s, 1H), 4.91 (s, 1H), 2.51 (s, 3H), 2.03 (s, 3H) ppm. **^{13}C NMR** (101 MHz, $CDCl_3$) δ 156.2, 148.7, 142.8, 138.5, 137.6, 121.3, 116.9, 24.0, 22.8 ppm. **LRMS** (DEP/EI-Orbitrap): m/z [%]: 167.0 (100), 151.9 (35), 132.0 (18), 117.0 (68). **HRMS** (EI-Orbitrap): m/z calcd for $C_9H_{10}ClN^+$: 167.0502; found: 167.0493. **IR** (Diamond-ATR, neat) $\tilde{\nu}_{max}$ (cm^{-1}): 3508 (m), 3484 (m), 3468 (m), 3444 (m), 3416 (m), 3411 (m), 3397 (m), 3275 (w), 1703 (vs), 1675 (m), 1668 (m), 1662 (m).

2,4-Dimethoxy-5-(prop-1-en-2-yl)pyrimidine (9n)

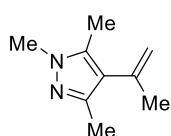
Using 5-bromo-2,4-dimethoxypyrimidine and prop-1-en-2-ylmagnesium bromide (**SM1**) according to general procedure **C** provided **9n** (0.74 mmol, 134 mg, 74%) as yellowish oil. General procedure **G (a)** provided **9n** in 44%. $R_f = 0.40$ (hexane/EtOAc 9:1, UV, PAA, KMnO_4). $^1\text{H NMR}$ (400 MHz, CDCl_3) δ 8.13 (s, 1H), 5.22 (s, 1H), 5.16 (s, 1H), 4.01 (s, 3H), 3.99 (s, 3H), 2.07 (s, 3H) ppm. $^{13}\text{C NMR}$ (101 MHz, CDCl_3) δ 168.4, 164.5, 156.5, 138.1, 117.6, 116.5, 54.9, 54.1, 22.7 ppm. **LRMS** (DEP/EI-Orbitrap): m/z [%]: 180.1 (100), 165.1 (57), 150.1 (39), 135.1 (36). **HRMS** (EI-Orbitrap): m/z calcd for $\text{C}_9\text{H}_{11}\text{N}_2\text{O}_2^+$: 179.0821; found: 179.0814. **IR** (Diamond-ATR, neat) $\tilde{\nu}_{\text{max}}$ (cm^{-1}): 3082 (vw), 2956 (w), 1700 (vw), 1684 (vw), 1662 (vw), 1652 (vw), 1587 (s), 1552 (s).

5-(Prop-1-en-2-yl)benzofuran (9o)

Using 5-bromobenzofuran and prop-1-en-2-ylmagnesium bromide (**SM1**) according to general procedure **C** provided **9o** (0.66 mmol, 104 mg, 66%) as colorless oil. $R_f = 0.80$ (hexane, UV, PAA, KMnO_4). $^1\text{H NMR}$ (400 MHz, CDCl_3) δ 7.68 (s, 1H), 7.62 – 7.61 (d, $J = 2.2$ Hz, 1H), 7.45 – 7.45 (m, 2H), 6.77 – 6.76 (d, $J = 2.1$ Hz, 1H), 5.36 (s, 1H), 5.08 (s, 1H), 2.22 (s, 3H) ppm. $^{13}\text{C NMR}$ (101 MHz, CDCl_3) δ 154.5, 145.4, 143.5, 136.5, 127.4, 122.3, 118.1, 111.9, 110.9, 106.8, 22.4 ppm. **LRMS** (DEP/EI-Orbitrap): m/z [%]: 158.1 (100), 143.1 (38), 129.1 (24), 115.1 (50). **HRMS** (EI-Orbitrap): m/z calcd for $\text{C}_{11}\text{H}_{10}\text{O}^+$: 158.0732; found: 158.0725. **IR** (Diamond-ATR, neat) $\tilde{\nu}_{\text{max}}$ (cm^{-1}): 3083 (vw), 2971 (w), 2858 (vw), 1772 (vw), 1705 (vw), 1652 (vw), 1628 (w), 1610 (w).

3-(Prop-1-en-2-yl)benzo[*b*]thiophene (9p)

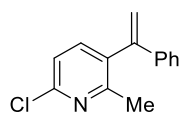
Using 3-bromobenzo[*b*]thiophene and prop-1-en-2-ylmagnesium bromide (**SM1**) according to general procedure **C** provided **9p** (0.62 mmol, 108 mg, 62%) as yellow oil. $R_f = 0.70$ (hexane, UV, PAA, KMnO_4). $^1\text{H NMR}$ (400 MHz, CDCl_3) δ 8.01 – 7.99 (d, $J = 7.5$ Hz, 1H), 7.88 – 7.86 (d, $J = 7.5$ Hz, 1H), 7.40 – 7.33 (m, 2H), 7.30 (s, 1H), 5.36 (s, 1H), 5.33 (s, 1H), 2.22 (s, 3H) ppm. $^{13}\text{C NMR}$ (101 MHz, CDCl_3) δ 140.8, 139.1, 139.0, 137.7, 124.4, 124.3, 123.6, 123.0, 122.7, 114.9, 24.1 ppm. **LRMS** (DEP/EI-Orbitrap): m/z [%]: 174.1 (100), 159.1 (26), 148.0 (14), 141.1 (60), 134.0 (25). **HRMS** (EI-Orbitrap): m/z calcd for $\text{C}_{11}\text{H}_{10}\text{S}^+$: 174.0503; found: 174.0496. **IR** (Diamond-ATR, neat) $\tilde{\nu}_{\text{max}}$ (cm^{-1}): 3065 (vw), 2969 (w), 2914 (vw), 2851 (vw), 1941 (vw), 1937 (vw), 1910 (vw), 1791 (vw), 1733 (vw), 1700 (vw), 1695 (vw), 1669 (w).

1,3,5-Trimethyl-4-(prop-1-en-2-yl)-1*H*-pyrazole (9q)

Using 4-bromo-1,3,5-trimethyl-1*H*-pyrazole and prop-1-en-2-ylmagnesium bromide (**SM1**) according to general procedure **C** provided **9q** (0.48 mmol, 72 mg, 48%) as yellowish oil. General procedure **G (a)** provided **9q** in 55%. $R_f = 0.20$ (pentane/Et₂O

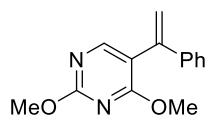
7:3, UV, PAA, KMnO₄). ¹H NMR (400 MHz, CDCl₃) δ 5.13 (s, 1H), 4.76 (s, 1H), 3.71 (s, 3H), 2.21 (s, 3H), 2.20 (s, 3H), 1.99 (s, 3H) ppm. ¹³C NMR (101 MHz, CDCl₃) δ 144.6, 137.8, 135.8, 120.4, 114.9, 35.9, 23.9, 12.9, 10.4 ppm. LRMS (DEP/EI-Orbitrap): *m/z* [%]: 150.1 (83), 135.0 (100), 93.9 (14). HRMS (EI-Orbitrap): *m/z* calcd for C₉H₁₄N₂⁺: 150.1157; found: 150.1150. IR (Diamond-ATR, neat) $\tilde{\nu}_{max}$ (cm⁻¹): 2923 (m), 2858 (w), 1634 (m), 1553 (m).

6-Chloro-2-methyl-3-(1-phenylvinyl)pyridine (9r)



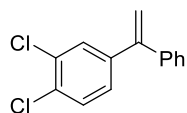
Using 3-bromo-6-chloro-2-methylpyridine and (1-phenylvinyl)magnesium bromide (**SM3**) according to general procedure C provided **9r** (0.70 mmol, 161 mg, 70%) as yellow oil. *R_f* = 0.20 (hexane/EtOAc 98:2, UV, PAA, KMnO₄). ¹H NMR (400 MHz, CDCl₃) δ 7.48 – 7.46 (d, *J* = 8.0 Hz, 1H), 7.33 – 7.30 (m, 3H), 7.24 – 7.20 (m, 3H), 5.84 (s, 1H), 5.23 (s, 1H), 2.28 (s, 3H) ppm. ¹³C NMR (101 MHz, CDCl₃) δ 157.8, 149.5, 146.6, 140.4, 139.4, 135.6, 128.8, 128.4, 128.3, 127.3, 126.5, 24.9 ppm. LRMS (DEP/EI-Orbitrap): *m/z* [%]: 229.0 (24), 214.0 (100), 178.0 (35), 165.0 (13). HRMS (EI-Orbitrap): *m/z* calcd for C₁₄H₁₂ClN⁺: 229.0658; found: 229.0654. IR (Diamond-ATR, neat) $\tilde{\nu}_{max}$ (cm⁻¹): 3081 (vw), 3056 (vw), 2977 (vw), 2925 (vw), 1809 (vw), 1700 (vw), 1684 (w), 1669 (vw).

2,4-Dimethoxy-5-(1-phenylvinyl)pyrimidine (9s)



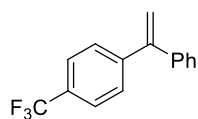
Using 5-bromo-2,4-dimethoxypyrimidine and (1-phenylvinyl)magnesium bromide (**SM3**) according to general procedure C provided **9s** (0.48 mmol, 116 mg, 48%) as yellow solid. General procedure G (a) provided **9s** in 41%. *R_f* = 0.20 (hexane/EtOAc 95:5, UV, PAA, KMnO₄). ¹H NMR (400 MHz, CDCl₃) δ 8.14 (s, 1H), 7.32 – 7.27 (m, 5H), 5.69 (s, 1H), 5.39 (s, 1H), 4.03 (s, 3H), 3.85 (s, 3H) ppm. ¹³C NMR (101 MHz, CDCl₃) δ 168.7, 164.9, 158.3, 141.9, 139.9, 128.3, 127.9, 126.5, 116.9, 116.3, 54.9, 54.0 ppm. LRMS (DEP/EI-Orbitrap): *m/z* [%]: 242.1 (100), 227.0 (93), 212.1 (18), 170.0 (13). HRMS (EI-Orbitrap): *m/z* calcd for C₁₄H₁₄N₂O₂⁺: 242.1055; found: 242.1053. IR (Diamond-ATR, neat) $\tilde{\nu}_{max}$ (cm⁻¹): 3370 (w), 2989 (w), 2956 (w), 2933 (w), 1591 (vs), 1574 (m), 1554 (vs). *Mp* (°C): 53–56.

1,2-Dichloro-4-(1-phenylvinyl)benzene (9t)*

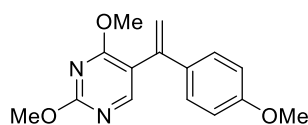


Using 4-bromo-1,2-dichlorobenzene and (1-phenylvinyl)magnesium bromide (**SM3**) according to general procedure C provided **9t** (0.76 mmol, 189 mg, 76%) as colorless oil. *R_f* = 0.50 (hexane, UV, PAA, KMnO₄). ¹H NMR (400 MHz, CDCl₃) δ 7.44 (d, *J* = 2.1 Hz, 1H), 7.40 (d, *J* = 8.3 Hz, 1H), 7.38 – 7.33 (m, 3H), 7.33 – 7.28 (m, 2H), 7.17 (dd, *J* = 8.3, 2.1 Hz, 1H), 5.50 (d, *J* = 0.9 Hz, 1H), 5.47 (d, *J* = 0.9 Hz, 1H) ppm. LRMS (DEP/EI-Orbitrap): *m/z* [%]: 248.1 (71), 213.1 (49), 178.1 (100), 152.1 (12), 88.1 (24). Analytical data in accordance to literature.²¹⁴

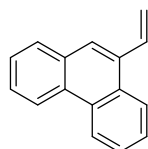
²¹⁴ P. K. Tiwari, B. SivaRaman, I. S. Aidhen, *Eur. J. Org. Chem.*, **2017**, 3594–3605.

1-(1-Phenylvinyl)-4-(trifluoromethyl)benzene (9u)

Using 1-bromo-4-(trifluoromethyl)benzene and (1-phenylvinyl)magnesium bromide (**SM3**) according to general procedure **C** provided **9u** (0.53 mmol, 132 mg, 53%) as colorless oil. $R_f = 0.74$ (hexane, UV, PAA, KMnO_4). $^1\text{H NMR}$ (400 MHz, CDCl_3) δ 7.60 (d, $J = 8.2$ Hz, 2H), 7.46 (d, $J = 8.1$ Hz, 2H), 7.39 – 7.30 (m, 5H), 5.57 (s, 1H), 5.53 (s, 1H) ppm. **LRMS** (DEP/EI-Orbitrap): m/z [%]: 248.1 (99), 233.0 (32), 178.1 (100), 151.1 (16), 89.0 (19), 77.0 (20), 51.0 (17). Analytical data in accordance to literature.²¹⁵

2,4-Dimethoxy-5-(1-(4-methoxyphenyl)vinyl)pyrimidine (9v)

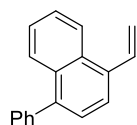
Using 5-bromo-2,4-dimethoxypyrimidine and (1-(4-methoxyphenyl)vinyl)magnesium bromide according to general procedure **C** provided **9v** (0.67 mmol, 183 mg, 67%) as colorless solid. $R_f = 0.30$ (hexane/EtOAc 8:2, UV, PAA, KMnO_4). $^1\text{H NMR}$ (400 MHz, CDCl_3) δ 8.14 (s, 1H), 7.21 – 7.19 (d, $J = 8.8$ Hz, 2H), 6.85 – 6.82 (d, $J = 8.8$ Hz, 2H), 5.61 (s, 1H), 5.27 (s, 1H), 4.02 (s, 3H), 3.86 (s, 3H), 3.81 (s, 3H) ppm. $^{13}\text{C NMR}$ (101 MHz, CDCl_3) δ 168.9, 165.0, 159.5, 158.3, 141.4, 132.6, 127.8, 116.7, 115.4, 113.8, 55.4, 55.0, 54.2 ppm. **LRMS** (DEP/EI-Orbitrap): m/z [%]: 272.1 (69), 257.1 (100), 200.1 (10), 173.1 (11). **HRMS** (EI-Orbitrap): m/z calcd for $\text{C}_{15}\text{H}_{16}\text{N}_2\text{O}_3^+$: 272.1161; found: 272.1156. **IR** (Diamond-ATR, neat) $\tilde{\nu}_{\text{max}}$ (cm^{-1}): 3091 (vw) 3033 (vw), 3006 (w), 2995 (w), 2958 (w), 2933 (w), 2837 (w), 1604 (m), 1591 (s). **Mp** ($^\circ\text{C}$): 52–55.

9-Vinylphenanthrene (10a)*

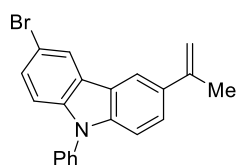
Using 9-bromophenanthrene and vinylmagnesium bromide (**SM2**) according to general procedure **D** provided **10a** (0.55 mmol, 112 mg, 55%) as colorless oil. $R_f = 0.56$ (hexane, UV, PAA, KMnO_4). $^1\text{H NMR}$ (400 MHz, CDCl_3) δ 8.75 (dd, $J = 7.8, 1.7$ Hz, 1H), 8.68 (d, $J = 8.0$ Hz, 1H), 8.19 (dd, $J = 7.7, 1.7$ Hz, 1H), 7.92 (dd, $J = 7.5, 1.7$ Hz, 1H), 7.88 (s, 1H), 7.73 – 7.58 (m, 4H), 7.50 (dd, $J = 17.1, 10.8$ Hz, 1H), 5.90 (dd, $J = 17.2, 1.7$ Hz, 1H), 5.56 (dd, $J = 10.8, 1.7$ Hz, 1H) ppm. $^{13}\text{C NMR}$ (101 MHz, CDCl_3) δ 135.2, 134.8, 131.9, 130.6, 130.4, 130.4, 128.8, 126.9, 126.8, 126.7, 126.6, 126.6, 124.7, 123.2, 122.6, 117.7 ppm. **LRMS** (DEP/EI-Orbitrap): m/z [%]: 203.1 (100), 176.1 (10), 150.1 (5), 101.1 (40), 88.0 (15), 75.0 (5), 63.1 (3). Analytical data in accordance to literature.²¹⁶

²¹⁵ D. S. Choi, J. H. Kim, U. S. Shin, R. R. Deshmukh, C. E. Song, *Chem. Commun.* **2007**, 3482–3484.

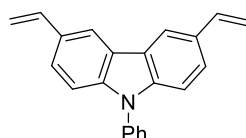
²¹⁶ K. T. Neumann, S. Klimeczyk, M. N. Burhardt, B. Bang-Andersen, T. Skrydstrup, A. T. Linhardt, *ACS Catal.* **2016**, *6*, 4710–4714.

1-Phenyl-4-vinylnaphthalene (10b)

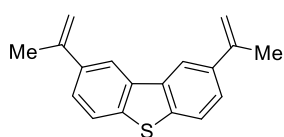
Using 1-bromo-4-phenylnaphthalene and vinylmagnesium bromide (**SM2**) according to general procedure **D** provided **10b** (0.70 mmol, 161 mg, 70%) as colorless oil. $R_f = 0.31$ (hexane, UV, PAA, KMnO_4). $^1\text{H NMR}$ (400 MHz, CDCl_3) δ 8.22 (d, $J = 8.5$ Hz, 1H), 7.96 (dd, $J = 8.5, 1.6$ Hz, 1H), 7.74 – 7.65 (m, 1H), 7.58 – 7.42 (m, 9H), 5.86 (dd, $J = 17.3, 1.6$ Hz, 1H), 5.54 (dd, $J = 10.9, 1.6$ Hz, 1H) ppm. $^{13}\text{C NMR}$ (101 MHz, CDCl_3) δ 140.9, 140.4, 135.3, 134.6, 131.8, 131.5, 130.2, 128.4, 127.4, 126.9, 126.8, 126.1, 126.0, 124.2, 123.4, 117.3 ppm. **LRMS** (DEP/EI-Orbitrap): m/z [%]: 230.2 (100), 215.2 (15), 202.1 (20), 153.1 (20), 113.1 (10), 101.1 (10). **HRMS** (EI-Orbitrap): m/z calcd for $\text{C}_{18}\text{H}_{14}^+$: 230.1096; found: 230.1092. **IR** (Diamond-ATR, neat) $\tilde{\nu}_{\text{max}}$ (cm^{-1}): 1492 (vw), 1443 (vw), 1377 (w), 984 (w), 912 (m), 843 (m), 766 (vs), 700 (s).

3-Bromo-9-phenyl-6-(prop-1-en-2-yl)-9H-carbazole (10c)

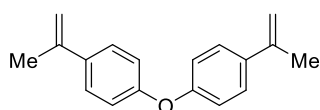
Using 3,6-dibromo-9-phenyl-9H-carbazole and prop-1-en-2-ylmagnesium bromide (**SM1**) according to general procedure **D** provided **10c** (1.20 mmol, 433 mg, 80%) as colorless oil. $R_f = 0.60$ (hexane/EtOAc 98:2, UV, PAA, KMnO_4). $^1\text{H NMR}$ (400 MHz, CDCl_3) δ 8.17 (d, $J = 1.8$ Hz, 1H), 8.06 (d, $J = 1.5$ Hz, 1H), 7.53 – 7.46 (m, 3H), 7.43 – 7.33 (m, 4H), 7.22 (d, $J = 8.6$ Hz, 1H), 7.15 (d, $J = 8.9$ Hz, 1H), 5.34 (s, 1H), 5.04 – 5.00 (m, 1H), 2.19 (s, 3H) ppm. $^{13}\text{C NMR}$ (101 MHz, CDCl_3) δ 143.5, 140.8, 140.0, 137.3, 134.0, 130.1, 128.7, 127.9, 127.0, 125.4, 124.7, 123.2, 122.3, 117.5, 112.9, 111.5, 109.8, 22.5 ppm. One carbon signal could not be detected. **LRMS** (DEP/EI-Orbitrap): m/z [%]: 361.1 (100), 348.0 (25), 267.1 (35), 241.1 (12), 133.6 (10). **HRMS** (EI-Orbitrap): m/z calcd for $\text{C}_{21}\text{H}_{16}\text{BrN}^+$: 361.0466; found: 361.0459. **IR** (Diamond-ATR, neat) $\tilde{\nu}_{\text{max}}$ (cm^{-1}): 3068 (w), 2966 (w), 2359 (m), 2341 (m), 2334 (m), 1624 (m), 1597 (m), 1500 (vs).

9-Phenyl-3,6-divinyl-9H-carbazole (10d)

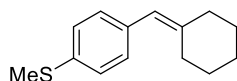
Using 3,6-dibromo-9-phenyl-9H-carbazole and vinylmagnesium bromide (**SM2**) according to general procedure **E** provided **10d** (0.63 mmol, 186 mg, 63%) as yellowish oil. $R_f = 0.50$ (hexane, UV, PAA, KMnO_4). $^1\text{H NMR}$ (400 MHz, CDCl_3) δ 8.21 (s, 2H), 7.65 – 7.47 (m, 7H), 7.37 (d, $J = 8.5$ Hz, 2H), 6.96 (dd, $J = 17.6, 10.9$ Hz, 2H), 5.85 (d, $J = 17.5$ Hz, 2H), 5.28 (d, $J = 10.9$ Hz, 2H) ppm. $^{13}\text{C NMR}$ (101 MHz, CDCl_3) δ 141.1, 137.5, 137.4, 130.2, 130.0, 127.6, 127.0, 124.5, 123.7, 118.4, 111.7, 110.0 ppm. **LRMS** (DEP/EI-Orbitrap): m/z [%]: 295.3 (100), 279.1 (5), 267.1 (10), 254.2 (2). **HRMS** (EI-Orbitrap): m/z calcd for $\text{C}_{22}\text{H}_{17}\text{N}^+$: 295.1361; found: 295.1353. **IR** (Diamond-ATR, neat) $\tilde{\nu}_{\text{max}}$ (cm^{-1}): 3040 (vw), 2959 (w), 2926 (w), 2869 (w), 2246 (vw), 1684 (w), 1626 (w), 1596 (m), 1569 (w), 1501 (s).

2,8-Di(prop-1-en-2-yl)dibenzo[*b,d*]thiophene (10e)

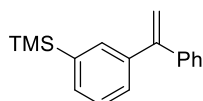
Using 2,8-dibromodibenzo[*b,d*]thiophene and prop-1-en-2-ylmagnesium bromide (**SM1**) according to general procedure **E** provided **10e** (0.61 mmol, 161 mg, 61%) as colorless oil. $R_f = 0.50$ (hexane, UV, PAA, KMnO_4). $^1\text{H NMR}$ (400 MHz, CDCl_3) δ 8.24 (d, $J = 1.7$ Hz, 2H), 7.79 (d, $J = 8.4$ Hz, 2H), 7.62 (dd, $J = 8.4, 1.8$ Hz, 2H), 5.54 (dd, $J = 1.5, 0.8$ Hz, 2H), 5.24 – 5.20 (m, 2H), 2.33 (s, 6H) ppm. $^{13}\text{C NMR}$ (101 MHz, CDCl_3) δ 143.3, 139.0, 138.0, 135.7, 124.7, 122.6, 118.4, 112.7, 22.3 ppm. **LRMS** (DEP/EI-Orbitrap): m/z [%]: 264.1 (100), 249.2 (30), 234.1 (10), 221.1 (15), 208.1 (35). **HRMS** (EI-Orbitrap): m/z calcd for $\text{C}_{18}\text{H}_{16}\text{S}^+$: 264.0973; found: 264.0969.

4,4'-Oxybis(prop-1-en-2-ylbenzene) (10f)

Using 4,4'-oxybis(bromobenzene) and prop-1-en-2-ylmagnesium bromide (**SM1**) prop-1-en-2-ylmagnesium bromide **E** provided **10f** (0.63 mmol, 158 mg, 63%) as colorless solid. $R_f = 0.15$ (hexane, UV, PAA, KMnO_4). $^1\text{H NMR}$ (400 MHz, CDCl_3) δ 7.44 (d, $J = 8.7$ Hz, 4H), 6.97 (d, $J = 8.7$ Hz, 4H), 5.33 (s, 2H), 5.05 (s, 2H), 2.14 (s, 6H) ppm. $^{13}\text{C NMR}$ (101 MHz, CDCl_3) δ 156.7, 142.5, 136.4, 127.0, 118.6, 111.9, 22.1 ppm. **LRMS** (DEP/EI-Orbitrap): m/z [%]: 251.1 (20), 250.1 (100), 235.1 (28), 165.1 (9), 115.1 (13). **HRMS** (EI-Orbitrap): m/z calcd for $\text{C}_{18}\text{H}_{18}\text{O}^+$: 250.1358 found: 250.1353. **IR** (Diamond-ATR, neat) $\tilde{\nu}_{max}$ (cm^{-1}): 2971 (w), 2251 (w), 1624 (w), 1596 (w). **Mp** ($^\circ\text{C}$): 99–101.

(4-(Cyclohexylidenemethyl)phenyl)(methyl)sulfane (11a)*

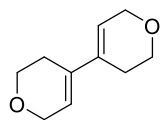
Using (4-bromophenyl)(methyl)sulfane and (cyclohexylidenemethyl)lithium (**SM6**) according to general procedure **F** provided **11a** (0.47 mmol, 103 mg, 47%) as colorless oil. $R_f = 0.30$ (hexane, UV, PAA, KMnO_4). $^1\text{H NMR}$ (400 MHz, CDCl_3) δ 7.23 – 7.18 (m, 2H), 7.15 – 7.10 (m, 2H), 6.17 (s, 1H), 2.48 (s, 3H), 2.39 – 2.33 (m, 2H), 2.27 – 2.21 (m, 2H), 1.67 – 1.51 (m, 6H) ppm. $^{13}\text{C NMR}$ (101 MHz, CDCl_3) δ 143.7, 135.6, 135.5, 129.5, 126.7, 121.5, 37.8, 29.6, 28.7, 28.0, 26.8, 16.3 ppm. **LRMS** (DEP/EI-Orbitrap): m/z [%]: 218.1 (100), 203.1 (2), 189.1 (5), 171.1 (5). **HRMS** (EI-Orbitrap): m/z calcd for $\text{C}_{14}\text{H}_{18}\text{S}^+$: 218.1129; found: 218.1119. **IR** (Diamond-ATR, neat) $\tilde{\nu}_{max}$ (cm^{-1}): n.d.

Trimethyl(3-(1-phenylvinyl)phenyl)silane (11b)

Using (3-bromophenyl)trimethylsilane and (1-phenylvinyl)lithium (**SM7**) according to general procedure **F** provided **11b** (0.26 mmol, 65 mg, 51%) as colorless oil. (1-phenylvinyl)lithium was prepared by treating (1-bromovinyl)benzene (1.5 equiv) with a solution of *n*-BuLi in hexanes (1.5 equiv) in Et_2O at -78 $^\circ\text{C}$ for 30 min. $R_f = 0.40$ (hexane, UV, PAA, KMnO_4). $^1\text{H NMR}$ (400 MHz, CDCl_3) δ 7.53 – 7.51 (m, 1H), 7.48 (dt, $J = 7.0, 1.4$ Hz, 1H), 7.38 – 7.28 (m, 7H), 5.49 (d, $J = 1.2$ Hz, 1H), 5.46 (d, $J = 1.2$ Hz, 1H), 0.26 (s, 9H) ppm. $^{13}\text{C NMR}$ (101 MHz,

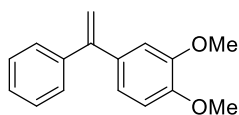
CDCl₃) δ 150.4, 141.6, 140.8, 140.5, 133.2, 132.9, 129.1, 128.3, 128.3, 127.8, 127.6, 114.4, -1.0 ppm. **LRMS** (DEP/EI-Orbitrap): m/z [%]: 252.1 (30), 237.1 (100), 178.1 (12), 75.1 (8). **HRMS** (EI-Orbitrap): m/z calcd for C₁₇H₂₀Si⁺: 252.1334; found: 252.1328. **IR** (Diamond-ATR, neat) $\tilde{\nu}_{max}$ (cm⁻¹): 3081 (vw), 3053 (vw), 3023 (vw), 2955 (w), 2896 (vw), 1610 (vw).

3,3',6,6'-Tetrahydro-2H,2'H-4,4'-bipyran (**11c**)^{*}



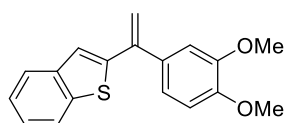
Under inert atmosphere, 4-bromo-3,6-dihydro-2H-pyran (2.0 mmol, 1.0 equiv) was dissolved in a reaction flask in THF (5.0 mL) and the solution was cooled down to -78 °C before adding a solution of *t*-BuLi in pentane (4.0 mmol, 2.0 equiv) dropwise. The mixture was stirred for 30 min before tributylborate (270 μ L, 1.0 mmol, 0.5 equiv) was added dropwise at -78 °C. The mixture was stirred for 30 min at -78 °C before warming to 0 °C and was then stirred for another 1 h. Then, after cooling back to -78 °C, iodine (1.52 g, 6.0 mmol, 3.0 equiv) dissolved in THF (2.0 mL), was added dropwise to the solution. After 20 min a suspension of sodium methoxide (405 mg, 7.5 mmol, 3.75 equiv) in methanol (2.0 mL) was added at once. The reaction was allowed to reach room temperature, after which it was completed, providing **11c** (0.88 mmol, 146 mg, 88%) after purification as greenish oil. R_f = 0.30 (hexane/Et₂O 8:2, UV, PAA, KMnO₄). ¹H NMR (400 MHz, C₆D₆) δ 5.31 (s, 2H), 4.09 (d, J = 2.1 Hz, 4H), 3.65 (t, J = 5.6 Hz, 4H), 2.03 – 1.91 (m, 4H) ppm. ¹³C NMR (101 MHz, C₆D₆) δ 133.5, 121.0, 65.8, 64.4, 25.5 ppm **LRMS** (DEP/EI-Orbitrap): m/z [%]: 166.1 (40), 137.1 (10), 121.1 (15). **HRMS** (EI-Orbitrap): m/z calcd for C₁₀H₁₄O₂⁺: 166.0994; found: 166.0988. **IR** (Diamond-ATR, neat) $\tilde{\nu}_{max}$ (cm⁻¹): 2927 (w), 2848 (w), 1724 (w), 1671 (vw), 1627 (w).

1,2-Dimethoxy-4-(1-phenylvinyl)benzene (**12a**)



Using (1-bromovinyl)benzene and (3,4-dimethoxyphenyl)lithium according to general procedure **G** (a) provided **12a** (0.50 mmol, 120 mg, 50%) as colorless oil. R_f = 0.40 (hexane/EtOAc 9:1, UV, PAA, KMnO₄). ¹H NMR (400 MHz, CDCl₃) δ 7.39 – 7.30 (m, 5H), 6.92 – 6.87 (m, 2H), 6.83 (d, J = 8.0 Hz, 1H), 5.40 (dd, J = 10.1, 1.3 Hz, 2H), 3.90 (s, 3H), 3.84 (s, 3H) ppm. ¹³C NMR (101 MHz, CDCl₃) δ 149.8, 148.9, 148.6, 141.7, 134.4, 128.4, 128.3, 127.9, 121.0, 113.3, 111.5, 110.8, 56.0, 56.0 ppm. **LRMS** (DEP/EI-Orbitrap): m/z [%]: 240.1 (100), 225.1 (10), 209.1 (5), 193.1 (10), 181.1 (10). **HRMS** (EI-Orbitrap): m/z calcd for C₁₆H₁₆O₂⁺: 240.1150; found: 240.1140. **IR** (Diamond-ATR, neat) $\tilde{\nu}_{max}$ (cm⁻¹): 3055 (vw), 2999 (w), 2934 (w), 2835 (w), 1601 (w).

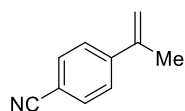
2-(1-(3,4-Dimethoxyphenyl)vinyl)benzo[*b*]thiophene (**12b**)



Using 2-(1-bromovinyl)benzo[*b*]thiophene and (3,4-dimethoxyphenyl)lithium according to general procedure **G** (a) provided **12b** (0.52 mmol, 154 mg, 52%) as colorless oil. R_f = 0.30 (hexane/EtOAc 9:1, UV, PAA, KMnO₄). ¹H NMR (400 MHz, CDCl₃) δ 7.82 – 7.76 (m, 1H), 7.68 – 7.64 (m, 1H), 7.36 – 7.28 (m, 2H), 7.13 (s, 1H), 7.06 (dd, J = 8.2, 2.1 Hz, 1H), 7.00 (d, J = 2.0 Hz, 1H), 6.90 (d, J = 8.3 Hz, 1H), 5.65 (s, 1H), 5.36 (s,

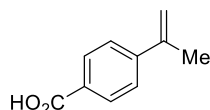
1H), 3.93 (s, 3H), 3.88 (s, 3H) ppm. ^{13}C NMR (101 MHz, CDCl_3) δ 149.2, 148.7, 145.1, 143.6, 140.2, 139.6, 133.4, 124.8, 124.5, 123.8, 123.6, 122.3, 121.1, 115.3, 111.8, 110.9, 56.1 ppm. One carbon signal could not be detected. LRMS (DEP/EI-Orbitrap): m/z [%]: 296.1 (100), 281.1 (10), 265.1 (10), 249.0 (10), 237.1 (5). HRMS (EI-Orbitrap): m/z calcd for $\text{C}_{18}\text{H}_{16}\text{O}_2\text{S}^+$: 296.0871; found: 296.0864. IR (Diamond-ATR, neat) $\tilde{\nu}_{\text{max}}$ (cm^{-1}): 3056 (vw), 3000 (w), 2933 (w), 2834 (w), 1667 (w), 1602 (w), 1578 (w), 1512 cm^{-1} (vs).

4-(Prop-1-en-2-yl)benzonitrile (12c)



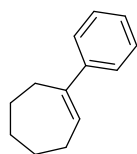
Using 2-bromoprop-1-ene and (4-cyanophenyl)lithium according to general procedure **G (a)** provided **12c** (0.35 mmol, 50 mg, 35%) as yellowish oil. R_f = 0.50 (hexane/EtOAc 9:1, UV, PAA, KMnO_4). ^1H NMR (400 MHz, CDCl_3) δ 7.60 (d, J = 8.5, 2H), 7.53 (d, J = 8.5, 2H), 5.46 (s, 1H), 5.25–5.24 (m, 1H), 2.15 (s, 3H) ppm. LRMS (DEP/EI-Orbitrap): m/z [%]: 143.1 (100), 127.9 (50), 116.0 (60). Analytical data in accordance to literature.²¹⁷

4-(Prop-1-en-2-yl)benzoic acid (12d)*



Using 2-bromoprop-1-ene and lithium (4-carboxylatophenyl)lithium according to general procedure **G (a)** provided **12d** (0.53 mmol, 86 mg, 53%) as colorless solid. R_f = 0.30 ($\text{CH}_2\text{Cl}_2/\text{MeOH}$ 99:1, UV, PAA, KMnO_4). ^1H NMR (400 MHz, CDCl_3) δ 8.08 (d, J = 8.0 Hz, 2H), 7.56 (d, J = 8.4 Hz, 2H), 5.50 (s, 1H), 5.24 – 5.21 (m, 1H), 2.19 (s, 3H) ppm. The carboxylic acid proton was not observed. LRMS (DEP/EI-Orbitrap): m/z [%]: 162.1 (5), 144.0 (5), 133.1 (5), 120.1 (50), 105.0 (100). Analytical data in accordance to literature.²¹⁸

1-Phenylcyclohept-1-ene (13)*



For the following preparation a modified procedure by Keay *et al.* was used.²¹⁹ In a dry Schlenk flask *N*-cycloheptylidene-4-methylbenzenesulfonohydrazide (1.0 mmol, 1.0 equiv) was added under nitrogen stream. Then, hexane (2 mL) was added resulting in a suspension. After cooling down to -78 °C, TMEDA (1 mL) was added and the mixture was further stirred for 10 min. Then, a solution of *n*-BuLi in hexanes (3.0 mmol, 3.0 equiv) was added at -78 °C resulting in a red colored solution. After 10 min of stirring, the reaction mixture was allowed to reach 0 °C for 15 min (N_2 evolution was observed) before cooling down to -78 °C again. $\text{B}(\text{O}n\text{-Bu})_3$ was added and after 5 min of stirring the solution was allowed to warm to 0 °C. The solvent was removed *in vacuo* with the Schlenk line. At 0 °C phenylmagnesium bromide (3.0 mmol, 3.0 equiv) was added. The resulting mixture was allowed to reach room temperature after 10 min and was stirred for 1 h. After cooling down to -78 °C, iodine (4.0 mmol, 4.0 equiv, dissolved in 4 mL THF) was added and

²¹⁷ G. Pratsch, L. E. Overman, *J. Org. Chem.* **2015**, *80*, 11388–11397.

²¹⁸ a) B. Yang, Z. Lu, *ACS Catal.*, **2017**, *7*, 8362–8365; b) R. L. Letsinger, S. B. Hamilton, *J. Am. Chem. Soc.* **1959**, *81*, 3009–3012.

²¹⁹ M. S. Passafaro, B. A. Keay, *Tetrahedron Lett.* **1996**, *37*, 429–432.

the reaction mixture stirred for 20 min, followed by portion wise addition of sodium methoxide (8.0 mmol, 8.0 equiv, dissolved in 5 mL MeOH). The resulting mixture was allowed to reach 0 °C after 10 min and was stirred for further 30 min. The reaction was then quenched by the addition of sat. aq. Na₂S₂O₃ and extracted with diethyl ether (3 × 20 mL). The combined organic phases were dried over MgSO₄, filtered and concentrated under reduced pressure. The crude product was purified by column chromatography on silica gel yielding **13** as a colorless liquid (0.29 mmol, 50 mg, 29 %). *R_f* = 0.89 (hexane, UV, PAA, KMnO₄). ¹H NMR (400 MHz, CDCl₃) δ 7.29 – 7.18 (m, 4H), 7.16 – 7.07 (m, 1H), 6.02 (t, *J* = 6.8 Hz, 1H), 2.59 – 2.45 (m, 2H), 2.29 – 2.15 (m, 2H), 1.76 (quint, *J* = 5.9 Hz, 2H), 1.61 – 1.52 (m, 2H), 1.52 – 1.40 (m, 2H) ppm. ¹³C NMR (101 MHz, CDCl₃) δ 145.1, 145.0, 130.6, 128.2, 126.4, 125.8, 33.0, 32.9, 29.0, 27.1, 26.9 ppm. LRMS (DEP/EI-Orbitrap): *m/z* [%]: 172.1 (50), 155.1 (9), 144.1 (74), 143.1 (34), 141.1 (15), 130.1 (23), 129.1 (100). HRMS (EI-Orbitrap): *m/z* calcd for C₁₃H₁₆⁺: 172.1252; found: 172.1246. IR (Diamond-ATR, neat) $\tilde{\nu}_{max}$ (cm⁻¹): 3056 (w), 3024 (w), 2916 (m), 2846 (w), 1639 (w).

3.5 Representative NMR Spectra

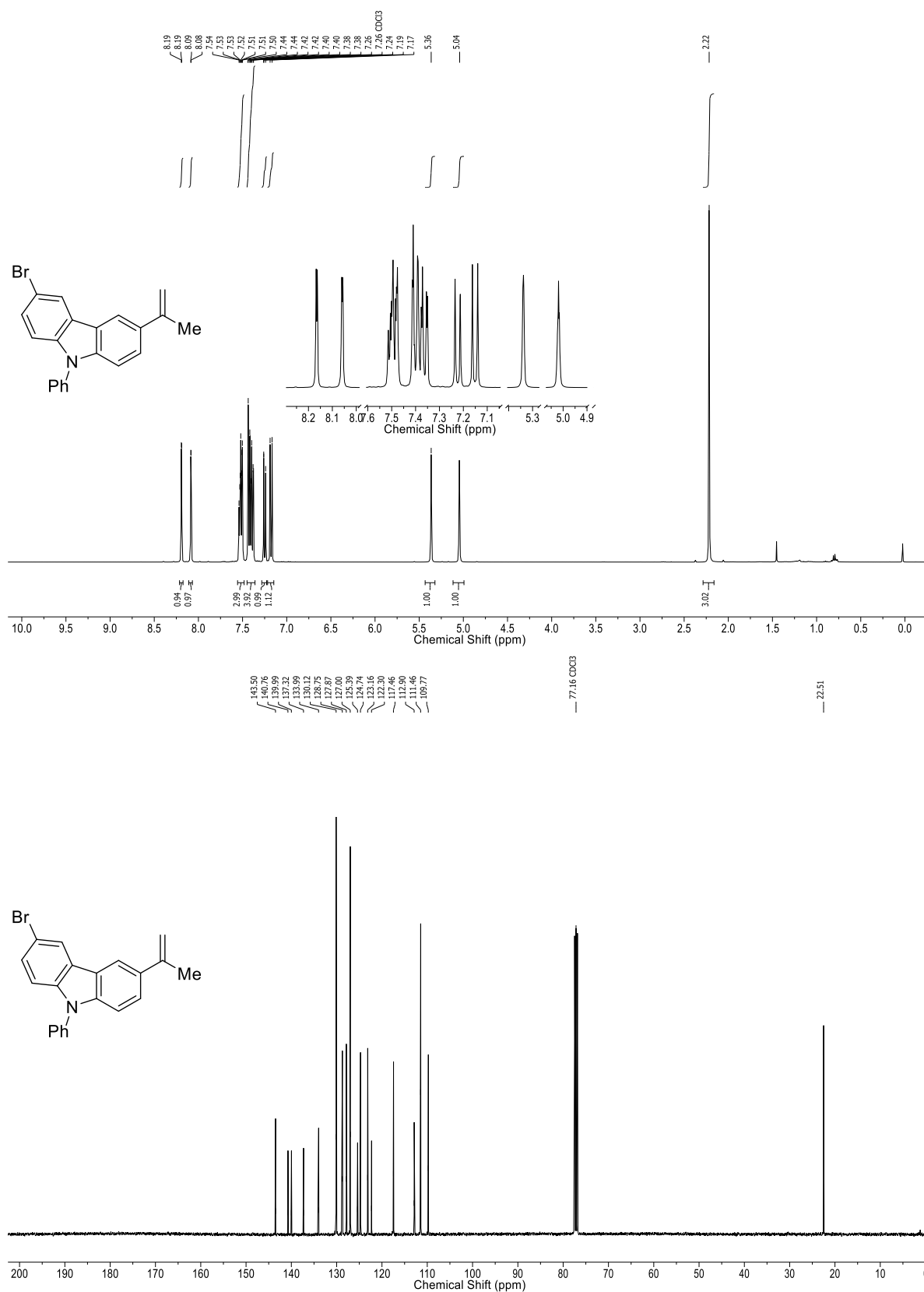


Figure 11: ^1H NMR (400 MHz, CDCl_3) and ^{13}C NMR (101 MHz, CDCl_3) of 3-Bromo-9-phenyl-6-(prop-1-en-2-yl)-9H-carbazole (10c).

4 Catalyst-Free Enantiospecific Olefination with *in situ* Generated Organocerium Species²²⁰

4.1 Synthesis of the Exchange Reagent

4.1.1 Preparation of CeCl₃•2LiCl (0.33 M in THF)

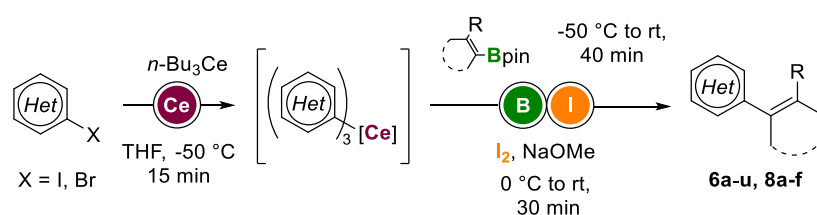
Adapted from a previously reported procedure,⁴⁹ commercially available CeCl₃•7H₂O (50.0 mmol, 18.63 g) was mixed with LiCl (100 mmol, 4.24 g) and water (20 mL) in a 500 mL Schlenk flask and the mixture was stirred vigorously for 4 h at room temperature under high vacuum. Stirring under vacuum was continued for 4 h at 40 °C, 4 h at 60 °C, 4 h at 80 °C, 4 h at 100 °C, 4 h at 120 °C, 4 h at 140 °C and lastly 4 h at 160 °C. The resulting solid was allowed to reach room temperature and 150 mL of dry THF were added. To the resulting slurry, molecular sieves (25.0 g, 4 Å) were added and the mixture was stirred vigorously for 24 h at room temperature. In a last step, the molecular sieves were filtered off *via* Schlenk-filtration under a nitrogen atmosphere, resulting in a clear and slightly orange solution of CeCl₃•2LiCl (0.33 M), which was stable for several months under nitrogen storage at room temperature.

4.1.2 Preparation of *n*-Bu₃Ce•5LiCl

A Schlenk flask was charged with CeCl₃•2LiCl (0.33 M, 0.33 mL, 0.11 mmol, 0.33 equiv) solution and cooled to –30 °C. A solution of *n*-BuLi in hexanes (2.32 M, 0.14 mL, 0.33 mmol, 1.00 equiv) was then added and the resulting yellow solution was stirred for 15 min at –30 °C before being used.

4.2 General Procedures

4.2.1 General Procedure H: Zweifel Olefination of (Hetero)Aromatic Halides with Vinyl 4,4,5,5-Tetramethyl-1,3,2-Dioxaborolanes using *n*-Bu₃Ce•5LiCl (6a–u, 8a–f)

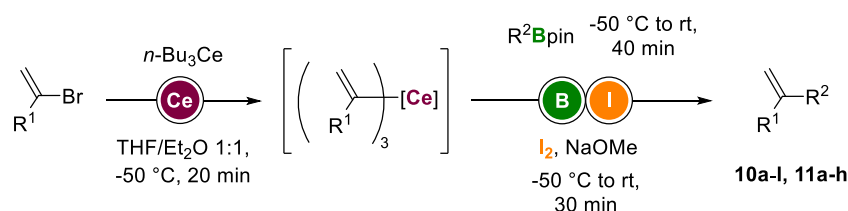


To a freshly prepared yellow solution of *n*-Bu₃Ce•5LiCl (0.11 mmol, 0.37 equiv) at –50 °C was added the (hetero)aryl iodide or bromide (0.30 mmol, 1.00 equiv, dissolved in 1.0 mL of THF) and stirred for 15 min. After complete exchange, which was followed by GC and GC-MS, the desired vinyl 4,4,5,5-tetramethyl-1,3,2-dioxaborolane (0.26 mmol, 0.85 equiv, dissolved in 1.0 mL of THF) was added and the resulting solution was stirred for 20 min at –50 °C. The solution was allowed to gradually warm to

²²⁰ The full supporting information can be found under the following link: <https://doi.org/10.1002/anie.201810327>

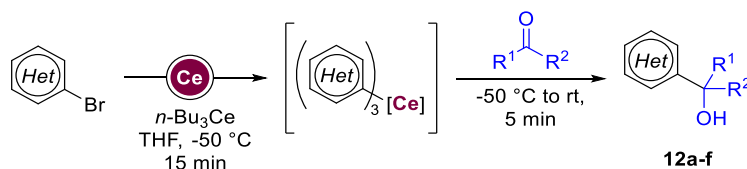
room temperature and further stirred for 20 min. After cooling down to 0 °C, sodium methoxide (1.50 mmol, 5.00 equiv, dissolved in 2 mL of MeOH) was first added, followed by dropwise addition of iodine (0.45 mmol, 1.50 equiv, dissolved in 1 mL of THF). The mixture was allowed to reach room temperature after 10 min and further stirred for 20 min. The reaction was then quenched by the addition of sat. aq. Na₂S₂O₃ and extracted with diethyl ether (3 × 15 mL). The combined organic phases were dried over MgSO₄, filtered and concentrated *in vacuo*. The crude product was purified by column chromatography on silica gel to yield the desired products **6a–u** and **8a–f**.

4.2.2 General procedure I: Zweifel Olefination of Vinyl Bromides with (Hetero)Aromatic (10a–l) and Aliphatic (11a–h) 4,4,5,5-Tetramethyl-1,3,2-Dioxaborolanes using *n*-Bu₃Ce•5LiCl



To a freshly prepared yellow solution of *n*-Bu₃Ce•5LiCl (0.11 mmol, 0.37 equiv) at –50 °C was added the desired vinyl bromide (0.30 mmol, 1.00 equiv, dissolved in 1.0 mL of THF/Et₂O 1:1) and stirred for 20 min. After complete exchange, which was followed by GC and GC-MS, the desired (hetero)aromatic or aliphatic 4,4,5,5-tetramethyl-1,3,2-dioxaborolane (0.26 mmol, 0.85 equiv, dissolved in 1.0 mL of THF) was added and the resulting solution was stirred for 20 min at –50 °C. The solution was allowed to gradually warm to room temperature and stirred for further 20 min. After cooling back to –50 °C, sodium methoxide (1.50 mmol, 5.00 equiv, dissolved in 2 mL of MeOH) was first added, followed by dropwise addition of iodine (0.45 mmol, 1.50 equiv, dissolved in 1 mL of THF). The mixture was allowed to reach room temperature after 10 min and further stirred for 20 min. The reaction was quenched by addition of sat. aq. Na₂S₂O₃ and extracted with diethyl ether (3 × 15 mL). The combined organic phases were dried over MgSO₄, filtered and concentrated *in vacuo*. The crude product was purified by column chromatography on silica gel to yield the desired products **10a–i** and **11a–h**.

4.2.3 General Procedure J: Synthesis of Tertiary Alcohols **12a–f** using *n*-Bu₃Ce•5LiCl



To a freshly prepared yellow solution of *n*-Bu₃Ce•5LiCl (0.15 mmol, 0.37 equiv) at –50 °C was added the (hetero)aryl bromide (0.40 mmol, 1.00 equiv, dissolved in 1.0 mL of THF) and stirred for 15 min. After complete exchange, which was followed by GC and GC-MS, the desired aliphatic or aromatic ketone (0.34 mmol, 0.85 equiv, dissolved in 1.0 mL of THF) was added and the resulting solution was

stirred for 5 min at $-50\text{ }^{\circ}\text{C}$ and then warmed to room temperature. The reaction was then quenched by the addition of sat. aq. NH_4Cl and extracted with EtOAc ($3 \times 15\text{ mL}$). The combined organic phases were dried over MgSO_4 , filtered and concentrated *in vacuo*. The crude product was purified by column chromatography on silica gel to yield the desired products **12a–f**.

4.3 Optimizations

Table 5: Optimizations on Br/Ce exchanges.

RLi	x (equiv)	$\text{R}_x\text{CeCl}_{3-x}$	conv. (%)
<i>n</i> -BuLi	1 (1.1)	<i>n</i> -BuCeCl ₂	97
<i>n</i> -BuLi	2 (2.2)	<i>n</i> -Bu ₂ CeCl	95
<i>n</i>-BuLi	3 (3.3)	<i>n</i>-Bu₃Ce	93
MeLi	1 (1.1)	MeCeCl ₂	90
MeLi	2 (2.2)	Me ₂ CeCl	38
MeLi	3 (3.3)	Me ₃ Ce	30
<i>s</i> -BuLi	1 (1.1)	<i>s</i> -BuCeCl ₂	n.d.
<i>s</i> -BuLi	2 (2.2)	<i>s</i> -Bu ₂ CeCl	78
<i>s</i> -BuLi	3 (3.3)	<i>s</i> -Bu ₃ Ce	55

Conversion rates of the 1-bromo-4-chlorobenzene were assessed by hydrolysis and GC analysis with *n*-undecane as an internal standard, see Table 5.

4.4 Experimental Data

4.4.1 Synthesis of 4,4,5,5-Tetramethyl-1,3,2-Dioxaborolanes

(*E*)-4,4,5,5-Tetramethyl-2-(1-phenylprop-1-en-1-yl)-1,3,2-dioxaborolane (SM9)

Following a procedure published by Tanaka *et al.*,²²¹ **SM9** was synthesized as a colorless oil (*E/Z* = 99:1, 0.25 mmol, 61 mg, 25%). R_f = 0.40 (hexane/EtOAc 99:1, UV, KMnO_4 , PAA). $^1\text{H NMR}$ (400 MHz, CDCl_3) δ 7.32 (t, J = 7.6 Hz, 2H), 7.23 – 7.12 (m, 3H), 6.72 (q, J = 7.0 Hz, 1H), 1.77 (d, J = 7.0 Hz, 3H), 1.27 (s, 12H) ppm. **LRMS** (DEP/EI-Orbitrap): m/z (%): 244.1 (29), 229.2 (10), 187.1 (81), 171.1 (11), 143.1 (100), 129.0 (11), 116.0 (59), 105.0 (69), 91.0 (22), 71.1 (14), 55.0 (15). Analytical data in accordance to literature.²²¹

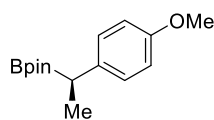
(*E*)-4,4,5,5-Tetramethyl-2-(pent-1-en-1-yl)-1,3,2-dioxaborolane (SM10)

Following a procedure published by Tanaka *et al.*,²²¹ **SM10** was synthesized as a colorless solid (*E/Z* = 88:12, 0.54 mmol, 106 mg, 54%). R_f = 0.30 (hexane/EtOAc 99:1, UV, KMnO_4 , PAA). $^1\text{H NMR}$ (400 MHz, CDCl_3) δ 6.63 (dt, J = 18.0, 6.4 Hz, 1H), 5.43 (dt, J = 18.0, 1.6 Hz, 1H),

²²¹ S. Tanaka, Y. Sairo, T. Yamamoto, T. Hattori, *Org. Lett.* **2018**, *20*, 1828–1831.

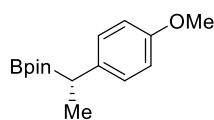
2.18 – 2.09 (m, 2H), 1.44 (h, $J = 7.4$ Hz, 2H), 1.26 (s, 12H), 0.91 (t, $J = 7.4$ Hz, 3H) ppm. **LRMS** (DEP/EI-Orbitrap): m/z (%): 196.2 (10), 181.1 (52), 153.1 (59), 139.1 (13), 110.1 (82), 97.1 (100), 85.1 (42), 69.1 (44), 55.1 (49). Analytical data in accordance to literature.²²¹

(R)-2-(1-(4-Methoxyphenyl)ethyl)-4,4,5,5-tetramethyl-1,3,2-dioxaborolane (SM11)



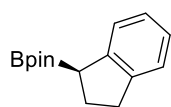
Following a procedure published by Noh *et al.*,²²² **SM11** was synthesized as a colorless oil (98% *ee*, 1.56 mmol, 408 mg, 52%). $R_f = 0.75$ (hexane/EtOAc 95:5, UV, KMnO₄, PAA). ¹H NMR (400 MHz, CDCl₃) δ 7.20 – 7.02 (m, 2H), 6.87 – 6.76 (m, 2H), 3.78 (s, 3H), 2.37 (q, $J = 7.5$ Hz, 1H), 1.30 (d, $J = 7.5$ Hz, 3H), 1.21 (s, 6H), 1.19 (s, 6H) ppm. **LRMS** (DEP/EI-Orbitrap): m/z (%): 262.1 (40), 247.2 (100), 161.0 (20), 147.0 (42), 135.1 (50), 121.1 (16), 91.0 (18). Analytical data in accordance to literature.²²²

(S)-2-(1-(4-Methoxyphenyl)ethyl)-4,4,5,5-tetramethyl-1,3,2-dioxaborolane (SM12)



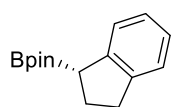
Following a procedure published by Noh *et al.*,²²² **SM12** was synthesized as a colorless oil (99% *ee*, 0.66 mmol, 173 mg, 66%). $R_f = 0.75$ (hexane/EtOAc 95:5, UV, KMnO₄, PAA). ¹H NMR (400 MHz, CDCl₃) δ 7.20 – 7.02 (m, 2H), 6.87 – 6.76 (m, 2H), 3.78 (s, 3H), 2.37 (q, $J = 7.5$ Hz, 1H), 1.30 (d, $J = 7.5$ Hz, 3H), 1.21 (s, 6H), 1.19 (s, 6H) ppm. **LRMS** (DEP/EI-Orbitrap): m/z (%): 262.1 (40), 247.2 (100), 161.0 (20), 147.0 (42), 135.1 (50), 121.1 (16), 91.0 (18). Analytical data in accordance to literature.²²²

(R)-2-(2,3-Dihydro-1H-inden-1-yl)-4,4,5,5-tetramethyl-1,3,2-dioxaborolane (SM13)



Following a procedure published by Noh *et al.*,²²² **SM13** was synthesized as a colorless oil (97% *ee*, 2.50 mmol, 610 mg, 50%). $R_f = 0.36$ (hexane/EtOAc 99:1, UV, KMnO₄, PAA). ¹H NMR (400 MHz, CDCl₃) δ 7.30 – 7.26 (m, 1H), 7.23 – 7.19 (m, 1H), 7.14 – 7.05 (m, 2H), 2.97 – 2.87 (m, 2H), 2.73 (t, $J = 8.7$ Hz, 1H), 2.28 – 2.17 (m, 1H), 2.14 – 2.03 (m, 1H), 1.26 (s, 6H), 1.25 (s, 6H) ppm. **LRMS** (DEP/EI-Orbitrap): m/z (%): 244.2 (30), 229.1 (10), 143.1 (33), 116.1 (100), 85.1 (75). Analytical data in accordance to literature.²²²

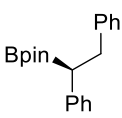
(S)-2-(2,3-Dihydro-1H-inden-1-yl)-4,4,5,5-tetramethyl-1,3,2-dioxaborolane (SM14)



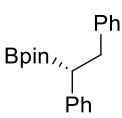
Following a procedure published by Noh *et al.*,²²² **SM14** was synthesized as a colorless oil (97% *ee*, 2.72 mmol, 665 mg, 54%). $R_f = 0.36$ (hexane/EtOAc 99:1, UV, KMnO₄, PAA). ¹H NMR (400 MHz, CDCl₃) δ 7.30 – 7.26 (m, 1H), 7.23 – 7.19 (m, 1H), 7.14 – 7.05 (m, 2H), 2.97 – 2.87 (m, 2H), 2.73 (t, $J = 8.7$ Hz, 1H), 2.28 – 2.17 (m, 1H), 2.14 – 2.03 (m, 1H), 1.26 (s, 6H), 1.25 (s, 6H) ppm. **LRMS** (DEP/EI-Orbitrap): m/z (%): 244.2 (30), 229.1 (10), 143.1 (33), 116.1 (100), 85.1 (75). Analytical data in accordance to literature.²²²

²²² D. Noh, S. K. Yoon, J. Won, J. Y. Lee, J. Yun, *Chem. Asian J.* **2011**, *6*, 1967–1969.

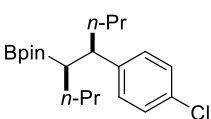
(S)-2-(1,2-Diphenylethyl)-4,4,5,5-tetramethyl-1,3,2-dioxaborolane (SM15)


 Following a procedure published by Noh *et al.*,²²² **SM15** was synthesized as a colorless oil (98% *ee*, 2.03 mmol, 620 mg, 70%). $R_f = 0.40$ (hexane/EtOAc 99:1, UV, KMnO₄, PAA). ¹H NMR (400 MHz, CDCl₃) δ 7.29 – 7.12 (m, 10H), 3.17 (dd, $J = 13.5, 9.8$ Hz, 1H), 2.98 (dd, $J = 13.4, 6.9$ Hz, 1H), 2.70 (dd, $J = 9.8, 6.8$ Hz, 1H), 1.12 (s, 6H), 1.11 (s, 6H) ppm. LRMS (DEP/EI-Orbitrap): m/z (%): 308.2 (13), 217.1 (100), 180.0 (15), 131.0 (20), 117.0 (48), 104.0 (20), 91.0 (75). Analytical data in accordance to literature.²²²

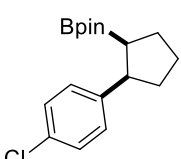
(R)-2-(1,2-Diphenylethyl)-4,4,5,5-tetramethyl-1,3,2-dioxaborolane (SM16)


 Following a procedure published by Noh *et al.*,²²² **SM16** was synthesized as a colorless oil (98% *ee*, 1.60 mmol, 500 mg, 54%). $R_f = 0.40$ (hexane/EtOAc 99:1, UV, KMnO₄, PAA). ¹H NMR (400 MHz, CDCl₃) δ 7.29 – 7.12 (m, 10H), 3.17 (dd, $J = 13.5, 9.8$ Hz, 1H), 2.98 (dd, $J = 13.4, 6.9$ Hz, 1H), 2.70 (dd, $J = 9.8, 6.8$ Hz, 1H), 1.12 (s, 6H), 1.11 (s, 6H) ppm. LRMS (DEP/EI-Orbitrap): m/z (%): 308.2 (13), 217.1 (100), 180.0 (15), 131.0 (20), 117.0 (48), 104.0 (20), 91.0 (75). Analytical data in accordance to literature.²²²

2-((4R,5R)-5-(4-Chlorophenyl)octan-4-yl)-4,4,5,5-tetramethyl-1,3,2-dioxaborolane (SM17)

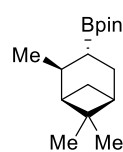

 Following a procedure published by Logan *et al.*,²²³ **SM17** was synthesized as a colorless solid ($dr > 99:1$, 0.54 mmol, 190 mg, 27%). $R_f = 0.33$ (hexane/EtOAc 99:1, UV, KMnO₄, PAA). ¹H NMR (400 MHz, CDCl₃) δ 7.20 (d, $J = 8.4$ Hz, 2H), 7.11 (d, $J = 8.4$ Hz, 2H), 2.54 (td, $J = 10.4, 3.5$ Hz, 1H), 1.88 – 1.74 (m, 1H), 1.60 – 1.50 (m, 1H), 1.44 – 1.20 (m, 7H), 0.98 (s, 6H), 0.96 (s, 6H), 0.91 (t, $J = 7.2$ Hz, 3H), 0.80 (t, $J = 7.3$ Hz, 3H) ppm. LRMS (DEP/EI-Orbitrap): m/z (%): 307.1 (10), 251.0 (12), 221.9 (13), 167.0 (30), 125.0 (100), 101.0 (20), 85.1 (30). Analytical data in accordance to literature.²²³

2-((1S,2R)-2-(4-Chlorophenyl)cyclopentyl)-4,4,5,5-tetramethyl-1,3,2-dioxaborolane (SM18)


 Following a procedure published by Logan *et al.*,²²³ **SM18** was synthesized as a colorless oil ($dr > 99:1$, 0.19 mmol, 57 mg, 38%). $R_f = 0.19$ (hexane/EtOAc 99:1, UV, KMnO₄, PAA). ¹H NMR (400 MHz, CDCl₃) δ 7.23 – 7.13 (m, 4H), 3.33 – 3.31 (m, 1H), 2.07 (dtd, $J = 11.8, 7.9, 3.5$ Hz, 1H), 1.96 – 1.72 (m, 5H), 1.70 – 1.59 (m, 1H), 0.98 (s, 6H), 0.94 (s, 6H) ppm. LRMS (DEP/EI-Orbitrap): m/z (%): 306.1 (13), 205.0 (12), 178.0 (66), 151.0 (30), 138.0 (35), 115.0 (40), 101.1 (28), 84.1 (100). Analytical data in accordance to literature.²²³

²²³ K. M. Logan, S. R. Sardini, S. D. White, M. K. Brown, *J. Am. Chem. Soc.* **2018**, *140*, 159–162.

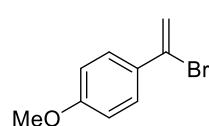
4,4,5,5-Tetramethyl-2-((1*R*,2*S*,3*R*,5*R*)-2,6,6-trimethylbicyclo[3.1.1]heptan-3-yl)-1,3,2-dioxaborolane (SM19)



Following a procedure published by Odachowski *et al.*,²²⁴ **SM19** was synthesized as a colorless oil (*dr* > 99:1, 2.27 mmol, 600 mg, 69%). R_f = 0.40 (hexane/EtOAc 98:2, UV, KMnO_4 , PAA). $^1\text{H NMR}$ (400 MHz, CDCl_3) δ 2.29 (dtd, J = 9.4, 6.2, 2.0 Hz, 1H), 2.17 – 2.09 (m, 1H), 2.08 – 1.99 (m, 1H), 1.91 – 1.79 (m, 2H), 1.75 (ddd, J = 6.7, 5.0, 2.0 Hz, 1H), 1.25 (s, 6H), 1.24 (s, 6H), 1.16 (s, 3H), 1.03 (s, 3H), 1.02 (s, 3H), 0.90 – 0.84 (m, 1H), 0.81 (d, J = 9.4 Hz, 1H) ppm. **LRMS** (DEP/EI-Orbitrap): m/z (%): 264.1 (8), 249.2 (10), 208.2 (40), 136.1 (59), 121.1 (32), 101.1 (51), 83.1 (100), 69.1 (40). Analytical data in accordance to literature.²²⁴

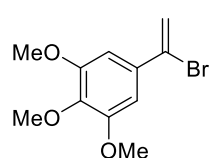
4.4.2 Synthesis of Vinyl Bromides

1-(1-Bromovinyl)-4-methoxybenzene (SM20)



Following a procedure published by Rosiak *et al.*,²²⁵ **SM20** was synthesized as a light-yellow oil (12.7 mmol, 2.7 g, 85%). R_f = 0.50 (hexane/EtOAc 99:1, UV, KMnO_4 , PAA). $^1\text{H NMR}$ (400 MHz, CDCl_3) δ 7.56 – 7.49 (m, 2H), 6.91 – 6.81 (m, 2H), 6.01 (d, J = 2.0 Hz, 1H), 5.67 (d, J = 2.0 Hz, 1H), 3.83 (s, 3H) ppm. **LRMS** (DEP/EI-Orbitrap): m/z (%): 213.9 (12), 133.0 (100), 118.0 (20), 103.0 (11), 89.0 (27), 77.0 (14), 63.0 (22). Analytical data in accordance to literature.²²⁵

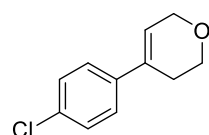
5-(1-Bromovinyl)-1,2,3-trimethoxybenzene (SM21)



Following a procedure published by Rosiak *et al.*,²²⁵ **SM21** was synthesized as an orange oil (3.78 mmol, 1.03 g, 85%). R_f = 0.35 (hexane/EtOAc 90:10, UV, KMnO_4 , PAA). $^1\text{H NMR}$ (400 MHz, CDCl_3) δ 6.81 (s, 2H), 6.05 (d, J = 2.0 Hz, 1H), 5.74 (d, J = 2.0 Hz, 1H), 3.89 (s, 6H), 3.86 (s, 3H) ppm. **LRMS** (DEP/EI-Orbitrap): m/z (%): 272.0 (25), 193.1 (100), 163.1 (19), 150.1 (15), 133.0 (13), 119.0 (11), 92.0 (12). Analytical data in accordance to literature.²²⁶

4.4.3 Remaining Experimental Data

4-4(Chlorophenyl)-3,6-dihydro-2*H*-pyran (6a)



Using 1-bromo-4-chlorobenzene and 2-(3,6-dihydro-2*H*-pyran-4-yl)-4,4,5,5-tetramethyl-1,3,2-dioxaborolane procedure **A** (0.45 mmol scale), provided **6a** (0.32 mmol, 63 mg, 86%) as a colorless oil. R_f = 0.22 (hexane/EtOAc 94:6, UV, KMnO_4 , PAA). $^1\text{H NMR}$ (400 MHz, CDCl_3) δ 7.37 – 7.27 (m, 4H), 6.13 – 6.09 (m, 1H), 4.33 – 4.30 (m, 2H),

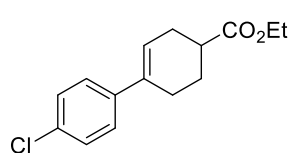
²²⁴ M. Odachowski, A. Bonet, S. Essafi, P. Conti-Ramsden, J. N. Harvey, D. Leonori, V. K. Aggarwal, *J. Am. Chem. Soc.* **2016**, *138*, 9521–9532.

²²⁵ A. Rosiak, W. Frey, J. Christoffers, *Eur. J. Org. Chem.* **2006**, 4044–4054.

²²⁶ A. Hamze, J.-D. Brion, M. Alami, *Org. Lett.* **2012**, *14*, 2782–2785.

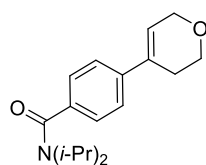
3.93 (t, $J = 5.5$ Hz, 2H), 2.49 (tt, $J = 5.6, 2.7$ Hz, 2H) ppm. ^{13}C NMR (101 MHz, CDCl_3) δ 138.8, 133.2, 133.1, 128.7, 126.1, 123.1, 65.9, 64.5, 27.2 ppm. LRMS (DEP/EI-Orbitrap): m/z (%): 194.0 (15), 176.0 (14), 159.1 (100), 141.1 (15), 131.0 (28), 129.1 (48), 115.1 (35). HRMS (EI-Orbitrap): m/z calcd for $\text{C}_{11}\text{H}_{11}\text{ClO}^+$: 194.0498; found: 194.0491. IR (Diamond-ATR, neat) $\tilde{\nu}_{\text{max}}$ (cm^{-1}): 3302 (vw), 3038 (vw), 2962 (w), 2924 (w), 2852 (w), 2829 (w), 2754 (vw), 1687 (vw), 1649 (vw), 1592 (w), 1491 (s), 1462 (w), 1426 (w), 1404 (m), 1385 (m), 1362 (m), 1284 (w), 1257 (w), 1229 (m), 1132 (vs), 1093 (vs), 1045 (m), 1012 (s), 975 (m), 853 (m), 807 (s), 731 (s).

Ethyl 4'-chloro-2,3,4,5-tetrahydro-[1,1'-biphenyl]-4-carboxylate (**6b**)

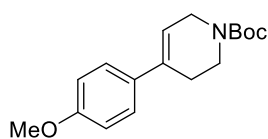


Using 1-bromo-4-chlorobenzene and ethyl 4-(4,4,5,5-tetramethyl-1,3,2-dioxaborolan-2-yl)cyclohex-3-ene-1-carboxylate according to general procedure **H**, provided **6b** (0.13 mmol, 34 mg, 50%) as a colorless oil. Fast decomposition of product **6b** to the carboxylic acid was observed by NMR spectroscopy. $R_f = 0.35$ (hexane/EtOAc 95:5, UV, KMnO_4 , PAA). ^1H NMR (400 MHz, CDCl_3) δ 7.33 – 7.23 (m, 4H), 6.14 – 6.04 (m, 1H), 4.17 (q, $J = 7.1$ Hz, 2H), 2.69 – 2.52 (m, 1H), 2.51 – 2.41 (m, 3H), 2.23 – 2.13 (m, 1H), 1.91 – 1.76 (m, 1H), 1.28 (t, $J = 7.1$ Hz, 3H) ppm. ^{13}C NMR (101 MHz, CDCl_3) δ 175.8, 140.3, 135.4, 132.7, 128.5, 126.4, 123.3, 60.6, 39.1, 28.3, 26.8, 25.7, 14.4 ppm. LRMS (DEP/EI-Orbitrap): m/z (%): 192.1 (32), 190.1 (100), 155.1 (45), 153.1 (28), 129.1 (15), 125.0 (34). HRMS (EI-Orbitrap): m/z calcd for $\text{C}_{15}\text{H}_{17}\text{ClO}_2^+$: 264.0917, found 264.0907. IR (Diamond-ATR, neat) $\tilde{\nu}_{\text{max}}$ (cm^{-1}): 2979 (w), 2958 (w), 2930 (w), 2840 (w), 1729 (vs), 1493 (m), 1436 (w), 1402 (w), 1378 (w), 1311 (w), 1255 (w), 1221 (m), 1175 (m), 1094 (m), 1032 (m), 1011 (w), 806 (m).

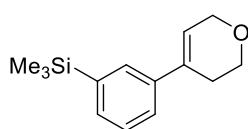
4-(3,6-Dihydro-2H-pyran-4-yl)-*N,N*-diisopropylbenzamide (**6c**)



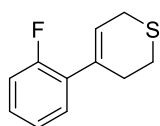
Using 4-iodo-*N,N*-diisopropylbenzamide and 2-(3,6-dihydro-2H-pyran-4-yl)-4,4,5,5-tetramethyl-1,3,2-dioxaborolane according to general procedure **H**, provided **6c** (0.14 mmol, 39 mg, 52%) as a colorless oil. $R_f = 0.15$ (hexane/EtOAc 80:20, UV, KMnO_4 , PAA). ^1H NMR (400 MHz, CDCl_3) δ 7.42 – 7.37 (m, 2H), 7.31 – 7.26 (m, 2H), 6.18 – 6.13 (m, 1H), 4.34 – 4.32 (m, 2H), 3.93 (t, $J = 5.4$ Hz, 2H), 3.89 – 3.39 (m, 2H), 2.58 – 2.45 (m, 2H), 1.71 – 0.98 (m, 12H) ppm. ^{13}C NMR (101 MHz, CDCl_3) δ 170.9, 140.6, 137.9, 133.7, 126.0, 124.8, 123.3, 66.0, 64.5, 51.2, 46.4, 27.2, 20.9 ppm. LRMS (DEP/EI-Orbitrap): m/z (%) = 287.1 (5), 244.1 (30), 187.1 (43), 97.1 (16), 71.1 (40), 57.1 (94), 43.0 (100). HRMS (DEP/EI-Orbitrap): m/z calcd for $\text{C}_{18}\text{H}_{25}\text{NO}_2^+$: 287.1885; found: 287.1870. IR (Diamond-ATR, neat) $\tilde{\nu}_{\text{max}}$ (cm^{-1}): 2966 (m), 2931 (m), 2878 (w), 2862 (w), 1722 (w), 1691 (w), 1625 (s), 1608 (s), 1512 (w), 1447 (s), 1440 (s), 1402 (m), 1370 (s), 1339 (vs), 1292 (m), 1261 (m), 1212 (m), 1185 (m), 1160 (m), 1135 (s), 1097 (m), 1077 (m), 1036 (m), 1017 (m), 989 (m), 975 (m), 939 (m), 917 (m), 877 (m), 849 (m), 827 (m), 762 (m), 730 (m).

***tert*-Butyl 4-(4-methoxyphenyl)-3,6-dihydropyridine-1(2*H*)-carboxylate (6d)**

Using 1-bromo-4-methoxybenzene and *tert*-butyl 4-(4,4,5,5-tetramethyl-1,3,2-dioxaborolan-2-yl)-3,6-dihydropyridine-1(2*H*)-carboxylate according to general procedure **H** (0.50 mmol scale), provided **6d** (0.26 mmol, 75 mg, 61%) as a light-yellow oil. R_f = 0.16 (hexane/EtOAc 95:5, UV, KMnO₄, PAA). ¹H NMR (400 MHz, CDCl₃) δ 7.34 – 7.27 (m, 2H), 6.90 – 6.83 (m, 2H), 5.94 (s, 1H), 4.05 (d, J = 1.6 Hz, 2H), 3.81 (s, 3H), 3.62 (t, J = 5.6 Hz, 2H), 2.49 (s, 2H), 1.49 (s, 9H) ppm. ¹³C NMR (101 MHz, CDCl₃) δ 159.0, 155.0, 133.4, 130.7, 126.1, 119.1, 113.8, 79.7, 55.4, 44.0, 39.9, 28.6, 27.6 ppm. LRMS (DEP/EI-Orbitrap): m/z (%): 232.1 (100), 202.1 (15), 188.1 (34), 160.0 (16), 145.0 (16), 115.0 (13), 57.0 (63), 41.0 (28). HRMS (EI-Orbitrap): m/z calcd for C₁₇H₂₃NO₃⁺: 289.1678; found: 289.1690. IR (Diamond-ATR, neat) $\tilde{\nu}_{max}$ (cm⁻¹): 3037 (vw), 3002 (vw), 2975 (w), 2932 (w), 2836 (w), 1693 (vs), 1608 (m), 1578 (vw), 1513 (s), 1478 (w), 1454 (m), 1421 (s), 1365 (m), 1339 (w), 1290 (m), 1278 (m), 1237 (vs), 1170 (s), 1114 (m), 1061 (w), 1036 (m), 988 (w), 988 (w), 971 (w), 938 (vw), 864 (w), 840 (w), 809 (w), 769 (w), 730 (vw).

(3-(3,6-Dihydro-2*H*-pyran-4-yl)phenyl)trimethylsilane (6e)

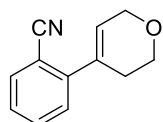
Using (3-bromophenyl)trimethylsilane and 2-(3,6-dihydro-2*H*-pyran-4-yl)-4,4,5,5-tetramethyl-1,3,2-dioxaborolane according to general procedure **H** (0.40 mmol scale), provided **6e** (0.23 mmol, 53 mg, 67%) as a colorless oil. R_f = 0.31 (hexane/EtOAc 95:5, UV, KMnO₄, PAA). ¹H NMR (400 MHz, CDCl₃) δ 7.54 (s, 1H), 7.46 – 7.41 (m, 1H), 7.40 – 7.31 (m, 2H), 6.12 (tt, J = 3.0, 1.6 Hz, 1H), 4.34 (q, J = 2.8 Hz, 2H), 3.95 (t, J = 5.5 Hz, 2H), 2.62 – 2.46 (m, 2H), 0.29 (s, 9H) ppm. ¹³C NMR (101 MHz, CDCl₃) δ 140.7, 139.7, 134.7, 132.5, 129.7, 128.0, 125.5, 122.6, 66.1, 64.7, 27.5, -1.0 ppm. LRMS (DEP/EI-Orbitrap): m/z (%): 231.1 (88), 217.1 (66), 187.1 (100), 155.1 (18), 143.1 (21), 142.1 (53), 128.1 (58), 115.1 (40), 75.0 (57). HRMS (EI-Orbitrap): m/z calcd for C₁₄H₂₀OSi⁺: 232.1283; found: 232.1278. IR (Diamond-ATR, neat) $\tilde{\nu}_{max}$ (cm⁻¹): 3055 (vw), 3024 (vw), 2953 (w), 2923 (w), 2895 (w), 2848 (w), 2810 (w), 1726 (vw), 1684 (vw), 1462 (vw), 1446 (vw), 1403 (w), 1384 (w), 1354 (w), 1313 (vw), 1261 (w), 1247 (m), 1229 (w), 1133 (m), 1120 (m), 1080 (w), 1046 (w), 1013 (w), 982 (w), 963 (w), 943 (w), 910 (w), 856 (s), 837 (vs), 794 (w), 778 (w), 753 (m), 736 (w), 692 (w).

4-(2-Fluorophenyl)-3,6-dihydro-2*H*-pyran (6f)

Using 1-bromo-2-fluorobenzene and 2-(3,6-dihydro-2*H*-thiopyran-4-yl)-4,4,5,5-tetramethyl-1,3,2-dioxaborolane according to general procedure **H** (0.50 mmol scale), provided **6f** (0.30 mmol, 58 mg, 70%) as a light-yellow oil. R_f = 0.20 (hexane/EtOAc 99:1, UV, KMnO₄, PAA). ¹H NMR (400 MHz, CDCl₃) δ 7.28 – 7.17 (m, 2H), 7.13 – 6.98 (m, 2H), 6.01 (tt, J = 4.1, 1.8 Hz, 1H), 3.33 (dt, J = 4.4, 2.3 Hz, 2H), 2.86 (t, J = 5.7 Hz, 2H), 2.71 – 2.60 (m, 2H) ppm. ¹³C NMR (101 MHz, CDCl₃) δ 159.9 (d, J = 247.0 Hz), 135.2 (d, J = 1.0 Hz), 131.4 (d, J = 14.1 Hz), 129.7 (d, J = 4.4 Hz), 128.7 (d, J = 8.3 Hz), 124.5 (d, J = 2.0 Hz), 124.2 (d, J = 3.5 Hz), 115.9 (d, J =

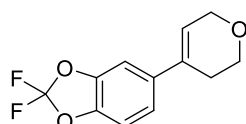
22.7 Hz), 29.6 (d, $J = 3.5$ Hz), 26.0, 25.3 ppm. **LRMS** (DEP/EI-Orbitrap): m/z (%): 194.1 (90), 191.0 (27), 165.0 (100), 159.1 (22), 147.1 (22), 133.0 (42), 109.0 (12). **HRMS** (EI-Orbitrap): m/z calcd for $C_{11}H_{11}FS^+$: 194.0565; found: 194.0559. **IR** (Diamond-ATR, neat) $\tilde{\nu}_{max}$ (cm^{-1}): 3058 (w), 3034 (w), 2956 (w), 2920 (m), 2893 (w), 2827 (w), 1654 (w), 1613 (w), 1577 (w), 1488 (s), 1449 (m), 1421 (w), 1348 (w), 1285 (w), 1264 (w), 1235 (m), 1205 (m), 1196 (m), 1144 (w), 1104 (m), 1035 (m), 1009 (m), 955 (m), 941 (m), 884 (m), 813 (m), 799 (m), 754 (vs).

2-(3,6-Dihydro-2H-pyran-4-yl)benzonitrile (**6g**)

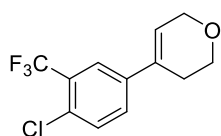


Using 2-bromobenzonitrile and 2-(3,6-dihydro-2H-pyran-4-yl)-4,4,5,5-tetramethyl-1,3,2-dioxaborolane according to general procedure **H** (0.50 mmol scale), provided **6g** (0.31 mmol, 57 mg, 72%) as a light-orange oil. $R_f = 0.26$ (hexane/EtOAc 85:15, UV, $KMnO_4$, PAA). **1H NMR** (400 MHz, $CDCl_3$) δ 7.70 – 7.64 (m, 1H), 7.55 (td, $J = 7.7, 1.4$ Hz, 1H), 7.39 – 7.30 (m, 2H), 6.08 (tt, $J = 2.9, 1.6$ Hz, 1H), 4.35 – 4.33 (m, 2H), 3.95 (t, $J = 5.4$ Hz, 2H), 2.57 – 2.48 (m, 2H) ppm. **^{13}C NMR** (101 MHz, $CDCl_3$) δ 145.8, 133.8, 133.2, 132.8, 128.4, 128.1, 127.5, 118.8, 110.4, 65.5, 64.3, 28.8 ppm. **LRMS** (DEP/EI-Orbitrap): m/z (%): 184.1 (35), 156.1 (100), 140.1 (16), 129.1 (34), 115.1 (18). **HRMS** (EI-Orbitrap): m/z calcd for $C_{12}H_{11}NO^+$: 185.0841; found: 185.0833. **IR** (Diamond-ATR, neat) $\tilde{\nu}_{max}$ (cm^{-1}): 3060 (w), 2964 (m), 2920 (w), 2865 (w), 2833 (w), 2748 (w), 2704 (w), 2223 (m), 1982 (w), 1950 (w), 1836 (w), 1718 (w), 1645 (w), 1593 (w), 1566 (w), 1484 (m), 1456 (w), 1437 (m), 1382 (m), 1361 (m), 1306 (w), 1286 (w), 1283 (w), 1267 (m), 1252 (w), 1227 (m), 1198 (m), 1182 (w), 1164 (w), 1131 (vs), 1106 (m), 1071 (m), 1046 (m), 1036 (m), 1012 (m), 979 (m), 958 (m), 950 (m), 939 (m), 847 (m), 836 (m), 760 (vs), 733 (s).

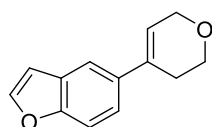
5-(3,6-Dihydro-2H-pyran-4-yl)-2,2-difluorobenzo[d][1,3]dioxole (**6h**)



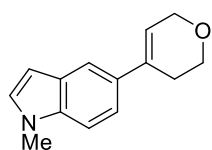
Using 5-bromo-2,2-difluorobenzo[d][1,3]dioxole and 2-(3,6-dihydro-2H-pyran-4-yl)-4,4,5,5-tetramethyl-1,3,2-dioxaborolane according to general procedure **H** (0.40 mmol scale), provided **6h** (0.22 mmol, 52 mg, 64%) as a colorless oil. $R_f = 0.42$ (hexane/EtOAc 90:10, UV, $KMnO_4$, PAA). **1H NMR** (400 MHz, $CDCl_3$) δ 7.13 – 7.05 (m, 2H), 7.04 – 6.97 (m, 1H), 6.06 (tt, $J = 3.0, 1.6$ Hz, 1H), 4.32 – 4.30 (m, 2H), 3.93 (t, $J = 5.4$ Hz, 2H), 2.55 – 2.39 (m, 2H) ppm. **^{13}C NMR** (101 MHz, $CDCl_3$) δ 144.1, 142.9, 137.0, 132.0 (t, $J = 255.5$ Hz), 131.6, 123.1, 120.0, 109.2, 106.2, 65.8, 64.3, 27.4 ppm. **LRMS** (DEP/EI-Orbitrap): m/z (%): 240.1 (100), 222.1 (53), 211.0 (32), 197.0 (33), 171.0 (34), 158.0 (44), 131.1 (30), 117.1 (23), 115.1 (85), 89.0 (29). **HRMS** (EI-Orbitrap): m/z calcd for $C_{12}H_{10}F_2O_3^+$: 240.0598; found: 240.0593. **IR** (Diamond-ATR, neat) $\tilde{\nu}_{max}$ (cm^{-1}): 2966 (w), 2924 (w), 2860 (vw), 2360 (w), 1733 (w), 1501 (m), 1447 (w), 1387 (w), 1371 (w), 1257 (s), 1238 (vs), 1181 (m), 1158 (m), 1131 (m), 1033 (w), 968 (w), 908 (w), 808(w).

4-(4-Chloro-3-(trifluoromethyl)phenyl)-3,6-dihydro-2H-pyran (6i)

Using 4-bromo-1-chloro-2-(trifluoromethyl)benzene and 2-(3,6-dihydro-2H-pyran-4-yl)-4,4,5,5-tetramethyl-1,3,2-dioxaborolane according to general procedure **H** (0.40 mmol scale), provided **6i** (0.21 mmol, 55 mg, 62%) as a colorless oil. $R_f = 0.35$ (hexane/EtOAc 90:10, UV, KMnO_4 , PAA). $^1\text{H NMR}$ (400 MHz, CDCl_3) δ 7.68 (s, 1H), 7.51 – 7.40 (m, 2H), 6.20 (tt, $J = 3.1, 1.6$ Hz, 1H), 4.35 – 4.32 (m, 2H), 3.94 (t, $J = 5.4$ Hz, 2H), 2.53 – 2.46 (m, 2H) ppm. $^{13}\text{C NMR}$ (101 MHz, CDCl_3) δ 139.2, 132.4, 131.6, 130.9 (q, $J = 1.8$ Hz), 128.9, 128.5 (q, $J = 31.1$ Hz), 124.8, 123.9 (q, $J = 5.3$ Hz), 123.0 (q, $J = 273.3$ Hz), 65.9, 64.3, 27.1 ppm. **LRMS** (DEP/EI-Orbitrap): m/z (%): 262.0 (15), 244.0 (25), 227.1 (100), 199.0 (32), 193.0 (29), 183.0 (26), 177.1 (49), 169.0 (22), 151.0 (19), 128.1 (40). **HRMS** (EI-Orbitrap): m/z calcd for $\text{C}_{12}\text{H}_{10}\text{ClF}_3\text{O}^+$: 262.0372; found: 262.0369. **IR** (Diamond-ATR, neat) $\tilde{\nu}_{max}$ (cm^{-1}): 2976 (vw), 2934 (vw), 2892 (vw), 1726 (w), 1696 (w), 1649 (vw), 1604 (w), 1575 (vw), 1482 (m), 1408 (w), 1388 (w), 1358 (w), 1320 (s), 1261 (m), 1255 (m), 1242 (m), 1177 (s), 1131 (vs), 1115 (s), 1051 (w), 1034 (m), 1011 (w), 957 (w), 944 (m), 905 (w), 853 (w), 832 (w), 815 (w), 733 (w), 724 (vw), 664 (m).

5-(3,6-Dihydro-2H-pyran-4-yl)benzofuran (6j)

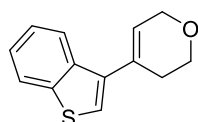
Using 5-bromobenzofuran and 2-(3,6-dihydro-2H-pyran-4-yl)-4,4,5,5-tetramethyl-1,3,2-dioxaborolane according to general procedure **H** (0.40 mmol scale), provided **6j** (0.25 mmol, 50 mg, 73%) as a colorless solid. $R_f = 0.22$ (hexane/EtOAc 95:5, UV, KMnO_4 , PAA). $^1\text{H NMR}$ (400 MHz, CDCl_3) δ 7.62 (d, $J = 2.2$ Hz, 1H), 7.60 (d, $J = 1.9$ Hz, 1H), 7.47 (d, $J = 8.6$ Hz, 1H), 7.37 (dd, $J = 8.6, 1.9$ Hz, 1H), 6.76 (dd, $J = 2.3, 0.9$ Hz, 1H), 6.10 (tt, $J = 3.0, 1.6$ Hz, 1H), 4.36 – 4.34 (m, 2H), 3.97 (t, $J = 5.5$ Hz, 2H), 2.62 – 2.54 (m, 2H) ppm. $^{13}\text{C NMR}$ (101 MHz, CDCl_3) δ 154.5, 145.6, 135.8, 134.5, 127.7, 122.0, 121.7, 117.4, 111.3, 106.9, 66.0, 64.7, 27.9 ppm. **LRMS** (DEP/EI-Orbitrap): m/z (%): 200.1 (61), 182.1 (68), 170.1 (61), 157.1 (26), 153.1 (40), 141.1 (100), 128.1 (39), 115.1 (50). **HRMS** (EI-Orbitrap): m/z calcd for $\text{C}_{13}\text{H}_{12}\text{O}_2^+$: 200.0837; found: 200.0832. **IR** (Diamond-ATR, neat) $\tilde{\nu}_{max}$ (cm^{-1}): 3146 (vw), 3114 (vw), 2964 (w), 2923 (w), 2850 (w), 2830 (w), 2812 (w), 2750 (vw), 1721 (vw), 1605 (vw), 1536 (w), 1467 (m), 1440 (w), 1427 (w), 1385 (w), 1370 (w), 1332 (w), 1276 (w), 1267 (m), 1238 (w), 1219 (m), 1130 (vs), 1111 (m), 1073 (w), 1043 (w), 1030 (m), 1011 (w), 982 (w), 965 (w), 945 (w), 878 (w), 870 (m), 850 (w), 804 (m), 764 (s), 736 (m). **Mp** ($^\circ\text{C}$) = 80–84.

5-(3,6-Dihydro-2H-pyran-4-yl)-1-methyl-1H-indole (6k)

Using 5-bromo-1-methyl-1H-indole and 2-(3,6-dihydro-2H-pyran-4-yl)-4,4,5,5-tetramethyl-1,3,2-dioxaborolane according to general procedure **H** (0.40 mmol scale), provided **6k** (0.24 mmol, 51 mg, 70%) as a colorless solid. $R_f = 0.27$ (hexane/EtOAc 90:10, UV, KMnO_4 , PAA). $^1\text{H NMR}$ (400 MHz, CDCl_3) δ 7.65 (s, 1H), 7.35 (dd, $J = 8.6, 1.7$ Hz, 1H), 7.29 (d, $J = 8.6$ Hz, 1H), 7.05 (d, $J = 3.1$ Hz, 1H), 6.49 (d, $J = 3.1$ Hz,

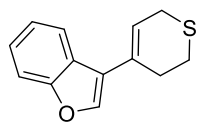
1H), 6.18 – 6.00 (m, 1H), 4.38 – 4.36 (m, 2H), 3.99 (t, $J = 5.5$ Hz, 2H), 3.79 (s, 3H), 2.71 – 2.53 (m, 2H) ppm. ^{13}C NMR (101 MHz, CDCl_3) δ 136.3, 135.0, 132.1, 129.4 (d, $J = 5.0$ Hz), 128.6, 120.6, 119.1, 117.1, 109.2, 101.4, 66.2, 64.8, 33.0, 28.0 ppm. LRMS (DEP/EI-Orbitrap): m/z (%): 213.1 (85), 195.1 (65), 182.1 (94), 167.1 (100), 157.1 (28), 144.1 (23), 131.1 (16), 115.1 (21). HRMS (EI-Orbitrap): m/z calcd for $\text{C}_{14}\text{H}_{15}\text{NO}^+$: 213.1154; found: 213.1145. IR (Diamond-ATR, neat) $\tilde{\nu}_{\text{max}}$ (cm^{-1}): 2981 (m), 2936 (m), 2837 (w), 1731 (vs), 1494 (m), 1434 (m), 1377 (m), 1315 (m), 1257 (m), 1222 (m), 1177 (s), 1094 (m), 1035 (m), 1012 (m), 916 (m), 807 (m), 733 (s). Mp ($^{\circ}\text{C}$) = 146–150.

4- (Benzo[*b*]thiophen-3-yl)-3,6-dihydro-2*H*-pyran (6l)

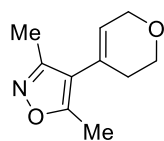


Using 3-bromobenzo[*b*]thiophene and 2-(3,6-dihydro-2*H*-pyran-4-yl)-4,4,5,5-tetramethyl-1,3,2-dioxaborolane according to general procedure **H** (0.50 mmol scale), provided **6l** (0.33 mmol, 72 mg, 78%) as a light-yellow oil. $R_f = 0.25$ (hexane/EtOAc 95:5, UV, KMnO_4 , PAA). ^1H NMR (400 MHz CDCl_3) δ 8.00 – 7.94 (m, 1H), 7.91 – 7.84 (m, 1H), 7.44 – 7.31 (m, 3H), 6.12 (tt, $J = 3.0, 1.6$ Hz, 1H), 4.40 – 4.38 (m, 2H), 4.00 (t, $J = 5.4$ Hz, 2H), 2.66 – 2.51 (m, 2H) ppm. ^{13}C NMR (101 MHz, CDCl_3) δ 140.8, 137.9, 137.5, 130.4, 125.0, 124.5, 124.3, 123.2, 123.1, 122.1, 65.7, 64.6, 29.5 ppm. LRMS (DEP/EI-Orbitrap): m/z (%): 216.1 (100), 187.0 (40), 173.0 (43), 160.0 (14), 147.0 (22), 134.0 (32), 115.1 (23). HRMS (EI-Orbitrap): m/z calcd for $\text{C}_{13}\text{H}_{12}\text{OS}^+$: 216.0609; found: 216.0603. IR (Diamond-ATR, neat) $\tilde{\nu}_{\text{max}}$ (cm^{-1}): 3096 (w), 3065 (w), 2963 (w), 2925 (w), 2851 (w), 2825 (w), 2751 (w), 1721 (m), 1670 (w), 1555 (w), 1496 (w), 1458 (m), 1426 (m), 1384 (m), 1332 (m), 1270 (w), 1261 (w), 1236 (w), 1165 (m), 1128 (s), 1072 (m), 1033 (m), 972 (m), 942 (m), 903 (m), 828 (m), 760 (vs), 733 (vs).

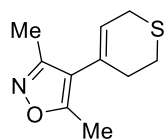
3-(3,6-Dihydro-2*H*-thiopyran-4-yl)benzofuran (6m)



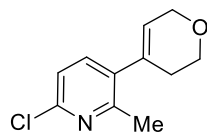
Using 3-bromobenzofuran and 2-(3,6-dihydro-2*H*-thiopyran-4-yl)-4,4,5,5-tetramethyl-1,3,2-dioxaborolane according to general procedure **H**, provided **6m** (0.08 mmol, 16 mg, 29%) as a light-yellow oil. $R_f = 0.43$ (hexane/EtOAc 98:2, UV, KMnO_4 , PAA). ^1H NMR (400 MHz, CDCl_3) δ 7.79 (dd, $J = 7.8, 1.5$ Hz, 1H), 7.61 (s, 1H), 7.51 (d, $J = 8.7$ Hz, 1H), 7.38 – 7.25 (m, 2H), 6.47 (tt, $J = 4.2, 1.8$ Hz, 1H), 3.41 (dt, $J = 4.4, 2.3$ Hz, 2H), 2.94 (t, $J = 5.8$ Hz, 2H), 2.79 – 2.60 (m, 2H) ppm. ^{13}C NMR (101 MHz, CDCl_3) δ 155.8, 141.1, 130.1, 125.9, 124.6, 123.3, 122.9, 121.8, 121.2, 111.9, 28.8, 26.1, 25.3 ppm. LRMS (DEP/EI-Orbitrap): m/z (%): 216.1 (60), 187.0 (100), 169.1 (22), 115.1 (23), 76.0 (10). HRMS (EI-Orbitrap): m/z calcd for $\text{C}_{13}\text{H}_{12}\text{OS}^+$: 216.0609; found: 216.0607. IR (Diamond-ATR, neat) $\tilde{\nu}_{\text{max}}$ (cm^{-1}): 2956 (w), 2918 (w), 2853 (w), 2360 (w), 1740 (w), 1550 (w), 1474 (w), 1451 (s), 1421 (w), 1380 (w), 1331 (w), 1288 (m), 1261 (w), 1207 (m), 1115 (m), 1100 (m), 1016 (w), 930 (w), 878 (w), 856 (m), 791 (w), 746 (vs).

4-(3,6-Dihydro-2H-pyran-4-yl)-3,5-dimethylisoxazole (6n)

Using 4-bromo-3,5-dimethylisoxazole and 2-(3,6-dihydro-2H-pyran-4-yl)-4,4,5,5-tetramethyl-1,3,2-dioxaborolane according to general procedure **H** (0.40 mmol scale), provided **6n** (0.22 mmol, 40 mg, 66%) as a colorless oil. $R_f = 0.22$ (hexane/EtOAc 80:20, UV, KMnO_4 , PAA). $^1\text{H NMR}$ (400 MHz, CDCl_3) δ 5.67 (tt, $J = 3.0, 1.7$ Hz, 1H), 4.28 – 4.26 (m, 2H), 3.88 (t, $J = 5.4$ Hz, 2H), 2.35 (s, 3H), 2.32 – 2.25 (m, 2H), 2.22 (s, 3H) ppm. $^{13}\text{C NMR}$ (101 MHz, CDCl_3) δ 164.8, 158.5, 126.9, 125.6, 116.7, 65.6, 64.3, 29.0, 11.9, 11.2 ppm. **LRMS** (DEP/EI-Orbitrap): m/z (%): 179.1 (100), 151.1 (32), 136.1 (81), 123.0 (31), 110.0 (70), 95.0 (67), 82.0 (33), 67.1 (25). **HRMS** (EI-Orbitrap): m/z calcd for $\text{C}_{10}\text{H}_{13}\text{NO}_2^+$: 179.0946; found: 179.0938. **IR** (Diamond-ATR, neat) $\tilde{\nu}_{\text{max}}$ (cm^{-1}): 2970 (w), 2926 (m), 2853 (w), 2824 (w), 1723 (vw), 1662 (w), 1621 (w), 1446 (m), 1421 (s), 1384 (m), 1277 (w), 1239 (m), 1221 (s), 1205 (w), 1132 (vs), 1039 (m), 1010 (w), 976 (m), 933 (w), 894 (w), 846 (m), 823 (w).

4-(3,6-Dihydro-2H-thiopyran-4-yl)-3,5-dimethylisoxazole (6o)

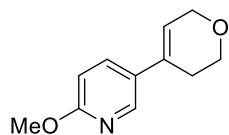
Using 4-bromo-3,5-dimethylisoxazole and 2-(3,6-dihydro-2H-thiopyran-4-yl)-4,4,5,5-tetramethyl-1,3,2-dioxaborolane according to general procedure **H**, provided **6o** (0.22 mmol, 43 mg, 87%) as a colorless oil. $R_f = 0.27$ (hexane/EtOAc 90:10, UV, KMnO_4 , PAA). $^1\text{H NMR}$ (400 MHz, CDCl_3) δ 5.79 (tt, $J = 4.1, 1.9$ Hz, 1H), 3.29 (dt, $J = 4.5, 2.4$ Hz, 2H), 2.83 (t, $J = 5.7$ Hz, 2H), 2.45 – 2.38 (m, 2H), 2.33 (s, 3H), 2.21 (s, 3H) ppm. $^{13}\text{C NMR}$ (101 MHz, CDCl_3) δ 164.8, 158.6, 128.8, 125.7, 118.4, 29.9, 25.9, 25.2, 11.7, 11.0 ppm. **LRMS** (DEP/EI-Orbitrap): m/z (%): 195.1 (82), 154.0 (83), 153.0 (100), 134.1 (20), 126.0 (25), 111.0 (45), 97.0 (12), 77.0 (16). **HRMS** (EI-Orbitrap): m/z calcd for $\text{C}_{10}\text{H}_{13}\text{NOS}^+$: 195.0718; found: 195.0710. **IR** (Diamond-ATR, neat) $\tilde{\nu}_{\text{max}}$ (cm^{-1}): 2960 (w), 2931 (w), 2887 (w), 2826 (w), 1662 (w), 1621 (m), 1493 (w), 1442 (m), 1420 (vs), 1381 (w), 1306 (w), 1282 (m), 1258 (w), 1220 (m), 1200 (w), 1170 (w), 1144 (w), 1062 (w), 1039 (w), 1004 (w), 977 (w), 944 (m), 888 (m), 804 (w).

6-Chloro-3-(3,6-dihydro-2H-pyran-4-yl)-2-methylpyridine (6p)

Using 3-bromo-6-chloro-2-methylpyridine and 2-(3,6-dihydro-2H-pyran-4-yl)-4,4,5,5-tetramethyl-1,3,2-dioxaborolane according to general procedure **H** (0.40 mmol scale), provided **6p** (0.25 mmol, 53 mg, 74%) as an orange solid. $R_f = 0.19$ (hexane/EtOAc 90:10, UV, KMnO_4 , PAA). $^1\text{H NMR}$ (400 MHz, CDCl_3) δ 7.34 (d, $J = 8.0$ Hz, 1H), 7.12 (d, $J = 8.0$ Hz, 1H), 5.68 (tt, $J = 2.8, 1.6$ Hz, 1H), 4.29 – 4.27 (m, 2H), 3.91 (t, $J = 5.4$ Hz, 2H), 2.50 (s, 3H), 2.37 – 2.25 (m, 2H) ppm. $^{13}\text{C NMR}$ (101 MHz, CDCl_3) δ 156.6, 148.8, 138.7, 136.1, 133.7, 126.7, 121.4, 65.5, 64.3, 29.6, 22.8 ppm. **LRMS** (DEP/EI-Orbitrap): m/z (%): 209.1 (14), 194.0 (20), 180.1 (19), 174.1 (57), 166.0 (100), 152.0 (42), 131.1 (48), 115.1 (21), 89.0 (15). **HRMS** (EI-Orbitrap): m/z calcd for $\text{C}_{11}\text{H}_{12}\text{ClNO}^+$: 209.0607; found: 209.0600. **IR** (Diamond-ATR, neat) $\tilde{\nu}_{\text{max}}$ (cm^{-1}): 2968 (w), 2927 (w), 2892 (w), 2851 (w), 2823 (w), 1575 (m), 1552 (m), 1444 (s), 1430 (s),

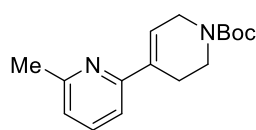
1383 (m), 1361 (w), 1274 (w), 1268 (w), 1228 (m), 1192 (m), 1131 (vs), 1037 (m), 976 (m), 910 (w), 875 (s), 844 (m), 819 (m), 730 (m). **Mp** (°C) = 99–103.

5-(3,6-Dihydro-2H-pyran-4-yl)-2-methoxypyridine (**6q**)



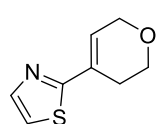
Using 5-bromo-2-methoxypyridine and 2-(3,6-dihydro-2H-pyran-4-yl)-4,4,5,5-tetramethyl-1,3,2-dioxaborolane according to general procedure **H** (0.40 mmol scale), provided **6q** (0.28 mmol, 53 mg, 82%) as a colorless oil. R_f = 0.29 (hexane/EtOAc 80:20, UV, KMnO₄, PAA). ¹H NMR (400 MHz, CDCl₃) δ 8.17 (d, J = 2.6 Hz, 1H), 7.60 (dd, J = 8.7, 2.6 Hz, 1H), 6.71 (d, J = 8.6 Hz, 1H), 6.03 (tt, J = 3.0, 1.6 Hz, 1H), 4.31 – 4.29 (m, 2H), 3.92 (t, J = 5.5 Hz, 2H), 3.92 (s, 3H), 2.54 – 2.37 (m, 2H) ppm. ¹³C NMR (101 MHz, CDCl₃) δ 163.6, 143.1, 135.3, 131.3, 129.2, 122.0, 110.6, 65.9, 64.4, 53.6, 27.1 ppm. **LRMS** (DEP/EI-Orbitrap): m/z (%): 191.1 (57), 162.1 (99), 148.1 (100), 134.1 (30), 123.1 (21), 103.1 (10), 77.0 (11). **HRMS** (EI-Orbitrap): m/z calcd for C₁₁H₁₃NO₂⁺: 191.0946; found: 191.0940. **IR** (Diamond-ATR, neat) $\tilde{\nu}_{max}$ (cm⁻¹): 3020 (vw), 2946 (w), 2927 (w), 2848 (w), 2818 (w), 2753 (vw), 1719 (vw), 1649 (vw), 1600 (s), 1563 (m), 1495 (vs), 1462 (m), 1445 (w), 1381 (s), 1352 (m), 1285 (vs), 1245 (s), 1229 (w), 1177 (w), 1130 (s), 1076 (w), 1045 (w), 1028 (s), 1020 (m), 1016 (m), 975 (w), 940 (w), 852 (m), 813 (m), 775 (w).

tert-Butyl 6-methyl-3'-6'-dihydro-[2,4'-bipyridine]-1'(2'*H*)-carboxylate (**6r**)



Using 2-bromo-6-methylpyridine and *tert*-butyl 4-(4,4,5,5-tetramethyl-1,3,2-dioxaborolan-2-yl)-3,6-dihydropyridine-1(2*H*)-carboxylate according to general procedure **H**, provided **6r** (0.38 mmol, 60 mg, 85%) as a light-yellow oil. R_f = 0.22 (hexane/EtOAc 80:20, UV, KMnO₄, PAA). ¹H NMR (400 MHz, CDCl₃) δ 7.52 (t, J = 7.7 Hz, 1H), 7.12 (d, J = 7.8 Hz, 1H), 7.00 (d, J = 7.6 Hz, 1H), 6.61 (tt, J = 3.5, 1.6 Hz, 1H), 4.13 – 4.11 (m, 2H), 3.68 – 3.58 (m, 2H), 2.66 – 2.57 (m, 2H), 2.53 (s, 3H), 1.48 (s, 9H) ppm. ¹³C NMR (101 MHz, CDCl₃) δ 157.8, 156.6, 155.0, 136.8, 135.5, 124.2, 121.7, 116.2, 79.7, 43.9, 40.5, 28.6, 26.2, 24.8 ppm. Signal splitting was observed, which was presumably caused by rotational barriers. **LRMS** (DEP/EI-Orbitrap): m/z (%): 218.1 (100), 201.1 (15), 173.1 (38), 158.1 (16), 144.1 (37), 131.1 (31), 57.1 (76), 41.0 (23). **HRMS** (EI-Orbitrap): m/z calcd for C₁₆H₂₂N₂O₂⁺: 274.1681; found: 274.1676. **IR** (Diamond-ATR, neat) $\tilde{\nu}_{max}$ (cm⁻¹): 3001 (vw), 2974 (w), 2925 (w), 2849 (vw), 2361 (vw), 1689 (vs), 1653 (w), 1584 (m), 1574 (m), 1478 (w), 1454 (s), 1415 (s), 1391 (m), 1364 (s), 1336 (m), 1294 (m), 1272 (m), 1236 (s), 1160 (vs), 1112 (s), 1075 (w), 1066 (w), 1039 (w), 983 (m), 976 (w), 949 (m), 865 (m), 825 (w), 789 (s), 766 (m).

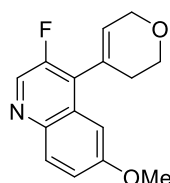
2-(3,6-Dihydro-2H-pyran-4-yl)thiazole (**6s**)



Using 2-bromothiazole and 2-(3,6-dihydro-2H-pyran-4-yl)-4,4,5,5-tetramethyl-1,3,2-dioxaborolane according to general procedure **H** (0.40 mmol scale), provided **6s** (0.18 mmol, 30 mg, 52%) as a light-yellow oil. R_f = 0.20 (hexane/EtOAc 80:20, UV,

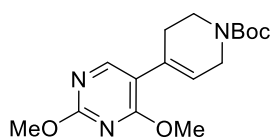
KMnO₄, PAA). ¹H NMR (400 MHz, CDCl₃) δ 7.75 (d, *J* = 3.3 Hz, 1H), 7.22 (d, *J* = 3.3 Hz, 1H), 6.60 (tt, *J* = 3.1, 1.6 Hz, 1H), 4.34 – 4.32 (m, 2H), 3.92 (t, *J* = 5.5 Hz, 2H), 2.73 – 2.65 (m, 2H) ppm. ¹³C NMR (101 MHz, CDCl₃) δ 168.9, 143.1, 130.1, 127.5, 117.9, 65.4, 64.2, 26.8 ppm. LRMS (DEP/EI-Orbitrap): *m/z* (%): 167.0 (72), 152.0 (31), 138.0 (100), 123.0 (70), 110.0 (34), 58.0 (14). HRMS (EI-Orbitrap): *m/z* calcd for C₈H₉NOS⁺: 167.0405; found: 167.0398. IR (Diamond-ATR, neat) $\tilde{\nu}_{max}$ (cm⁻¹): 3120 (w), 3081 (w), 2970 (w), 2927 (w), 2856 (w), 2816 (w), 1720 (w), 1647 (vw), 1485 (m), 1462 (w), 1440 (w), 1422 (w), 1383 (w), 1358 (w), 1316 (w), 1278 (w), 1242 (w), 1220 (w), 1147 (m), 1122 (vs), 1073 (w), 1056 (w), 1034 (w), 972 (w), 911 (w), 872 (w), 843 (m), 724 (w).

4-(3,6-Dihydro-2H-pyran-4-yl)-3-fluoro-6-methoxyquinoline (6t)



Using 3-fluoro-4-iodo-6-methoxyquinoline and 2-(3,6-dihydro-2H-pyran-4-yl)-4,4,5,5-tetramethyl-1,3,2-dioxaborolane according to general procedure H (0.50 mmol scale), provided **6t** (0.25 mmol, 64 mg, 58%) as a light-yellow oil. *R*_f = 0.21 (hexane/EtOAc 80:20, UV, KMnO₄, PAA). ¹H NMR (400 MHz, CDCl₃) δ 8.62 (d, *J* = 1.2 Hz, 1H), 7.99 (d, *J* = 9.2 Hz, 1H), 7.32 (dd, *J* = 9.2, 2.8 Hz, 1H), 7.20 (d, *J* = 2.8 Hz, 1H), 5.91 (td, *J* = 2.7, 1.4 Hz, 1H), 4.43 – 4.41 (m, 2H), 4.03 (t, *J* = 5.4 Hz, 2H), 3.91 (s, 3H), 2.51 – 2.40 (m, 2H) ppm. ¹³C NMR (101 MHz, CDCl₃) δ 158.8, 153.3 (d, *J* = 253.0 Hz), 141.9 (d, *J* = 2.4 Hz), 138.6 (d, *J* = 28.9 Hz), 131.5, 130.7 (d, *J* = 13.5 Hz), 129.1, 128.7 (d, *J* = 3.0 Hz), 127.4, 120.7 (d, *J* = 2.8 Hz), 103.2 (d, *J* = 5.5 Hz), 65.5, 64.4, 55.7, 29.0 (d, *J* = 1.8 Hz) ppm. LRMS (DEP/EI-Orbitrap): *m/z* (%): 259.1 (89), 228.1 (16), 214.1 (100), 198.1 (29), 185.1 (41), 172.1 (41), 159.0 (12). HRMS (EI-Orbitrap): *m/z* calcd for C₁₅H₁₄FNO₂⁺: 259.1009; found: 259.1004. IR (Diamond-ATR, neat) $\tilde{\nu}_{max}$ (cm⁻¹): 2962 (w), 2930 (w), 2848 (w), 2832 (w), 1621 (s), 1505 (s), 1468 (m), 1426 (m), 1383 (w), 1353 (m), 1310 (m), 1268 (m), 1223 (vs), 1206 (m), 1153 (m), 1130 (s), 1028 (m), 974 (w), 947 (w), 907 (w), 831 (m), 791 (m).

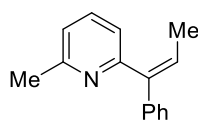
tert-Butyl 4-(2,4-dimethoxypyrimidin-5-yl)-3,6-dihydropyridine-1(2H)-carboxylate (6u)



Using 5-bromo-2,4-dimethoxypyrimidine and *tert*-butyl 4-(4,4,5,5-tetramethyl-1,3,2-dioxaborolan-2-yl)-3,6-dihydropyridine-1(2H)-carboxylate according to general procedure H, provided **6u** (0.22 mmol, 72 mg, 88%) as a colorless oil. This experiment was redone on a gram scale (5.0 mmol), resulting in almost the same yield of product **6u** (3.66 mmol, 1.18 g, 86%). *R*_f = 0.17 (hexane/EtOAc 80:20, UV, KMnO₄, PAA). ¹H NMR (400 MHz, CDCl₃) δ 8.06 (s, 1H), 5.86 (s, 1H), 4.06 – 4.01 (m, 2H), 3.98 (s, 3H), 3.98 (s, 3H), 3.58 (t, *J* = 5.7 Hz, 2H), 2.41 (s, 2H), 1.48 (s, 9H) ppm. ¹³C NMR (101 MHz, CDCl₃) δ 168.3, 164.4, 156.1, 155.0, 130.3, 124.2, 116.9, 79.8, 54.9, 54.1, 43.8, 40.4, 28.6, 28.2 ppm. Signal splitting was observed, which was presumably caused by rotational barriers. LRMS (DEP/EI-Orbitrap): *m/z* (%): 264.1 (100), 220.1 (37), 192.1 (15), 57.1 (99), 43.0 (58). HRMS (EI-Orbitrap): *m/z* calcd for C₁₂H₁₄N₃O₄⁺ [M-*t*-Bu]⁺: 264.0984; found: 264.1025. IR (Diamond-ATR, neat) $\tilde{\nu}_{max}$ (cm⁻¹): 3000 (w),

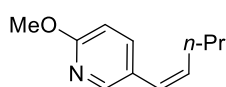
2980 (w), 2929 (w), 2859 (w), 1695 (s), 1592 (s), 1556 (s), 1468 (s), 1396 (vs), 1363 (s), 1338 (m), 1291 (m), 1232 (s), 1169 (s), 1113 (m), 1080 (m), 1056 (w), 1015 (m), 986 (w), 968 (w), 862 (w), 827 (w), 797 (w), 771 (w).

(Z)-2-Methyl-6-(1-phenylprop-1-en-1-yl)pyridine (8a)



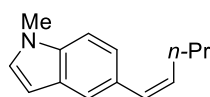
Using 2-bromo-6-methylpyridine and (*E*)-4,4,5,5-tetramethyl-2-(1-phenylprop-1-en-1-yl)-1,3,2-dioxaborolane (**SM9**) according to general procedure **H**, provided **8a** (0.14 mmol, 29 mg, 54%) as a colorless oil. $R_f = 0.16$ (hexane/EtOAc 95:5, UV, KMnO_4 , PAA). $^1\text{H NMR}$ (400 MHz, CDCl_3) δ 7.63 (t, $J = 7.7$ Hz, 1H), 7.37 – 7.21 (m, 5H), 7.13 (d, $J = 7.7$ Hz, 1H), 7.04 (d, $J = 7.7$ Hz, 1H), 6.34 (q, $J = 7.1$ Hz, 1H), 2.65 (s, 3H), 1.85 (d, $J = 7.1$ Hz, 3H) ppm. $^{13}\text{C NMR}$ (101 MHz, CDCl_3) δ 158.5, 158.3, 142.1, 141.8, 136.4, 128.2, 127.2, 126.9, 126.6, 122.2, 121.3, 24.9, 15.7 ppm. **LRMS** (DEP/EI-Orbitrap): m/z (%): 209.1 (30), 208.1 (100), 194.1 (12), 193.1 (18), 107.1 (11). **HRMS** (EI-Orbitrap): m/z calcd for $\text{C}_{15}\text{H}_{15}\text{N}^+$: 209.1204; found: 209.1199. **IR** (Diamond-ATR, neat) $\tilde{\nu}_{max}$ (cm^{-1}): 3079 (w), 3057 (w), 3021 (w), 2975 (w), 2919 (w), 2854 (w), 1882 (vw), 1631 (vw), 1583 (m), 1571 (s), 1494 (m), 1456 (m), 1443 (s), 1373 (w), 1354 (w), 1247 (w), 1192 (w), 1153 (w), 1091 (w), 1075 (w), 1032 (w), 990 (w), 965 (w), 908 (s), 843 (w), 796 (s), 758 (vs), 729 (vs), 696 (vs).

(Z)-2-Methoxy-5-(pent-1-en-1-yl)pyridine (8b)



Using 5-bromo-2-methoxypyridine and (*E*)-4,4,5,5-tetramethyl-2-(pent-1-en-1-yl)-1,3,2-dioxaborolane (**SM10**) according to general procedure **H**, provided **8b** (*E/Z* = 12:88, 0.18 mmol, 32 mg, 70%) as a colorless oil. $R_f = 0.10$ (hexane/EtOAc 98:2, UV, KMnO_4 , PAA). $^1\text{H NMR}$ (400 MHz, CDCl_3) δ 8.09 (d, $J = 2.4$ Hz, 1H), 7.49 (dd, $J = 8.5, 2.4$ Hz, 1H), 6.76 – 6.63 (m, 1H), 6.28 (dt, $J = 11.6, 1.8$ Hz, 1H), 5.67 (dt, $J = 11.6, 7.3$ Hz, 1H), 3.93 (s, 3H), 2.26 (qd, $J = 7.4, 1.8$ Hz, 2H), 1.52 – 1.43 (m, 2H), 0.93 (t, $J = 7.4$ Hz, 3H) ppm. $^{13}\text{C NMR}$ (101 MHz, CDCl_3) δ 162.7, 146.8, 139.1, 133.4, 126.9, 125.1, 110.4, 53.6, 30.8, 23.2, 14.0 ppm. **LRMS** (DEP/EI-Orbitrap): m/z (%): 177.1 (31), 148.1 (100), 133.1 (40), 120.1 (16), 105.1 (14), 91.1 (10). **HRMS** (EI-Orbitrap): m/z calcd for $\text{C}_{11}\text{H}_{15}\text{NO}^+$: 177.1154; found: 177.1149. **IR** (Diamond-ATR, neat) $\tilde{\nu}_{max}$ (cm^{-1}): 3009 (w), 2960 (m), 2929 (w), 2875 (w), 1601 (m), 1562 (w), 1492 (vs), 1463 (w), 1408 (w), 1368 (m), 1306 (m), 1288 (m), 1260 (m), 1126 (w), 1027 (m), 927 (w), 830 (w).

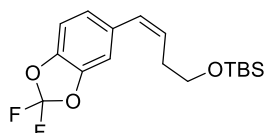
(Z)-1-Methyl-5-(pent-1-en-1-yl)-1H-indole (8c)



Using 5-bromo-1-methyl-1H-indole and (*E*)-4,4,5,5-tetramethyl-2-(pent-1-en-1-yl)-1,3,2-dioxaborolane (**SM10**) according to general procedure **H**, provided **8c** (*E/Z* = 12:88, 0.21 mmol, 43 mg, 84%) as a colorless oil. $R_f = 0.17$ (hexane/EtOAc 100:0, UV, KMnO_4 , PAA). $^1\text{H NMR}$ (400 MHz, CDCl_3) δ 7.58 (s, 1H), 7.30 (dt, $J = 8.4, 0.8$ Hz, 1H), 7.21 (dd, $J = 8.5, 1.6$ Hz, 1H), 7.06 (d, $J = 3.1$ Hz, 1H), 6.58 (dt, $J = 11.7, 1.9$ Hz, 1H), 6.50 (dd, $J = 3.1, 0.8$ Hz, 1H), 5.63 (dt, $J = 11.6, 7.1$ Hz, 1H), 3.80 (s, 3H), 2.42 (qd, $J = 7.3, 1.9$ Hz, 2H), 1.58 – 1.47

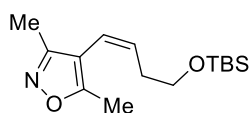
(m, 2H), 0.98 (t, $J = 7.4$ Hz, 3H) ppm. $^{13}\text{C NMR}$ (101 MHz, CDCl_3) δ 135.7, 131.0, 129.9, 129.4, 129.3, 128.5, 123.2, 121.0, 108.9, 101.2, 33.0, 30.9, 23.5, 14.1 ppm. **LRMS** (DEP/EI-Orbitrap): m/z (%): 199.1 (41), 170.1 (100), 168.1 (25), 155.1 (28), 128.1 (10). **HRMS** (EI-Orbitrap): m/z calcd for $\text{C}_{14}\text{H}_{17}\text{N}^+$: 199.1361; found: 199.1357. **IR** (Diamond-ATR, neat) $\tilde{\nu}_{\text{max}}$ (cm^{-1}): 3000 (m), 2960 (vs), 2927 (s), 2872 (m), 1616 (m), 1513 (s), 1491 (s), 1422 (m), 1377 (m), 1335 (m), 1245 (s), 1154 (m), 1096 (m), 1078 (m), 886 (m), 804 (s), 708 (s).

(Z)-tert-Butyl((4-(2,2-difluorobenzo[d][1,3]dioxol-5-yl)but-3-en-1-yl)oxy)dimethylsilane (8d)

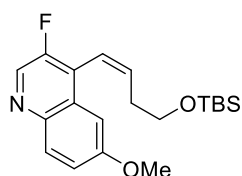


Using 5-bromo-2,2-difluorobenzo[d][1,3]dioxole and (*E*)-tert-butyl dimethyl((4-(4,4,5,5-tetramethyl-1,3,2-dioxaborolan-2-yl)but-3-en-1-yl)oxy)silane according to general procedure **H**, provided **8d** (0.23 mmol, 78 mg, 89%) as a colorless oil. $R_f = 0.44$ (hexane/EtOAc 98:2, UV, KMnO_4 , PAA). $^1\text{H NMR}$ (400 MHz, CDCl_3) δ 7.09 (s, 1H), 7.00 (s, 2H), 6.45 (dt, $J = 11.7, 1.8$ Hz, 1H), 5.71 (dt, $J = 11.6, 7.4$ Hz, 1H), 3.73 (t, $J = 6.4$ Hz, 2H), 2.54 – 2.47 (m, 2H), 0.90 (s, 9H), 0.06 (s, 6H) ppm. $^{13}\text{C NMR}$ (101 MHz, CDCl_3) δ 143.7, 142.3, 133.7 (t, $J = 50.0$ Hz), 131.6, 129.9, 129.2, 124.1, 109.8, 109.0, 62.6, 32.0, 25.9, 18.4, -5.3 ppm. **LRMS** (DEP/EI-Orbitrap): m/z (%): 285.1 (100), 173.1 (14), 146.1 (10), 115.1 (30), 89.0 (14), 73.0 (20). **HRMS** (ESI pos): calcd for $\text{C}_{16}\text{H}_{21}\text{F}_2\text{O}_3\text{Si}^+ [\text{M-Me}]^+$: 327.1228; found: 327.1216. **IR** (Diamond-ATR, neat) $\tilde{\nu}_{\text{max}}$ (cm^{-1}): 3017 (vw), 2954 (w), 2929 (w), 2896 (w), 2885 (w), 2857 (w), 1616 (vw), 1497 (m), 1472 (w), 1446 (w), 1388 (w), 1361 (w), 1237 (vs), 1154 (s), 1100 (s), 1034 (m), 1006 (w), 937 (m), 900 (w), 870 (w), 835 (s), 775 (s), 744 (w), 704 (w).

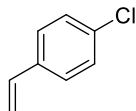
(Z)-4-(4-((tert-Butyldimethylsilyl)oxy)but-1-en-1-yl)-3,5-dimethylisoxazole (8e)



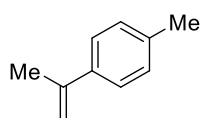
Using 4-bromo-3,5-dimethylisoxazole and (*E*)-tert-butyl dimethyl((4-(4,4,5,5-tetramethyl-1,3,2-dioxaborolan-2-yl)but-3-en-1-yl)oxy)silane according to general procedure **H**, provided **8e** (0.18 mmol, 51 mg, 71%) as a colorless oil. $R_f = 0.16$ (hexane/EtOAc 98:2, UV, KMnO_4 , PAA). $^1\text{H NMR}$ (400 MHz, CDCl_3) δ 5.98 (d, $J = 11.2$ Hz, 1H), 5.89 – 5.80 (m, 1H), 3.63 (t, $J = 6.5$ Hz, 2H), 2.27 (s, 3H), 2.21 – 2.13 (m, 2H), 2.15 (s, 3H), 0.87 (s, 9H), 0.03 (s, 6H) ppm. $^{13}\text{C NMR}$ (101 MHz, CDCl_3) δ 164.8, 159.5, 133.8, 117.6, 112.4, 62.5, 32.9, 26.1, 18.5, 12.0, 10.6, -5.2 ppm. **LRMS** (DEP/EI-Orbitrap): m/z (%): 224.1 (78), 208.1 (31), 183.1 (24), 153.1 (23), 136.1 (16), 109.1 (18), 89.0 (27), 75.0 (100). **HRMS** (EI-Orbitrap): m/z calcd for $\text{C}_{11}\text{H}_{18}\text{NO}_2\text{Si}^+ [\text{M-}t\text{-Bu}]^+$: 224.1107; found: 224.1106. **IR** (Diamond-ATR, neat) $\tilde{\nu}_{\text{max}}$ (cm^{-1}): 3010 (vw), 2954 (w), 2928 (w), 2857 (w), 1472 (w), 1447 (w), 1422 (w), 1393 (w), 1361 (w), 1256 (w), 1182 (w), 1105 (m), 906 (s), 837 (m), 776 (w), 729 (vs).

(Z)-4-(4-((*tert*-Butyldimethylsilyloxy)but-1-en-1-yl)-3-fluoro-6-methoxyquinoline (8f)

Using 3-fluoro-4-iodo-6-methoxyquinoline and (*E*)-*tert*-butyldimethyl((4-(4,4,5,5-tetramethyl-1,3,2-dioxaborolan-2-yl)but-3-en-1-yl)oxy)silane according to general procedure **H**, provided **8f** (0.18 mmol, 66 mg, 72%) as a colorless oil. $R_f = 0.38$ (hexane/EtOAc 90:10, UV, KMnO_4 , PAA). $^1\text{H NMR}$ (400 MHz, CDCl_3) δ 8.63 (d, $J = 1.2$ Hz, 1H), 7.99 (d, $J = 9.2$ Hz, 1H), 7.31 (dd, $J = 9.2, 2.8$ Hz, 1H), 7.09 (d, $J = 2.8$ Hz, 1H), 6.52 (dq, $J = 11.5, 1.5$ Hz, 1H), 6.32 – 6.23 (m, 1H), 3.92 (s, 3H), 3.66 (t, $J = 6.5$ Hz, 2H), 2.25 – 2.18 (m, 2H), 0.84 (s, 9H), -0.01 (s, 6H) ppm. $^{13}\text{C NMR}$ (101 MHz, CDCl_3) δ 158.7, 153.3 (d, $J = 253.4$ Hz), 141.5 (d, $J = 2.3$ Hz), 138.6 (d, $J = 25.4$ Hz), 136.2, 131.4, 129.1 (d, $J = 3.1$ Hz), 126.0 (d, $J = 13.8$ Hz), 121.0, 119.1, 102.9, 62.2, 55.7 (d, $J = 11.6$ Hz), 33.6, 26.0 (d, $J = 5.3$ Hz), 18.4, -5.2 ppm. **LRMS** (DEP/EI-Orbitrap): m/z (%): 304.1 (69), 289.1 (18), 273.1 (13), 261.1 (21), 210.1 (100), 195.1 (25), 184.1 (18), 167.1 (44), 152.1 (14), 73.0 (45). **HRMS** (EI-Orbitrap): m/z calcd for $\text{C}_{20}\text{H}_{28}\text{FNO}_2\text{Si}^+$: 361.1873; found: 361.1865. **IR** (Diamond-ATR, neat) $\tilde{\nu}_{\text{max}}$ (cm^{-1}): 3007 (vw), 2953 (m), 2928 (m), 2907 (w), 2903 (w), 2897 (w), 2890 (w), 2885 (w), 2881 (w), 2876 (w), 2873 (w), 2857 (m), 1621 (m), 1505 (s), 1467 (m), 1427 (m), 1357 (m), 1303 (w), 1264 (m), 1258 (m), 1227 (vs), 1197 (m), 1175 (w), 1142 (m), 1096 (s), 1071 (w), 1031 (m), 1005 (w), 939 (w), 926 (w), 907 (m), 831 (vs), 811 (m), 800 (m), 776 (s), 730 (s).

1-Chloro-4-vinylbenzene (10a)

Using vinyl bromide (1 M in THF) and 2-(4-chlorophenyl)-4,4,5,5-tetramethyl-1,3,2-dioxaborolane according to general procedure **I** (1.50 mmol scale), provided **10a** (0.88 mmol, 122 mg, 69%) as a light-yellow oil. General procedure **I** was slightly changed for product **10a** to maximize the conversion of the vinyl bromide. Therefore, the freshly prepared *n*-Bu₃Ce•5LiCl solution was concentrated *in vacuo* to about 0.50 M at -30 °C prior to the addition of the vinyl bromide. $R_f = 0.70$ (hexane/EtOAc 100:0, UV, KMnO_4 , PAA). $^1\text{H NMR}$ (400 MHz, CDCl_3) δ 7.32 – 7.22 (m, 4H), 6.62 (dd, $J = 17.6, 10.9$ Hz, 1H), 5.68 (d, $J = 17.5$ Hz, 1H), 5.22 (d, $J = 10.9$ Hz, 1H) ppm. **LRMS** (DEP/EI-Orbitrap): m/z (%): 138.1 (100), 103.1 (76), 77.1 (31). Analytical data in accordance to literature.²²⁷

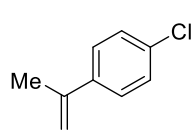
1-Methyl-4-(prop-1-en-2-yl)benzene (10b)

Using 2-bromoprop-1-ene and 4,4,5,5-tetramethyl-2-(*p*-tolyl)-1,3,2-dioxaborolane according to general procedure **I** (0.40 mmol scale), provided **10b** (0.22 mmol, 29 mg, 64%) as a colorless oil. $R_f = 0.73$ (hexane/EtOAc 100:0, UV, KMnO_4 , PAA). $^1\text{H NMR}$ (400 MHz, CDCl_3) δ 7.39 (d, $J = 8.2$ Hz, 2H), 7.16 (d, $J = 8.0$ Hz, 2H), 5.36 (s, 1H),

²²⁷ S. Rej, S. Pramanik, H. Tsurugi, K. Mashima, *Chem. Comm.* **2017**, 53, 13157–13160.

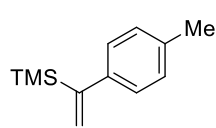
5.06 – 5.04 (m, 1H), 2.36 (s, 3H), 2.16 (s, 3H) ppm. **LRMS** (DEP/EI-Orbitrap): m/z (%): 132.1 (95), 117.1 (100), 91.1 (55), 65.1 (24). Analytical data in accordance to literature.²²⁸

1-Chloro-4-(prop-1-en-2-yl)benzene (**10b'**)



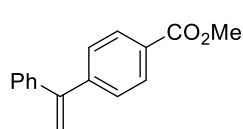
Using 2-bromoprop-1-ene and 2-(4-chlorophenyl)-4,4,5,5-tetramethyl-1,3,2-dioxaborolane according to general procedure **I** (0.40 mmol scale), provided **10b'** (0.23 mmol, 35 mg, 68%) as a colorless oil. R_f = 0.73 (hexane/EtOAc 100:0, UV, KMnO₄, PAA). **¹H NMR** (400 MHz, CDCl₃) δ 7.42 – 7.37 (m, 2H), 7.32 – 7.27 (m, 2H), 5.35 (s, 1H), 5.12 – 5.09 (m, 1H), 2.13 (s, 3H) ppm. **LRMS** (DEP/EI-Orbitrap): m/z (%): 152.1 (100), 137.1 (41), 117.1 (80), 102.1 (30), 75.1 (20). Analytical data in accordance to literature.²²⁸

Trimethyl(1-(*p*-tolyl)vinyl)silane (**10c**)



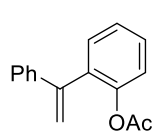
Using (1-bromovinyl)trimethylsilane and 4,4,5,5-tetramethyl-2-(*p*-tolyl)-1,3,2-dioxaborolane according to general procedure **I**, provided **10c** (0.11 mmol, 21 mg, 44%) as a colorless oil. R_f = 0.60 (hexane/EtOAc 100:0, UV, KMnO₄, PAA). **¹H NMR** (400 MHz, CDCl₃) δ 7.16 – 7.07 (m, 4H), 5.83 (d, J = 3.0 Hz, 1H), 5.59 (d, J = 3.0 Hz, 1H), 2.36 (s, 3H), 0.19 (s, 9H) ppm. **LRMS** (DEP/EI-Orbitrap): m/z (%): 190.1 (70), 175.0 (100), 158.8 (35), 149.0 (81), 115.1 (73), 90.9 (32), 73.0 (100). Analytical data in accordance to literature.²²⁹

Methyl 4-(1-phenylvinyl)benzoate (**10d**)



Using (1-bromovinyl)benzene and methyl 4-(4,4,5,5-tetramethyl-1,3,2-dioxaborolan-2-yl)benzoate according to general procedure **I**, provided **10d** (0.15 mmol, 36 mg, 60%) as a colorless solid. R_f = 0.20 (hexane/EtOAc 98:2, UV, KMnO₄, PAA). **¹H NMR** (400 MHz, CDCl₃) δ 8.04 – 7.97 (m, 2H), 7.44 – 7.39 (m, 2H), 7.37 – 7.28 (m, 5H), 5.57 – 5.52 (m, 2H), 3.93 (s, 3H) ppm. **¹³C NMR** (101 MHz, CDCl₃) δ 167.1, 149.4, 146.2, 140.9, 129.7, 129.5, 128.5, 128.4, 128.3, 128.1, 116.0, 52.3 ppm. **LRMS** (DEP/EI-Orbitrap): m/z (%): 238.1 (71), 207.1 (58), 178.1 (100), 152.1 (17), 89.0 (14), 76.0 (10). **HRMS** (EI-Orbitrap): m/z calcd for C₁₆H₁₄O₂⁺: 238.0994; found: 238.0989. **IR** (Diamond-ATR, neat) $\tilde{\nu}_{max}$ (cm⁻¹): 3085 (vw), 3062 (vw), 3024 (vw), 2998 (vw), 2949 (w), 1720 (vs), 1608 (w), 1493 (w), 1435 (m), 1404 (w), 1312 (w), 1280 (vs), 1181 (w), 1150 (w), 1107 (m), 1017 (w), 968 (vw), 905 (w), 864 (w), 781 (w), 776 (m), 719 (w), 701 (m). **Mp** (°C) = 76–80.

2-(1-Phenylvinyl)phenyl acetate (**10e**)



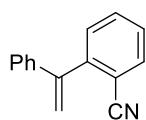
Using (1-bromovinyl)benzene and 2-(4,4,5,5-tetramethyl-1,3,2-dioxaborolan-2-yl)phenyl acetate according to general procedure **I**, provided **10e** (0.11 mmol, 27 mg, 44%) as a colorless oil. R_f = 0.16 (hexane/EtOAc 98:2, UV, KMnO₄, PAA). **¹H NMR** (400 MHz,

²²⁸ A. Cabre, G. Sciortino, G. Ujaque, X. Verdaguier, A. Lledos, A. Riera, *Org. Lett.* **2018**, *20*, 5747–5751.

²²⁹ H. A. Laub, H. Mayr, *Chem. Eur. J.* **2014**, *20*, 1103–1110.

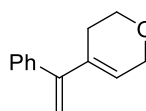
CDCl₃) δ 7.42 – 7.35 (m, 2H), 7.33 – 7.24 (m, 6H), 7.09 (d, J = 8.0 Hz, 1H), 5.67 (d, J = 1.2 Hz, 1H), 5.36 (d, J = 1.2 Hz, 1H), 1.78 (s, 3H) ppm. ¹³C NMR (101 MHz, CDCl₃) δ 169.1, 148.2, 146.4, 140.9, 134.7, 131.4, 129.0, 128.4, 127.9, 127.0, 126.2, 123.1, 116.9, 20.4 ppm. LRMS (DEP/EI-Orbitrap): m/z (%): 238.1 (1), 223.1 (6), 195.1 (100), 181.1 (39), 165.1 (24), 152.1 (11). HRMS (EI-Orbitrap): m/z calcd for C₁₆H₁₄O₂⁺: 238.0994; found: 238.0988. IR (Diamond-ATR, neat) $\tilde{\nu}_{max}$ (cm⁻¹): 3085 (vw), 3056 (vw), 3029 (vw), 2930 (vw), 1814 (vw), 1766 (s), 1749 (w), 1614 (vw), 1602 (w), 1575 (vw), 1494 (w), 1483 (w), 1447 (w), 1367 (m), 1327 (vw), 1191 (vs), 1150 (w), 1101 (w), 1081 (w), 1065 (w), 1027 (w), 1009 (w), 945 (vw), 913 (m), 840 (vw), 810 (w), 781 (w), 764 (m), 705 (w).

2-(1-Phenylvinyl)benzonitrile (10f)

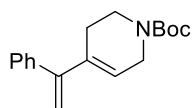


Using (1-bromovinyl)benzene and 2-(4,4,5,5-tetramethyl-1,3,2-dioxaborolan-2-yl)benzonitrile according to general procedure I, provided **10f** (0.18 mmol, 36 mg, 69%) as a colorless oil. R_f = 0.19 (hexane/EtOAc 98:2, UV, KMnO₄, PAA). ¹H NMR (400 MHz, CDCl₃) δ 7.71 (dd, J = 7.8, 1.4 Hz, 1H), 7.57 (td, J = 7.7, 1.4 Hz, 1H), 7.43 (td, J = 7.6, 1.2 Hz, 1H), 7.39 – 7.35 (m, 1H), 7.35 – 7.30 (m, 3H), 7.29 – 7.23 (m, 2H), 5.88 (s, 1H), 5.49 (s, 1H) ppm. ¹³C NMR (101 MHz, CDCl₃) δ 146.6, 145.9, 139.9, 133.5, 132.6, 130.5, 128.6, 128.4, 128.1, 127.5, 118.3, 118.2, 112.5 ppm. LRMS (DEP/EI-Orbitrap): m/z (%): 205.1 (100), 190.1 (24), 178.1 (10), 102.0 (10), 88.0 (11). HRMS (EI-Orbitrap): m/z calcd for C₁₅H₁₁N⁺: 205.0891; found: 205.0879. IR (Diamond-ATR, neat) $\tilde{\nu}_{max}$ (cm⁻¹): 3086 (w), 3067 (w), 3027 (w), 2225 (m), 1611 (w), 1595 (w), 1575 (w), 1565 (w), 1495 (m), 1484 (m), 1442 (m), 1326 (w), 1310 (w), 1264 (w), 1158 (w), 1028 (w), 912 (m), 770 (vs), 699 (s).

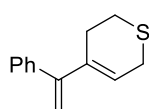
4-(1-Phenylvinyl)-3,6-dihydro-2H-pyran (10g)



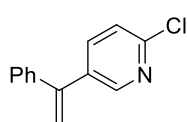
Using (1-bromovinyl)benzene and 2-(3,6-dihydro-2H-pyran-4-yl)-4,4,5,5-tetramethyl-1,3,2-dioxaborolane according to general procedure I, provided **10g** (0.18 mmol, 33 mg, 70%) as a colorless oil. R_f = 0.32 (hexane/EtOAc 98:2, UV, KMnO₄, PAA). ¹H NMR (400 MHz, CDCl₃) δ 7.38 – 7.27 (m, 5H), 5.61 – 5.56 (m, 1H), 5.25 (s, 1H), 5.07 (s, 1H), 4.22 – 4.20 (m, 2H), 3.89 (t, J = 5.5 Hz, 2H), 2.43 – 2.33 (m, 2H) ppm. ¹³C NMR (101 MHz, CDCl₃) δ 149.9, 141.2, 134.7, 128.9, 128.1, 127.4, 126.7, 112.4, 65.9, 64.5, 26.5 ppm. LRMS (DEP/EI-Orbitrap): m/z (%): 186.1 (24), 171.1 (11), 156.1 (28), 141.1 (75), 128.1 (100), 115.1 (60), 103.1 (25), 91.1 (20), 83.0 (60). HRMS (EI-Orbitrap): m/z calcd for C₁₃H₁₄O⁺: 186.1045; found: 186.1037. IR (Diamond-ATR, neat) $\tilde{\nu}_{max}$ (cm⁻¹): 2977 (s), 2936 (m), 2886 (m), 1712 (m), 1698 (m), 1606 (m), 1589 (m), 1514 (m), 1474 (vs), 1454 (vs), 1443 (vs), 1381 (s), 1372 (s), 1328 (vs), 1273 (s), 1217 (s), 1144 (vs), 1009 (s), 981 (s), 951 (s), 927 (m), 851 (s), 755 (s), 672 (s).

***tert*-Butyl 4-(1-phenylvinyl)-3,6-dihydropyridine-1(2*H*)-carboxylate (10h)**

Using (1-bromovinyl)benzene and *tert*-butyl 4-(4,4,5,5-tetramethyl-1,3,2-dioxaborolan-2-yl)-3,6-dihydropyridine-1(2*H*)-carboxylate according to general procedure **I**, provided **10h** (0.18 mmol, 52 mg, 72%) as a colorless oil. $R_f = 0.10$ (hexane/EtOAc 99:1, UV, KMnO_4 , PAA). $^1\text{H NMR}$ (400 MHz, CDCl_3) δ 7.33 – 7.27 (m, 2H), 7.25 – 7.20 (m, 2H), 5.51 (s, 1H), 5.21 (s, 1H), 5.05 (s, 1H), 3.96 – 3.91 (m, 2H), 3.56 (t, $J = 5.7$ Hz, 2H), 2.37 – 2.31 (m, 2H), 1.45 (s, 9H) ppm. $^{13}\text{C NMR}$ (101 MHz, CDCl_3) δ 155.0, 150.1, 141.2, 135.7, 128.8, 128.1, 127.4, 124.9, 112.6, 79.8, 43.7, 40.5, 28.6, 26.5 ppm. Signal splitting was observed, which was presumably caused by rotational barriers. **LRMS** (DEP/EI-Orbitrap): m/z (%): 229.1 (51), 212.1 (11), 185.1 (13), 168.5 (10), 155.0 (14), 141.0 (13), 126.1 (29), 115.0 (10), 82.0 (42). **HRMS** (EI-Orbitrap): m/z calcd for $\text{C}_{18}\text{H}_{23}\text{NO}_2^+$: 285.1729; found: 285.1723. **IR** (Diamond-ATR, neat) $\tilde{\nu}_{\text{max}}$ (cm^{-1}): 2973 (w), 2931 (w), 2859 (vw), 1695 (vs), 1601 (w), 1476 (w), 1419 (m), 1392 (m), 1365 (m), 1337 (w), 1281 (w), 1240 (m), 1169 (s), 1113 (m), 1068 (w), 982 (w), 956 (w), 893 (w), 866 (w), 833 (w), 773 (w), 702 (m).

4-(1-Phenylvinyl)-3,6-dihydro-2*H*-thiopyran (10i)

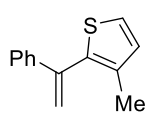
Using (1-bromovinyl)benzene and 2-(3,6-dihydro-2*H*-thiopyran-4-yl)-4,4,5,5-tetramethyl-1,3,2-dioxaborolane according to general procedure **I**, provided **10i** (0.17 mmol, 35 mg, 68%) as a colorless oil. $R_f = 0.20$ (hexane/EtOAc 99:1, UV, KMnO_4 , PAA). $^1\text{H NMR}$ (400 MHz, CDCl_3) δ 7.38 – 7.24 (m, 5H), 5.84 (tt, $J = 4.1, 1.7$ Hz, 1H), 5.26 (s, 1H), 5.10 (s, 1H), 3.26 (dt, $J = 4.4, 2.2$ Hz, 2H), 2.83 (t, $J = 5.8$ Hz, 2H), 2.56 – 2.48 (m, 2H) ppm. $^{13}\text{C NMR}$ (101 MHz, CDCl_3) δ 151.8, 141.2, 138.5, 128.6, 128.2, 127.4, 124.9, 112.3, 27.6, 26.3, 25.4 ppm. **LRMS** (DEP/EI-Orbitrap): m/z (%): 202.0 (38), 187.0 (36), 173.1 (30), 155.0 (100), 141.0 (70), 128.1 (59), 115.0 (48), 99.0 (55), 77.0 (70). **HRMS** (EI-Orbitrap): m/z calcd for $\text{C}_{13}\text{H}_{14}\text{S}^+$: 202.0816; found: 202.0824. **IR** (Diamond-ATR, neat) $\tilde{\nu}_{\text{max}}$ (cm^{-1}): 3087 (w), 3055 (w), 3024 (w), 2953 (w), 2923 (w), 1675 (w), 1599 (w), 1492 (m), 1444 (m), 1422 (w), 1287 (w), 1259 (w), 1065 (w), 1027 (m), 905 (w), 884 (w), 778 (m), 762 (m), 700 (vs).

2-Chloro-5-(1-phenylvinyl)pyridine (10j)

Using (1-bromovinyl)benzene and 2-chloro-5-(4,4,5,5-tetramethyl-1,3,2-dioxaborolan-2-yl)pyridine according to general procedure **I**, provided **10j** (0.20 mmol, 44 mg, 80%) as a colorless oil. $R_f = 0.33$ (hexane/EtOAc 97:3, UV, KMnO_4 , PAA). $^1\text{H NMR}$ (400 MHz, CDCl_3) δ 8.40 (d, $J = 2.4$ Hz, 1H), 7.57 (dd, $J = 8.3, 2.5$ Hz, 1H), 7.40 – 7.32 (m, 3H), 7.32 – 7.27 (m, 3H), 5.58 (s, 1H), 5.50 (s, 1H) ppm. $^{13}\text{C NMR}$ (101 MHz, CDCl_3) δ 150.8, 149.2, 145.9, 140.0, 138.5, 136.2, 128.7, 128.5, 128.1, 123.8, 116.4 ppm. **LRMS** (DEP/EI-Orbitrap): m/z (%): 214.0 (100), 200.0 (50), 180.1 (94), 178.1 (75), 151.1 (34), 90.0 (10), 76.0 (12). **HRMS** (EI-Orbitrap): m/z calcd for $\text{C}_{13}\text{H}_{10}\text{ClN}^+$: 215.0502; found: 215.0496. **IR** (Diamond-ATR, neat) $\tilde{\nu}_{\text{max}}$ (cm^{-1}): 3087 (w),

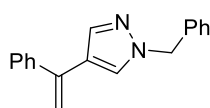
3061 (w), 3027 (w), 1613 (w), 1581 (m), 1552 (w), 1494 (m), 1459 (vs), 1444 (m), 1358 (m), 1320 (w), 1308 (w), 1287 (w), 1157 (m), 1139 (w), 1104 (s), 1018 (m), 906 (m), 837 (m), 778 (s), 758 (m), 748 (w), 705 (m).

3-Methyl-2-(1-phenylvinyl)thiophene (10k)



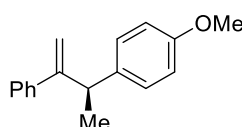
Using (1-bromovinyl)benzene and 4,4,5,5-tetramethyl-2-(3-methylthiophen-2-yl)-1,3,2-dioxaborolane according to general procedure I, provided **10k** (0.19 mmol, 38 mg, 75%) as a colorless oil. $R_f = 0.49$ (hexane/EtOAc 100:0, UV, KMnO_4 , PAA). $^1\text{H NMR}$ (400 MHz, CDCl_3) δ 7.40 – 7.29 (m, 5H), 7.18 (d, $J = 5.1$ Hz, 1H), 6.88 (d, $J = 5.1$ Hz, 1H), 5.65 (d, $J = 1.3$ Hz, 1H), 5.41 (d, $J = 1.3$ Hz, 1H), 1.99 (s, 3H) ppm. $^{13}\text{C NMR}$ (101 MHz, CDCl_3) δ 142.7, 141.1, 137.5, 135.2, 130.7, 128.4, 128.0, 127.4, 123.5, 117.2, 15.2 ppm. LRMS (DEP/EI-Orbitrap): m/z (%): 200.0 (18), 185.0 (100), 152.1 (15), 141.1 (8), 115.1 (6). HRMS (EI-Orbitrap): m/z calcd for $\text{C}_{13}\text{H}_{12}\text{S}^+$: 200.0660; found: 200.0652. IR (Diamond-ATR, neat) $\tilde{\nu}_{\text{max}}$ (cm^{-1}): 3095 (vw), 3078 (w), 3055 (w), 3020 (w), 2942 (w), 2921 (w), 2859 (vw), 1758 (vw), 1606 (w), 1573 (w), 1491 (m), 1445 (m), 1381 (w), 1366 (w), 1316 (w), 1302 (w), 1227 (w), 1181 (vw), 1156 (vw), 1134 (vw), 1073 (w), 1048 (w), 1027 (w), 1006 (w), 934 (w), 899 (m), 839 (w), 796 (w), 775 (s), 699 (vs).

1-Benzyl-4-(1-phenylvinyl)-1H-pyrazole (10l)



Using (1-bromovinyl)benzene and 1-benzyl-4-(4,4,5,5-tetramethyl-1,3,2-dioxaborolan-2-yl)-1H-pyrazole according to general procedure I, provided **10l** (0.19 mmol, 49 mg, 74%) as a light-yellow oil. $R_f = 0.28$ (hexane/EtOAc 90:10, UV, KMnO_4 , PAA). $^1\text{H NMR}$ (400 MHz, CDCl_3) δ 7.58 (s, 1H), 7.41 – 7.35 (m, 2H), 7.34 – 7.24 (m, 7H), 7.23 – 7.15 (m, 2H), 5.37 (d, $J = 1.3$ Hz, 1H), 5.24 (s, 2H), 5.15 (d, $J = 1.3$ Hz, 1H) ppm. $^{13}\text{C NMR}$ (101 MHz, CDCl_3) δ 141.6, 140.9, 138.6, 136.5, 129.0, 128.4, 128.3, 128.2, 128.0, 127.8, 127.7, 123.6, 111.5, 56.2 ppm. LRMS (DEP/EI-Orbitrap): m/z (%): 260.1 (86), 259.1 (50), 181.1 (6), 169.1 (20), 115.1 (13), 91.1 (100), 65.0 (11). HRMS (EI-Orbitrap): m/z calcd for $\text{C}_{18}\text{H}_{16}\text{N}_2^+$: 260.1313; found: 260.1310. IR (Diamond-ATR, neat) $\tilde{\nu}_{\text{max}}$ (cm^{-1}): 3087 (w), 3061 (w), 3029 (w), 2931 (vw), 1608 (w), 1572 (w), 1550 (w), 1493 (m), 1455 (m), 1442 (m), 1430 (w), 1389 (w), 1357 (w), 1282 (w), 1253 (m), 1159 (w), 1137 (w), 1073 (w), 1028 (w), 997 (m), 888 (m), 859 (w), 810 (w), 776 (s), 720 (s), 696 (vs).

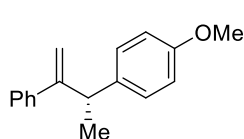
(R)-1-Methoxy-4-(3-phenylbut-3-en-2-yl)benzene (11a)



Using (1-bromovinyl)benzene and (*R*)-2-(1-(4-methoxyphenyl)ethyl)-4,4,5,5-tetramethyl-1,3,2-dioxaborolane (**SM11**) according to general procedure I (0.40 mmol scale), provided **11a** (0.32 mmol, 75 mg, 93%) as a light-yellow oil. $R_f = 0.16$ (hexane/EtOAc 99:1, UV, KMnO_4 , PAA). $^1\text{H NMR}$ (400 MHz, CDCl_3) δ 7.37 – 7.17 (m, 7H), 6.88 – 6.81 (m, 2H), 5.43 (s, 1H), 5.19 – 5.17 (m, 1H), 4.03 (q, $J = 7.1$ Hz, 1H), 3.80 (s, 3H), 1.49 (d, $J = 7.1$ Hz, 3H) ppm. $^{13}\text{C NMR}$ (101 MHz, CDCl_3) δ 157.9, 153.0, 142.4, 137.2, 128.7, 128.2, 127.2, 126.8, 113.8, 112.9, 55.3, 43.4, 21.9 ppm. LRMS (DEP/EI-Orbitrap): m/z (%): 238.1 (27), 223.1 (44),

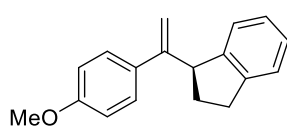
207.1 (10), 165.1 (8), 135.1 (100), 115.1 (11), 105.1 (15), 91.1 (9). **HRMS** (EI-Orbitrap): m/z calcd for $C_{17}H_{18}O^+$: 238.1358; found: 238.1351. $[\alpha]_D^{22}$: -72.08 ($\beta = 0.99$, CH_2Cl_2). **Chiral HPLC**: 98% *ee* (*er* 98.9:1.1), OB-H column, *i*-PrOH:heptane = 0.5:99.5, 1.0 mL/min, 30 °C. **IR** (Diamond-ATR, neat) $\tilde{\nu}_{max}$ (cm^{-1}): 3090 (vw), 3056 (vw), 3029 (w), 3002 (vw), 2964 (w), 2930 (w), 2903 (w), 2877 (vw), 2834 (w), 1623 (w), 1609 (w), 1583 (w), 1573 (w), 1510 (vs), 1493 (w), 1461 (w), 1442 (w), 1368 (w), 1301 (w), 1245 (s), 1177 (m), 1109 (w), 1070 (w), 1036 (m), 1000 (vw), 902 (w), 830 (m), 811 (w), 779 (m), 755 (w), 700 (m).

(S)-1-Methoxy-4-(3-phenylbut-3-en-2-yl)benzene (ent-11a)



Using (1-bromovinyl)benzene and (*S*)-2-(1-(4-methoxyphenyl)ethyl)-4,4,5,5-tetramethyl-1,3,2-dioxaborolane (**SM12**) according to general procedure **I** (0.40 mmol scale), provided **ent-11a** (0.33 mmol, 78 mg, 96%) as a light-yellow oil. $R_f = 0.16$ (hexane/EtOAc 99:1, UV, $KMnO_4$, PAA). 1H NMR (400 MHz, $CDCl_3$) δ 7.37 – 7.17 (m, 7H), 6.88 – 6.81 (m, 2H), 5.43 (s, 1H), 5.19 – 5.17 (m, 1H), 4.03 (q, $J = 7.1$ Hz, 1H), 3.80 (s, 3H), 1.49 (d, $J = 7.1$ Hz, 3H) ppm. ^{13}C NMR (101 MHz, $CDCl_3$) δ 157.9, 153.0, 142.4, 137.2, 128.7, 128.2, 127.2, 126.8, 113.8, 112.9, 55.3, 43.4, 21.9 ppm. **LRMS** (DEP/EI-Orbitrap): m/z (%): 238.1 (27), 223.1 (44), 207.1 (10), 165.1 (8), 135.1 (100), 115.1 (11), 105.1 (15), 91.1 (9). **HRMS** (EI-Orbitrap): m/z calcd for $C_{17}H_{18}O^+$: 238.1358; found: 238.1351. $[\alpha]_D^{22}$: +73.74 ($\beta = 0.87$, CH_2Cl_2). **Chiral HPLC**: 99% *ee* (*er* 99.5:0.5), OB-H column, *i*-PrOH:heptane = 0.5:99.5, 1.0 mL/min, 30 °C. **IR** (Diamond-ATR, neat) $\tilde{\nu}_{max}$ (cm^{-1}): 3090 (vw), 3056 (vw), 3029 (w), 3002 (vw), 2964 (w), 2930 (w), 2903 (w), 2877 (vw), 2834 (w), 1623 (w), 1609 (w), 1583 (w), 1573 (w), 1510 (vs), 1493 (w), 1461 (w), 1442 (w), 1368 (w), 1301 (w), 1245 (s), 1177 (m), 1109 (w), 1070 (w), 1036 (m), 1000 (vw), 902 (w), 830 (m), 811 (w), 779 (m), 755 (w), 700 (m).

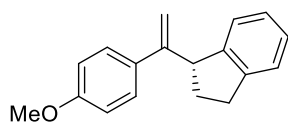
(S)-1-(1-(4-Methoxyphenyl)vinyl)-2,3-dihydro-1H-indene (11b)



Using 1-(1-bromovinyl)-4-methoxybenzene (**SM20**) and (*R*)-2-(2,3-dihydro-1H-inden-1-yl)-4,4,5,5-tetramethyl-1,3,2-dioxaborolane (**SM13**) according to general procedure **I** (0.40 mmol scale), provided **11b** (0.33 mmol, 83 mg, 98%) as a colorless oil. $R_f = 0.15$ (hexane/EtOAc 100:0, UV, $KMnO_4$, PAA). 1H NMR (400 MHz, $CDCl_3$) δ 7.36 – 7.31 (m, 2H), 7.29 – 7.24 (m, 1H), 7.22 – 7.14 (m, 3H), 6.89 – 6.81 (m, 2H), 5.29 (d, $J = 1.3$ Hz, 1H), 4.85 – 4.82 (m, 1H), 4.31 (t, $J = 7.5$ Hz, 1H), 3.82 (s, 3H), 3.02 – 2.82 (m, 2H), 2.47 – 2.31 (m, 1H), 2.04 – 1.90 (m, 1H) ppm. ^{13}C NMR (101 MHz, $CDCl_3$) δ 159.1, 150.7, 145.8, 144.6, 134.3, 127.9, 126.7, 126.3, 125.2, 124.6, 113.7, 112.1, 55.4, 50.7, 33.1, 31.5 ppm. Signal splitting was observed, which was presumably caused by rotational barriers. **LRMS** (DEP/EI-Orbitrap): m/z (%): 250.1 (16), 235.1 (26), 225.0 (100), 209.0 (45), 191.0 (19), 151.0 (11), 133.1 (94), 115.1 (56), 91.1 (12). **HRMS** (EI-Orbitrap): m/z calcd for $C_{18}H_{18}O^+$: 250.1358; found: 250.1351. $[\alpha]_D^{20}$: +89.18 ($\beta = 0.92$, CH_2Cl_2). **Chiral HPLC**: 98% *ee* (*er* 98.7:1.3), OD-H column, EtOAc:heptane = 0.5:99.5,

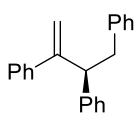
1.0 mL/min, 30 °C. **IR** (Diamond-ATR, neat) $\tilde{\nu}_{max}$ (cm⁻¹): 3068 (w), 3033 (w), 3005 (w), 2955 (w), 2931 (w), 2838 (w), 1606 (m), 1510 (vs), 1476 (w), 1458 (m), 1441 (w), 1295 (m), 1245 (s), 1179 (m), 1034 (m), 896 (w), 835 (m), 750 (m).

(R)-1-(1-(4-Methoxyphenyl)vinyl)-2,3-dihydro-1H-indene (ent-11b)

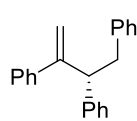


Using 1-(1-bromovinyl)-4-methoxybenzene (**SM20**) and (*S*)-2-(2,3-dihydro-1*H*-inden-1-yl)-4,4,5,5-tetramethyl-1,3,2-dioxaborolane (**SM14**) according to general procedure **I** (0.40 mmol scale), provided **ent-11b** (0.32 mmol, 81 mg, 95%) as a colorless oil. R_f = 0.15 (hexane/EtOAc 100:0, UV, KMnO₄, PAA). **¹H NMR** (400 MHz, CDCl₃) δ 7.36 – 7.31 (m, 2H), 7.29 – 7.24 (m, 1H), 7.22 – 7.14 (m, 3H), 6.89 – 6.81 (m, 2H), 5.29 (d, J = 1.3 Hz, 1H), 4.85 – 4.82 (m, 1H), 4.31 (t, J = 7.5 Hz, 1H), 3.82 (s, 3H), 3.02 – 2.82 (m, 2H), 2.47 – 2.31 (m, 1H), 2.04 – 1.90 (m, 1H) ppm. **¹³C NMR** (101 MHz, CDCl₃) δ 159.1, 150.7, 145.8, 144.6, 134.3, 127.9, 126.7, 126.3, 125.2, 124.6, 113.7, 112.1, 55.4, 50.7, 33.1, 31.5 ppm. Signal splitting was observed, which was presumably caused by rotational barriers. **LRMS** (DEP/EI-Orbitrap): m/z (%): 250.1 (16), 235.1 (26), 225.0 (100), 209.0 (45), 191.0 (19), 151.0 (11), 133.1 (94), 115.1 (56), 91.1 (12). **HRMS** (EI-Orbitrap): m/z calcd for C₁₈H₁₈O⁺: 250.1358; found: 250.1351. $[\alpha]_D^{20}$: -88.34 (β = 1.18, CH₂Cl₂). **Chiral HPLC**: 96% *ee* (*er* 98.0:2.0), OD-H column, EtOAc:heptane = 0.5:99.5, 1.0 mL/min, 30 °C. **IR** (Diamond-ATR, neat) $\tilde{\nu}_{max}$ (cm⁻¹): 3068 (w), 3033 (w), 3005 (w), 2955 (w), 2931 (w), 2838 (w), 1606 (m), 1510 (vs), 1476 (w), 1458 (m), 1441 (w), 1295 (m), 1245 (s), 1179 (m), 1034 (m), 896 (w), 835 (m), 750 (m).

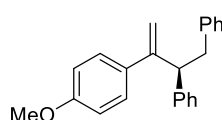
(S)-But-3-ene-1,2,3-triyltribenzene (11c)



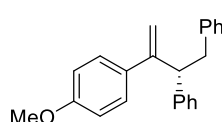
Using (1-bromovinyl)benzene and (*S*)-2-(1,2-diphenylethyl)-4,4,5,5-tetramethyl-1,3,2-dioxaborolane (**SM15**) according to general procedure **I**, provided **11c** (0.19 mmol, 53 mg, 73%) as a colorless oil. R_f = 0.20 (hexane/EtOAc 100:0, UV, KMnO₄, PAA). **¹H NMR** (400 MHz, CDCl₃) δ 7.35 – 7.15 (m, 13H), 7.12 – 7.03 (m, 2H), 5.53 (s, 1H), 5.38 (s, 1H), 4.23 – 4.14 (m, 1H), 3.35 (dd, J = 13.7, 6.4 Hz, 1H), 3.14 (dd, J = 13.7, 8.9 Hz, 1H) ppm. **¹³C NMR** (101 MHz, CDCl₃) δ 151.2, 142.6, 142.5, 140.5, 129.2, 128.4, 128.3, 128.2, 128.2, 127.3, 126.9, 126.4, 126.0, 113.9, 52.2, 41.9 ppm. **LRMS** (DEP/EI-Orbitrap): m/z (%): 284.2 (14), 206.1 (11), 193.1 (100), 189.1 (8), 178.1 (52), 165.1 (13), 115.1 (71), 91.1 (16). **HRMS** (EI-Orbitrap): m/z calcd for C₂₂H₂₀⁺: 284.1565; found: 284.1558. $[\alpha]_D^{20}$: +208.07 (β = 1.19, CH₂Cl₂). **Chiral HPLC**: 99% *ee* (*er* 99.7:0.3), OD-H column, EtOAc:heptane = 0:100, 1.0 mL/min, 30 °C. **IR** (Diamond-ATR, neat) $\tilde{\nu}_{max}$ (cm⁻¹): 3083 (w), 3059 (w), 3025 (w), 3003 (w), 2921 (w), 2855 (w), 1944 (vw), 1879 (vw), 1805 (w), 1625 (w), 1599 (w), 1573 (w), 1493 (m), 1452 (m), 1443 (w), 1296 (w), 1262 (w), 1179 (w), 1155 (w), 1071 (w), 1029 (w), 965 (w), 901 (m), 777 (m), 745 (m), 696 (vs).

(R)-But-3-ene-1,2,3-triyltribenzene (*ent*-11c)

Using (1-bromovinyl)benzene and (*R*)-2-(1,2-diphenylethyl)-4,4,5,5-tetramethyl-1,3,2-dioxaborolane (**SM16**) according to general procedure **I**, provided **ent-11c** (0.13 mmol, 37 mg, 51%) as a colorless oil. $R_f = 0.20$ (hexane/EtOAc 100:0, UV, KMnO_4 , PAA). $^1\text{H NMR}$ (400 MHz, CDCl_3) δ 7.35 – 7.15 (m, 13H), 7.12 – 7.03 (m, 2H), 5.53 (s, 1H), 5.38 (s, 1H), 4.23 – 4.14 (m, 1H), 3.35 (dd, $J = 13.7, 6.4$ Hz, 1H), 3.14 (dd, $J = 13.7, 8.9$ Hz, 1H) ppm. $^{13}\text{C NMR}$ (101 MHz, CDCl_3) δ 151.2, 142.6, 142.5, 140.5, 129.2, 128.4, 128.3, 128.2, 128.2, 127.3, 126.9, 126.4, 126.0, 113.9, 52.2, 41.9 ppm. **LRMS** (DEP/EI-Orbitrap): m/z (%): 284.2 (14), 206.1 (11), 193.1 (100), 189.1 (8), 178.1 (52), 165.1 (13), 115.1 (71), 91.1 (16). **HRMS** (EI-Orbitrap): m/z calcd for $\text{C}_{22}\text{H}_{20}^+$: 284.1565; found: 284.1558. $[\alpha]_D^{20}$: -180.73 ($\beta = 0.97$, CH_2Cl_2). **Chiral HPLC**: 97% *ee* (*er* 98.5:1.5), OD-H column, EtOAc:heptane = 0:100, 1.0 mL/min, 30 °C. **IR** (Diamond-ATR, neat) $\tilde{\nu}_{max}$ (cm^{-1}): 3083 (w), 3059 (w), 3025 (w), 3003 (w), 2921 (w), 2855 (w), 1944 (vw), 1879 (vw), 1805 (w), 1625 (w), 1599 (w), 1573 (w), 1493 (m), 1452 (m), 1443 (w), 1296 (w), 1262 (w), 1179 (w), 1155 (w), 1071 (w), 1029 (w), 965 (w), 901 (m), 777 (m), 745 (m), 696 (vs).

(S)-(3-(4-Methoxyphenyl)but-3-ene-1,2-diyl)dibenzene (11d)

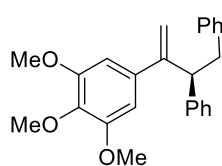
Using 1-(1-bromovinyl)-4-methoxybenzene (**SM20**) and (*S*)-2-(1,2-diphenylethyl)-4,4,5,5-tetramethyl-1,3,2-dioxaborolane (**SM15**) according to general procedure **I** (0.40 mmol scale), provided **11d** (0.24 mmol, 75 mg, 70%) as a colorless oil. $R_f = 0.15$ (hexane/EtOAc 99:1, UV, KMnO_4 , PAA). $^1\text{H NMR}$ (400 MHz, CDCl_3) δ 7.23 – 7.09 (m, 10H), 7.03 – 6.97 (m, 2H), 6.78 – 6.72 (m, 2H), 5.41 (s, 1H), 5.24 (s, 1H), 4.11 – 4.04 (m, 1H), 3.75 (s, 3H), 3.27 (dd, $J = 13.7, 6.3$ Hz, 1H), 3.06 (dd, $J = 13.7, 8.9$ Hz, 1H) ppm. $^{13}\text{C NMR}$ (101 MHz, CDCl_3) δ 158.9, 150.4, 142.8, 140.6, 134.9, 129.2, 128.4, 128.3, 128.1, 127.9, 126.4, 126.0, 113.6, 112.6, 55.3, 52.2, 41.9 ppm. **LRMS** (DEP/EI-Orbitrap): m/z (%): 314.2 (21), 281.1 (16), 223.1 (100), 207.0 (84), 191.1 (27), 178.1 (79), 165.1 (66), 152.1 (21), 115.1 (93), 91.1 (52). **HRMS** (EI-Orbitrap): m/z calcd for $\text{C}_{23}\text{H}_{22}\text{O}^+$: 314.1671; found: 314.1665. $[\alpha]_D^{20}$: +145.62 ($\beta = 1.78$, CH_2Cl_2). **Chiral HPLC**: 92% *ee* (*er* 96.0:4.0), OD-H column, EtOAc:heptane = 1.0:99.0, 1.0 mL/min, 30 °C. **IR** (Diamond-ATR, neat) $\tilde{\nu}_{max}$ (cm^{-1}): 3078 (w), 3065 (w), 3026 (w), 3001 (w), 2944 (w), 2833 (w), 1670 (w), 1606 (m), 1511 (vs), 1495 (m), 1453 (m), 1292 (m), 1248 (s), 1178 (m), 1069 (w), 1032 (m), 900 (w), 835 (m), 759 (m), 700 (s).

(R)-(3-(4-Methoxyphenyl)but-3-ene-1,2-diyl)dibenzene (*ent*-11d)

Using 1-(1-bromovinyl)-4-methoxybenzene (**SM20**) and (*R*)-2-(1,2-diphenylethyl)-4,4,5,5-tetramethyl-1,3,2-dioxaborolane (**SM16**) according to general procedure **I**, provided **ent-11d** (0.19 mmol, 59 mg, 73%) as a colorless oil. $R_f = 0.17$ (hexane/EtOAc 99:1, UV, KMnO_4 , PAA). $^1\text{H NMR}$ (400 MHz, CDCl_3) δ 7.23 – 7.09 (m, 10H), 7.03 – 6.97 (m, 2H), 6.78 – 6.72 (m, 2H), 5.41 (s, 1H), 5.24 (s, 1H), 4.11 – 4.04 (m, 1H), 3.75 (s, 3H),

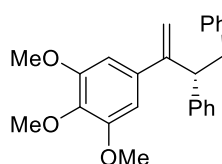
3.27 (dd, $J = 13.7, 6.3$ Hz, 1H), 3.06 (dd, $J = 13.7, 8.9$ Hz, 1H) ppm. $^{13}\text{C NMR}$ (101 MHz, CDCl_3) δ 158.9, 150.4, 142.8, 140.6, 134.9, 129.2, 128.4, 128.3, 128.1, 127.9, 126.4, 126.0, 113.6, 112.6, 55.3, 52.2, 41.9 ppm. **LRMS** (DEP/EI-Orbitrap): m/z (%): 314.2 (21), 281.1 (16), 223.1 (100), 207.0 (84), 191.1 (27), 178.1 (79), 165.1 (66), 152.1 (21), 115.1 (93), 91.1 (52). **HRMS** (EI-Orbitrap): m/z calcd for $\text{C}_{23}\text{H}_{22}\text{O}^+$: 314.1671; found: 314.1665. $[\alpha]_{\text{D}}^{20}$: -135.74 ($\beta = 1.22, \text{CH}_2\text{Cl}_2$). **Chiral HPLC**: 89% *ee* (*er* 94.5:5.5), OD-H column, EtOAc:heptane = 1.0:99.0, 1.0 mL/min, 30 °C. **IR** (Diamond-ATR, neat) $\tilde{\nu}_{\text{max}}$ (cm^{-1}): 3078 (w), 3065 (w), 3026 (w), 3001 (w), 2944 (w), 2833 (w), 1670 (w), 1606 (m), 1511 (vs), 1495 (m), 1453 (m), 1292 (m), 1248 (s), 1178 (m), 1069 (w), 1032 (m), 900 (w), 835 (m), 759 (m), 700 (s).

(S)-(3-(3,4,5-Trimethoxyphenyl)but-3-ene-1,2-diyl)dibenzene (11e)



Using 5-(1-bromovinyl)-1,2,3-trimethoxybenzene (**SM21**) and (*S*)-2-(1,2-diphenylethyl)-4,4,5,5-tetramethyl-1,3,2-dioxaborolane (**SM15**) according to general procedure **I** (0.40 mmol scale), provided **11e** (0.27 mmol, 102 mg, 80%) as a colorless oil. $R_f = 0.19$ (hexane/EtOAc 95:5, UV, KMnO_4 , PAA). $^1\text{H NMR}$ (400 MHz, CDCl_3) δ 7.25 – 7.11 (m, 8H), 7.04 – 6.98 (m, 2H), 6.36 (s, 2H), 5.43 (s, 1H), 5.30 (s, 1H), 4.02 (t, $J = 7.6$ Hz, 1H), 3.79 (s, 3H), 3.71 (s, 6H), 3.25 (dd, $J = 13.6, 6.8$ Hz, 1H), 3.09 (dd, $J = 13.6, 8.4$ Hz, 1H) ppm. $^{13}\text{C NMR}$ (101 MHz, CDCl_3) δ 152.8, 151.1, 143.0, 140.4, 138.3, 137.4, 129.3, 128.4, 128.3, 128.2, 126.6, 126.1, 113.8, 104.2, 61.0, 56.1, 52.7, 41.8 ppm. **LRMS** (DEP/EI-Orbitrap): m/z (%): 374.2 (38), 283.1 (39), 252.1 (40), 237.1 (25), 225.0 (21), 207.0 (39), 193.1 (17), 178.1 (47), 165.1 (60), 152.1 (28), 115.1 (100), 91.1 (56). **HRMS** (EI-Orbitrap): m/z calcd for $\text{C}_{25}\text{H}_{26}\text{O}_3^+$: 374.1882; found: 374.1876. $[\alpha]_{\text{D}}^{20}$: +118.70 ($\beta = 0.77, \text{CH}_2\text{Cl}_2$). **Chiral HPLC**: 95% *ee* (*er* 97.5:2.5), OD-H column, EtOAc:heptane = 10:90, 1.0 mL/min, 30 °C. **IR** (Diamond-ATR, neat) $\tilde{\nu}_{\text{max}}$ (cm^{-1}): 3083 (w), 3061 (w), 3029 (w), 2998 (w), 2934 (w), 2834 (w), 1579 (m), 1504 (m), 1496 (m), 1461 (m), 1453 (m), 1410 (m), 1334 (m), 1240 (m), 1180 (w), 1173 (w), 1127 (vs), 1007 (w), 905 (m), 840 (w), 731 (m), 701 (m).

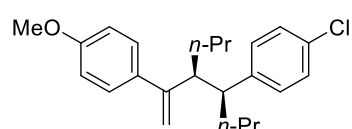
(R)-(3-(3,4,5-Trimethoxyphenyl)but-3-ene-1,2-diyl)dibenzene (ent-11e)



Using 5-(1-bromovinyl)-1,2,3-trimethoxybenzene (**SM21**) and (*R*)-2-(1,2-diphenylethyl)-4,4,5,5-tetramethyl-1,3,2-dioxaborolane (**SM16**) according to general procedure **I** (0.40 mmol scale), provided **ent-11e** (0.29 mmol, 108 mg, 85%) as a colorless oil. $R_f = 0.19$ (hexane/EtOAc 95:5, UV, KMnO_4 , PAA). $^1\text{H NMR}$ (400 MHz, CDCl_3) δ 7.25 – 7.11 (m, 8H), 7.04 – 6.98 (m, 2H), 6.36 (s, 2H), 5.43 (s, 1H), 5.30 (s, 1H), 4.02 (t, $J = 7.6$ Hz, 1H), 3.79 (s, 3H), 3.71 (s, 6H), 3.25 (dd, $J = 13.6, 6.8$ Hz, 1H), 3.09 (dd, $J = 13.6, 8.4$ Hz, 1H) ppm. $^{13}\text{C NMR}$ (101 MHz, CDCl_3) δ 152.8, 151.1, 143.0, 140.4, 138.3, 137.4, 129.3, 128.4, 128.3, 128.2, 126.6, 126.1, 113.8, 104.2, 61.0, 56.1, 52.7, 41.8 ppm. **LRMS** (DEP/EI-Orbitrap): m/z (%): 374.2 (38), 283.1 (39), 252.1 (40), 237.1 (25), 225.0 (21), 207.0 (39), 193.1 (17), 178.1 (47), 165.1

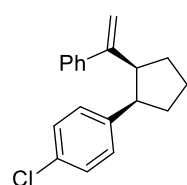
(60), 152.1 (28), 115.1 (100), 91.1 (56). **HRMS** (EI-Orbitrap): m/z calcd for $C_{25}H_{26}O_3^+$: 374.1882; found: 374.1876. $[\alpha]_D^{20}$: -118.21 ($\beta = 1.45$, CH_2Cl_2). **Chiral HPLC**: 99% *ee* (*er* 99.5:0.5), OD-H column, EtOAc:heptane = 10:90, 1.0 mL/min, 30 °C. **IR** (Diamond-ATR, neat) $\tilde{\nu}_{max}$ (cm^{-1}): 3083 (w), 3061 (w), 3029 (w), 2998 (w), 2934 (w), 2834 (w), 1579 (m), 1504 (m), 1496 (m), 1461 (m), 1453 (m), 1410 (m), 1334 (m), 1240 (m), 1180 (w), 1173 (w), 1127 (vs), 1007 (w), 905 (m), 840 (w), 731 (m), 701 (m).

1-Chloro-4-((4*S*,5*S*)-5-(1-(4-methoxyphenyl)vinyl)octan-4-yl)benzene (**11f**)

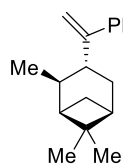


Using 1-(1-bromovinyl)-4-methoxybenzene (**SM20**) and 2-((4*R*,5*R*)-5-(4-chlorophenyl)octan-4-yl)-4,4,5,5-tetramethyl-1,3,2-dioxaborolane (**SM17**) according to general procedure **I**, provided **11f** (*dr* > 99:1, 0.20 mmol, 70 mg, 77%) as a colorless oil. $R_f = 0.16$ (hexane/EtOAc 100:0, UV, $KMnO_4$, PAA). **¹H NMR** (400 MHz, $CDCl_3$) δ 7.16 – 7.11 (m, 2H), 7.10 – 7.04 (m, 2H), 6.94 (d, $J = 8.4$ Hz, 2H), 6.84 – 6.75 (m, 2H), 5.14 (d, $J = 1.0$ Hz, 1H), 4.79 (s, 1H), 3.81 (s, 3H), 2.78 – 2.68 (m, 1H), 2.66 – 2.56 (m, 1H), 1.75 – 1.58 (m, 2H), 1.58 – 1.40 (m, 3H), 1.31 – 1.15 (m, 1H), 1.13 – 1.01 (m, 1H), 1.01 – 0.93 (m, 1H), 0.89 (t, $J = 7.2$ Hz, 3H), 0.77 (t, $J = 7.3$ Hz, 3H) ppm. **¹³C NMR** (101 MHz, $CDCl_3$) δ 158.8, 150.3, 142.8, 136.8, 131.3, 130.2, 127.8, 127.8, 113.5, 113.1, 55.4, 50.4, 49.1, 33.7, 33.4, 20.9, 20.8, 14.6, 14.2 ppm. **LRMS** (DEP/EI-Orbitrap): m/z (%): 225.0 (16), 207.0 (18), 166.1 (11), 151.0 (14), 131.1 (20), 125.0 (100), 115.1 (30), 91.1 (12). **HRMS** (EI-Orbitrap): m/z calcd for $C_{23}H_{29}ClO^+$: 356.1907; found: 356.1902. **IR** (Diamond-ATR, neat) $\tilde{\nu}_{max}$ (cm^{-1}): 3088 (vw), 3039 (vw), 2954 (m), 2931 (w), 2870 (w), 2835 (vw), 1607 (m), 1573 (w), 1509 (s), 1490 (m), 1464 (m), 1456 (w), 1441 (w), 1409 (w), 1377 (w), 1292 (w), 1244 (s), 1177 (m), 1113 (w), 1093 (m), 1035 (m), 1014 (m), 905 (s), 832 (s), 802 (m), 729 (vs).

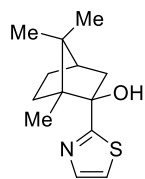
1-Chloro-4-((1*R*,2*S*)-2-(1-phenylvinyl)cyclopentyl)benzene (**11g**)



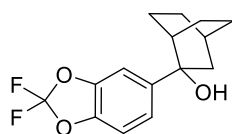
Using (1-bromovinyl)benzene and 2-((1*S*,2*R*)-2-(4-chlorophenyl)cyclopentyl)-4,4,5,5-tetramethyl-1,3,2-dioxaborolane (**SM18**) according to general procedure **I**, provided **11g** (*dr* > 99:1, 0.13 mmol, 38 mg, 52%) as a colorless oil. $R_f = 0.50$ (hexane/EtOAc 97:3, UV, $KMnO_4$, PAA). **¹H NMR** (400 MHz, $CDCl_3$) δ 7.26 – 7.18 (m, 3H), 7.13 – 7.07 (m, 2H), 7.05 – 6.98 (m, 2H), 6.70 – 6.62 (m, 2H), 5.04 (s, 1H), 4.79 (s, 1H), 3.49 – 3.40 (m, 1H), 3.29 (td, $J = 8.0, 4.4$ Hz, 1H), 2.33 – 2.17 (m, 1H), 2.08 – 1.75 (m, 5H) ppm. **¹³C NMR** (101 MHz, $CDCl_3$) δ 149.1, 142.9, 142.8, 131.2, 130.0, 128.1, 127.4, 127.1, 126.5, 113.2, 49.2, 46.9, 33.2, 29.8, 24.1 ppm. **LRMS** (DEP/EI-Orbitrap): m/z (%): 282.1 (7), 207.0 (21), 157.1 (13), 143.1 (20), 129.1 (100), 115.1 (38), 103.1 (16), 91.1 (20). **HRMS** (EI-Orbitrap): m/z calcd for $C_{19}H_{19}Cl^+$: 282.1175; found: 282.1167. **IR** (Diamond-ATR, neat) $\tilde{\nu}_{max}$ (cm^{-1}): 3091 (vw), 3058 (w), 3027 (w), 2954 (m), 2871 (w), 2365 (w), 2338 (w), 1626 (w), 1596 (w), 1573 (w), 1492 (vs), 1443 (w), 1410 (w), 1305 (w), 1184 (vw), 1091 (m), 1014 (m), 905 (m), 817 (m), 776 (s), 731 (m), 701 (s).

(1*R*,2*R*,3*R*,5*R*)-2,6,6-Trimethyl-3-(1-phenylvinyl)bicyclo[3.1.1]heptane (11h)

Using (1-bromovinyl)benzene and 4,4,5,5-tetramethyl-2-((1*R*,2*S*,3*R*,5*R*)-2,6,6-trimethylbicyclo[3.1.1]heptan-3-yl)-1,3,2-dioxaborolane (**SM19**) according to general procedure **I** (0.40 mmol scale), provided **11h** (*dr* > 99:1, 0.21 mmol, 51 mg, 63%) as a colorless oil. *R_f* = 0.70 (hexane/EtOAc 100:0, UV, KMnO₄, PAA). ¹H NMR (400 MHz, CDCl₃) δ 7.39 – 7.23 (m, 5H), 5.16 (d, *J* = 4.0 Hz, 2H), 2.99 (dt, *J* = 9.8, 8.0 Hz, 1H), 2.38 – 2.17 (m, 3H), 1.96 – 1.90 (m, 1H), 1.86 (td, *J* = 5.8, 1.9 Hz, 1H), 1.70 (ddd, *J* = 13.6, 7.7, 2.4 Hz, 1H), 1.23 (s, 3H), 1.11 (s, 3H), 1.03 (d, *J* = 7.1 Hz, 3H), 0.85 (d, *J* = 9.5 Hz, 1H) ppm. ¹³C NMR (101 MHz, CDCl₃) δ 156.4, 144.2, 128.2, 127.3, 127.1, 111.3, 48.3, 42.7, 42.0, 41.8, 39.1, 36.0, 34.5, 28.5, 23.2, 21.8 ppm. LRMS (DEP/EI-Orbitrap): *m/z* (%): 240.2 (8), 197.1 (15), 185.1 (32), 169.1 (20), 155.1 (21), 143.1 (45), 129.1 (50), 115.1 (31), 93.1 (80), 83.1 (100), 69.1 (28), 55.1 (61). HRMS (EI-Orbitrap): *m/z* calcd for C₁₈H₂₄⁺: 240.1878; found: 240.1872. [α]_D²⁰: -18.98 (β = 1.48, CH₂Cl₂). IR (Diamond-ATR, neat) $\tilde{\nu}_{max}$ (cm⁻¹): 3078 (w), 3054 (w), 3018 (w), 2984 (m), 2950 (m), 2918 (m), 2900 (s), 2869 (m), 1625 (w), 1599 (w), 1573 (w), 1491 (w), 1470 (w), 1452 (m), 1442 (w), 1384 (w), 1372 (w), 1266 (w), 1217 (vw), 1147 (w), 1072 (w), 1027 (w), 1009 (vw), 891 (m), 780 (w), 770 (m), 701 (vs).

(-)-1,7,7-Trimethyl-2-(thiazol-2-yl)bicyclo[2.2.1]heptan-2-ol (12a)

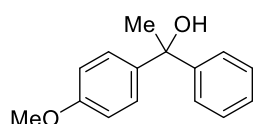
Using 2-bromothiazole and (+)-camphor according to general procedure **J** (0.40 mmol scale), provided **12a** (*dr* > 99:1, 0.34 mmol, 82 mg, 86%) as a yellow solid. *R_f* = 0.56 (hexane/EtOAc 80:20, UV, KMnO₄, PAA). ¹H NMR (400 MHz, CDCl₃) δ 7.72 (d, *J* = 3.3 Hz, 1H), 7.24 (d, *J* = 3.3 Hz, 1H), 3.09 (s, 1H), 2.37 – 2.33 (m, 2H), 1.91 – 1.87 (m, 1H), 1.79 – 1.67 (m, 1H), 1.37 – 1.24 (m, 2H), 1.19 (s, 3H), 1.02 (s, 3H, OH), 0.91 (s, 3H), 0.88 – 0.79 (m, 1H) ppm. ¹³C NMR (101 MHz, CDCl₃) δ 177.8, 142.1, 118.8, 83.5, 54.4, 50.1, 47.1, 45.4, 31.0, 26.8, 21.4, 21.2, 9.9 ppm. LRMS (DEP/EI-Orbitrap): *m/z* (%): 237.2 (20), 209.2 (10), 176.1 (9), 128.1 (100), 112.0 (21), 95.1 (80), 86.0 (40). HRMS (EI-Orbitrap): *m/z* calcd for C₁₃H₁₉NOS⁺: 237.1187; found: 237.1183. [α]_D²²: -57.28 (β = 1.10, CH₂Cl₂). IR (Diamond-ATR, neat) $\tilde{\nu}_{max}$ (cm⁻¹): 3421 (br/m), 2987 (m), 2952 (vs), 2934 (s), 2882 (m), 2874 (m), 1492 (m), 1479 (m), 1454 (s), 1422 (m), 1389 (s), 1370 (m), 1274 (w), 1253 (w), 1220 (m), 1197 (w), 1157 (m), 1131 (m), 1114 (m), 1095 (m), 1069 (vs), 1057 (s), 1007 (m), 970 (m), 951 (m), 943 (m), 910 (m), 866 (m), 801 (m), 723 (vs). *Mp* (°C) = 58–61.

2-(2,2-Difluorobenzo[*d*][1,3]dioxol-5-yl)bicyclo[2.2.2]octan-2-ol (12b)

Using 5-bromo-2,2-difluorobenzo[*d*][1,3]dioxole and bicyclo[2.2.2]octan-2-one according to general procedure **J** (0.40 mmol scale), provided **12b** (0.22 mmol, 63 mg, 66%) as a colorless oil. *R_f* = 0.38 (hexane/EtOAc 90:10, UV, KMnO₄, PAA). ¹H NMR (400 MHz, C₆D₆) δ 6.96 (d, *J* = 1.8 Hz, 1H), 6.75 (dd, *J* = 8.5, 1.8 Hz, 1H), 6.44 (d, *J* = 8.4 Hz, 1H), 2.24 – 2.14 (m, 1H, OH), 1.87 (dt, *J* = 14.3, 2.6 Hz, 1H), 1.70 – 1.56 (m, 2H), 1.49 – 1.34 (m, 3H), 1.32 – 1.22 (m, 2H), 1.22 – 1.09 (m, 2H), 1.08 – 0.97 (m, 2H) ppm. ¹³C NMR (101 MHz,

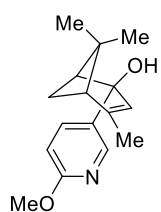
C_6D_6) δ 145.4, 144.1, 142.6, 132.6 (t, $J = 254.0$ Hz), 121.4, 108.4, 108.4, 74.5, 42.5, 36.5, 26.2, 25.2, 24.3, 22.3, 21.3 ppm. **LRMS** (DEP/EI-Orbitrap): m/z (%): 282.1 (13), 264.1 (33), 236.1 (96), 200.1 (100), 185.1 (56), 171.0 (31), 141.1 (32), 115.1 (32). **HRMS** (EI-Orbitrap): m/z calcd for $C_{15}H_{16}F_2O_3^+$: 282.1068; found: 282.1063. **IR** (Diamond-ATR, neat) $\tilde{\nu}_{max}$ (cm^{-1}): 3413 (br/w), 2941 (w), 2917 (w), 2867 (w), 1620 (vw), 1494 (m), 1476 (w), 1456 (w), 1436 (w), 1238 (vs), 1153 (s), 1085 (w), 1032 (m), 1012 (w), 982 (w), 939 (w), 935 (w), 906 (w), 869 (w), 859 (w), 812 (w).

1-(4-Methoxyphenyl)-1-phenylethan-1-ol (**12c**)



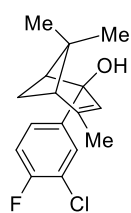
Using 1-bromo-4-methoxybenzene and acetophenone according to general procedure **J** (0.40 mmol scale), provided **12c** (0.28 mmol, 63 mg, 81%) as a colorless oil. $R_f = 0.17$ (hexane/EtOAc 95:5, UV, $KMnO_4$, PAA). **1H NMR** (400 MHz, $CDCl_3$) δ 7.40 – 7.34 (m, 2H), 7.31 – 7.25 (m, 4H), 7.23 – 7.17 (m, 1H), 6.84 – 6.77 (m, 2H), 3.75 (s, 3H), 2.16 (s, 1H, OH), 1.90 (s, 3H) ppm. **LRMS** (DEP/EI-Orbitrap): m/z (%): 210.1 (100), 195.0 (70), 165.1 (71), 152.0 (47), 115.0 (13), 89.0 (13). Analytical data in accordance to literature.⁴⁹

(-)-2-(6-Methoxypyridin-3-yl)-4,6,6-trimethylbicyclo[3.1.1]hept-3-en-2-ol (**12d**)



Using 5-bromo-2-methoxypyridine and (-)-verbenone according to general procedure **J** (0.40 mmol scale), provided **12d** ($dr > 99:1$, 0.29 mmol, 74 mg, 84%) as a colorless solid. $R_f = 0.36$ (hexane/EtOAc 80:20, UV, $KMnO_4$, PAA). **1H NMR** (400 MHz, C_6D_6) δ 8.43 (d, $J = 2.4$ Hz, 1H), 7.58 (dd, $J = 8.6, 2.5$ Hz, 1H), 6.70 (d, $J = 8.6$ Hz, 1H), 5.25 – 5.19 (m, 1H), 3.88 (s, 3H), 2.21 (td, $J = 6.0, 2.1$ Hz, 1H), 2.01 (ddd, $J = 9.5, 6.1, 5.3$ Hz, 1H), 1.77 – 1.73 (m, 1H), 1.60 (s, 1H), 1.58 (d, $J = 1.6$ Hz, 3H), 1.25 (d, $J = 9.5$ Hz, 1H), 1.21 (s, 3H), 1.15 (s, 3H) ppm. **^{13}C NMR** (101 MHz, C_6D_6) δ 163.8, 147.1, 145.8, 137.7, 136.2, 120.9, 110.5, 77.5, 53.9, 53.3, 47.5, 43.4, 34.0, 27.3, 23.5, 22.8 ppm. **LRMS** (DEP/EI-Orbitrap): m/z (%): 241.2 (81), 226.2 (78), 198.1 (100), 184.1 (25), 154.1 (20), 128.1 (25), 115.1 (31), 91.1 (11). **HRMS** (EI-Orbitrap): m/z calcd for $C_{16}H_{21}NO_2^+$: 259.1572; found: 259.1565. $[\alpha]_D^{22}$: -66.01 ($\beta = 1.01$, CH_2Cl_2). **IR** (Diamond-ATR, neat) $\tilde{\nu}_{max}$ (cm^{-1}): 3373 (br/w), 2973 (m), 2921 (m), 2867 (w), 1603 (m), 1571 (m), 1491 (vs), 1462 (w), 1442 (m), 1433 (w), 1376 (m), 1333 (w), 1287 (s), 1250 (m), 1230 (w), 1167 (w), 1129 (w), 1121 (w), 1052 (m), 1030 (m), 1022 (m), 1008 (m), 957 (m), 831 (m). **Mp** ($^{\circ}C$) = 97–100.

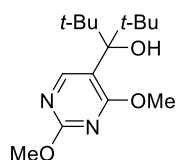
(+)-2-(3-Chloro-4-fluorophenyl)-4,6,6-trimethylbicyclo[3.1.1]hept-3-en-2-ol (**12e**)



Using 4-bromo-2-chloro-1-fluorobenzene and (-)-verbenone according to general procedure **J** (0.40 mmol scale), provided **12e** ($dr > 99:1$, 0.27 mmol, 75 mg, 79%) as a light-yellow oil. $R_f = 0.54$ (hexane/EtOAc 80:20, UV, $KMnO_4$, PAA). **1H NMR** (400 MHz, $CDCl_3$) δ 7.50 (dd, $J = 7.2, 2.2$ Hz, 1H), 7.32 (ddd, $J = 8.5, 4.6, 2.2$ Hz, 1H), 7.07 (t, $J = 8.7$ Hz, 1H), 5.43 (s, 1H), 2.32 – 2.21 (m, 2H), 2.14 (s, 1H, OH), 2.06 (t, $J = 5.4$ Hz, 1H), 1.86 (d, $J = 1.5$ Hz, 3H), 1.40 (s, 3H), 1.26 (d, $J = 9.2$ Hz, 1H), 1.21 (s, 3H) ppm. **^{13}C NMR** (101 MHz, $CDCl_3$) δ 157.2 (d, $J = 248.1$ Hz), 148.6, 144.3, 129.3, 126.7 (d, $J = 7.1$ Hz), 120.0, 116.0, 115.8, 78.8,

54.0, 47.4, 43.9, 34.0, 27.2, 23.4, 23.1 ppm. **LRMS** (DEP/EI-Orbitrap): m/z (%): 280.1 (9), 262.1 (60), 247.1 (52), 219.1 (100), 197.1 (54), 183.1 (93), 170.1 (30), 157.0 (68), 133.1 (25), 91.1 (29). **HRMS** (EI-Orbitrap): m/z calcd for $C_{16}H_{18}ClFO^+$: 280.1030; found: 280.1025. $[\alpha]_D^{22}$: +4.50 ($\beta = 1.19$, CH_2Cl_2). **IR** (Diamond-ATR, neat) $\tilde{\nu}_{max}$ (cm^{-1}): 3413 (br/w), 2975 (m), 2925 (m), 2869 (w), 1654 (w), 1599 (w), 1590 (w), 1496 (vs), 1443 (w), 1391 (m), 1366 (w), 1333 (w), 1261 (m), 1246 (s), 1166 (w), 1131 (w), 1059 (m), 1048 (m), 1008 (m), 994 (m), 966 (w), 908 (m), 896 (w), 888 (w), 819 (m).

3-(2,4-Dimethoxypyrimidin-5-yl)-2,2,4,4-tetramethylpentan-3-ol (**12f**)



Using 5-bromo-2,4-dimethoxypyrimidine and hexamethylacetone according to general procedure **J** (0.40 mmol scale), provided **12f** (0.24 mmol, 67 mg, 70%) as a colorless solid. $R_f = 0.21$ (hexane/EtOAc 90:10, UV, $KMnO_4$, PAA). **1H NMR** (400 MHz, $CDCl_3$) δ 8.71 (s, 1H), 4.00 (s, 3H), 3.95 (s, 3H), 1.89 (s, 1H, OH), 1.08 (s, 18H) ppm. **^{13}C NMR** (101 MHz, $CDCl_3$) δ 167.8, 164.1, 160.8, 119.0, 84.3, 54.8, 52.8, 42.4, 29.3 ppm. **LRMS** (DEP/EI-Orbitrap): m/z (%): 225.2 (80), 207.2 (10), 167.1 (10), 141.1 (100), 109.1 (8), 57.1 (25). **HRMS** (EI-Orbitrap): m/z calcd for $C_{11}H_{17}N_2O_3^+ [M-t-Bu]^+$: 225.1239; found: 225.1237. **IR** (Diamond-ATR, neat) $\tilde{\nu}_{max}$ (cm^{-1}): 3386 (br/m), 2961 (m), 2920 (m), 2874 (m), 2359 (m), 2341 (m), 1579 (s), 1558 (s), 1473 (s), 1462 (s), 1395 (vs), 1319 (m), 1279 (m), 1241 (m), 1195 (m), 1139 (m), 1074 (m), 1060 (m), 1017 (s), 924 (m). **Mp** ($^{\circ}C$) = 143–147.

4.5 Raman Spectroscopy²³⁰

4.5.1 Measurements

Raman spectroscopy was performed at $-50\text{ }^{\circ}\text{C}$ in a sealed glass vessel under argon atmosphere. The sample was concentrated under high vacuum prior to measuring to give maximum intensities (Figure 12).

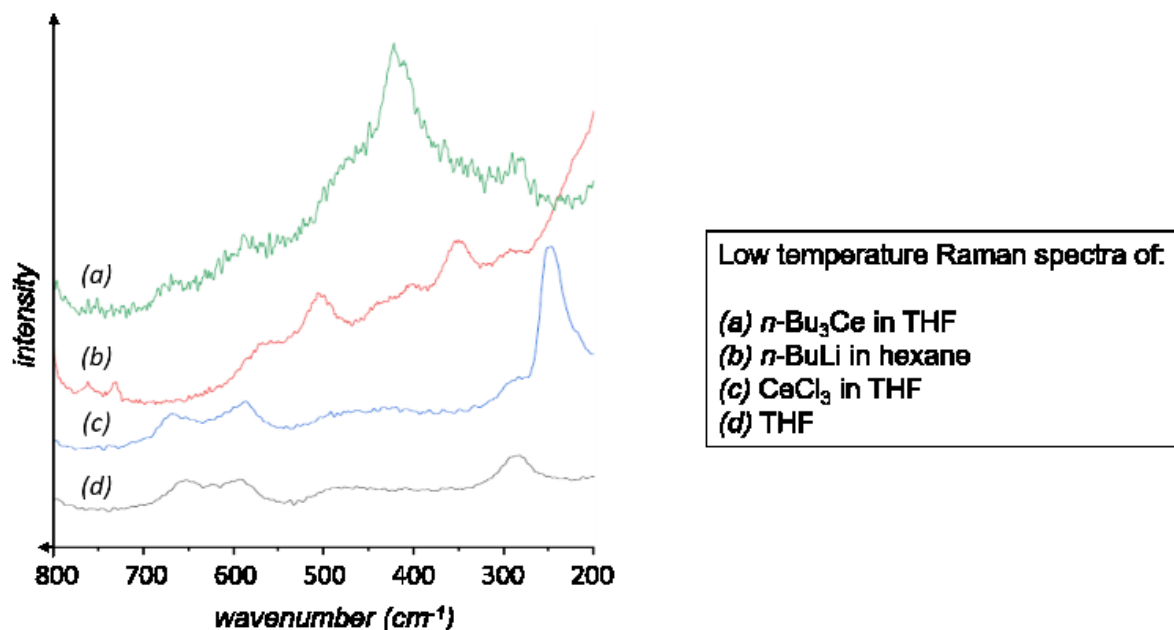


Figure 12: Comparative Raman spectra of different metallic salts and organometallic species.

The Raman spectra of the reaction mixture show a significant Raman line at 420 cm^{-1} , indicating a carbon stretching mode. This observation and the absence of CeCl_3 and $n\text{-BuLi}$ vibrations point to the existence of a cerium carbon species. In addition, comparable Raman frequencies of other alkylic metal complexes can be found in the literature.²³¹ No further significant Raman lines or shifts compared to the $n\text{-BuLi}$ were observed in the Raman spectrum of “ $n\text{-Bu}_3\text{Ce}$ ”.

²³⁰ Raman measurements and theoretical calculations were performed by Dr. Florian Zischka, Department of Chemistry, LMU Munich.

²³¹ K. Nakamoto, *Infrared and Raman Spectra of Inorganic and Coordination Compounds, Part B: Applications in Coordination, Organometallic, and Bioinorganic Chemistry*, 6th Ed., Wiley & Sons, Hoboken, USA, 2009, 275–331.

4.7.2 Calculations

In order to gain insights on the vibrational frequencies of the Ce-C stretching modes, the gas phase structure of $R_x\text{CeCl}_{3-x}$ ($x=3$) was calculated with the Program Gaussian 09 Revision B. 01 as an example. The equilibrium geometry and the vibrational frequencies were calculated at the B3LYP/aug-cc-pvdz level of theory for H and C atoms.²³² For the calculation of cerium the Effective Core Potential MWB28 was employed. The vibrational analysis exhibits no negative frequencies, indicating a true minimum on the energy hypersurface. Calculated vibrational frequencies were scaled with an empirical factor of 0.97 according to the NIST CCCB Data Base (<https://cccbdb.nist.gov/vibscalejust.asp>).

The theoretical calculations predict the ν_s (Ce-C) at 452 cm^{-1} and two degenerated antisymmetric Ce-C stretching modes at 446 cm^{-1} . The calculated frequencies are in reasonable agreement with the observed Raman line at 420 cm^{-1} . The two discussed Ce-C modes, showing only a small difference in frequency, may be a good explanation of the broad Raman line observed in the experiment. The calculated equilibrium geometry is depicted in Table 6.

Calculated vibrational frequencies (B3LYP/aug-cc-pvdz/MWB28) of $R_x\text{CeCl}_{3-x}$ ($x=3$) in cm^{-1} (IR Absorption/Raman Intensity):

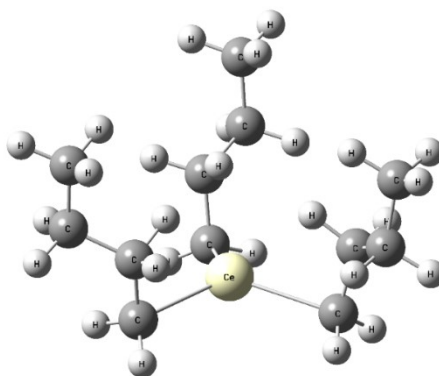
3096 (32/111), 3096 (43/126), 3096 (48/133), 3088 (98/23), 3088 (107/12), 3087 (24/61), 3082 (20/118), 3080 (27/122), 3079 (12/131), 3059 (4/93), 3059 (2/61), 3059 (2/61), 3033 (33/47), 3032 (37/39), 3030 (45/30), 3021 (4/505), 3021 (11/155), 3021 (9/63), 3019 (66/222), 3019 (4/24), 3019 (8/40), 3000 (24/134), 2998 (22/112), 2997 (20/93), 2574 (147/70), 2566 (231/19), 2563 (244/10), 1480 (6/0), 1480 (4/0), 1479 (4/0), 1474 (3/2), 1474 (6/5), 1474 (8/7), 1465 (1/2), 1464 (1/4), 1464 (0/12), 1463 (3/16), 1462 (3/8), 1459 (3/6), 1431 (3/4), 1428 (1/1), 1428 (1/1), 1390 (11/0), 1390 (2/0), 1390 (0/0), 1376 (7/10), 1375 (7/8), 1374 (1/14), 1334 (7/4), 1332 (9/4), 1331 (4/4), 1299 (8/1), 1298 (9/3), 1298 (9/3), 1272 (1/0), 1271 (1/0), 1270 (1/0), 1189 (4/5), 1189 (4/4), 1188 (3/5), 1108 (0/39), 1107 (3/6), 1107 (2/7), 1064 (8/3), 1064 (7/4), 1064 (4/15), 1021 (3/8), 1021 (3/6), 1020 (3/7), 990 (2/1), 990 (2/1), 989 (3/0), 920 (46/98), 919 (7/27), 918 (6/25), 847 (42/18), 842 (1/9), 842 (1/11), 832 (10/18), 827 (3/17), 826 (4/18), 725 (0/0), 724 (0/0), 724 (0/1), 466 (4/3), 461 (60/1), 461 (60/1), 427 (27/2), 424 (29/2), 416 (20/20), 372 (12/1), 370 (11/1), 319 (0/0), 266 (23/1), 265 (24/1), 257 (1/8), 235 (0/0), 234 (0/0), 234 (0/0), 201 (5/1), 199 (5/2), 197 (5/1), 106 (2/0), 98 (1/1), 98 (1/1), 70 (0/2), 69 (0/2), 67 (0/1), 59 (1/2), 58 (1/2), 26 (0/0), 20 (0/0), 13 (0/1), 12 (0/1).

²³² a) A. D. Becke, *J. Chem. Phys.* **1993**, *98*, 5648–5652; b) E. R. Davidson, *Chem. Phys. Lett.* **1996**, *260*, 514–518; c) T. H. Dunning, *J. Chem. Phys.* **1989**, *90*, 1007–1023; d) R. A. Kendall, T. H. Dunning, R. J. Harrison, *J. Chem. Phys.* **1992**, *96*, 6796–6806; e) K. A. Peterson, D. E. Woon, T. H. Dunning, *J. Chem. Phys.* **1994**, *100*, 7410–7415; f) D. E. Woon, T. H. Dunning, *J. Chem. Phys.* **1993**, *98*, 1358–1371.

Scaled calculated vibrational frequencies (B3LYP/aug-cc-pvdz/MWB28) of “ R_xCeCl_{3-x} ($x=3$)” in cm^{-1} . Calculated frequencies were scaled with an empirical factor of 0.97 according to the NIST CCCB Data Base (<https://cccbdb.nist.gov/vibscalejust.asp>).

3004, 3004, 3004, 2996, 2996, 2995, 2990, 2989, 2988, 2969, 2968, 2968, 2943, 2941, 2940, 2932, 2931, 2931, 2930, 2929, 2929, 2912, 2909, 2908, 2495, 2488, 2486, 1436, 1436, 1435, 1431, 1430, 1430, 1422, 1421, 1420, 1419, 1419, 1416, 1389, 1386, 1385, 1349, 1349, 1348, 1334, 1333, 1332, 1292, 1292, 1291, 1260, 1259, 1257, 1233, 1233, 1232, 1154, 1153, 1153, 1075, 1074, 1074, 1033, 1032, 1031, 992, 990, 990, 961, 960, 959, 893, 892, 891, 823, 818, 817, 807, 803, 802, 704, 703, 702, 452, 448, 447, 418, 412, 404, 364, 360, 315, 260, 257, 250, 233, 230, 228, 197, 192, 192, 104, 97, 97, 71, 69, 68, 60, 55, 27, 22, 13, 11.

Table 6: Cartesian coordinates of the equilibrium geometry of R_xCeCl_{3-x} ($x=3$) calculated at B3LYP/aug-cc-pvdz/MWB28 and depicted structure of the calculated molecule.



Atom Number	Label	X	Y	Z	Element
1	C1	0.0503	24.194	-13.276	C
2	H2	10.360	27.309	-17.149	H
3	H3	-0.7303	29.255	-19.123	H
4	Ce4	-0.0035	-0.0124	-0.9505	Ce
5	C5	-0.0729	27.011	0.1667	C
6	H6	-10.892	30.428	0.4185	H
7	H7	0.0281	17.489	0.7895	H
8	C8	0.9544	36.671	0.7797	C
9	H9	0.8317	46.452	0.2908	H
10	H10	19.661	33.193	0.5174	H
11	C11	0.8355	38.221	22.984	C
12	H12	15.854	45.247	26.879	H
13	H13	-0.1572	42.019	25.827	H
14	H14	0.9839	28.599	28.121	H

15	C15	20.909	-12.603	-13.184	C
16	H16	29.132	-0.836	-19.112	H
17	H17	18.800	-22.771	-16.938	H
18	C18	24.039	-12.752	0.1745	C
19	H19	31.949	-0.5479	0.4166	H
20	H20	15.246	-0.8982	0.7989	H
21	C21	27.575	-26.351	0.7995	C
22	H22	36.749	-30.013	0.3149	H
23	H23	19.671	-33.581	0.5429	H
24	C24	29.489	-25.922	23.183	C
25	H25	32.063	-35.836	27.164	H
26	H26	37.571	-19.001	25.979	H
27	H27	20.324	-22.576	28.280	H
28	C28	-21.528	-11.679	-13.069	C
29	H29	-22.203	-21.044	-18.781	H
30	H30	-29.086	-0.4649	-16.996	H
31	C31	-23.325	-13.934	0.1911	C
32	H32	-20.848	-24.328	0.4599	H
33	H33	-15.823	-0.79	0.805	H
34	C34	-36.970	-10.259	0.7985	C
35	H35	-44.603	-16.594	0.3223	H
36	H36	-39.407	0.0107	0.5167	H
37	C37	-37.632	-11.795	23.206	C
38	H38	-47.560	-0.9088	27.061	H
39	H39	-35.582	-22.164	26.258	H
40	H40	-30.256	-0.5329	28.201	H

4.6 Representative NMR Spectra

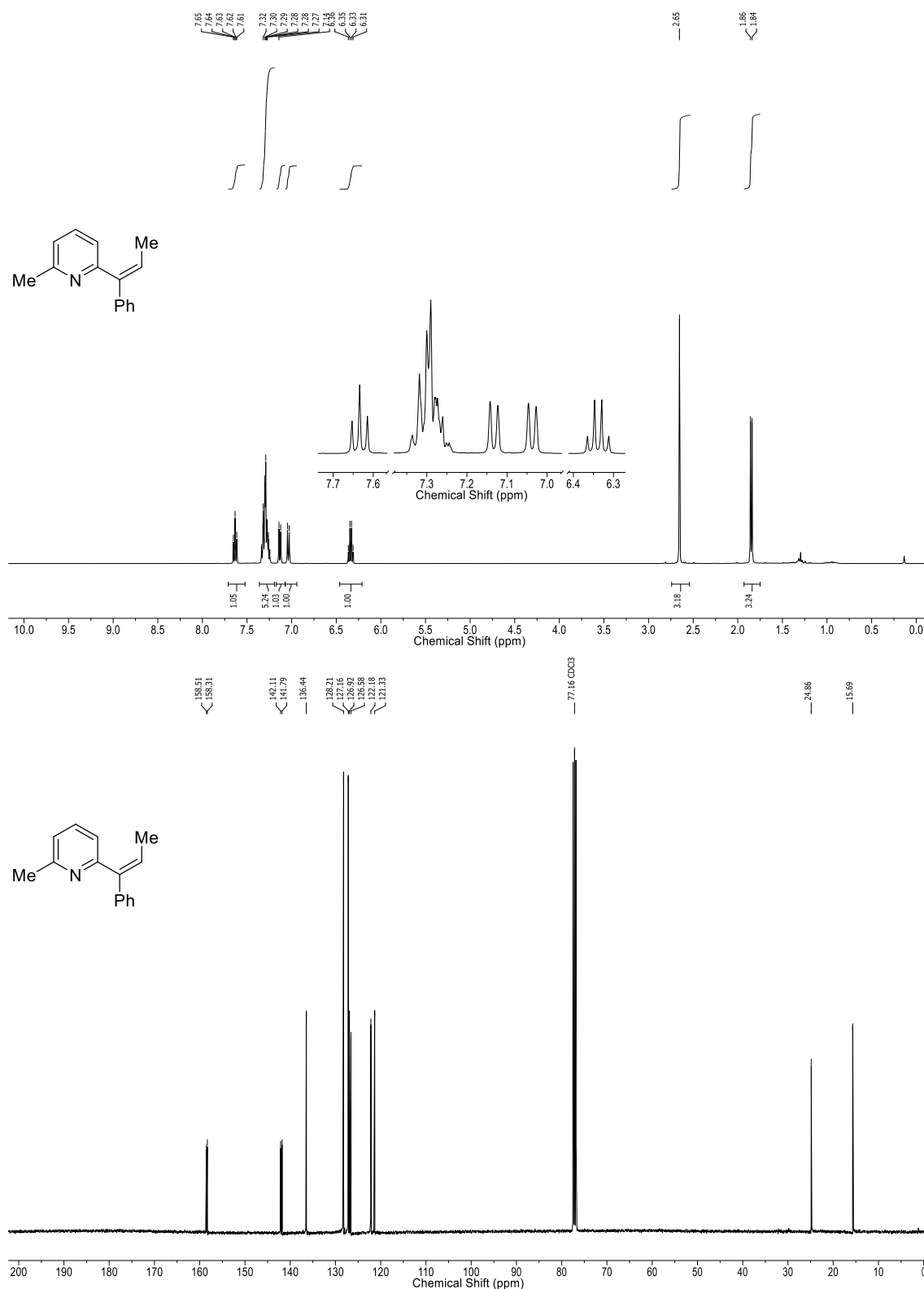


Figure 13: ¹H NMR (400 MHz, CDCl₃) and ¹³C NMR (101 MHz, CDCl₃) of (Z)-2-Methyl-6-(1-phenylprop-1-en-1-yl)pyridine (**8a**).

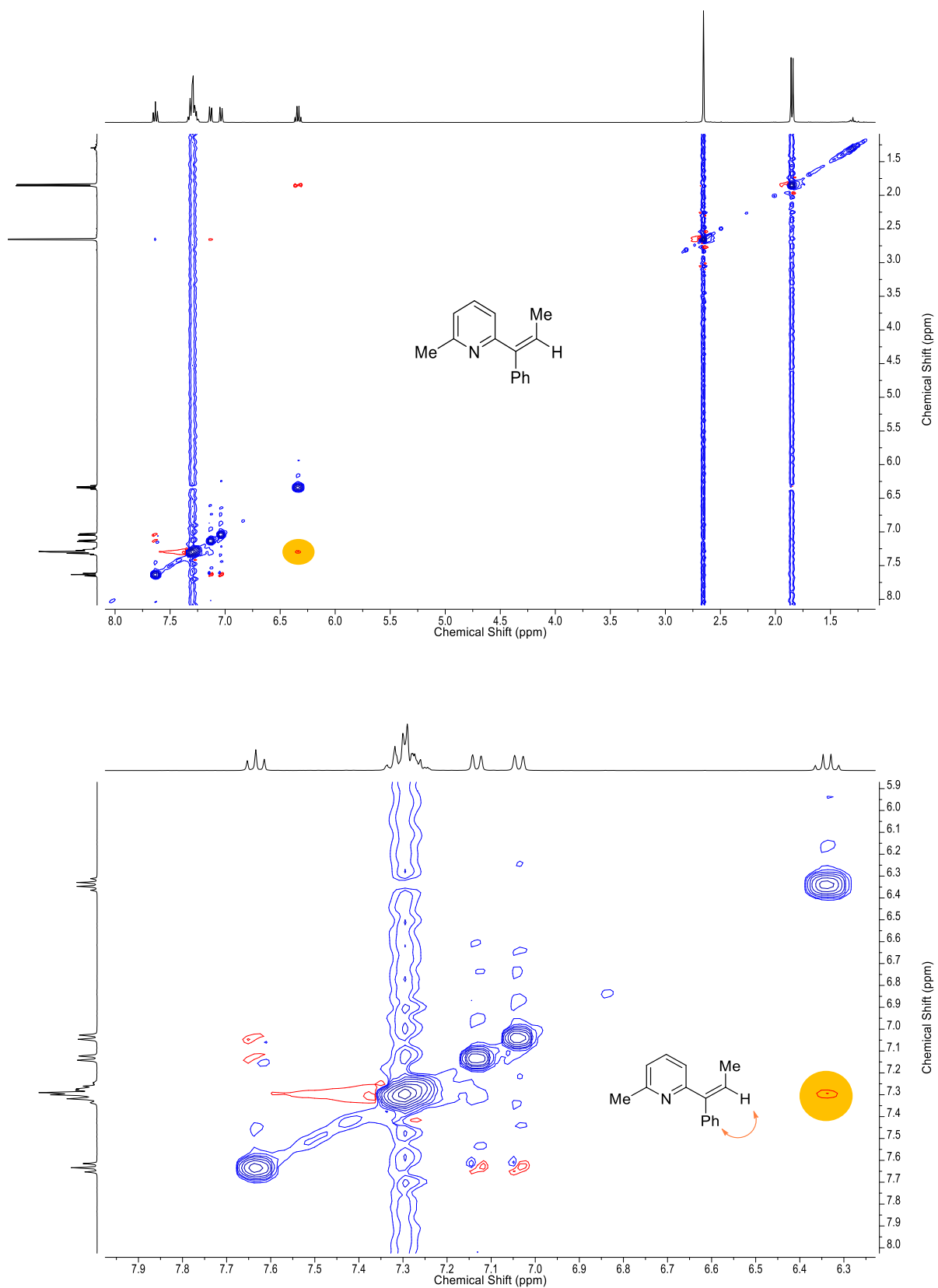


Figure 14: NOESY, observed NOEs (top) and zoom on relevant NOESY area (bottom) of (Z)-2-Methyl-6-(1-phenylprop-1-en-1-yl)pyridine (**8a**).

4.7 Chiral HPLC Analysis

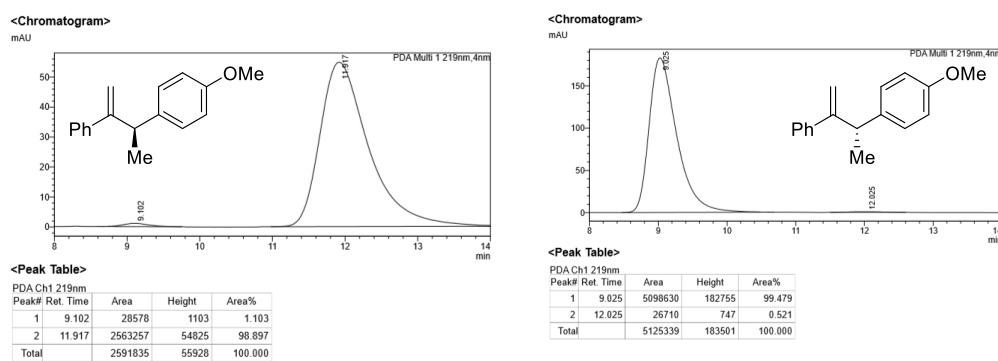


Figure 15: HPLC chromatogram, peak table and footprint for (*R*) and (*S*)-1-Methoxy-4-(3-phenylbut-3-en-2-yl)benzene (11a and *ent*-11a).

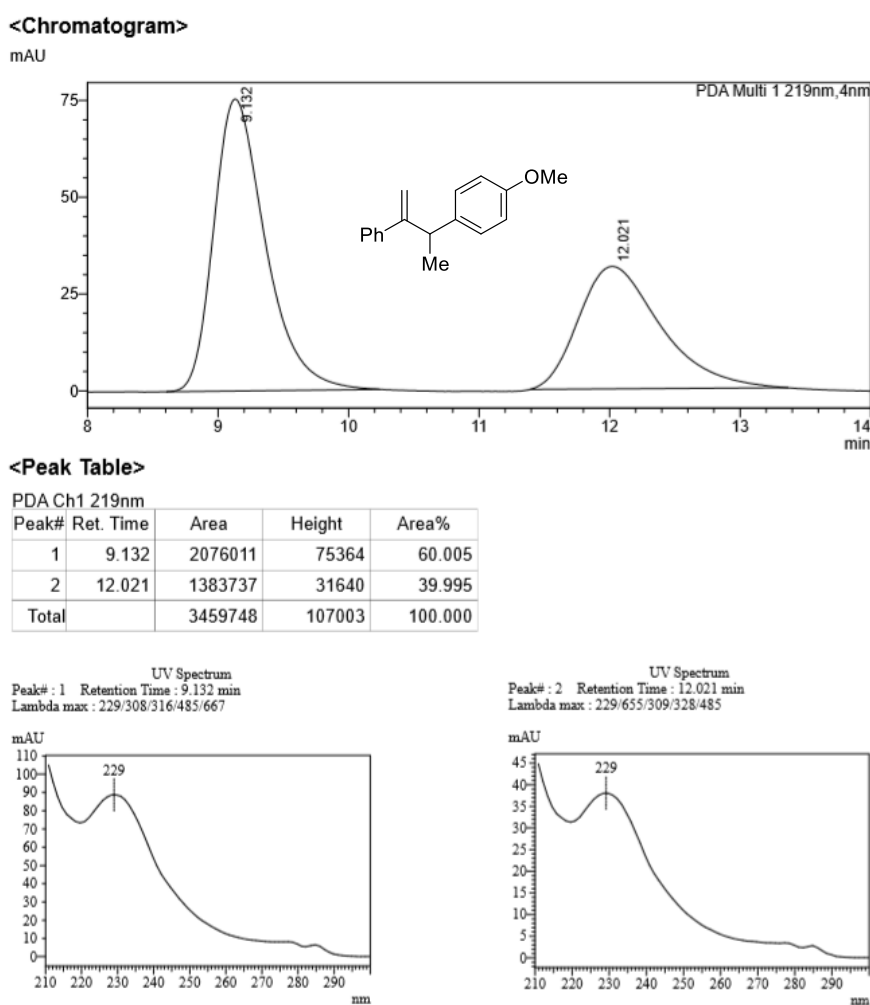


Figure 16: HPLC chromatogram, peak table and footprint for racemic 1-Methoxy-4-(3-phenylbut-3-en-2-yl)benzene (11a and *ent*-11a).

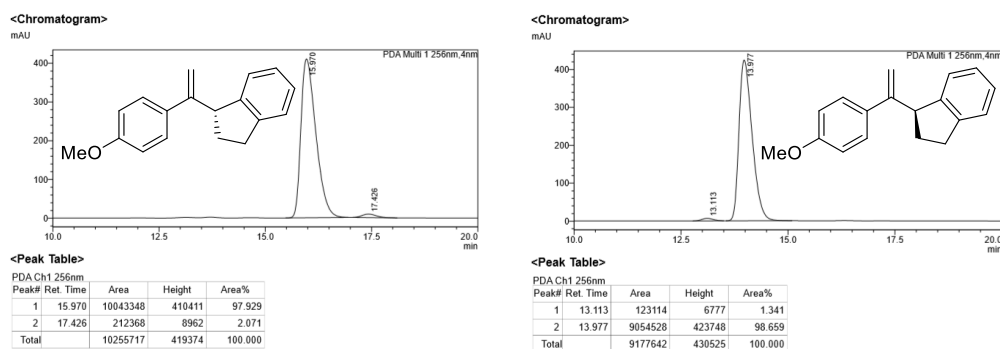


Figure 17: HPLC chromatogram, peak table and footprint for (*R*) and (*S*)-1-(1-(4-Methoxyphenyl)vinyl)-2,3-dihydro-1*H*-indene (*ent*-**11b** and **11b**).

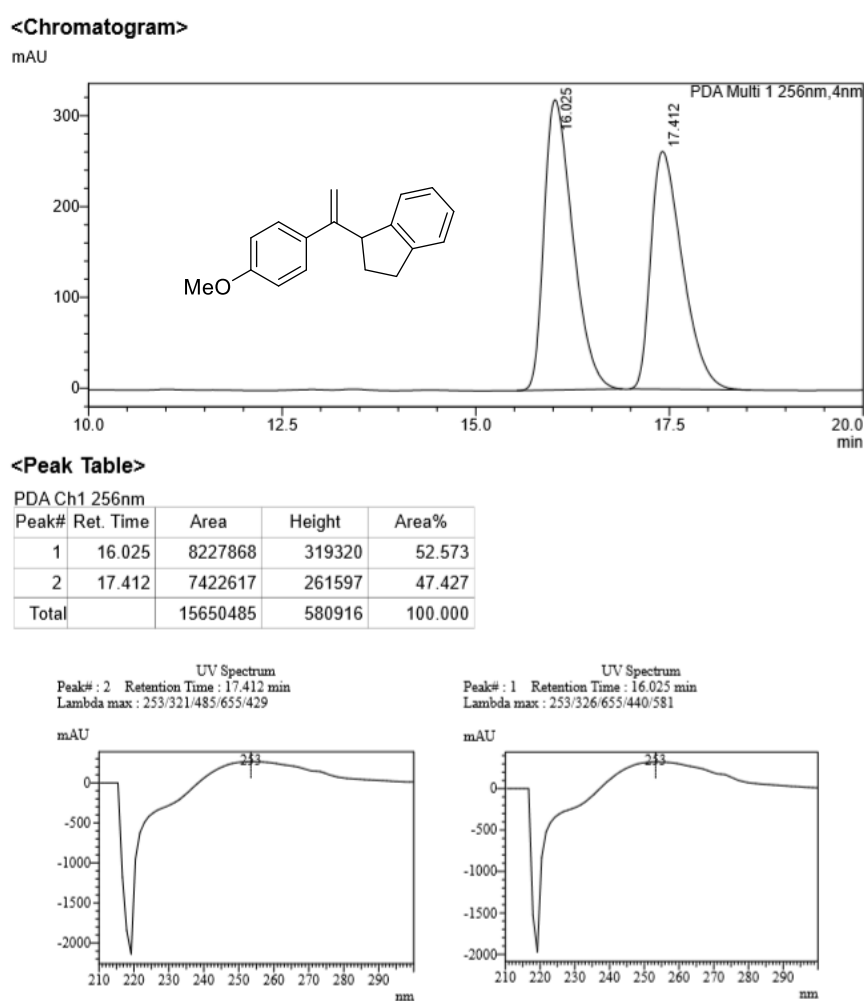


Figure 18: HPLC chromatogram, peak table and footprint for racemic 1-(1-(4-Methoxyphenyl)vinyl)-2,3-dihydro-1*H*-indene (*ent*-**11b** and **11b**).

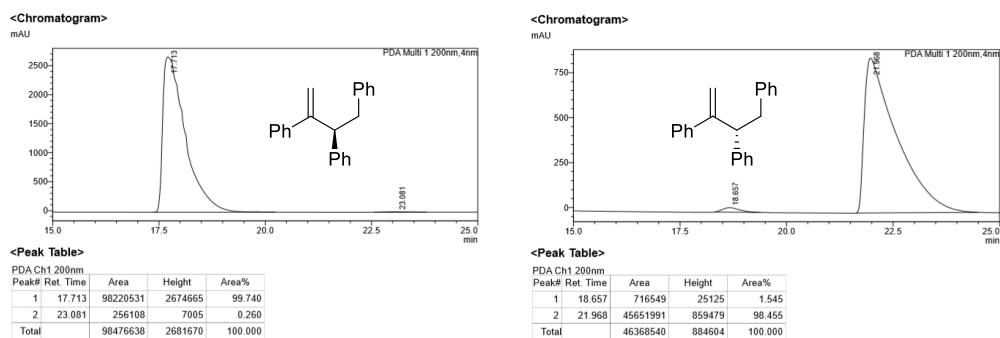


Figure 19: HPLC chromatogram, peak table and footprint for (*S*) and (*R*)-But-3-ene-1,2,3-triyltribenzene (**11c** and *ent*-**11c**).

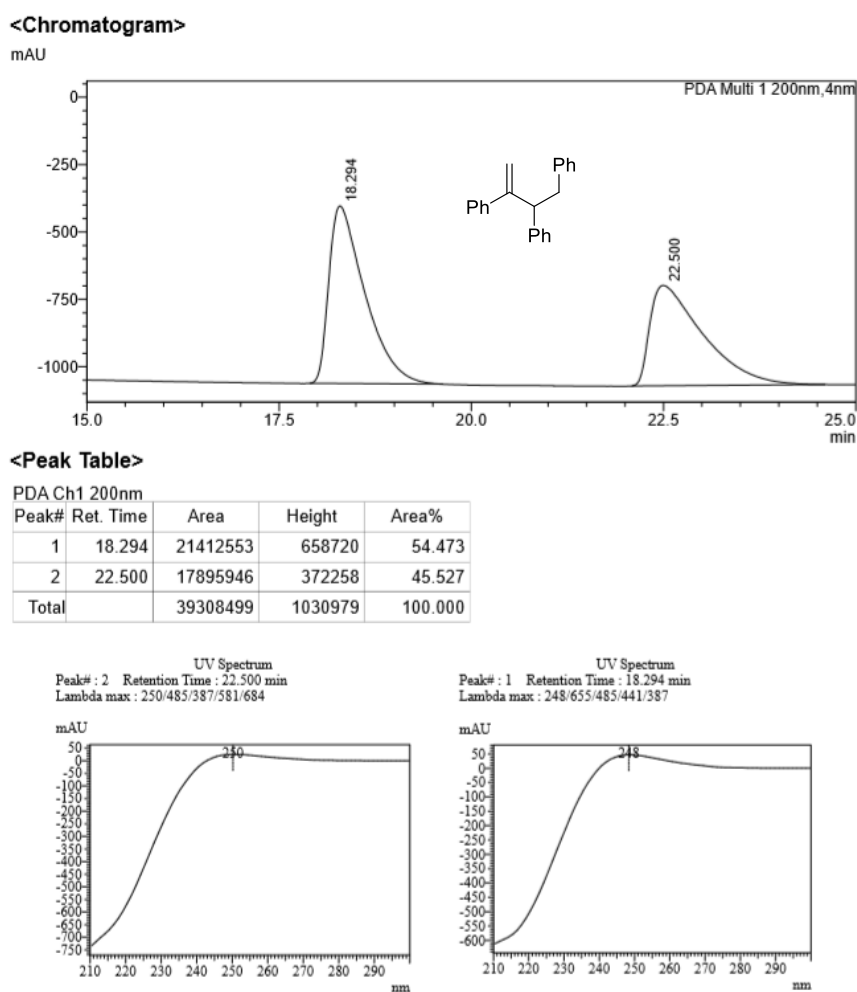


Figure 20: HPLC chromatogram, peak table and footprint for racemic But-3-ene-1,2,3-triyltribenzene (**11c** and *ent*-**11c**).

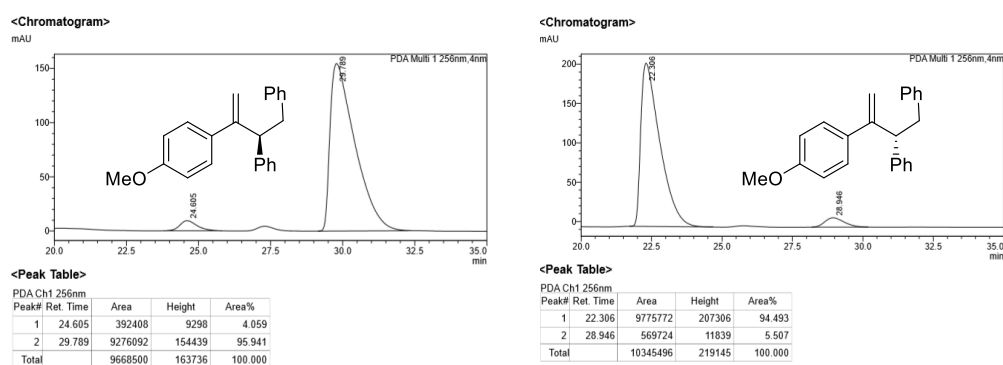


Figure 21: HPLC chromatogram, peak table and footprint for (S) and (R)-(3-(4-Methoxyphenyl)but-3-ene-1,2-diyl)dibenzene (**11d** and *ent*-**11d**).

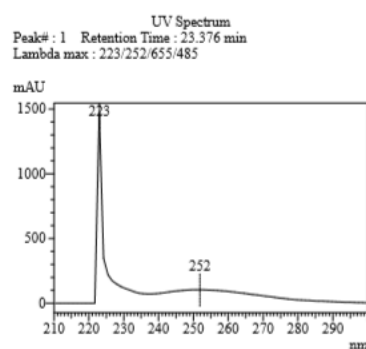
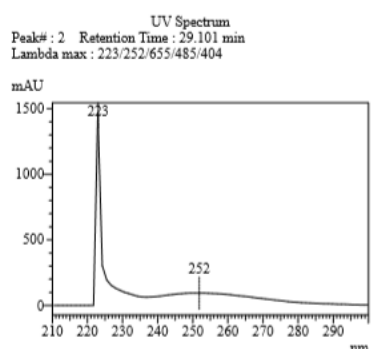
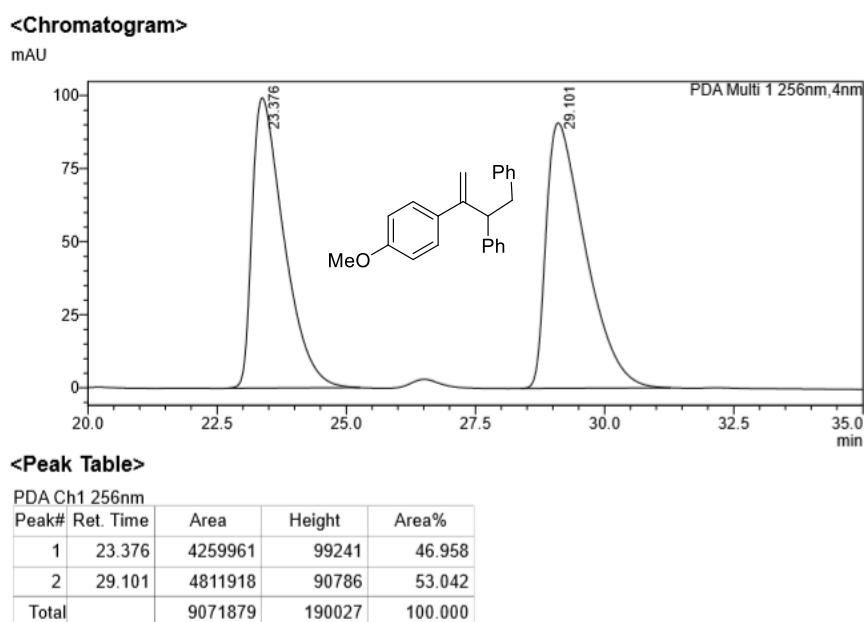


Figure 22: HPLC chromatogram, peak table and footprint for racemic (3-(4-Methoxyphenyl)but-3-ene-1,2-diyl)dibenzene (**11d** and *ent*-**11d**).

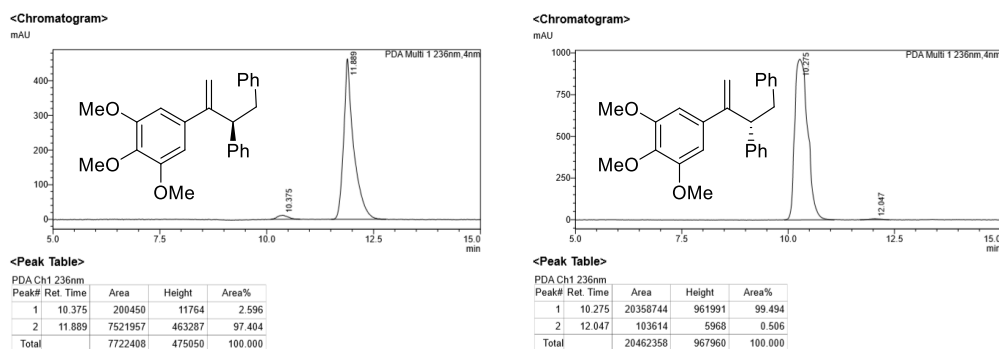


Figure 23: HPLC chromatogram, peak table and footprint for (*S*) and (*R*)-3-(3,4,5-Trimethoxyphenyl)but-3-ene-1,2-diyl)dibenzene (**11e** and *ent*-**11e**).

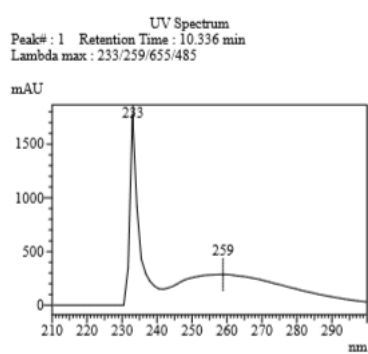
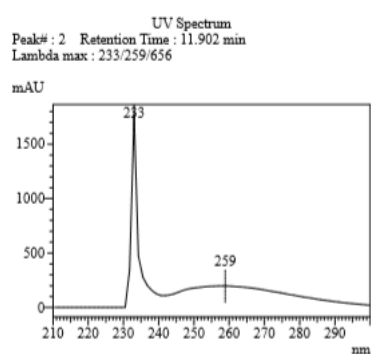
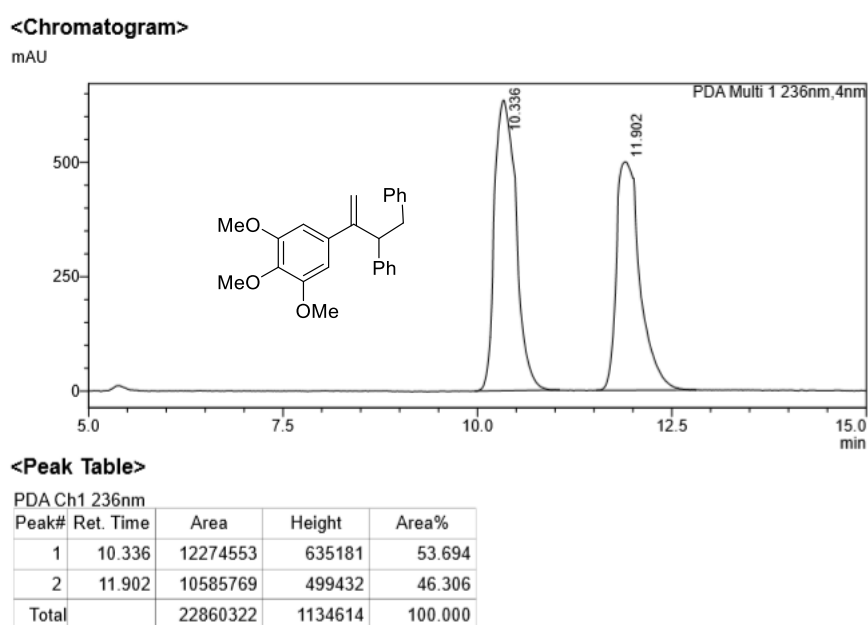
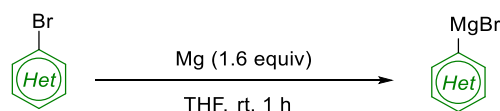


Figure 24: HPLC chromatogram, peak table and footprint for racemic 3-(3,4,5-Trimethoxyphenyl)but-3-ene-1,2-diyl)dibenzene (**11e** and *ent*-**11e**).

5 Electrochemical Synthesis of Biaryls *via* Oxidative Intramolecular Coupling of Tetra(hetero)arylborates²³³

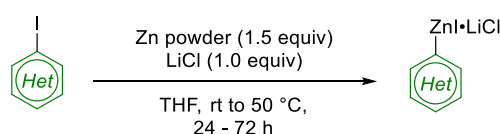
5.1 General Procedures

5.1.1 General Procedure K: Synthesis of Aryl Grignard Reagents



A Schlenk flask was charged with magnesium turnings (972 mg, 40 mmol, 1.6 equiv) and dried *in vacuo* using a heat gun (600 °C, 2 × 5 min). After addition of THF (2.0 mL) and 1,2-dibromoethane (2 drops), the mixture was heated to boil with a heat gun to activate the magnesium. The corresponding aryl bromide (25 mmol, 1.0 equiv) was dissolved in THF (23.0 mL for approximately 1 M solution or 48.0 mL for 0.5 M solution) and added to the activated magnesium suspension dropwise. After completion of the addition, the mixture was stirred for one hour at room temperature to yield a THF-solution of the arylmagnesium reagents.

5.1.2 General Procedure L: Synthesis of Arylzinc Reagents

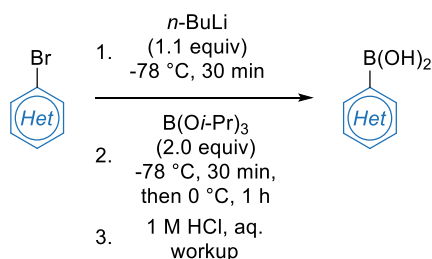


According to a previously reported procedure,²³⁴ a Schlenk flask was charged with LiCl (212 mg, 5.0 mmol, 1.0 equiv) and dried *in vacuo* using a heat gun (500 °C, 2 × 5 min). Zinc powder (490 mg, 7.5 mmol, 1.5 equiv) was added and the flask was dried again *in vacuo* (350 °C, 2 × 5 min). After addition of THF (5.0 mL), 1,2-dibromoethane (2 drops) and TMSCl (5 drops), the mixture was heated to boil with a heat gun to activate the zinc. The corresponding aryl iodide (5.0 mmol, 1.0 equiv) was added neat to the activated zinc suspension at room temperature and the reaction was stirred at 50 °C until complete consumption of the aryl iodide was observed by GC analysis.

²³³ The full supporting information can be found under the following link: <https://doi.org/10.1021/jacs.9b12300>

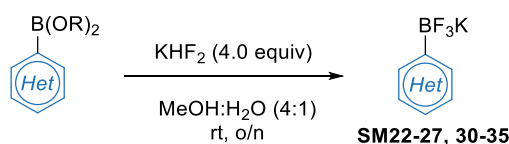
²³⁴ A. Krasovskiy, V. Malakhov, A. Gavryushin, P. Knochel, *Angew. Chem.* **2006**, *118*, 6186–6190.

5.1.3 General Procedure M: Preparation of Aryl Boronic Acids starting from Aryl Bromides



Adapted from a previously reported procedure,²³⁵ commercially available aryl bromides (5.0 mmol, 1.0 equiv) were dissolved in 20 mL of THF and cooled to $-78\text{ }^{\circ}\text{C}$. A solution of $n\text{-BuLi}$ in hexanes (5.5 mmol, 2.43 M, 1.1 equiv) was added dropwise and the reaction stirred for 30 min. $\text{B}(\text{O}i\text{-Pr})_3$ was then added dropwise (10 mmol, 2.0 equiv) and the reaction stirred for further 30 min. The reaction was then allowed to reach $0\text{ }^{\circ}\text{C}$ and was stirred at that temperature for one hour. The reaction was then quenched with 1 M HCl (40 mL) and extracted with EtOAc ($3 \times 50\text{ mL}$). The combined organic phases were dried over MgSO_4 , filtered and concentrated under reduced pressure. The crude product was used without further purification in general procedure N.

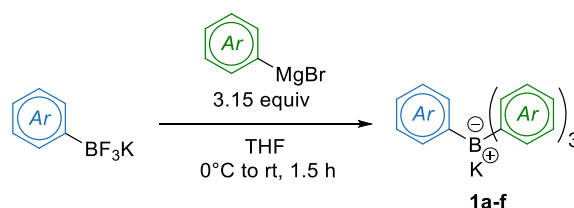
5.1.4 General Procedure N: Preparation of Potassium Trifluoroborate Salts starting from Aryl Boronic Esters and Acids



Adapted from a previously reported procedure,²³⁵ 5.0 mmol (1.0 equiv) of commercially available Aryl pinacol boronic esters, boronic acids or crude intermediates from general procedure M were dissolved in 15 mL of a 4:1 (v/v) mixture of MeOH and H_2O . The mixture was cooled to $0\text{ }^{\circ}\text{C}$ and KHF_2 (4.0 equiv) was added neat. The mixture was vigorously stirred at room temperature overnight and then concentrated under reduced pressure. The remaining solids were extracted with boiling acetone ($2 \times 50\text{ mL}$) and twice with acetone at room temperature ($2 \times 50\text{ mL}$). The acetone was removed under reduced pressure and the remaining solid was dissolved in a minimum amount of boiling acetone, before being treated with diethyl ether, resulting in the precipitation of a colorless solid. The solids were filtered, washed with diethyl ether and dried *in vacuo* to yield potassium aryltrifluoroborate salts **SM22–27** and **SM30–35**. (Note: A recrystallization in hexanes/acetone mixtures was performed in cases, where the desired potassium trifluoroborate salt was not pure by $^1\text{H NMR}$.)

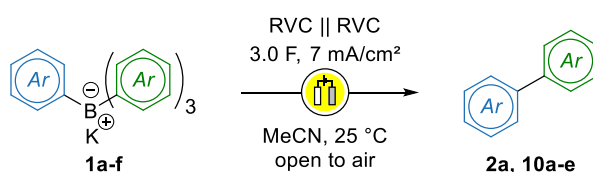
²³⁵ S. Darses, G. Michaud, J.-P. Genet, *Eur. J. Org. Chem.* **1999**, 1875–1883.

5.1.5 General Procedure O: Preparation of Tetra(hetero)arylborate Salts (TABs)



A 25 mL Schlenk flask was charged with the corresponding potassium trifluoroborate salt (3.0 mmol, 1.0 equiv) and 6 mL of THF were added. The mixture was cooled to 0 °C and the desired aryl Grignard reagent (9.45 mmol, 3.15 equiv) was added dropwise over 30 min *via* syringe pump. The reaction was allowed to warm to room temperature and was stirred one hour. The reaction was then quenched with 5 mL of sat. aq. K₂CO₃ solution and extracted with EtOAc (3 × 40 mL). The combined organic phases were filtered and concentrated under reduced pressure. The crude solid product was washed with cold diethyl or diisopropyl ether, filtered and dried *in vacuo* to afford TABs **1a–f**. (Note: The final TABs are very soluble in most organic solvents. Therefore, complete removal of residual EtOAc *in vacuo* is essential for their solidification. Only small amounts of ether are necessary in the washing step, since TABs are also slightly soluble in ethers.)

5.1.6 General Procedure P: Electrochemical Oxidation of TABs into Biaryls

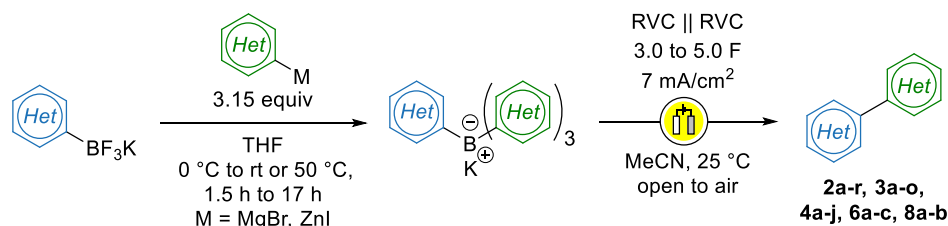


A 10 mL IKA glass vial was charged with 0.40 mmol (1.0 equiv) TAB salt **1a–f** and dissolved in 8 mL of HPLC-grade MeCN. The reaction was started using the IKA ElectraSyn 2.0 with RVC as working and counter electrode under galvanostatic conditions (5 mA, 3.0 F, 700 rpm stirring). The crude mixture was then treated with water and extracted with diethyl ether (3 × 15 mL). The combined organic phases were dried over MgSO₄, filtered and concentrated under reduced pressure. The crude product was purified by column chromatography on silica gel to yield the desired products **2a** and **10a–e**.

a) Adaptation for potentiostatic oxidation of compound **1a**

A 10 mL IKA glass vial was charged with 0.40 mmol (1.0 equiv) TAB salt **1a**, 2.0 mmol (5.0 equiv) of LiClO₄ and dissolved in 8 mL of HPLC-grade MeCN. The reaction was started using the IKA ElectraSyn 2.0 with RVC as working and counter electrode under potentiostatic conditions (1.6 V, 3.0 F, 700 rpm stirring, 60 seconds alternating mode). The crude was then treated with water and extracted with diethyl ether (3 × 15 mL). The combined organic phases were dried over MgSO₄, filtered and concentrated under reduced pressure. The crude product was purified by column chromatography on silica gel to yield the desired product **2a**.

5.1.7 General Procedure Q (Two-pot Procedure): Synthesis of Biaryls starting from Potassium Aryltrifluoroborate Salts



A 25 mL Schlenk flask was charged with the corresponding potassium trifluoroborate salt (0.40 mmol, 1.0 equiv) and 2 mL of THF were added. The mixture was cooled to 0 °C and a solution of the desired aryl Grignard reagent (1.26 mmol, 3.15 equiv) was added dropwise over 30 min *via* syringe pump. The reaction was allowed to warm to room temperature and was stirred one hour. The reaction was then quenched with 5 mL of sat. aq. K_2CO_3 solution and extracted with EtOAc (3 × 40 mL). The combined organic phases were filtered and concentrated under reduced pressure. The crude product was then dissolved in 8 mL of HPLC-grade MeCN and transferred into a 10 mL IKA glass vial. Following general procedure P, products **2a–q**, **3a–g**, **3i–o**, **4c–j** and **8a–b** were isolated.

b) Adaptation for the Use of Arylzinc Reagents

After addition of the arylzinc species (instead of the aryl Grignard reagent as described above) *via* syringe pump, the reaction was heated to 50 °C for 16 hours to ensure full conversion of the potassium trifluoroborate salt into the desired TAB salt. general procedure Q was then followed to give products **2r**, **3h**, **4a–b**, **6a–c**.

5.2 Formation of TAB Salt **1a** by ^{11}B NMR

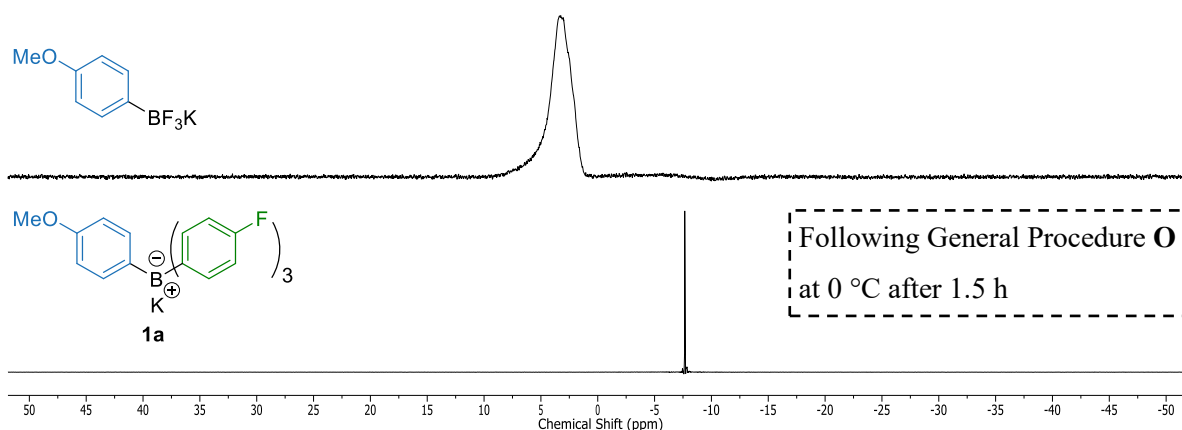


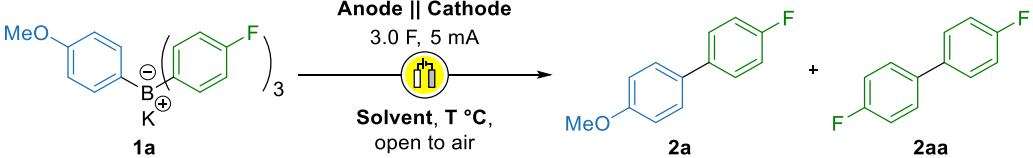
Figure 25: ^{11}B NMR analysis of the TAB salt formation to yield **1a**.

As depicted in Figure 25, a smooth transformation of the starting trifluoro(4-methoxyphenyl)borate into the desired TAB salt **1a** was observed in the crude ^{11}B NMR, which was measured as a 1:1 THF:CD₃CN (v/v) mixture following general procedure O.

5.3 Optimizations

5.3.1 Conditions for the Electrochemical Coupling

Table 7: Screening of different electrode materials and solvents.



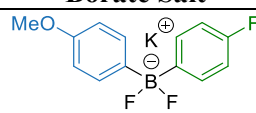
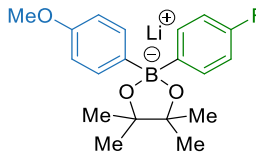
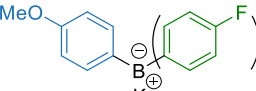
Anode Cathode	Solvent	T (°C)	conv. (%) 2a:2aa
Graphite Graphite	MeCN	25	80:7
GCE GCE ²³⁶	MeCN	25	81:4
RVC RVC	MeCN	25	82:5 (79% isolated)
RVC Platinum	MeCN	25	80:6
RVC RVC	EtOH	25	81:4
RVC RVC	THF	25	50:14
RVC RVC	MeCN	70	82:17

Conversion rates into 4-fluoro-4'-methoxy-1,1'-biphenyl (**2a**) were assessed by hydrolysis and GC analysis with *n*-undecane as an internal standard. As seen in Table 7, the oxidation process can be performed with different carbon or platinum electrode setups, resulting in good conversion and selectivity ratios. In addition, the oxidation process can also be performed in environmentally friendly solvents such as ethanol with only marginal conversion loss.

5.3.2 Attempted Oxidations with Dummy Ligands

Table 8: Screening of different salt materials.



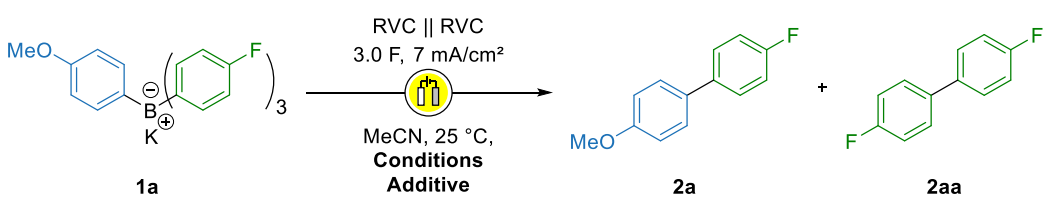
Borate Salt	conv. (%) 2a:2aa
	0:0
	0:0
	82:5

²³⁶ Glassy carbon electrodes.

As seen in Table 8, the oxidation process only leads to the desired product formation when TAB salts are used. Other substituents on the tetracoordinated boron atom such as pinacol or fluoride do not result in any product formation by GC analysis.

5.3.3 Attempted Oxidations with Dummy Ligands

Table 9: Screening of different additives during the electrochemical oxidation.

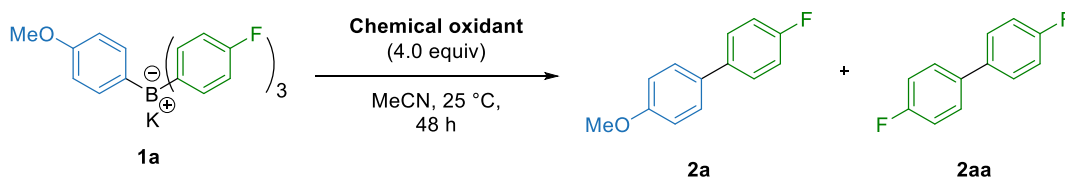


Conditions	Additive	conv. (%) 2a:2aa
Open to air	0.1 M LiClO ₄	63:3
Open to air	-	82:5
O ₂ balloon	-	75:4
Open to air	1,4-Naphthochinon (2 equiv)	82:6
Open to air	TBHP (2 equiv)	55:2
Open to air	CCl ₃ Br (2 equiv)	40:10
N ₂ balloon (inert)	-	80:5
Open to air	H ₂ O (2 mol%)	81:4
Open to air	H ₂ O (5 mol%)	81:4
Open to air	BHT (2 equiv)	79:4
Open to air	TEMPO (2.0 equiv)	80:4
Open to air	<i>t</i> -BuOH (5.0 equiv)	82:5

As seen in Table 9, electrolyte slows the reaction down significantly. In addition, externally added oxidants do not improve conversion rates and small amounts of water have no impact on the conversion rates. Lastly, no radical species could be trapped by using TEMPO or BHT as trapping agents.

5.3.4 Oxidative Couplings with Chemical Oxidants

Table 10: Screening of different chemical oxidants.



Chemical oxidant	conv. (%) 2a:2aa
Ceric ammonium nitrate (CAN)	34:14
Phenyliodine(II) diacetate (PIDA)	35:9
Ferrocenium tetrafluoroborate	68:7
Iodine	0:0
NBS	0:0

As seen in Table 10, the oxidation process can also be performed using several equivalents of chemical oxidants instead of the presented electrochemical oxidation. Best results are achieved using ferrocenium tetrafluoroborate, where a decent selectivity for the formation of biaryl **2a** was observed. Two-electron oxidants such as Iodine or NBS do not result in any biaryl coupling products.

5.4 NMR Experiments

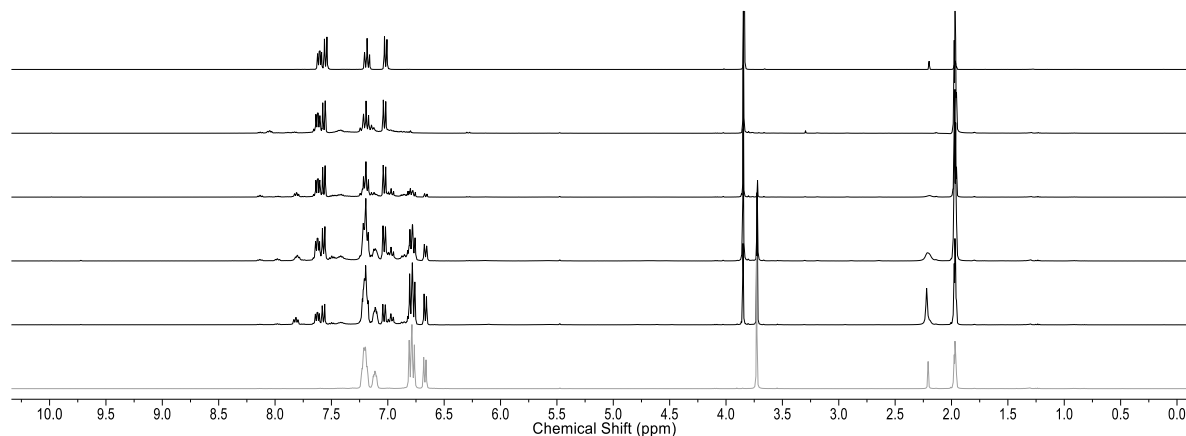
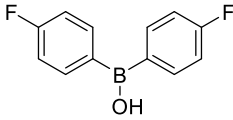


Figure 26: ^1H NMR analysis of the electrochemical oxidation in CD_3CN .

As seen in Figure 26, the TAB salt **1a** is consumed after approximately 2.5 F. In addition, the crude NMR shows only marginal side product formation. The residual water within the CD_3CN is consumed within the oxidative process, which indicates that it is essential for the formation of the aryl borinic acid, which is the main side product of the transformation. Interestingly, the borinic acid seems to be consumed during the electrochemical process, probably due to oxidation into the corresponding boronic acid. However, it can still be isolated after 3.0 F as a colorless solid in 33% yield and gives further indication for the plausibility of the proposed mechanism of this electrochemical process. Figure 27 shows the ^1H and ^{11}B NMR of the isolated boronic acid.

Bis(4-fluorophenyl)(hydroxy)borane (**2ab**)

 $R_f = 0.51$ (DCM/MeOH 100:0, UV, KMnO_4 , PAA). ^1H NMR (400 MHz, CDCl_3) δ 7.78 (dd, $J = 8.2, 6.3$ Hz, 4H), 7.14 (dd, $J = 8.8, 8.8$ Hz, 4H), 5.85 (s, 1H) ppm. ^{11}B NMR (128 MHz, CDCl_3) δ 39.61 ppm. Analytical data in accordance to literature.²³⁷

²³⁷ X. Chen, H. Ke, Y. Chen, C. Guan, G. Zou, *J. Org. Chem.* **2012**, *77*, 7572–7578.

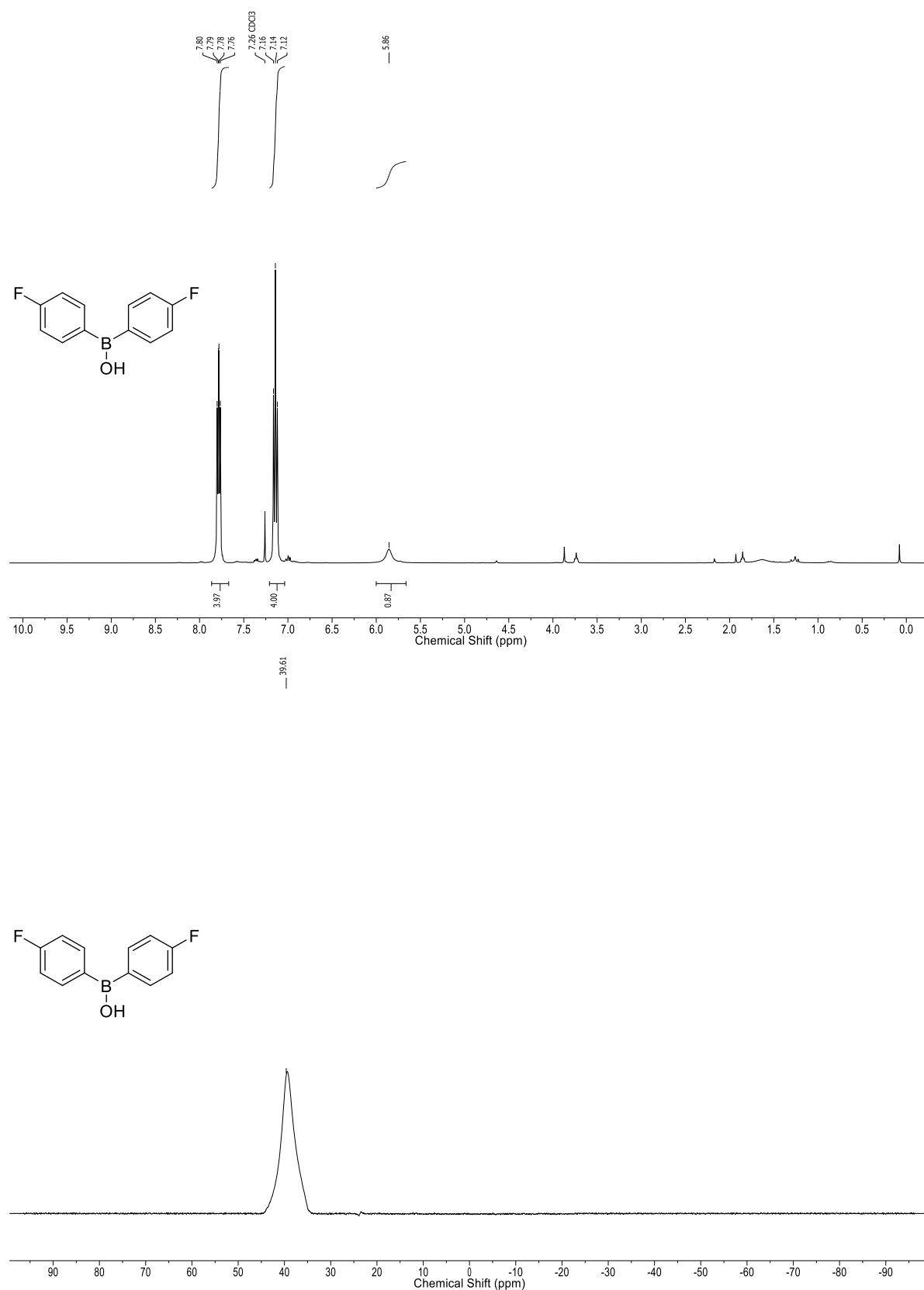
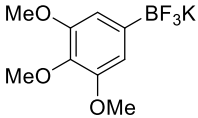


Figure 27: ¹H NMR (400 MHz, CDCl₃) and ¹¹B NMR (128 MHz, CDCl₃) of acid **2ab**.

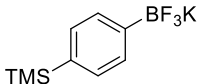
5.5 Experimental Data

5.5.1 Synthesis of Potassium Aryl Trifluoroborate Salts

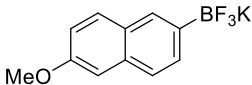
Potassium trifluoro(3,4,5-trimethoxyphenyl)borate (SM22)


 Using 5-bromo-1,2,3-trimethoxybenzene according to general procedure **M** (10.0 mmol scale), provided **SM22** (6.57 mmol, 1.81 g, 66%) as a colorless solid. **¹H NMR** (400 MHz, CD₃CN) δ 6.69 (s, 2H), 3.78 (s, 6H), 3.66 (s, 3H) ppm. **HRMS** (ESI-Quadrupole): *m/z* calcd for C₉H₁₁BF₃O₃⁻ [M-K]: 235.0759; found: 235.0757. Analytical data in accordance to literature.²³⁸

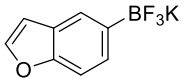
Potassium trifluoro(4-(trimethylsilyl)phenyl)borate (SM23)


 Using (4-(trimethylsilyl)phenyl)boronic acid according to general procedure **N** (4.33 mmol scale), provided **SM23** (4.26 mmol, 1.09 g, 98%) as a colorless solid. **¹H NMR** (400 MHz, CD₃CN) δ 7.42 (d, *J* = 7.3 Hz, 2H), 7.35 (d, *J* = 6.3 Hz, 2H), 0.22 (s, 9H) ppm. **HRMS** (ESI-Quadrupole): *m/z* calcd for C₉H₁₃BF₃Si⁻ [M-K]: 217.0837; found: 217.0835. Analytical data in accordance to literature.²³⁹

Potassium trifluoro(6-methoxynaphthalen-2-yl)borate (SM24)


 Using 2-bromo-6-methoxynaphthalene according to general procedure **M** (5.0 mmol scale), provided **SM24** (3.97 mmol, 1.05 g, 79%) as a colorless solid. **¹H NMR** (400 MHz, CD₃CN) δ 7.82 (s, 1H), 7.69 (d, *J* = 8.9 Hz, 1H), 7.60 – 7.55 (m, 2H), 7.16 (d, *J* = 2.6 Hz, 1H), 7.02 (dd, *J* = 8.9, 2.6 Hz, 1H), 3.87 (s, 3H) ppm. **HRMS** (ESI-Quadrupole): *m/z* calcd for C₁₁H₉BF₃O⁻ [M-K]: 225.0704; found: 225.0702. Analytical data in accordance to literature.²⁴⁰

Potassium benzofuran-5-yltrifluoroborate (SM25)

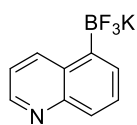

 Using 5-bromobenzofuran according to general procedure **M** (4.7 mmol scale), provided **SM25** (1.58 mmol, 354 mg, 34%) as a colorless solid. **¹H NMR** (400 MHz, CD₃CN) δ 7.67 (s, 1H), 7.61 (d, *J* = 2.2 Hz, 1H), 7.41 (d, *J* = 7.1 Hz, 1H), 7.32 (d, *J* = 8.0 Hz, 1H), 6.75 (dd, *J* = 2.2, 1.0 Hz, 1H) ppm. **HRMS** (ESI-Quadrupole): *m/z* calcd for C₈H₅BF₃O⁻ [M-K]: 185.0391; found: 185.0389. Analytical data in accordance to literature.²⁴¹

²³⁸ E. F. Santos-Filho, J. C. Sousa, N. M. M. Bezerra, P. H. Menezes, *Tetrahedron Lett.* **2011**, 52, 5288–5291.

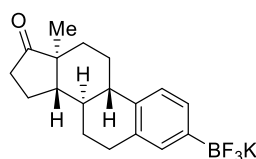
²³⁹ N. M. Ellis, G. A. Molander, *J. Org. Chem.* **2006**, 71, 7491–7493.

²⁴⁰ J. Lindh, J. Sävmarker, P. Nilsson, P. J. R. Sjöberg, M. Larhed, *Chem. Eur. J.* **2009**, 15, 4630–4636.

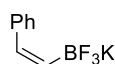
²⁴¹ L. N. Cavalcanti, C. García-García, G. A. Molander, *J. Org. Chem.* **2013**, 78, 6427–6439.

Potassium trifluoro(quinolin-5-yl)borate (SM26)

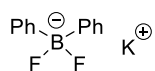
Using 5-bromoquinoline according to general procedure **M** (5.0 mmol scale), provided **SM26** (1.32 mmol, 310 mg, 26%) as a light-yellow solid. $^1\text{H NMR}$ (400 MHz, CD_3CN) δ 8.92 (d, $J = 8.5$ Hz, 1H), 8.77 (dd, $J = 4.4, 1.8$ Hz, 1H), 7.82 (d, $J = 8.3$ Hz, 1H), 7.75 (d, $J = 6.7$ Hz, 1H), 7.62 (t, $J = 7.5$ Hz, 1H), 7.42 (dd, $J = 8.5, 4.3$ Hz, 1H) ppm. **HRMS** (ESI-Quadrupole): m/z calcd for $\text{C}_9\text{H}_6\text{BF}_3\text{N}^- [\text{M-K}]^-$: 196.0551; found: 196.0549. Analytical data in accordance to literature.²³⁹

Potassium 3-deoxyestrone-3-trifluoroborate (SM27)

Using 3-deoxyestrone-3-boronic acid pinacol ester²⁴⁰ according to general procedure **N** (2.9 mmol scale), provided **SM27** (1.42 mmol, 510 mg, 49%) as a colorless solid. $^1\text{H NMR}$ (400 MHz, CD_3CN) δ 7.16 (d, $J = 7.7$ Hz, 1H), 7.13 (s, 1H), 7.08 (d, $J = 7.7$ Hz, 1H), 2.91 – 2.79 (m, 2H), 2.48 – 2.36 (m, 2H), 2.29 – 2.20 (m, 1H), 2.12 – 1.96 (m, 3H), 1.86 – 1.79 (m, 1H), 1.66 – 1.33 (m, 6H), 0.88 (s, 3H) ppm. **HRMS** (ESI-Quadrupole): m/z calcd for $\text{C}_{18}\text{H}_{21}\text{BF}_3\text{O}^- [\text{M-K}]^-$: 321.1643; found: 321.1644. Analytical data in accordance to literature.²⁴²

Potassium (Z)-styryltrifluoroborate (SM28)

Following a procedure published by Molander *et al.* (5.0 mmol scale),²⁴³ provided **SM28** (2.67 mmol, 0.56 g, 53%) as a colorless solid. $^1\text{H NMR}$ (400 MHz, $(\text{CD}_3)_2\text{CO}$) δ 7.68 – 7.63 (m, 2H), 7.16 (t, $J = 7.7$ Hz, 2H), 7.07 – 7.00 (m, 1H), 6.61 – 6.47 (m, 1H), 5.70 (m, 1H) ppm. **HRMS** (ESI-Quadrupole): m/z calcd for $\text{C}_8\text{H}_7\text{BF}_3^- [\text{M-K}]^-$: 171.0593; found: 171.0598. Analytical data in accordance to literature.²⁴³

Potassium difluorodiphenylborate (SM29)

Following a procedure published by Ito *et al.* (10.0 mmol scale),²⁴⁴ provided **SM29** (7.85 mmol, 1.90 g, 79%) as a colorless solid. $^1\text{H NMR}$ (400 MHz, $\text{DMSO}-d_6$) δ 7.33 (d, $J = 6.7$ Hz, 4H), 7.02 (t, $J = 7.3$ Hz, 4H), 6.95 – 6.87 (m, 2H) ppm. **HRMS** (ESI-Quadrupole): m/z calcd for $\text{C}_{12}\text{H}_{10}\text{BF}_2^- [\text{M-K}]^-$: 203.0849; found: 203.0847. Analytical data in accordance to literature.²⁴⁴

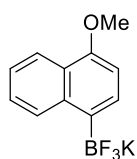
²⁴² D. van der Born, C. Sewing, J. (Koos) D. M. Herscheid, A. D. Windhorst, R. V. A. Orru, D. J. Vugts, *Angew. Chem. Int. Ed.* **2014**, *53*, 11046–11050.

²⁴³ G. A. Molander, C. R. Bernardi, *J. Org. Chem.* **2002**, *67*, 8424–8429.

²⁴⁴ T. Ito, T. Iwai, T. Mizuno, Y. Ishino, *Synlett* **2003**, *10*, 1435–1438.

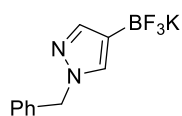
5.5.2 Characterization of Potassium Aryl Trifluoroborate Salts

Potassium trifluoro(4-methoxynaphthalen-1-yl)borate (SM30)



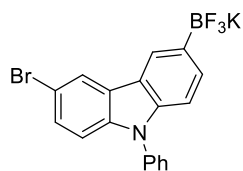
Using 1-bromo-4-methoxynaphthalene according to general procedure **M** (5.0 mmol scale), provided **SM30** (3.82 mmol, 1.10 g, 76%) as a colorless solid. $^1\text{H NMR}$ (400 MHz, CD_3CN) δ 8.43 – 8.33 (m, 1H), 8.16 – 8.10 (m, 1H), 7.55 (d, $J = 7.6$ Hz, 1H), 7.43 – 7.30 (m, 2H), 6.79 (d, $J = 7.6$ Hz, 1H), 3.95 (s, 3H) ppm. $^{13}\text{C NMR}$ (101 MHz, CD_3CN) δ 154.6, 138.6, 130.7, 129.7, 126.2, 125.3, 124.4, 121.9, 104.3, 55.7 ppm. The signal for the carbon atom adjacent to the boron center was not observed. $^{11}\text{B NMR}$ (128 MHz, CD_3CN) δ 3.88 (q, $J = 56.2$ Hz) ppm. $^{19}\text{F NMR}$ (377 MHz, CD_3CN) δ -137.40 – -138.18 (m) ppm. **HRMS** (ESI-Quadrupole): m/z calcd for $\text{C}_{11}\text{H}_9\text{BF}_3\text{O}^-$ [M-K] $^-$: 225.0704; found: 225.0702. **IR** (Diamond-ATR, neat) $\tilde{\nu}_{\text{max}}$ (cm^{-1}): 1580 (m), 1509 (m), 1460 (w), 1448 (w), 1421 (m), 1366 (w), 1315 (m), 1243 (w), 1220 (m), 1194 (m), 1154 (s), 1096 (m), 1072 (m), 1060 (s), 1028 (m), 1004 (m), 986 (s), 963 (m), 942 (m), 931 (m), 906 (s), 885 (s), 872 (m), 844 (w), 824 (s), 791 (m), 766 (vs). **Mp** ($^\circ\text{C}$) = 248–252.

Potassium (1-benzyl-1*H*-pyrazol-4-yl)trifluoroborate (SM31)



Using 1-benzyl-4-(4,4,5,5-tetramethyl-1,3,2-dioxaborolan-2-yl)-1*H*-pyrazole according to general procedure **N** (3.5 mmol scale), provided **SM31** (1.00 mmol, 264 mg, 28%) as a colorless solid. $^1\text{H NMR}$ (400 MHz, CD_3CN) δ 7.35 – 7.29 (m, 2H), 7.28 – 7.22 (m, 3H), 7.21 – 7.16 (m, 2H), 5.21 (s, 2H) ppm. $^{13}\text{C NMR}$ (101 MHz, CD_3CN) δ 143.4, 139.8, 132.2, 129.3, 128.3, 128.2, 55.4 ppm. The signal for the carbon atom adjacent to the boron center was not observed. $^{11}\text{B NMR}$ (128 MHz, CD_3CN) δ 3.04 (q, $J = 52.6$ Hz) ppm. $^{19}\text{F NMR}$ (377 MHz, CD_3CN) δ -136.25 – -136.87 (m) ppm. **HRMS** (ESI-Quadrupole): m/z calcd for $\text{C}_{10}\text{H}_9\text{BF}_3\text{N}_2^-$ [M-K] $^-$: 225.0816; found: 225.0815. **IR** (Diamond-ATR, neat) $\tilde{\nu}_{\text{max}}$ (cm^{-1}): 1541 (m), 1455 (w), 1434 (w), 1356 (w), 1336 (w), 1204 (m), 1173 (m), 1161 (m), 1078 (w), 1064 (w), 1050 (m), 1027 (m), 1006 (m), 979 (m), 971 (m), 919 (vs), 900 (s), 857 (s), 814 (m), 807 (m), 790 (w), 776 (w), 759 (w), 749 (w), 719 (vs). **Mp** ($^\circ\text{C}$) = 222–227.

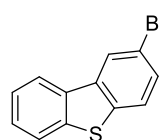
Potassium (6-bromo-9-phenyl-9*H*-carbazol-3-yl)trifluoroborate (SM32)



Using 3,6-dibromo-9-phenyl-9*H*-carbazole according to general procedure **M** (5.0 mmol scale), provided **SM32** (4.55 mmol, 1.94 g, 90%) as a light-brown solid. $^1\text{H NMR}$ (400 MHz, CD_3CN) δ 8.33 (d, $J = 2.0$ Hz, 1H), 8.25 (s, 1H), 7.67 – 7.56 (m, 5H), 7.52 – 7.46 (m, 1H), 7.43 (dd, $J = 8.7, 2.0$ Hz, 1H), 7.28 (d, $J = 8.7$ Hz, 1H), 7.24 (d, $J = 8.2$ Hz, 1H) ppm. $^{13}\text{C NMR}$ (101 MHz, CD_3CN) δ 141.3, 140.0, 138.5, 131.9, 130.8, 128.3, 128.3, 127.6, 126.9, 123.9, 123.6, 122.2, 112.4, 111.9, 109.1 ppm. The signal for the carbon atom adjacent to the boron center was not observed. $^{11}\text{B NMR}$ (128 MHz, CD_3CN) δ 3.76 (br, s) ppm. $^{19}\text{F NMR}$ (377 MHz, CD_3CN) δ -140.89 (br, s) ppm. **HRMS** (ESI-Quadrupole): m/z calcd for $\text{C}_{18}\text{H}_{11}\text{BBrF}_3\text{N}^-$ [M-K] $^-$: 388.0126; found: 388.0126. **IR** (Diamond-ATR, neat) $\tilde{\nu}_{\text{max}}$ (cm^{-1}): 1622 (w),

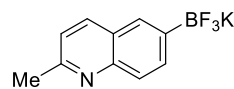
1597 (m), 1501 (s), 1478 (m), 1466 (m), 1436 (m), 1360 (w), 1279 (m), 1270 (s), 1230 (m), 1197 (s), 1174 (m), 1160 (m), 1137 (w), 1119 (w), 1074 (w), 1056 (m), 970 (vs), 935 (vs), 893 (s), 812 (vs), 758 (s). **Mp** (°C) = 296–300.

Potassium dibenzo[*b,d*]thiophen-2-yltrifluoroborate (SM33)



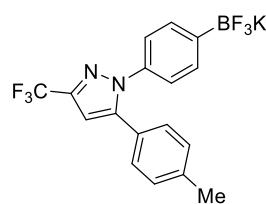
Using 2-bromodibenzo[*b,d*]thiophene according to general procedure **M** (5.0 mmol scale), provided **SM33** (2.41 mmol, 700 mg, 48%) as a colorless solid. **¹H NMR** (400 MHz, CD₃CN) δ 8.34 (s, 1H), 8.29 – 8.23 (m, 1H), 7.91 – 7.85 (m, 1H), 7.74 (dt, *J* = 7.9, 0.7 Hz, 1H), 7.62 (d, *J* = 6.8 Hz, 1H), 7.48 – 7.40 (m, 2H) ppm. **¹³C NMR** (101 MHz, CD₃CN) δ 139.7, 137.4, 137.2, 135.1, 132.1, 126.9, 125.2, 125.1, 123.5, 122.4, 121.7 ppm. The signal for the carbon atom adjacent to the boron center was not observed. **¹¹B NMR** (128 MHz, CD₃CN) δ 3.55 (q, *J* = 56.4 Hz) ppm. **¹⁹F NMR** (377 MHz, CD₃CN) δ -141.42 – -142.10 (m) ppm. **HRMS** (ESI-Quadrupole): *m/z* calcd for C₁₂H₇BF₃S⁻ [M-K]⁻: 251.0319; found: 251.0318. **IR** (Diamond-ATR, neat) $\tilde{\nu}_{max}$ (cm⁻¹): 1601 (w), 1589 (w), 1466 (w), 1431 (w), 1400 (w), 1320 (w), 1271 (m), 1230 (m), 1194 (m), 1151 (m), 1136 (w), 1078 (m), 1067 (m), 1020 (m), 958 (s), 936 (vs), 926 (vs), 900 (m), 882 (s), 820 (s), 800 (s), 765 (vs), 736 (s). **Mp** (°C) = 268–272.

Potassium trifluoro(2-methylquinolin-6-yl)borate (SM34)



Using 6-bromo-2-methylquinoline according to general procedure **M** (5.0 mmol scale), provided **SM34** (3.25 mmol, 810 mg, 65%) as a colorless solid. **¹H NMR** (400 MHz, CD₃CN) δ 8.11 (d, *J* = 8.3 Hz, 1H), 7.89 (s, 1H), 7.84 (d, *J* = 7.0 Hz, 1H), 7.74 (d, *J* = 7.3 Hz, 1H), 7.27 (d, *J* = 8.4 Hz, 1H), 2.65 (s, 3H) ppm. **¹³C NMR** (101 MHz, CD₃CN) δ 157.7, 147.4, 137.5, 135.3, 130.4, 127.0, 126.1, 121.8, 24.9 ppm. The signal for the carbon atom adjacent to the boron center was not observed. **¹¹B NMR** (128 MHz, CD₃CN) δ 3.30 (q, *J* = 53.7 Hz) ppm. **¹⁹F NMR** (377 MHz, CD₃CN) δ -141.95 – -142.48 (m) ppm. **HRMS** (ESI-Quadrupole): *m/z* calcd for C₁₀H₈BF₃N⁻ [M-K]⁻: 210.0707; found: 210.0706. **IR** (Diamond-ATR, neat) $\tilde{\nu}_{max}$ (cm⁻¹): 1646 (w), 1621 (w), 1593 (w), 1567 (w), 1558 (w), 1532 (m), 1476 (m), 1464 (m), 1448 (m), 1439 (m), 1384 (m), 1336 (w), 1226 (s), 1174 (s), 1150 (m), 1135 (m), 1123 (m), 1072 (w), 1035 (m), 1002 (s), 983 (s), 960 (s), 942 (vs), 884 (vs), 842 (m), 830 (s), 819 (s), 798 (s). **Mp** (°C) >300.

Potassium trifluoro(4-(5-(*p*-tolyl)-3-(trifluoromethyl)-1*H*-pyrazol-1-yl)phenyl)borate (SM35)

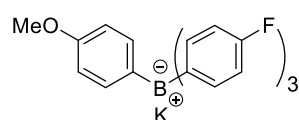


Using 1-(4-bromophenyl)-5-(*p*-tolyl)-3-(trifluoromethyl)-1*H*-pyrazole according to general procedure **M** (9.5 mmol scale), provided **SM35** (7.35 mmol, 3.01 g, 77%) as a colorless solid. **¹H NMR** (400 MHz, CD₃CN) δ 7.49 – 7.43 (m, 2H), 7.16 – 7.14 (m, 4H), 7.08 (d, *J* = 7.6 Hz, 2H), 6.85 (s, 1H), 2.32 (s, 3H) ppm. **¹³C NMR** (101 MHz, CD₃CN) δ 145.9, 142.5 (q, *J* = 37.6 Hz), 140.0, 138.0, 132.8, 130.0, 129.7, 127.4, 124.8, 122.8 (q, *J* = 267.6 Hz), 105.6, 21.1 ppm. The signal for the carbon atom adjacent to the boron center was not observed. **¹¹B NMR** (128 MHz, CD₃CN) δ 3.16 (br,

s) ppm. ^{19}F NMR (377 MHz, CD_3CN) δ -62.52, -142.26 – -142.89 (m) ppm. **HRMS** (ESI-Quadrupole): m/z calcd for $\text{C}_{17}\text{H}_{12}\text{BF}_6\text{N}_2^- [\text{M-K}]^-$: 369.1003; found: 369.1007. **IR** (Diamond-ATR, neat) $\tilde{\nu}_{\text{max}}$ (cm^{-1}): 1604 (w), 1506 (w), 1473 (m), 1449 (m), 1396 (w), 1376 (w), 1275 (w), 1233 (s), 1210 (s), 1160 (s), 1128 (s), 1097 (m), 1067 (w), 978 (s), 954 (vs), 866 (w), 831 (s), 802 (s), 772 (w), 753 (m), 732 (m). **Mp** ($^\circ\text{C}$) = 295–299.

5.5.3 Characterization of TAB Salts

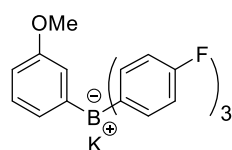
Potassium tris(4-fluorophenyl)(4-methoxyphenyl)borate (**1a**)



Using potassium 4-methoxyphenyltrifluoroborate and a solution of 4-fluorophenylmagnesium bromide in THF according to general procedure **O** (3.0 mmol scale), provided **1a** (2.49 mmol, 1.10 g, 83%) as a colorless solid.

^1H NMR (400 MHz, CD_3CN) δ 7.21 – 7.13 (m, 6H), 7.11 – 7.04 (m, 2H), 6.79 – 6.71 (m, 6H), 6.66 – 6.61 (m, 2H), 3.70 (s, 3H) ppm. ^{13}C NMR (101 MHz, CD_3CN) δ 161.9, 160.4 (d, $J = 3.5$ Hz), 159.9 (d, $J = 3.3$ Hz), 159.6, 159.4 (d, $J = 3.3$ Hz), 158.9 (d, $J = 3.3$ Hz), 156.7, 137.4 (ddd, $J = 5.4, 3.3, 1.6$ Hz), 137.0 (dd, $J = 3.4, 1.6$ Hz), 112.8 (dd, $J = 6.1, 3.0$ Hz), 112.6 (dd, $J = 6.1, 3.0$ Hz), 112.4 (dd, $J = 6.0, 2.9$ Hz), 55.2 ppm. The signals for the carbon atoms adjacent to the boron center were not observed. ^{11}B NMR (128 MHz, CD_3CN) δ -7.66 ppm. ^{19}F NMR (377 MHz, CD_3CN) δ -124.85 (tt, $J = 10.2, 7.0$ Hz) ppm. **HRMS** (ESI-Quadrupole): m/z calcd for $\text{C}_{25}\text{H}_{19}\text{BF}_3\text{O}^- [\text{M-K}]^-$: 403.1487; found: 403.1486. **IR** (Diamond-ATR, neat) $\tilde{\nu}_{\text{ax}}$ (cm^{-1}): 1579 (m), 1486 (s), 1462 (w), 1272 (w), 1259 (w), 1244 (w), 1218 (s), 1176 (w), 1159 (s), 1147 (w), 1086 (w), 1035 (w), 1015 (w), 841 (m), 816 (vs), 787 (w), 775 (w). **Mp** ($^\circ\text{C}$) >300.

Potassium tris(4-fluorophenyl)(3-methoxyphenyl)borate (**1b**)

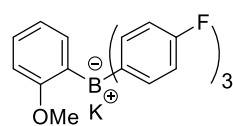


Using potassium 3-methoxyphenyltrifluoroborate and a solution of 4-fluorophenylmagnesium bromide in THF according to general procedure **O** (3.0 mmol scale), provided **1b** (2.10 mmol, 929 mg, 70%) as a colorless solid. ^1H NMR

(400 MHz, CD_3CN) δ 7.23 – 7.14 (m, 6H), 6.96 (t, $J = 7.6$ Hz, 1H), 6.81 – 6.71 (m, 8H), 6.46 (ddd, $J = 7.9, 2.9, 1.0$ Hz, 1H), 3.62 (s, 3H) ppm. ^{13}C NMR (101 MHz, CD_3CN) δ 161.9, 159.9 (d, $J = 3.5$ Hz), 159.6, 159.4 (d, $J = 3.3$ Hz), 158.9 (q, $J = 3.4$ Hz), 158.4 (d, $J = 3.4$ Hz), 137.4 (ddd, $J = 5.5, 3.5, 1.8$ Hz), 129.3 – 129.0 (m), 127.3 (dd, $J = 6.3, 3.1$ Hz), 122.3 – 122.2 (m), 112.8 (dd, $J = 6.2, 3.0$ Hz), 112.6 (dd, $J = 6.1, 3.0$ Hz), 107.5, 54.9 ppm. The signals for the carbon atoms adjacent to the boron center were not observed. ^{11}B NMR (128 MHz, CD_3CN) δ -7.34 ppm. ^{19}F NMR (377 MHz, CD_3CN) δ -124.64 (tt, $J = 10.2, 7.0$ Hz) ppm. **HRMS** (ESI-Quadrupole): m/z calcd for $\text{C}_{25}\text{H}_{19}\text{BF}_3\text{O}^- [\text{M-K}]^-$: 403.1487; found: 403.1485. **IR** (Diamond-ATR, neat) $\tilde{\nu}_{\text{max}}$ (cm^{-1}): 1703 (w), 1578 (s), 1568 (m), 1487 (s), 1476 (m), 1468 (m), 1455 (m), 1447 (m), 1401 (m), 1377 (m), 1279 (m), 1245 (s), 1216 (vs), 1188 (m), 1156 (vs), 1122 (m), 1087 (m), 1068 (w), 1038 (m), 1014 (m), 993 (w), 940 (w),

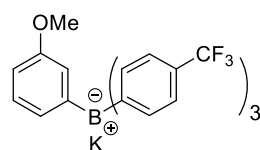
896 (w), 862 (w), 824 (s), 814 (vs), 798 (s), 778 (s), 770 (vs), 747 (m), 738 (m), 717 (m), 705 (s). **Mp** (°C) >300.

Potassium tris(4-fluorophenyl)(2-methoxyphenyl)borate (**1c**)



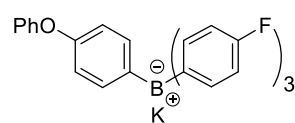
Using potassium 2-methoxyphenyltrifluoroborate and a solution of 4-fluorophenylmagnesium bromide in THF according to general procedure **O** (3.0 mmol scale), provided **1c** (1.61 mmol, 712 mg, 54%) as a colorless solid. **¹H NMR** (400 MHz, CD₃CN) δ 7.14 – 7.06 (m, 6H), 7.00 – 6.94 (m, 2H), 6.76 – 6.67 (m, 8H), 3.16 (s, 3H) ppm. **¹³C NMR** (101 MHz, CD₃CN) δ 164.5, 161.7, 160.0 (d, *J* = 3.3 Hz), 159.5 (d, *J* = 3.5 Hz), 159.4, 159.0 (d, *J* = 3.3 Hz), 158.5 (d, *J* = 3.3 Hz), 137.5 – 137.2 (m), 137.0, 125.5, 120.2 (dd, *J* = 5.4, 2.5 Hz), 112.4 (dd, *J* = 6.2, 2.9 Hz), 112.2 (dd, *J* = 6.1, 2.9 Hz), 111.7, 55.1 ppm. The signals for the carbon atoms adjacent to the boron center were not observed. **¹¹B NMR** (128 MHz, CD₃CN) δ -8.04 ppm. **¹⁹F NMR** (377 MHz, CD₃CN) δ -125.38 (tt, *J* = 10.3, 7.0 Hz) ppm. **HRMS** (ESI-Quadrupole): *m/z* calcd for C₂₅H₁₉BF₃O⁻ [M-K]⁻: 403.1487; found: 403.1485. **IR** (Diamond-ATR, neat) $\tilde{\nu}_{max}$ (cm⁻¹): 1578 (m), 1487 (m), 1465 (w), 1262 (w), 1222 (m), 1218 (m), 1161 (m), 1085 (w), 1026 (w), 1014 (w), 848 (w), 835 (m), 817 (vs), 793 (w), 779 (m), 766 (w), 746 (w). **Mp** (°C) >300.

Potassium tris(4-(trifluoromethyl)phenyl)(3-methoxyphenyl)borate (**1d**)



Using potassium 3-methoxyphenyltrifluoroborate and a solution of 4-(trifluoromethyl)phenylmagnesium bromide in THF according to general procedure **O** (3.0 mmol scale), provided **1d** (2.01 mmol, 1.19 g, 67%) as a light-orange solid. **¹H NMR** (400 MHz, CD₃CN) δ 7.48 – 7.40 (m, 6H), 7.35 (d, *J* = 7.9 Hz, 6H), 7.01 (t, *J* = 7.7 Hz, 1H), 6.83 – 6.79 (m, 1H), 6.76 (ddq, *J* = 4.1, 3.0, 1.5 Hz, 1H), 6.51 (ddd, *J* = 8.0, 2.8, 1.0 Hz, 1H), 3.64 (s, 3H) ppm. **¹³C NMR** (101 MHz, CD₃CN) δ 169.7, 169.3, 168.8, 168.3, 164.4, 163.9, 163.4, 162.9, 159.2 (dd, *J* = 6.9, 3.3 Hz), 136.4, 129.0, 127.9 (q, *J* = 3.0 Hz), 126.5 (q, *J* = 269.7 Hz), 124.85 (q, *J* = 31.1 Hz), 123.3 – 123.1 (m), 122.2, 108.1, 55.0 ppm. The signals for the carbon atoms adjacent to the boron center were not observed. **¹¹B NMR** (128 MHz, CD₃CN) δ -6.59 ppm. **¹⁹F NMR** (377 MHz, CD₃CN) δ -62.02 ppm. **HRMS** (ESI-Quadrupole): *m/z* calcd for C₂₈H₁₉BF₉O⁻ [M-K]⁻: 553.1391; found: 553.1396. **IR** (Diamond-ATR, neat) $\tilde{\nu}_{max}$ (cm⁻¹): 3307 (br, m), 1597 (m), 1319 (vs), 1281 (m), 1224 (m), 1158 (s), 1121 (s), 1102 (s), 1060 (s), 1045 (m), 1016 (s), 961 (m), 844 (m), 823 (s), 800 (m), 788 (s), 767 (m), 756 (s), 746 (m), 730 (s). **Mp** (°C) >300.

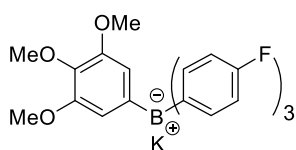
Potassium tris(4-fluorophenyl)(4-phenoxyphenyl)borate (**1e**)



Using potassium 4-phenoxyphenyltrifluoroborate and a solution of 4-fluorophenylmagnesium bromide in THF according to general procedure **O** (3.0 mmol scale), provided **1e** (1.20 mmol, 605 mg, 40%) as a colorless solid. **¹H NMR** (400 MHz, CD₃CN) δ 7.35 – 7.28 (m, 2H), 7.25 – 7.16 (m, 8H), 7.05 – 6.99 (m, 1H), 6.97 – 6.91 (m, 2H), 6.82 – 6.70 (m, 8H) ppm. **¹³C NMR** (101 MHz, CD₃CN) δ 162.1, 160.1 (d, *J* =

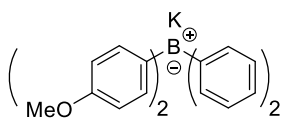
3.2 Hz), 159.8, 159.7, 159.6 (d, $J = 3.2$ Hz), 159.1 (d, $J = 2.9$ Hz), 158.6 (d, $J = 3.5$ Hz), 153.2, 137.6 – 137.4 (m), 130.5, 122.89, 118.4, 118.0 (dd, $J = 6.0, 3.0$ Hz), 112.9 (dd, $J = 6.1, 3.1$ Hz), 112.7 (dd, $J = 6.1, 3.0$ Hz) ppm. The signals for the carbon atoms adjacent to the boron center were not observed. ^{11}B NMR (128 MHz, CD_3CN) δ -7.55 ppm. ^{19}F NMR (377 MHz, CD_3CN) δ -124.62 (tt, $J = 10.3, 7.0$ Hz) ppm. HRMS (ESI-Quadrupole): m/z calcd for $\text{C}_{30}\text{H}_{21}\text{BF}_3\text{O}^-$ [M-K]: 465.1643; found: 465.1647. IR (Diamond-ATR, neat) $\tilde{\nu}_{\text{max}}$ (cm^{-1}): 1578 (m), 1483 (s), 1456 (w), 1388 (w), 1261 (w), 1241 (m), 1232 (m), 1218 (s), 1158 (s), 1086 (w), 1014 (w), 942 (w), 903 (w), 869 (w), 839 (m), 816 (vs), 794 (w), 781 (m), 750 (m), 708 (w), 693 (m). Mp ($^\circ\text{C}$) >300.

Potassium tris(4-fluorophenyl)(2,3,4 trimethoxyphenyl)borate (1f)



Using potassium 2,3,4-trimethoxyphenyltrifluoroborate and a solution of 4-fluorophenylmagnesium bromide in THF according to general procedure **O** (3.0 mmol scale), provided **1f** (1.49 mmol, 748 mg, 50%) as a colorless solid. ^1H NMR (400 MHz, CD_3CN) δ 7.21 (dddd, $J = 8.7, 6.9, 5.1, 2.6$ Hz, 6H), 6.80 – 6.73 (m, 6H), 6.53 (dd, $J = 5.8, 2.9$ Hz, 2H), 3.65 (s, 3H), 3.58 (s, 6H) ppm. ^{13}C NMR (101 MHz, CD_3CN) δ 162.0, 160.0 (d, $J = 3.1$ Hz), 159.7, 159.5 (d, $J = 3.0$ Hz), 159.0 (d, $J = 3.6$ Hz), 158.5 (d, $J = 3.8$ Hz), 152.1 (dd, $J = 7.7, 3.8$ Hz), 137.5 (ddd, $J = 5.6, 3.5, 1.7$ Hz), 134.9, 113.8 – 113.6 (m), 112.9 (dd, $J = 6.2, 3.0$ Hz), 112.7 (dd, $J = 6.1, 3.0$ Hz), 60.6, 56.3 ppm. The signals for the carbon atoms adjacent to the boron center were not observed. ^{11}B NMR (128 MHz, CD_3CN) δ -7.16 ppm. ^{19}F NMR (377 MHz, CD_3CN) δ -124.67 (tt, $J = 10.4, 7.0$ Hz). HRMS (ESI-Quadrupole): m/z calcd for $\text{C}_{27}\text{H}_{23}\text{BF}_3\text{O}_3^-$ [M-K]: 463.1698; found: 463.1700. IR (Diamond-ATR, neat) $\tilde{\nu}_{\text{max}}$ (cm^{-1}): 1578 (m), 1562 (w), 1487 (s), 1466 (w), 1443 (w), 1434 (w), 1393 (m), 1296 (w), 1290 (m), 1260 (w), 1244 (w), 1236 (w), 1217 (m), 1206 (m), 1193 (m), 1158 (s), 1136 (w), 1104 (vs), 1088 (m), 1016 (m), 996 (m), 973 (m), 845 (w), 814 (vs), 782 (w), 727 (m), 686 (m). Mp ($^\circ\text{C}$) = 272–276 (decomposition).

Potassium bis(4-methoxyphenyl)diphenylborate (1g)

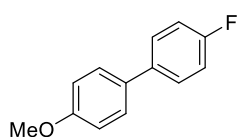


A 25 mL Schlenk flask was charged with Potassium difluorodiphenylborate (**SM29**) (3.0 mmol, 1.0 equiv, 726 mg) and 6.0 mL of THF were added. The mixture was cooled to 0 $^\circ\text{C}$ and a solution of (4-methoxyphenyl)magnesium bromide (6.3 mmol, 2.1 equiv, 6.8 mL, 0.93 M) in THF was added dropwise over 30 min *via* syringe pump. The reaction was allowed to warm to room temperature and was stirred one hour. The reaction was then quenched with 5 mL of sat. aq. K_2CO_3 solution and extracted with EtOAc (3×40 mL). The combined organic phases were filtered and concentrated under reduced pressure. The crude solid product was washed with cold diethyl ether, filtered and dried *in vacuo* to afford TAB **1g** as a colorless solid (2.46 mmol, 1.04 g, 83%). ^1H NMR (400 MHz, CD_3CN) δ 7.28 – 7.21 (m, 4H), 7.14 (tt, $J = 5.2, 2.4$ Hz, 4H), 7.00 (t, $J = 7.4$ Hz, 4H), 6.84 (t, $J = 7.2$ Hz, 2H), 6.62 (d, $J = 8.3$ Hz, 4H), 3.70 (s, 6H) ppm. ^{13}C NMR (101 MHz, CD_3CN) δ 165.2 (dd, $J = 98.4, 49.2$ Hz), 156.4, 155.8 (dd, $J = 100.3, 50.2$ Hz), 137.2

(dd, $J = 3.3, 1.7$ Hz), 136.5 (q, $J = 1.5$ Hz), 126.4 (dd, $J = 5.5, 2.6$ Hz), 122.6, 112.2 (dd, $J = 5.9, 2.9$ Hz), 55.2 ppm. The signals for the carbon atoms adjacent to the boron center were not observed. ^{11}B NMR (128 MHz, CD_3CN) δ -7.20 ppm. HRMS (ESI-Quadrupole): m/z calcd for $\text{C}_{26}\text{H}_{24}\text{BO}_2^-$ [M-K]: 379.1875; found: 379.1874. IR (Diamond-ATR, neat) $\tilde{\nu}_{\text{max}}$ (cm^{-1}): 1590 (m), 1578 (w), 1493 (m), 1461 (w), 1438 (w), 1427 (w), 1271 (m), 1251 (m), 1232 (m), 1184 (m), 1174 (s), 1152 (m), 1127 (w), 1120 (w), 1098 (w), 1036 (m), 866 (w), 844 (w), 822 (w), 807 (vs), 785 (m), 762 (m), 732 (s), 724 (s), 709 (vs). Mp ($^\circ\text{C}$) >300.

5.5.4 Characterization of Bi(hetero)aryls

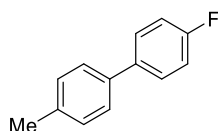
4-Fluoro-4'-methoxy-1,1'-biphenyl (2a)



Using potassium trifluoro(4-methoxyphenyl)borate and a solution of (4-fluorophenyl)magnesium bromide in THF according to general procedure **Q** (0.40 mmol scale), provided **2a** (0.25 mmol, 50 mg, 62%) as a colorless solid.

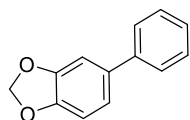
Using potassium tris(4-fluorophenyl)(4-methoxyphenyl)borate (**1a**) according to general procedure **P** (0.40 mmol scale), provided **2a** (0.32 mmol, 64 mg, 79%) as a colorless solid. For the decagram-scale reaction see chapter 5.6. $R_f = 0.21$ (hexane/EtOAc 99:1, UV, KMnO_4 , PAA). ^1H NMR (400 MHz, CDCl_3) δ 7.53 – 7.44 (m, 4H), 7.15 – 7.07 (m, 2H), 7.01 – 6.94 (m, 2H), 3.85 (s, 3H) ppm. LRMS (DEP/EI-Orbitrap): m/z (%): 202.1 (100), 187.1 (69), 159.1 (71), 133.1 (46), 107.1 (10). Analytical data in accordance to literature.²⁴⁵

4-Fluoro-4'-methyl-1,1'-biphenyl (2b)



Using potassium trifluoro(*p*-tolyl)borate and a solution of (4-fluorophenyl)magnesium bromide in THF according to general procedure **Q** (0.40 mmol scale), provided **2b** (0.21 mmol, 39 mg, 52%) as a colorless solid. $R_f = 0.80$ (hexane/EtOAc 100:0, UV, KMnO_4 , PAA). ^1H NMR (400 MHz, CDCl_3) δ 7.56 – 7.49 (m, 2H), 7.47 – 7.42 (m, 2H), 7.25 (d, $J = 8.1$ Hz, 2H), 7.15 – 7.08 (m, 2H), 2.40 (s, 3H) ppm. LRMS (DEP/EI-Orbitrap): m/z (%): 186.0 (100), 165.0 (48), 133.0 (18), 91.1 (11). Analytical data in accordance to literature.²⁴⁶

5-Phenylbenzo[*d*][1,3]dioxole (2c)



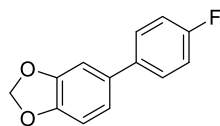
Using potassium benzo[*d*][1,3]dioxol-5-yltrifluoroborate and a solution of phenylmagnesium bromide in THF according to general procedure **Q** (0.40 mmol scale), provided **2c** (0.21 mmol, 42 mg, 53%) as a colorless solid. $R_f = 0.22$ (hexane/EtOAc 100:0, UV, KMnO_4 , PAA). ^1H NMR (400 MHz, CDCl_3) δ 7.56 – 7.52 (m, 2H), 7.46 – 7.40 (m, 2H), 7.36 – 7.31 (m, 1H), 7.11 – 7.09 (m, 1H), 7.07 (d, $J = 1.8$ Hz, 1H), 6.91 (dd, $J = 7.9, 0.6$ Hz, 1H), 6.01

²⁴⁵ W. Erb, M. Albini, J. Rouden, J. Blanchet, *J. Org. Chem.* **2014**, *79*, 10568–10580.

²⁴⁶ T. Agrawal, S. P. Cook, *Org. Lett.* **2014**, *16*, 5080–5083.

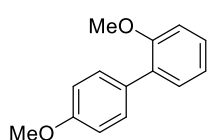
(s, 2H) ppm. **LRMS** (DEP/EI-Orbitrap): m/z (%): 198.0 (100), 139.0 (60), 115.0 (10), 98.7 (13). Analytical data in accordance to literature.²⁴⁷

5-(4-Fluorophenyl)benzo[*d*][1,3]dioxole (**2d**)



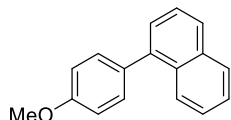
Using potassium benzo[*d*][1,3]dioxol-5-yltrifluoroborate and a solution of (4-fluorophenyl)magnesium bromide in THF according to general procedure **Q** (0.50 mmol scale), provided **2d** (0.28 mmol, 60 mg, 57%) as a colorless solid. R_f = 0.30 (hexane/EtOAc 98:2, UV, KMnO₄, PAA). ¹H NMR (400 MHz, CDCl₃) δ 7.49 – 7.43 (m, 2H), 7.14 – 7.07 (m, 2H), 7.03 – 7.01 (m, 1H), 6.99 (d, J = 1.8 Hz, 1H), 6.88 (d, J = 7.9 Hz, 1H), 6.00 (s, 2H) ppm. **LRMS** (DEP/EI-Orbitrap): m/z (%): 216.0 (100), 157.0 (57), 138.0 (11), 133.0 (10), 107.8 (14). Analytical data in accordance to literature.²⁴⁷

2,4'-Dimethoxy-1,1'-biphenyl (**2e**)



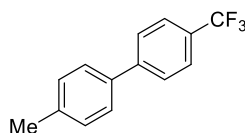
Using potassium trifluoro(4-methoxyphenyl)borate and a solution of (2-methoxyphenyl)magnesium bromide in THF according to general procedure **Q** (0.40 mmol scale), provided **2e** (0.21 mmol, 45 mg, 53%) as a colorless solid. R_f = 0.42 (hexane/EtOAc 98:2, UV, KMnO₄, PAA). ¹H NMR (400 MHz, CDCl₃) 7.53 – 7.47 (m, 2H), 7.35 – 7.29 (m, 2H), 7.07 – 7.02 (m, 1H), 7.01 – 6.96 (m, 3H), 3.87 (s, 3H), 3.83 (s, 3H) ppm. **LRMS** (DEP/EI-Orbitrap): m/z (%): 214.1 (100), 199.1 (33), 184.0 (30), 168.0 (22), 139.0 (22), 128.0 (37), 115.0 (15). Analytical data in accordance to literature.²⁴⁸

1-(4-Methoxyphenyl)naphthalene (**2f**)



Using potassium trifluoro(4-methoxyphenyl)borate and a solution of naphthalen-1-ylmagnesium bromide in THF according to general procedure **Q** (0.50 mmol scale), provided **2f** (0.33 mmol, 77 mg, 66%) as a colorless solid. R_f = 0.44 (hexane/EtOAc 98:2, UV, KMnO₄, PAA). ¹H NMR (400 MHz, CDCl₃) δ 7.98 (d, J = 8.3 Hz, 1H), 7.96 – 7.92 (m, 1H), 7.88 (dt, J = 8.2, 1.1 Hz, 1H), 7.58 – 7.50 (m, 2H), 7.49 – 7.43 (m, 4H), 7.10 – 7.04 (m, 2H), 3.92 (s, 3H) ppm. **LRMS** (DEP/EI-Orbitrap): m/z (%): 234.1 (100), 219.1 (31), 203.1 (11), 189.1 (48), 163.1 (10), 94.6 (11). Analytical data in accordance to literature.²⁴⁹

4-Methyl-4'-(trifluoromethyl)-1,1'-biphenyl (**2g**)



Using potassium trifluoro(*p*-tolyl)borate and a solution of (4-(trifluoromethyl)phenyl)magnesium bromide in THF according to general procedure **Q** (0.40 mmol scale), provided **2g** (0.33 mmol, 77 mg, 82%) as a colorless solid. R_f = 0.79 (hexane/EtOAc 100:0, UV, KMnO₄, PAA). ¹H NMR (400 MHz, CDCl₃) δ 7.70 – 7.68 (m,

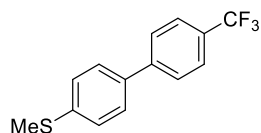
²⁴⁷ F. Mäsing, H. Nüsse, J. Klingauf, A. Studer, *Org. Lett.* **2018**, *20*, 752–755.

²⁴⁸ J. M. Quibell, G. Duan, G. J. P. Perry, I. Larrosa, *Chem. Comm.* **2019**, *55*, 6445–6448.

²⁴⁹ Y.-Y. Chua, H. A. Duong, *Chem. Comm.* **2016**, *52*, 1466–1469.

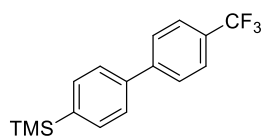
4H), 7.54 – 7.49 (m, 2H), 7.32 – 7.28 (m, 2H), 2.43 (s, 3H) ppm. **LRMS** (DEP/EI-Orbitrap): m/z (%): 236.1 (100), 217.1 (10), 167.1 (42), 165.1 (40), 152.1 (11), 91.1 (10). Analytical data in accordance to literature.²⁵⁰

Methyl(4'-(trifluoromethyl)-[1,1'-biphenyl]-4-yl)sulfane (**2h**)



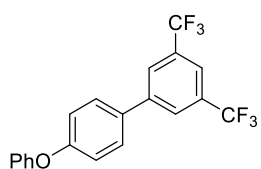
Using potassium trifluoro(4-(methylthio)phenyl)borate and a solution of (4-(trifluoromethyl)phenyl)magnesium bromide in THF according to general procedure **Q** (0.50 mmol scale), provided **2h** (0.29 mmol, 78 mg, 58%) as a colorless solid. R_f = 0.26 (hexane/EtOAc 99:1, UV, KMnO₄, PAA). **¹H NMR** (400 MHz, CDCl₃) δ 7.71 – 7.64 (m, 4H), 7.56 – 7.50 (m, 2H), 7.37 – 7.33 (m, 2H), 2.54 (s, 3H) ppm. **¹³C NMR** (101 MHz, CDCl₃) δ 144.1, 139.2, 136.4, 129.3 (q, J = 32.4 Hz), 127.7, 127.1, 126.9, 125.9 (q, J = 3.8 Hz), 124.4 (q, J = 271.9 Hz), 15.7 ppm. **LRMS** (DEP/EI-Orbitrap): m/z (%): 268.1 (100), 233.0 (12), 222.0 (20), 201.1 (10), 184.0 (27), 152.1 (17). **HRMS** (EI-Orbitrap): m/z calcd for C₁₄H₁₁F₃S⁺: 268.0534; found: 268.0528. **IR** (Diamond-ATR, neat) $\tilde{\nu}_{max}$ (cm⁻¹): 1734 (w), 1715 (m), 1684 (w), 1616 (w), 1595 (w), 1490 (w), 1437 (w), 1418 (w), 1396 (w), 1362 (m), 1327 (s), 1279 (w), 1262 (w), 1221 (m), 1171 (m), 1129 (s), 1114 (s), 1102 (s), 1074 (s), 1014 (w), 1001 (w), 973 (w), 958 (w), 852 (w), 813 (vs), 740 (w). **Mp** (°C) = 133–137.

Trimethyl(4'-(trifluoromethyl)-[1,1'-biphenyl]-4-yl)silane (**2i**)



Using potassium trifluoro(4-(trimethylsilyl)phenyl)borate (**SM23**) and a solution of (4-(trifluoromethyl)phenyl)magnesium bromide in THF according to general procedure **Q** (0.50 mmol scale), provided **2i** (0.31 mmol, 90 mg, 62%) as a colorless oil. R_f = 0.52 (hexane/EtOAc 100:0, UV, KMnO₄, PAA). **¹H NMR** (400 MHz, CDCl₃) δ 7.70 (s, 4H), 7.66 – 7.63 (m, 2H), 7.61 – 7.57 (m, 2H), 0.32 (s, 9H) ppm. **¹³C NMR** (101 MHz, CDCl₃) δ 144.8, 140.7, 140.2, 134.2, 129.5 (q, J = 32.5 Hz), 127.6, 126.7, 125.9 (q, J = 3.8 Hz), 123.1 (q, J = 271.9 Hz), -1.0 ppm. **LRMS** (DEP/EI-Orbitrap): m/z (%): 294.1 (12), 279.1 (100), 263.1 (10), 203.1 (18). **HRMS** (EI-Orbitrap): m/z calcd for C₁₆H₁₇F₃Si⁺: 294.1052; found: 294.1047. **IR** (Diamond-ATR, neat) $\tilde{\nu}_{max}$ (cm⁻¹): n.d.

4'-Phenoxy-3,5-bis(trifluoromethyl)-1,1'-biphenyl (**2j**)

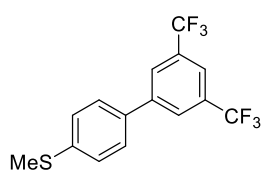


Using potassium trifluoro(4-phenoxyphenyl)borate and a solution of (3,5-bis(trifluoromethyl)phenyl)magnesium bromide in THF according to general procedure **Q** (0.50 mmol scale), provided **2j** (0.43 mmol, 166 mg, 87%) as a colorless oil. R_f = 0.30 (hexane/EtOAc 100:0, UV, KMnO₄, PAA). **¹H NMR** (400 MHz, CDCl₃) δ 7.99 (s, 2H), 7.84 (s, 1H), 7.61 – 7.55 (m, 2H), 7.43 – 7.37 (m, 2H), 7.20 – 7.15 (m, 1H), 7.15 – 7.11 (m, 2H), 7.11 – 7.06 (m, 2H) ppm. **¹³C NMR** (101 MHz, CDCl₃) δ 158.5, 156.6,

²⁵⁰ J. Tang, A. Biafora, L. J. Goossen, *Angew. Chem. Int. Ed.* **2015**, *54*, 13130–13133.

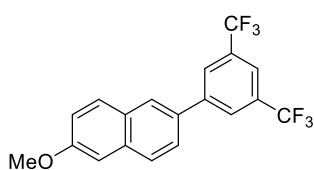
142.8, 133.1, 132.2 (q, $J = 33.2$ Hz), 130.1, 128.8, 127.2 – 126.9 (m), 124.1, 123.5 (q, $J = 272.7$ Hz), 120.7 (qq, $J = 3.8$ Hz), 119.5, 119.3 ppm. **LRMS** (DEP/EI-Orbitrap): m/z (%): 382.1 (100), 354.1 (22), 277.0 (18), 237.0 (11), 219.0 (18), 215.1 (18), 188.0 (21), 182.0 (11), 141.1 (11), 77.0 (41). **HRMS** (EI-Orbitrap): m/z calcd for $C_{20}H_{12}F_6O^+$: 382.0792; found: 382.0786. **IR** (Diamond-ATR, neat) $\tilde{\nu}_{max}$ (cm^{-1}): 1610 (w), 1591 (m), 1513 (m), 1490 (m), 1466 (m), 1380 (s), 1276 (vs), 1261 (m), 1243 (s), 1202 (m), 1173 (s), 1127 (vs), 1109 (m), 1070 (w), 1058 (m), 897 (m), 872 (m), 842 (m), 834 (m), 788 (w), 752 (m), 714 (m), 705 (m), 693 (m), 682 (m).

(3',5'-Bis(trifluoromethyl)-[1,1'-biphenyl]-4-yl)(methyl)sulfane (**2k**)



Using potassium trifluoro(4-(methylthio)phenyl)borate and a solution of (3,5-bis(trifluoromethyl)phenyl)magnesium bromide in THF according to general procedure **Q** (0.50 mmol scale), provided **2k** (0.33 mmol, 110 mg, 66%) as a colorless solid. (Note: Only 1 F was used in the electrochemical oxidation, as more electrons lead to oxidation of the desired product into the undesired sulfoxide.) $R_f = 0.41$ (hexane/EtOAc 100:0, UV, $KMnO_4$, PAA). **1H NMR** (400 MHz, $CDCl_3$) δ 7.99 (d, $J = 1.7$ Hz, 2H), 7.84 (s, 1H), 7.57 – 7.51 (m, 2H), 7.39 – 7.34 (m, 2H), 2.54 (s, 3H) ppm. **^{13}C NMR** (101 MHz, $CDCl_3$) δ 142.8, 140.3, 134.7, 132.3 (q, $J = 33.2$ Hz), 127.6, 126.9, 126.9, 123.5 (q, $J = 272.8$ Hz), 120.9 (qq, $J = 3.8$ Hz), 15.6 ppm. **LRMS** (DEP/EI-Orbitrap): m/z (%): 336.0 (100), 321.0 (31), 301.0 (20), 290.1 (11), 252.0 (11). **HRMS** (EI-Orbitrap): m/z calcd for $C_{15}H_{10}F_6S^+$: 336.0407; found: 336.0402. **IR** (Diamond-ATR, neat) $\tilde{\nu}_{max}$ (cm^{-1}): 1717 (m), 1707 (w), 1700 (w), 1684 (w), 1654 (w), 1559 (w), 1541 (w), 1507 (w), 1458 (w), 1382 (s), 1279 (vs), 1262 (w), 1221 (w), 1179 (m), 1132 (s), 1109 (w), 1054 (m), 897 (w), 846 (w), 819 (w), 682 (m). **Mp** ($^{\circ}C$) = 66–70.

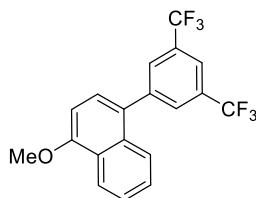
2-(3,5-Bis(trifluoromethyl)phenyl)-6-methoxynaphthalene (**2l**)



Using potassium trifluoro(6-methoxynaphthalen-2-yl)borate (**SM24**) and a solution of (3,5-bis(trifluoromethyl)phenyl)magnesium bromide in THF according to general procedure **Q** (0.50 mmol scale), provided **2l** (0.15 mmol, 55 mg, 30%) as a colorless oil. $R_f = 0.43$ (hexane/EtOAc 98:2, UV, $KMnO_4$, PAA). **1H NMR** (400 MHz, $CDCl_3$) δ 8.12 (s, 2H), 8.01 (d, $J = 1.9$ Hz, 1H), 7.90 – 7.82 (m, 3H), 7.70 (dd, $J = 8.5, 1.9$ Hz, 1H), 7.23 (dd, $J = 8.9, 2.5$ Hz, 1H), 7.19 (d, $J = 2.5$ Hz, 1H), 3.96 (s, 3H) ppm. **^{13}C NMR** (101 MHz, $CDCl_3$) δ 158.6, 143.5, 134.7, 133.3, 132.2 (q, $J = 33.2$ Hz), 130.0, 129.1, 128.1, 127.3, 126.5, 125.3, 123.6 (q, $J = 272.7$ Hz), 120.7 (qq, $J = 3.8$ Hz), 120.0, 105.7, 55.5 ppm. **LRMS** (DEP/EI-Orbitrap): m/z (%): 370.1 (75), 327.1 (100), 299.1 (14), 281.1 (18), 238.1 (21), 225.0 (60), 207.0 (41), 189.1 (25), 151.0 (14), 73.0 (22). **HRMS** (EI-Orbitrap): m/z calcd for $C_{19}H_{12}F_6O^+$: 370.0792; found: 370.0784. **IR** (Diamond-ATR, neat) $\tilde{\nu}_{max}$ (cm^{-1}): 1716 (w), 1616 (w), 1595 (w), 1559 (w), 1540 (w), 1490 (w), 1438 (w), 1418 (w), 1396 (w), 1362 (w), 1329 (m), 1279 (w),

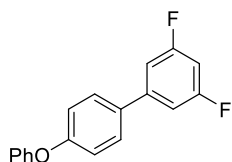
1262 (w), 1220 (w), 1172 (m), 1133 (s), 1114 (vs), 1102 (s), 1075 (m), 1014 (w), 1001 (w), 973 (w), 958 (w), 852 (w), 813 (vs), 740 (w), 674 (w).

1-(3,5-Bis(trifluoromethyl)phenyl)-4-methoxynaphthalene (**2m**)



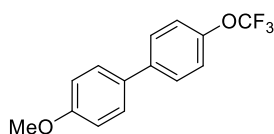
Using potassium trifluoro(4-methoxynaphthalen-1-yl)borate (**SM30**) and a solution of (3,5-bis(trifluoromethyl)phenyl)magnesium bromide in THF according to general procedure **Q** (0.40 mmol scale), provided **2m** (0.23 mmol, 85 mg, 58%) as a colorless oil. $R_f = 0.51$ (hexane/EtOAc 100:0, UV, KMnO_4 , PAA). $^1\text{H NMR}$ (400 MHz, CDCl_3) δ 8.41 – 8.37 (m, 1H), 7.94 (s, 2H), 7.93 (s, 1H), 7.71 – 7.66 (m, 1H), 7.58 – 7.49 (m, 2H), 7.35 (d, $J = 7.9$ Hz, 1H), 6.90 (d, $J = 7.9$ Hz, 1H), 4.07 (s, 3H) ppm. $^{13}\text{C NMR}$ (101 MHz, CDCl_3) δ 156.2, 143.2, 132.0, 131.8 (q, $J = 33.2$ Hz), 130.6 – 130.3 (m), 129.4, 127.8, 127.6, 125.9, 125.8, 124.6, 122.8, 122.2 (q, $J = 272.6$ Hz), 120.9 (qq, $J = 3.8$ Hz), 103.4, 55.8 ppm. **LRMS** (DEP/EI-Orbitrap): m/z (%): 370.1 (100), 355.1 (37), 327.1 (74), 307.1 (17), 301.0 (11), 238.1 (18), 189.1 (17). **HRMS** (EI-Orbitrap): m/z calcd for $\text{C}_{19}\text{H}_{12}\text{F}_6\text{O}^+$: 370.0792; found: 370.0782. **IR** (Diamond-ATR, neat) $\tilde{\nu}_{max}$ (cm^{-1}): 1718 (w), 1700 (w), 1684 (w), 1654 (m), 1588 (w), 1559 (m), 1540 (m), 1522 (w), 1516 (w), 1508 (m), 1458 (m), 1424 (w), 1420 (w), 1365 (m), 1278 (vs), 1246 (w), 1173 (m), 1131 (s), 1116 (m), 1106 (w), 1087 (w), 1005 (w), 899 (w), 847 (w), 816 (w), 766 (w), 709 (w).

3,5-Difluoro-4'-phenoxy-1,1'-biphenyl (**2n**)



Using potassium trifluoro(4-phenoxyphenyl)borate and a solution of (3,5-difluorophenyl)magnesium bromide in THF according to general procedure **Q** (0.50 mmol scale), provided **2n** (0.25 mmol, 71 mg, 50%) as a colorless oil. $R_f = 0.33$ (hexane/EtOAc 100:0, UV, KMnO_4 , PAA). $^1\text{H NMR}$ (400 MHz, CDCl_3) δ 7.54 – 7.49 (m, 2H), 7.42 – 7.35 (m, 2H), 7.20 – 7.14 (m, 1H), 7.12 – 7.05 (m, 6H), 6.78 (tt, $J = 8.9$, 2.3 Hz, 1H) ppm. $^{13}\text{C NMR}$ (101 MHz, CDCl_3) δ 163.4 (dd, $J = 247.8$, 13.2 Hz), 158.0, 156.8, 144.0 (t, $J = 9.6$ Hz), 133.8 (t, $J = 2.6$ Hz), 130.0, 128.5, 123.9, 119.4, 119.1, 109.7 (dd, $J = 18.6$, 7.2 Hz), 102.3 (t, $J = 25.5$ Hz) ppm. **LRMS** (DEP/EI-Orbitrap): m/z (%): 282.1 (100), 254.1 (16), 233.1 (25), 188.0 (31), 177.1 (39), 168.0 (11), 151.0 (59), 77.0 (49). **HRMS** (EI-Orbitrap): m/z calcd for $\text{C}_{18}\text{H}_{12}\text{F}_2\text{O}^+$: 282.0856; found: 282.0848. **IR** (Diamond-ATR, neat) $\tilde{\nu}_{max}$ (cm^{-1}): n.d.

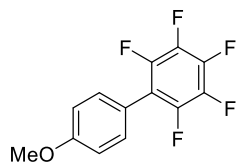
4-Methoxy-4'-(trifluoromethoxy)-1,1'-biphenyl (**2o**)



Using potassium trifluoro(4-methoxyphenyl)borate and a solution of (4-(trifluoromethoxy)phenyl)magnesium bromide in THF according to general procedure **Q** (0.40 mmol scale), provided **2o** (0.28 mmol, 76 mg, 71%) as a colorless solid. $R_f = 0.35$ (hexane/EtOAc 98:2, UV, KMnO_4 , PAA). $^1\text{H NMR}$ (400 MHz, CDCl_3) δ 7.56 – 7.50 (m, 2H), 7.50 – 7.44 (m, 2H), 7.24 (d, $J = 7.3$ Hz, 2H), 7.01 – 6.91 (m, 2H), 3.83 (s, 3H) ppm.

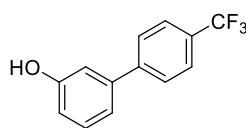
LRMS (DEP/EI-Orbitrap): m/z (%): 268.0 (100), 253.0 (37), 225.0 (42), 199.0 (16), 139.0 (13), 128.0 (21), 69.0 (18). Analytical data in accordance to literature.²⁵¹

2,3,4,5,6-Pentafluoro-4'-methoxy-1,1'-biphenyl (**2p**)



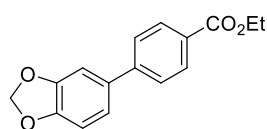
Using potassium trifluoro(4-methoxyphenyl)borate and a solution of (perfluorophenyl)magnesium bromide in THF according to general procedure **Q** (0.50 mmol scale), provided **2p** (0.07 mmol, 19 mg, 14%) as a colorless solid. R_f = 0.37 (hexane/EtOAc 98:2, UV, KMnO₄, PAA). ¹H NMR (400 MHz, CDCl₃) δ 7.39 – 7.33 (m, 2H), 7.04 – 6.99 (m, 2H), 3.87 (s, 3H) ppm. **LRMS** (DEP/EI-Orbitrap): m/z (%): 274.0 (100), 259.0 (11), 231.0 (83), 205.0 (27), 181.0 (12). Analytical data in accordance to literature.²⁵²

4'-(Trifluoromethyl)-[1,1'-biphenyl]-3-ol (**2q**)



Using potassium trifluoro(3-hydroxyphenyl)borate and a solution of (4-(trifluoromethyl)phenyl)magnesium bromide in THF according to general procedure **Q** (0.40 mmol scale), provided **2q** (0.16 mmol, 38 mg, 40%) as a colorless solid. (Note: general procedure **Q** was modified, as 4.2 equiv (1.68 mmol) of Grignard reagent were used, since the alcohol had to be deprotonated first.) R_f = 0.30 (hexane/EtOAc 90:10, UV, KMnO₄, PAA). ¹H NMR (400 MHz, CDCl₃) δ 7.71 – 7.63 (m, 4H), 7.35 (t, J = 7.9 Hz, 1H), 7.18 (dt, J = 7.8, 1.3 Hz, 1H), 7.08 (dd, J = 2.5, 1.7 Hz, 1H), 6.89 (ddd, J = 8.1, 2.6, 0.9 Hz, 1H), 5.12 (s, 1H, OH) ppm. **LRMS** (DEP/EI-Orbitrap): m/z (%): 238.0 (100), 219.0 (10), 209.0 (11), 141.0 (12), 115.0 (10). Analytical data in accordance to literature.²⁵³

Ethyl 4-(benzo[d][1,3]dioxol-5-yl)benzoate (**2r**)



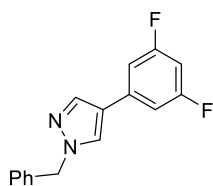
Using potassium benzo[d][1,3]dioxol-5-yltrifluoroborate and a solution of (4-(ethoxycarbonyl)phenyl)zinc iodide in THF according to general procedure **Q** (0.50 mmol scale), provided **2r** (0.27 mmol, 73 mg, 54%) as a colorless solid. R_f = 0.35 (hexane/EtOAc 98:2, UV, KMnO₄, PAA). ¹H NMR (400 MHz, CDCl₃) δ 8.11 – 8.04 (m, 2H), 7.60 – 7.54 (m, 2H), 7.13 – 7.07 (m, 2H), 6.92 – 6.88 (m, 1H), 6.01 (s, 2H), 4.39 (q, J = 7.1 Hz, 2H), 1.41 (t, J = 7.1 Hz, 3H) ppm. **LRMS** (DEP/EI-Orbitrap): m/z (%): 270.1 (100), 242.1 (42), 225.0 (79), 167.0 (11), 139.1 (89), 112.1 (21). Analytical data in accordance to literature.²⁵⁴

²⁵¹ I. R. Baxendale, C. M. Griffiths-Jones, S. V. Ley, G. K. Tranmer, *Chem. Eur. J.* **2006**, *12*, 4407–4416.

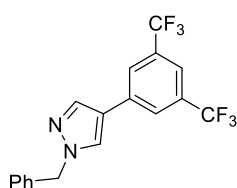
²⁵² Y. Nakamura, N. Yosgikai, L. Illies, E. Nakamura, *Org. Lett.* **2012**, *14*, 3316–3319.

²⁵³ J. Luo, S. Preciado, I. Larrosa, *Chem. Comm.* **2015**, *51*, 3127–3130.

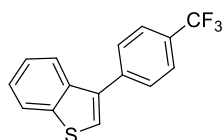
²⁵⁴ M. Ketels, M. A. Ganiek, N. Weidmann, P. Knochel, *Angew. Chem. Int. Ed.* **2017**, *56*, 12770–12773.

1-Benzyl-4-(3,5-difluorophenyl)-1H-pyrazole (3a)

Using potassium (1-benzyl-1H-pyrazol-4-yl)trifluoroborate (**SM31**) and a solution of (3,5-difluorophenyl)magnesium bromide in THF according to general procedure **Q** (0.40 mmol scale), provided **3a** (0.19 mmol, 52 mg, 48%) as a colorless solid. $R_f = 0.25$ (hexane/EtOAc 90:10, UV, KMnO₄, PAA). ¹H NMR (400 MHz, CDCl₃) δ 7.71 (s, 1H), 7.53 (s, 1H), 7.34 – 7.24 (m, 3H), 7.22 – 7.17 (m, 2H), 6.90 – 6.83 (m, 2H), 6.56 (tt, $J = 9.0, 2.3$ Hz, 1H), 5.26 (s, 2H) ppm. ¹³C NMR (101 MHz, CDCl₃) δ 163.5 (dd, $J = 247.4, 13.4$ Hz), 137.2, 136.0, 135.9 (t, $J = 10.4$ Hz), 129.1, 128.5, 128.0, 126.8, 121.9 (t, $J = 2.9$ Hz), 108.2 (dd, $J = 19.0, 6.9$ Hz), 101.6 (t, $J = 25.5$ Hz), 56.5 ppm. LRMS (DEP/EI-Orbitrap): m/z (%): 270.1 (48), 269.1 (100), 242.1 (10), 91.1 (97), 65.0 (10). HRMS (EI-Orbitrap): m/z calcd for C₁₆H₁₂F₂N₂⁺: 270.0969; found: 270.0970. IR (Diamond-ATR, neat) $\tilde{\nu}_{max}$ (cm⁻¹): 1709 (s), 1624 (s), 1591 (s), 1576 (m), 1570 (m), 1560 (w), 1540 (w), 1521 (w), 1507 (w), 1498 (w), 1465 (m), 1457 (m), 1436 (m), 1431 (m), 1420 (m), 1386 (m), 1361 (s), 1277 (w), 1221 (s), 1173 (m), 1116 (vs), 1091 (w), 1079 (w), 1030 (w), 1008 (w), 996 (m), 984 (s), 849 (s), 829 (vs), 780 (w), 714 (s). Mp (°C) = 66–70.

1-Benzyl-4-(3,5-bis(trifluoromethyl)phenyl)-1H-pyrazole (3b)

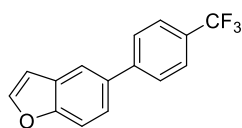
Using potassium (1-benzyl-1H-pyrazol-4-yl)trifluoroborate (**SM31**) and a solution of (3,5-bis(trifluoromethyl)phenyl)magnesium bromide in THF according to general procedure **Q** (0.50 mmol scale), provided **3b** (0.38 mmol, 139 mg, 75%) as a colorless solid. $R_f = 0.14$ (hexane/EtOAc 95:5, UV, KMnO₄, PAA). ¹H NMR (400 MHz, CDCl₃) δ 7.87 (d, $J = 18.5$ Hz, 3H), 7.72 (d, $J = 15.5$ Hz, 2H), 7.43 – 7.33 (m, 3H), 7.32 – 7.25 (m, 2H), 5.37 (s, 2H) ppm. ¹³C NMR (101 MHz, CDCl₃) δ 137.2, 135.9, 134.9, 132.3 (q, $J = 33.2$ Hz), 129.2, 128.6, 128.0, 127.0, 125.4, 123.4 (q, $J = 272.7$ Hz), 121.2, 119.9 (qq, $J = 3.9$ Hz), 56.7 ppm. LRMS (DEP/EI-Orbitrap): m/z (%): 369.1 (100), 351.1 (11), 293.0 (10), 91.1 (56), 65.0 (13). HRMS (EI-Orbitrap): m/z calcd for C₁₈H₁₂F₆N₂⁺: 370.0905; found: 370.0883. IR (Diamond-ATR, neat) $\tilde{\nu}_{max}$ (cm⁻¹): 1700 (w), 1684 (w), 1654 (w), 1559 (w), 1541 (w), 1507 (w), 1458 (w), 1383 (m), 1277 (vs), 1264 (w), 1213 (w), 1176 (m), 1126 (s), 1110 (m), 1055 (w), 897 (w), 847 (w), 832 (w), 818 (m). Mp (°C) = 125–128.

3-(4-(Trifluoromethyl)phenyl)benzo[*b*]thiophene (3c)

Using potassium benzo[*b*]thiophen-3-yltrifluoroborate and a solution of (4-(trifluoromethyl)phenyl)magnesium bromide in THF according to general procedure **Q** (0.40 mmol scale), provided **3c** (0.21 mmol, 58 mg, 52%) as a colorless oil. $R_f = 0.60$ (hexane/EtOAc 100:0, UV, KMnO₄, PAA). ¹H NMR (400 MHz, CDCl₃) δ 7.98 – 7.92 (m, 1H), 7.92 – 7.86 (m, 1H), 7.76 (d, $J = 8.4$ Hz, 2H), 7.71 (d, $J = 8.4$ Hz, 2H), 7.48 (s, 1H), 7.46 – 7.40 (m,

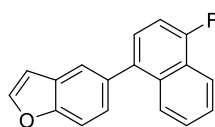
2H) ppm. **LRMS** (DEP/EI-Orbitrap): m/z (%): 278.0 (100), 259.0 (10), 233.0 (17), 208.0 (15), 165.1 (15). Analytical data in accordance to literature.²⁵⁵

5-(4-(Trifluoromethyl)phenyl)benzofuran (3d)



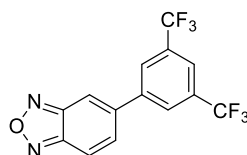
Using potassium benzofuran-5-yltrifluoroborate (**SM25**) and a solution of (4-(trifluoromethyl)phenyl)magnesium bromide in THF according to general procedure **Q** (0.40 mmol scale), provided **3d** (0.27 mmol, 70 mg, 67%) as a colorless solid. R_f = 0.43 (hexane/EtOAc 100:0, UV, KMnO₄, PAA). ¹H NMR (400 MHz, CDCl₃) δ 7.81 (d, J = 1.7 Hz, 1H), 7.74 – 7.68 (m, 4H), 7.69 (d, J = 2.1 Hz, 1H), 7.60 (d, J = 8.6 Hz, 1H), 7.53 (dd, J = 8.6, 1.9 Hz, 1H), 6.84 (dd, J = 2.2, 0.8 Hz, 1H) ppm. **LRMS** (DEP/EI-Orbitrap): m/z (%): 262.0 (100), 243.0 (10), 233.0 (12), 183.0 (10), 165.0 (26). Analytical data in accordance to literature.²⁵⁶

5-(4-Fluoronaphthalen-1-yl)benzofuran (3e)



Using potassium benzofuran-5-yltrifluoroborate (**SM25**) and a solution of (4-fluoronaphthalen-1-yl)magnesium bromide in THF according to general procedure **Q** (0.40 mmol scale), provided **3e** (0.15 mmol, 40 mg, 38%) as a colorless oil. R_f = 0.48 (hexane/EtOAc 100:0, UV, KMnO₄, PAA). ¹H NMR (400 MHz, CDCl₃) δ 8.24 (d, J = 8.5 Hz, 1H), 7.96 – 7.91 (m, 1H), 7.76 (d, J = 2.2 Hz, 1H), 7.72 (d, J = 1.7 Hz, 1H), 7.66 (dt, J = 8.4, 0.8 Hz, 1H), 7.61 (ddd, J = 8.3, 6.8, 1.2 Hz, 1H), 7.53 (ddd, J = 8.3, 6.8, 1.3 Hz, 1H), 7.45 – 7.40 (m, 2H), 7.27 (dd, J = 20.7, 18.3 Hz, 1H), 6.89 (dd, J = 2.3, 1.0 Hz, 1H) ppm. ¹³C NMR (101 MHz, CDCl₃) δ 158.3 (d, J = 251.5 Hz), 154.5, 145.8, 136.6 (d, J = 4.5 Hz), 135.0, 133.4 (d, J = 4.6 Hz), 127.7, 127.0, 126.9, 126.8, 126.3 (d, J = 2.7 Hz), 126.2 (d, J = 1.9 Hz), 123.9 (d, J = 16.3 Hz), 122.7, 120.9 (d, J = 5.6 Hz), 111.2, 109.0 (d, J = 19.8 Hz), 106.8 ppm. **LRMS** (DEP/EI-Orbitrap): m/z (%): 262.1 (76), 233.1 (100), 231.1 (21), 207.1 (11), 103.5 (10). **HRMS** (EI-Orbitrap): m/z calcd for C₁₈H₁₁FO⁺: 262.0794; found: 262.0790. **IR** (Diamond-ATR, neat) $\tilde{\nu}_{max}$ (cm⁻¹): 1717 (w), 1700 (w), 1684 (w), 1654 (w), 1630 (w), 1601 (m), 1590 (w), 1577 (w), 1559 (w), 1540 (w), 1534 (w), 1522 (w), 1509 (m), 1474 (w), 1458 (s), 1437 (w), 1421 (w), 1392 (s), 1374 (w), 1329 (w), 1291 (m), 1262 (m), 1225 (s), 1184 (m), 1156 (w), 1144 (w), 1131 (m), 1110 (m), 1082 (w), 1042 (m), 1031 (m), 1019 (w), 964 (w), 889 (w), 867 (m), 833 (m), 814 (s), 785 (m), 764 (vs), 739 (vs).

5-(3,5-Bis(trifluoromethyl)phenyl)benzo[*c*][1,2,5]oxadiazole (3f)



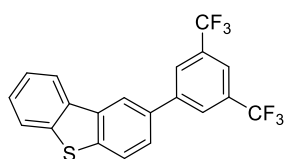
Using potassium benzo[*c*][1,2,5]oxadiazol-5-yltrifluoroborate and a solution of (3,5-bis(trifluoromethyl)phenyl)magnesium bromide in THF according to general procedure **Q** (0.40 mmol scale), provided **3f** (0.23 mmol, 76 mg, 57%) as a colorless solid. R_f = 0.48 (hexane/EtOAc 98:2, UV, KMnO₄, PAA). ¹H NMR

²⁵⁵ K. Funaki, T. Sato, S. Oi, *Org. Lett.* **2012**, *14*, 6186–6189.

²⁵⁶ H. Saito, S. Otsuka, K. Nogi, H. Yorimitsu, *J. Am. Chem. Soc.* **2016**, *138*, 15315–15318.

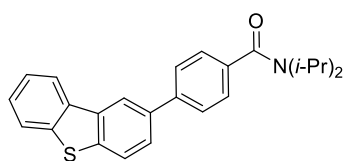
(400 MHz, CDCl₃) δ 8.09 (s, 2H), 8.08 – 8.06 (m, 1H), 8.03 (dd, $J = 9.3, 0.9$ Hz, 1H), 7.99 (s, 1H), 7.70 (dd, $J = 9.3, 1.5$ Hz, 1H) ppm. ¹³C NMR (101 MHz, CDCl₃) 149.5, 148.7, 141.5, 141.1, 132.9 (q, $J = 33.7$ Hz), 131.8, 127.6, 123.2 (q, $J = 272.9$ Hz), 122.9 (qq, $J = 3.7$ Hz), 118.1, 114.9 ppm. LRMS (DEP/EI-Orbitrap): m/z (%): 332.0 (100), 312.0 (34), 302.0 (22), 282.0 (61), 265.0 (24), 237.0 (16), 213.0 (30), 164.0 (13). HRMS (EI-Orbitrap): m/z calcd for C₁₄H₆F₆N₂O⁺: 332.0384; found: 332.0378. IR (Diamond-ATR, neat) $\tilde{\nu}_{max}$ (cm⁻¹): 1628 (w), 1620 (vw), 1540 (w), 1520 (w), 1460 (w), 1382 (m), 1373 (m), 1364 (m), 1326 (w), 1310 (m), 1276 (vs), 1237 (m), 1171 (s), 1123 (vs), 1110 (vs), 1043 (s), 1012 (w), 905 (m), 884 (m), 848 (m), 815 (s), 768 (m), 722 (m), 705 (m), 684 (s). Mp (°C) = 97–101.

2-(3,5-Bis(trifluoromethyl)phenyl)dibenzo[*b,d*]thiophene (3g)



Using potassium dibenzo[*b,d*]thiophen-2-yltrifluoroborate (SM33) and a solution of (3,5-bis(trifluoromethyl)phenyl)magnesium bromide in THF according to general procedure Q (0.40 mmol scale), provided **3g** (0.23 mmol, 89 mg, 56%) as a colorless solid. $R_f = 0.53$ (hexane/EtOAc 100:0, UV, KMnO₄, PAA). ¹H NMR (400 MHz, CDCl₃) δ 8.32 (d, $J = 1.6$ Hz, 1H), 8.29 – 8.22 (m, 1H), 8.13 (s, 2H), 7.96 (d, $J = 8.3$ Hz, 1H), 7.93 – 7.90 (m, 1H), 7.90 – 7.86 (m, 1H), 7.67 (dd, $J = 8.3, 1.9$ Hz, 1H), 7.54 – 7.48 (m, 2H) ppm. ¹³C NMR (101 MHz, CDCl₃) δ 143.4, 140.3, 140.1, 136.5, 135.2, 134.8, 132.4 (q, $J = 33.3$ Hz), 127.5, 127.5, 125.8, 124.8, 123.7, 123.6 (q, $J = 272.8$ Hz), 123.1, 121.9, 121.0 (qq, $J = 3.8$ Hz), 120.2 ppm. LRMS (DEP/EI-Orbitrap): m/z (%): 396.0 (100), 326.0 (10), 258.0 (10), 198.0 (14), 163.4 (12). HRMS (EI-Orbitrap): m/z calcd for C₂₀H₁₀F₆S⁺: 396.0407; found: 396.0399. IR (Diamond-ATR, neat) $\tilde{\nu}_{max}$ (cm⁻¹): 1717 (w), 1618 (w), 1459 (w), 1450 (w), 1434 (w), 1411 (w), 1374 (s), 1326 (w), 1308 (w), 1273 (vs), 1246 (w), 1223 (m), 1170 (s), 1121 (vs), 1108 (s), 1072 (m), 1049 (s), 1024 (m), 898 (m), 881 (m), 874 (m), 846 (m), 813 (m), 762 (s), 732 (m), 726 (m), 716 (w), 704 (m), 692 (m), 682 (s). Mp (°C) = 119–124.

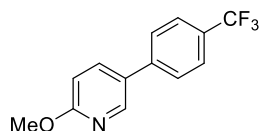
4-(Dibenzo[*b,d*]thiophen-2-yl)-*N,N*-diisopropylbenzamide (3h)



Using potassium dibenzo[*b,d*]thiophen-2-yltrifluoroborate (SM33) and a solution of (4-(diisopropylcarbamoyl)phenyl)zinc iodide in THF according to general procedure Q (0.40 mmol scale), provided **3h** (0.22 mmol, 85 mg, 56%) as a colorless oil. $R_f = 0.35$ (hexane/EtOAc 80:20, UV, KMnO₄, PAA). ¹H NMR (400 MHz, CDCl₃) δ 8.34 (d, $J = 1.5$ Hz, 1H), 8.24 – 8.19 (m, 1H), 7.90 (d, $J = 8.3$ Hz, 1H), 7.89 – 7.84 (m, 1H), 7.74 – 7.70 (m, 2H), 7.68 (dd, $J = 8.3, 1.8$ Hz, 1H), 7.51 – 7.42 (m, 4H), 4.12 – 3.41 (m, 2H), 1.81 – 1.01 (m, 12H) ppm. ¹³C NMR (101 MHz, CDCl₃) δ 170.9, 141.6, 140.0, 138.9, 137.9, 137.2, 136.2, 135.5, 127.5, 127.0, 126.4, 126.1, 124.6, 123.2, 123.0, 121.7, 120.1, 51.2, 46.3, 20.9 ppm. Signal splitting was observed, which was presumably caused by rotational barriers. LRMS (DEP/EI-Orbitrap): m/z (%): 387.2 (20), 344.1 (36), 287.1 (92), 258.1 (39), 143.5 (11), 61.0 (15). HRMS (EI-Orbitrap): m/z calcd for C₂₅H₂₅NOS⁺: 387.1657; found: 387.1646. IR

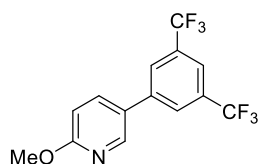
(Diamond-ATR, neat) $\tilde{\nu}_{max}$ (cm⁻¹): 2967 (w), 2930 (w), 2873 (w), 1610 (m), 1515 (w), 1466 (w), 1441 (m), 1432 (m), 1378 (m), 1370 (m), 1340 (s), 1291 (w), 1252 (w), 1225 (w), 1212 (w), 1192 (w), 1159 (w), 1136 (w), 1097 (w), 1082 (w), 1070 (w), 1037 (w), 1025 (w), 1017 (w), 1006 (w), 906 (s), 878 (w), 852 (w), 838 (w), 822 (w), 811 (m), 763 (m), 725 (vs).

2-Methoxy-5-(4-(trifluoromethyl)phenyl)pyridine (**3i**)

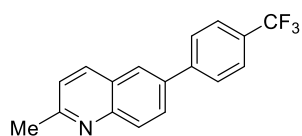


Using potassium trifluoro(6-methoxypyridin-3-yl)borate and a solution of (4-(trifluoromethyl)phenyl)magnesium bromide in THF according to general procedure **Q** (0.40 mmol scale), provided **3i** (0.24 mmol, 60 mg, 59%) as a colorless solid. R_f = 0.37 (hexane/EtOAc 95:5, UV, KMnO₄, PAA). ¹H NMR (400 MHz, CDCl₃) δ 8.41 (dd, J = 2.6, 0.8 Hz, 1H), 7.80 (dd, J = 8.6, 2.6 Hz, 1H), 7.72 – 7.67 (m, 2H), 7.65 – 7.60 (m, 2H), 6.85 (dd, J = 8.6, 0.8 Hz, 1H), 3.99 (s, 3H) ppm. ¹³C NMR (101 MHz, CDCl₃) δ 164.3, 145.4, 141.6, 137.6, 129.5 (q, J = 32.5 Hz), 128.8, 127.0, 126.1 (q, J = 3.8 Hz), 124.3 (q, J = 271.9 Hz), 111.3, 53.8 ppm. LRMS (DEP/EI-Orbitrap): m/z (%): 252.1 (100), 224.1 (42), 222.1 (28), 202.0 (13), 183.0 (10), 154.1 (17). HRMS (EI-Orbitrap): m/z calcd for C₁₃H₁₀F₃NO⁺: 253.0714; found: 253.0712. IR (Diamond-ATR, neat) $\tilde{\nu}_{max}$ (cm⁻¹): 3058 (w), 3019 (w), 2980 (w), 2947 (w), 2905 (w), 1617 (w), 1608 (m), 1582 (w), 1566 (w), 1529 (w), 1490 (m), 1460 (w), 1444 (w), 1438 (w), 1418 (m), 1374 (m), 1334 (s), 1327 (s), 1314 (m), 1293 (s), 1280 (m), 1252 (m), 1196 (w), 1178 (w), 1161 (s), 1145 (m), 1108 (vs), 1073 (s), 1042 (m), 1016 (s), 999 (m), 972 (w), 959 (w), 939 (w), 853 (w), 831 (s), 714 (m). Mp (°C) = 54–58.

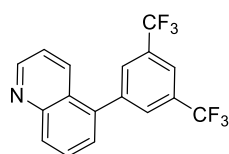
5-(3,5-Bis(trifluoromethyl)phenyl)-2-methoxypyridine (**3j**)



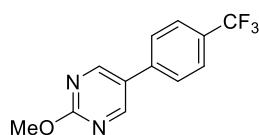
Using potassium trifluoro(6-methoxypyridin-3-yl)borate and a solution of (3,5-bis(trifluoromethyl)phenyl)magnesium bromide in THF according to general procedure **Q** (0.50 mmol scale), provided **3j** (0.24 mmol, 77 mg, 48%) as a colorless oil. R_f = 0.46 (hexane/EtOAc 95:5, UV, KMnO₄, PAA). ¹H NMR (400 MHz, CDCl₃) δ 8.41 (dd, J = 2.6, 0.8 Hz, 1H), 7.94 (s, 2H), 7.85 (s, 1H), 7.81 (dd, J = 8.6, 2.6 Hz, 1H), 6.87 (dd, J = 8.7, 0.8 Hz, 1H), 4.00 (s, 3H) ppm. ¹³C NMR (101 MHz, CDCl₃) δ 164.7, 145.6, 140.3, 137.4, 132.5 (q, J = 33.3 Hz), 127.4, 126.8, 123.4 (q, J = 272.8 Hz), 121.1 (qq, J = 3.8 Hz), 111.6, 53.9 ppm. LRMS (DEP/EI-Orbitrap): m/z (%): 320.1 (100), 302.1 (14), 292.1 (47), 270.0 (24), 222.1 (12), 202.0 (14), 182.1 (11). HRMS (EI-Orbitrap): m/z calcd for C₁₄H₉F₆NO⁺: 321.0588; found: 321.0578. IR (Diamond-ATR, neat) $\tilde{\nu}_{max}$ (cm⁻¹): 1604 (m), 1568 (w), 1504 (m), 1466 (m), 1455 (w), 1436 (w), 1383 (m), 1368 (s), 1314 (w), 1274 (vs), 1171 (s), 1123 (vs), 1108 (s), 1062 (s), 1021 (s), 1012 (m), 894 (s), 846 (m), 830 (s), 798 (w), 760 (w), 717 (m), 704 (s), 682 (s).

2-Methyl-6-(4-(trifluoromethyl)phenyl)quinoline (3k)

Using potassium trifluoro(2-methylquinolin-6-yl)borate (**SM34**) and a solution of (4-(trifluoromethyl)phenyl)magnesium bromide in THF according to general procedure **Q** (0.40 mmol scale), provided **3k** (0.21 mmol, 60 mg, 52%) as a colorless solid. $R_f = 0.15$ (hexane/EtOAc 90:10, UV, KMnO_4 , PAA). $^1\text{H NMR}$ (400 MHz, CDCl_3) δ 8.10 (dd, $J = 8.5, 4.9$ Hz, 2H), 7.96 (d, $J = 2.0$ Hz, 1H), 7.92 (dd, $J = 8.7, 2.1$ Hz, 1H), 7.79 (d, $J = 7.9$ Hz, 2H), 7.73 (d, $J = 8.3$ Hz, 2H), 7.33 (d, $J = 8.4$ Hz, 1H), 2.77 (s, 3H) ppm. $^{13}\text{C NMR}$ (101 MHz, CDCl_3) δ 159.8, 147.6, 144.1, 137.0, 136.6, 130.0 (d, $J = 32.5$ Hz), 129.5, 128.9, 127.7, 126.7, 126.0 (q, $J = 3.7$ Hz), 126.0, 124.4 (q, $J = 272.0$ Hz), 122.8, 25.6 ppm. **LRMS** (DEP/EI-Orbitrap): m/z (%): 287.1 (100), 268.1 (8), 217.1 (7), 176.0 (8), 143.5 (9), 118.5 (9). **HRMS** (EI-Orbitrap): m/z calcd for $\text{C}_{17}\text{H}_{12}\text{F}_3\text{N}^+$: 287.0922; found: 287.0917. **IR** (Diamond-ATR, neat) $\tilde{\nu}_{\text{max}}$ (cm^{-1}): 1615 (m), 1600 (m), 1576 (w), 1494 (m), 1439 (w), 1415 (w), 1389 (w), 1371 (vw), 1322 (s), 1284 (m), 1258 (m), 1225 (m), 1166 (s), 1158 (s), 1104 (vs), 1067 (s), 1028 (m), 1014 (m), 984 (w), 964 (m), 950 (m), 904 (m), 892 (m), 850 (m), 826 (s), 775 (w), 736 (m). **Mp** ($^\circ\text{C}$) = 117–121.

5-(3,5-Bis(trifluoromethyl)phenyl)quinoline (3l)

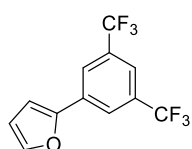
Using potassium trifluoro(quinolin-5-yl)borate (**SM26**) and a solution of (3,5-bis(trifluoromethyl)phenyl)magnesium bromide in THF according to general procedure **Q** (0.40 mmol scale), provided **3l** (0.16 mmol, 54 mg, 41%) as a colorless solid. $R_f = 0.34$ (hexane/EtOAc 80:20, UV, KMnO_4 , PAA). $^1\text{H NMR}$ (400 MHz, CDCl_3) δ 8.99 (dd, $J = 4.2, 1.7$ Hz, 1H), 8.22 (dt, $J = 8.6, 1.0$ Hz, 1H), 8.05 (dt, $J = 8.5, 1.2$ Hz, 1H), 7.99 (s, 1H), 7.94 (s, 2H), 7.81 (dd, $J = 8.6, 7.1$ Hz, 1H), 7.54 (dd, $J = 7.1, 1.2$ Hz, 1H), 7.45 (dd, $J = 8.6, 4.2$ Hz, 1H) ppm. $^{13}\text{C NMR}$ (101 MHz, CDCl_3) δ 150.9, 148.6, 141.6, 137.2, 133.2, 132.1 (q, $J = 33.4$ Hz), 130.7, 130.2, 129.1, 128.0, 126.3, 123.4 (q, $J = 272.9$ Hz), 122.1, 121.8 (qq, $J = 3.8$ Hz) ppm. **LRMS** (DEP/EI-Orbitrap): m/z (%): 341.1 (100), 272.1 (47), 252.1 (10), 225.1 (11), 203.1 (10). **HRMS** (EI-Orbitrap): m/z calcd for $\text{C}_{17}\text{H}_9\text{F}_6\text{N}^+$: 341.0639; found: 341.0632. **IR** (Diamond-ATR, neat) $\tilde{\nu}_{\text{max}}$ (cm^{-1}): 1505 (w), 1374 (m), 1360 (w), 1285 (s), 1204 (w), 1170 (s), 1115 (vs), 1062 (w), 1042 (w), 902 (m), 873 (w), 848 (w), 828 (w), 803 (m), 714 (m), 706 (m), 688 (m). **Mp** ($^\circ\text{C}$) = 119–121.

2-Methoxy-5-(4-(trifluoromethyl)phenyl)pyrimidine (3m)

Using potassium trifluoro(2-methoxypyrimidin-5-yl)borate and a solution of (4-(trifluoromethyl)phenyl)magnesium bromide in THF according to general procedure **Q** (0.40 mmol scale), provided **3m** (0.15 mmol, 37 mg, 37%) as a colorless solid. $R_f = 0.20$ (hexane/EtOAc 90:10, UV, KMnO_4 , PAA). $^1\text{H NMR}$ (400 MHz, CDCl_3) δ 8.74 (s, 2H), 7.74 (d, $J = 7.8$ Hz, 2H), 7.64 (d, $J = 7.5$ Hz, 2H), 4.08 (s, 3H) ppm. $^{13}\text{C NMR}$ (101 MHz, CDCl_3) δ 165.7, 157.6, 138.2, 130.5 (q, $J = 32.7$ Hz), 127.1, 127.0, 126.4 (q, $J = 3.8$ Hz), 124.1 (q, $J = 272.2$ Hz), 55.4 ppm. **LRMS** (DEP/EI-Orbitrap): m/z (%): 254.1 (68), 225.1 (100), 198.1 (27), 169.0

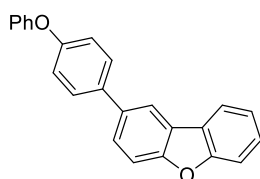
(12), 155.1 (43), 151.0 (14). **HRMS** (EI-Orbitrap): m/z calcd for $C_{12}H_9F_3N_2O^+$: 254.0667; found: 254.0662. **IR** (Diamond-ATR, neat) $\tilde{\nu}_{max}$ (cm^{-1}): 1750 (w), 1710 (vs), 1619 (w), 1598 (w), 1551 (w), 1525 (w), 1475 (m), 1436 (w), 1419 (m), 1361 (s), 1326 (s), 1304 (m), 1278 (w), 1221 (s), 1204 (w), 1167 (m), 1156 (m), 1126 (m), 1115 (m), 1098 (m), 1080 (m), 1065 (m), 1034 (m), 1020 (w), 999 (w), 901 (w), 853 (w), 838 (m), 798 (w), 716 (w). **Mp** ($^{\circ}C$) = 103–107.

2-(3,5-Bis(trifluoromethyl)phenyl)furan (3n)



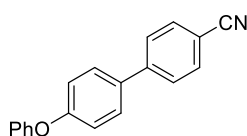
Using potassium trifluoro(furan-2-yl)borate and a solution of (3,5-bis(trifluoromethyl)phenyl)magnesium bromide in THF according to general procedure **Q** (0.50 mmol scale), provided **3n** (0.13 mmol, 35 mg, 25%) as a colorless solid. (Note: This product could only be isolated in 70% purity, as no separation from the undesired homocoupled product was possible.) R_f = 0.58 (hexane/EtOAc 100:0, UV, $KMnO_4$, PAA). **1H NMR** (400 MHz, $CDCl_3$) δ 8.07 (s, 2H), 7.73 (s, 1H), 7.55 (dd, J = 1.9, 0.7 Hz, 1H), 6.85 (dd, J = 3.4, 0.7 Hz, 1H), 6.55 (dd, J = 3.5, 1.8 Hz, 1H) ppm. **LRMS** (DEP/EI-Orbitrap): m/z (%): 280.0 (100), 261.0 (17), 251.0 (39), 183.0 (35), 133.0 (10). Analytical data in accordance to literature.²⁵⁷

2-(4-Phenoxyphenyl)dibenzo[*b,d*]furan (3o)



Using potassium trifluoro(4-phenoxyphenyl)borate and a solution of dibenzo[*b,d*]furan-2-ylmagnesium bromide in THF according to general procedure **Q** (0.40 mmol scale), provided **3o** (0.26 mmol, 88 mg, 66%) as a colorless solid. R_f = 0.51 (hexane/EtOAc 98:2, UV, $KMnO_4$, PAA). **1H NMR** (400 MHz, $CDCl_3$) δ 8.12 (dd, J = 1.9, 0.7 Hz, 1H), 8.00 (ddd, J = 7.7, 1.4, 0.7 Hz, 1H), 7.68 – 7.58 (m, 5H), 7.48 (ddd, J = 8.4, 7.3, 1.4 Hz, 1H), 7.40 – 7.34 (m, 3H), 7.16 – 7.06 (m, 5H) ppm. **^{13}C NMR** (101 MHz, $CDCl_3$) δ 157.4, 156.8, 156.8, 155.8, 136.6, 135.9, 130.0, 128.9, 127.5, 126.6, 124.9, 124.4, 123.5, 123.0, 120.9, 119.4, 119.1, 112.0 ppm. **LRMS** (DEP/EI-Orbitrap): m/z (%): 336.1 (100), 259.1 (10), 231.1 (14), 202.1 (10), 77.1 (9). **HRMS** (EI-Orbitrap): m/z calcd for $C_{24}H_{16}O_2^+$: 336.1150; found: 336.1145. **IR** (Diamond-ATR, neat) $\tilde{\nu}_{max}$ (cm^{-1}): 1750 (w), 1734 (w), 1710 (s), 1684 (w), 1654 (w), 1559 (w), 1540 (w), 1508 (w), 1489 (w), 1473 (w), 1466 (w), 1457 (w), 1447 (w), 1436 (w), 1430 (w), 1419 (w), 1361 (m), 1221 (m), 1197 (w), 1092 (w), 915 (m), 842 (w), 814 (w), 728 (vs). **Mp** ($^{\circ}C$) = 140–145.

4'-Phenoxy-[1,1'-biphenyl]-4-carbonitrile (4a)

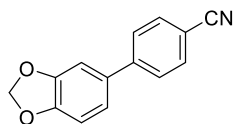


Using potassium trifluoro(4-phenoxyphenyl)borate and a solution of (4-cyanophenyl)zinc iodide in THF according to general procedure **Q** (0.50 mmol scale), provided **4a** (0.23 mmol, 62 mg, 46%) as a colorless oil. R_f = 0.14 (hexane/EtOAc 98:2, UV, $KMnO_4$, PAA). **1H NMR** (400 MHz, $CDCl_3$) δ 7.74 – 7.69 (m, 2H), 7.68 – 7.63

²⁵⁷ G. E. Morton, A. G. M. Barrett, *J. Org. Chem.* **2005**, *70*, 3525–3529.

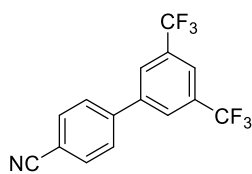
(m, 2H), 7.58 – 7.52 (m, 2H), 7.41 – 7.35 (m, 2H), 7.16 (ddt, $J = 8.5, 7.2, 1.1$ Hz, 1H), 7.12 – 7.05 (m, 4H) ppm. **LRMS** (DEP/EI-Orbitrap): m/z (%): 271.1 (100), 242.1 (12), 207.0 (86), 190.9 (12), 166.1 (17), 140.1 (19), 77.0 (36). Analytical data in accordance to literature.²⁵⁸

4-(Benzo[*d*][1,3]dioxol-5-yl)benzonitrile (**4b**)



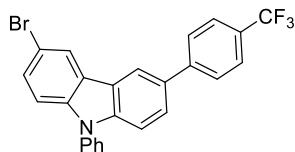
Using potassium benzo[*d*][1,3]dioxol-5-yltrifluoroborate and a solution of (4-cyanophenyl)zinc iodide in THF according to general procedure **Q** (0.50 mmol scale), provided **4b** (0.19 mmol, 42 mg, 38%) as a colorless oil. $R_f = 0.30$ (hexane/EtOAc 98:2, UV, KMnO₄, PAA). ¹H NMR (400 MHz, CDCl₃) δ 7.72 – 7.66 (m, 2H), 7.63 – 7.58 (m, 2H), 7.09 – 7.04 (m, 2H), 6.91 (d, $J = 7.9$ Hz, 1H), 6.03 (s, 2H) ppm. **LRMS** (DEP/EI-Orbitrap): m/z (%): 223.0 (100), 164.0 (43), 138.0 (17), 111.2 (18). Analytical data in accordance to literature.²⁵⁹

3',5'-Bis(trifluoromethyl)-[1,1'-biphenyl]-4-carbonitrile (**4c**)



Using potassium trifluoro(4-benzonitrile)borate and a solution of (3,5-bis(trifluoromethyl)phenyl)magnesium bromide in THF according to general procedure **Q** (0.40 mmol scale), provided **4c** (0.21 mmol, 66 mg, 66%) as a colorless solid. $R_f = 0.33$ (hexane/EtOAc 98:2, UV, KMnO₄, PAA). ¹H NMR (400 MHz, CDCl₃) δ 8.02 (s, 2H), 7.94 (s, 1H), 7.85 – 7.78 (m, 2H), 7.77 – 7.69 (m, 2H) ppm. **LRMS** (DEP/EI-Orbitrap): m/z (%): 315.0 (100), 296.0 (19), 226.0 (22), 177.0 (15). Analytical data in accordance to literature.²⁶⁰

3-Bromo-9-phenyl-6-(4-(trifluoromethyl)phenyl)-9*H*-carbazole (**4d**)



Using potassium (6-bromo-9-phenyl-9*H*-carbazol-3-yl)trifluoroborate (**SM32**) and a solution of (4-(trifluoromethyl)phenyl)magnesium bromide in THF according to general procedure **Q** (0.40 mmol scale), provided **4d** (0.26 mmol, 120 mg, 64%) as a colorless solid. $R_f = 0.50$ (hexane/EtOAc 98:2, UV, KMnO₄, PAA). ¹H NMR (400 MHz, CDCl₃) δ 8.33 – 8.29 (m, 2H), 7.80 (d, $J = 8.4$ Hz, 2H), 7.73 (d, $J = 8.3$ Hz, 2H), 7.69 – 7.61 (m, 3H), 7.57 – 7.49 (m, 4H), 7.47 (d, $J = 8.6$ Hz, 1H), 7.30 (d, $J = 8.7$ Hz, 1H) ppm. ¹³C NMR (101 MHz, CDCl₃) δ 145.3, 141.2, 140.2, 137.1, 132.4, 130.3, 129.2, 128.9 (q, $J = 32.4$ Hz), 128.2, 127.6, 127.1, 126.2, 125.9 (q, $J = 3.8$ Hz), 125.1, 124.6 (q, $J = 271.9$ Hz), 123.3, 123.0, 119.3, 113.2, 111.7, 110.7 ppm. **LRMS** (DEP/EI-Orbitrap): m/z (%): 467.0 (100), 465.0 (97), 385.1 (18), 233.5 (10), 43.1 (35). **HRMS** (EI-Orbitrap): m/z calcd for C₂₅H₁₅BrF₃N⁺: 465.0340; found: 465.0339. **IR** (Diamond-ATR, neat) $\tilde{\nu}_{max}$ (cm⁻¹): 1716 (w), 1700 (w), 1684 (w), 1616 (m), 1598 (m), 1559 (w), 1541 (w), 1522 (w), 1500 (s), 1478 (m), 1456 (w), 1439 (m), 1420 (w), 1404 (w), 1363 (m), 1323 (vs), 1286 (m), 1252 (w), 1234 (m), 1193 (w), 1164 (m), 1120 (s), 1111 (s), 1070 (s), 1059

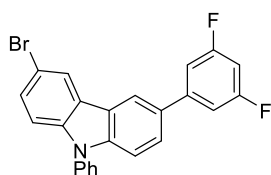
²⁵⁸ S. Yang, C. Wu, H. Zhou, Y. Yang, Y. Zhao, C. Wang, W. Yang, J. Xu, *Adv. Synth. Catal.* **2013**, 355, 53–58.

²⁵⁹ J. M. Hammann, F. H. Lutter, D. Haas, P. Knochel, *Angew. Chem. Int. Ed.* **2017**, 56, 1082–1086.

²⁶⁰ G. A. Molander, B. Biolatto, *J. Org. Chem.* **2003**, 68, 4302–4314.

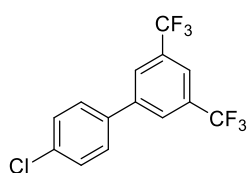
(w), 1028 (w), 1018 (w), 1012 (w), 941 (w), 871 (w), 848 (m), 809 (m), 761 (m), 710 (w), 698 (m). **Mp** (°C) = 138–141.

3-Bromo-6-(3,5-difluorophenyl)-9-phenyl-9H-carbazole (4e)



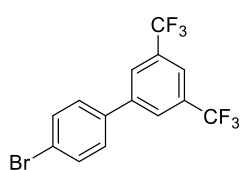
Using potassium (6-bromo-9-phenyl-9H-carbazol-3-yl)trifluoroborate (**SM32**) and a solution of (3,5-difluorophenyl)magnesium bromide in THF according to general procedure **Q** (0.40 mmol scale), provided **4e** (0.18 mmol, 80 mg, 46%) as a colorless solid. $R_f = 0.40$ (hexane/EtOAc 98:2, UV, KMnO_4 , PAA). $^1\text{H NMR}$ (400 MHz, CDCl_3) δ 8.30 (d, $J = 1.9$ Hz, 1H), 8.25 (d, $J = 1.8$ Hz, 1H), 7.67 – 7.59 (m, 3H), 7.56 – 7.49 (m, 4H), 7.44 (d, $J = 8.5$ Hz, 1H), 7.29 (d, $J = 8.7$ Hz, 1H), 7.24 – 7.17 (m, 2H), 6.79 (tt, $J = 8.9, 2.3$ Hz, 1H) ppm. $^{13}\text{C NMR}$ (101 MHz, CDCl_3) δ 163.5 (dd, $J = 247.6, 13.3$ Hz), 145.1 (t, $J = 9.6$ Hz), 141.3, 140.2, 137.1, 131.5 (t, $J = 2.5$ Hz), 130.2, 129.3, 128.2, 127.1, 125.9, 125.1, 123.3, 123.0, 119.1, 113.2, 111.7, 110.6, 110.0 (dd, $J = 18.2, 6.6$ Hz), 102.0 (t, $J = 25.5$ Hz) ppm. **LRMS** (DEP/EI-Orbitrap): m/z (%): 435.0 (100), 433.0 (97), 353.1 (23), 216.5 (12), 166.5 (10), 123.0 (12), 74.1 (75), 59.0 (91). **HRMS** (EI-Orbitrap): m/z calcd for $\text{C}_{24}\text{H}_{14}\text{BrF}_2\text{N}^+$: 433.0278; found: 433.0272. **IR** (Diamond-ATR, neat) $\tilde{\nu}_{max}$ (cm^{-1}): 1750 (w), 1734 (w), 1717 (m), 1700 (w), 1684 (w), 1654 (m), 1647 (w), 1635 (m), 1619 (s), 1592 (s), 1576 (m), 1570 (w), 1559 (m), 1541 (m), 1522 (w), 1501 (vs), 1472 (m), 1465 (s), 1457 (s), 1436 (m), 1420 (w), 1363 (m), 1339 (w), 1321 (w), 1283 (m), 1266 (m), 1234 (m), 1196 (m), 1173 (w), 1116 (s), 1063 (w), 1056 (w), 1026 (w), 988 (m), 937 (vw), 905 (w), 857 (m), 835 (w), 810 (m), 790 (w), 761 (m), 699 (m). **Mp** (°C) = 174–178.

4'-Chloro-3,5-bis(trifluoromethyl)-1,1'-biphenyl (4f)



Using potassium trifluoro(4-chlorophenyl)borate and a solution of (3,5-bis(trifluoromethyl)phenyl)magnesium bromide in THF according to general procedure **Q** (0.40 mmol scale), provided **4f** (0.32 mmol, 104 mg, 80%) as a colorless oil. (Note: This product could only be isolated in 90% purity, as no separation from the undesired homocoupled product was possible.) $R_f = 0.67$ (hexane/EtOAc 100:0, UV, KMnO_4 , PAA). $^1\text{H NMR}$ (400 MHz, CDCl_3) δ 7.98 (s, 2H), 7.88 (s, 1H), 7.58 – 7.52 (m, 2H), 7.51 – 7.45 (m, 2H) ppm. **LRMS** (DEP/EI-Orbitrap): m/z (%): 324.0 (100), 305.0 (15), 269.0 (25), 220.1 (26). Analytical data in accordance to literature.²⁶¹

4'-Bromo-3,5-bis(trifluoromethyl)-1,1'-biphenyl (4g)

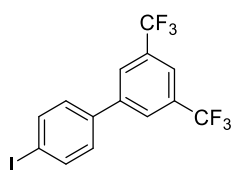


Using potassium (4-bromophenyl)trifluoroborate and a solution of (3,5-bis(trifluoromethyl)phenyl)magnesium bromide in THF according to general procedure **Q** (0.50 mmol scale), provided **4g** (0.25 mmol, 90 mg, 49%) as a colorless oil. (Note: This product could only be isolated in 80% purity, as no separation

²⁶¹ Y.-N. Wang, X.-Q. Guo, X.-H. Zhu, R. Zhong, L.-H. Cai, X.-F. Huo, *Chem. Commun.* **2012**, 48, 10437–10439.

from the undesired homocoupled product was possible.) $R_f = 0.62$ (hexane/EtOAc 100:0, UV, KMnO_4 , PAA). $^1\text{H NMR}$ (400 MHz, CDCl_3) δ 7.98 (s, 2H), 7.88 (s, 1H), 7.68 – 7.61 (m, 2H), 7.53 – 7.45 (m, 2H) ppm. $^{13}\text{C NMR}$ (101 MHz, CDCl_3) δ 142.3, 137.2, 132.6, 133.7 (q, $J = 33.3$ Hz), 128.9, 127.2 – 127.1 (m), 123.6, 123.4 (q, $J = 272.8$ Hz), 121.4 (qq, $J = 3.8$ Hz) ppm. **LRMS** (DEP/EI-Orbitrap): m/z (%): 370.0 (76), 368.0 (77), 269.0 (100), 219.0 (56), 201.1 (19), 199.0 (13), 170.1 (11). **HRMS** (EI-Orbitrap): m/z calcd for $\text{C}_{14}\text{H}_7\text{BrF}_6^+$: 367.9635; found: 367.9630. **IR** (Diamond-ATR, neat) $\tilde{\nu}_{\text{max}}$ (cm^{-1}): 1465 (w), 1381 (s), 1349 (m), 1274 (vs), 1258 (s), 1170 (s), 1125 (vs), 1107 (s), 1076 (s), 1052 (s), 1010 (m), 898 (s), 847 (m), 821 (s), 728 (m), 716 (w), 704 (s), 682 (s).

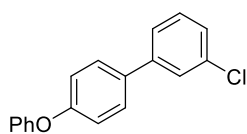
4'-Iodo-3,5-bis(trifluoromethyl)-1,1'-biphenyl (4h)



Using potassium trifluoro(4-iodophenyl)borate and a solution of (3,5-bis(trifluoromethyl)phenyl)magnesium bromide in THF according to general procedure **Q** (0.40 mmol scale), provided **4h** (0.31 mmol, 129 mg, 78%) as a colorless solid.

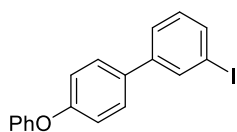
$R_f = 0.75$ (hexane/EtOAc 100:0, UV, KMnO_4 , PAA). $^1\text{H NMR}$ (400 MHz, CDCl_3) δ 7.97 (s, 2H), 7.87 (s, 1H), 7.86 – 7.82 (m, 2H), 7.37 – 7.32 (m, 2H) ppm. $^{13}\text{C NMR}$ (101 MHz, CDCl_3) δ 142.4, 138.6, 137.8, 132.5 (q, $J = 33.4$ Hz), 129.1, 127.1 (q, $J = 2.8$ Hz), 123.4 (q, $J = 272.9$ Hz), 121.5 (dt, $J = 7.7, 3.8$ Hz), 95.2 ppm. **LRMS** (DEP/EI-Orbitrap): m/z (%): 416.0 (100), 397.0 (10), 269.0 (59), 220.0 (34), 201.0 (12). **HRMS** (EI-Orbitrap): m/z calcd for $\text{C}_{14}\text{H}_7\text{F}_6\text{I}^+$: 415.9497; found: 415.9492. **IR** (Diamond-ATR, neat) $\tilde{\nu}_{\text{max}}$ (cm^{-1}): 1381 (m), 1273 (s), 1195 (m), 1186 (m), 1166 (m), 1128 (vs), 1111 (m), 1051 (w), 1005 (w), 902 (m), 846 (w), 823 (s), 727 (w), 704 (m), 682 (m). **Mp** ($^\circ\text{C}$) = 68–70.

3-Chloro-4'-phenoxy-1,1'-biphenyl (4i)

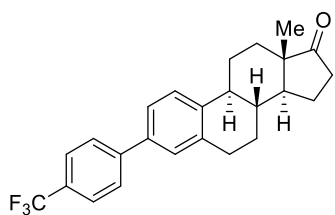


Using potassium trifluoro(4-phenoxyphenyl)borate and a solution of (3-chlorophenyl)magnesium bromide in THF according to general procedure **Q** (0.40 mmol scale), provided **4i** (0.31 mmol, 87 mg, 77%) as a colorless solid. R_f

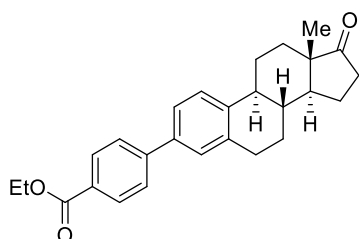
= 0.18 (hexane/EtOAc 100:0, UV, KMnO_4 , PAA). $^1\text{H NMR}$ (400 MHz, CDCl_3) δ 7.57 (t, $J = 1.8$ Hz, 1H), 7.56 – 7.51 (m, 2H), 7.45 (dt, $J = 7.6, 1.5$ Hz, 1H), 7.42 – 7.34 (m, 3H), 7.34 – 7.29 (m, 1H), 7.19 – 7.13 (m, 1H), 7.12 – 7.06 (m, 4H) ppm. $^{13}\text{C NMR}$ (101 MHz, CDCl_3) δ 157.5, 157.0, 142.5, 134.82, 134.79, 130.1, 130.0, 128.6, 127.1, 125.1, 123.7, 119.3, 119.1 ppm. One carbon signal could not be detected. **LRMS** (DEP/EI-Orbitrap): m/z (%): 280.1 (100), 252.1 (11), 217.1 (14), 207.0 (22), 152.1 (13). **HRMS** (EI-Orbitrap): m/z calcd for $\text{C}_{18}\text{H}_{13}\text{ClO}^+$: 280.0655; found: 280.0650. **IR** (Diamond-ATR, neat) $\tilde{\nu}_{\text{max}}$ (cm^{-1}): 3066 (w), 3037 (w), 1607 (w), 1594 (m), 1588 (s), 1563 (w), 1539 (w), 1510 (s), 1488 (vs), 1473 (s), 1430 (w), 1419 (vw), 1394 (w), 1332 (w), 1303 (w), 1279 (w), 1233 (vs), 1202 (m), 1169 (m), 1099 (m), 1081 (w), 1071 (w), 1036 (w), 1023 (w), 1011 (w), 1004 (w), 997 (w), 870 (m), 837 (m), 805 (w), 782 (s), 746 (s), 731 (w), 724 (w), 691 (s), 673 (w). **Mp** ($^\circ\text{C}$) = 46–48.

3-Iodo-4'-phenoxy-1,1'-biphenyl (4j)

Using potassium trifluoro(4-phenoxyphenyl)borate and a solution of (3-iodophenyl)magnesium iodide in THF according to general procedure **Q** (0.40 mmol scale), provided **4j** (0.24 mmol, 88 mg, 60%) as a colorless solid. $R_f = 0.28$ (hexane/EtOAc 100:0, UV, KMnO_4 , PAA). $^1\text{H NMR}$ (400 MHz, CDCl_3) δ 7.93 (t, $J = 1.8$ Hz, 1H), 7.67 (dt, $J = 7.8, 1.3$ Hz, 1H), 7.55 – 7.49 (m, 3H), 7.41 – 7.34 (m, 2H), 7.20 – 7.12 (m, 2H), 7.12 – 7.04 (m, 4H) ppm. $^{13}\text{C NMR}$ (101 MHz, CDCl_3) δ 157.5, 157.0, 142.9, 136.0, 134.7, 130.6, 130.0, 128.6, 126.3, 123.7, 119.3, 119.1, 95.0 ppm. One carbon signal could not be detected. **LRMS** (DEP/EI-Orbitrap): m/z (%): 372.0 (100), 207.0 (14), 152.1 (48), 139.1 (14). **HRMS** (EI-Orbitrap): m/z calcd for $\text{C}_{18}\text{H}_{13}\text{IO}^+$: 372.0011; found: 372.0005. **IR** (Diamond-ATR, neat) $\tilde{\nu}_{max}$ (cm^{-1}): 3036 (w), 1610 (w), 1587 (s), 1554 (m), 1509 (s), 1487 (vs), 1468 (s), 1455 (m), 1425 (w), 1389 (w), 1332 (w), 1303 (w), 1278 (w), 1232 (vs), 1201 (m), 1166 (m), 1108 (w), 1070 (w), 1025 (w), 1010 (w), 992 (m), 907 (w), 903 (w), 870 (m), 837 (m), 801 (w), 780 (s), 757 (m), 745 (w), 731 (m), 719 (w), 690 (s), 654 (m). **Mp** ($^\circ\text{C}$) = 75–77.

3-(4-(Trifluoromethyl)phenyl)-3-deoxyestrone (6a)

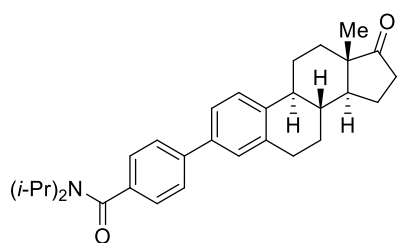
Using potassium 3-deoxyestrone-3-trifluoroborate (**SM27**) and a solution of (4-(trifluoromethyl)phenyl)zinc iodide in THF according to general procedure **Q** (0.40 mmol scale), provided **6a** (0.26 mmol, 103 mg, 65%) as a colorless solid. $R_f = 0.17$ (hexane/EtOAc 95:5, UV, KMnO_4 , PAA). $^1\text{H NMR}$ (400 MHz, CDCl_3) δ 7.68 (s, 4H), 7.42 – 7.40 (m, 2H), 7.35 (s, 1H), 3.05 – 2.98 (m, 2H), 2.58 – 2.44 (m, 2H), 2.37 (td, $J = 10.9, 4.1$ Hz, 1H), 2.23 – 2.14 (m, 1H), 2.14 – 2.04 (m, 2H), 2.01 (dt, $J = 12.5, 2.9$ Hz, 1H), 1.72 – 1.45 (m, 6H), 0.94 (s, 3H) ppm. $^{13}\text{C NMR}$ (101 MHz, CDCl_3) δ 221.0, 144.7, 140.1, 137.4, 137.4, 129.3 (q, $J = 32.4$ Hz), 128.0, 127.3, 126.2, 125.8 (q, $J = 3.8$ Hz), 124.8, 127.2 (q, $J = 270.8$ Hz), 50.7, 48.1, 44.5, 38.3, 36.0, 31.7, 29.7, 26.6, 25.9, 21.8, 14.0 ppm. **LRMS** (DEP/EI-Orbitrap): m/z (%): 398.2 (100), 365.2 (11), 354.2 (36), 341.2 (29), 300.1 (26), 288.1 (25), 274.1 (22), 207.0 (47). **HRMS** (EI-Orbitrap): m/z calcd for $\text{C}_{25}\text{H}_{25}\text{F}_3\text{O}^+$: 398.1858; found: 398.1850. **IR** (Diamond-ATR, neat) $\tilde{\nu}_{max}$ (cm^{-1}): 2940 (w), 2924 (w), 1736 (s), 1615 (m), 1320 (vs), 1258 (m), 1163 (s), 1126 (s), 1114 (s), 1108 (s), 1088 (m), 1068 (s), 1056 (s), 1042 (m), 1014 (m), 1007 (m), 958 (w), 865 (w), 850 (m), 842 (m), 824 (s), 800 (m). **Mp** ($^\circ\text{C}$) = 170–175.

3-(4-(Ethoxycarbonyl)phenyl)-3-deoxyestrone (6b)

Using potassium 3-deoxyestrone-3-trifluoroborate (**SM27**) and a solution of (4-(ethoxycarbonyl)phenyl)zinc iodide in THF according to general procedure **Q** (0.40 mmol scale), provided **6b** (0.22 mmol, 89 mg, 55%) as a colorless solid. $R_f = 0.51$ (hexane/EtOAc 80:20, UV, KMnO_4 , PAA). $^1\text{H NMR}$ (400 MHz, CDCl_3) δ 8.12 – 8.06 (m, 2H),

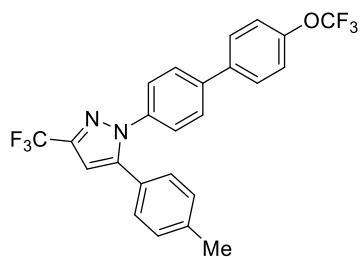
7.68 – 7.61 (m, 2H), 7.45 – 7.33 (m, 3H), 4.40 (q, $J = 7.1$ Hz, 2H), 3.03 – 2.98 (m, 2H), 2.57 – 2.44 (m, 2H), 2.36 (td, $J = 10.8, 4.0$ Hz, 1H), 2.22 – 2.13 (m, 1H), 2.13 – 2.04 (m, 2H), 2.03 – 1.96 (m, 1H), 1.72 – 1.46 (m, 6H), 1.41 (t, $J = 7.1$ Hz, 3H), 0.93 (s, 3H) ppm. ^{13}C NMR (101 MHz, CDCl_3) δ 220.9, 166.7, 145.5, 140.1, 137.7, 137.3, 130.2, 129.2, 128.0, 126.9, 126.2, 124.8, 61.1, 50.7, 48.1, 44.5, 38.3, 36.0, 31.7, 29.7, 26.6, 25.9, 21.8, 14.5, 14.0 ppm. LRMS (DEP/EI-Orbitrap): m/z (%): 402.2 (100), 357.2 (10), 345.2 (10), 304.1 (8), 278.1 (7). HRMS (EI-Orbitrap): m/z calcd for $\text{C}_{27}\text{H}_{30}\text{O}_3^+$: 402.2195; found: 402.2189. IR (Diamond-ATR, neat) $\tilde{\nu}_{\text{max}}$ (cm^{-1}): 2979 (w), 2931 (m), 2872 (w), 1737 (s), 1710 (vs), 1608 (m), 1576 (w), 1492 (w), 1473 (w), 1465 (w), 1454 (m), 1424 (w), 1405 (w), 1395 (m), 1367 (m), 1338 (w), 1313 (w), 1270 (vs), 1218 (w), 1177 (m), 1102 (s), 1086 (m), 1057 (m), 1042 (w), 1020 (m), 1009 (m), 965 (w), 910 (m), 894 (w), 860 (m), 847 (m), 822 (m), 768 (s), 730 (s), 703 (m). Mp ($^{\circ}\text{C}$) = 155–159.

3-(4-(*N,N*-Diisopropylbenzamide)-3-deoxyestrone (6c)



Using potassium 3-deoxyestrone-3-trifluoroborate (SM27) and a solution of (4-(diisopropylcarbamoyl)phenyl)zinc iodide in THF according to general procedure Q (0.40 mmol scale), provided **6c** (0.19 mmol, 84 mg, 47%) as a colorless solid. $R_f = 0.25$ (hexane/EtOAc 80:20, UV, KMnO_4 , PAA). ^1H NMR (400 MHz, CDCl_3) δ 7.58 (d, $J = 8.2$ Hz, 2H), 7.40 – 7.37 (m, 3H), 7.35 (d, $J = 7.9$ Hz, 2H), 4.07 – 3.39 (m, br, 2H), 2.99 (dd, $J = 9.2, 4.2$ Hz, 2H), 2.57 – 2.43 (m, 2H), 2.36 (td, $J = 10.8, 4.0$ Hz, 1H), 2.22 – 2.13 (m, 1H), 2.11 – 2.03 (m, 2H), 2.02 – 1.96 (m, 1H), 1.73 – 1.43 (m, 6H), 1.74 – 1.04 (m, 12H), 0.93 (s, 3H) ppm. ^{13}C NMR (101 MHz, CDCl_3) δ 220.9, 171.0, 141.4, 139.4, 138.1, 137.6, 137.1, 127.8, 127.1, 126.2, 126.0, 124.6, 51.1, 50.6, 48.1, 46.3, 44.5, 38.3, 36.0, 31.7, 29.6, 26.6, 25.9, 21.7, 20.9, 13.9 ppm. Signal splitting was observed, which was presumably caused by rotational barriers. LRMS (DEP/EI-Orbitrap): m/z (%): 457.3 (17), 414.2 (62), 357.2 (100), 165.1 (12). HRMS (EI-Orbitrap): m/z calcd for $\text{C}_{31}\text{H}_{39}\text{NO}_2^+$: 457.2981; found: 457.2983. IR (Diamond-ATR, neat) $\tilde{\nu}_{\text{max}}$ (cm^{-1}): 2962 (w), 2925 (w), 2873 (w), 1736 (s), 1621 (vs), 1468 (m), 1437 (m), 1369 (m), 1338 (s), 1294 (w), 1260 (w), 1254 (w), 1212 (m), 1203 (w), 1161 (m), 1153 (m), 1136 (w), 1083 (w), 1039 (m), 1013 (m), 963 (w), 917 (w), 856 (w), 844 (m), 832 (m), 821 (vs), 785 (w), 763 (s). Mp ($^{\circ}\text{C}$) = 275–280 (decomposition).

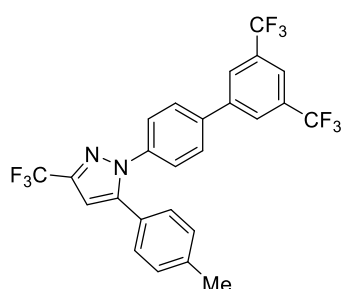
5-(*p*-Tolyl)-1-(4'-(trifluoromethoxy)-[1,1'-biphenyl]-4-yl)-3-(trifluoromethyl)-1*H*-pyrazole (8a)



Using potassium trifluoro(4-(5-(*p*-tolyl)-3-(trifluoromethyl)-1*H*-pyrazol-1-yl)phenyl)borate (SM35) and a solution of (4-(trifluoromethoxy)phenyl)magnesium bromide in THF according to general procedure Q (0.40 mmol scale), provided **8a** (0.22 mmol, 100 mg, 54%) as a colorless oil. $R_f = 0.23$ (hexane/EtOAc 98:2, UV, KMnO_4 , PAA). ^1H NMR (400 MHz, CDCl_3) δ 7.62 – 7.57 (m, 2H), 7.57 – 7.52 (m, 2H),

7.43 – 7.37 (m, 2H), 7.32 – 7.27 (m, 2H), 7.16 (s, 4H), 6.74 (s, 1H), 2.37 (s, 3H) ppm. ^{13}C NMR (101 MHz, CDCl_3) δ 149.1 (q, $J = 1.8$ Hz), 144.9, 143.5 (q, $J = 38.3$ Hz), 139.8, 139.4, 138.9, 138.7, 129.6, 128.9, 128.6, 127.8, 126.4, 125.9, 121.5, 121.4 (q, $J = 269.0$ Hz), 120.6 (q, $J = 257.4$ Hz), 105.7 (q, $J = 2.2$ Hz), 21.5 ppm. LRMS (DEP/EI-Orbitrap): m/z (%): 462.1 (100), 441.1 (13), 178.1 (12), 139.1 (15), 57.1 (11), 44.0 (49). HRMS (EI-Orbitrap): m/z calcd for $\text{C}_{24}\text{H}_{16}\text{F}_6\text{N}_2\text{O}^+$: 462.1167; found: 462.1662. IR (Diamond-ATR, neat) $\tilde{\nu}_{\text{max}}$ (cm^{-1}): 1498 (m), 1473 (m), 1448 (w), 1377 (m), 1259 (vs), 1236 (vs), 1212 (s), 1161 (vs), 1134 (s), 1097 (m), 1008 (w), 978 (m), 922 (w), 859 (w), 836 (m), 826 (m), 808 (m).

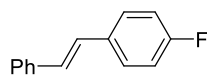
1-(3',5'-Bis(trifluoromethyl)-[1,1'-biphenyl]-4-yl)-5-(*p*-tolyl)-3-(trifluoromethyl)-1*H*-pyrazole (8b)



Using potassium trifluoro(4-(5-(*p*-tolyl)-3-(trifluoromethyl)-1*H*-pyrazol-1-yl)phenyl)borate (**SM35**) and a solution of (3,5-bis(trifluoromethyl)phenyl)magnesium bromide in THF according to general procedure **Q** (0.40 mmol scale), provided **8b** (0.22 mmol, 110 mg, 55%) as a colorless oil. $R_f = 0.48$ (hexane/EtOAc 98:2, UV, KMnO_4 , PAA). ^1H NMR (400 MHz, CDCl_3) δ 8.01 (s, 2H), 7.89 (s, 1H), 7.64 – 7.59 (m, 2H), 7.50 – 7.44 (m, 2H), 7.20 – 7.14 (m, 4H), 6.75 (s, 1H), 2.38 (s, 3H) ppm. ^{13}C NMR (101 MHz, CDCl_3) δ 145.1, 143.7 (q, $J = 38.4$ Hz), 142.0, 139.9, 139.6, 138.1, 132.4 (q, $J = 33.3$ Hz), 129.7, 128.9, 123.0, 127.3, 126.0, 126.1, 123.4 (q, $J = 272.8$ Hz), 121.6 (qq, $J = 3.8$ Hz), 121.4 (q, $J = 269.0$ Hz), 106.0 (q, $J = 2.0$ Hz), 21.5 ppm. LRMS (DEP/EI-Orbitrap): m/z (%): 514.1 (100), 499.1 (12), 493.1 (36), 479.1 (13), 301.1 (10), 237.1 (11). HRMS (EI-Orbitrap): m/z calcd for $\text{C}_{25}\text{H}_{15}\text{F}_9\text{N}_2^+$: 514.1092; found: 514.1086. IR (Diamond-ATR, neat) $\tilde{\nu}_{\text{max}}$ (cm^{-1}): 1525 (w), 1513 (w), 1472 (m), 1448 (w), 1408 (w), 1384 (s), 1278 (vs), 1262 (m), 1237 (m), 1164 (s), 1131 (vs), 1110 (m), 1097 (m), 1071 (w), 1053 (w), 977 (m), 900 (w), 850 (w), 838 (m), 808 (w), 751 (w), 733 (w), 705 (w), 682 (m).

5.5.5 Synthesis of compound 9a

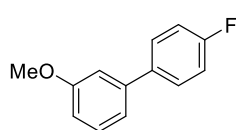
(*E*)-1-Fluoro-4-styrylbenzene (9a)



A 25 mL Schlenk flask was charged with (*E/Z*)-trifluoro(styryl)borate (0.4 mmol, 1.0 equiv) and 2 mL of THF were added. The mixture was cooled to 0 °C and the desired aryl Grignard reagent (1.20 mmol, 3.0 equiv) was added dropwise over 30 min *via* syringe pump. The reaction was quenched after 5 min with 5 mL of sat. aq. K_2CO_3 solution and extracted with EtOAc (3 \times 40 mL). The combined organic phases were filtered and concentrated under reduced pressure. The crude product was then dissolved in 8 mL of HPLC-grade MeCN and transferred into a 10 mL IKA glass vial. The reaction was started using the IKA ElectraSyn 2.0 with RVC as working and counter electrode (5 mA, 3.0 F, 700 rpm stirring). The crude was then treated with water and extracted with diethyl ether (3 \times 15 mL). The combined organic phases were dried over MgSO_4 , filtered and

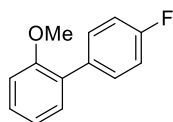
concentrated under reduced pressure. The crude product was purified by column chromatography on silica gel to yield the desired product **9a**. Using potassium (*E*)-trifluoro(styryl)borate and a solution of (4-fluorophenyl)magnesium bromide in THF according to the procedure mentioned above, provided **9a** (0.27 mmol, 54 mg, 68%, *E/Z* = 99:1) as colorless solid. Using potassium (*Z*)-trifluoro(styryl)borate (**SM28**) and a solution of (4-fluorophenyl)magnesium bromide in THF according to the procedure mentioned above, provided **9a** (0.22 mmol, 44 mg, 55%, *E/Z* = 98:2) as colorless solid. ¹H NMR (400 MHz, CDCl₃) δ 7.46-7.35 (m, 4H), 7.27 (t, *J* = 7.7 Hz, 2H), 7.21-7.13 (m, 1H), 7.03-6.92 (m, 4H) ppm. LRMS (DEP/EI-Orbitrap): *m/z* (%): 198.0 (100), 183.0 (45), 177.0 (20). Analytical data in accordance to literature.²⁶²

4'-Fluoro-3-methoxy-1,1'-biphenyl (**10a**)



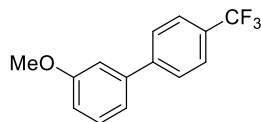
Using potassium trifluoro(3-methoxyphenyl)borate and a solution of (4-fluorophenyl)magnesium bromide in THF according to general procedure **P** (0.40 mmol scale), provided **10a** (0.18 mmol, 36 mg, 46%) as a colorless solid. *R_f* = 0.46 (hexane/EtOAc 98:2, UV, KMnO₄, PAA). ¹H NMR (400 MHz, CDCl₃) δ 7.58 – 7.52 (m, 2H), 7.36 (t, *J* = 7.9 Hz, 1H), 7.18 – 7.06 (m, 4H), 6.91 (ddd, *J* = 8.3, 2.6, 1.0 Hz, 1H), 3.87 (s, 3H) ppm. LRMS (DEP/EI-Orbitrap): *m/z* (%): 202.1 (100), 172.1 (24), 159.1 (35), 133.1 (30). Analytical data in accordance to literature.²⁶³

4'-Fluoro-2-methoxy-1,1'-biphenyl (**10b**)



Using potassium trifluoro(2-methoxyphenyl)borate and a solution of (4-fluorophenyl)magnesium bromide in THF according to general procedure **P** (0.40 mmol scale), provided **10b** (0.07 mmol, 14 mg, 18%) as a colorless solid. *R_f* = 0.21 (hexane/EtOAc 99:1, UV, KMnO₄, PAA). ¹H NMR (400 MHz, CDCl₃) δ 7.54 – 7.43 (m, 2H), 7.37 – 7.27 (m, 2H), 7.19 – 7.08 (m, 2H), 7.06 – 6.97 (m, 2H), 3.82 (s, 3H) ppm. LRMS (DEP/EI-Orbitrap): *m/z* (%): 202.0 (100), 187.0 (58), 170.0 (13), 159.0 (54), 133.0 (46). Analytical data in accordance to literature.²⁶⁴

3-Methoxy-4'-(trifluoromethyl)-1,1'-biphenyl (**10c**)



Using potassium trifluoro(3-methoxyphenyl)borate and a solution of (4-(trifluoromethyl)phenyl)magnesium bromide in THF according to general procedure **P** (0.40 mmol scale), provided **10c** (0.28 mmol, 70 mg, 70%) as a colorless solid. *R_f* = 0.36 (hexane/EtOAc 98:2, UV, KMnO₄, PAA). ¹H NMR (400 MHz, CDCl₃) δ 7.69 (s, 4H), 7.40 (t, *J* = 7.9 Hz, 1H), 7.19 (d, *J* = 7.7 Hz, 1H), 7.15 – 7.11 (m, 1H), 6.96 (dd, *J* = 8.2, 2.0 Hz,

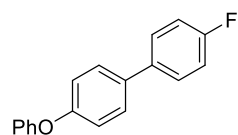
²⁶² A. L. Isfahani, I. Mohammadpoor-Baltork, V. Mirkhani, A. R. Khosropour, M. Moghadam, S. Tangestaninejad, R. Kia, *Adv. Synth. Catal.* **2013**, *355*, 957–972.

²⁶³ J.-F. Soule, H. Miyamura, S. Kobayashi, *J. Am. Chem. Soc.* **2013**, *11*, 7899–7906.

²⁶⁴ Q. Simpson, M. J. G. Sinclair, D. W. Lupton, A. B. Chaplin, J. F. Hooper, *Org. Lett.* **2018**, *20*, 5537–5540.

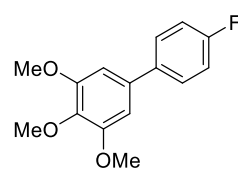
1H), 3.88 (s, 3H) ppm. **LRMS** (DEP/EI-Orbitrap): *m/z* (%): 252.1 (100), 222.0 (21), 209.0 (24), 183.0 (16), 152.0 (10), 139.0 (11). Analytical data in accordance to literature.²⁶⁵

4-Fluoro-4'-phenoxy-1,1'-biphenyl (10d)



Using potassium trifluoro(4-phenoxyphenyl)borate and a solution of (4-fluorophenyl)magnesium bromide in THF according to general procedure **P** (0.35 mmol scale), provided **10d** (0.24 mmol, 63 mg, 67%) as a colorless solid. $R_f = 0.34$ (hexane/EtOAc 98:2, UV, KMnO₄, PAA). ¹H NMR (400 MHz, CDCl₃) δ 7.55 – 7.48 (m, 4H), 7.40 – 7.33 (m, 2H), 7.16 – 7.10 (m, 3H), 7.10 – 7.04 (m, 4H) ppm. **LRMS** (DEP/EI-Orbitrap): *m/z* (%): 264.1 (100), 187.0 (10), 170.0 (17), 159.0 (18), 133.0 (16), 77.0 (13). Analytical data in accordance to literature.^{170c}

4'-Fluoro-3,4,5-trimethoxy-1,1'-biphenyl (10e)



Using potassium trifluoro(3,4,5-trimethoxyphenyl)borate (**SM22**) and a solution of (4-fluorophenyl)magnesium bromide in THF according to general procedure **P** (0.40 mmol scale), provided **10e** (0.27 mmol, 70 mg, 67%) as a colorless solid. $R_f = 0.25$ (hexane/EtOAc 98:2, UV, KMnO₄, PAA). ¹H NMR (400 MHz, CDCl₃) δ 7.54 – 7.47 (m, 2H), 7.15 – 7.08 (m, 2H), 6.72 (s, 2H), 3.92 (s, 6H), 3.89 (s, 3H) ppm. **LRMS** (DEP/EI-Orbitrap): *m/z* (%): 262.1 (93), 247.0 (82), 219.0 (36), 189.0 (36), 159.0 (30), 133.0 (100). Analytical data in accordance to literature.²⁵¹

5.6 Decagram Scale Reaction of 2a

Figure 28 shows a pictorial guide toward the synthesis of product **2a** on a decagram scale. First, a round bottom flask was charged with 75 mmol potassium trifluoro(4-methoxyphenyl)borate, 400 mL THF, a sufficiently powerful stirring bar and topped with a dropping funnel containing 237 mmol of freshly prepared 4-fluorophenyl magnesium bromide (approximately 1 M). The solution was cooled down to 0 °C and the Grignard was added dropwise over 4 h (**A**). After warming to room temperature and stirring for additional two hours, a colorless solid was formed (**B**). The typical workup (see General Procedures) yielded crude TAB salt **1a** (**C**), which was then dissolved in 650 mL ethanol and transferred into a 1000 mL plastic beaker with respective RVC electrodes (7.0 x 8.0 x 0.5 cm). The reaction was electrified using an Atlas 0931 Potentiostat in a simple two-electrode setup at 60 mA current until 3 F were reached (**D**). The solvent was then removed, and the crude mixture filtrated through a silica plug using hexanes/EtOAc (98:2) as eluent (**E**), which – after solvent evaporation – yielded pure compound **2a** (**F**). After a simple wash with 1 M HCl, water and acetone, the RVC electrodes were easily recovered (**G**).

²⁶⁵ V. Salamanca, A. Toledo, A. C. Albéniz, *J. Am. Chem. Soc.* **2018**, *140*, 6959–6963.

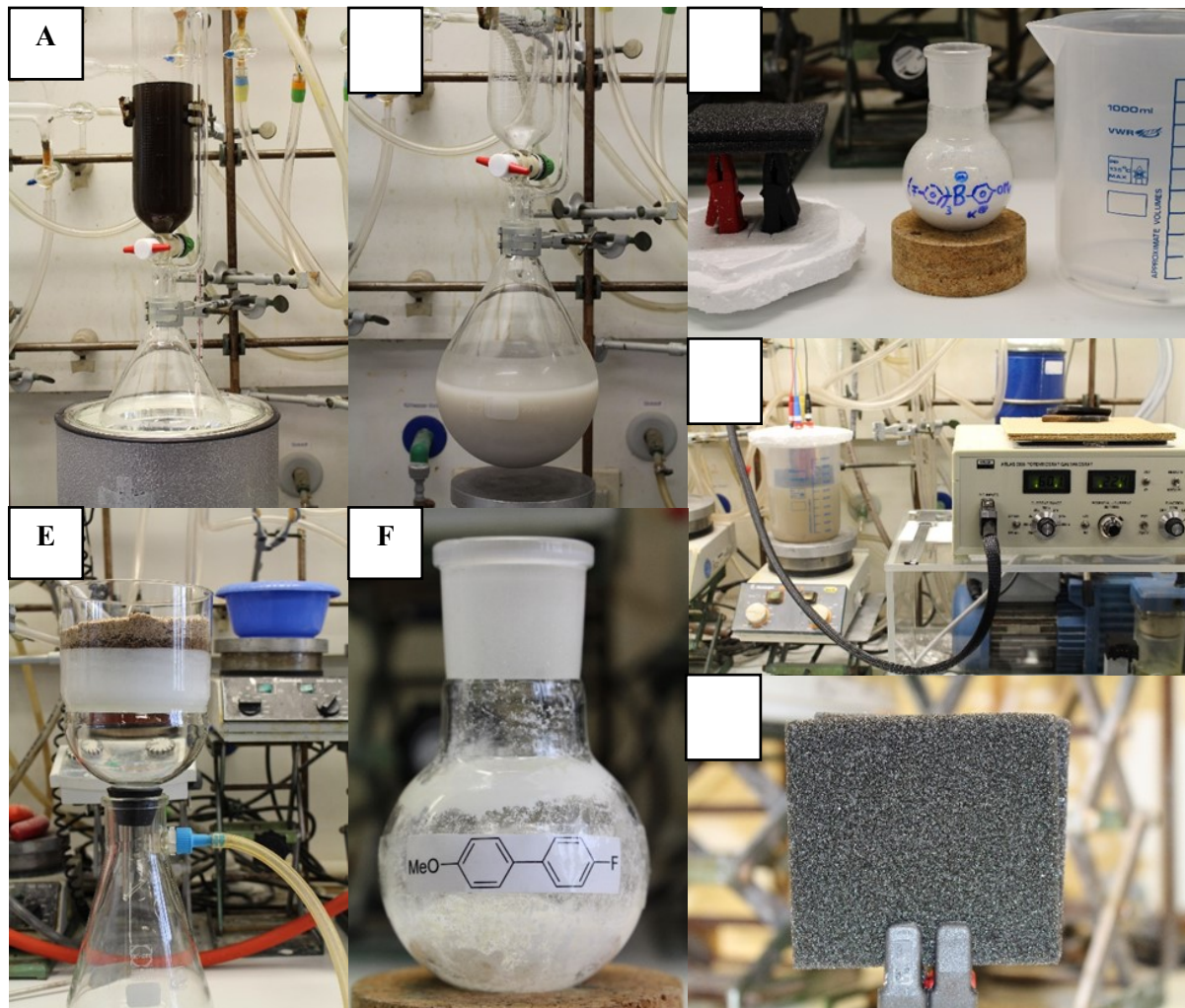
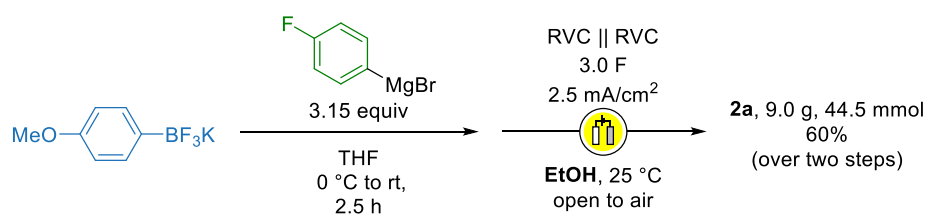
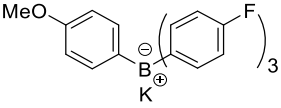
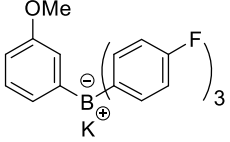
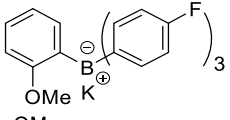
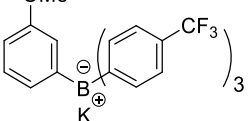
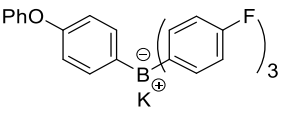
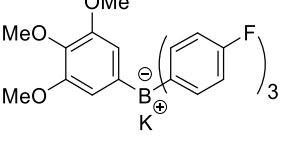
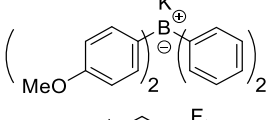
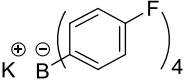


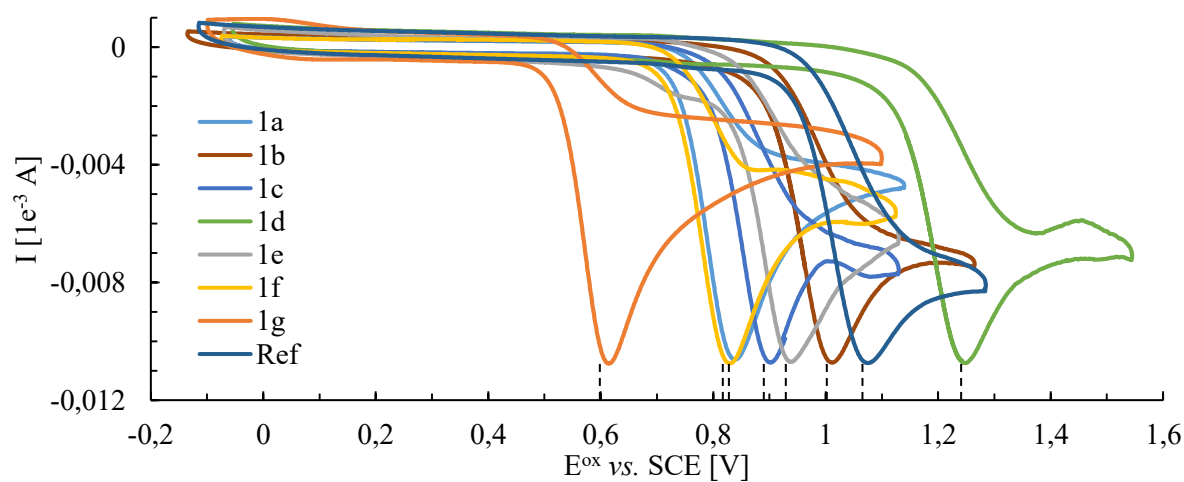
Figure 28: Pictorial guide toward the synthesis of product **2a** on a decagram scale.

5.7 Cyclic Voltammetry

The oxidation potentials were determined in acetonitrile on a CH Instruments 630E electrochemical analyzer using a 2 mm diameter platinum working electrode, a platinum wire counter electrode and an Ag wire pseudo-reference electrode applying a scan rate of 0.1 V/s. Cyclic voltammetry measurements were performed in acetonitrile containing 0.1 M NBu_4ClO_4 with the TAB salts (**1a–g**) ($c \approx 3.4 \times 10^{-4}$ M) and ferrocene ($c = 3.8 \times 10^{-4}$ M) as an internal standard. The $E_{1/2}(\text{fc}^+/\text{fc in MeCN}) = +0.382$ V was used to calibrate E_p^{ox} (in MeCN) vs. SCE. The results are summarized in Table 11 and Figure 29.

Table 11: Determined oxidation potentials of TAB salts **1a–g** vs. SCE.

TAB salt	TAB structure	E_p^{Ox} vs. SCE / V
1a		0.84
1b		1.01
1c		0.90
1d		1.24
1e		0.94
1f		0.83
1g		0.62
KB((p-F)phenyl)₄ reference		1.08

**Figure 29:** Graphical summary of measured E_p^{Ox} vs. SCE of TAB salts **1a–g**.

5.8 Calculations²⁶⁶

Calculations were performed at the equation-of-motion ionization potential coupled-cluster singles and doubles (EOM-IP-CCSD) level of theory and using density functional theory (DFT) with the ω B97X-D3 functional. The 6-31G* basis set was used in all calculations if not indicated otherwise. (EOM-IP)-CCSD calculations (Table 12) were performed for isolated molecules in gas phase, DFT calculations were performed in gas phase (Table 13) and additionally taking into account the solvent (acetonitrile) by means of the polarizable continuum (PCM) approach (Table 14 and Table 15).²⁶⁷ Non-equilibrium solvent effects upon ionization were either disregarded (Table 14) or taken into account by means of the state-specific approach (Table 15).²⁶⁸ Molecular structures of the TAB anions were optimized at the ω B97X-D3/6-31G*/PCM level of theory.²⁶⁹ Core electrons were frozen in all CCSD and EOM-IP-CCSD calculations.²⁷⁰ All calculations were performed with the Q-Chem program package, release 5.0.²⁷¹ The energy differences shown in Table 12–Table 15 confirm most of the trends observed in experiment. For the three isomers **1a–c**, all calculations agree with cyclic voltammetry measurements (see Section 5.7) that the species with the methoxy group in *meta*-position has the highest oxidation potential while that with the methoxy group in *para*-position has the lowest oxidation potential. All calculations also agree with experiment that molecule **1g** is easier to oxidize than the three preceding species and that molecule **1d** is harder to oxidize. However, experiment and theory disagree about the oxidation potential of molecules **1e** and **1f**. Notably, solvent effects make a sizable impact, especially on the oxidation potential of molecule **1e**, but no theoretical approach reproduces the trends measured for these two species. To characterize the change in the electronic structure upon oxidation of the TAB anions, spin and charge densities (Table 16 and Table 17) were computed based on Mulliken population analysis.²⁷² Since this approach is known to suffer from a heavy basis-set dependence, partial charges were additionally computed using the ChElPG (Charges from the electrostatic potential on a grid) approach (Table 18).²⁷³ These results illustrate that the single electron-rich aromatic ring is selectively oxidized in all cases while the charge and spin densities of the other aromatic rings change only insignificantly. This fact is also visualized in Figure 30 by means of the spin density of molecule **1a**. The sole exception is again molecule **1e**, where all approaches agree on an unselective oxidation to which

²⁶⁶ Calculations were performed by Dr. Thomas Jagau, Department of Chemistry, LMU Munich.

²⁶⁷ J. Tomasi, B. Mennucci, R. Cammi, *Chem. Rev.* **2005**, *105*, 2999–3094.

²⁶⁸ a) M. Cossi, V. Barone, *J. Phys. Chem. A* **2000**, *104*, 10614–10622. b) Z.-Q. You, J.-M. Mewes, A. Dreuw, J. M. Herbert, *J. Chem. Phys.* **2015**, *143*, 204104.

²⁶⁹ a) J.-D. Chai, M. Head-Gordon, *J. Chem. Phys.* **2008**, *128*, 084106. b) J.-D. Chai, M. Head-Gordon, *Phys. Chem. Chem. Phys.* **2008**, *10*, 6615–6620. c) S. Grimme, J. Antony, S. Ehrlich, H. Krieg, *J. Chem. Phys.* **2010**, *132*, 154104.

²⁷⁰ I. Shavitt, R. J. Bartlett, *Many Body Methods in Chemistry and Physics. MBPT and Coupled-Cluster Theory*, Cambridge University Press, Cambridge, UK, **2009**.

²⁷¹ Y. Shao, *et al.*, *Mol. Phys.* **2015**, *113*, 184–215.

²⁷² F. Jensen, *Introduction to Computational Chemistry*, Wiley, New York, USA, **1994**.

²⁷³ a) C. M. Breneman, K. B. Wiberg, *J. Comput. Chem.* **1990**, *11*, 361–373. b) J. M. Herbert, L.D. Jacobson, K. U. Lao, M. A. Rohrdanz, *Phys. Chem. Chem. Phys.* **2012**, *14*, 7679–7699.

all four rings contribute equally. However, additional ω B97X-D3 calculations with the larger 6-311G** basis set call this result into question: Here, Mulliken population analysis and the ChEIPG approach agree that neither of the four aromatic rings connected to the boron atom is oxidized but instead the remote phenoxy unit. This points to the possibility that the oxidation of molecule **1e** proceeds through a different mechanism than that of the other species and may also be related to the disagreement between theory and experiment about the oxidation potential of molecule **1e**. Notably, results do not change significantly for all other molecules when going from 6-31G* to 6-311G**.

Table 12: Total energies (in atomic units) of closed-shell TAB anions (**1a–g**) and the corresponding neutral radicals computed at the CCSD/6-31G* and EOM-IP-CCSD/6-31G* levels of theory, respectively. Energy differences (in eV) are also shown.

TAB salt	$E_t(\text{Anionic})$ (a.u.)	$E_t(\text{Radical})$ (a.u.)	ΔE (eV)
KBPh ₄ reference	-948.477575	-948.3275427	4.08
1a	-1359.736341	-1359.587152	4.06
1b	-1359.739393	-1359.580906	4.31
1c	-1359.734564	-1359.581572	4.16
1d	-2071.475102	-2071.305966	4.60
1e	-1550.895685	-1550.729427	4.52
1f	-1588.125960	-1587.970440	4.23
1g	-1176.874745	-1176.734463	3.82

Table 13: Total energies (in atomic units) of closed-shell TAB anions (**1a–g**) and the corresponding neutral radicals computed at the ω B97X-D3/6-31G* level of theory. Energy differences (in eV) are also shown.

TAB salt	$E_t(\text{Anionic})$ (a.u.)	$E_t(\text{Radical})$ (a.u.)	ΔE (eV)
KBPh ₄ reference	-951.253221	-951.094822	4.31
1a	-1363.38385	-1363.227497	4.26
1b	-1363.38719	-1363.221982	4.50
1c	-1363.38271	-1363.222669	4.36
1d	-2076.64802	-2076.472911	4.77
1e	-1555.07616	-1554.903011	4.71
1f	-1592.35686	-1592.195301	4.40
1g	-1180.23428	-1180.083084	4.11

Table 14: Total energies (in atomic units) of closed-shell TAB anions (**1a–g**) and the corresponding neutral radicals computed at the ω B97X-D3/6-31G*/PCM level of theory. The solvent reaction field is equilibrated in all calculations. Energy differences (in eV) are also shown.

TAB salt	$E_t(\text{Anionic})$ (a.u.)	$E_t(\text{Radical})$ (a.u.)	ΔE (eV)
KBPh ₄ reference	-951.325714	-951.104965	6.01
1a	-1363.451318	-1363.252960	5.40
1b	-1363.453315	-1363.248214	5.58
1c	-1363.451734	-1363.250999	5.46
1d	-2076.708309	-2076.501594	5.63
1e	-1555.141062	-1554.916474	6.11
1f	-1592.427566	-1592.223624	5.55
1g	-1180.311780	-1180.114435	5.37

Table 15: Total energies (in atomic units) of closed-shell TAB anions (**1a–g**) and the corresponding neutral radicals computed at the ω B97X-D3/6-31G*/PCM level of theory. The state-specific approach is used to describe non-equilibrium solvent effects upon ionization. Energy differences (in eV) are also shown.

TAB salt	$E_t(\text{Anionic})$ (a.u.)	$E_t(\text{Radical})$ (a.u.)	ΔE (eV)
KBPh ₄ reference	-951.325714	-951.075570	6.81
1a	-1363.451318	-1363.218253	6.34
1b	-1363.453315	-1363.211345	6.58
1c	-1363.451734	-1363.215351	6.43
1d	-2076.708309	-2076.465110	6.62
1e	-1555.141062	-1554.890363	6.82
1f	-1592.427566	-1592.189655	6.47
1g	-1180.311780	-1180.079829	6.31

Table 16: Spin densities of neutral TAB radicals computed from Mulliken population analysis at the ω B97X-D3/6-31G*/PCM level of theory. The values represent the sums of the spin densities associated with the carbon atoms of the four aromatic rings.

TAB salt	Spin density e-poor Ar ¹	Spin density e-rich Ar ²
KBPh ₄ reference	0.27/0.24/0.24/0.26	-
1a	0.01/0.03/0.05	0.78
1b	0.00/0.01/0.02	0.82
1c	0.00/0.02/0.02	0.78
1d	0.00/0.01/0.01	0.82
1e	0.21/0.25/0.29	0.25
1f	0.01/0.01/0.03	0.79
1g	0.01/0.04	0.05/0.79

Table 17: Differences in charge density between TAB anions and neutral radicals computed from Mulliken population analysis at the ω B97X-D3/6-31G*/PCM level of theory. The values represent the sums of the charge density differences associated with the carbon atoms of the four aromatic rings.

TAB salt	Δ Charge density e-poor Ar ¹	Δ Charge density e-rich Ar ²
KBPh ₄ reference	0.09/0.09/0.09/0.10	-
1a	0.01/0.02/0.02	0.33
1b	0.00/0.01/0.02	0.35
1c	0.01/0.01/0.02	0.34
1d	0.00/0.01/0.01	0.35
1e	0.09/0.10/0.12	0.11
1f	0.00/0.01/0.03	0.38
1g	0.01/0.01	0.03/0.33

Table 18: Differences in charge density between TAB anions and neutral radicals computed from charges from the electrostatic potential on a grid (ChElPG) at the ω B97X-D3/6-31G*/PCM level of theory. The values represent the sums of the charge density differences associated with the carbon atoms of the four aromatic rings.

TAB salt	Δ Charge density e-poor Ar ¹	Δ Charge density e-rich Ar ²
KBPh ₄ reference	-0.21, -0.20, -0.20, -0.19	-
1a	-0.03, -0.04, -0.06	-0.60
1b	-0.02, -0.02, -0.03	-0.63
1c	-0.03, -0.03, -0.04	-0.61
1d	-0.02, -0.03, -0.03	-0.63
1e	-0.19, -0.21, -0.20	-0.17
1f	-0.02, -0.03, -0.04	-0.59
1g	-0.03, -0.03	-0.04, -0.60

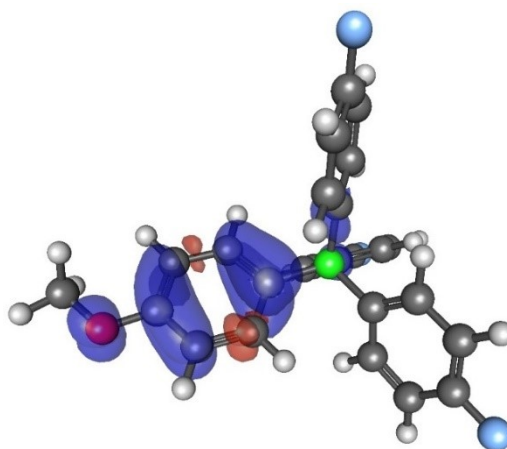
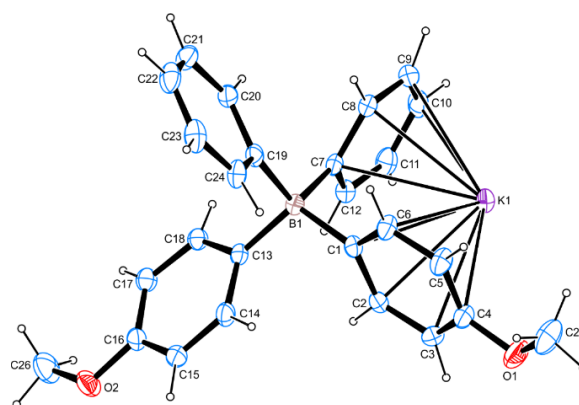


Figure 30: Spin density for the neutral TAB radical (from **1a**) computed at the ω B97X-D3/6-31G*/PCM level of theory and plotted at an *iso*value of 0.015.

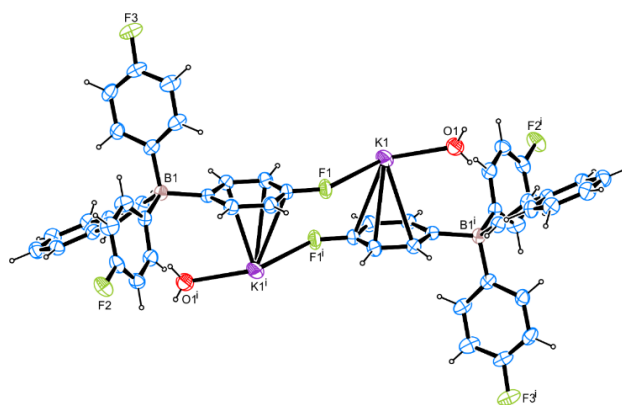
5.9 Single X-Ray Diffraction

Supporting Information available: Crystallographic data have been deposited with the Cambridge Crystallographic Data Centre: CCDC-1954369 for **1g**, CCDC-1964338 for **1h**. Copies of the data can be obtained free of charge: <https://www.ccdc.cam.ac.uk/structures/>.

Table 19: Crystallographic data for compound **1g**.²⁷⁴

Compound 1g			
net formula	$C_{26}H_{24}BKO_2$	absorption correction	Multi-Scan
$M_r/g\ mol^{-1}$	418.36	transmission factor range	0.93–0.99
crystal size/mm	$0.100 \times 0.040 \times 0.040$	refls. measured	19433
T/K	109.(2)	R_{int}	0.0359
radiation	MoK α	mean $\sigma(I)/I$	0.0321
diffractometer	'Bruker D8 Venture TXS'	θ range	2.649–27.101
crystal system	monoclinic	observed refls.	4348
space group	'P 1 21 1'	x, y (weighting scheme)	0.0300, 0.3433
$a/\text{\AA}$	7.8292(3)	hydrogen refinement	constr
$b/\text{\AA}$	11.0341(4)	Flack parameter	0.21(4)
$c/\text{\AA}$	12.7149(6)	refls in refinement	4734
$\alpha/^\circ$	90	parameters	274
$\beta/^\circ$	100.8430(10)	restraints	6
$\gamma/^\circ$	90	$R(F_{obs})$	0.0312
$V/\text{\AA}^3$	1078.81(8)	$R_w(F^2)$	0.0746
Z	2	S	1.040
calc. density/ $g\ cm^{-3}$	1.288	shift/error _{max}	0.001
μ/mm^{-1}	0.266	max electron density/ $e\ \text{\AA}^{-3}$	0.273
net formula	$C_{26}H_{24}BKO_2$	min electron density/ $e\ \text{\AA}^{-3}$	–0.189

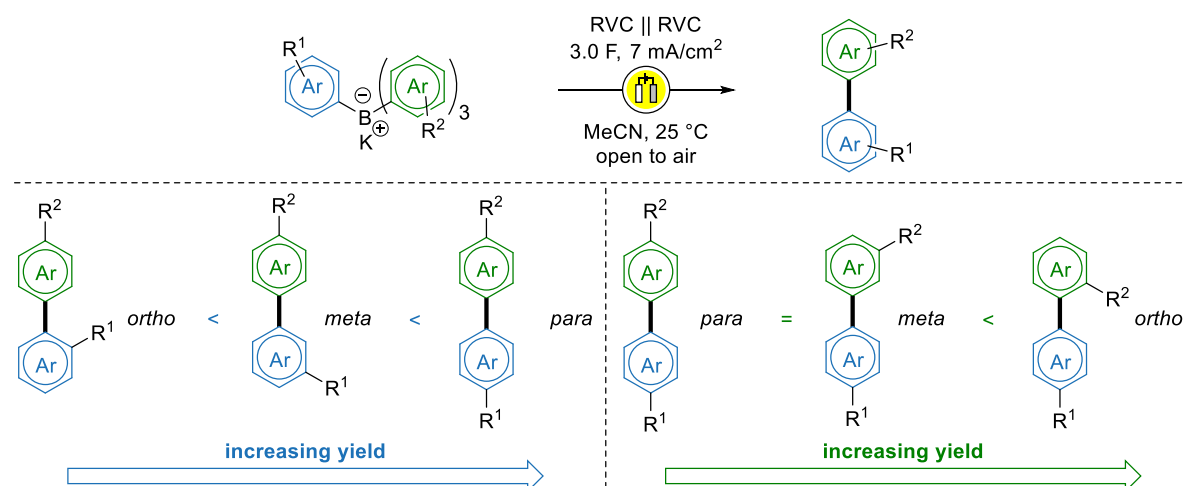
²⁷⁴ Refined as inversion twin, BASF 0.21.

Table 20: Crystallographic data for compound **1h**.²⁷⁵

Compound 1h			
net formula	$C_{26}H_{21.56}BF_3KO_{1.28}$	absorption correction	Multi-Scan
$M_r/g\ mol^{-1}$	461.42	transmission factor range	0.96–0.99
crystal size/mm	$0.070 \times 0.050 \times 0.030$	refls. measured	19826
T/K	102.(2)	R_{int}	0.0309
radiation	MoK α	mean $\sigma(I)/I$	0.0293
diffractometer	'Bruker D8 Venture TXS'	θ range	2.887–27.101
crystal system	triclinic	observed refls.	4217
space group	'P -1'	x, y (weighting scheme)	0.0605, 1.4236
$a/\text{\AA}$	9.8924(4)	hydrogen refinement	mixed
$b/\text{\AA}$	10.0377(4)	refls in refinement	4955
$c/\text{\AA}$	11.5787(4)	parameters	302
$\alpha/^\circ$	82.5670(10)	restraints	0
$\beta/^\circ$	81.2960(10)	$R(F_{obs})$	0.0566
$\gamma/^\circ$	88.2120(10)	$R_w(F^2)$	0.1499
$V/\text{\AA}^3$	1126.86(7)	S	1.054
Z	2	shift/error $_{max}$	0.001
calc. density/ $g\ cm^{-3}$	1.360	max electron density/ $e\ \text{\AA}^{-3}$	1.214
μ/mm^{-1}	0.278	min electron density/ $e\ \text{\AA}^{-3}$	-1.115

²⁷⁵ H(C) constr, H(O1) refall, H(O2) not considered in refinement The sof of O2 has been refined freely and results in a value of 0.28. The hydrogen atoms bound to this O could not be located and have not been considered in the refinement. This water-O-atom is not depicted in the table above.

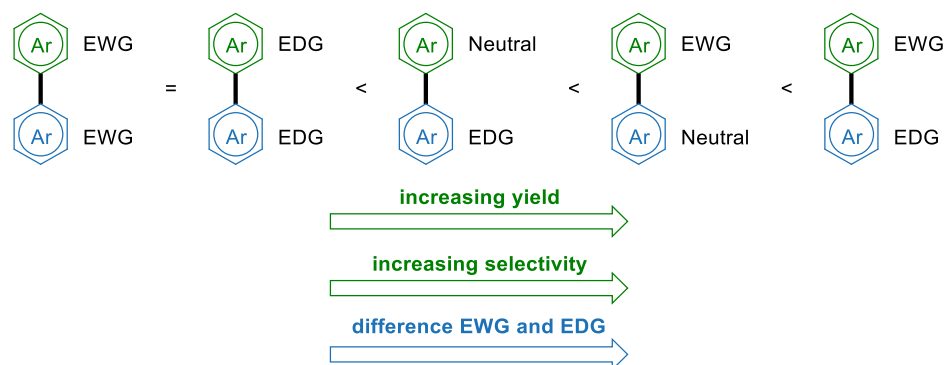
5.10 Unsuccessful Transformations and Limitations



Scheme 45: Substitution effects on heterocoupling selectivity.

As seen in Scheme 45, the yields generally increase from *o*- to *m*- to *p*-substitution on the more electron-rich aromatic, presumably due to steric interactions. This trend is inverted when substituting the more electron-poor aromatics, as *o*-substituted systems give the best yield. In addition, best heterocoupling selectivity is obtained for TABs with great difference in electronic structure (Scheme 46), meaning that aromatics with donating groups (EDG, highlighted blue) are most selectively coupled with aromatics with electron-withdrawing groups (EWG, highlighted green).

Couplings with unsubstituted heteroaromatics such as pyrroles, thiophenes and furans are challenging, mainly due to polymerization side reactions. Lastly, pyridyl patterns as electron-poor coupling partners were not tolerated, as TAB salt formation was never observed with pyridyl organometallics. This was attributed to preferred coordination of the pyridine moiety to the potassium aryl trifluoroborate salt, which results in the inhibition of its reactivity.



Scheme 46: Electronic effects on heterocoupling selectivity.

5.11 Representative NMR Spectra

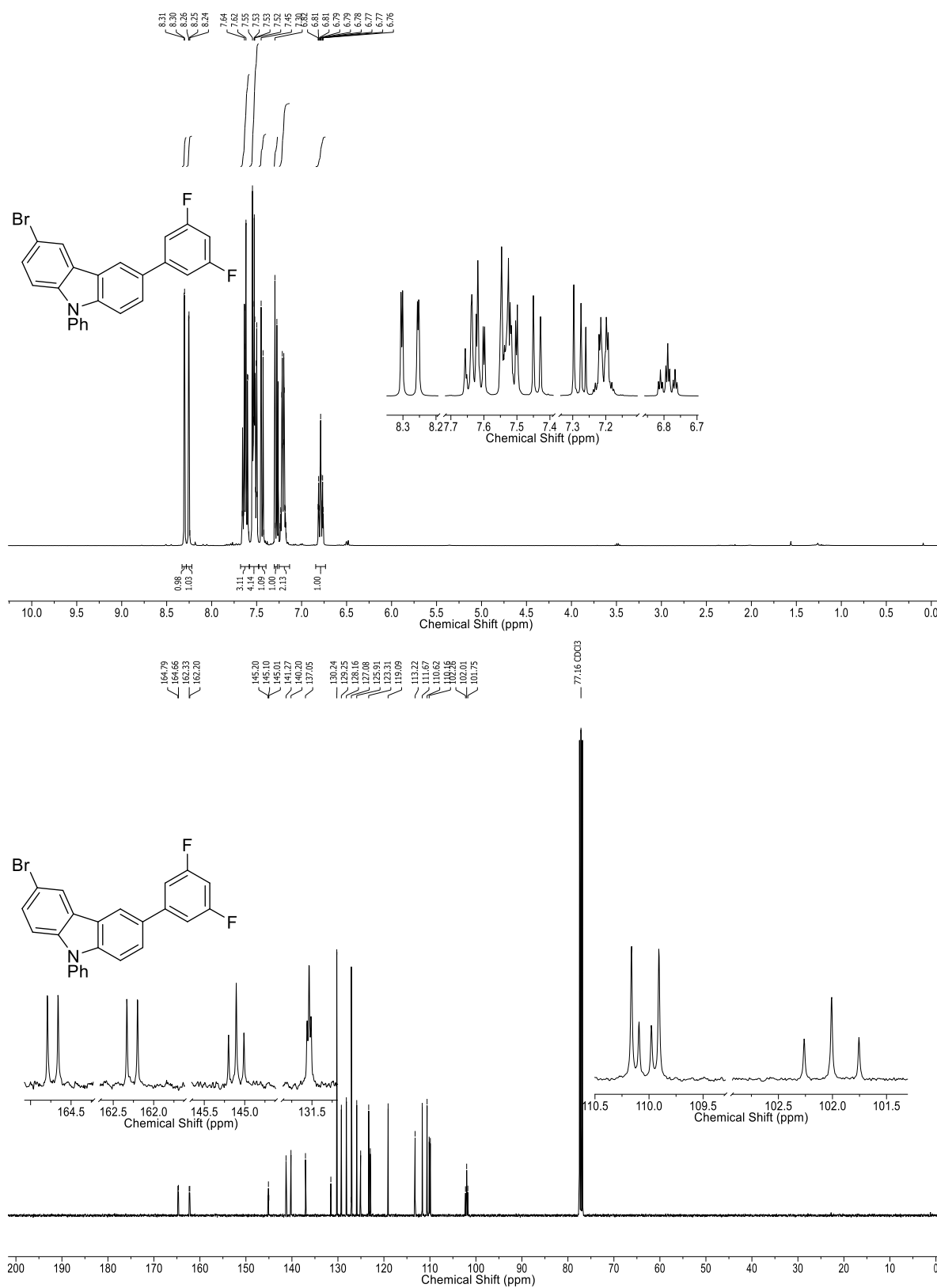


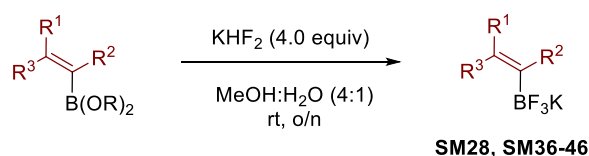
Figure 31: ^1H NMR (400 MHz, CDCl_3) and ^{13}C NMR (101 MHz, CDCl_3) for 3-Bromo-6-(3,5-difluorophenyl)-9-phenyl-9H-carbazole (**4e**).

6 Electro-Olefination – a Catalyst Free Stereoconvergent Strategy for the Functionalization of Alkenes²⁷⁶

6.1 General Procedures

For the synthesis of aryl Grignard and arylzinc reagents, see chapter 5.1.1 and 5.1.2 of the experimental part.

6.1.1 General Procedure R: Preparation of Potassium Alkenyl Trifluoroborate Salts



Adapted from a previously reported procedure,²³⁸ 5.0 mmol (1.0 equiv) of commercially available alkenyl boronic pinacol esters and boronic acids were dissolved in 15 mL of a 4:1 (v/v) mixture of MeOH and H₂O. The mixture was cooled to 0 °C and KHF₂ (20 mmol, 4.0 equiv) was added neat. The mixture was vigorously stirred at room temperature overnight and then concentrated under reduced pressure. The remaining solids were extracted with boiling acetone (2 × 50 mL) and twice with acetone at room temperature (2 × 50 mL). The acetone was removed under reduced pressure, the remaining solid was dissolved in a minimum amount of boiling acetone and precipitated by the addition of diethyl ether. The colorless solids were filtered, washed with diethyl ether and dried *in vacuo* to yield potassium alkenyl trifluoroborate salts **SM28** and **SM36–47**. (Note: Literature known potassium alkenyl trifluoroborate salts were synthesized according to the same procedure and used without further purification, see Figure 32).

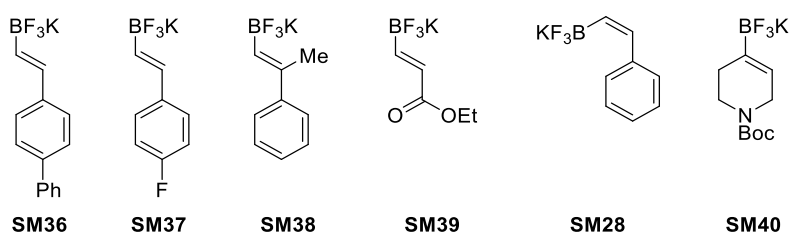


Figure 32: Literature known trifluoroborate salts. Analytical data in accordance to literature for **SM36**²⁷⁷, **SM37**²⁷⁸, **SM38**²⁷⁹, **SM39**²⁸⁰, **SM28**²⁴³, **SM40**²⁷⁷.

²⁷⁶ The full supporting information can be found under the following link: <https://doi.org/10.1002/chem.202001394>. This project was conducted in equal contribution with A. N. Baumann.

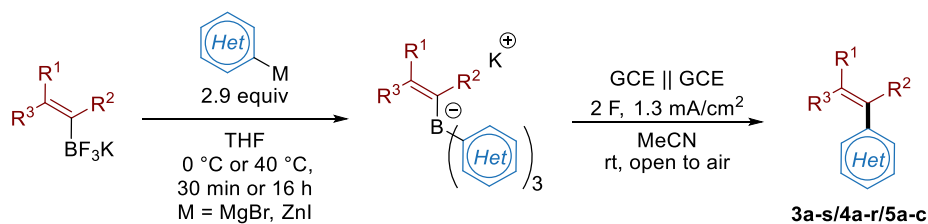
²⁷⁷ M. Pisset, D. Oehlich, F. Rombouts, G. A. Molander, *J. Org. Chem.* **2013**, *78*, 12837–12843.

²⁷⁸ B. Gopula, C.-W. Chiang, W.-Z. Lee, T.-S. Kuo, P.-Y. Wu, J. P. Henschke, H.-L. Wu, *Org. Lett.* **2014**, *16*, 632–635.

²⁷⁹ J. J. Molloy, J. B. Metternich, C. G. Daniliuc, A. J. B. Watson, R. Gilmour, *Angew. Chem. Int. Ed.* **2018**, *57*, 3168–3172.

²⁸⁰ C. Feng, H. Wang, L. Xu, P. Li, *Org. Biomol. Chem.* **2015**, *13*, 7136–7139.

6.1.2 General Procedure S: Two-pot Procedure for the Synthesis of Functionalized Alkenes starting from Potassium Alkenyl Trifluoroborate Salts

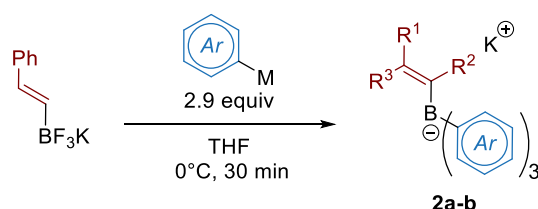


A 25 mL Schlenk flask was charged with the corresponding potassium trifluoroborate salt (0.4 mmol, 1.0 equiv) and 2 mL of THF were added. The mixture was cooled to 0 °C and a solution of the aryl Grignard reagent **A** in THF (1.16 mmol, 2.9 equiv) was added dropwise over 30 min *via* syringe pump. After addition, the reaction mixture was allowed to stir for further 10 min at 0 °C and was then quenched with 5 mL of H₂O and extracted with EtOAc (3 × 40 mL). If no phase separation was observed, 5 mL of sat. aq. K₂CO₃ solution was added. The combined organic phases were filtered and concentrated under reduced pressure (no higher temperature than 40 °C). The crude tetraorganoborate was then dissolved in 8 mL of HPLC-grade MeCN and transferred into a 10 mL IKA glass vial. The reaction was started using the IKA ElectraSyn 2.0 with GCE (glassy carbon electrodes) as working and counter electrodes (5 mA, 2.0 F, 1.3 mA/cm², 700 rpm stirring). The crude mixture was then treated with water and extracted with diethyl ether (3 × 15 mL). The combined organic phases were dried over MgSO₄, filtered, concentrated under reduced pressure and purified by flash-column chromatography on silica gel with the appropriate solvent mixture to obtain pure **3a–b**, **3d–k**, **3m–s/4a–r/5a–c**.

a) Adaptation for the use of arylzinc reagents

After addition of a solution of the arylzinc species in THF (instead of the aryl Grignard reagent as described above) *via* syringe pump, the reaction was heated to 40 °C for 16 hours to ensure full conversion of the potassium trifluoroborate salt into the desired ATB salt. General Procedure **S** was then followed to give products **3c** and **3l**.

6.1.3 General Procedure T: Procedure for the Isolation of Functionalized ATB Salts starting from Potassium Alkenyl Trifluoroborate Salts



A 50 mL Schlenk flask was charged with (*E*)-trifluoro(styryl)borate (3.0 mmol, 1.0 equiv) and 9 mL of THF were added. The mixture was cooled to 0 °C and the corresponding solution of the aryl Grignard reagent **A** in THF (9.0 mmol, 3.0 equiv) was added dropwise over 30 min *via* syringe pump. After

addition, the reaction mixture was allowed to stir for further 10 min at 0 °C and was then quenched with 5 mL of H₂O and extracted with EtOAc (3 × 40 mL). If no phase separation was observed, 5 mL of sat. aq. K₂CO₃ solution was added. The combined organic phases were filtered and concentrated under reduced pressure (no higher temperature than 40 °C). The resulting oil was then layered with hexane (20 mL) and sonicated at 0 °C for 10 min. The hexane was decanted, and the process repeated two more times, until a colorless solid was obtained. (Note: ATB salts are highly soluble in EtOAc and therefore solidification can be challenging.) The solids were then again sonicated in hexane, the fine white powder was then filtered and washed with hexanes (2 × 10 mL) and dried *in vacuo* to yield ATB salts **2a–b**.

6.2 Formation of ATB salt **2a** by ¹¹B NMR

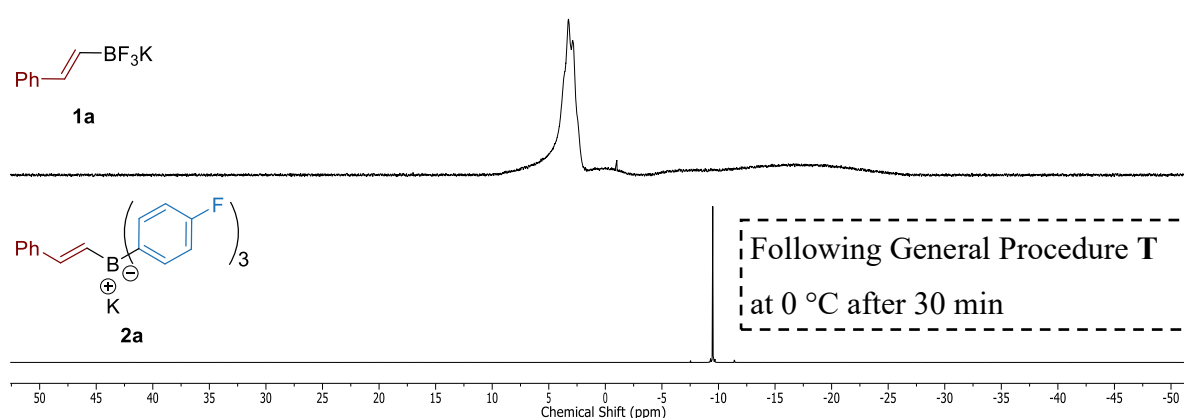
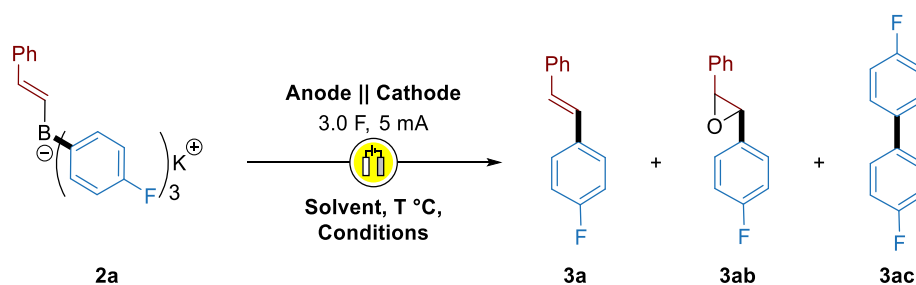


Figure 33: ¹¹B NMR analysis of the TAB salt formation to yield **2a**.

As depicted in Figure 33, a smooth transformation of the starting (*E*)-trifluoro(styryl)borate into the desired ATB salt **2a** was observed in the crude ¹¹B NMR, which was measured as a 1:1 THF:CD₃CN mixture following general procedure **T**.

6.3 Optimizations

Conversion rates into (*E*)-1-fluoro-4-styrylbenzene (**3a**) were assessed by hydrolysis and GC analysis with *n*-undecane as an internal standard. As seen in Table 21, the oxidation process can be performed with different carbon electrode setups, resulting in good conversion and selectivity ratios. In addition, the oxidation process can also be performed in environmentally friendly solvents such as ethanol with only marginal conversion loss.

Table 21: Screening of different electrode materials, solvents and conditions.

Anode Cathode	Solvent	Conditions	T (°C)	conv. (%) 3a:3ab:3ac
Graphite Graphite	MeCN	Open to air no Electrolyte	25	77:5:2
RVC RVC	MeCN	Open to air no Electrolyte	25	80:10:3
GCE GCE	MeCN	Open to air no Electrolyte	25	82:5:5 (isolated 75%)
GCE GCE	MeCN	N ₂ -atmosphere no Electrolyte	25	65:2:3
GCE GCE	MeCN	O ₂ -atmosphere no Electrolyte	25	30:37:4
GCE GCE	MeCN	Open to air with LiClO ₄ [0.1 M]	25	75:4:3
GCE GCE	EtOH	Open to air no Electrolyte	25	78:5:5
RVC RVC	EtOH	Open to air no Electrolyte	25	73:9:1

6.4 Experimental Data

6.4.1 Synthesis of Potassium Alkenyl Trifluoroborates

Potassium (*Z*)-trifluoro(2-(6-methoxynaphthalen-2-yl)vinyl)borate (SM41)

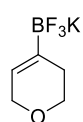


Using (*Z*)-2-(2-(6-methoxynaphthalen-2-yl)vinyl)-4,4,5,5-tetramethyl-1,3,2-dioxaborolane according to general procedure **R**, provided **SM41** (4.09 mmol, 1.186 g, 48%) as brownish solid. ¹H NMR (400 MHz, CD₃CN) δ 7.97 (dd, *J* = 8.6, 1.7 Hz, 1H), 7.81 (s, 1H), 7.66 (dd, *J* = 18.2, 8.8 Hz, 2H), 7.19 (d, *J* = 2.6 Hz, 1H), 7.07 (dd, *J* = 8.9, 2.6 Hz, 1H), 6.73 (d, *J* = 15.0 Hz, 1H), 5.70 (dq, *J* = 15.2, 6.6 Hz, 1H), 3.88 (s, 3H) ppm.

¹³C NMR (101 MHz, CD₃CN) δ 158.1, 137.9, 136.7, 134.2, 130.2, 129.8, 128.8, 127.7, 126.5, 119.0, 106.6, 55.9 ppm. The signal for the carbon atom adjacent to the boron center was not observed. ¹¹B NMR (128 MHz, CD₃CN) δ 2.43 (q, *J* = 54.7 Hz) ppm. HRMS (ESI-Quadrupole): *m/z* calcd for C₁₃H₁₁OBF₃KNa⁺ [M+Na]⁺: 313.0390; found: 313.0385. IR (Diamond-ATR, neat) $\tilde{\nu}_{max}$ (cm⁻¹): 1686 (m), 1680 (m), 1623 (m), 1605 (m), 1482 (m), 1390 (m), 1292 (w), 1268 (m), 1258 (m), 1210 (m), 1196 (m), 1186 (m), 1164 (s), 1118 (m), 1108 (m), 1090 (s), 1084 (s), 1067 (s), 1060 (s), 1050 (s), 1030 (vs), 990 (s), 982 (s), 966 (s), 958 (s), 950 (s), 934 (s), 881 (m), 860 (s), 854 (s), 834 (m), 804 (s), 780 (m), 768 (m), 758 (m). Mp (°C) = 160–182 (decomposition).

Potassium cyclopent-1-en-1-yltrifluoroborate (SM42)

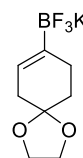
Using 2-(cyclopent-1-en-1-yl)-4,4,5,5-tetramethyl-1,3,2-dioxaborolane according to general procedure **R**, provided **SM42** (3.76 mmol, 658 mg, 84%) as colorless solid. $^1\text{H NMR}$ (400 MHz, CD_3CN) δ 5.48 (s, 1H), 2.25 – 2.19 (m, 2H), 1.94 (quint, $J = 2.5$ Hz, 2H), 1.69 (quint, $J = 7.5$ Hz, 2H) ppm. $^{13}\text{C NMR}$ (101 MHz, CD_3CN) δ 128.8, 36.2, 34.5, 24.8 ppm. The signal for the carbon atom adjacent to the boron center was not observed. $^{11}\text{B NMR}$ (128 MHz, CD_3CN) δ 2.71 (q, $J = 57.1$ Hz) ppm. **HRMS** (ESI-Quadrupole): m/z calcd for $\text{C}_5\text{H}_7\text{BF}_3^-$ [M-K]: 135.0593; found: 135.0597. **IR** (Diamond-ATR, neat) $\tilde{\nu}_{\text{max}}$ (cm^{-1}): 2948 (w), 2843 (w), 1620 (w), 1291 (w), 1224 (w), 1152 (m), 1038 (m), 1021 (m), 980 (m), 949 (s), 916 (vs), 885 (s), 840 (m), 806 (m). **Mp** ($^\circ\text{C}$) = 200–210 (decomposition).

Potassium (3,6-dihydro-2H-pyran-4-yl)trifluoroborate (SM43)

Using 2-(3,6-dihydro-2H-pyran-4-yl)-4,4,5,5-tetramethyl-1,3,2-dioxaborolane according to general procedure **R**, provided **SM43** (6.84 mmol, 1.30 g, 68%) as colorless solid. $^1\text{H NMR}$ (400 MHz, CD_3CN) δ 5.55 (s, 1H), 3.96 (qd, $J = 2.6, 1.3$ Hz, 2H), 3.61 (t, $J = 5.5$ Hz, 2H), 2.00 (dq, $J = 5.6, 2.8$ Hz, 2H) ppm. $^{13}\text{C NMR}$ (101 MHz, CD_3CN) δ 123.8, 66.6, 65.7, 27.8 ppm. The signal for the carbon atom adjacent to the boron center was not observed. $^{11}\text{B NMR}$ (128 MHz, CD_3CN) δ 2.49 (q, $J = 56.0$ Hz) ppm. **HRMS** (ESI-Quadrupole): m/z calcd for $\text{C}_5\text{H}_7\text{OBF}_3^-$ [M-K]: 151.0542; found: 151.0547. **IR** (Diamond-ATR, neat) $\tilde{\nu}_{\text{max}}$ (cm^{-1}): 1239 (m), 1211 (m), 1176 (s), 1114 (m), 1066 (m), 1035 (s), 1005 (s), 989 (s), 965 (s), 939 (vs), 919 (vs), 841 (s), 813 (m), 760 (m). **Mp** ($^\circ\text{C}$) = 190–192.

Potassium (3,6-dihydro-2H-thiopyran-4-yl)trifluoroborate (SM44)

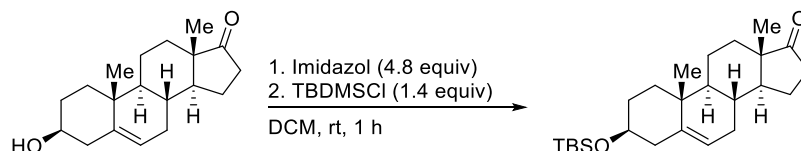
Using 2-(3,6-dihydro-2H-thiopyran-4-yl)-4,4,5,5-tetramethyl-1,3,2-dioxaborolane according to general procedure **R**, provided **SM44** (3.49 mmol, 718 mg, 84%) as colorless solid. $^1\text{H NMR}$ (400 MHz, CD_3CN) δ 5.79 (s, 1H), 3.06 – 2.97 (m, 2H), 2.60 (t, $J = 5.8$ Hz, 2H), 2.22 – 2.17 (m, 2H) ppm. $^{13}\text{C NMR}$ (101 MHz, CD_3CN) δ 120.7, 27.3, 26.1, 25.9 ppm. The signal for the carbon atom adjacent to the boron center was not observed. $^{11}\text{B NMR}$ (128 MHz, CD_3CN) n. d. **HRMS** (ESI-Quadrupole): m/z calcd for $\text{C}_5\text{H}_7\text{SBF}_3^-$ [M-K]: 167.0314; found: 167.0318. **IR** (Diamond-ATR, neat) $\tilde{\nu}_{\text{max}}$ (cm^{-1}): n.d.

Potassium trifluoro(1,4-dioxaspiro[4.5]dec-7-en-8-yl)borate (SM45)

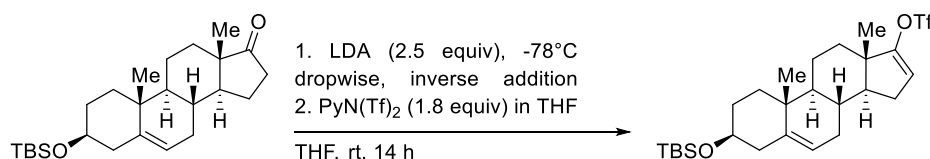
Using 4,4,5,5-tetramethyl-2-(1,4-dioxaspiro[4.5]dec-7-en-8-yl)-1,3,2-dioxaborolane according to general procedure **R**, provided **SM45** (3.43 mmol, 843 mg, 59%) as colorless solid. $^1\text{H NMR}$ (400 MHz, CD_3CN) δ 5.47 (s, 1H), 3.88 (s, 4H), 2.14 – 2.07 (m, 4H), 1.58 (t, $J = 6.4$ Hz, 2H) ppm. $^{13}\text{C NMR}$ (101 MHz, CD_3CN) δ 121.9, 109.6, 64.6, 37.0, 32.2, 27.1 ppm. The signal for the carbon atom adjacent to the boron center was not observed. $^{11}\text{B NMR}$ (128 MHz, CD_3CN) δ

2.61 (q, $J = 56.4$ Hz) ppm. **HRMS** (ESI-Quadrupole): m/z calcd for $C_8H_{11}O_2BF_3^-$ [M-K]: 207.0804; found: 207.0809. **IR** (Diamond-ATR, neat) $\tilde{\nu}_{max}$ (cm^{-1}): 1693 (w), 1209 (w), 1201 (w), 1170 (w), 1150 (m), 1128 (m), 1108 (m), 1058 (m), 1048 (m), 1010 (s), 941 (vs), 894 (s), 857 (m), 816 (w), 812 (w), 789 (m). **Mp** ($^{\circ}C$) = 185–188.

6.4.2 Experimental Procedures for the Synthesis of SM46



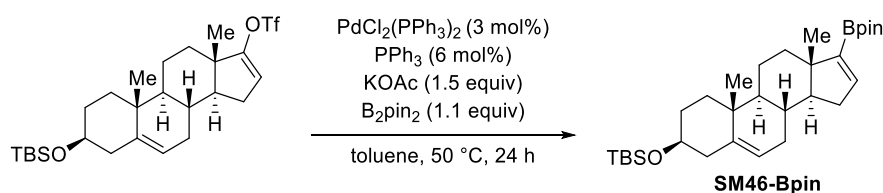
3-TBS-5-DHEA was prepared according to Pérez *et al.*²⁸¹ To a suspension of 5-dehydroepiandrosterone (15.0 mmol, 4.33 g) in DCM (50 mL) was added imidazole (72.0 mmol, 4.90 g). When a clear solution had formed, TBSCl (21.0 mmol, 3.16 g, 1.4 equiv) was added. The mixture was stirred at room temperature for 2 h and then concentrated *in vacuo*. The crude product was dissolved in DCM (50 mL) and washed with 1 M HCl (2×50 mL) and water (2×50 mL). The organic phase was dried over $MgSO_4$ and evaporated *in vacuo*. The colorless solid was dried under high vacuum at $60^{\circ}C$ to obtain the pure product in 90% yield (13.5 mmol, 5.4 g), which was used without further purification for the following step.



3-TBS-5-DHEA triflate was prepared according to procedures from Lopez *et al.*²⁸² A solution of LDA was freshly prepared by dropwise addition of a solution of *n*-BuLi in hexanes (11.5 mmol, 4.64 mL, 2.47 M, 2.3 equiv) to a solution of DIPA (12.5 mmol, 1.26 g, 1.75 mL, 2.5 equiv) in THF at $-78^{\circ}C$. To this solution, a suspension of 3-TBS-5-DHEA (5.00 mmol, 2.01 g) in THF (25 mL) was added dropwise at $-78^{\circ}C$. After stirring for 1 h, a solution of $PyN(Tf)_2$ (9.00 mmol, 3.22 g, 1.8 equiv) in THF (12.5 mL) was added dropwise at $-78^{\circ}C$. The reaction mixture was stirred at room temperature overnight and then filtered over silica gel and washed with DCM (2×50 mL). The filtrate was concentrated *in vacuo*. The resulting colorless solid was purified *via* flash-column chromatography (hexanes/EtOAc 98:2) to give the product in 80% yield (4.0 mmol, 2.13 g), which was directly engaged in the next step.

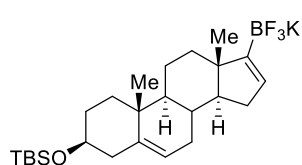
²⁸¹ A. Pérez Encabo, J. A. Turiel Hernandez, F. J. Gallo Nieto, A. Lorente Bonde-Larsen, C. M. Sandoval Rodríguez, *C07J* 41/00, **2013**.

²⁸² B. López-Pérez, M. A. Maestro, A. Mourino, *Chem. Commun.* **2017**, 53, 8144–8147.



3-TBS-5-DHEA alkenylboronic acid pinacol ester was prepared according to procedures from Tagaki *et al.*²⁸³ A dried flask was charged with 3-TBS-5-DHEA alkenyl triflate (1.24 mmol, 661 mg), $\text{PdCl}_2(\text{PPh}_3)_2$ (0.037 mmol, 26 mg, 3 mol%), PPh_3 (0.074 mmol, 19 mg, 6 mol%), B_2pin_2 (1.36 mmol, 345 mg, 1.1 equiv) and toluene (7.5 mL). After adding KOAc (1.85 mmol, 182 mg, 1.5 equiv), the flask was flushed with nitrogen, sealed and stirred at 50 °C for 24 h. The mixture was filtered over MgSO_4 , washed with THF (20 mL) and concentrated *in vacuo*. The resulting colorless solid was purified *via* flash-column chromatography (hexanes/ EtOAc 95:5) to give the product in **SM46-Bpin** 86% yield (1.0 mmol, 512 mg). $R_f = 0.60$ (hexane/ EtOAc 95:5, UV, KMnO_4). $^1\text{H NMR}$ (400 MHz, CDCl_3) δ 6.50 (dd, $J = 3.1, 1.6$ Hz, 1H), 5.35 – 5.31 (m, 1H), 3.48 (tt, $J = 10.9, 4.7$ Hz, 1H), 2.34 – 2.22 (m, 1H), 2.22 – 2.05 (m, 3H), 2.05 – 1.89 (m, 2H), 1.81 (dt, $J = 13.4, 3.6$ Hz, 1H), 1.76 – 1.45 (m, 8H), 1.41 – 1.27 (m, 3H), 1.25 (s, 12H), 1.03 (s, 3H), 0.89 (s, 9H), 0.06 (s, 6H) ppm. $^{13}\text{C NMR}$ (101 MHz, CDCl_3) δ 146.1, 142.1, 121.2, 82.8, 72.8, 57.0, 53.6, 51.0, 47.8, 43.0, 37.5, 37.0, 35.9, 33.8, 32.2, 30.8, 26.1, 25.0, 24.9, 21.0, 19.5, 18.5, 16.8, –4.5 ppm. **LRMS** (DEP/EI-Orbitrap): m/z (%): 455.3 (100) [$\text{M}-t\text{-Bu}$]⁺.

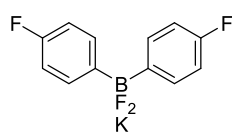
Potassium ((3*S*,9*S*,10*R*,13*S*,14*S*)-3-((*tert*-butyldimethylsilyl)oxy)-10,13-dimethyl-2,3,4,7,8,9,10,11,12,13,14,15-dodecahydro-1*H*-cyclopenta[*a*]phenanthren-17-yl)trifluoroborate (SM46)



Using *tert*-butyl(((3*S*,9*S*,10*R*,13*S*,14*S*)-10,13-dimethyl-17-(4,4,5,5-tetramethyl-1,3,2-dioxaborolan-2-yl)-2,3,4,7,8,9,10,11,12,13,14,15-dodecahydro-1*H*-cyclopenta[*a*]phenanthren-3-yl)oxy)dimethylsilane according to general procedure **R**, provided **SM46** (0.5 mmol, 246 mg, 50%) as colorless solid. Due to high insolubility in many different deuterated solvents like CDCl_3 , $\text{DMSO}-d_6$, $(\text{CD}_3)_2\text{CO}$, C_6D_6 , and CD_3CN , NMR spectral analysis was not enough to determine the exact proton shifts and couplings. $^{11}\text{B NMR}$ (128 MHz, CD_3CN) δ 2.09 (br, s) ppm. **HRMS** (ESI-Quadrupole): m/z calcd for $\text{C}_{25}\text{H}_{41}\text{BF}_3\text{OSi}^-$ [$\text{M}-\text{K}$]: 453.2977; found: 453.2981. **IR** (Diamond-ATR, neat) $\tilde{\nu}_{\text{max}}$ (cm^{-1}): 2970 (w), 2960 (w), 2949 (w), 2930 (m), 2897 (w), 2857 (w), 2828 (w), 1608 (w), 1584 (w), 1470 (w), 1459 (w), 1437 (w), 1381 (w), 1368 (w), 1270 (w), 1250 (w), 1206 (w), 1195 (w), 1165 (w), 1146 (w), 1133 (w), 1087 (s), 1044 (w), 1004 (m), 993 (m), 982 (m), 952 (s), 945 (s), 930 (s), 919 (s), 908 (m), 887 (m), 874 (m), 863 (s), 838 (vs), 820 (m), 803 (m), 776 (s), 738 (m), 715 (w), 689 (w), 674 (w). **Mp** (°C) >300.

²⁸³ J. Takagi, K. Takahashi, T. Ishiyama, N. Miyaura, *J. Am. Chem. Soc.* **2002**, *124*, 8001–8006.

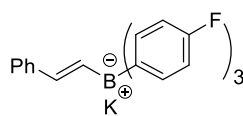
6.4.3 Synthesis of Potassium difluorobis(4-fluorophenyl) borate (SM47)



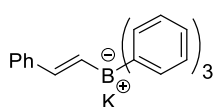
Adapted from a previously reported procedure,²⁴⁴ 15.0 mL of (4-fluorophenyl)magnesium bromide (0.7 M, 10.5 mmol, 2.1 equiv) were cooled to 0 °C. *Triisopropyl borate* (5.0 mmol, 1.0 equiv, 1.15 mL) was slowly added *via* syringe pump over 30 min. The mixture was allowed to reach room temperature and stirred overnight. The slurry was then quenched with 2 mL of 2 M HCl and extracted with EtOAc (3 × 30 mL). The organic phases were combined, dried over MgSO₄ and concentrated *in vacuo*. After column chromatography in DCM (*R_f* = 0.60) the corresponding borinic acid was isolated as an orange oil. The crude product was then directly redissolved in MeOH (20 mL) and KHF₂ (15.0 mmol, 1.17 g) was added in one portion at 0 °C. The reaction was stirred at room temperature overnight and the solvent removed afterwards. The solids were extracted with boiling acetone (4 × 20 mL) and the combined organic phases were dried *in vacuo*. The colorless solid was then filtered off and washed with diethyl ether (3 × 20 mL) to yield the desired product **SM47** (3.12 mmol, 867 mg, 62%). ¹H NMR (400 MHz, CD₃CN) δ 7.44 – 7.34 (m, 2H), 6.90 – 6.81 (m, 2H) ppm. ¹³C NMR (101 MHz, CD₃CN) δ 162.2 (d, *J* = 237.8 Hz), 133.8 (dt, *J* = 6.9, 3.6 Hz), 113.7 (d, *J* = 18.6 Hz) ppm. The signals for the carbon atoms adjacent to the boron center were not observed. ¹¹B NMR (128 MHz, CD₃CN) δ 6.84 (t, *J* = 71.4 Hz) ppm. HRMS (ESI-Quadrupole): *m/z* calcd for C₁₂H₈BF₄⁻ [M-K]⁻: 239.0655; found: 239.0660. IR (Diamond-ATR, neat) $\tilde{\nu}_{max}$ (cm⁻¹): 1594 (m), 1499 (w), 1389 (vw), 1301 (w), 1270 (w), 1228 (m), 1207 (m), 1193 (m), 1166 (m), 1158 (m), 1152 (m), 1090 (w), 1018 (w), 961 (w), 929 (m), 911 (m), 894 (s), 872 (m), 832 (s), 822 (vs), 800 (m), 715 (w). Mp (°C) = 193–196.

6.4.4 Characterization of ATB Salts

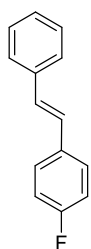
(*E*)-Tris(4-fluorophenyl)(styryl)borate (2a)



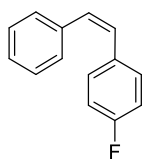
Using potassium (*E*)-trifluoro(styryl)borate and a solution of (4-fluorophenyl)magnesium bromide in THF according to general procedure **T**, provided **2a** (2.61 mmol, 1.14 g, 87%) as colorless solid. ¹H NMR (400 MHz, (CD₃)₂CO) δ 7.59 (d, *J* = 17.8 Hz, 1H), 7.34 – 7.28 (m, 2H), 7.24 – 7.13 (m, 8H), 7.01 – 6.92 (m, 1H), 6.76 – 6.68 (m, 6H), 6.13 (ddd, *J* = 17.8, 6.9, 3.3 Hz, 1H) ppm. ¹³C NMR (101 MHz, (CD₃)₂CO) δ 160.9 (d, *J* = 236.1 Hz), 160.1 (d, *J* = 3.4 Hz), 159.6 (d, *J* = 3.4 Hz), 159.1 (d, *J* = 4.0 Hz), 158.6 (d, *J* = 4.3 Hz), 158.0, 157.5, 143.7 (dd, *J* = 8.6, 4.3 Hz), 137.0 (ddd, *J* = 5.5, 3.5, 1.6 Hz), 131.6, 128.7, 126.0, 125.0, 112.5 (ddd, *J* = 17.7, 6.1, 2.9 Hz) ppm. The signals for the carbon atoms adjacent to the boron center were not observed. ¹¹B NMR (128 MHz, CD₃CN) δ -9.49 ppm. HRMS (ESI-Quadrupole): *m/z* calcd for C₂₆H₁₉BF₃⁻ [M-K]⁻: 399.1532; found: 399.1538. IR (Diamond-ATR, neat) $\tilde{\nu}_{max}$ (cm⁻¹): 1579 (m), 1487 (s), 1218 (s), 1157 (s), 1086 (w), 1012 (m), 966 (w), 827 (s), 817 (vs), 782 (w), 744 (m), 722 (m), 696 (m). Mp (°C) = 279–282 (decomposition).

(E)-Tris(phenyl)(styryl)borate (2b)

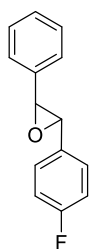
Using potassium (*E*)-trifluoro(styryl)borate and a solution of phenylmagnesium bromide in THF according to general procedure **T**, provided **2b** (2.47 mmol, 949 mg, 82%) as colorless powder. ¹H NMR (400 MHz, (CD₃)₂CO) δ 7.71 (d, *J* = 17.8 Hz, 1H), 7.34 – 7.27 (m, 8H), 7.18 – 7.11 (m, 2H), 6.99 – 6.92 (m, 7H), 6.83 – 6.77 (m, 3H), 6.20 (ddd, *J* = 17.8, 6.7, 3.3 Hz, 1H) ppm. ¹³C NMR (101 MHz, (CD₃)₂CO) δ 165.5, 165.0, 164.5, 164.1, 160.4, 159.9, 159.4, 158.9, 144.2 (dd, *J* = 8.5, 4.1 Hz), 136.4 (dd, *J* = 2.9, 1.4 Hz), 131.2, 128.7, 126.2 (dd, *J* = 5.6, 2.7 Hz), 125.9, 124.6, 122.4 ppm. The signals for the carbon atoms adjacent to the boron center were not observed. ¹¹B NMR (128 MHz, CD₃CN) δ -8.75 ppm. HRMS (ESI-Quadrupole): *m/z* calcd for C₂₆H₂₂B⁻ [M-K]: 345.1815; found: 345.1824. IR (Diamond-ATR, neat) $\tilde{\nu}_{max}$ (cm⁻¹): 1742 (w), 1596 (w), 1578 (w), 1493 (w), 1477 (w), 1444 (w), 1428 (w), 1261 (w), 1236 (w), 1185 (w), 1152 (w), 1070 (w), 1030 (w), 1011 (w), 1006 (w), 958 (w), 912 (w), 874 (w), 818 (w), 768 (m), 756 (m), 739 (s), 723 (m), 712 (vs), 696 (s). **Mp** (°C) >300.

6.4.5 Characterization of Olefinated (Hetero)Arenes**(E)-1-Fluoro-4-styrylbenzene (3a/3m)**

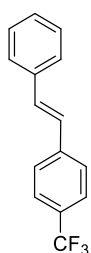
Using potassium (*E*)-trifluoro(styryl)borate and a solution of (4-fluorophenyl)magnesium bromide in THF according to general procedure **S**, provided **3a** (0.27 mmol, 54 mg, 68%, *E/Z* = 99:1) as colorless solid. Using potassium (*Z*)-trifluoro(styryl)borate (**SM28**) and a solution of (4-fluorophenyl)magnesium bromide in THF according to general procedure **S**, provided **3m** (0.22 mmol, 44 mg, 55%, *E/Z* = 98:2) as a colorless solid. Using the purified tetraorganoborate **2a** under the optimized conditions for the electrochemical transformation, **3a** (0.30 mmol, 59 mg, 75%, *E/Z* = 99:1) was provided as a colorless solid. Zweifel Olefination: A 25 mL Schlenk flask was charged with the (*Z*)-trifluoro(styryl)borate (**SM28**) (0.2 mmol, 1.0 equiv, 42 mg) and 1 mL of THF was added. The mixture was cooled to 0 °C and a solution of (4-fluorophenyl)magnesium bromide in THF (0.6 mmol, 3.0 equiv) was added dropwise over 30 min *via* syringe pump. After addition, the reaction mixture was allowed to stir for further 10 min at 0 °C, after which 1.2 mL of NaOMe (0.5 M in MeOH, 0.6 mmol, 3.0 equiv) were added. Iodine (0.3 mmol, 1.5 equiv, 76 mg) was dissolved in 1 mL THF and added dropwise to the mixture, which was then further stirred at 0 °C for 30 min. The slurry was then quenched with sat. aq. Na₂S₂O₃ solution (2 mL) and extracted with EtOAc (3 × 10 mL). The combined organic phases were dried over MgSO₄, filtered, concentrated under reduced pressure and purified by flash-column chromatography on silica gel in hexane (*R_f* = 0.37 (hexane/EtOAc 100:0, UV, KMnO₄)) to yield product **3a** (0.22 mmol, 44 mg, 55%, *E/Z* = 99:1) as colorless solid. ¹H NMR (400 MHz, CDCl₃) δ 7.46 – 7.35 (m, 4H), 7.27 (t, *J* = 7.7 Hz, 2H), 7.21 – 7.13 (m, 1H), 7.03 – 6.92 (m, 4H) ppm. LRMS (DEP/EI-Orbitrap): *m/z* (%): 198.0 (100), 183.0 (45), 177.0 (20). Analytical data in accordance to literature.²⁶²

(Z)-1-Fluoro-4-styrylbenzene ((Z)-3a)

Zweifel Olefination: A 25 mL Schlenk flask was charged with (*E*)-Tris(4-fluorophenyl)(styryl)borate **2a** (0.2 mmol, 1.0 equiv, 88 mg) and 1 mL of THF was added. 1.2 mL of NaOMe (0.5 M in MeOH, 0.6 mmol, 3.0 equiv) were added in one portion. Iodine (0.3 mmol, 1.5 equiv, 76 mg) was dissolved in 1 mL THF and added dropwise to the mixture, which was then further stirred at 0 °C for 30 min. The slurry was then quenched with sat. aq. Na₂S₂O₃ solution (2 mL) and extracted with EtOAc (3 × 10 mL). The combined organic phases were dried over MgSO₄, filtered, concentrated under reduced pressure and purified by flash-column chromatography on silica gel in hexane (*R_f* = 0.37 (hexane/EtOAc 100:0, UV, KMnO₄)) to yield product (*Z*)-**3a** (0.17 mmol, 34 mg, 86%, *E/Z* = 1:99) as colorless solid. ¹H NMR (400 MHz, CDCl₃) δ 7.28 – 7.16 (m, 7H), 6.95 – 6.87 (m, 2H), 6.60 (d, *J* = 12.2 Hz, 1H), 6.55 (d, *J* = 12.2 Hz, 1H) ppm. LRMS (DEP/EI-Orbitrap): *m/z* (%): 198.0 (100), 183.0 (45), 177.0 (20). Analytical data in accordance to literature.²⁸⁴

trans*-2-(4-fluorophenyl)-3-phenyloxirane (3ab)

Using potassium (*E*)-trifluoro(styryl)borate and a solution of (4-fluorophenyl)magnesium bromide in THF according to general procedure **S** under O₂ atmosphere, provided **3ab** (0.15 mmol, 32 mg, 37%) as yellowish oil. *R_f* = 0.21 (hexane/EtOAc 100:0, UV, KMnO₄, PAA). ¹H NMR (400 MHz, CDCl₃) δ 7.44 – 7.28 (m, 7H), 7.08 (tt, *J* = 8.8, 2.5 Hz, 2H), 3.86 (d, *J* = 1.8 Hz, 1H), 3.84 (d, *J* = 1.8 Hz, 1H) ppm. LRMS (DEP/EI-Orbitrap): *m/z* (%): 214.0 (20), 196.0 (20), 185.0 (100), 165.0 (70). Analytical data in accordance to literature.²⁸⁵

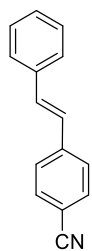
(*E*)-1-Styryl-4-(trifluoromethyl)benzene (3b)*

Using potassium (*E*)-trifluoro(styryl)borate and a solution of (4-(trifluoromethyl)phenyl)magnesium bromide in THF according to general procedure **S**, provided **3b** (0.28 mmol, 68 mg, 69%, *E/Z* = 99:1) as colorless solid. ¹H NMR (400 MHz, CDCl₃) δ 7.61 (s, 4H), 7.56 – 7.52 (m, 2H), 7.43 – 7.37 (m, 2H), 7.33 – 7.27 (m, 1H), 7.20 (d, *J* = 16.4 Hz, 1H), 7.12 (d, *J* = 16.4 Hz, 1H) ppm. LRMS (DEP/EI-Orbitrap): *m/z* (%): 248.0 (100), 233.0 (15), 227.0 (25). Analytical data in accordance to literature.²⁸⁶

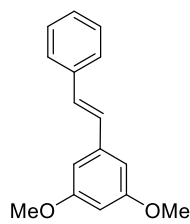
²⁸⁴ M. Das, D. F. O'Shea, *Org. Lett.* **2016**, *18*, 336–339.

²⁸⁵ T. Niwa, M. Nakada, *J. Am. Chem. Soc.* **2012**, *134*, 13538–13541.

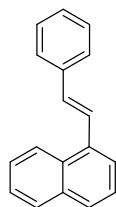
²⁸⁶ S. W. Youn, B. S. Kim, A. R. Jagdale, *J. Am. Chem. Soc.* **2012**, *134*, 11308–11311.

(E)-4-Styrylbenzotrile (3c)

Using potassium (*E*)-trifluoro(styryl)borate and a solution of (4-cyanophenyl)zinc(II) iodide in THF according to general procedure **S**, provided **3c** (0.12 mmol, 24 mg, 29%, *E/Z* = 99:1) as colorless solid. ¹H NMR (400 MHz, CDCl₃) δ 7.69 – 7.61 (m, 2H), 7.61 – 7.57 (m, 2H), 7.56 – 7.52 (m, 2H), 7.43 – 7.37 (m, 2H), 7.36 – 7.29 (m, 1H), 7.22 (d, *J* = 16.3 Hz, 1H), 7.09 (d, *J* = 16.3 Hz, 1H) ppm. LRMS (DEP/EI-Orbitrap): *m/z* (%): 205.1 (100), 190.0 (50), 176.0 (20). Analytical data in accordance to literature.²⁸⁷

(E)-1,3-Dimethoxy-5-styrylbenzene (3d)

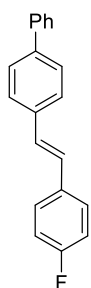
Using potassium (*E*)-(styryl)trifluoroborate and a solution of (3,5-dimethoxyphenyl)magnesium bromide in THF according to general procedure **S**, provided **3d** (0.21 mmol, 50 mg, 42%) as colorless solid. *R_f* = 0.50 (hexane/EtOAc 9:1, UV, KMnO₄). ¹H NMR (400 MHz, CDCl₃) δ 7.54 – 7.49 (m, 2H), 7.39 – 7.34 (m, 2H), 7.30 – 7.24 (m, 1H), 7.10 (d, *J* = 16.3 Hz, 1H), 7.04 (d, *J* = 16.3 Hz, 1H), 6.68 (d, *J* = 2.3 Hz, 2H), 6.40 (t, *J* = 2.3 Hz, 1H), 3.84 (s, 6H) ppm. LRMS (DEP/EI-Orbitrap): *m/z* (%): 240.1 (100), 224.0 (10), 209.0 (20). HRMS (EI-Orbitrap): *m/z* calcd. for C₁₆H₁₆O₂⁺: 240.1150; found: 240.1143. Analytical data in accordance to literature.²⁸⁸

(E)-1-Styrylnaphthalene (3e/3q)

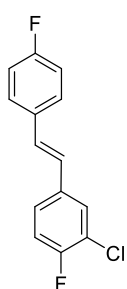
Using potassium (*E*)-trifluoro(styryl)borate and a solution of naphthalen-1-ylmagnesium bromide in THF according to general procedure **S**, provided **3e** (0.30 mmol, 68 mg, 74%, *E/Z* = 99:1) as colorless solid. Using potassium (*Z*)-trifluoro(styryl)borate (**SM28**) and a solution of naphthalen-1-ylmagnesium bromide in THF according to general procedure **S**, provided **3q** (0.17 mmol, 37 mg, 43%, *E/Z* = 93:7) as colorless solid. ¹H NMR (400 MHz, CDCl₃) δ 8.23 (d, *J* = 8.0 Hz, 1H), 7.93 – 7.86 (m, 2H), 7.82 (d, *J* = 8.2 Hz, 1H), 7.76 (d, *J* = 6.1 Hz, 1H), 7.65 – 7.60 (m, 2H), 7.58 – 7.48 (m, 3H), 7.42 (t, *J* = 7.7 Hz, 2H), 7.34 – 7.29 (m, 1H), 7.17 (d, *J* = 16.0 Hz, 1H) ppm. LRMS (DEP/EI-Orbitrap): *m/z* (%): 229.1 (100), 215.1 (15), 202.1 (10). Analytical data in accordance to literature.²⁸⁴

²⁸⁷ H. Li, J. Lü, J. Lin, Y. Huang, M. Cao, R. Cao, *Chem. Eur. J.* **2013**, *19*, 15661–15668.

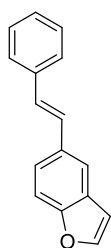
²⁸⁸ J. Yang, C. Wang, Y. Sun, X. Man, J. Li, F. Sun, *Chem. Commun.* **2019**, *55*, 1903–1906.

(E)-4-(4-Fluorostyryl)-1,1'-biphenyl (3f)*

Using potassium (*E*)-(2-([1,1'-biphenyl]-4-yl)vinyl)trifluoroborate (**SM36**) and a solution of (4-fluorophenyl)magnesium bromide in THF according to general procedure **S**, provided **3f** (0.28 mmol, 78 mg, 71%, *E/Z* = 99:1) as colorless solid. ¹H NMR (400 MHz, CDCl₃) δ 7.69 – 7.55 (m, 6H), 7.55 – 7.42 (m, 4H), 7.40 – 7.31 (m, 1H), 7.15 – 7.00 (m, 4H) ppm. LRMS (DEP/EI-Orbitrap): *m/z* (%): 274.1 (100), 259.0 (10), 252.1 (15). Analytical data in accordance to literature.²⁸⁹

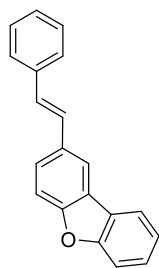
(E)-2-Chloro-1-fluoro-4-(4-fluorostyryl)benzene (3g)

Using potassium (*E*)-trifluoro(4-fluorostyryl)borate (**SM37**) and a solution of (3-chloro-4-fluorophenyl)magnesium bromide in THF according to general procedure **S**, provided **3g** (0.22 mmol, 55 mg, 55%, *E/Z* = 99:1) as colorless oil. *R_f* = 0.40 (hexane, UV, KMnO₄). ¹H NMR (400 MHz, CDCl₃) δ 7.53 (dd, *J* = 7.0, 2.2 Hz, 1H), 7.48 – 7.43 (m, 2H), 7.33 (ddd, *J* = 8.6, 4.6, 2.2 Hz, 1H), 7.12 (t, *J* = 8.7 Hz, 1H), 7.06 (t, *J* = 8.7 Hz, 2H), 6.99 (d, *J* = 16.3 Hz, 1H), 6.90 (d, *J* = 16.3 Hz, 1H) ppm. ¹³C NMR (101 MHz, CDCl₃) δ 162.7 (d, *J* = 247.8 Hz), 157.6 (d, *J* = 249.8 Hz), 134.7 (d, *J* = 3.9 Hz), 133.0 (d, *J* = 3.4 Hz), 128.7 (d, *J* = 2.4 Hz), 128.3, 128.2, 126.2 (d, *J* = 7.0 Hz), 126.1 (t, *J* = 2.1 Hz), 121.5 (d, *J* = 18.1 Hz), 116.9 (d, *J* = 21.5 Hz), 115.9 (d, *J* = 21.7 Hz) ppm. LRMS (DEP/EI-Orbitrap): *m/z* (%): 250.0 (95), 235.0 (15), 214.1 (100), 195.1 (30). HRMS (EI-Orbitrap): *m/z* calcd. for C₁₄H₉ClF₂⁺: 250.0361; found: 250.0354. IR (Diamond-ATR, neat) $\tilde{\nu}_{max}$ (cm⁻¹): 2942 (vs), 2929 (vs), 2892 (s), 2866 (vs), 1502 (vs), 1463 (s), 1254 (m), 1202 (s), 1148 (m), 1096 (s), 1059 (m), 1037 (s), 1017 (s), 1004 (s), 993 (s), 981 (s), 942 (m), 931 (m), 919 (m), 906 (m), 884 (s), 863 (m), 830 (s), 810 (m), 804 (m), 775 (m), 739 (m), 709 (m), 677 (s), 668 (s), 662 (s).

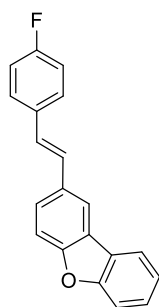
(E)-5-Styrylbenzofuran (3h)

Using potassium (*E*)-trifluoro(styryl)borate and a solution of benzofuran-5-ylmagnesium bromide in THF according to general procedure **S**, provided **3h** (0.25 mmol, 55 mg, 63%, *E/Z* = 99:1) as colorless oil. *R_f* = 0.30 (hexane, UV, PAA, KMnO₄). ¹H NMR (400 MHz, CDCl₃) δ 7.72 (s, 1H), 7.62 (d, *J* = 2.2 Hz, 1H), 7.55 – 7.47 (m, 4H), 7.37 (t, *J* = 7.7 Hz, 2H), 7.31 – 7.19 (m, 2H), 7.10 (d, *J* = 16.3 Hz, 1H), 6.78 (d, *J* = 2.2 Hz, 1H) ppm. ¹³C NMR (101 MHz, CDCl₃) δ 154.8, 145.7, 137.6, 132.6, 129.1, 128.8, 128.0, 127.8, 127.5, 126.5, 123.1, 119.4, 111.7, 106.8 ppm. LRMS (DEP/EI-Orbitrap): *m/z* (%): 220.0 (100), 204.9 (10), 191.0 (60). HRMS (EI-Orbitrap): *m/z* calcd. for C₁₆H₁₂O⁺: 220.0888; found: 220.0882. IR (Diamond-ATR, neat) $\tilde{\nu}_{max}$ (cm⁻¹): 1464 (w), 1450 (w), 1253 (w), 1197 (w), 1125 (m), 1105 (m), 1028 (m), 967 (m), 887 (m), 809 (s), 769 (s), 736 (vs), 693 (s).

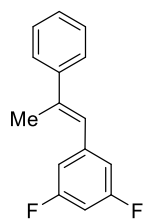
²⁸⁹ Y. Liu, P. Liu, Y. Wei, *Chin. J. Chem.* **2017**, *35*, 1141–1148.

(E)-2-Styryldibenzo[*b,d*]furan (3i/3s)*

Using potassium (*E*)-trifluoro(styryl)borate and a solution of dibenzo[*b,d*]furan-2-ylmagnesium bromide in THF according to general procedure **S**, provided **3i** (0.23 mmol, 62 mg, 57%, *E/Z* = 99:1) as colorless solid. Using potassium (*Z*)-trifluoro(styryl)borate (**SM28**) and a solution of dibenzo[*b,d*]furan-2-ylmagnesium bromide in THF according to general procedure **S**, provided **3s** (0.24 mmol, 65 mg, 60%, *E/Z* = 96:4) as colorless solid. ¹H NMR (400 MHz, CDCl₃) δ 8.09 (d, *J* = 1.8 Hz, 1H), 7.99 (dd, *J* = 7.8, 1.3 Hz, 1H), 7.64 (dd, *J* = 8.5, 1.8 Hz, 1H), 7.61 – 7.53 (m, 4H), 7.48 (ddd, *J* = 8.4, 7.3, 1.4 Hz, 1H), 7.43 – 7.35 (m, 3H), 7.32 – 7.25 (m, 2H), 7.17 (d, *J* = 16.3 Hz, 1H) ppm. LRMS (DEP/EI-Orbitrap): *m/z* (%): 270.1 (100), 255.0 (10), 239.0 (20). Analytical data in accordance to literature.²⁹⁰

(E)-2-(4-Fluorostyryl)dibenzo[*b,d*]furan (3j)

Using potassium (*E*)-trifluoro(4-fluorostyryl)borate (**SM37**) and a solution of dibenzo[*b,d*]furan-2-ylmagnesium bromide in THF according to general procedure **S**, provided **3j** (0.27 mmol, 78 mg, 68%, *E/Z* = 99:1) as colorless oil. *R*_f = 0.30 (hexane, UV, PAA, KMnO₄). ¹H NMR (400 MHz, CDCl₃) δ 8.07 (d, *J* = 1.8 Hz, 1H), 7.98 (d, *J* = 6.9 Hz, 1H), 7.62 (dd, *J* = 8.6, 1.8 Hz, 1H), 7.60 – 7.45 (m, 5H), 7.37 (td, *J* = 7.5, 1.0 Hz, 1H), 7.18 (d, *J* = 16.3 Hz, 1H), 7.14 – 7.05 (m, 3H) ppm. ¹³C NMR (101 MHz, CDCl₃) δ 162.40 (d, *J* = 246.9 Hz), 156.8, 156.0, 133.74 (d, *J* = 3.3 Hz), 132.4, 128.53 (d, *J* = 2.5 Hz), 128.00 (d, *J* = 7.8 Hz), 127.5, 126.9, 126.0, 124.9, 124.2, 123.0, 120.8, 118.5, 115.8 (d, *J* = 21.6 Hz), 112.0, 111.9 ppm. LRMS (DEP/EI-Orbitrap): *m/z* (%): 288.1 (100), 273.0 (5), 257.1 (30). HRMS (EI-Orbitrap): *m/z* calcd. for C₂₀H₁₃FO⁺: 288.0950; found: 288.0945. IR (Diamond-ATR, neat) $\tilde{\nu}_{max}$ (cm⁻¹): 3041 (w), 1710 (m), 1601 (m), 1508 (s), 1473 (m), 1450 (s), 1431 (m), 1414 (m), 1360 (m), 1349 (m), 1329 (w), 1304 (w), 1296 (w), 1261 (w), 1226 (s), 1210 (m), 1196 (s), 1168 (m), 1159 (m), 1141 (m), 1122 (m), 1100 (m), 1022 (m), 1004 (w), 972 (m), 961 (s), 940 (m), 926 (m), 908 (w), 893 (m), 857 (m), 841 (m), 824 (vs), 812 (s), 790 (m), 766 (m), 752 (s), 741 (vs), 726 (s), 710 (m), 683 (w), 665 (w), 656 (w).

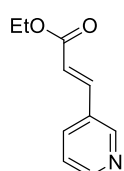
(E)-1,3-Difluoro-5-(2-phenylprop-1-en-1-yl)benzene (3k)

Using potassium (*E*)-trifluoro(2-phenylprop-1-en-1-yl)borate (**SM38**) and a solution of (3,5-difluorophenyl)magnesium bromide in THF according to general procedure **S**, provided **3k** (0.28 mmol, 64 mg, 70%, *E/Z* = 99:1) as colorless oil. *R*_f = 0.60 (hexane, UV, PAA, KMnO₄). ¹H NMR (400 MHz, CDCl₃) δ 7.56 – 7.46 (m, 2H), 7.43 – 7.36 (m, 2H), 7.35 – 7.29 (m, 1H), 6.94 – 6.83 (m, 2H), 6.74 – 6.66 (m, 2H), 2.28 (d, *J* = 1.4 Hz,

²⁹⁰ C. Wang, I. Piel, F. Glorius, *J. Am. Chem. Soc.* **2009**, *131*, 4194–4195.

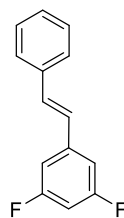
3H) ppm. ^{13}C NMR (101 MHz, CDCl_3) δ 162.97 (dd, $J = 247.4, 13.2$ Hz), 143.4, 141.62 (t, $J = 9.7$ Hz), 140.1, 128.6, 127.9, 126.2, 125.80 (t, $J = 2.6$ Hz), 112.21 – 111.70 (m), 102.01 (t, $J = 25.5$ Hz), 17.8 ppm. **LRMS** (DEP/EI-Orbitrap): m/z (%): 230.1 (100), 215.1 (80), 195.1 (20). **HRMS** (EI-Orbitrap): m/z calcd. for $\text{C}_{14}\text{H}_{15}\text{FO}_2^+$: 230.0907; found: 230.0896. **IR** (Diamond-ATR, neat) $\tilde{\nu}_{\text{max}}$ (cm^{-1}): n.d.

Ethyl (*E*)-3-(pyridin-3-yl)acrylate (**3l**)



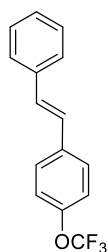
Using potassium (*E*)-(3-ethoxy-3-oxoprop-1-en-1-yl)trifluoroborate (**SM39**) and a solution of pyridin-3-ylzinc(II) iodide in THF according to general procedure **S**, provided **3l** (0.10 mmol, 18 mg, 25%, $E/Z = 99:1$) as colorless oil. $R_f = 0.25$ (hexane/EtOAc 6:4, UV, PAA). ^1H NMR (400 MHz, CDCl_3) δ 8.75 (d, $J = 2.2$ Hz, 1H), 8.61 (dd, $J = 4.8, 1.6$ Hz, 1H), 7.84 (dt, $J = 7.9, 2.0$ Hz, 1H), 7.67 (d, $J = 16.1$ Hz, 1H), 7.37 – 7.31 (m, 1H), 6.51 (d, $J = 16.1$ Hz, 1H), 4.28 (q, $J = 7.1$ Hz, 2H), 1.35 (t, $J = 7.1$ Hz, 3H) ppm. ^{13}C NMR (101 MHz, CDCl_3) δ 166.5, 151.1, 149.9, 141.0, 134.3, 130.4, 123.9, 120.6, 61.0, 14.4 ppm. **HRMS** (EI-Orbitrap): m/z calcd. for $\text{C}_{10}\text{H}_{11}\text{NO}_2^+$: 177.0790; found: 177.0782. **IR** (Diamond-ATR, neat) $\tilde{\nu}_{\text{max}}$ (cm^{-1}): 2963 (m), 2956 (m), 2926 (m), 2853 (m), 1717 (vs), 1685 (w), 1653 (w), 1642 (m), 1508 (m), 1472 (m), 1465 (m), 1457 (m), 1418 (m), 1388 (w), 1367 (m), 1312 (m), 1278 (m), 1262 (s), 1218 (m), 1184 (s), 1127 (m), 1120 (m), 1096 (m), 1074 (m), 1066 (m), 1043 (m), 1026 (m), 983 (m), 806 (m), 718 (w), 712 (w), 700 (m), 668 (w), 662 (w).

(*E*)-1,3-difluoro-5-styrylbenzene (**3n**)*

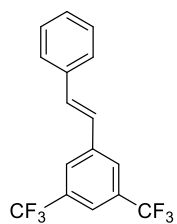


Using potassium (*Z*)-trifluoro(styryl)borate (**SM28**) and a solution of (3,5-difluorophenyl)magnesium bromide in THF according to general procedure **S**, provided **3n** (0.26 mmol, 56 mg, 65%, $E/Z = 90:10$) as colorless solid. ^1H NMR (400 MHz, CDCl_3) δ 7.56 – 7.48 (m, 2H), 7.43 – 7.35 (m, 2H), 7.35 – 7.28 (m, 1H), 7.11 (d, $J = 16.2$ Hz, 1H), 7.05 – 6.97 (m, 3H), 6.71 (tt, $J = 8.8, 2.3$ Hz, 1H) ppm. ^{13}C NMR (101 MHz, CDCl_3) δ 163.41 (dd, $J = 247.5, 13.2$ Hz), 140.88 (t, $J = 9.6$ Hz), 136.4, 131.4, 129.0, 128.5, 126.9, 126.62 (t, $J = 2.9$ Hz), 109.46 – 108.89 (m), 102.85 (t, $J = 25.7$ Hz) ppm. **LRMS** (DEP/EI-Orbitrap): m/z (%): 216.1 (100), 201.1 (50), 195.1 (30). Analytical data in accordance to literature.²⁹¹

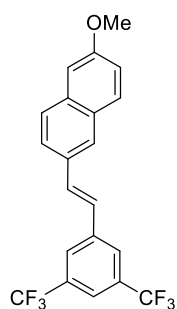
²⁹¹ T. Ismail, S. Shafi, J. Srinivas, D. Sarkar, Y. Qurishi, J. Khazir, M. S. Alam, H. M. S. Kumar, *Bioorg. Chem.* **2016**, *64*, 97–102.

(E)-1-Styryl-4-(trifluoromethoxy)benzene (3o)

Using potassium (*Z*)-trifluoro(styryl)borate (**SM28**) and a solution of (4-(trifluoromethoxy)phenyl)magnesium bromide in THF according to general procedure **S**, provided **3o** (0.24 mmol, 64 mg, 60%, *E/Z* = 97:3) as colorless solid. ¹H NMR (400 MHz, CDCl₃) δ 7.57 – 7.49 (m, 4H), 7.42 – 7.34 (m, 2H), 7.33 – 7.27 (m, 1H), 7.24 – 7.19 (m, 2H), 7.09 (s, 2H) ppm. LRMS (DEP/EI-Orbitrap): *m/z* (%): 264.1 (100), 249.0 (10), 179.1 (50). Analytical data in accordance to literature.²⁹²

(E)-1-Styryl-3,5-bis(trifluoromethyl)benzene (3p)

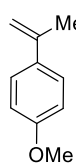
Using potassium (*Z*)-trifluoro(styryl)borate (**SM28**) and a solution of (3,5-bis(trifluoromethyl)phenyl)magnesium bromide in THF according to general procedure **S**, provided **3p** (0.24 mmol, 76 mg, 60%, *E/Z* = 90:10) as colorless solid. ¹H NMR (400 MHz, CDCl₃) δ 7.92 (s, 2H), 7.75 (s, 1H), 7.59 – 7.53 (m, 2H), 7.46 – 7.38 (m, 2H), 7.38 – 7.31 (m, 1H), 7.25 (d, *J* = 16.4 Hz, 1H), 7.13 (d, *J* = 16.4 Hz, 1H) ppm. LRMS (DEP/EI-Orbitrap): *m/z* (%): 316.1 (100), 301.1 (15), 275.1 (10). Analytical data in accordance to literature.²⁹³

(E)-2-(3,5-Bis(trifluoromethyl)styryl)-6-methoxynaphthalene (3r)

Using potassium (*Z*)-trifluoro(2-(6-methoxynaphthalen-2-yl)vinyl)borate (**SM41**) and a solution of (3,5-bis(trifluoromethyl)phenyl)magnesium bromide in THF according to general procedure **S**, provided **3r** (0.22 mmol, 89 mg, 56%, *E/Z* = 84:16) as colorless oil. *R_f* = 0.25 (hexane, UV, PAA, KMnO₄). ¹H NMR (400 MHz, CDCl₃) δ 7.94 (s, 2H), 7.85 (s, 1H), 7.77 – 7.68 (m, 4H), 7.38 (d, *J* = 16.3 Hz, 1H), 7.24 (d, *J* = 15.1 Hz, 1H), 7.19 – 7.12 (m, 2H), 3.94 (s, 3H) ppm. ¹³C NMR (101 MHz, CDCl₃) δ 158.4, 139.8, 134.9, 132.8, 132.13 (q, *J* = 33.1 Hz), 131.5, 129.9, 129.1, 127.8, 127.6, 126.2, 124.8, 123.9, 122.2, 120.7 (qq, *J* = 3.9 Hz), 119.5, 106.1, 55.5 ppm. LRMS (DEP/EI-Orbitrap): *m/z* (%): 396.1 (100), 381.0 (5), 353.0 (10), 333.0 (5). HRMS (EI-Orbitrap): *m/z* calcd. for C₂₁H₁₄F₆O₂⁺: 396.0949; found: 396.0949. IR (Diamond-ATR, neat) $\tilde{\nu}_{max}$ (cm⁻¹): 1626 (m), 1611 (m), 1602 (m), 1484 (m), 1467 (w), 1392 (m), 1373 (s), 1274 (vs), 1248 (m), 1218 (w), 1204 (m), 1170 (s), 1123 (vs), 1107 (s), 1032 (m), 1000 (w), 957 (m), 943 (m), 888 (s), 853 (m), 844 (m), 810 (m), 699 (m), 682 (s), 666 (m).

²⁹² K. Kanagaraj, K. Pitchumani, *Chem. Eur. J.* **2013**, *19*, 14425–14431.

²⁹³ L. Yu, Y. Huang, Z. Wie, Y. Ding, C. Su, Q. Xu, *J. Org. Chem.* **2015**, *80*, 8677–8683.

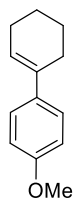
1-Methoxy-4-(prop-1-en-2-yl)benzene (4a)*

Using potassium trifluoro(prop-1-en-2-yl)borate and a solution of (4-methoxyphenyl)magnesium bromide in THF according to general procedure S, provided **4a** (0.16 mmol, 24 mg, 41%) as colorless oil. $^1\text{H NMR}$ (400 MHz, CDCl_3) δ 7.45 – 7.37 (m, 2H), 6.91 – 6.82 (m, 2H), 5.29 (dd, $J = 1.6, 0.8$ Hz, 1H), 5.04 – 4.96 (m, 1H), 3.82 (s, 3H), 2.13 (dd, $J = 1.5, 0.8$ Hz, 3H) ppm.

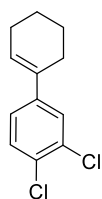
LRMS (DEP/EI-Orbitrap): m/z (%): 148.0 (100), 133.0 (80), 127.8 (5). Analytical data in accordance to literature.²¹¹

1-(Cyclopent-1-en-1-yl)-3,5-bis(trifluoromethyl)benzene (4b)

Using potassium cyclopent-1-en-1-yltrifluoroborate (**SM42**) and a solution of (3,5-bis(trifluoromethyl)phenyl)magnesium bromide in THF according to general procedure S, provided **4b** (0.21 mmol, 58 mg, 52%) as colorless oil. $R_f = 0.60$ (hexane, UV, PAA). $^1\text{H NMR}$ (400 MHz, CDCl_3) δ 7.81 (s, 2H), 7.70 (s, 1H), 6.39 (td, $J = 2.7, 1.4$ Hz, 1H), 2.78 – 2.71 (m, 2H), 2.62 – 2.56 (m, 2H), 2.08 (quint, $J = 7.6$ Hz, 2H) ppm. $^{13}\text{C NMR}$ (101 MHz, CDCl_3) δ 140.3, 138.9, 131.6 (q, $J = 32.9$ Hz), 130.7, 125.5, 123.5 (q, $J = 272.5$ Hz), 120.3 (q, $J = 3.9$ Hz), 33.7, 33.2, 23.4 ppm. **LRMS** (DEP/EI-Orbitrap): m/z (%): 280.1 (100), 261.1 (50), 245.1 (40), 211.1 (100), 191.1 (45), 142.1 (25). **HRMS** (EI-Orbitrap): m/z calcd. for $\text{C}_{13}\text{H}_{10}\text{F}_6^+$: 280.0687; found: 280.0680. **IR** (Diamond-ATR, neat) $\tilde{\nu}_{max}$ (cm^{-1}): 2959 (vw), 2929 (vw), 2852 (vw), 1703 (vw), 1626 (vw), 1468 (w), 1384 (m), 1331 (w), 1277 (vs), 1171 (s), 1129 (vs), 1108 (m), 1046 (w), 1016 (w), 994 (w), 960 (w), 945 (vw), 895 (m), 888 (m), 843 (w), 770 (vw), 758 (vw), 700 (m), 682 (m).

4'-Methoxy-2,3,4,5-tetrahydro-1,1'-biphenyl (4c)

Using potassium cyclohex-1-en-1-yltrifluoroborate and a solution of (4-methoxyphenyl)magnesium bromide in THF according to general procedure S, provided **4c** (0.28 mmol, 53 mg, 71%) as colorless oil. $^1\text{H NMR}$ (400 MHz, CDCl_3) δ 7.36 – 7.29 (m, 2H), 6.90 – 6.82 (m, 2H), 6.03 (tt, $J = 3.9, 1.7$ Hz, 1H), 3.81 (s, 3H), 2.38 (dtd, $J = 6.1, 3.2, 2.6, 1.4$ Hz, 2H), 2.19 (dddd, $J = 8.7, 6.3, 4.4, 2.5$ Hz, 2H), 1.82 – 1.72 (m, 2H), 1.68 – 1.61 (m, 2H) ppm. **LRMS** (DEP/EI-Orbitrap): m/z (%): 188.1 (100), 184.0 (5), 173.1 (15), 159.0 (50). Analytical data in accordance to literature.²⁹⁴

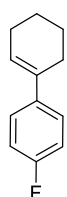
3',4'-Dichloro-2,3,4,5-tetrahydro-1,1'-biphenyl (4d)

Using potassium cyclohex-1-en-1-yltrifluoroborate and a solution of (3,4-dichlorophenyl)magnesium bromide in THF according to general procedure S, provided **4d** (0.21 mmol, 48 mg, 53%) as colorless oil. $R_f = 0.80$ (hexane, UV, PAA, KMnO_4). $^1\text{H NMR}$ (400 MHz, CDCl_3) δ 7.44 (d, $J = 2.2$ Hz, 1H), 7.35 (d, $J = 8.4$ Hz, 1H), 7.20 (dd, $J = 8.4,$

²⁹⁴ M. O. Ganiu, A.-H. Cleveland, J. L. Paul, R. Kartika, *Org. Lett.* **2019**, *21*, 5611–5615.

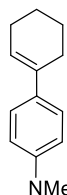
2.2 Hz, 1H), 6.13 (td, $J = 4.0, 1.9$ Hz, 1H), 2.33 (tdd, $J = 6.2, 2.5, 1.7$ Hz, 2H), 2.20 (dddd, $J = 9.2, 6.7, 4.7, 2.7$ Hz, 2H), 1.82 – 1.72 (m, 2H), 1.70 – 1.58 (m, 2H) ppm. ^{13}C NMR (101 MHz, CDCl_3) δ 142.0, 134.8, 132.3, 130.2, 130.1, 127.0, 126.7, 123.5, 27.3, 26.0, 23.0, 22.0 ppm. LRMS (DEP/EI-Orbitrap): m/z (%): 226.0 (70), 211.0 (20), 191.0 (60), 163.0 (100). HRMS (EI-Orbitrap): m/z calcd. for $\text{C}_{12}\text{H}_{12}\text{Cl}_2^+$: 226.0316; found: 226.0309. IR (Diamond-ATR, neat) $\tilde{\nu}_{\text{max}}$ (cm^{-1}): 2927 (w), 2848 (w), 1724 (w), 1627 (w), 1463 (w), 1447 (w), 1425 (w), 1384 (w), 1363 (w), 1353 (w), 1311 (w), 1279 (w), 1261 (w), 1236 (m), 1128 (vs), 1076 (w), 1042 (m), 969 (m), 947 (m), 916 (w), 904 (m), 863 (w), 844 (m), 802 (w), 773 (w), 762 (w), 746 (w).

4'-Fluoro-2,3,4,5-tetrahydro-1,1'-biphenyl (4e)



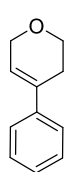
Using potassium cyclohex-1-en-1-yltrifluoroborate and a solution of (4-fluorophenyl)magnesium bromide in THF according to general procedure, provided **4e** (0.30 mmol, 53 mg, 75%) as colorless oil. ^1H NMR (400 MHz, CDCl_3) δ 7.41 – 7.29 (m, 2H), 7.03 – 6.92 (m, 2H), 6.06 (tt, $J = 3.9, 1.8$ Hz, 1H), 2.37 (ddq, $J = 6.3, 4.3, 2.2$ Hz, 2H), 2.20 (dtt, $J = 8.8, 6.1, 2.6$ Hz, 2H), 1.85 – 1.74 (m, 2H), 1.70 – 1.60 (m, 2H) ppm. LRMS (DEP/EI-Orbitrap): m/z (%): 176.1 (100), 161.0 (50), 147.0 (100). Analytical data in accordance to literature.²⁹⁵

N,N-dimethyl-2',3',4',5'-tetrahydro-[1,1'-biphenyl]-4-amine (4f)*



Using potassium cyclohex-1-en-1-yltrifluoroborate and a solution of (4-(dimethylamino)phenyl)magnesium bromide in THF according to general procedure **S**, provided **4f** (0.20 mmol, 40 mg, 70%) as colorless oil. ^1H NMR (400 MHz, CDCl_3) δ 7.34 – 7.27 (m, 2H), 6.74 – 6.65 (m, 2H), 6.00 (tt, $J = 4.0, 1.7$ Hz, 1H), 2.94 (s, 6H), 2.38 (ddt, $J = 6.2, 3.9, 2.0$ Hz, 2H), 2.19 (dtd, $J = 8.2, 4.0, 2.2$ Hz, 2H), 1.82 – 1.72 (m, 2H), 1.69 – 1.59 (m, 2H) ppm. LRMS (DEP/EI-Orbitrap): m/z (%): 201.1 (100), 197.1 (40), 186.1 (5). Analytical data in accordance to literature.²⁹⁶

4-Phenyl-3,6-dihydro-2H-pyran (4g)



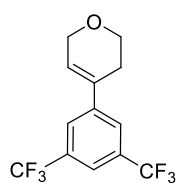
Using potassium (3,6-dihydro-2H-pyran-4-yl)trifluoroborate (**SM43**) and a solution of phenylmagnesium bromide in THF according to general procedure **S**, provided **4g** (0.24 mmol, 38 mg, 60%) as colorless oil. ^1H NMR (400 MHz, CDCl_3) δ 7.42 – 7.38 (m, 2H), 7.37 – 7.32 (m, 2H), 7.30 – 7.24 (m, 1H), 6.13 (tt, $J = 3.0, 1.6$ Hz, 1H), 4.33 (q, $J = 2.8$ Hz, 2H), 3.94 (t, $J = 5.5$ Hz, 2H), 2.74 – 2.34 (m, 2H) ppm. LRMS (DEP/EI-Orbitrap): m/z (%): 160.1 (100), 145.1 (10), 131.1 (100). Analytical data in accordance to literature.²⁹⁷

²⁹⁵ K. Ishizuka, H. Seike, T. Hatakeyama, M. Nakamura, *J. Am. Chem. Soc.* **2010**, *132*, 13117–13119.

²⁹⁶ W. D. Oosterbaan, P. C. M. van Gerven, C. A. van Walree, M. Koeberg, J. J. Piet, R. W. A. Havenith, J. W. Zwicker, L. W. Jenneskens, R. Gleiter, *Eur. J. Org. Chem.* **2003**, 3117–3130.

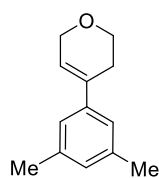
²⁹⁷ B. Guo, G. Schwarzwald, J. T. Njardarson, *Angew. Chem. Int. Ed.* **2012**, *51*, 5675–5678.

4-(3,5-Bis(trifluoromethyl)phenyl)-3,6-dihydro-2H-pyran (4h)



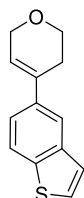
Using potassium (3,6-dihydro-2H-pyran-4-yl)trifluoroborate (**SM43**) and a solution of (3,5-bis(trifluoromethyl)phenyl)magnesium bromide in THF according to general procedure **S**, provided **4h** (0.22 mmol, 64 mg, 54%) as colorless oil. $R_f = 0.30$ (hexane/EtOAc 9:1, UV, PAA, KMnO_4). $^1\text{H NMR}$ (400 MHz, CDCl_3) δ 7.80 (s, 2H), 7.76 (s, 1H), 6.31 (tt, $J = 3.0, 1.6$ Hz, 1H), 4.36 (q, $J = 2.9$ Hz, 2H), 3.96 (t, $J = 5.4$ Hz, 2H), 2.59 – 2.51 (m, 2H) ppm. $^{13}\text{C NMR}$ (101 MHz, CDCl_3) δ 142.3, 132.3, 131.89 (q, $J = 33.1$ Hz), 126.3, 125.05 – 124.76 (m), 123.51 (d, $J = 271.9$ Hz), 121.09 – 120.83 (m), 65.8, 64.2, 27.1 ppm. **LRMS** (DEP/EI-Orbitrap): m/z (%): 296.1 (100), 278.1 (70), 267.1 (80), 254.1 (20). **HRMS** (EI-Orbitrap): m/z calcd. for $\text{C}_{13}\text{H}_{10}\text{F}_6^+$: 296.0636; found: 296.0628. **IR** (Diamond-ATR, neat) $\tilde{\nu}_{max}$ (cm^{-1}): 1710 (m), 1621 (vw), 1470 (vw), 1356 (m), 1275 (vs), 1224 (w), 1171 (s), 1123 (vs), 1053 (m), 1021 (m), 963 (w), 940 (m), 899 (m), 879 (w), 844 (m), 810 (w), 725 (w), 701 (m), 681 (s).

4-(3,5-Dimethylphenyl)-3,6-dihydro-2H-pyran (4i)



Using potassium (3,6-dihydro-2H-pyran-4-yl)trifluoroborate (**SM43**) and a solution of (3,5-dimethylphenyl)magnesium bromide in THF according to general procedure **S**, provided **4i** (0.22 mmol, 64 mg, 54%) as colorless oil. $R_f = 0.35$ (hexane/EtOAc 98:2, UV, KMnO_4). $^1\text{H NMR}$ (400 MHz, CDCl_3) δ 7.02 (s, 2H), 6.92 (s, 1H), 6.09 (tt, $J = 3.1, 1.6$ Hz, 1H), 4.32 (q, $J = 2.8$ Hz, 2H), 3.93 (t, $J = 5.5$ Hz, 2H), 2.54 – 2.48 (m, 2H), 2.33 (s, 6H) ppm. $^{13}\text{C NMR}$ (101 MHz, CDCl_3) δ 140.5, 138.0, 134.4, 129.1, 122.8, 122.2, 66.0, 64.7, 27.5, 21.5 ppm. **LRMS** (DEP/EI-Orbitrap): m/z (%): 188.1 (100), 173.1 (90), 159.1 (35), 145.1 (100). **HRMS** (EI-Orbitrap): m/z calcd. for $\text{C}_{13}\text{H}_{16}\text{O}^+$: 188.1201; found: 188.1206. **IR** (Diamond-ATR, neat) $\tilde{\nu}_{max}$ (cm^{-1}): 2948 (m), 2920 (s), 2894 (m), 1722 (s), 1685 (m), 1602 (s), 1464 (m), 1450 (m), 1444 (m), 1423 (m), 1385 (m), 1363 (m), 1309 (m), 1295 (m), 1280 (m), 1269 (m), 1260 (m), 1242 (m), 1223 (m), 1183 (m), 1160 (m), 1137 (vs), 1084 (s), 1060 (s), 1044 (s), 1017 (m), 995 (m), 974 (m), 966 (m), 951 (s), 881 (m), 849 (s), 818 (m), 699 (m), 688 (m).

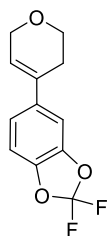
4-(Benzo[*b*]thiophen-5-yl)-3,6-dihydro-2H-pyran (4j)*



Using potassium (3,6-dihydro-2H-pyran-4-yl)trifluoroborate (**SM43**) and a solution of benzo[*b*]thiophen-5-ylmagnesium bromide in THF according to general procedure **S**, provided **4j** (0.09 mmol, 20 mg, 23%) as colorless oil. $R_f = 0.60$ (hexane/EtOAc 98:2, UV, PAA, KMnO_4). $^1\text{H NMR}$ (400 MHz, CDCl_3) δ 7.74 – 7.68 (m, 2H), 7.37 – 7.29 (m, 2H), 7.23 (d, $J = 5.5$ Hz, 1H), 6.09 (tt, $J = 3.0, 1.6$ Hz, 1H), 4.26 (q, $J = 2.8$ Hz, 2H), 3.88 (t, $J = 5.5$ Hz, 2H), 2.59 – 2.46 (m, 2H) ppm. $^{13}\text{C NMR}$ (101 MHz, CDCl_3) δ 140.8, 140.0, 138.7, 136.9, 134.3, 124.2, 122.6, 122.4, 121.7, 119.7, 66.1, 64.7, 27.7 ppm. **HRMS** (EI-Orbitrap): m/z calcd. for $\text{C}_{13}\text{H}_{12}\text{OS}^+$: 216.0609; found: 216.0604. **IR** (Diamond-ATR, neat) $\tilde{\nu}_{max}$ (cm^{-1}): 3253 (w), 3099 (w), 2922 (m), 2853 (m), 1596 (m), 1565 (w), 1503 (w), 1415 (m), 1340 (s), 1328 (s), 1303 (m), 1253 (s), 1231 (m), 1188 (m), 1183

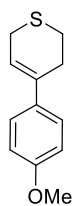
(m), 1146 (m), 1140 (m), 1089 (s), 1046 (s), 1017 (m), 944 (m), 917 (m), 906 (m), 900 (m), 889 (m), 862 (m), 849 (m), 830 (s), 803 (s), 768 (m), 748 (s), 737 (s), 723 (s), 690 (vs).

5-(3,6-Dihydro-2*H*-pyran-4-yl)-2,2-difluorobenzo[*d*][1,3]dioxole (4k)

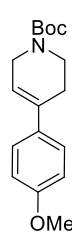


Using potassium (3,6-dihydro-2*H*-pyran-4-yl)trifluoroborate (**SM43**) and a solution of (2,2-difluorobenzo[*d*][1,3]dioxol-5-yl)magnesium bromide in THF according to general procedure **S**, provided **4k** (0.12 mmol, 27 mg, 29%) as colorless oil. $R_f = 0.30$ (hexane/EtOAc 98:2, UV, PAA). $^1\text{H NMR}$ (400 MHz, CDCl_3) δ 7.11 – 7.06 (m, 2H), 7.03 – 6.99 (m, 1H), 6.06 (tt, $J = 3.0, 1.6$ Hz, 1H), 4.31 (q, $J = 2.8$ Hz, 2H), 3.93 (t, $J = 5.4$ Hz, 2H), 2.47 (ttd, $J = 5.5, 2.7, 1.6$ Hz, 2H) ppm. $^{13}\text{C NMR}$ (101 MHz, CDCl_3) δ 144.2, 143.0, 137.1, 133.3, 131.8 (t, $J = 255.1$ Hz), 123.3, 120.1, 109.3, 106.3, 65.9, 64.5, 27.6 ppm. **LRMS** (DEP/EI-Orbitrap): m/z (%): 240.0 (70), 222.0 (20), 196.9 (25), 158.0 (50). **HRMS** (EI-Orbitrap): m/z calcd. for $\text{C}_{12}\text{H}_{10}\text{F}_2\text{O}_3^+$: 240.0598; found: 240.0592. **IR** (Diamond-ATR, neat) $\tilde{\nu}_{max}$ (cm^{-1}): 3248 (w), 3099 (w), 2961 (w), 2923 (w), 2853 (w), 1597 (m), 1565 (m), 1502 (m), 1451 (w), 1421 (m), 1346 (s), 1328 (m), 1303 (m), 1261 (s), 1238 (vs), 1183 (s), 1145 (s), 1088 (s), 1046 (s), 1035 (s), 944 (m), 916 (m), 908 (m), 889 (m), 862 (m), 849 (m), 830 (s), 810 (s), 803 (s), 767 (m), 748 (s), 737 (m), 723 (s), 690 (vs).

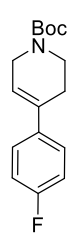
4-(4-Methoxyphenyl)-3,6-dihydro-2*H*-thiopyran (4l)



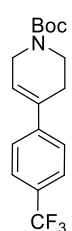
Using potassium (3,6-dihydro-2*H*-thiopyran-4-yl)trifluoroborate (**SM44**) and a solution of (4-methoxyphenyl)magnesium bromide in THF according to general procedure **S**, provided **4l** (0.31 mmol, 63 mg, 77%) as colorless oil. The yield was calculated by $^1\text{H NMR}$ analysis since the hydrolysis product of (4-methoxyphenyl)magnesium bromide (anisole) was not separable from the olefinic product *via* column chromatography. $R_f = 0.50$ (hexane/EtOAc 98:2, UV, PAA). $^1\text{H NMR}$ (400 MHz, CDCl_3) δ 7.30 – 7.25 (m, 2H), 6.89 – 6.84 (m, 2H), 6.12 – 6.08 (m, 1H), 3.81 (s, 3H), 3.33 (dt, $J = 4.5, 2.3$ Hz, 2H), 2.88 (t, $J = 5.8$ Hz, 2H), 2.70 – 2.64 (m, 2H) ppm. $^{13}\text{C NMR}$ (101 MHz, CDCl_3) δ 159.0, 137.7, 135.6, 126.7, 120.3, 113.8, 55.4, 28.8, 26.4, 25.3 ppm. **LRMS** (DEP/EI-Orbitrap): m/z (%): 206.1 (100), 191.0 (5), 177.0 (60), 147.1 (75). **HRMS** (EI-Orbitrap): m/z calcd. for $\text{C}_{12}\text{H}_{14}\text{OS}^+$: 206.0765; found: 206.0765. **IR** (Diamond-ATR, neat) $\tilde{\nu}_{max}$ (cm^{-1}): 3248 (w), 2999 (w), 2934 (w), 2835 (w), 1601 (w), 1578 (w), 1511 (vs), 1493 (m), 1463 (m), 1453 (m), 1443 (m), 1414 (m), 1340 (w), 1322 (w), 1309 (w), 1252 (vs), 1229 (vs), 1179 (m), 1134 (s), 1086 (w), 1071 (vw), 1026 (s), 926 (w), 895 (w), 862 (m), 814 (m), 800 (w), 779 (s), 765 (m), 738 (w), 698 (m), 656 (w).

tert*-Butyl 4-(4-methoxyphenyl)-3,6-dihydropyridine-1(2*H*)-carboxylate (4m)

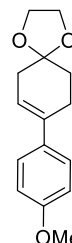
Using potassium (1-(*tert*-butoxycarbonyl)-1,2,3,6-tetrahydropyridin-4-yl)trifluoroborate (**SM40**) and a solution of (4-methoxyphenyl)magnesium bromide in THF according to general procedure **S**, provided **4m** (0.21 mmol, 60 mg, 52%) as colorless oil. ¹H NMR (400 MHz, CDCl₃) δ 7.35 – 7.29 (m, 2H), 6.93 – 6.83 (m, 2H), 6.00 – 5.88 (m, 1H), 4.08 – 4.03 (m, 2H), 3.81 (s, 3H), 3.63 (t, *J* = 5.7 Hz, 2H), 2.53 – 2.45 (m, 2H), 1.49 (s, 9H) ppm. LRMS (DEP/EI-Orbitrap): *m/z* (%): 232.1 (100), 202.1 (15), 188.1 (34), 160.0 (16). Analytical data in accordance to literature.²⁹⁸

tert*-Butyl 4-(4-fluorophenyl)-3,6-dihydropyridine-1(2*H*)-carboxylate (4n)

Using potassium (1-(*tert*-butoxycarbonyl)-1,2,3,6-tetrahydropyridin-4-yl)trifluoroborate (**SM40**) and a solution of (4-fluorophenyl)magnesium bromide in THF according to general procedure **S**, provided **4n** (0.22 mmol, 62 mg, 56%) as colorless oil. ¹H NMR (400 MHz, CDCl₃) δ 7.37 – 7.29 (m, 2H), 7.06 – 6.98 (m, 2H), 6.02 – 5.91 (m, 1H), 4.09 – 4.02 (m, 2H), 3.63 (t, *J* = 5.7 Hz, 2H), 2.53 – 2.44 (m, 2H), 1.49 (s, 9H) ppm. LRMS (DEP/EI-Orbitrap): *m/z* (%): 220.1 (100), 204.1 (15), 177.1 (70). Analytical data in accordance to literature.²⁹⁹

***tert*-Butyl 4-(4-(trifluoromethyl)phenyl)-3,6-dihydropyridine-1(2*H*)-carboxylate (4o)**

Using potassium (1-(*tert*-butoxycarbonyl)-1,2,3,6-tetrahydropyridin-4-yl)trifluoroborate (**SM40**) and a solution of (4-(trifluoromethyl)phenyl)magnesium bromide in THF according to general procedure **S**, provided **4o** (0.17 mmol, 56 mg, 43%) as colorless oil. ¹H NMR (400 MHz, CDCl₃) δ 7.58 (d, *J* = 8.7 Hz, 2H), 7.46 (d, *J* = 8.1 Hz, 2H), 6.15 – 6.08 (m, 1H), 4.15 – 4.00 (m, 2H), 3.65 (t, *J* = 5.7 Hz, 2H), 2.58 – 2.50 (m, 2H), 1.49 (s, 9H) ppm. LRMS (DEP/EI-Orbitrap): *m/z* (%): 271.1 (100), 254.1 (15), 227.1 (90). Analytical data in accordance to literature.³⁰⁰

8-(4-Methoxyphenyl)-1,4-dioxaspiro[4.5]dec-7-ene (4p)

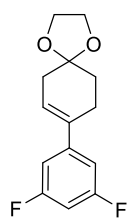
Using potassium trifluoro(1,4-dioxaspiro[4.5]dec-7-en-8-yl)borate (**SM45**) and a solution of (4-methoxyphenyl)magnesium bromide in THF according to general procedure **S**, provided **4p** (0.35 mmol, 86 mg, 87%) as colorless oil. ¹H NMR (400 MHz, CDCl₃) δ 7.35 – 7.31 (m, 2H), 6.88 – 6.81 (m, 2H), 5.90 (td, *J* = 3.9, 2.0 Hz, 1H), 4.02 (s, 4H), 3.80 (s, 3H), 2.66 – 2.60 (m, 2H), 2.51 – 2.42 (m, 2H), 1.92 (t, *J* = 6.5 Hz, 2H) ppm. LRMS (DEP/EI-Orbitrap): *m/z* (%): 246.1 (40), 231.0 (2), 160.1 (100). Analytical data in accordance to literature.³⁰¹

²⁹⁸ The full characterization can be found in chapter 4.4 of the experimental part (molecule **6d**).

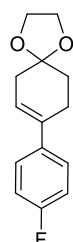
²⁹⁹ D. J. Wustrow, L. D. Wise, *Synthesis* **1991**, *11*, 993–995.

³⁰⁰ Merck & Co., US6303593, **2001**, B1.

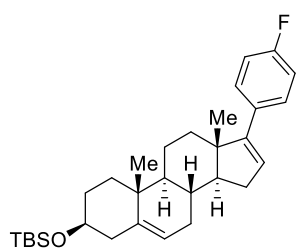
³⁰¹ A. J. Pearson, I. C. Richards, D. V. Gardner, *J. Org. Chem.* **1984**, *49*, 3887–3891.

8-(3,5-Difluorophenyl)-1,4-dioxaspiro[4.5]dec-7-ene (4q)

Using potassium trifluoro(1,4-dioxaspiro[4.5]dec-7-en-8-yl)borate (**SM45**) and a solution of (3,5-difluorophenyl)magnesium bromide in THF according to general procedure **S**, provided **4q** (0.16 mmol, 40 mg, 40%) as colorless oil. $R_f = 0.10$ (hexane/EtOAc 98:2, UV, PAA). $^1\text{H NMR}$ (400 MHz, CDCl_3) δ 6.95 – 6.85 (m, 2H), 6.66 (tt, $J = 8.8, 2.3$ Hz, 1H), 6.05 (tt, $J = 4.0, 1.6$ Hz, 1H), 4.02 (s, 4H), 2.63 – 2.56 (m, 2H), 2.49 – 2.44 (m, 2H), 1.91 (t, $J = 6.6$ Hz, 2H) ppm. $^{13}\text{C NMR}$ (101 MHz, CDCl_3) δ 163.1 (dd, $J = 246.8, 13.3$ Hz), 144.9 (t, $J = 9.2$ Hz), 134.6 (t, $J = 2.6$ Hz), 124.0, 108.3 – 107.9 (m), 107.6, 102.1 (t, $J = 25.6$ Hz), 64.7, 36.2, 31.3, 26.6 ppm. **LRMS** (DEP/EI-Orbitrap): m/z (%): 252.1 (35), 237.0 (5), 164.0 (15), 151.0 (15), 86.0 (100). **HRMS** (EI-Orbitrap): m/z calcd. for $\text{C}_{14}\text{H}_{14}\text{F}_2\text{O}_2^+$: 252.0962; found: 252.0956. **IR** (Diamond-ATR, neat) $\tilde{\nu}_{max}$ (cm^{-1}): 2942 (vs), 2929 (vs), 2892 (s), 2866 (vs), 1502 (vs), 1463 (s), 1254 (m), 1202 (s), 1148 (m), 1096 (s), 1059 (m), 1037 (s), 1017 (s), 1004 (s), 993 (s), 981 (s), 942 (m), 931 (m), 919 (m), 884 (s), 863 (m), 830 (s), 810 (m), 804 (m), 775 (m), 709 (m), 677 (s), 668 (s), 662 (s).

8-(4-Fluorophenyl)-1,4-dioxaspiro[4.5]dec-7-ene (4r)*

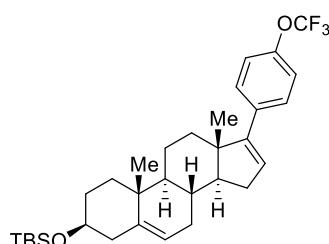
Using potassium trifluoro(1,4-dioxaspiro[4.5]dec-7-en-8-yl)borate (**SM45**) and a solution of (4-fluorophenyl)magnesium bromide in THF according to general procedure **S**, provided **4r** (0.34 mmol, 80 mg, 86%) as colorless oil. $R_f = 0.15$ (hexane/EtOAc 98:2, UV, PAA). $^1\text{H NMR}$ (400 MHz, CDCl_3) δ 7.38 – 7.31 (m, 2H), 7.02 – 6.95 (m, 2H), 5.93 (tt, $J = 3.9, 1.6$ Hz, 1H), 4.02 (s, 4H), 2.63 (tq, $J = 6.4, 2.1$ Hz, 2H), 2.48 – 2.44 (m, 2H), 1.92 (t, $J = 6.5$ Hz, 2H) ppm. $^{13}\text{C NMR}$ (101 MHz, CDCl_3) δ 162.1 (d, $J = 245.4$ Hz), 137.7 (d, $J = 3.2$ Hz), 135.5, 126.8 (d, $J = 7.8$ Hz), 121.6 (d, $J = 1.4$ Hz), 115.1 (d, $J = 21.2$ Hz), 107.8, 64.6, 36.2, 31.4, 27.1 ppm. **LRMS** (DEP/EI-Orbitrap): m/z (%): 234.1 (25), 219.1 (5), 146.0 (20), 133.0 (20), 86.0 (100). **HRMS** (EI-Orbitrap): m/z calcd. for $\text{C}_{14}\text{H}_{15}\text{FO}_2^+$: 234.1056; found: 234.1049. **IR** (Diamond-ATR, neat) $\tilde{\nu}_{max}$ (cm^{-1}): 3406 (w), 2925 (w), 1709 (s), 1599 (m), 1509 (m), 1500 (m), 1412 (m), 1360 (s), 1277 (m), 1261 (m), 1221 (vs), 1158 (s), 1092 (s), 1031 (s), 1014 (s), 946 (m), 931 (m), 900 (m), 881 (m), 828 (s), 811 (s), 748 (m), 682 (m), 668 (m).

***tert*-Butyl(((3*S*,8*R*,9*S*,10*R*,13*S*,14*S*)-17-(4-fluorophenyl)-10,13-dimethyl-2,3,4,7,8,9,10,11,12,13,14,15-dodecahydro-1*H*-cyclopenta[*a*]phenanthren-3-yl)oxy)dime-thylsilane (5a)**

Using potassium ((3*S*,8*S*,9*S*,10*R*,13*S*,14*S*)-3-((*tert*-butyldimethylsilyl)oxy)-10,13-dimethyl-2,3,4,7,8,9,10,11,12,13,14,15-dodecahydro-1*H*-cyclopenta[*a*]phenanthren-17-yl)trifluoroborate (**SM46**) and a solution of (4-fluorophenyl)magnesium bromide in THF according to general procedure **S**, provided **5a** (0.25 mmol, 121mg, 63%) as colorless oil. $R_f = 0.20$ (hexane/EtOAc 98:2, UV, PAA, KMnO_4). $^1\text{H NMR}$ (400 MHz, CDCl_3) δ 7.32 (dd, $J = 8.7, 5.5$ Hz, 2H),

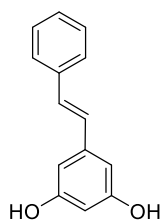
7.01 – 6.95 (m, 2H), 5.85 (dd, $J = 3.4, 1.8$ Hz, 1H), 5.38 – 5.33 (m, 1H), 3.50 (tt, $J = 11.0, 4.7$ Hz, 1H), 2.34 – 2.15 (m, 3H), 2.09 – 1.96 (m, 3H), 1.85 – 1.41 (m, 10H), 1.33 – 1.20 (m, 1H), 1.06 (s, 3H), 1.03 (s, 3H), 0.90 (s, 9H), 0.07 (s, 6H) ppm. ^{13}C NMR (101 MHz, CDCl_3) δ 161.9 (d, $J = 245.4$ Hz), 153.8, 141.9, 133.4 (d, $J = 3.5$ Hz), 128.2 (d, $J = 7.7$ Hz), 127.1, 120.9, 114.9 (d, $J = 21.0$ Hz), 72.6, 57.7, 50.5, 50.4, 47.2, 42.9, 37.3, 36.8, 35.4, 32.1, 31.6, 30.5, 26.0, 20.9, 19.4, 18.3, 16.6, -4.4 ppm. LRMS (DEP/EI-Orbitrap): m/z (%): 423.3 (50), 348.2 (5), 207.0 (100). HRMS (EI-Orbitrap): m/z calcd. for $\text{C}_{31}\text{H}_{45}\text{FOSi}^+$: 480.3224; found: 480.3211. IR (Diamond-ATR, neat) $\tilde{\nu}_{\text{max}}$ (cm^{-1}): 2929 (m), 2900 (m), 2855 (m), 1714 (w), 1600 (w), 1507 (m), 1471 (w), 1462 (m), 1437 (w), 1408 (w), 1380 (w), 1371 (w), 1361 (w), 1294 (w), 1250 (m), 1227 (m), 1159 (m), 1089 (s), 1006 (m), 959 (w), 938 (w), 925 (w), 888 (m), 870 (m), 835 (vs), 806 (s), 774 (s), 736 (w), 718 (w), 668 (m).

***tert*-Butyl(((3*S*,8*R*,9*S*,10*R*,13*S*,14*S*)-10,13-dimethyl-17-(4-(trifluoromethoxy)phenyl)-2,3,4,7,8,9,10,11,12,13,14,15-dodecahydro-1*H*-cyclopenta[*a*]phenanthren-3-yl)oxy)dime-thylsilane (5b)**



Using potassium ((3*S*,8*S*,9*S*,10*R*,13*S*,14*S*)-3-((*tert*-butyldimethylsilyl)oxy)-10,13-dimethyl-2,3,4,7,8,9,10,11,12,13,14,15-dodecahydro-1*H*-cyclopenta[*a*]phenanthren-17-yl)trifluoroborate (SM46) and a solution of (4-fluorophenyl)magnesium bromide in THF according to general procedure S, provided **5b** (0.28 mmol, 153 mg, 70%) as colorless oil. $R_f = 0.30$ (hexane/EtOAc 98:2, UV, PAA, KMnO_4). ^1H NMR (400 MHz, CDCl_3) δ 7.42 – 7.35 (m, 2H), 7.16 – 7.09 (m, 2H), 5.92 (dd, $J = 3.3, 1.8$ Hz, 1H), 5.38 – 5.33 (m, 1H), 3.49 (tt, $J = 11.0, 4.7$ Hz, 1H), 2.35 – 2.16 (m, 3H), 2.09 – 1.97 (m, 3H), 1.87 – 1.41 (m, 10H), 1.30 – 1.21 (m, 1H), 1.06 (s, 3H), 1.04 (s, 3H), 0.89 (s, 9H), 0.06 (s, 6H) ppm. ^{13}C NMR (101 MHz, CDCl_3) δ 153.7, 148.1, 142.0, 136.2, 128.4, 128.0, 121.0, 120.8, 120.6 (q, $J = 256.7$ Hz), 77.2, 72.7, 57.8, 50.6, 47.4, 43.0, 37.4, 36.9, 35.5, 32.2, 31.7, 30.6, 26.1, 21.0, 19.5, 18.4, 16.7, -4.4 ppm. LRMS (DEP/EI-Orbitrap): m/z (%): 489.2 (100), 413.1 (5), 329.1 (10). HRMS (EI-Orbitrap): m/z calcd. for $\text{C}_{32}\text{H}_{45}\text{F}_3\text{O}_2\text{Si}^+$: 546.3141; found: 546.3138. IR (Diamond-ATR, neat) $\tilde{\nu}_{\text{max}}$ (cm^{-1}): 2959 (w), 2936 (w), 2930 (w), 2897 (w), 2857 (w), 1749 (w), 1712 (s), 1602 (w), 1507 (w), 1470 (w), 1458 (w), 1437 (w), 1428 (w), 1382 (m), 1361 (s), 1257 (s), 1220 (vs), 1166 (m), 1085 (s), 1062 (m), 1048 (m), 1019 (m), 1003 (m), 957 (m), 937 (m), 922 (m), 911 (m), 888 (s), 869 (s), 838 (s), 815 (m), 802 (m), 771 (m), 734 (m), 672 (m).

(*E*)-5-Styrylbenzene-1,3-diol (pinosylvin) (5c)

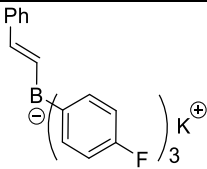
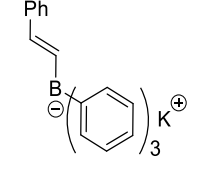
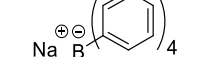


Using potassium (*E*)-trifluoro(styryl)borate and a solution of (3,5-dimethoxyphenyl)magnesium bromide in THF according to general procedure S, provided (*E*)-1,3-dimethoxy-5-styrylbenzene. For deprotection of the alcohol, the crude compound was dissolved in CH_2Cl_2 (4 mL) after electrochemical oxidation, cooled down to -20 °C and treated with a solution of BBr_3 (1.6 mmol, 4.0 equiv) dissolved in 1 mL CH_2Cl_2 .

The reaction was allowed to reach room temperature. After completion, the reaction was treated with water and extracted with dichloromethane (3×10 mL) and washed with a solution of sat. aq. NaCl (1×10 mL). The combined organic phases were dried over MgSO_4 , filtered and concentrated *in vacuo*. The crude was purified by flash-column chromatography with appropriate solvent mixture to provide **5c** (0.23 mmol, 62 mg, 57%, *E/Z* = 99:1) as colorless solid. $^1\text{H NMR}$ (400 MHz, CDCl_3) δ 7.51 – 7.46 (m, 2H), 7.39 – 7.33 (m, 2H), 7.29 – 7.26 (m, 1H), 7.05 (d, $J = 16.3$ Hz, 1H), 6.96 (d, $J = 16.3$ Hz, 1H), 6.58 (d, $J = 2.2$ Hz, 2H), 6.28 (t, $J = 2.2$ Hz, 1H), 4.76 (s, 2H, OH) ppm. **HRMS** (EI-Orbitrap): m/z calcd. for $\text{C}_{14}\text{H}_{12}\text{O}_2^+$: 212.0837; found: 212.0830. Analytical data in accordance to literature.²⁸⁸

6.5 Cyclic Voltammetry

Table 22: Determined Oxidation potentials of ATB salts **2a–b** vs. SCE.

ATB salt	ATB structure	E_p^{Ox} vs. SCE / V
2a		0.81
2b		0.67
NaBPh₄ reference (2c)		0.82

The results of cyclic voltammetry experiments are summarized in Table 22 and Figure 34. The oxidation potentials were determined in acetonitrile on a CH Instruments 630E electrochemical analyzer using a 2 mm diameter platinum working electrode, a platinum wire counter electrode and an Ag wire pseudo-reference electrode applying a scan rate of 0.1 V/s. Cyclic voltammetry measurements were performed in acetonitrile containing 0.1 M NBu_4ClO_4 with the ATB salts (**2a–b**) ($c \approx 3.4 \times 10^{-4}$ M) and ferrocene ($c = 3.8 \times 10^{-4}$ M) as an internal standard. The $E_{1/2}(\text{fc}^+/\text{fc})$ in MeCN) = +0.382 V was used to calibrate E_p^{Ox} (in MeCN) vs. SCE.

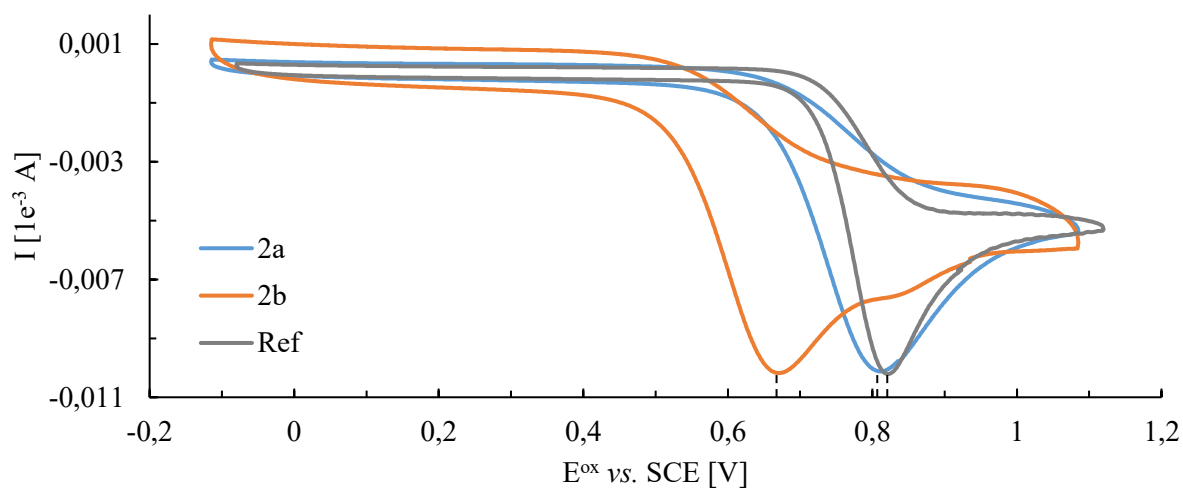


Figure 34: Graphical summary of measured E_p^{ox} vs. SCE of ATB salts **2a–b** and NaBPh₄ reference.

6.6 Calculations²⁶⁶

Calculations were performed at the equation-of-motion ionization potential coupled-cluster singles and doubles (EOM-IP-CCSD) level of theory and using density functional theory (DFT) with the ω B97X-D3 functional. The 6-31G* basis set was used in all calculations if not indicated otherwise. (EOM-IP)-CCSD calculations (Table 23) were performed for isolated molecules in gas phase, DFT calculations were performed in gas phase (Table 24) and additionally taking into account the solvent (acetonitrile) by means of the polarizable continuum (PCM) approach (Table 25 and Table 26).²⁶⁷ Non-equilibrium solvent effects upon ionization were either disregarded (Table 25) or taken into account by means of the state-specific approach (Table 26).²⁶⁸ Molecular structures of the ATB anions were optimized at the ω B97X-D3/6-31G*/PCM level of theory.²⁶⁹ Core electrons were frozen in all CCSD and EOM-IP-CCSD calculations.²⁷⁰ All calculations were performed with the Q-Chem program package, release 5.0.²⁷¹ The energy differences shown in Table 23–Table 26 support most of the trends observed in experiments. For the both ATB salts **2a–b**, the calculations agree with cyclic voltammetry measurements (see Section 4) that the species with the styryl group (**2b**) shows a lower oxidation potential than the tetraphenylborate anion. This effect is however nullified, when the phenyl substituents are exchanged for more electron-deficient *p*-fluorophenyl residues (**2a**), which results in a higher oxidation potential for this ATB salt compared to **2b** and an almost identical oxidation potential as the tetraphenylborate anion. To characterize the change in the electronic structure upon oxidation of the ATB anions, spin and charge densities (Table 27 and Table 28) were computed based on Mulliken population analysis.²⁷² Since this approach is known to suffer from a heavy basis-set dependence, partial charges were additionally computed using the ChEIPG (Charges from the electrostatic potential on a grid) approach (Table 29).²⁷³ These results illustrate that the single styryl moiety is selectively oxidized in all cases while the charge and spin densities of the other aromatic rings change only insignificantly. This fact is

also visualized in Figure 35 and by means of the spin densities of molecules **2a–b**. Notably, results do not change significantly for all other molecules when going from 6-31G* to 6-311G**.

Table 23: Total energies (in atomic units) of closed-shell ATB anions (**2a–b**) and NaBPh₄ reference and the corresponding neutral radicals computed at the CCSD/6-31G* and EOM-IP-CCSD/6-31G* levels of theory, respectively. Energy differences (in eV) are also shown.

ATB salt	$E_t(\text{Anionic})$ (a.u.)	$E_t(\text{Radical})$ (a.u.)	ΔE (eV)
NaBPh ₄ reference	-948.477575	-948.3275427	4.08
2a	-1322.690426	-1322.534683	4.24
2b	-1025.630332	-1025.484670	3.96

Table 24: Total energies (in atomic units) of closed-shell ATB anions (**2a–b**) and NaBPh₄ reference and the corresponding neutral radicals computed at the ω B97X-D3/6-31G* level of theory. Energy differences (in eV) are also shown.

ATB salt	$E_t(\text{Anionic})$ (a.u.)	$E_t(\text{Radical})$ (a.u.)	ΔE (eV)
KBPh ₄ reference	-951.253221	-951.094822	4.31
2a	-1326.271536	-1326.112552	4.33
2b	-1028.631710	-1028.481268	4.09

Table 25: Total energies (in atomic units) of closed-shell ATB anions (**2a–b**) and NaBPh₄ reference and the corresponding neutral radicals computed at the ω B97X-D3/6-31G*/PCM level of theory. The solvent reaction field is equilibrated in all calculations. Energy differences (in eV) are also shown.

ATB salt	$E_t(\text{Anionic})$ (a.u.)	$E_t(\text{Radical})$ (a.u.)	ΔE (eV)
KBPh ₄ reference	-951.325714	-951.104965	6.01
2a	-1326.336968	-1326.136995	5.44
2b	-1028.704321	-1028.505684	5.41

Table 26: Total energies (in atomic units) of closed-shell ATB anions (**2a–b**) and NaBPh₄ reference and the corresponding neutral radicals computed at the ω B97X-D3/6-31G*/PCM level of theory. The state-specific approach is used to describe non-equilibrium solvent effects upon ionization. Energy differences (in eV) are also shown.

ATB salt	$E_t(\text{Anionic})$ (a.u.)	$E_t(\text{Radical})$ (a.u.)	ΔE (eV)
KBPh ₄ reference	-951.325714	-951.075570	6.81
2a	-1326.336968	-1326.103329	6.36
2b	-1028.704321	-1028.472163	6.32

Table 27: Spin densities of neutral ATB (**2a–b**) and NaBPh₄ reference radicals computed from Mulliken population analysis at the ω B97X-D3/6-31G*/PCM level of theory. The values represent the sums of the spin densities associated with the carbon atoms of the four aromatic rings.

ATB salt	Spin densities Ar ¹	Spin density Ar ² /vinyl
KBPh ₄ reference	0.27/0.24/0.24/0.26	-
2a	0.00/0.03/0.06	0.37/0.61
2b	0.00/0.03/0.07	0.33/0.62

Table 28: Differences in charge density between ATB (**2a–b**) and NaBPh₄ reference anions and neutral radicals computed from Mulliken population analysis at the ω B97X-D3/6-31G*/PCM level of theory. The values represent the sums of the charge density differences associated with the carbon atoms of the four aromatic rings.

ATB salt	Δ Charge density Ar ¹	Δ Charge density Ar ² /vinyl
KBPh ₄ reference	0.09/0.09/0.09/0.10	-
2a	0.02/0.01/0.04	0.19/0.17
2b	0.02/0.01/0.03	0.18/0.17

Table 29: Differences in charge density between ATB (**2a–b**) and NaBPh₄ reference anions and neutral radicals computed from charges from the electrostatic potential on a grid (ChEIPG) at the ω B97X-D3/6-31G*/PCM level of theory. The values represent the sums of the charge density differences associated with the carbon atoms of the four aromatic rings.

ATB salt	Δ Charge density Ar ¹	Δ Charge density Ar ² /vinyl
KBPh ₄ reference	-0.21, -0.20, -0.20, -0.19	-
2a	-0.02/-0.01/-0.05,	-0.29/-0.56
2b	-0.03/-0.01/-0.06	-0.28/-0.47

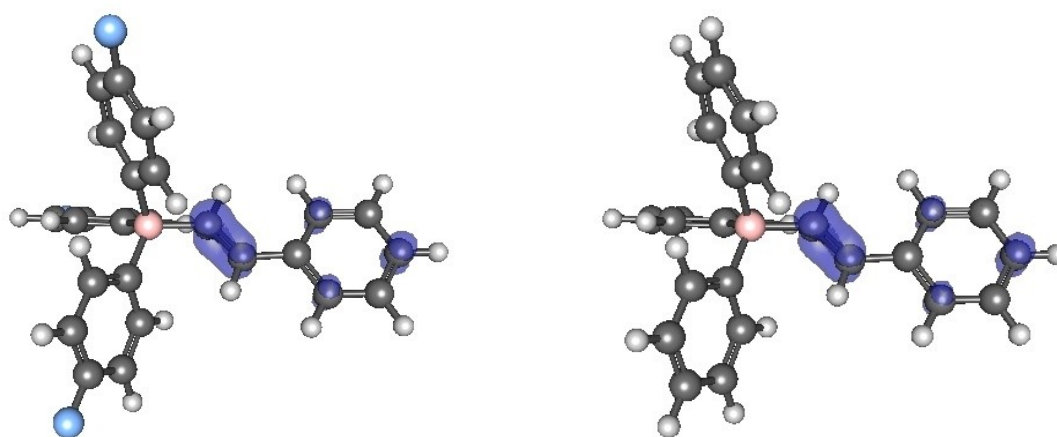


Figure 35: Spin density of the neutral ATB radical for **2a** (left) and **2b** (right) computed at the ω B97X-D3/6-31G*/PCM level of theory and plotted at an *isovalue* of 0.015.

6.7 Single Crystal X-Ray Diffraction

The structure determination of compound **2a** was already presented and can be found in chapter 5.9 of the experimental part.

6.8 Representative NMR Spectra

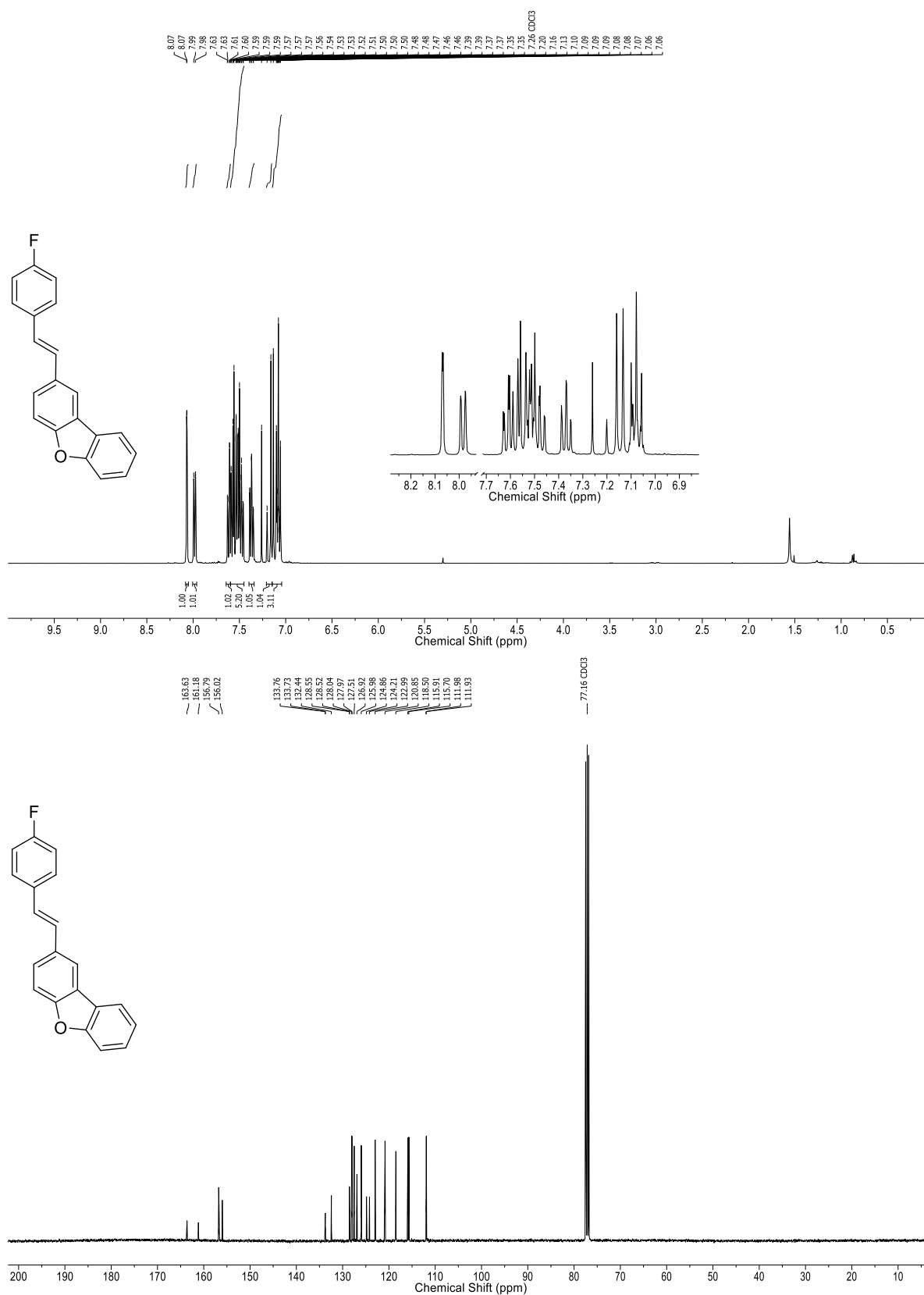


Figure 36: ¹H NMR (400 MHz, CDCl₃) and ¹³C NMR (101 MHz, CDCl₃) for (*E*)-2-(4-Fluorostyryl)dibenzo[*b,d*]furan (**3j**).